A formula for evaluating colour differences for thread sewn into fabric samples

Thorsten Steder

Submitted in accordance with the requirements for the degree of
Doctor of Philosophy

The University of Leeds

School of Chemistry

Department of Colour Science

AUGUST 2012

The candidate confirms that the work submitted is his own and that appropriate credit has been given where reference has been made to the work of others.

Acknowledgements

I would like to thank the University of Leeds for giving me the opportunity for studying a funded degree of Doctor of Philosophy. I would also like to thank Professor Mike Wilson, Dean for the Faculty of Mathematics and Physical Science, for his help during the last stages of this project. I am thankful for the valuable feedback I have received from my external examiner, Dr. Philipp Urban von der Technischen Universität in Darmstadt, and my internal examiner, Dr. Jim Nobbs from the University of Leeds, during my viva examination.

I would like to thank Coats plc. for providing physical colour difference sample pairs; for letting me visit one of their dye houses, and also for their valuable contributions during Experiment B. I believe that some of the results can significantly contribute to a better understanding of how colour appearance phenomena can alter our perception of visual colour differences.

I thank all of my observers who were helping me unconditionally at any time with my experiments. Especially, I would like to thank the Korean Church in Leeds, Rev Dongil Kim, for providing a shelter - and this not only - for those who are from abroad studying here in the UK.

Thank you to Hyunhi, Dagmar, Susanna, Gerhard, and Stephan especially for your help at the beginning of my journey, which after more than ten years comes herewith finally to an end.

Thorsten Steder, 30/01/2013

Abstract

Coats plc.'s research efforts during the 1970's led to a breakthrough in colour difference predictions. The result was a new colour difference formula 'JPC_{79}', which was tested in a commercial environment providing fewer wrong decisions when compared with the best colour matcher from a group at Coats plc. The formula was designed from a large number of thread winding card samples from which colour difference pairs were formed. The formula was later modified and became a standard in the textile industry known as the CMC(*l*:*c*) colour difference formula.

However, visual colour differences for two thread winding card samples, judged in a viewing cabinet side-by-side, may not reflect on a real world scenario, for instance, when a thread is to be matched while stitched upon or within another kind of material, such as a fabric or leather sample. It was therefore of interest to assess such a scenario by using thread end products. Preparing those sample pairs can be time consuming and expensive. Therefore, it was also of interest to assess substitutes on a digital screen with the aim to find a suitable correlation between two methods.

The CMC formula is the preferred equation for calculating colour differences for matching textile samples. The question here was whether the equation can also be used for predicting visual colour differences that were obtained from assessments of end products without compromising its prediction performances.

The primary findings for this project and experimental setups are; (**1**) that the variation in sample type and presentation can alter the perception of colour differences in human observers, significantly; (**2**) it is generally possible to use digital substitutes for psychophysical experiments as such following the same trends as they occur from physical samples that are assessed in a viewing cabinet, (**3**) advanced colour difference formulae can predict those visual colour differences obtained from assessments for end-products once they are optimised (parametric functions), and an overall size parametric factor is applied for various 'thread sewn into fabric samples'.

Table of Contents

List of Tables

List of Graphs

List of Images

List of Figures

List of Abbreviations

LCD	liquid crystal display
CCT	correlated colour temperature
ST	Single Needle Lockstitch type sample
BH	Buttonhole stitch type sample
TWC	Thread Winding card sample
JND	Just noticeable difference
UCS	Uniform chromaticity scale
ULS	Uniform lightness scale
NBS	National Bureau of Standards
mse	mean standard error

Chapter 1

"*Insects produce flowers. Flowers produce the colour-sense in insects. The colour sense produces a taste for colour. The taste for colour produces butterflies and brilliant beetles. Birds and mammals produce fruits. Fruits produce a taste for colour in birds and mammals. The taste for colour produces the external hues of hummingbirds, parrots, and monkeys. Man's frugivorous ancestry produces in him a similar taste; and that taste produces the various final results of the chromatic arts."* (G. Allen[1])

1.1 Colour vision

1.1.1 It is known that vision evolved over time. The mechanism of colour vision consists of two subsystems. One system was described as an ancient neural channel that carried chromatic signals overlaid by a 'modern' system adding further colour information to be interpreted by the brain. Amongst rods, there are three classes of cone cells, which can be found present in a human retina. The cells light sensitivities are strongest in the violet/blue, yellow/green and green/red region. Each individual cone's output depends on the total number of photons that are absorbed by molecules from the photosensitive pigments in the cones. What vary amongst cones are the sensitivities for specific wavelengths and the ratios of photon catches between them. Each cone then signals the total numbers of photons absorbed per unit time for further interpretation. According to Mollon, the information produced by each class of cone is one-dimensional only depending on the absorbed photons in each of the cone cells[2].

1.1.2 A basic colour vision is produced, when the signals of cones in the middle wavelength range ('M' – cones) are compared with signals (or ratios) from cones in the short wavelength range ('S' – cones). This type of colour vision is said to be similar to the vision of dichromate observers, who have one of the 'M' – or 'L' - cone pigments missing. The small amount of 'S' – cones in the retina, when compared to the amount of 'M' – cones, limited the cones ability to detect fine texture, local discontinuities, and/or edges in a visual scene well. It is primarily a subsystem for basic colour vision[3].

1.1.3 The overlaid 'modern' subsystem of colour vision is reserved to primates as described by Jacobs[4]. This was likely to have occurred after a gene duplication, which may have generated and developed a 'new' cone type, extending their sensitivities further up to the red part of the spectrum[5]. The 'M' – and 'L' – cones exhibit rather similar properties. This 'younger' subsystem compares neural information between 'M' - and 'L' – cones with each other. The spatial resolution given by these cones is said to be good. All cone signals are then processed

through a nerve system being either added or subtracted from each other so to form a luminance and two chromatic information channels, according to Viénot and Walraven[6].

1.1.4 This particular arrangement of photo pigments in primates with their peaks around 430, 530 and 560 nanometres maximized the contrast between fruit and foliage. The contrast was at its best when the fruit was ripe (becomes reddish in colour against a greenish colour of leaves when the fruit contained its highest content of sugars). This was to distinguish between '*... form and size but also in properties such as ripe and unripe, eatable and uneatable, flowers with honey and without, against sky, earth or foliage…'* and has developed our 'sense of colour' as a means of survival[7].

The result of this twofold evolutionary subsystem is a sensation in the brain of a continuous range of hues and lightness.

1.2 Early colour science

1.2.1 'Colour Science' had its first known modern recognition in the seventeenth century, when Newton analytically started to use sets of prism to investigate sunlight. He placed a prism in front of a window shutter's hole from which sunlight emerged into a darkened room. A small aperture in a wooden board was placed directly behind the first prism, so to allow only a narrow part of the incoming and yet refracted sunlight to pass through it. A second aperture, from a distant second wooden board, narrowed this beam further down. A second prism placed just behind the second aperture refracted the partial beam furthermore and projected it onto a white wall in a darkened room[8]. The experimental setup permitted Newton to project different parts of the sunlight onto a wall by rotating the first prism in its long axis. The light that was refracted strongest by the first prism was also refracted strongest by the second prism. A red and violet colour emerged on the wall for the weakest and strongest refracted portions of the beam. It was not possible to change a small bandwidth of rays or 'quasi – monochromatic' colours any further once a colour was isolated. Newton identified seven pure spectral colours as red, orange, yellow, green, blue, indigo, and violet, which also can be seen in a rainbow. Yet, there was no 'white' light to be isolated from the spectrum of the sunlight beam. However, a white light emerged on the wall again, when those separated parts of the incident sunlight were re-combined together[2].

1.2.2 Trichromacy, or three component theory, which describes colour vision occurred in opposition to Newton's seven primary colour theory. Le Blon published in 1725 a paper that explained trichromatic colour printing. His work on experimental colour printing secured him a patent in 'printing paintings' long before trichromacy colour vision theory gathered attention to a wider audience, according to Lilien[9].

1.2.3 Other sources, which contributed to the theory of trichromacy, were known as astronomer Mayer[10] and Lambert[11], who designed a three dimensional colour order systems by pigment mixtures of yellow, blue and red (and black and white) pigments. These were early attempts of ordering colours into a systematic way or, in other words, into a 'colour by numbers' system.

1.2.4 Palmer[12], Young[13], von Helmholtz[14], amongst others provided insights towards the development of an additive trichromatic colour mixing theory, in which only three coloured lights (primaries often chosen as red, green, blue or violet) with varying intensities were needed to match any other coloured stimuli. Palmer's theory of colour vision was based on the existence of three rays of light and three corresponding particles (molecules) in the retina, each class only excited by one of the rays. Also, he invented a daylight substitute using a blue coloured glass chamber for oil lamps[2]. Young was one of the first who adopted a wave theory of light suggesting that the physical variable of light was wavelength (physical description) and continuous in its form, whereas trichromacy of colour matching was due to the physiology of the human visual system (visually description). He assumed that colour vision was produced by light that excited three different nerve fibres in the retina. He also became known for his study on interference, and his mapping of colours to the underlying physical variable. Von Helmholtz described differences between absorptive colour mixing (commonly referred to as subtractive) using pigments, and the additive nature of a mixture of coloured lights. He used a mixture of yellow and blue pigments for the centre of a disk whereas the outer area was separated into a yellow and a blue section. The spinning disk revealed a dark 'greenish' colour for the mixture of paints, whereas the individual yellow and blue paint sections appeared greyish to the observer. The inner circle gave rise to its dark greenish appearance due to a physical mixture of blue and yellow pigments before entering the eye. A blue paint absorbs and reflects partly green and most of the red wavelength spectrum. Yellow paint absorbs most of the blue, only part of the green, and reflects most of the red spectrum. Since pigments were said not to be ideal block absorbers, it is likely that some light in the green wavelength range is reflected back from the disk. A lighter grey colour was perceived from two light stimuli entering the eyes due to additive mechanism of cone responses in the short and middle/long wavelength range (reflected blue light consists not of red/green light; reflected yellow light consists of red and green light). The combined signals can appear from grey to white depending on the intensity of the individual signals.

1.2.5 Grassmann formulated laws[a] of additive colour mixtures in 1853[15]. These are summed up in the trichromatic generalisation, which states that *'...over a wide range of conditions of observations, many colour stimuli can be matched in color completely in by additive mixtures of three fixed primary stimuli whose radiant powers have been suitable adjusted...'* as described by Wyszecki and Stiles[16]. A colour sensation was for Grassmann of three-dimensional form corresponding to hue, brightness, and saturation; or, in physical form as wavelength, intensity, and purity. Also, he argued that each colour on a colour circle should have an associated complementary colour. Von Helmholtz[14] was able to draw a chromaticity diagram, based on measurements, so to find complementary lights for green in the purple mixture of red and violet from the end of the spectrum.

1.2.6 Maxwell[17,18] was also concerned with additive colour mixing. He designed a spinning device (Maxwell's disk) consisting of two disks (an inner and outer radial disk). The complete outer radial disk consisted of three circular paint colour patches (those areas were adjustable in size for each colour; i.e. red, green, blue) and an inner black and white circular paint patch (with adjustable areas). The goal was to match the appearances given by the inner with the outer disk by varying the areas of the red, green, and blue patches (subtractive method resulting probably in '1/3' of the brightness of an additive mixture of a red, green, and blue light stimuli) while the disks were rotating around its centre blending all separate areas together. Once a *partitive* match was achieved, it was possible to describe this match in mathematical form as given in *Equation 1* (**Eq. 1**).

Eq. 1: $.15\mathrm{R} + .35\mathrm{G} + .50\mathrm{B} = .40\mathrm{W} + .60\mathrm{D}$**,** where

'R', 'G', and 'B' refers to the red, green, and blue coloured area, and 'W' or 'D' refers to the disk's black ('W') or white ('D') painted area. The decimals refer to amounts or areas in degrees normalised to unity, which are needed to match any given amount of black and white. Varying the amounts of black and white will alter the brightness of the resulting grey shade. Maxwell[19] also invented a device that allowed a match of daylight with a mixture of three monochromatic lights. By varying the intensities of those primaries, he was able to match any given wavelength of a light stimulus. The intensities needed to match each colour throughout the visible wavelength range were then plotted in a diagram, which was regarded as an early attempt to construct colour-matching functions from his wife's matching observations.

---

[a] see page 78

1.2.7 The Young-Helmholtz three-component colour vision theory assumed the existence of three different cone types mainly differing in their spectral sensitivities. The degree of responses from light in the short, medium, and long wavelength range of the cones produced a sensation of colour. They assumed that the sensation of colour was transmitted directly from the cones unaltered to the brain. The foundation was based on empirically obtained colour matching results (2° degree observer) of additive mixture from light stimuli[20].

1.3 Colour vision phenomena and opponency

1.3.1 However, some phenomena could not be explained by this theory; for instance, (**a**) why a blue light mixed with a yellow light appeared as a white light to the observer, or (**b**) why a yellow colour sensation was given by the additive mixture of red and green light, and (**c**) why a greenish after image occurred once the eye rested against a white area after a prolonged sensation from a saturated red patch.

1.3.2 Other phenomena were associated with simultaneous contrast when objects, which were placed on a green background, appeared redder (and vice versa). Objects, placed on a blue background, appeared yellower and vice versa as described by Fairchild[21]. The hypothesis of 'opponent' colour responses was less prominent at that time, but successfully explained colour vision in humans and some of the appearance phenomena, which were not explained by trichromacy[22].

1.3.3 Hering proposed in 1878 an opponent–colour (four colour) theory[23], in which three photoreceptors react in an opponent fashion producing either; a red (but not green), or green (but not red), blue (but not yellow), or yellow (but not blue) and a brightness sensation ranging black to white, respectively. Those visual processes generated neural signals accounting for colours described as; red, yellow, green and blue; intermediates such as; red-yellow, yellow-green, green-blue, and blue-red but not bluish-yellow, yellow-bluish, reddish-green or greenish-red.

1.3.4 Both, trichromacy and opponent colour vision theory, were empirically derived and yet, if seen alone, have failed to explain one or another important colour-vision phenomena albeit contradicting each other. However, it was not well understood which phenomenon actually occurred in the retina, according to Ohta and Robertson[24]. Around 1930, it was understood that phenomena such as colour matching, discrimination, appearance and chromatic adaptation results could be explained and predicted by combining both theories[22].

1.4 Zone system

1.4.1 Müller published in 1922 and 1929 his view on the matter and introduced a zone theory[25,26]. The first zone was designed in accordance to the principles of 'Young-Helmholtz' trichromacy theory. Colour vision was introduced by absorption of photons in one of the three cones. Three different cone types, which were sensitive in the short, medium, and long wavelengths range, were initiating colour vision through absorption of photons by photopigments in the cones, as such transforming gains of energy into electrical signals (photochemical stage).

1.4.2 A neural network transfers those signals to new information resulting in one achromatic and two chromatic signals (intermediate chemical stage). This process was designed to be closely related to Hering's opponent colour vision theory. The third zone (excitation of nerve fibres) refers to the cortex in the brain receiving signals, which are interpreted either by visual experiences (memory) or other visual information, such as spatial and temporal occurrences. Judd (1949, 1951) provided further information as how to develop models that can describe mathematically those processes that takes place in each zone[27]. A graphical representation of the first and third process inherent in the zone theory can be seen in *Figure 1* and *2*. Mathematical models, in respect to colour matching functions for two processes, are given in *Equation 1* (Cone Receptor Stage) and *Equation 2* (Neural Coding) for each cone class.

1.4.3 Jameson and Hurvich work[28,29] in the 1950s is based on chromatic response functions, which are linear related to colour matching functions. Their mathematical model of the response functions is similar to Judd's model (*Equation 2*) for the third zone stage in Müller and/or Adam's[30,31] interpretation of the zone theory. In this method, a colour such as bluish-green will be altered either by yellow or red to cancel out the blue or green part, so to derive unique blue or green. A unique red, green, yellow, and blue stimuli are then identified for each observer. Monochromatic lights were then presented to those observers, who were asked to cancel out hues, in order to derive unique hues. Stimuli related to the short wavelength range are altered by adding unique green to cancel out redness; unique red to cancel out green, and unique blue to cancel out red. Those cancellation amounts (or energies) necessary for cancellation of hues are then recorded at each wavelength. This method derives opponent spectral sensitivities curves similar as seen in *Figure 2*[32]. Other colour vision theories included, for instance, the 'retinex' theory described and invented by Land[33] in 1974.

Eq. 2: $\bar{p}_1(\lambda) = 3.1956\bar{x}(\lambda) + 2.4478\bar{y}(\lambda) - 0.6434\bar{z}(\lambda)$

$\bar{p}_2(\lambda) = -2.5455\bar{x}(\lambda) + 7.0492\bar{y}(\lambda) + 0.4963\bar{z}(\lambda)$

$\bar{p}_3(\lambda) = 5.0000\bar{z}(\lambda)$

Eq. 3: $\beta_1(\lambda) = 6.325[\bar{x}(\lambda) - \bar{y}(\lambda)]$

$\beta_2(\lambda) = 2.004[\bar{y}(\lambda) - \bar{z}(\lambda)]$

$\beta_3(\lambda) = \bar{y}(\lambda)$, where

'$\bar{x}$', '$\bar{y}$', and '$\bar{z}$' refers to the individual CIE colour matching functions for the CIE 1931 standard observer. The relationship between the relative spectral response against wavelength for each cone type, and the relative spectral response for six neural sensations of grey from black to white, red or green, and yellow or blue are given in *Figure 1* and *2*. *Figure 1* shows the 'spectral responsivities' of the cones derived from *Equation 1*. The coefficients were determined from König's fundamentals[34]. The curves 'p_1 (λ)', 'p_2 (λ)', and 'p_3 (λ)' refer to the long, medium, and short cone receptor sensitivities, which are plotted against wavelength (nm). The red/green curve 'b_1(λ)' refers to a photoreceptor responding positive to red and negative to green signals (at 550 nm -4 green and +2 yellow = greenish/yellow sensation), the yellow/blue or 'b_2(λ)' curve refers to a photoreceptor responding positive to yellow and negative to blue signals (at 450 nm -3.3 blue +2 red = reddish/blue sensation), and 'b_3(λ)' refers to the luminance or black/white channel similar to CIE '$\bar{y}$' - colour matching function.

1.4.4 Evidence was collected to support both theories, especially backed up by the progress in measurement techniques since the 1960's (electro-retinography for the study of electrical properties inherent in biological cells and nervous systems). According to Ohta and Robertson[35], it is possible to record electrical responses in cones using detectors in size of a fraction of a micrometre. Measurements of trichromatic responses of carp cones were taken (*Figure 3*) by introducing coloured lights to the cones. The electrical responses of each cone depend on wavelength and approximately matched the spectral response function in *Figure 1*. This gave further evidence in favour for the 'Young-Helmholtz' trichromacy theory at the cone level stage. When measurements were taken inaccurately, in fact just before the actual location of the cones, measured responses revealed electrical signals producing opponency patterns coming from cells transmitting signals to the brain (*Figure 4*). Recent research has indeed found evidence that the cone responses are additive in nature, and that electric signals produced in cones are undergoing an opponent process once they are transmitted through the nerve cells.

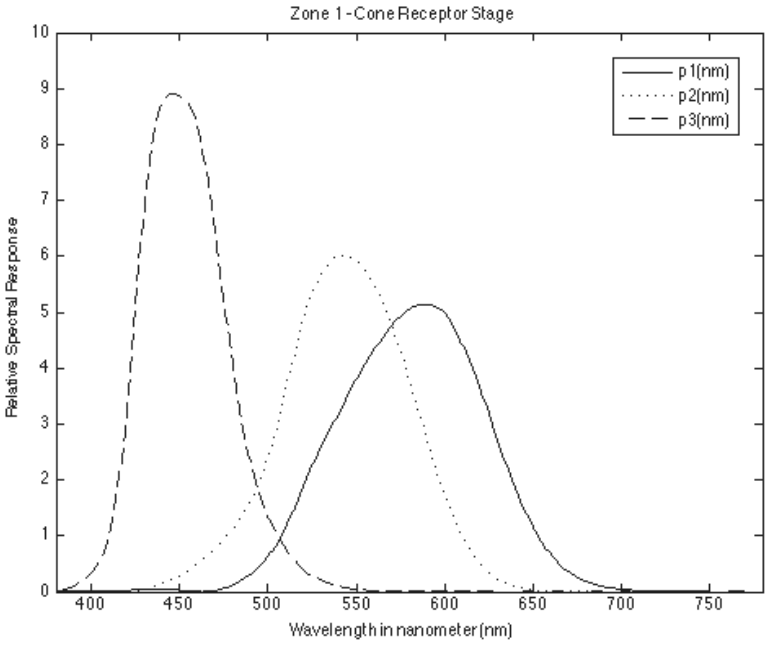

***Figure 1*: Müller and Judd color vision zone theory – Zone 1 Trichromacy; Data taken from Wyszecki and Stiles (2000), page 637.**

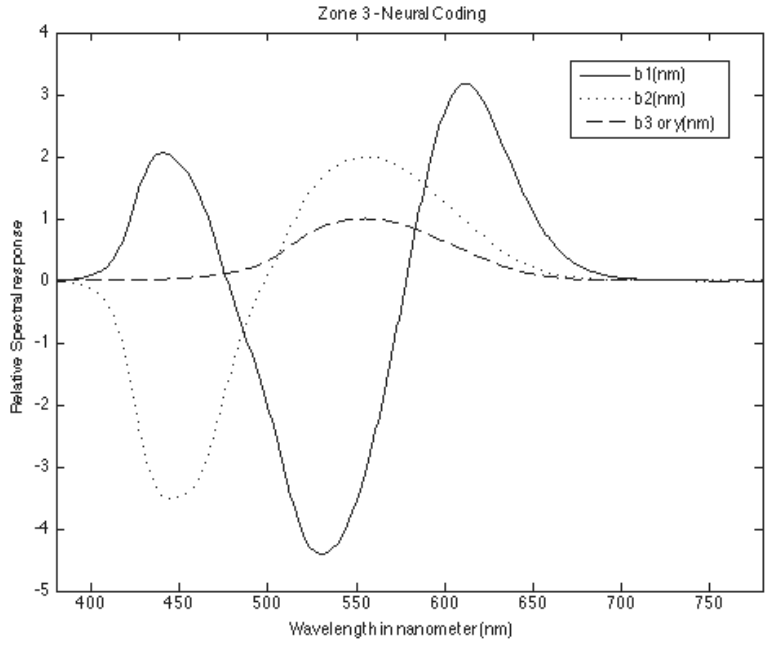

***Figure 2*: Müller and Judd color vision zone theory – Zone 3 Opponent theory; Data taken from Wyszecki and Stiles (2000), page 637.**

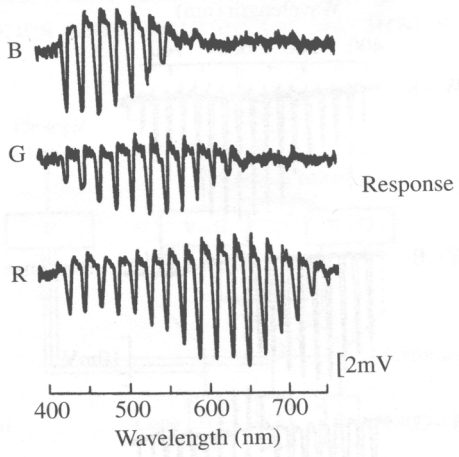

***Figure 3*: Trichromatic responses from carp cones (Tomita *et al.*, 1967). Source: Ohta and Robertson (2005), page 43.**

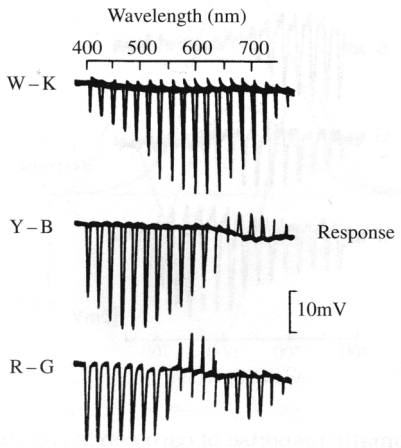

***Figure 4*: Electrical responses in the carp retina (Tomita, 1963). Source: Ohta and Robertson (2005), page 43.**

1.5 Photometry and colorimetry

1.5.1 However, Grassman's work manifested in his trichromatic generalisation[36] (and its stronger form given by Wyszecki and Stiles[16]); early attempts of Maxwell[19] so to construct colour matching functions; later work of Gibson and Tendall[37]; Guild[38] and Wright[39] contributed to the foundation of a photometric and colorimetric system. Those systems were provided in 1924 by introducing a standard photometric observer (Commission Internationale de Photométrie), and by introducing a standard colorimetric observer in 1931 by the CIE (Commission Internationale de l'Eclairage), respectively. 'Photometry', or '*…the measurement of light according to perceived brightness to the human eye'*, and 'Colorimetry', or '*…quantification of how colour was perceived by a human observer',* therefore, couples objective physics of light stimuli with subjective perception from human observers under

restricted viewing conditions, as described by Lee[40]. Psychophysical colour stimuli are represented in its physical form as spectral power or radiant intensity distributions. A reduced numerical form is given as 'XYZ' – tristimulus values (as to how this light stimuli is recorded by the photoreceptors in the eyes). The concept of a 'Standard Photometric Observer' is defined in the form of a spectral luminance efficiency function 'V(λ)' for daylight but also for low light level or scotopic vision 'V'(λ)'. This function couples radiometric measures (i.e. as how much radiant intensity per small wavelength bandwidth was contained in a light stimuli) with the sensation it produces in the observer's eyes.

1.5.2 In order to reduce measurements of spectral power or radiant intensity distributions for any colour stimuli to the effect it has on the colour perception of human observers, it is necessary to know the fundamental sensitivity functions of the photoreceptors in the eyes (*Figure 3*). It was not possible at that time to measure cone responses in the retina by direct means. However, using linear transformations of these response functions served well to describe them. Several monochromatic light stimuli in one half of a 2° degree viewing field over the visible wavelength range were matched in appearance while varying radiant power of three primary stimuli (red, green, and red) viewed in the second 2° degree viewing field. Those obtained colour matching functions '$\bar{r}(\lambda)$','$\bar{g}(\lambda)$', and '$\bar{g}(\lambda)$' for the short, medium, and long wavelength range were standardised and resulted in the CIE 1931 2° Standard Colorimetric Observer (CIE 1964 10° Supplementary Standard Colorimetric Observer for colour matching with a field of view larger than 4° angular subtense). Negative loops in the long wavelength range functions was one reason for the CIE to transform 'real' primaries, which were used during matching tasks, to a set of imaginary primaries ('X', 'Y', 'Z'). The 'new' colour matching functions '$\bar{x}(\lambda)$', '$\bar{y}(\lambda)$', '$\bar{z}(\lambda)$' for the CIE 2° Standard Colorimetric Observer included a photometric term since '$\bar{y}(\lambda)$' was equal to the luminance function 'V(λ)'.

1.5.3 Psychophysics is concerned with colour matches of light stimuli. If two samples differ in physical characteristics (different spectral radiant power distributions), but produce the same sensation in the eyes of a human observer, then they are said to be metameric. The CIE colorimetric fundamentals are related to these phenomena, and as such are many other applications in *Colour Science* today, for instance, in additive or subtractive colour mixing applications in the television or colorant industry, according to Schanda[41].

1.6 Modern colour science

1.6.1 If we want to quantify the difference between two stimuli that do not match, then colour difference evaluation is concerned. Colour difference formulae belong to advanced colorimetry. The CIE also provides other concepts, which are of importance in colorimetry:

(**1**) *CIE Standard Colorimetric Observer* representing the ideal colour matching functions from the average observer from a large population,

(**2**) *CIE Standard Illuminants* for defining light sources in terms of relative spectral power distributions that can be used for the measurement of object colours,

(**3**) Methods of calculating *CIE illuminants*,

(**4**) *CIE Standard Sources*, such as a CIE Source 'A' being realised by a gas filled coiled tungsten filament lamp operating at '2856' K,

(**5**) Calculation of *CIE XYZ-tristimulus values,* standardised viewing and illumination conditions,

(**6**) *CIE Uniform Colour Space* and *Uniform Chromaticity Diagram*,

(**7**) *Colour Difference Formulae*,

(**8**) *CIE Metamerism Index* for change in illuminant,

(**9**) *CIE Colour Rendering Index* for assessing the quality of a light source in comparison to a standard light source judged by samples colour appearance changes if seen under both illuminations,

(**10**) calculation of *chromaticity coordinates* and *dominant wavelength*, *excitation purity* and *colorimetric purity* as colour appearance descriptors for saturation and hue of a colour, and

(**11**) maximum values of *luminous efficacy* and *optimal colours* for a defined set of viewing conditions.

1.6.2 The CIE has now evolved beyond the fundamental principles established in 1931. Colorimetry was initially concerned with colour matching and to some extent with predicting *small* colour differences, when two stimuli did not match with each other. However, as discussed by Lee[40], it cannot describe alone what colour a human observer actually sees. Colorimetry specifies the physical aspect of a colour stimulus under specific viewing conditions; but not, how a colour appears to an observer. Also, tristimulus values are strictly related to colour measurements but may ignore factors such as texture, gloss, and surface characteristics. Two samples with the same tristimulus values may therefore produce a different colour sensation to the eyes of an observer caused by a change of material, surface structure,

texture, surround and background, illumination, and/or viewing conditions, as explained by Rigg[42].

1.6.3 Important aspects in respect to the viewing field, which influences a colour appearance of a stimuli, are specified and described by Hunt[43,44] and Fairchild[21] as; (**a**) the colour stimulus of about 2° angular subtense (the object), (**b**) the proximal field around the object with an angular subtense from 3° to 4° degree (**c**) the background with an angular subtense from 5° to 10° degree, (**d**) the surround outside the background (entire environment a colour is viewed in), and (**e**) the adapting field as the total environment including (**a**) – (**d**) that extend in all directions. Expansions to the CIE system nowadays belong amongst others to;

(**12**) *Chromatic Adaption Transforms* ('CAT') to predict light and chromatic adaption in the form of corresponding colours[45],

(**13**) *Colour Appearance Models* ('CAM') and *Spaces*, capable of predicting colours viewed across a wide range of viewing conditions[46],

(**14**) also to be used for colour difference predictions from three appearance attributes, such as chromatic content combined with lightness and hue[47],

(**14**) new fundamental *Cone Response Functions* ('CRF'), which specify colours in a 'LMS'- space instead of in a 'XYZ' - tristimulus colour space,

(**15**) this approach can also be extended to derive a *cone fundamental chromaticity diagram*, *colour differences*, and *appearance measures* in the future, if vision science is of predominant interest[6].

1.6.4 Other areas of interests in colorimetry are reported as (**a**) the underestimation of luminance at wavelengths below 460 nm for the 1931 CIE Standard Observer, (**b**) to derive improved colour matching functions, (**c**) the standard deviate observer, (**d**) standard daylight illuminants, (**e**) colour difference evaluation for images, and (**f**) visual appearance measurements, according Hunt[48]. Schanda[41] has classified colour difference formulae, specification of metamerism, chromatic adaption transforms, colour appearance models, perceptual uniform appearance colour spaces, amongst others as advanced colorimetric applications, that are of interest in colour science today.

1.7 Project background

1.7.1 It is desired to enhance colour uniformity since the early years of colour reproductions as such to match a product in colour as close as possibly with the original sample. To communicate a colour specification of a reproduction was often a challenge. How to specify a colour unambiguously amongst people and plants, which were involved in a manufacturing process, often required clarification. Colour order systems, in which colours are ordered in a systematic manner, were an early attempt to improve colour communication. Systems that aims to order colours in accordance to certain attributes can be classified mainly into three groups; (**a**) systems, which are based on additive colour mixing of colour stimuli, (**b**) systems based on colorant mixtures of dyes or pigments, and (**c**) colour order systems based on colour perception or colour appearance systems. Prominent colour appearance examples are known as the 'Munsell Color System', 'DIN Colour System', 'NCS' system, or 'OSA Colour System' amongst others.

1.7.2 Those systems could be of conceptual form (colour order system), or a collection of physical samples (colour atlas). It became a custom in industry to produce a catalogue containing physical production samples, which could then be presented to a buyer. These shades or cards were labelled and ordered systematically in terms of its hue (colour), chroma (saturation), and lightness attributes. It can provide a visual idea of a product and how it would look alike in certain viewing conditions. It also provides an unambiguous specification system that can be used as a communication tool between people. However, the success of this 'colour by numbers' attempt is not only dependend on a good reproduction of the original sample (standard) but also depends on the viewing conditions, in which they those samples are seen.

1.8 Visual matching

1.8.1 Professional colourists were trained to use their eyes for specifying matches between a standard and reproduction samples. Colour discrimination of human observers are generally said to be precise enough for typical matching assignments. However, those matches can be subjective, especially if only one individual observer selects whether a match is successfully produced, or not. In fact, individual colour sensitivity functions vary significantly amongst observers. Other influences that can alter matching results are associated, for instance, with colour defective vision, fatigue, and/or with the emotional state of a colour matcher.

1.9 Colour measurement

1.9.1 The development of colour measurement instruments in the 20th century enabled colourists to obtain spectral power or radiant distribution data, which were then used to determine the unique physical colour aspects of a sample. Also, tristimulus colorimeters were introduced, which included red, green and blue filters simulating those sensitivities curves from an ideal average human observer (colour matching functions). Methods were provided with the introduction of a colorimetric system by the CIE in 1931 as how to measure, calculate, and communicate a colour by numerically means. Those methods found a wider audience in industry giving its objective foundation. Whether, and how these instrumentally obtained colour information for two samples that differ in colour, could be related to perceived colour differences from a human observer, needed still to be established. Also, it became evident that observations made in reference to the magnitude of a colour difference resulted in larger variations than if made in reference for matching two colours, as described by the CIE[49].

1.10 Colour difference formula

1.10.1 It also became meaningful to derive colour difference tolerances so to accept small variations between a standard colour and its reproduction due to the possible limitations that can be an inherent in any reproduction systems. So, to which extent will a perceived colour difference be acceptable to the designer or buyer of a product? And, how will these human observer limits be interpreted with those results that are obtained from instrumental measurements? One answer to this question is to correlate results from psychophysical experiments with those results that are obtained from instrumental measurements, according to Witt[50]. Psychophysical experiments are concerned with the study of psychological responses from human observers obtained from physical stimuli, in our case, from samples that differ in colour. Since the 1930s, researchers tried to find appropriate colour difference metrics for a range of industrial applications. Being able to identify the magnitude and direction of a colour difference as perceived differences in lightness, chroma, or hue can provide useful information. Those directions can then be used to adjust parameters that are generally used in a reproduction process. The CIE 'XYZ' - tristimulus values can be regarded as a three-dimensional colour space. A rectangular distance measure between 'XYZ' - coordinates from two samples in a 'XYZ' tristimulus colour space can provide a numerical colour difference value, as McLaren explained it. The Pythagoras theorem applied to the 'XYZ' values of a standard and batch sample can be seen in *Equation 4*.

Eq. 4: $\Delta E = [(\Delta X)^2 + (\Delta Y)^2 + (\Delta Z)^2]^{0.5}$, where

‘ΔE’ signified 'difference in sensation’ for the individual ‘XYZ’ - tristimulus values. These values are parameter for colour specification seen under restricted viewing conditions (normally derived form light stimuli surrounded by a neutral colour), so that two colours that visually match each other, will also exhibit the same ‘XYZ’ - tristimulus values. However, ‘X’- and ‘Z’- tristimulus values are not correlated well with colour appearance attributes such as hue or chroma. The appearance of a colour depends not only on a stimulus alone, but also depends on the surround and the state of adaption of the eye that can be caused by a change of illumination[52].

1.10.2 The CIE recommended a mathematically transformation from ‘X’, ’Y’, and ‘Z’ - tristimulus values (‘XYZ’) to trichromatic coefficients. Relative ‘x’, ‘y’, and ‘z’ - chromaticity coordinates represented relative amounts of ‘XYZ’ - tristimulus values. Plotting a colour sample’s ‘xy’ – chromaticity coordinates in a chromaticity diagram can provide location and *approximately* appearance correlates in regards to dominant wavelength (hue) and excitation purity (saturation). A more complete colour description was obtained once luminance, in the form of the ‘Y’ - tristimulus value for a sample, was added to the chromaticness information. For instance, the ‘xy’ - chromaticity coordinates for an orange and brown colour can be the same, according to Hunter and Pointer[53], just because the *relative* relationship between ‘XYZ’ – tristimulus values were the same between these two colours. The ‘Y’ – tristimulus value from both samples would then describe whether one or the other sample was brighter or darker in appearance, when compared with each other. Also, it seemed to be meaningful to use a distance measure between two samples in the ‘xy’ - diagram as a measure of colour difference.

1.11 MacAdam’s matching ellipses

1.11.1 MacAdam[54], who extensively conducted experiments regarding the uniformity of the ‘xy’ – chromaticity diagram, asked one observer to match ‘25’ light stimuli at a constant luminance level across the colour space. Colour matching for each colour centre was constrained to a series of different directions in the chromaticity diagram. A colour stimuli, seen in one half of a 2° degree bipartite viewing field in a colorimeter, was matched by adjusting a mix of individual radiant intensities of three primary stimuli in the second ‘half’ of the viewing field, until the sum of their contributions appeared similar to the standard colour stimuli seen in the other half.

1.11.2 The viewing conditions were chosen so that ‘*object-viewing mode’* was simulated with a surround of 42° degrees. The surround field of the setting was of the same chromaticity as given for the ‘*CIE illuminant C’* with a luminance of ‘24’ cd/m^{-2}, according to Wyszecki and Stiles[55]. It was then possible to determine the standard deviations (or errors) from all fluctuation

measures around each colour centre. More experiments were conducted yet to identify at which primary stimuli settings those matching colours (batches) just started to appear differently to the observer when compared with a standard stimulus. Those stimuli '*mismatches'* refer to 'threshold or just noticeable differences' ('JND'). They were three times larger than the standard deviations obtained from matching various colour stimuli.

1.11.3 The important finding was the fact that the standard deviation of fluctuation of those colour matches around each standard colour in the CIE 'xy' – chromaticity diagram was described by an elliptical form. However, sizes and orientations from these fitted ellipses for all stimuli differed significantly throughout the diagram. For instance, a distance measure for the same perceptual perceived colour difference in the green region of the diagram was approximately 10 times larger than the distance for the same perceptual perceived colour difference in the blue region. A uniform tristimulus colour space would provide a diagram, in which 'JND' ellipses were of similar size and orientation towards each dominant and secondary primary stimulus. Furthermore, in an ideal perceptual equidistant colour space, all plots would theoretically being described as circles despite their location in the diagram[55]. More experimental data were obtained from several observers and, on average, they agreed well with those results that were obtained from MacAdam. However, there were larger variations found between results from different observers, according to Wright[57], and Wright & Pitt[58].

1.12 Uniform colour scales

1.12.1 After the introduction of the CIE colour specification system in 1931, researchers tried to establish more uniform colour or chromaticity scales/spaces ('UCS'). There are mainly four different types of scales in psychophysical experiments employed for deriving uniform scales. The nominal scale is used for equality (only naming can be performed); the ordinal scale (for determination of greater or less of a particular attribute, though not necessarily evenly spaced); the interval scale for the determination of equality of differences (no zero point is defined but differences for instance between unit '3' and '4' are similar to the difference between unit '8' and '9'); and the ratio scale (included a meaningful zero point and equality of ratios, also multiplication and division can be performed), according to Fairchild[59] and Lee[60].

1.12.2 Interval and ratio scales are useful for quantifying attributes of colour perception. Deriving a formula for three-dimensional colour scales are generally constructed from a chromaticness and lightness scale. They are often altered in such a way that equal unit differences in one scale are equivalent to the unit differences in another scale (for instance, one chroma unit compared to one lightness unit), according to Wyszecki and Stiles[61]. The success of scaling between one-dimensional uniform colour scales depends on the methods that are used.

Prominent methods for 'just noticeable differences' in brightness matching are described by '*Weber'* or '*Fechner's law'* (the greater a magnitude of a stimuli, the greater the size of a 'just perceptible difference'). A useful method in ratio scaling is the magnitude estimation in colour perception studies.

1.12.3 Most of the new uniform colour or chromaticity scales were initially based on CIE 'XYZ' – tristimulus values or 'xy' – chromaticity coordinates. Other scales were designed by transforming CIE 'XYZ' tristimulus or chromaticity coordinates values to new scales describing equally perceived differences from material colour samples in one of the three colour attributes. One group of workers used simple linear transformations, whereas others took Munsell's Color Order system, or other colour vision theories, as the underlying principle to achieve better perceptual uniformity. The main differences between Munsell's colour order system and the CIE colour specification system is on one hand the achievement of visual equally perceived distances between surface colours in terms of appearance attributes, and the need for colour stimuli matches and specifications on the other hand.

1.13 Munsell Renotation System

1.13.1 Munsell produced a colour atlas (over '1500' glossy or '1300' matt coloured paint chips) with numerical classifications for '10' principle hues and '10' steps of value. More colours were formed for a specific hue/value combination by increasing chroma in equal steps until the colour was saturated. Munsell chose scales such as that one step in 'V' (lightness) equalled two steps in chroma 'C' and three steps in hue 'H'[62]. Samples were measured with a spectrophotometer and specified by their corresponding CIE 'XYZ' – tristimulus values in regards to CIE Illuminant 'C', and the CIE 2° Standard Observer. Participants were then asked to scale coloured chips between two samples against a neutral grey background until they achieved equally perceived differences to either side. This equally spacing of three colour attributes (lightness, chroma, and hue) was determined by a large number of visual experiments. The relationship between instrumentally computed Munsell colours, and visual equally spaced estimates, became the '*Munsell Renotation System'* as described by Newhall, Nickerson, and Judd[63] in 1943. The system became for many researchers the experimental basis for deriving uniform colour scales.

1.14 Judd – Maxwell Triangle

1.14.1 Judd[64,65] tried to achieve uniform scales for spacing colours in terms of dominant wavelength and purity, as described by Kühni[65]. Empirically derived transformations from colour matching functions to Judd's uniform scale became known as the 'Judd - Maxwell Triangle'. The triangle was derived from chromatic threshold differences obtained from using

light stimuli. The aim was to build an equilateral diagram, in which a small chromatic difference of two stimuli (equal brightness) was proportional to the distance between any two points in the triangle. Any colour stimuli was then transformed from its individual CIE '$\bar{x}, \bar{y}, \bar{z}$' - colour matching function - values by a '3 x 3' transformation matrix (coefficients derived from empirical experiments) to '$\bar{r}, \bar{g}, \bar{b}$' - tristimulus specifications.

1.14.2 Those obtained tristimulus values were then transformed to fractional parts of total '$\bar{r}, \bar{g}, \bar{b}$' – values; each of them a distance measure perpendicular to one side of the triangle. Applications for the determination of chromaticity differences were found in the quantification of colour grading in illuminants, grading of cottonseed oil, or grading of lubricating oil[64]. However, using this triangle for determining chromatic differences would require plotting triangular coordinates, according to Smith[67].

1.15 MacAdam

1.51.1 MacAdam devised 'Judd's Maxwell Triangle' using rectangular coordinates for a two-coordinate system in an attempt to simplify the determination of uniform scales procedures. This let to MacAdam's 'uv' – chromaticity diagram, in which two axes are oriented in an opponent red/green and yellow/blue direction[68]. His chromaticity diagram was adopted in 1960 by the CIE and succeeded by the CIE uniform '*u*'*v*'' - chromaticity diagram in 1976. Nevertheless, the final chromaticity diagram is still not perceptual uniform and causes problems in practice. MacAdam's enlarged matching ellipses (by ten times) plotted in the '*u*'*v*'' – diagram (1976) can be seen in *Figure 5*.

1.16 Hunter

1.16.1 Hunter[69] made use of a modified Judd[70] system and took on Hering's opponent colour vision theory[71] as the underlying principle for his uniform colour scale model. Six colours (red/green, yellow/blue, black/white) were ordered in opponent scales. This space or scales were achieved by mathematically transforming; **(1)** CIE 'Y' – tristimulus value in a non-linear way ('$U_Y = kY^{0.5}$') to fit Munsell's ('V') lightness function, and **(2)** transformation of CIE 'xy' – chromaticity coordinates to obtain a red/green ('α') and blue/yellow scale ('β'), according to Berns[72]. Also, a constant 'k' was introduced to express the relative importance of the lightness scale against chromatic components. These transformations of tri-colorimetric data resulted in a three dimensional, approximated visually uniform, object colour space (*L*', *α*', *β*'). Scofield[73] used Hunter's 'L, α, β' - system yet changed scaling factors for all three dimensions (i.e. '$L = 10^{*}Y^{0.5}$').

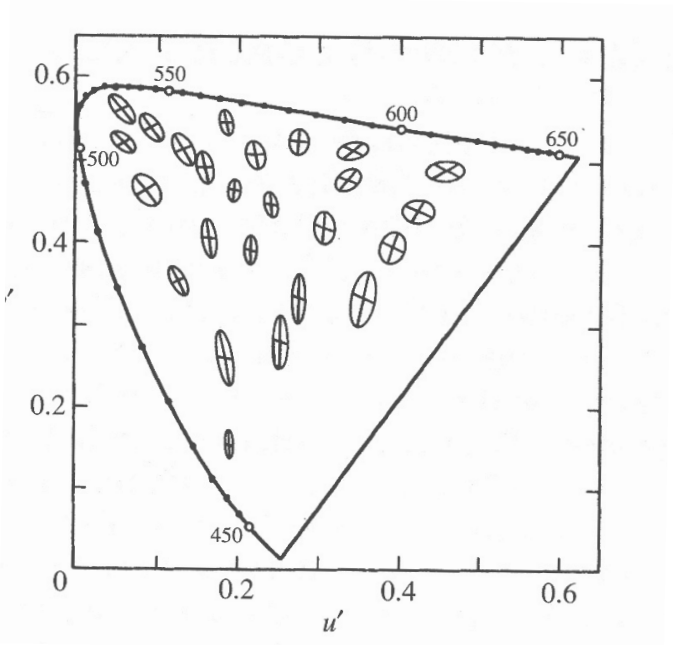

***Figure 5*: MacAdam's ellipses (1942) plotted in the CIE u'v' – chromaticity diagram (Ohta and Robertson, 2005, p. 121)**

1.17 Adam's chromatic value space and diagram

1.17.1 Adam's chromatic value space and chromatic value diagram linked 'Young – Helmholtz' trichromatic theory (assumption of the excitation of the red, green, and blue cone sensitivities that are sent and interpreted by the brain directly) with Hering's[23] opponent colour vision theory. Adam assumed that nerves in the retina connect the green/red and green/blue sensitive cones with each other. The signals are then proportional to the differences between the red/green and blue/green signals. The sensitivity of the green cone in the CIE system is represented by the CIE '$\overline{y}$' - colour matching function representing the lightness information for a stimuli. The resulting CIE 'Y' - tristimulus values are not linearly related to 'quasi' perceptual uniform Munsell's 'V' units.

1.17.2 Newhall *et al.*[63] fitted a fifth order polynomial function. Adams argued, that a sensation only for the red, or a sensation only for the blue cone, could be related to CIE 'X' - and 'Z' - tristimulus value in a similar way as the lightness sensation to Munsell's values with the same fifth order polynomial function ('Y = V_Y'). The mathematical representation for the activity of the nervous system became then ('X = V_X - V_Y') and ('Z = V_Y – V_Z'). This represented the chromatic content according to Hering's opponent colours theory defined and plotted in a uniform chromaticity scale ('UCS').

1.18 Nickerson

1.18.1 Nickerson applied factors to a uniform lightness scale ('ULS'). A combination of UCS and ULS became then the Adams-Nickerson uniform colour space and colour difference formula ('ANLAB'). The important contribution here was to find the appropriate scaling factors between red/green, yellow/blue, and lightness/darkness scales. A multiplication factor of '0.4' for the yellow/blue opponent function scaled for equally perceived steps in red/green. The lightness scale factor was determined as '0.23', and also an overall factor of '42' for both opponent and lightness scales were needed so to fit all scales to provide perceptual equal stepped chroma, hue, and lightness units in regards to for Munsell's Renotation system, as described by McLaren[74].

1.18.2 Minor modifications resulted in the CIELAB colour space and formula in 1976. Two important findings are observed and associated with this method; **(1)** chromaticity ellipses are transformed to almost circle like shapes, **(2)** circle sizes are almost the same for dark, medium, and light colours[67]. Adams' Chromatic Valence System follows a similar pattern, however, differences are taken before the non-linear lightness function is applied[75]. Enlarged uniformity of chromaticity spacing in the CIE 'xy' - chromaticity diagram and Hunter's 'αβ' – diagram can be seen in *Figure 6* and *7*.

1.19 Summary

Generally, and as described so far, different methods are used for deriving more perceptible uniform colour spaces or scales often confined to no more than three attributes. Either, chromaticity and lightness scales are suitably combined, or a lightness scale is used together with opponent axes, so to derive equally units of perception. Of importance is, that uniform colour spaces or scales derived from such methods, could also be used to design colour difference formulae. A early attempt was to relate visual colour difference assessments to the Munsell's 'V' - lightness scale, which later became known as the 'Grey Scale Method'. Changes in colour between two specimens are then related to the nearest difference between a series of grey scale patches. A general method was reported by the *Fastness Test Committee* of the Society of Dyers and Colourists in 1948 (which became later *F.T.C.C.*) and described in more detail by McLaren[76]. It became also a Standard for assessing colour changes and staining; a British (BSI) and international standard (ISO) for assessing a change in colour with a grey scale (AATCC Procedure 1[77] and 2[78] (ASTM D2616-12[79]; BS EN 20105 A02:1995[80]; ISO 105 A02:1993[80]).

1.20 Groups of colour difference scales

1.20.1 Colour difference scales after 1931 can be broadly classified into four groups. The first group (**1**) is related to Munsell's colour order system, whereas the second group (**2**) can be associated with Judd's and Hunter's work initially based on the CIE colorimetric system ('Y' – tristimulus and 'xy' - chromaticity coordinates) modified to fit equally perceived Munsell's colour scales. The third group (**3**) is based on either MacAdam's threshold data (derived from 'Y' and 'xy' – chromaticity coordinates), or MacAdam's chromaticity diagram derived from Judd's Maxwell triangle (empirical transformation from CIE colour matching functions). Finally, the fourth group (**4**) is based on Adams 'Chromatic Value' and 'Valence' systems also derived from CIE 'XYZ' - tristimulus values (assumption of cones responses being similar to the CIE colour matching functions) with the aim to derive scales that are as perceptual equally spaced as Munsell's colour scales are.

1.21 Group 1

1.21.1 The 'Nickerson Index of Fading' was an early attempt to index colour differences. Nickerson[81] measured perceptually dyed cotton, woollen, and silk materials differences with the aid of Munsell's scales mainly in terms of their fading properties (how does a material change its colour properties when it is exposed to light over a prolonged period of time). The differences in perceptual measurements in each of the Munsell attributes (lightness, chroma, and hue) were given weights (for instance, derived from experimental data such as one step in Munsell 'V' equalled two steps of chroma and three steps of hue) according to the judgements of observers in terms of their degree of fading, according to Hunter and Harold[82]. The summation of these components provided an 'index' of the total difference between coloured specimens. Also, it was important, that the extent and direction in which a change in colour occurred, was identified.

1.21.2 Balinkin[83] revised and transformed the formula according to Euclidean geometry in terms of measured distances in Munsell's cylindrical-coordinate system such as '*…distances between two points is the square root of the sum of squares of the distances between them along three mutually perpendicular axis.'* as described by Billmeyer and Saltzman[84].

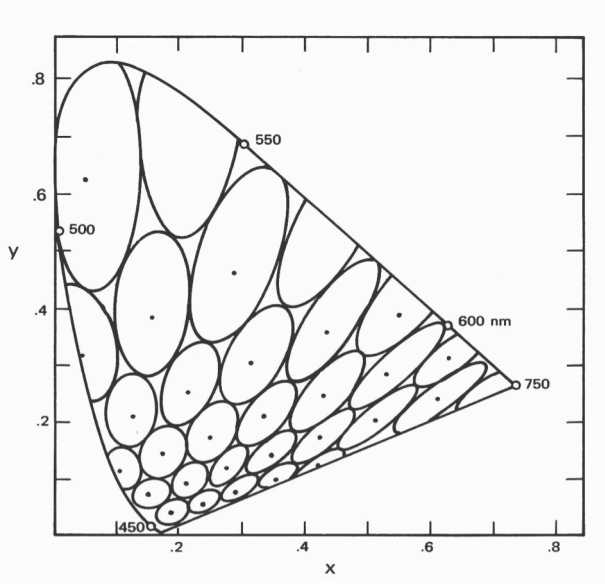

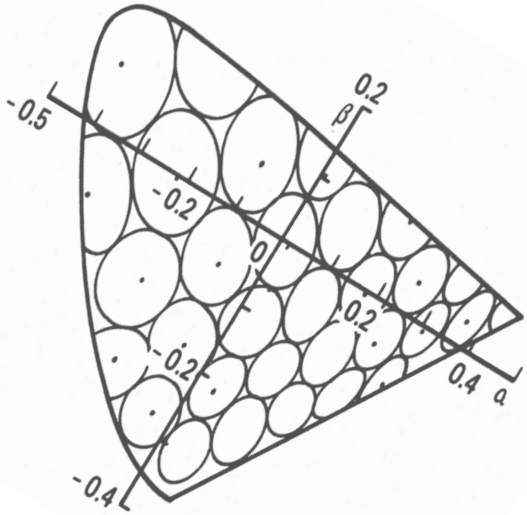

Figure 6 **(top) and** ***Figure 7*** **(bottom) showing same uniform spacing but transformed to Hunter alpha/beta diagram (Hunter and Harold, 1987, p. 128 – 132)**

1.21.3 Nickerson and Stultz[85] also developed a colour difference tolerance measure ('Tolerance Index') for the fit of mainly yellowish/green, weak olive/green, light yellow/brown, pale brown, weak brown, brown/ grey, reddish/brown, white and black camouflage patches. Other workers concentrated mainly on just perceptible differences given more weight to Munsell's 'V' values, as designed by Bellamy and Newhall[86].

1.21.4 Godlove[87] was concerned with fading properties and textile dyeing. He confirmed that there was no weighting or scale factor changes necessary for hue in relation to chroma, as derived by Bellamy and Newhall. However, the relationships between Munsell's 'V' and chroma 'C' units differ significantly amongst researchers. Godlove's experimental results showed a relationship of one step in Munsell 'V' value to four steps of Munsell's 'C' chroma compared to Davidson's ratio of one 'V' to three steps of 'C' units.

1.22 Group 2

1.22.1 The 'second group' of colour difference measurements has its origin from Judd's Maxwell triangle[b]. His threshold discrimination differences in wavelength and purity formed the basis for the perceptual equally spaced chromaticity triangle. Judd's work was initial concerned with dye house commercial colour matches (surface colours and acceptable data). His idea on colour difference formulae for surface colours were '*…that Euclidean distances between points in a colour solid should be proportional to the perceptibility of colour differences between these two colours represented by the points*.' The average commercially acceptable colour difference became the Judd ('NBS') unit of colour difference in 1939 derived from 'Judd's Maxwell Triangle'.

1.22.2 In 1940, Hunter[c] focused his work on the development of a tristimulus colorimeter. He took Judd's triangle method as a starting point for transforming tristimulus readings to a chromaticity scale, which was as perceptual equally uniform as a choice of ten Munsell colours. Readings were transformed in an opponent fashion (similar to Adam's chromatic value system), and a lightness scale was introduced. Functions were added to compensate for the visual change in chromaticity differences inherent with a change in lightness. His collaboration with Judd on a project on porcelain panels resulted in a formula (Judd-Hunter 'NBS' unit of colour difference), which included 'unique factors' to compensate for characteristics such as gloss factor and/or proximity. One unit was about four times the size compared to a threshold unit

---

[b] see page 17: General Information: Judd

[c] see page 18: General Information: Hunter

under ideal conditions. Differences smaller than '1' NBS unit were said to be not important in commercial applications, according to Hunter and Harold[82].

1.22.3 Hunter's formula ('L', 'a_L', 'b_L') consists of a square root lightness approximation to fit the Munsell 'V' value function ('$10^* Y^{1/2}$') and two opponent scales, which are calculated from CIE 'XYZ' – tristimulus values. The 'Y' tristimulus value is either subtracted or added to form the opponent scales. The green/redness ('b_L') scale is stretched by a factor of '2.5' when compared with the blue/yellow ('a_L') scale. Both scales are also multiplied by a factor of '7' so to bring them perceptually into alignment with the lightness scale.

1.23 Group 3

1.23.1 MacAdam's data from his original discrimination experiments obtained from one observer using chromatic light stimuli matches were used to identify the variation or standard deviation of the fluctuation between matches in all directions[88]. Similar ellipses were derived by Brown[89] for twenty-two colour standards from twelve observers, and Rich, Billmeyer and Howe[90] who obtained similar results from fifteen observers judging four sets of colour surface samples. MacAdam's chromaticity coordinate scatters and their observed 'standard deviations of colour matching' derived from twenty-five colour centres were modelled by an ellipse equation. The corresponding ellipses coefficients were determined. They differed in a systematic way mainly depending on their position in the chromaticity diagram. Families of contours were interpolated and drawn in the 'I.C.I.' - diagram as a tool to identify ellipses coefficients 'g_{11}', 'g_{12}', and 'g_{22}' for two stimuli differing in chromaticity coordinates. The chromatic colour differences between two stimuli were then calculated using an ellipse equation and those coefficients. The unit of a chromaticness difference was then given as the 'standard deviation of colour matching', as described by Silberstein[91].

1.23.2 Davidson and Friede[92] determined a commercially accepted limit of '$2^{1/2}$' MacAdam's units of chromaticity differences for wool flannel panels. Graphical techniques, which enabled the user to derive MacAdam's units from CIE data, were later developed by Simon and Godwin[93] and Foster[94]. Also, other charts were introduced that included methods to derive lightness differences. The most important formula, which was based on MacAdam's ellipses, was developed by Friele[51].

1.23.3 Friele took on Müller's stage zone theory[25,26] following a trichromatic, and two opponent processes, as a model for human vision. The first stage described how CIE 'XYZ' -tristimulus values were converted to cone sensitivity functions. In the second (intermediate) and third stage, opponent differences in chromaticness and lightness were calculated from cone sensitivity functions. Factors were included that changed the size of ellipses according to luminance

reflectance. Friele optimized MacAdam and Silberstein's initial parameter yet also changed the primaries (especially green) to achieve variations in size, shape, and orientation of the threshold ellipses. Scaling factors were included. Also, different threshold values for the three processes (red/green, yellow/blue, and lightness discrimination) were applied to the formula. These thresholds were mainly determined by the magnitude of colour differences that were considered. The lightness factor value varied according to the application for what the colour difference formula was actually used for (either for threshold or commercial purposes).

1.23.4 Further improvement was achieved from combined efforts including; (**a**) MacAdam[9] optimising Friele's equation, and (**b**) Chickering[96] optimising thus-modified Friele parameter resulting in the 'FMC-1' formula. Also, Chickering[97] developed a new colour difference formulae ('FMC-2') because of discrepancies in the magnitudes for 'FMC-1's' chromaticness and lightness differences when compared with the results for the same samples obtained from graphical techniques developed by Simon[98] and Godwin[93,99], according to Billmeyer and Saltzman[83]. The 'FMC-2' formula became popular because it was provided in the form of software that was linked to a computer. However, neither 'FMC-2' nor any other formulae based on MacAdam treshold data were represented in CIE's 1976 recommendations.

1.24 Group 4

1.24.1 The 'fourth group' is based on Adam's 'Chromatic Value' and 'Chromatic Valence' scales[32,75]. Those systems[d] were initially developed to prove Adam's opponent colour vision theory. Nickerson and Stultz[85] modified Adam's chromatic value formula by optimising parameter to fit their own colour measurement and colour difference data. Saunderson and Milner[100] introduced the 'zeta-space', in which opponent transformations from CIE 'XYZ' - tristimulus values are introduced without scaling for Munsell's 'V' – function. However, new factors were introduced that were derived from samples at various radial degree settings in Adam's chromatic value diagram. A colour difference was then calculated from those values obtained from two opponent equations, and a third scale describing Munsell 'V' units. A ruler and methods were provided as how to calculate a colour difference in the 'zeta' - system.

1.24.2 Nickerson[101,102] proposed in 1950 constants to approximate Judd 'NBS' units (Adam's original chromatic value scale was described by ten units between black and white). This became known as the 'Adams - Nickerson LAB' colour difference formula ('ANLAB'). Further refinements were then only applied to the multiplying constants rather than structure of the formula.

---

[d] see page 19

1.24.3 Glasser, McKinney, Reilly, and Schnelle[103] wanted to achieve a simple coordinate system (1958) accurately representing colours in an isotropic colour solid using an approach with less excessive computational efforts. The starting point was a modified Adams system, in which the Munsell 'V' - function was replaced by a cube-root function ('$25.29^{*}L=Y^{1/3}$-18.38'). In addition, a cube root function was also applied to the opponent 'a' and 'b' – scales. The performance was said to be similar to the modifications introduced by Adams, or Saunderson – Milner. Most of the derived colour scales after 1931 were of two-dimensional form (chromaticity coordinates) whereas, at a later stage, a third dimension (lightness) was added. A non-linear fitting of 'Y' - tristimulus values to Munsell's 'V' - values was achieved; (**a**) by applying a square root function[104], followed (**b**) by a fifth order polynomial function[63], until (**c**) a cube-root function was used with similar results when compared with (**b**) [38].

1.25 Uniform colour scales and formulae after 1960

1.25.1 Several new visual datasets were generated in the 1960s; industry being the main driving force reflecting on the need to establish reliable quality control measures that could be used by producers and buyers as well. Relative inexpensive colour measurement instruments became available and with it the desire to design colour differences formulae for various industrial applications. Datasets were produced consisting of, for instance, wool textile samples (acceptability data between production match and standard), blue paint samples (acceptability percentage), '500' textile samples (acceptability by sixteen colourists), '113' polyester/cotton fabrics (acceptability), '555' glossy paint samples (categorical from no difference to large differences), and many more. More than twelve formulae were developed and used in industry in the beginning of the 1960s, according to Kühni[105]. Generally, formulae differed from each other in the way they were derived from. Some were derived from CIE's 'XYZ' – tristimulus space or chromaticity values, which were adjusted to fit equal perceived distances in one of the colour spaces, or following a specific colour vision theory. Data were generated using different types of colour samples, such as light stimuli in matching procedures, or surface colours in combination with a standard light source. The tasks given to observers differed in ways such as either to match colours; deriving just noticeable colour differences ('JND'); scale colours according to specified attributes; or deriving acceptability colour differences for production samples for particular branches in industry[106].

1.26 CIE 1964 $U^*V^*W^*$ colour space and chromaticity diagram

1.26.1 In an attempt to promote '*uniformity of practice'* the CIE extended the 1960 'uv' – chromaticity diagram (adopted from MacAdam's 1937 'uv' – rectangular uniform chromaticity diagram) into three dimensions by introducing a cube-root lightness function, which in fact was very similar to Glasser's[103] original function. This became later the CIE 1964 $U^*V^*W^*$ colour space and colour difference equation[107] based on Judd's and MacAdam's threshold criterion so to provide a '*…more homogeneous, equidistant colour space and formula*'. The 'uv' - chromaticity diagram is used especially in conjunction with the definition of correlated colour temperature and for the evaluation of colour rendering performances of light sources, according to Ohta and Robertson[108]. However McLaren[109] described this equation as less reliable than others, especially when used in industry[110]. Therefore, the CIE recommended testing and comparing; **(a)** the modified cube root formula as suggested from Glasser *et al.*[103], **(b)** the Munsell Renotation formula[87], and **(c)** Chickering's 'FCM-2'[97] formula with the 1964 CIE colour difference formula.

1.27 Testing colour difference formulae

1.27.1 Eight professional shade passers tested '287' dyed carpet yarns in regards to deriving *acceptable* matches for nineteen standards. Rather than relying on analysis from scatter plots (colour difference 'ΔE' against 'number of acceptability as a percentage measure' equals '%A'), the CIE asked for a formula that was based on a 'most reliable' criteria. The correlation coefficient between 'ΔE' and '%A' was such a criteria that could be used to make quantified decisions on reliability. However, none of these equations were regarded as more reliable than one or another at a 10% significance level, although many workers regarded the 'FCM-2' formula, which was derived to fit MacAdam's ellipses, as the one that performed best. New tests were conducted and analysis revealed correlation coefficients that were significant different amongst formulae. Coates, Day, Provost, and Rigg[111] assessed the accuracy of colour difference formulae such as ANLAB50 or CIE $U^*V^*W^*$ in regards to industrial colour tolerance work. They estimated errors from all formulae and also concluded, that the results from most standard colour difference equations, were not satisfactory. The reason for these results was mainly based on the fact that different experimental conditions were used for collecting data. Therefore, it seemed to be clear why MacAdam's ellipses may be suitable for determining small colour differences between light stimuli, but may not be suitable for determining larger colour differences between surface colours.

1.27.2 Nevertheless, most of the cube-root colour difference formulae and ANLAB42 were regarded as significant more reliable than most of the standard formulae at that time. The textile

committee recommended a modification of the ANLAB42 formula in 1971 ('ANLAB40') as being considered and evaluated as an international standard 'ISO' equation for colour difference determination for textiles and plastic samples. The equation included Judd's fifth order polynomial lightness scale. A colour difference was defined between two specimens as the distance of their positions in ANLAB's uniform colour space, according to McLaren and Rigg[112,113].

1.27.3 McDonald[114] investigated in 1974 the entire ANLAB50 colour space in terms of how numerical colour differences varied with perceptual obtained colour differences by means of a grey scale method. He discovered that the correlation between both methods was improved when a scaling factor was introduced to the original formula. This scaling factor for two samples, for which a colour difference value was to be calculated, depended only on average saturation. It meant, that a calculated colour difference needed to decrease in magnitude with increasing perceptual colour differences caused by increasing saturation levels. Furthermore, McLaren[109] found out that optimised pass/fail boundaries ('50%A') also varied systematically with lightness and hue angle of the standards. Therefore, he introduced factors to all three colour difference directions according to lightness, chroma, and hue position of the standards. Other workers followed similar approaches, in which existing formulae where optimized against one or more datasets, according to Kühni[115] and Friele[116].

1.28 Modern requirements for colour difference formulae

1.28.1 The CIE itself wanted at least two principals to be addressed by a colour difference formula; (**a**) to produce uniform colour differences for all directions and colours, and (**b**) it should be capable of being used over a range of experimental conditions and material characteristics. An idealistic solution was to derive a universal formula for all materials and viewing conditions. Since, the ANLAB formula was likely to be biased towards a textile shade pass match (acceptability matches), the CIE focused primarily on perceptibility matches avoiding possibly variations in biases amongst industries. MacAdam[117] proposed to the CIE in 1973 a cube root version of the ANLAB40 formula, in which Judd's polynomial Munsell Value function was replaced, accordingly. This formula was tested in terms of perceptibility data obtained partly from observers with no prior experiences in acceptability matching. However, their results were not significant different when compared to those from observers with experiences in acceptability matching tasks. The reliability measure (correlation coefficient – assuming a linear relationship between computed colour differences and per cent acceptability) showed, that the CIELAB 1976 colour difference equation was amongst the best for perceptibility matches between surface colours. Therefore, it was recommended by the CIE to

be used instead of the ANLAB40 formula. CIELAB colour differences units were around 10% higher than ANLAB40 colour difference units[113].

1.29 CIELAB and CIELUV colour space and formulae

1.29.1 However, the 1976 CIELAB colour space is derived from CIE 'XYZ' – tristimulus values scaled in a non-linear opponent fashion using a cube root approach. This implies a non-linear distortion of the chromaticity diagram, according to Smith[118]. Industry using additive mixture of lights (such as in the television industry) favoured a colour space with an associated 'more uniform' chromaticity diagram, in which straight lines of dominant and complementary wavelengths, are maintained. The display industry made use of this space since additive mixtures from red, green, and blue primary phosphors are the underlying principle of additive colour reproduction (Grassman's additivity laws). The CIE therefore followed Eastwood's recommendation[119] in 1973 to modify the CIE 1964 $U^*V^*W^*$ colour space and formula by scaling the 1964 'v' chromaticity coordinate by a factor of '1.5', and changing the 1964 lightness scale's letter $'U^{*'}$ by $'L^{*'}$. According to Witt[120], this changes the '*…elongation in the direction of 'v', which improved uniformity without disturbing additivity rules'*. A relative perceived colour difference between two colour stimuli of similar luminance can then be represented as a Euclidean distance between coordinates in the '*u*'*v*'' – chromaticity diagram. This implies samples of similar sizes, viewed in identical surroundings, by an observer photopically adapted to a field with the chromaticity of a CIE standard illuminant. Correlates of lightness are described by a cube root transformation of CIE 'Y' - tristimulus values. A complete colour difference description, including the difference in lightness follows, accordingly. The CIE recommended in 1976 to use two new colour spaces (CIE 1976 $L^*a^*b^*$ and CIE 1976 CIE $L^*u^*v^*$) and associated colour difference formulae (CEN 2011a[121], CEN 2011b[122]).

1.29.2 CIELAB is derived from a theoretical model based on the fundamentals of colour perception that can include, for instance, cone excitation (CIE colour matching functions served as relative linear combinations of cone responses), chromatic adaption transforms (CIE $L^*a^*b^*$ taking ratios of 'XYZ' - tristimulus values relative to a reference white), and others to describe mechanism that can influence colour perception as described by the CIE[49] in 1995. The new colour spaces are approximately perceptual uniform and have a three – dimensional form. The colour difference formula could be described with rectangular, or polar coordinates. Colour attributes given in polar form are in close arrangement with Munsell's attributes of lightness, chroma, and hue. Describing a colour difference as metric lightness, hue-angle, and metric chroma are said to be advantageous over rectangular measures. A unit of colour difference refers to '$\Delta E'$ derived from the Greek word 'delta' and German word 'Empfindung' that

translates to ‘difference in sensation’. A colour difference of ‘1’ ‘ΔE^*_{ab}’ is said to be just noticeably.

1.30 Testing CIELAB and CIELUV

1.30.1 The 1976 CIE $L^*a^*b^*$ (CIELAB) colour difference formula was tested in the colorant industry and revealed that pass/fail contours around the standards were still of elliptical form, and differed in size and orientations[113]. Kühni[123] analysed five industrial visual colour tolerance datasets and confirmed that ellipses sizes were dependent on saturation. Generally, by fitting ellipses to various visual object colour difference data sets, following observations were made in regards to CIELAB’s 1976 colour space and ‘$a^*b^{*'}$ - diagram; (**a**) unit chromatic contours were generally described as ellipses pointing towards the neutral point, (**b**) ellipses increased in size as a function of metric chroma (chromatic crispening effect), (**c**) ellipsoids increased in size in the lightness direction the further they were away from the metric lightness of the surround (lightness crispening effect), (**d**) hue differences were not linearly related to hue angle differences but as such so in a non-linear more complex form, (**e**) ellipses were tilted counter clockwise near the CIE ‘b^*’ negative axis, and (**f**) unit contours at the neutral point were also of elliptical form[124]**.**

1.30.2 It is also believed that inconsistencies amongst results were caused by variations in experimental setups and differences in physical materials, which were used for those samples. The CIE proposed therefore recommendations and guidelines for colour difference evaluations. Those are mainly concerned with; (**g**) studies related to five colour centres such as mid grey/light, yellow/medium red, and green/darker blue latter four at medium chroma; (**h**) evaluation of parametric effects on colour difference perception using clear and defined experimental conditions; (**i**) obtaining reliable reference datasets; and (**j**) development and adoption of new colour difference formulae, as suggested by Robertson[125] in 1978. So far, experimental colorimetric stimuli matches are made in isolation of other colours (unrelated colours). In the contrary, colour matches in industry are often made using objects that are seen in different contexts (related colours). Those additional variables that are introduced by changing the experimental conditions are described as ‘parametric effects’.

1.30.3 Poor correlation between instrumental and visual results were discussed and described as; (**a**) uniform colour scales differed markedly in dimensions; (**b**) mode of observation (aperture, object, illuminates); (**c**) magnitude of colour differences; (**d**) level of illumination; (**e**) colour of illumination; (**f**) size and flatness of samples; (**g**) presence of gloss; (**h**) presence of texture; (**i**) surrounding and backgrounds for the samples; and (**j**) gap between samples to be matched (see CIE[126]). Human factors were related to; (**a**) prior experience of observer; (**b**) prior adaption to

observing situations; and (**c**) colour difference perceptibility and commercially acceptability did not correlate well since; (**ci**) hue difference were less accepted compared to lightness and chroma differences, (**cii**) mismatches on the yellow side of standards were more often rejected, and (**ciii**) acceptance criteria varied markedly amongst industries, according to Hunter and Harold[127].

1.31 JPC_{79} colour difference formula

1.31.1 A major contribution after 1976 was the introduction of the 'JPC_{79}' colour difference formula. This formula is a modification and further development of ANLAB. Prior work by McLaren[128] and McDonald[114] resulted in better correlation with visual results. McDonald's main idea was to compare; (**1**) visual matching data 'ΔV' (obtained from colour difference pairs contrasted against four grey scale gradings) with measured data obtained from the same sample pairs, and (**2**) to compare 'ΔV' from each of the four gradings against the saturation, hue, or lightness level/position for each colour difference pair (average of two samples). Models were established that described mathematically those relationships. A goodness of fit measure explained the variations between visual colour differences and, for instance, saturation levels described as the distance from the neutral point. In an ideal situation those relationships would have resulted in a ratio of '1' between observed colour differences and increasing saturation, lightness level, or hue position of the sample pair. The most significant discovery was the fact that a calculated colour difference did not accounted for decreasing perceptual colour differences with increasing saturation level. The original formula needed than to be rescaled so to obtain similar 'ΔE' values for the same colour difference samples despite a change in saturation level. The formula became of the form '$\Delta E_M = \Delta E^*(1+0.0022^*r)$' whereas 'r' defined the saturation level of a sample as the distance from the neutral point. The correlation coefficients as a measure of performance increased to '-0.68', compared to '-0.58' for ANLAB50, and '-0.54' for the CIE 1964 $U^*V^*W^*$ formula.

1.31.2 Following this approach further, McDonald produced industrial thread samples for fifty-five colour centres over four lightness levels judged by eight professional colour matchers. A second colour difference data set resulting in over '8500' judgements against '600' colour centres obtained from one observer in a dye house was added. The results showed that hue and metric chroma dimension of a tolerance ellipsoid increased in size with increasing metric chroma for various difference samples throughout the colour space. Also, the lightness dimension increased with the increase of lightness values, and hue dimensions were altered in regards to hue positions (McDonald[129,130,131,132]; Alman, Berns, Snyder, and Larsen[133]). All

values for the JPC_{79} formula were calculated from ANLAB (43.909) making comparisons with results obtained from CIELAB's colour difference formula more meaningful.

1.31.3 Three anomalies were discovered in the structure of the JPC_{79} formula; (**a**) once dark colours approached zero the scaling function also approached zero so that ratios between '$\Delta L/L_t$' became very large; (**b**) some neutral samples gave different colour difference values although they appeared similar; and (**c**) anomalous hue angles for low tristimulus values. Clarke *et al.* (1984) modified 'L_t' values for standard samples with lightness values smaller than '16'. They were fixed to a value of '1.022', as suggested by McDonald. The ratio between 'ΔE_{JPC}' against 'ΔV' for neutral samples ranged from '0.12' to '3.21' before, and '0.37' to '1.14' after modification.

1.31.4 Hue discrimination should be independent of hue for near neutral colours. This was corrected implementing a sharp break at a chroma limit of '0.638'. However it was a gradual transition that was required to avoid anomalous results for samples just crossing the chroma limit, as described by Smith[134]. Function 'H_t' was then redefined by changing 'T_n' applying a new function 'f' to provide a gradual transition between chroma and hue. The modifications improved calculation for dark and near neutral colours. Also, different relative lightness and chroma tolerances (l:c) were suggested either as linear parametric factors for controlling relative sensitivities to lightness, chroma against hue differences for different object substrates (in regards to the ratio an assessor tolerated equally perceptual differences in each component for instance in leather, paint, or textiles different pairs), or for the determination of perceptibility or acceptability data. Often, the relative tolerance weighting for 'l' was chosen to be '1' or '2' for perceptibility and acceptability colour difference data, respectively. Perceptibility results were obtained from paint samples and acceptability results from textile samples.

1.32 CMC colour difference formula

1.32.1 New results from acceptability judgements suggested various values for each relative tolerance weighting, according to Hunter and Harold[135]. Weighting functions (*accounting for variation in perceived colour difference magnitude with variation in CIELAB location of the colour difference standard* – 'CIE TC1 – 29') for component differences 'L_T', 'C_T', and 'H_T' were then replaced with 'S_L', 'S_C', and 'S_H' indicating the length of half semi axes of the ellipsoid defining 'ΔE_{CMC}' units, according to Clarke, McDonald, and Rigg[136]. The Colour Measurement Committee ('CMC') of the Society of Dyers and Colourists ('SDC') proposed this as the new formula ('CMC'), which became an ISO standard for textile applications in 1995.

1.32.2 The formula was tested against available experimental data. The performance of fit was extended to three measures; (**1**) correlation coefficient 'r' as a measure of tendency for 'ΔE' to increase with increasing visual colour differences; (**2**) 'ΔE' (calculated or predicted colour difference) and 'ΔV' (visual or perceived colour difference) should ideally lie on a straight line (perfect agreement), - the correlation coefficient ('CV') as a percentage measure of the root mean square deviations of the points from this perfect line from the mean 'ΔE' can provide a measure independent of unit; and (**3**) 'ΔE' should be proportional to 'ΔV' and the ratio of both should be a constant. The logarithms of ratios provided then a standard deviation of the log(ΔE:ΔV). However, the results showed various 'best' values for weightings 'l' and 'c' depending on the measures that were used. However, more important was the fact that CMC performed significantly better than CIELAB and JPC_{79}, when small colour difference datasets for surface colours were judged.

1.33 BFD colour difference formula

1.33.1 More formulae were derived mainly to improve existing formulae. The BFD formula was derived from thirteen available combined acceptability and perceptibility (yet scaled) datasets, consisting mainly of paint and textile samples (including one ink and thread winding card samples set). The formula introduced a term that rotated ellipses in the blue region away from the neutral point in CIE's 'a^*b^*' - diagram. The amount of rotation was dependent on chroma and hue position. Calculated ellipses from JPC_{79} or CMC in the blue region were pointing towards the neutral point in the 'a^*b^*' – diagram, whereas experimental ellipses did not. The main difference for experimental ellipsoids in the CIE 'xy' - chromaticity diagram was their size probably caused by different observer groups and scaling techniques as described by Luo and Rigg[137,138], and Kühni[66].

1.33.2 Relative sizes were then adjusted, and unreliable subsets deleted from the original set. Little differences were found between perceptibility and acceptability ellipses. The BFD formula was regarded as an optimised CMC formula with modified constants for a combined dataset. Improvement was especially reported for small perceptibility colour differences. The formula was tested together with twelve other formulae using measures of fit as described for the CMC formula, but with an addition of a measure of overall agreement 'V_{AB}' between 'ΔE' and 'ΔV'. Also, all measures ('r', 'CV', 'γ', 'V_{ab}') were combined into one overall performance measure 'P_f'. This measure revealed that BFD(1:1) and BFD(1.5:1) performed best amongst all twelve formulae for perceptibility and acceptability data, respectively; BFD outperforming CMC, according to Luo and Rigg[139].

1.34 SVF colour difference formula

1.34.1 Seim and Valberg[140] fitted a formula ('SVF') to Munsell's renotation system based on cone sensitivities. Physiological assumptions about signal processing in the eyes were taken as the underlying principles for the determination of colour differences such as; (**a**) absorption of quanta is linear but cone excitation and receptor signals are not, (**b**) relative sensitivities of three cone types were determined by the achromatic adapting stimulus using von Kries coefficient rules, which accounts for the nonlinear transformations of the resulting cone excitations, and (**c**) chromatic signal processing can be approximated by linear opponent combinations of hyperbolic functions. Spectral tristimulus values were converted to cone sensitivities and centred on white. The lightness value was represented by a close fit to Munsell's 'V' function and opponent colour signals were calculated following Adam's approach in two steps. The formula was said to be a good fit to Munsell's system.

1.35 New coordinate guidelines for colour difference evaluation

1.35.1 New sets of visual data were generated being primarily bounded to the set of guidelines for coordinated research issued by the CIE[125] in 1978. Cheung and Rigg[141] established a supratreshold small colour difference dataset of dyed wool fabric judged under tungsten and artificial daylight according to a standard difference pair; Badu and Rigg[142] prepared large colour difference nylon dyeings and glossy paint samples judged against a grey scale; Witt[143] used a threshold experiment for glossy acrylic paint samples under artificial daylight to determine whether a colour difference was perceived, or not; Alman *et al.*[133] and Berns *et al.*[144] designed nine colour centres from glossy acrylic lacquer paints determining whether a colour difference was smaller or larger compared to a near grey anchor colour difference pair. The anchor sample pair differed in lightness with a commercial magnitude of '1.02' 'ΔE^*_{ab}'. This colour difference tolerance dataset was then extended to cover nineteen colour centres judged by fifty observers.

1.36 CIELAB 1992 colour difference formula

1.36.1 Völtz[145] reported in 1991 areas of improvement for individual components for the CIELAB colour difference formula, especially if they were used and applied to pigment coatings. Discrepancies occurred between perceived brightness and 'ΔL^*' values, and between perceived saturation differences and 'ΔC^*_{ab}' values. Accordingly, the CIE proposed a new formula ('CIELAB 1992') for testing. *CIELAB* 1992 included weighting parameters (parametric factors) depending on the application and/or differences in reference conditions.

1.36.2 The formula was based on CMC, but the correction terms were limited only to the chroma effect, so that unsaturated and achromatic colour differences remained unaltered. Testing was required with the aim to establish further discussion and suitable parameter for relative sensitivity between lightness, chroma, and hue scales. The reference conditions were chosen such as to replicate daylight conditions; illuminance of 1000 lux; surrounding grey of 'L^*50'; sample size over 4° subtense; using sample pairs with nearest possible contact between them, and being of visual homogeneous texture.

1.37 CIELCH colour difference formula

1.37.1 Alman[146] proposed a provisional recommendation (1993) at a meeting of the 'CIE TC1 – 29' working group. This formula 'CIELCH' was based on CIELAB as described by Völtz. It included parametric factors ('k_L', 'k_C', 'k_H') that were set to unity for above described basic experimental conditions. Berns[147] tested CIELCH and provided test results in terms of statistical and graphical analyses. He also provided linear equations accounting for systematic trends between perceived and predicted colour differences. Three equal visual tolerance ellipses (or ellipsoids) prepared from surface colours by Luo and Rigg[137], Witt[143], and Berns[144] were converted to 'ΔL^*', 'Δa^*', 'Δb^*', 'ΔC^*' and 'ΔH^*' - tolerances. Plots of 'ΔL^*' against 'L^*' revealed only a random relationship in the case of Luo and Rigg's dataset, and little changes with increasing lightness level for all other datasets.

1.37.2 This was possibly explained by the use of different types of sample sets and the variation in the viewing conditions. A lightness weighting function was therefore not considered. However, the position of chroma 'C^*_{ab}' influenced significantly 'ΔC^*_{ab}', but had only a *small* influence on 'ΔH^*_{ab}'. Similar results were achieved in the work of McLaren and McDonald (CIELAB and ANLAB). Next, hue angle trends were evaluated by correcting 'ΔH^*_{ab}' for *small* chroma dependencies by dividing 'ΔH^*_{ab}' with the 'S_C' weighting function. The results for all three datasets were said to be of random nature and as such not considered for further considerations. A test on CMC revealed that the 'S_L' function had no significant influence on the overall colour difference formula performance and, therefore, CIELCH's 'S_L' function was set to unity. Also, it was concluded that weighting function should be of linear form. Witt[148] tested the CIELCH formula (which became later the CIE_{94} formula) using textile samples in terms of pass/fail observations. Ninety-four standards and forty-four batches were produced in all directions of the DIN colour order system. The results showed an increase in 'ΔC^*_{ab}' against 'C^*_{ab}', and also an increase in 'ΔH^*_{ab}' against 'ΔC^*_{ab}'. However, a plot of lightness differences against CIELAB lightness 'L^*' resulted in scattered data with just little trend with increasing lightness levels. Setting all parametric functions to unity revealed no better performance, when

compared with results obtained from to the CIELAB colour difference formula. However, the performances became significantly better once the weighting function 'k_L' was set to a value of '2'. The results for chroma and hue dependency were similar to the results that were obtained from Luo and Rigg using the CMC formula.

1.37.3 The correlation coefficients between predicted and calculated data for the *Hohenstein* textile samples were less than the coefficients reported by Luo and Rigg mainly caused by the large scatter of 'ΔL^*' against 'L^*' data. It was concluded that the 'k_L' weighting factor must vary depending on the application and samples that were to be judged. Also, evidence was given to the fact that CIE_{94} formula did not perform significantly better than CMC. Whether these results were just valid for the evaluation of textile colour difference samples was not completely verified at that time.

1.38 CIE new guidelines for testing colour difference formulae

1.38.1 The CIE published in 1995 guidelines, described by Witt[149], for testing the CIE_{94} formula with the aim to develop an international standard for most industrial applications. Analysis was conducted to investigate the quality of fit for dependence on metric chroma, hue angle, metric hue difference, and lightness. Following the CIE's 1978 guidelines and other published results, in which especially the heterogeneity of experimental results were questioned, it was decided that more information were needed for the investigation of; (**a**) the correlation of colour differences in sample pairs with change of illuminant, (**b**) the effect of background between light and dark or chromatic content, (**c**) to establish a correlation between object mode simulation (display) and true object mode for colour difference judgements, (**d**) sample size, and (**e**) surface texture .

1.38.2 The number of colour centres was extended to nineteen. Also, it was desired to consider all sorts of variability in the analysis of results. That included measurement uncertainty, within and between observer judgement variability, and an estimate for the overall variability of results. Further improvement in colour difference evaluation was regarded as necessary, for instance, by developing new formulae starting from a physiological basis. CIE_{94} was tested in the following years and compared with other formulae. Again, workers reported that evidence in performance gains in textile pass/fail colour difference evaluation was insufficient so to justify a change from CMC to CIE_{94}, according to McDonald and Smith[150].

1.38.3 Heggie, Wardman, and Luo[151] reported that there were regions within the CIELAB colour space (yellow/orange and blue) where CIE_{94} failed to account for inconsistencies in experimental visual data. Also, it was suggested that the Colour Measurement Committee (CMC) should closely work together with the CIE following the aim to establish new

recommendations for colour difference evaluation. The author particularly highlighted those results that '*…were obtained from lightness differences'*, and results that were obtained from '*…neutral and saturated blue colours*.[152],

1.39 Optimisation of colour difference formulae

1.39.1 Kühni[153,154] analysed equal hue distances in the Munsell, OSA-UCS, and NCS colour order systems concluding that Munsell's value function, which was applied to the Adam-Nickerson formula (also adopted for CIELAB) for fitting the lightness function and both opponent scales, was not appropriate. The linearization in CIELAB was obtained by a cube root function. A better linearization for opponent scales was achieved by varying the power values for the opponent scales. It was suggested to use a power of '0.50' for the blue, '0.33' for the yellow scale, and '0.75' for the redness/greenness for fitting experimentally determined uniform hue steps around Munsell's hue circle. Also, the curvature of unique blue chroma lines needed to be reduced by adjusting CIE 'X' - tristimulus with 'Z' - tristimulus values. This method was necessary for adjusting the lobes of the CIE '$\overline{x}$' – colour matching function allowing the direction of the constant hue axis primarily for bluish colours to be aligned with CIELAB's yellow/blue axis. The same method applied to the redness/greenness axis was reported to be not significant. Kim and Nobbs[155] provided analytical solutions for this problem.

1.39.2 A similar approach was used to optimize the CIE_{94} formula. Five datasets were considered from which the 'RIT – Dupont' and 'Witt' - data set were reported as the most suitable for optimization (consisting mostly of paint samples). The choice of various power functions applied to various colour difference datasets did not result in significant performance gains. Also, the CIE_{94} weighting functions 'S_L' and 'S_H' did not improve the prediction performance for some datasets. However, an adjustment of the CIE 'X' - tristimulus values, and a 'S_L' function that was dependent on the surround conditions, should be included in CIE_{94}'s formula, according to Kühni[153]. Thomsen[156] derived a Euclidean colour space by simple adjustments to CIELAB's 'a^*' and 'b^*' – axes. More data were made available by the authors Kim and Nobbs[155], Pointer and Attridge[157], Witt[158], and Guan and Luo[159].

1.40 LCD colour difference formula

1.41.1 Kim and Nobbs designed new weighting functions for each colour difference direction. Complex sinusoidal functions were added to the 'S_C' and 'S_H' weighting functions. The datasets consisted of small colour differences for matte paint and glossy paint samples, large colour difference pairs made from printed ink, and small to medium colour difference paint samples. A

grey scale method, and a near neutral reference pair for 'larger or smaller' assessment of visual colour differences, were employed. The LCD formula improved the correlation between visual and calculated colour differences for some datasets, according to Kühni[66].

1.41 Pointer and Attridge

1.41.1 Pointer and Attridge designed a colour difference sample set (colour difference magnitude ranged from '1' 'ΔE^*_{uv}' to '36' 'ΔE^*_{uv}' units) that was made from glossy reflecting print samples. Linear regression was considered to be the most suitable method to weight visual with calculated colour difference data. However, the authors concluded that for their dataset a power law function following '*Steven's law'* was more suitable.

1.42 Witt

1.42.1 Witt assumed additive linear extension along the axes in constant proportions of a threshold ellipsoid. Paint samples were produced as a linear defined extensions ('x', 'y', and 'Y') of ellipsoids directions in chroma, hue, and lightness consisting of low to moderate colour differences assessed by using the grey scale method. Although, linear regression fittings to the data were nearly described as in linear form, the author concluded, that perceptual colour differences were not just simple linear extension from thresholds ellipsoids in all three main directions of a colour space.

1.43 GLAB colour difference formula

1.43.1 Guan and Luo[160] produced a dataset consisting of large magnitude colour differences for wool pairs (average '12' 'ΔE^*_{ab}') to be judged using a pair comparison and a grey scale method. Data were combined with other large magnitude data sets and those results that were obtained from the grey scale method compared with each other. The geometric mean for this comparison, between a batch and standard sample for the difference in lightness and chroma, was used for calculating 'S_L', 'S_C', 'S_H' weighting functions for the CMC and CIE_{94} formula. The CIE_{94} formula served as the basic structure to develop an optimised formula ('GLAB') in terms of new weighting functions. CIELAB performed best for predicting large colour differences, whereas GLAB was preferred for predicting a combined dataset. By considering various experimental results, it became evident, that those differences in formulae performances depended also on the magnitude of a colour difference pair.

1.44 Lightness weighting functions

1.44.1 So far, starting with McLaren and McDonald's investigations, evidence was collected to confirm that experimental visual colour differences revealed a dependency on chroma (most significant part), and hue position of the standard sample. It was therefore decided to scale calculated colour differences with those perceived judgments in accordance to the position of the samples in the CIELAB colour space. This scaling improved the correlation between calculated and perceived differences, especially if those results were compared with CIELAB or CIELUV colour difference calculations. However, investigations of lightness colour difference dependency on lightness level did not follow a clear, or systematic, trend.

1.44.2 In 1999, Nobbs[161] investigated several lightness difference weighting functions ('S_L'). Five weighting functions of the form; (**a**) sloping line, (**b**) constant followed by sloping line, (**c**) constant followed by a quadratic curve, (**d**) V-shape form, and (**e**) a quadratic equation were investigated and also compared with CIE_{94}'s, CMC's, and Leeds 'LCD's' lightness functions. Several datasets were used for analysis satisfying following conditions; (**1**) chroma difference contribution to the overall colour difference was small '$(\Delta C^*_{ab}/\Delta E^*_{ab})^2 \leq 0.25$)'; (**2**) hue difference contribution was small '$(\Delta H^*_{ab}/\Delta E^*_{ab})^2 \leq 0.25$)'; and (**c**) total colour difference 'ΔE^*_{ab}' was less or equal to '5' 'ΔE^*_{ab}' units. All data subsets ('ΔL^*', 'ΔC^*_{ab}', 'ΔH^*_{ab}') were tested for bias with each other. Nobbs considered 'RIT' glossy paint, Leeds 'GS' matt paint – grey scale -, Leeds 'PC' matte paint – pair comparison -, Witt glossy paint, Bradford 'CA' - textile data, and a Bradford 'CP' combined dataset for evaluating the dependency of the 'S_L' weighting function on lightness 'L^*' of the standards. Equations were used that allowed statistical methods to be applied for testing the significance for different types of relationships. It was evident, that a simple sloping line performed best, if textile samples were of concern; and a double slope or quadratic slope equation fitted paint samples best. The relationship of 'S_L' on 'L^*' for paint samples included a feature that was always at minimum around a lightness value 'L^*' equal to '50'. The weighting value increased to '1.5' – '2' for lower and larger lightness values of the standards. Textiles samples followed a similar trend for larger lightness values of the standards, but not so for lower values.

1.44.3 Two equations were suggested compromising on the fact that textile and paint colour difference pairs would have otherwise resulted in two different 'S_L' functions for standard lightness samples below 'L^*' '50' values. The compromised 'S_L' weighting function was described by a constant ('1.22' or '1.26') for standard 'L^*' samples below or equal to '50', and a sloping line for standard samples greater than '50'. The author suggested to carry out more experiments focusing especially on the lightness dependence of 'S_L' in the range from 'L^*' '0' to '50'.

1.44.4 A new colour difference dataset was collected according to the CIE technical committee 'TC 1 – 47' (hue and lightness dependent correction) in collaboration with the *Society of Dyers and Colourists* (Colour Measurement Committee) to test different lightness scales. The University of Keele and the Colour & Imaging Institute at the University of Derby carried out these experiments. The questions that ought to be answered were; (**a**) which data set represented the true visual results, (**b**) which formula should be used for industrial applications, and (**c**) whether variations in the lightness weighting results were caused by experimental differences and/or caused by the magnitude of the lightness standard samples. Two hundred and eight matte and glossy Munsell neutral paint samples mainly differing mainly in lightness were produced and used for visual estimation with the aid of a matte grey scale. Several lightness functions 'S_L' (CMC, BFD, CIE94, and CIELAB) were then applied to predict those new and also previous datasets. Also, it was said that both lightness sample sets (matte and glossy) would describe and represent typical texture differences. All samples were divided into three subgroups depending on their colour difference magnitude.

1.44.5 The main general trend suggested that smaller perceptual lightness differences were recorded at low and larger lightness values of the standards, whereas larger differences were perceived for lightness differences at 'L^*50'. The lightness of the background of the viewing field in the experimental set up was approximately at 'L^*50'. Earlier suggestions to fit a 'V'-shape-weighting function to a lightness differences dataset was adopted and resulted in a new lightness difference formula[162]. However, no new textile colour difference samples were included.

1.45 Colour difference formulae at the beginning of a new century

1.45.1 Most formulae after 1976 were non - vectorial transformations from CIELAB's colour space. CIE reporter Witt[163] described in 1999 new aspects in the evaluation of colour difference formulae. The procedure of weighting colour difference components should be replaced by a new definition of basic coordinates that can form a uniform colour space, as it was intended with the introduction of the CIELAB colour space in 1976.

1.45.2 Two ideas were proposed to be considered for further considerations; (**1**) the modified model of Rohner and Rich[164] (1996 - DCI_{95} formula), who applied an integration method (weights on chroma and hue differences were integrated directly into the calculation of 'a^*' and 'b^*' - values), which became later the DIN_{99} formula. It was suggested to apply all existing datasets to optimize essential parameters. Generally, CIELAB coordinates were the point to start from; followed by a grey correction; logarithmic transformations for the chroma and lightness

scales; a size factor that was applied to scale total numerical with visual colour differences, and the ratio between changes in lightness compared to hue/chroma changes was also accounted for.

1.45.3 The second idea was to follow (**2**) suggestions from Kühni[153,154] by modifying the CIE '$\overline{xyz}$' - colour matching functions into cone sensitivity functions that define mathematically the opponent colour coordinates. Witt[163] also suggested combining both methods.

1.46 DIN_{99} colour difference formulae

1.46.1 Cui *et al.*[165] optimized the DIN_{99} formula to achieve better prediction performances. The authors started with Germans standard DIN_{99} formula (DIN 6176:2000[166]) applying four datasets (and a combined dataset) consisting of mainly glossy paint and textile samples. Their first modification was achieved by; (**1**) optimizing all parameters within the original DIN_{99} formula for the combined dataset until a better correlation with visual results was achieved (DIN_{99b}). Further modifications were introduced by (**2**) following suggestions from Kühni[154] to adjust CIE 'X' - tristimulus values by subtracting small amounts of the 'Y' - tristimulus values with the result of improved predictions for blue chromatic differences; scaling the 'b^*' axis by a factor of '0.94', and omitting DIN_{99}'s original rotation term for the 'a^*' and 'b^*' - axes (DIN_{99c}); or, (**2a**) by using (**2**) and optimising DIN_{99}'s rotation term (DIN_{99d}). The strongest deviation between CIELAB and DIN_{99} scales occurred in plots between chroma scales 'C_{99}' and 'C^*_{ab}' for the modified DIN_{99c} and DIN_{99d} formulae mainly caused by the modification of 'X' – tristimulus values. The modified versions of the formulae DIN_{99b}, DIN_{99c}, and DIN_{99d} improved predictions for small colour differences compared to CIELAB, CMC, and CIE_{94}, according to Kühni[154] and Richter & Witt[167].

1.47 $CIEDE_{2000}$ colour difference formula

1.47.1 In June 2000, members of the 'CIE TC1 - 47' committee proposed a draft version of a new colour difference formula '$CIEDE_{2000}$' ('ΔE_{00}' units). Explicitly, Luo[168] clarified on the fact that the 'S_L' function ('V' - shape) was '*…consistent for both textile and paint data sets.'* Four corrections were implemented since the introduction of the 1976 CIELAB colour difference formula to derive the new $CIEDE_{2000}$ formula. Starting with the implementation of empirically corrections to improve visual with numerical colour differences by implementing; …

1.47.2 …weighting functions for lightness, chroma, and hue colour difference components compensating for the non-uniformity of the CIELAB colour space; chroma colour difference dependency on increasing chroma level was the most significant parameter, as discovered by McLaren and McDonald during their work on colour difference formula work in the 1970 and

1980s (see CIE[169]). Several researches modified those weighting functions for the *CIEDE*$_{2000}$ formula depending on the data sets that were used during those experiments. Especially, the lightness weighting function differed significantly compared to *CIE*$_{94}$'s 'S_L' function. The chroma and hue colour difference dependencies on chroma level and hue position generally followed CIE94's 'S_C' and 'S_H' weighting functions, however with the addition of a correction for 'S_H', according to the hue angle of the colour difference pair to be considered[170].

1.47.3 Similar approaches and corrections on hue colour difference dependencies on hue angle were employed in the CMC, BFD, and LCD formulae. The *CIEDE*$_{2000}$ 'T' function (for hue colour difference dependency on hue angle) was revised by Berns while considering several datasets (Qiao, Berns, Reniff, and Montag[171], Luo and Rigg[137], Maier[172], Witt and Döring[173], Witt[143], Alman et al.[133]). All of them were constraint to hue differences and some of them were combined into a larger dataset. The materials that were used consisted of printed samples, plain wool serge[174], acrylic-lacquer paints, and painted colour samples. Qiao and Luo's hue dataset were sampled uniformly in accordance to hue angle 'h_{ab}'. Both datasets were mainly generated to provide samples with lightness values of either 'L^*40', 'L^*50', or 'L^*60'. Colorimetric calculations referred to the 1964 Standard Observer and illuminant D65. A fourth order, rather than fifth order sine series, as in the case of the BFD formula, was used to describe hue colour difference dependency on hue angle. The *CIEDE*$_{2000}$ optimised 'T' - function was derived from those datasets especially since the quality criterion was rather towards uniform sampling than visual precision. Also, it became evident that;

1.47.4 …other parameters, than the non-uniformity of the CIELAB colour space, were influencing experimental results (CIE[126]). The variation in experimental conditions and material variables also changed the sensitivities of an observer towards one of the three colour difference components in colour difference judgments. Parametric factors 'k_L', 'k_C', 'k_H' were introduced and added as weights according to those changes in sensation. Parametric factors compensated for the fact as how a change, for instance, in one unit in the lightness direction was tolerated by the observer compared to a change in one unit of chroma and/or hue differences. Parametric factors for the reference conditions (CIE[175]) should be set to unity such as '$k_L = k_C = k_H$' equals '1'. A prominent formula used in the textile industry was the CMC formula, in which colour differences in the lightness direction was generally tolerated twice as much as chroma differences;

1.47.5 …also, the 'a^*' - axis (red-green opponent) was increased by a factor in relation to the 'b^*' axis as such similar to the process applied to the development of the *DIN*$_{99}$ formula; however, having its largest effect for low chroma values and a descending effect up to a chroma value of approximately 'C^*_{ab} 30'. This method transformed near achromatic ellipses into circles

by elongating the length of the 'a*' – coordinates, according to Witt[176]. The prediction for neutral and near neutral colours was said to have improved;

1.47.6 …a rotation term 'R_T' developed originally by Luo and Rigg[138] for the BFD formula was added as a term in the *CIEDE*$_{2000}$ formula but with the addition of parametric factors 'k_C' and 'k_H'. This was said to be necessary since visual colour difference data showed an interaction between chroma and hue differences in the blue region of the CIELAB colour space. Experimental ellipses in the high chroma blue area of the colour space were tilted away from the neutral point. This made it necessary to adjust calculated ellipses with the inclusion of the 'R_T' term. The difference between *CIEDE*$_{2000}$(k_L:k_C:k_H) and CMC(*l:c*), or *CIE*$_{94}$(k_L:k_C:k_H) was in the prediction performance for neutral and high chromatic blue samples. The formula was derived from combining four datasets; (**a**) RIT – DuPont[133], (**b**) Witt[158], (**c**) Kim and Nobbs[155], and (**d**) BFD-P (perceptibility) data[139].

1.48 Testing *CIEDE*$_{2000}$

1.48.1 Alman[177] described statistical significance tests methods for each of the terms in the *CIEDE*$_{2000}$ formula compared with; (**1**) the full *CIEDE*$_{2000}$ colour difference model, and (**2**) CIELAB, *CIE*$_{94}$, CMC, BFD, and the LCD formulae. Especially, the new '*a*'' - axis correction term was in question. Luo, Cui, and Rigg[178] used a combined dataset for determining the significance of the new terms using magnitude scaled numerical colour difference data compared with visual data to determine the error (residuals). 'F' – test was employed, and the results obtained for each term followed generally those directions that were reported in earlier work reported by McLaren and McDonald. The order here in terms of significance from largest to smallest was in the form; 'S_C' < 'S_H' < 'S_L'. The 'F' – test values obtained from the combined dataset for 'S_L', 'S_C', 'S_H', hue angle 'T'- function, rotation function 'R_T', and for rescaling the 'a*' - axis were 0.880, 0.463, 0.759, 0.987, 0.889, 0.919, respectively (99% certainty). Colour difference dependency on chroma and hue was significant, whereas hue colour difference dependency on hue angle (expressed and approximated mathematically in the form of the 'T' - function) and rescaling of the '*a**'- axis were close to a possibly critical 'F'- value while assuming a normal distribution for all residuals.

1.48.2 Melgosa[179] confirmed those results using the same combined dataset for the determination of significance (95% certainty). Colour difference dependency on chroma was determined as the most significant term, but also all other corrections were classified as significant, if compared with the original *CIEDE*$_{2000}$ colour difference formula. Melgosa gave chroma corrections an arbitrary value of 100% so that scores for hue and lightness corrections, rotation term 'R_T', and neutral sample corrections resulted in values of '29', '8', '8', and '6'.

1.48.3 The $CIEDE_{2000}$ formula was the last of a series of formulae that accounted for the non-uniformity of the CIELAB colour space. The CIELAB formula was a modified version of the ANLAB formula that originated from Adam's work in the 1940s. The $CIEDE_{2000}$ formula included four new terms. Whether the original method of scaling opponent axes and coordinates resulted in an appropriate definition of equally perceived coordinate units of chroma and hue, and whether the original lightness scale was defined by an unambiguous mathematical equation that enabled the user to relate CIE 'Y' - tristimulus values with equally perceptual lightness values values for various neutral backgrounds, was not clearly answered. The new $CIEDE_{2000}$ lightness function was optimised for neutral backgrounds of approximately CIE 'L^* 50' and was, therefore, likely to perform best within those experimental conditions. It was also required to define experimental conditions in a strict sense whenever results needed to be reproduced. The inclusion of parametric factors, which were accounting for changes in relative sensitivities of the observers to colour difference components, became necessary as a wide range of experiments for surface colours indicated. Parametric factors were quantified, since colour perception was affected significantly by a change of illuminants, by the size of the samples, by the magnitude of colour differences, background colour, texture of the surface colours, and other deviations from the reference conditions (CIE[49,126,168]).

1.48.4 The CIE committees 'CIE TC 1 - 63' and 'TC 1 - 81' objectives were then to test the performance of the new $CIEDE_{2000}$ colour difference formula. Also, it was suggested that future improvements in industrial colour-difference evaluation '*…needed a colour space with improved uniformity thus comparable with perceptual results.'* The CIE established therefore a new technical committee, 'TC 1 - 55*' Uniform Colour Space for Industrial Colour-Difference Evaluation* with the aim to carry out this work. Rather, correcting for the non-uniformity of the CIELAB colour space, researcher were now asked to focus their efforts on obtaining a more perceptual uniform colour space. A colour difference measure could then be determined by defining a vector distances within a colour space.

1.49 Colour appearance colour spaces and formulae

1.49.1 Generally, a colour space was constructed by scaling equal lightness difference steps from object colours with the same perceived step differences in chroma and hue. Only object colours with the same lightness values were considered once scaling was satisfactory. Colours in an equal-luminance plane were then transformed (linear or non-linear) in a way in which distances between them were exactly the same and also referred to the same perceived colour differences. This arrangement could be either made of (**a**) equilateral triangles (six neighbouring

colours having the same distances from a base colour, or made of (**b**) polar coordinates. A colour solid could be then constructed at different lightness levels from black to white.

1.49.2 The *Munsell Notation* system was such a colour order system. This system was based on perceptual experiments, in which the equality of visual spacing of matte or glossy paint chips was the main objective. One perceptual step (or difference) in Munsell's lightness 'V' - scale equalled approximately two (some researchers believe three steps) difference steps in Munsell's Chroma 'C' – scale (at level '5'), and three steps difference units in Munsell's Hue 'H' scale. This spacing within a cylindrical system for hue differences increased with increasing chroma level of the samples. Also, the magnitude of the spacing between each colour attribute level was generally too large to be used for practical industrial colour difference estimation. A method of interpolation between two steps of colour attributes was said to be inaccurate, according to Newhall *et al.*[63].

1.49.3 Perceptual uniformity meant then dealing with a colour space of non - Euclidean form. Kühni[180] reminded on the fact that the surround lightness effect was not appropriately described and included in colour difference formulae. The luminance of the background colour (controlling adaptive state of the observer's eye; the magnitude of influence is determined by the size of the colour samples) was considered as the most important parameter influencing the spacing of a lightness scale[181,182]. Furthermore, Takasaki's experiments showed that a grey background enhanced the sensitivity of observer's eyes to lightness differences between grey samples once their luminance values were close to that of the background colour. This was explained by the term 'induction', in which the excitation strength from the background was inversely and partly induced on the sample area, so to change its overall brightness appearance, as explained by Hurvich and Jameson[183].

1.49.4 Once an approximate uniform scaling from observations of surface colours (i.e. Munsell colours) in terms of lightness, hue, and chroma was achieved, it was possible to determine their CIE 'XYZ' - tristimulus values. They were then transformed to new tristimulus values, which then defined a distorted space. A popular transformation, from CIE 'XYZ' - tristimulus values from approximate perceptual uniform colour scales, was the Adams-chromatic value diagram. The diagram was also the basis (after several modifications) for the introduction of the CIE 1976 ($L^*a^*b^*$) space. A similar approach initiated by Judd[65] based on chromaticity spacing of monochromatic stimuli, just noticeably differences, and spacing of chromaticity of dominant wavelengths let to a uniform chromaticity scale diagram (UCS - diagram). CIE 'xy' - chromaticity were linear transformed (coefficients determined from experimental results) to obtain new x'y' – chromaticity to be drawn in a coordinate system and diagram. Modifications finally let to the *CIE 1960 UCS diagram,* which was succeeded in 1976 by the *CIE 1976 UCS*

diagram[e]. These colour spaces also included colour difference formulae, either being related to perceptual uniform scaling of Munsell's Renotation system in the case of CIELAB, or relating to threshold experiments ('JND') from colour stimuli matches as in the case of CIELUV.

1.49.5 An approximation of a triangular system is known as the OSA colour appearance system (Optical Society of America). The OSA colour atlas included 558 coloured paint chips for deriving the best possible uniform colour spacing according to a cub octahedron lattice for global and local uniformity, as explained by Hunt and Pointer[184]. Twelve neighbouring colours surrounded each colour, all of them perceptually equal in distance. Lightness determination was related to CIE 1964 'XYZ' - tristimulus values, and followed generally Semmelroth's formula[181,182] that takes crispening effects of colour differences for a neutral background with a relative reflectance value of '30' into account. Lattice coordinates were determined ('j', 'g') in an opponent fashion either to derive; yellow/brown, blue, green, and/or reddish/purple colours. A colour difference formula ('ΔE_{OSA}' units) was also constructed from those colour attributes but reported to be unsuitable for small colour differences, since lattice points or samples in the OSA colour space were twenty times the size of just noticeable colour differences.

1.49.6 Huertas, Melgosa, and Oleari[185] used the OSA colour space to derive a new formula ('ΔE_{GP}' units) for small to medium colour differences. The BFD - P, BFD - A, and COM dataset were used to optimise 'E_{GP}' colour difference formula parameters. They were scaled in regards to OSA lightness, chroma, and hue (10^2); weighting functions 'S_C' and 'S_H' were optimised using linear functions of chroma 'C_{OSA}'; and parametric factors 'k_L', 'k_C', and 'k_H' were set to '1'. Oleari, Melgosa, and Huertas[186] modified further the OSA colour space and introduced a logarithmic compression for the chroma and lightness scale (see also DIN_{99}[f] and Thomsen[g]), so to produce a new space with an associated colour difference formula ('ΔE_E' units).

1.49.7 Berns and Zue[187] derived a new colour difference formula that was based on $CIECAM_{02}$, which included a logarithmic compression of chroma; Urban, Rosen, Berns, and Schleicher[188] transformed a colour space formed by a non-Euclidean colour difference formula ($CIEDE_{2000}$ and $CIECAM_{02}$) into a Euclidean colour space using a computational multigrid optimisation technique.

---

[e] see page 86 'UCS'

[f] see page 41: DIN_{99}

[g] see page 37: Thomsen's modification of CIELAB

1.49.8 Urban argues that, if an isometric transformation (or almost isometric) in an Euclidean space can be found, then calculations for colour differences would become simpler since geodesics are straight lines with a possibly advantage to be also appropriate for calculating larger colour differences. This method resulted in colour look up tables (CLUT) transforming a non – Euclidean into Euclidean space for lightness (1-D LUT) and 'chroma and hue' (2-D LUT) coordinates.

1.49.9 Another approach was to design a colour difference formula from a colour appearance model based on models of colour vision[189]. CIELAB was regarded as a colour appearance model in its simplest form (normalised by the reference white including viewing field for the 1931 and 1964 Standard Observer). This space can also describe a colour difference in a single set of viewing conditions not too different from average daylight. Descriptors were defined by using three colour attributes normally given as the difference either in lightness, chroma, and/or hue. Models for predicting the appearance of colours were given by Hunt[190], Nayatani, Takahama, and Sobagaki[191], Fairchild and Berns[192], and Kuo, Luo, and Bez[193]. They can describe, for instance, how a colour stimulus will look alike under various viewing conditions. Model output descriptor attributes were described as brightness; ('Q'), lightness ('J'), colourfulness ('M'), chroma ('C'), saturation ('s'), hue angle ('h'), and hue composition ('H'). Especially, changes in the proximal field, surround, background, and adapting field did influences the appearance of a stimulus.

1.49.10 Various researchers studied colour appearance phenomena; some of them included in the latest CAM model $CIECAM_{02}$[47] such as; (**1**) chromatic adaption transforms[46] for deriving corresponding colours that appeared similar to those original colours when viewed under a different illuminant (an early example was given by von Kries); (**2**) Hunt effect[194] describing light and dark adaption in relation to different viewing conditions an eye was adapted to with the effect that a colour with the same lightness and chroma value increased in colourfulness ('M') with increasing luminance level; and, that for the same colour sample but with varying chroma values, the contrast between them increased also with increasing luminance level; (**3**) Stevens effect[195] showed that perceived brightness of a sample increased with increasing illuminance level; and, that also the brightness contrast between samples with varying lightness values increased with increasing illuminance level; (**4**) surround effect, described by Bartleson and Breneman[196], as how a perceived contrast in colourfulness and brightness also increased with increasing illuminance level of the background surround; and (**5**) lightness contrast effect, investigated by Luo, Gao, and Sciviner[197], so to describe how a colour was perceived lighter in appearance when seen against a dark background. Other simultaneous contrast effects were detected, when different coloured background had a significant influence on the colour appearance in lightness and hue of a sample.

1.49.11 Li *et al.*[198] tested colour appearance models using three data sets (combined SCD[h], LCD, and Bradford Illuminant A 'BFA' dataset) derived from small and large colour differences (Zhu, OSA, Guan, BFD Badu Data – BFDB -, Pointer and Attridge, Munsell data, and combined SCD). Li suggested that a polar space was performing best for determining a colour difference between two samples in $CIECAM_{02}$ colour space. Three $CIECAM_{02}$ colour attributes according to lightness ('J'), colourfulness ('M'), and hue angle ('h') were used to fit both datasets. The '$M^{'}$ term in the formula (colourfulness) was derived from a typical chroma weighting function equation (see 'S_C' included in the CMC[i] formula); however, also a logarithmic term was included in the case of $CIECAM_{02}$'s '$M^{'}$ - function. The results and coefficients obtained after optimisation for those datasets were then applied to $CIECAM_{02}$'s red/green ($a^{'}$) and yellow/blue ($b^{'}$) - axes. This colour difference formula included also a 'k_L' weighting function, and optimised coefficients for small, large, and for a combined dataset. The correlation result between visual and numerical, or predicted, results for a large colour difference dataset was similar, when compared with the results for the CIELAB, Kuehni, SVF, OSA, GLAB, IPT, and $CIECAM_{02}$ formulae, as reported by the authors conducting those experiments (an average PF/3 value of 25.2 with a standard deviation 'STD' of 1.4). Testing the combined small colour difference dataset resulted in an average PF/3 value of 33.5 (STD of 3.5) omitting results from CIELAB's 1976 formula. The magnitude of the colour difference of a sample pair caused a significant variation in prediction performances amongst formulae[199].

1.49.12 In conclusion, more than 70 years of research was put to the test resulting in the latest $CIEDE_{2000}$ colour difference formula. However, the long series of improvements, mainly accounting for the non- uniformity of the CIELAB colour space, may have now exceeded the limits for what the colour space was originally intended for. A colour difference formula should describe the same perceptual colour differences as the same vector distance independent of location in a uniform colour space. It is now believed that further improvements in colour difference predictions can only then be achieved, if the colour space as such is of perceptually uniform three - dimensional nature, as it was intended with the introduction of the 1976 CIELAB colour space and formula. Nevertheless, the CIE colorimetric system was successfully adopted in industries. The implementation of the system is summarised in CIE's technical report publication from 2004[17].

---

[h] BFD, RIT-DuPont, Leeds, and Witt dataset

[i] see page 32 and 94

1.49.13 Colour spaces and formulae diagram

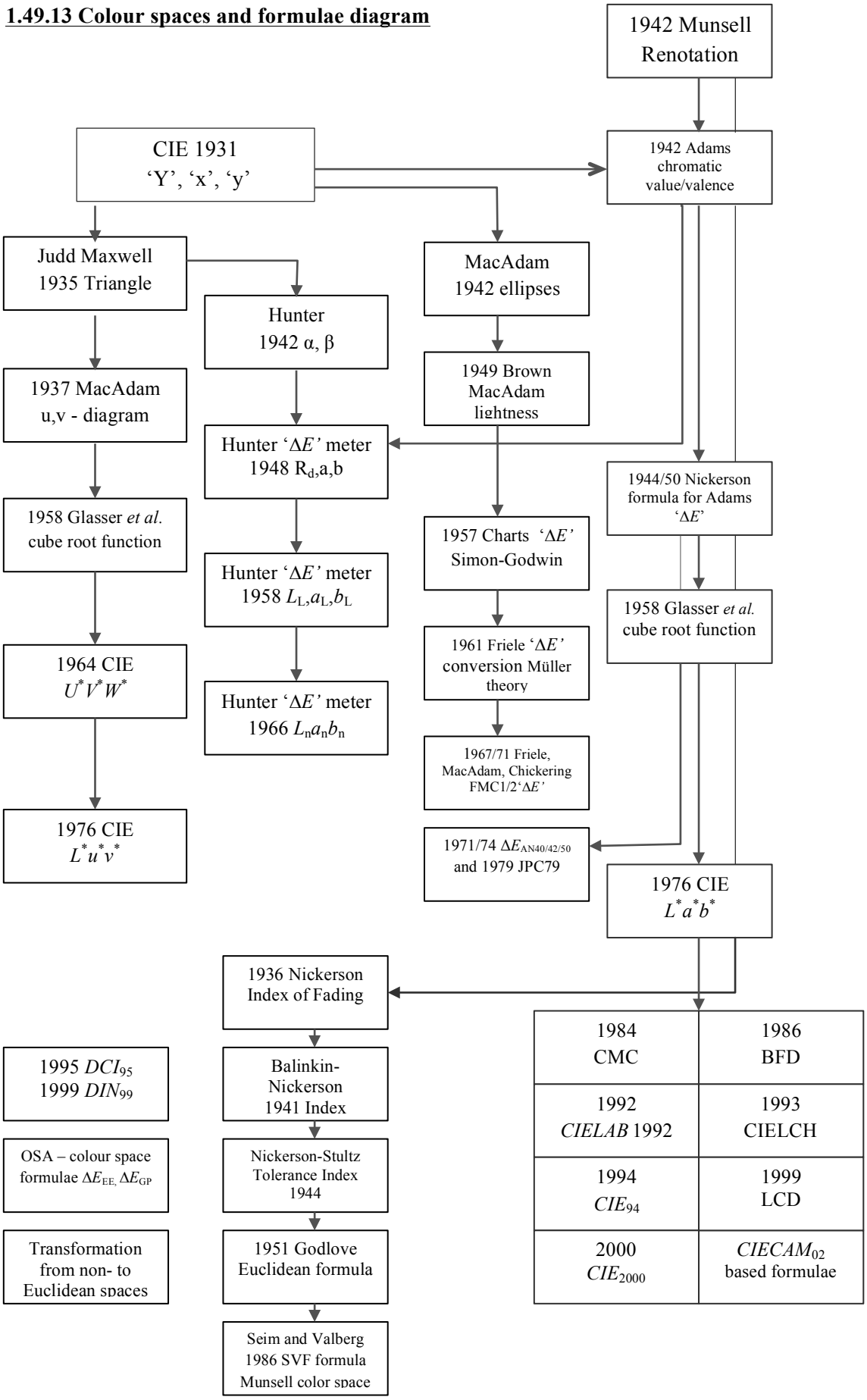

1.5 Project considerations

1.5.1 This project was sponsored by a manufacturer of industrial purpose spun polyester sewing and needlework threads (Coats plc.). It is an essential requirement in the textile industry to produce a coloured product exactly to a client's specification. Quality control measures are a prime concern and tool in the textile industry as such being used to insure that a product is successfully produced. Colorimetry is applied in textile applications, for instance, for characterisation of colorants in the CIELAB colour space, quality control measures with the help of colour difference formulae, for fastness evaluation, recipe formulation, and many other applications.

1.5.2. Historically, a professional dyer worked closely together with a designer of textiles to ensure that a good subjective match was achieved. The matching procedure follows generally certain rules and conventions normally specified by the dyeing and matching process. However, this has not always guaranteed a good match especially when we consider the subjective nature of a human observer in a colour matching assignment. Often an example of a desired product is provided so to avoid colour miscommunication. The dyer is then able to use his or her knowledge and expertise to determine the right recipe to match the colour of a physical example of a desired product (standard) according to a client's needs.

1.5.3 In modern colorimetry, it is the use of colour measurement instruments, software to compute colorant recipes, and a colour difference formula that is used to determine the success of a reproduction given its objective foundation. The quality controller prefers a single colour difference number representing a simple tolerance limit for pass/fail decisions. If, measurement methods and viewing conditions between industry and buyer are established and put into practice to agreed standards, than a mismatch between standard and reproduction is generally minimized (CIE 2004c[175], AATCC Evaluation Procedure 9[200], ASTM E308-08[201], ASTM D2616-12[79]). Only twenty dye houses in Europe before 1976 were employing instrumental measures for conducting colour quality control work, according to McDonald[202]. However, in 1989 most of the larger textile companies throughout Europe used instrumental quality control methods often so provided by companies that were selling measuring instruments and buying textile products (Datacolor and Marks & Spencer in the UK). Nowadays, Coats plc in-house quality control assignments rely entirely on instrumental measurements for controlling colour reproduction-performances[203]

1.5.4 Thread cones are generally dyed and produced to exact specifications as quantified and given in CIELAB $L^*a^*b^*$ - values. A manufacturer of blue shirts may order 5000 meter of spun polyester sewing threads of a blue shade. This order, communicated to a dye house manager, will be produced initially as a small trial lot. If, this small 'blue colour thread lot' is considered

to be dyed successfully, then the same recipe is used to produce the reminder of that order. Initial and further success is in this case determined by those colour specifications that are obtained for the reproduction sample compared to the original sample while using instrumental measurement methods. These measurements results are then used in combination with a colour difference formula that then describes the reproduction performance with a numerical value ('ΔE' unit) whenever a batch sample differs from a standard in colour. In order to obtain a colour specification for a thread sample it is necessary to measure a 'dyed' thread. A spectrophotometer is normally used in the textile industry so to obtain reflectance values for a sample in the visible wavelength range. Common industrial practice in the thread producing industry is to wind this thread around a winding card. This is primarily done so to align individual threads side by side and, given a sufficient quantity, to obtain opaque samples. Generally, an individual thread's size is normally smaller in size than most measuring apertures in spectrophotometric instruments. With this method, it is possible to obtain reflectance values from thread samples, and also to calculate and specify colorimetric values. The CMC(2:1) colour difference formula ('ΔE_{CMC}' units) is the preferred equation to calculate numerically colour differences between batch (reproduction) and standard samples (original)

1.5.5. An exact match in a reproduction process can be - but is not always – achieved. That's why producers and buyers of products established quality control measures, which specifies tolerances or deviations from the original values, which are still commercially accepted. In this case, a manufacturer provided a maximum total colour difference tolerance limit of '1.2' 'ΔE_{CMC}(2:1)' units, or a tolerance of '0.8' 'ΔE_{CMC}(2:1)' units, if a colour difference measure between two samples was solely determined by a difference in hue for products to be regarded as successfully produced. However, even when numerical colour specifications for two samples match or just differ slightly with each other, a corresponding reproduction samples does not always appear acceptable to the eye of an observer, especially in those cases when a thread is seen in an 'end-product' (for instance, a blue shirt). A colour difference value in our case is predicted by using a colour difference formula together with measurement results that is obtained from a 'thread winding card' and a 'fabric' sample. A fabric sample serves as a standard sample (a blue coloured background in contrast to a homogeneous grey reference background generally used in visual colour difference evaluation), and a stitched thread that is regarded as the batch sample (upon the blue fabric sample varying in size and form). Colour appearance phenomena can alter the colour difference perception of an observer. This altering in visual perception can occur, for instance, only by the difference in texture content of a fabric sample, viewing direction of a sample, lubrication of a thread, or type of stitch that is used (scattered and specular reflected light within and upon the fibres of a fabric sample). These

differences in colour appearance may occur to the eye but may not be 'visible' to the eye of a colour measurement instrument.

1.5.6 The overall appearance can be generally described by chromatic attributes (lightness, chroma, and hue) but also by geometric attributes such as; gloss, haze, shape, texture, and direction of the incident light. Conventional colour difference formulae were so far designed from experimental data in which a standard patch was compared with a batch sample site-by-site in contact, both samples similar in size, of homogeneous texture, viewed in well defined viewing conditions. Obtaining a visual colour difference value from a thread, which is stitched into a fabric sample, alters these reference conditions significantly (CIE 1995[49], 2004c[175]). Therefore, it was of interest to conduct psychophysical experiments comparing calculated with experimentally obtained visual colour differences from 'thread sewn into fabric' samples. Coats plc. concern was mainly of commercial interest as such to determine whether these new experimental results are in line with already established industrial colour difference tolerance limits using instrumental quality control measures. Three types of sample datasets, differing in size and orientation, were produced and displayed to observers during psychophysical experiments (Thread Winding Cards 'TWC', Single Needle Lockstitch 'ST', and Buttonhole stitch type 'BH' samples). Visual experimental results were analysed and contrasted with numerical results obtained from advanced colour difference formulae such as; CIELAB, BFD, LCD, CIE_{94}, DIN_{99c}, $CIEDE_{2000}$, OSA-E_{GP}, $CIECAM_{02}$ - SCD and the standard formula that is normally used in the textile industry - CMC.

1.5.7 Existing formulae were optimized with the aim to improve correlation between visual and corresponding numerical predictions. Parametric factors, describing the influences on colour perception due to the type of stitch (size) and presentation mode (orientation), were quantified. Obtaining quantitative data from psychophysical experiments require a large number of physical samples to be produced to exact defined colour specifications. This is time consuming and also expensive to achieve. Therefore, it was also of interest to determine whether digital substitutes from physical 'thread sewn into fabric' - samples can be used for psychophysical experiments providing results that are comparable with those that were obtained from physical samples.

1.6 Aims of Study

1.6.1 Aim 1

To conduct psychophysical experiments using ‘thread sewn into fabric’ samples to investigate if and how visual colour differences were altered due to the use of different stitch types and presentation modes.

1.6.2 Aim 2

To develop a characterisation model that can reproduce visual colour differences from physical ‘thread sewn into fabric’ - samples realistically on a digital screen.

1.6.3 Aim 3

To develop a colour difference formula that correlates better with visual colour difference results obtained from ‘thread sewn into fabric’ samples when compared with conventional settings in the textile manufacturing industry.

Chapter 2

The Oxford English Dictionary describes colour *'...as the property possessed by an object of producing different sensations on the eye as a result of the way it reflects or emits light.'* This included physical actions such as to produce a stimulus in the form of light and subjective results that are referred to as how the stimuli in the eye and brain will be processed and interpreted. Therefore, we can regard colour as a complex perception, which can be described in its simplest form *'...as the interaction of a light source, object and observer.'*[204]

2.1 Light

2.1.1 The sun is a natural radiant energy source. The sun's light can be of direct or indirect form when the sunlight produces scattered radiation in the earth's atmosphere. Daylight is altered, for instance, by absorption and scattering according to the angle of the sun in the sky, humidity, dust, gas molecules, or cloud conditions in the atmosphere.

2.1.2 A simple description says that light is made of electromagnetic waves carrying energy, which is visible to our eyes (radiant energy in units of Joule 'J' or given in electron volts 'eV'). These waves vibrate at right angles in comparison to their travel directions. The distance between two sinusoidal peaks is called the wavelength (λ) of radiation. The number of waves passing through any point in space in a second determines the frequency (unit is hertz 'Hz'). Both, frequency and wavelength determine the colour of a light source and its radiation. The intensity of light is given by the amplitude or lateral displacement from the travelling direction, according to Jacobson[205].

2.2 Radiation

2.2.1 Radiation can be explained and described by 'not continuous' amounts of quanta called photons (smallest unit of light) in the energetic process of absorption and emission. The energy of light or photons can be absorbed and emitted by an electron, atom, or groups of atoms (molecules), but only within certain energy quantities. The photon energy depends on wavelength (or frequency of radiation) and can be calculated using Planck's equation as seen in *Equation 5*.

Eq. 5: $E = hc/\lambda$, where

'h' refers to Planck's constant (6.626176 x 10^{-34} Joule seconds), 'c' refers to the velocity of light in a vacuum, and 'λ' (lambda) is the wavelength. 'E' refers to the smallest amount of energy in a photon, which is absorbed by a single atom or molecule as described by Sinclair[206].

2.2.2 The energy of light absorbed or emitted at shorter wavelengths (blue/ultraviolet) is higher than energy at longer wavelengths (towards red/infrared). This has two possible consequences; (**1**) at lower energy levels atoms and molecules starts to move once they are radiated. The result is in an increase of temperature or heat, whereas (**2**) at higher radiation levels atoms ionize by removing electrons with a possibly result of destroying molecules, according to Nassau[207]. Also, a change in energy can have an effect on a light's radiation that passes from one material into another (i.e. air/glass). The diffraction or bending of light is stronger at shorter wavelengths. A graphical description of a system that absorbs and emits quanta of light (or photons) can be seen in *Figure 8*.

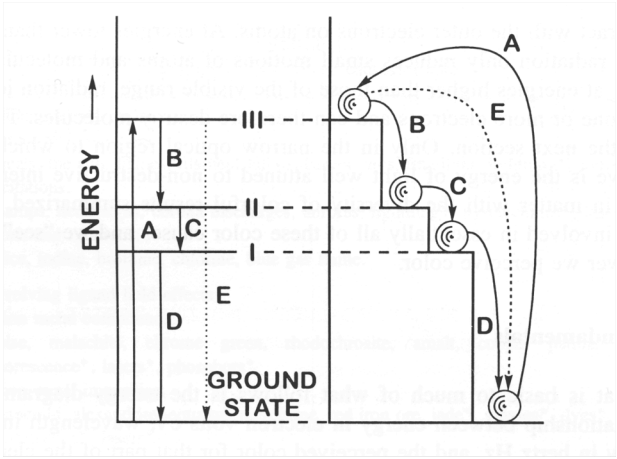

***Figure 8*: Energy level system describing a raise in energy (up to level III) and a stepwise decline back to ground state while releasing or emitting photons. Source: K.Nassau, 'The Fifteen Causes of Colour', page 128**

2.2.3 The specific characteristic of light can be described in energy terms given by the amount of photon dose in units of electron volts (eV = 1.602 x 10^{-19} Joule 'J') For instance, the sunlight emission at the surface peaks near a wavelength of 550 nm thus producing radiant energy of 2.25 eV. The photon energy spans a range from 3.26 eV to 1.59 eV in the wavelength range between 380 to 780 nm from blue to red for 'quasi' monochromatic light.

2.3 Photometric measurements

2.3.1 Other physical terms can be used such as power, intensity, existence, irradiance or radiance, as described by Lee[208]. When wavelengths are weighted in regards to their effect on the human visual system than quantities are measured in lumen (luminous flux), candela per square meter (luminance), or lux (illuminance). Altogether, there are four classes of measurements available to quantify light. 'Actinometry' is measured in photon units and 'Radiometry' is specified in energy units. 'Photometry' reduces the values of the spectrum of a light stimulus to a number that describes the effectiveness of it on the human visual system. 'Colorimetry' reduces the spectrum of a light stimulus into three numbers. Table 1 shows the units, symbols, and label of a specific measurement for the first three classes, according to Packer and Williams[209].

	Actinometry	***Radiometry***	***Photometry***
Amount of Light	Photon dose photons Q_p	Radiant energy joules (J) Q_e	Luminous energy lumens·s Q_v
Amount per unit time	Photon flux photons·s^{-1} P_P	Radiant flux J_s^{-1} watts (W) P_e	Luminous flux lumens (lm) P_V
Amount per unit time per unit solid angle	Photon flux intensity photon·s^{-1}·sr^{-1} I_P	Radiant intensity W·sr^{-1} I_e	Luminous intensity lm·sr^{-1} I_V
Amount per unit time per unit area	Photon flux irradiance photons·s^{-1}·m^{-2} E_p	Irradiance W·m^{-2} E_e	Illuminance lm·m^{-2} (lx) E_V
Amount per unit time per unit solid angle per unit area	Photon flux radiance photons·s^{-1}·sr^{-1}·m^{-2} L_p	Radiance W·sr^{-1}·m^{-2} L_e	Luminance lm·sr^{-1}·m^{-2} cd·m^{-2} L_V

***Table 1*: Three systems of measurement, name, unit, and symbol**

2.3.2 *Radiant energy (unit joules 'J')* defines the total energy emitted by a stimulus without any references of time and direction (no geometry); *radiant flux ($J.s^{-1}$ joule per second, or watts 'W')* adds a time component and direction; *radiant intensity (watts steradian^{-1})* specifies direction and angular density, in which the power of light rays is emitted from a points source; *irradiance or radiant flux per unit area (watts per m^{-2})* is associated with surfaces or volumes and specifies how much power is present on each location on a surface, and *radiance (watts per m^{-2})* describe how much power is emitted from each location of a surface.

2.3.3 Their associated partners can be found in 'Actinometry' and 'Photometry'. If, light sources are of broadband form, than it is necessary to describe them on a wavelength basis by adding the word 'spectral' to the unit (wavelength in nanometre 'λ'). Radiance describes the total amount of light that, for instance, is reflected from a sample, or how much light is emitted from the sun into the direction of a solid angle. Radiant intensity is more of a theoretical concept that refers to point sources (stars to some extent), but is also used to derive other terms in 'Radiometry'.

2.4 Light sources

2.4.1 What we see is known as light and, in the case of the sun, is perceived as 'white' light. Most light sources are of thermal form. Once they are heated, they start to glow from a reddish to an almost bluish/white colour at high temperatures emitting a spectrum of radiation. The light we see are photons released from electrons, atoms, or molecules as a by-product of heat energy caused by vibration. Light and radiation can also be produced artificially. Most common lights such as a tungsten filament lamp or sun light (incandescence light sources) are produced when solids or liquids emit light by making them 'incandescence' by raising their temperature higher than 1000 K. Light can also be produced by electric gas discharge when, for instance, a high voltage applied to a gas (addition of energy) can produce a current that enhances ionisation and movement between electrons and ions. Once electrons collide with the atoms of a gas (electrical excitation), they are transformed to a higher state for a short period of time (i.e. 1 x 10^{-12} seconds) before they return to their ground state by emitting photons or quanta of light, according to Wyszecki and Stiles[210].

2.4.2 In the case of fluorescent lamps, light is produced when this excess of energy is released as radiant energy or photon power mainly in the ultraviolet region (around 253.7 nm). These photons excite phosphor coatings in the tube that releases energy of longer wavelengths (colour depends on phosphors and activators). Light produced in this way can be described by its distinctive narrow spectral lines in the visible spectrum. These distinctive spectral 'spikes' in the case of sodium vapour street lighting results in a yellow/orange cast (two peaks in the yellow region at 589 and 589.7 nanometre), or bluish/green light from mercury vapour lamps omitting no light in the red region of the spectrum.

2.4.3 Colour rendering or appearance, when an object is viewed under those lighting conditions compared to a reference light source, is poor but sufficient for street or car park illumination[211]. Other lamps are for critical colour matching purposes more suitable. For instance, filtered high gas pressure xenon lamps provide a continuous emission amongst the ultraviolet and visible wavelength range; xenon lamps are also used for flash photography, or for projectors in cinemas because of its near daylight qualities. The pressure of the gas and other design properties in xenon lamps provide a continuous spectrum over the visible range, and also its colour[212].

2.4.4 Light emitting diodes produces light (electroluminescence) in narrow band wavelength ranges compared to sodium, or mercury vapour lamps. A combination of red (649 nm), green (570 nm), and blue light diodes (450-470 nm) can also produce a white light. They operate at low voltages and have high-energy efficacy (performance input voltage compared to output luminance) and are, therefore, used for laptop or televisions screens. The shortage and access of electrons on a semiconductor caused by impurities (n- and p- type material – gallium arsenide or

gallium phosphide) forces the electrons and holes to combine with a result of releasing photons. The peak energy depends on the semiconductor material and impurities. White LEDs emit blue light in the range of 450-470 nm. Normally, phosphors are added that emit light in the yellow wavelength range so that the combined light appear white. The correlated colour temperature is around 6500 K, but can vary with the type of LED that is used for designing the light source, according to Hunt and Pointer[213]. The relative spectral power distributions from low-pressure sodium vapour, high-pressure mercury gas discharge lamp, and a white LED light source can be seen in *Figure 9*.

2.5 Graphical representations of light sources

2.5.1 A viewing cabinet with a light source that simulates average daylight was used throughout this project for psychophysical experiments. *Figure 10* shows the relative spectral power distribution of a daylight simulator and average natural daylight 'D65' as described by the CIE[214,215].

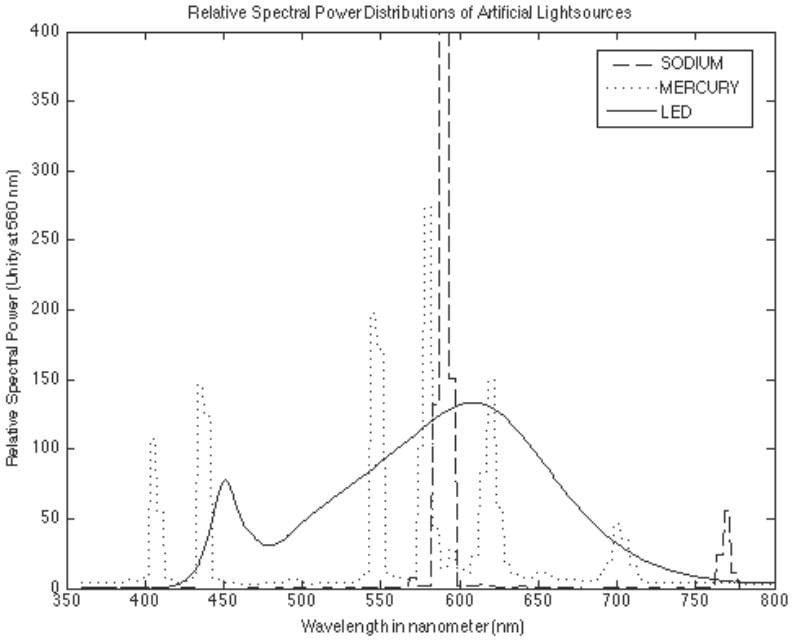

***Figure 9*: Relative Spectral Power Distributions from Illuminants: Data from gas discharge lamps 1. Low pressure sodium lamps (SOX). 2. High pressure mercury lamp (MBF), Philips LED Endura MR16B lamp plotted over the visible wavelength range. Data source: Hunt, R.W.G. and Pointer, M.R., Measuring Colour, 4th edition, 2011, page 371-373; http//research.ng.-london.org.uk**

Differences can be seen in *Figure 10* between the spectral power distribution of natural daylight and a 'daylight simulator' (a fluorescent tube lamp as described in BSI950:Part-1:1967[216]); (**1**) distinctive narrow band peaks in the blue and green wavelength regions caused by the gas and phosphors that were used for designing this fluorescent lamp, (**2**) a loss of energy at shorter and

longer wavelengths (blue/ultraviolet and red/infrared) when compared with natural average daylight, and (**3**) daylight is scatter back into space merely at shorter wavelengths around 440 nm, and some red light is absorbed in the red and infrared regions around 760 nm and 810 nm.

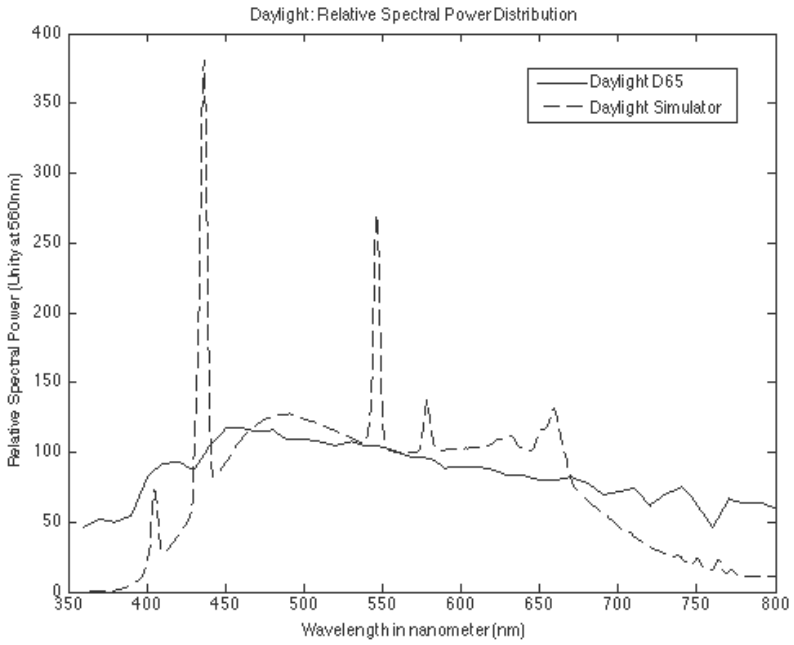

***Figure 10*: Relative Spectral Power Distribution of daylight and a daylight simulator (broadband fluorescent daylight simulator F8 used in a viewing cabinet) normalised to 100 at 560nm and plotted against wavelength.**

2.6 Colour temperature

2.6.1 Another important property of light is described as its colour temperature, distribution temperature, and/or correlated colour temperature (units in Kelvin 'K') to which extent its colour quality is approximately similar or correlated to a temperature and chromaticity of a black body radiator. The energy emitted from the walls of a cavity through a small aperture is regarded as a black body radiator. Other names are Planckian -, full-, or thermal radiator. A black body does not absorb, reflect, or transmit incident radiant energy and appears therefore black at low temperatures. Once, it is heated, it starts to glow and emit radiation in the form of quanta/photons[217]. This distinctive radiant or '*spectral power distribution'* ('SPD') can be characterised just by its temperature, according to Wyszecki and Stiles[218]. If a colour temperature is known, than it is possible to calculate the spectral radiant existence of a blackbody at temperature 'T' in Kelvin radiated into a hemisphere at wavelength 'λ' (in metre) using Planck's Radiation Law (*Equation 6*).

Eq. 6: $M_{e,\lambda}(\lambda, T) = c_1 \lambda^{-5} (e^{\frac{c_2}{T\lambda}} - 1)^{-1}$ $(W.m^{-3})$, where

'c1' = 3.74183 x 10^{-16} W m^2, and 'c2' = 1.4388 x 10^{-2} m K. The chromaticity coordinates of different black body temperatures ('T' defined by spectral power distributions, or spectral radiant existence, using Planck's law for the determination of CIE chromaticity coordinates) can be drawn in a chromaticity diagram (open circles – *Figure 11*). The lower curve refers to the Planckian locus, which is interpolated between chromaticity coordinates from several colour temperatures. All other circles refer to measured spectral radiant power distributions, and 'associated' calculated 'xy' – chromaticity coordinates, for various daylight phases. The *distribution temperature* refers to a source that has got the same spectral power distribution than a Planckian radiator. It can therefore be characterised by the distribution temperature of the Planckian radiator that matches the source. When a SPD of a source is different from a Planckian radiator but falls on this Planckian locus (non full radiator), then it can be described by the colour temperature of a similar Planckian radiator. If the source's chromaticity coordinates falls close to the Planckian locus, than the correlated colour temperature that is most similar to the Planckian's colour temperature could describe it[219]. Typical global correlated colour temperature values, for clear to overcast daylight from the sun and sky, can be between 5000 and 7000 K. A domestic tungsten or tungsten - halogen lamp can operate at a correlated colour temperature of 2800 and 3500 kelvin (less intensity in the short wavelength range). The light of a candle flame correlates to a colour temperature of approximately 1900 'K'. A higher temperature corresponds to an increasing bluish/white sensation compared to an orange/red sensation produced from lower colour temperatures.

2.7 Categories of light sources

2.7.1 Light sources can be categorised mainly into (**1**) solids, (**2**) liquids, and (**3**) gaseous form.

(**1**) Solids mainly refer to incandescence sources subdivided into (**a**) thermal radiators (black body and nearly black body radiators) that includes interactions with chemical energy (wood fire, candle, oil lamp), or electrical energy (carbon arc lamps, or incandescence lamps such as vacuum or gas filled lamps); (**b**) selective radiators using chemical or electrical energy. Other solids refer to luminescence sources subdivided into photo luminance (fluorescence, phosphorescence, solid state laser), electroluminescence (fluorescence and light emitting diode), and chemical luminescence interactions (phosphorus),

(**2**) Liquids are mainly subdivided into incandescence sources (molten iron and lava), luminescence sources such as photoluminescence (fluorescence, phosphorescence, laser), and chemical luminescence (light stick).

(**3**) Gaseous sources are mainly in incandescence form (sun, stars) and luminescence sources. Luminescence can be divided into (**a**) interactions with chemical energy, and (**b**)

electrical energy. Electrical energy is either produced by glow discharge (low and high pressure), or arc discharge such as low-pressure sodium lamps, mercury lamps, gas laser, or high pressure mercury, xenon, or metal halide lamps, according to Sinclair[220] and Hunt[221].

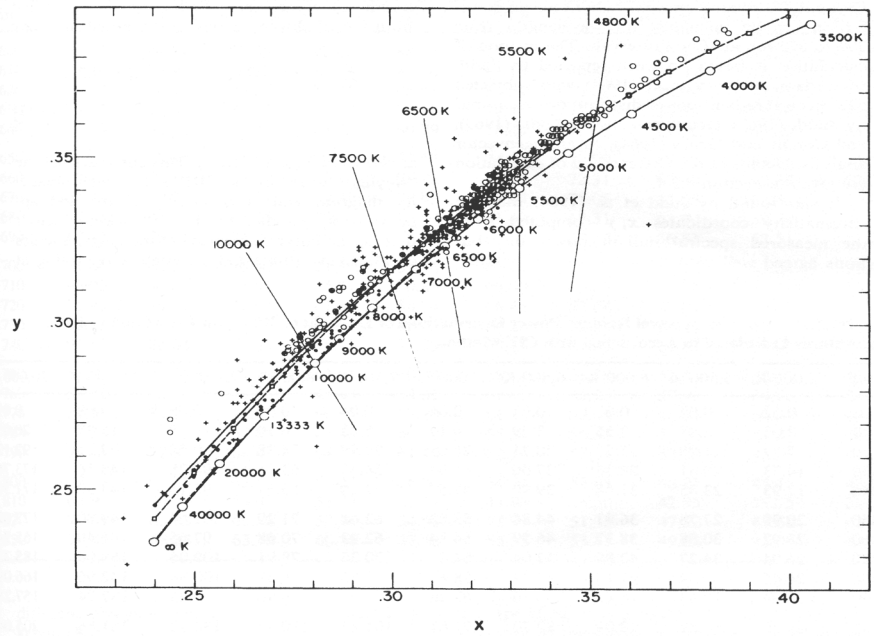

***Figure 11*: Chromaticity points of various measured daylights (upper) compared to locus of Planck's radiation law (lower). Source: Wyszecki & Stiles, page 7, data from Budde[222], Condit and Grum[223], and Henderson and Hodgkiss[224].**

2.7.2 The CIE (Commission Internationale de l'Eclairage) specifies SPDs for natural light sources related to various daylight phases and correlated 'T_c', or equivalent chromaticity coordinates (CIE 1970[214], CIE 1972[225], CIE 1986[226]). Judd *et al.*[227] have given methods as how to calculate relative spectral power distributions of daylight for any chromaticity or correlated colour temperature in the range from 4000 – 25000 T_c. The daylight locus in the 'x,y' - chromaticity diagram in *Figure 11* can be estimated using *Equation 7*.

Eq. 7: $$y_d = -3.000x_D^2 + 2.870x_D - 0.275$$

2.8 Coloured objects

2.8.1 A colour of an object is produced when light in the form of photons was partially absorbed, reflected, refracted, scattered and/or diffracted by matter before entering the eyes. This is known as the interaction between light and charged particles associated with a substance of which a physical object consists. Matter or physical materials can be free atoms, molecules, atom clusters, molecular clusters, and so on. The electromagnetic wave of the light forces the

oscillation of charged particles in atoms or molecules. Electrons absorb light energy and can be excited to higher energy states (*Figure 8*)[j]. The energy needed for state transition of an outer electron is from '1' to '10' eV provided and carried by light in the UV, visible, and infrared wavelength region. Principle effects of light to interact with matter can be seen in cases of absorption, scattering, reflection, refraction, diffraction, transmission, and chemical changes according to Lee[228].

2.8.2 When a light does not enter directly our eyes, then it is normally reflected or transmitted by an object. Reflectance is determined by the shape and material of the object. It can be of specular, diffuse, or mixed nature when some radiant energy is returned in the same wavelength range, as it was incident on the object (CIE[229]). Specular reflection refers to mirror like reflection; this is the case when all light is reflected without changing the content of the incident light. Diffuse reflection occurs on a macroscopic level, and mixed reflection is a combination of both types.

2.8.3 If we want to consider a colour of an object in physical terms, than it can be described by its spectral radiance, reflectance, or transmittance curve over a defined wavelength range. As an example, we consider a daylight simulator and measure the spectral radiance reflected from a blue fabric sample in a viewing cabinet with a tele-spectroradiometer over the wavelength range from 360 – 830 nm. The colour of this fabric sample can be described by the ratio of the incident and reflected radiation (as the sum of scattered and/or reflected light from or within the surface integrated over a defined wavelength range). *Figure 10*[k] shows the spectral radiant energy distribution of the daylight simulator with a correlated colour temperature of approximately 5800 K; the spectral reflectance curve (scaled to fit *Figure 12* – only the distribution shape is here of interest) obtained from a blue fabric sample, and the resulting spectral radiance curve obtained from the sample when it was measured in the viewing cabinet. The shape of the spectral radiance distribution (in W sr^{-1} m^{-2} per wavelength over the visible wavelength range) from a batch fabric sample (*Figure 12*, '---') was similar compared to the spectral radiance distribution from the incident light ('…'). What has changed was the height at each wavelength interval (correlates to the amount of spectral radiance at that particular wavelength interval) from the overall distribution, and that to an extent as how the incident light was reflected, scattered and absorbed by it. The sample's reflectance values over the visible wavelength range (360 - 830 nm) was obtained from a spectrophotometer and provided reflectance ratios of approximately 15% from the incident light between 380 – 500 nm, almost

---

[j] see page 55

[k] see page 59

zero reflectance between 580 – 630 nm, and increasing reflectance values around 670 nm and longer wavelengths (up to 65% of the incident light at small wavelength intervals). These data suggested that only light in the blue and red/purple wavelength range from the incident daylight simulator source was partly scattered and reflected back. In the contrary, incident light in the wavelength range from approximately 580 – 630 nm (yellow/orange/red) was strongly absorbed. The result of this absorption band, caused by a cyan compound, was defined by the blue appearance of the fabric sample in the viewing cabinet illuminated by a daylight source.

2.8.4 However, the curve shown in *Figure 12* does not provide any information about the sample's surface characteristics, for instance, whether it was of matt, glossy, or textured nature. The material used for the fabric sample, the surface structure, thickness, and backing material determines these attributes. Also of equally importance is the method that was used to illuminate the sample (determined by the incident angle of radiation, or number of light sources that were used to enhance or decrease texture content).

2.8.5 The substances that modify light in textiles or paints are known as dye or pigment colorants. They are characterised by their selective absorption or scattering power, respectively. Dyes do not scatter but absorb light; white fibres and textiles diffusely reflect light because of numerous boundaries within a textile's micro-fibril structure. Synthetic fibres scatter light because pigments were applied to them ('titanium dioxide'). The interplay between combined diffuse and specular reflection of incident light within a textile sample, and the absorption wavelength band of a dye applied to it, determines the resulting reflection.

2.8.6 Electrons in atoms and molecules are arranged in orbits around the nucleus. If two orbital electrons from two atoms form a stable pair than a chemical bond forms a molecule. Most dyes and pigments absorb light because of electron transit between orbitals in a molecule. This absorption depends on the chemical structure of a dye and incident light that penetrates it. If, the differences in energy levels between orbitals are equal to the energy of the incident light, than energy is absorbed. This defines absorption as a wavelength or wavelength bandwidth. Each of an atom's orbitals can be occupied by two electrons (Pauli Exclusion Principle), whereas a molecular orbital includes two single occupied outer orbital from two or more atoms. These molecular orbitals can be of various types and energy levels. Most organic molecules have their bonding and non-bonding orbitals (lone pair electrons) fully occupied with electrons (anti-bonding orbitals are empty) in the dark (ground state).

2.8.7 If absorption takes place in the visible wavelength range, for instance, by turning on a light source, a bonding electron and associated non-bonding electron are promoted to an anti-bonding orbital with the result, as described by Allen[230], of being promoted to an excited state. Generally, molecules become excited by absorption of photons due to the increase of energy.

Also, they can lose energy. The differences of energy levels between ground and excited state defines the wavelength of absorption.

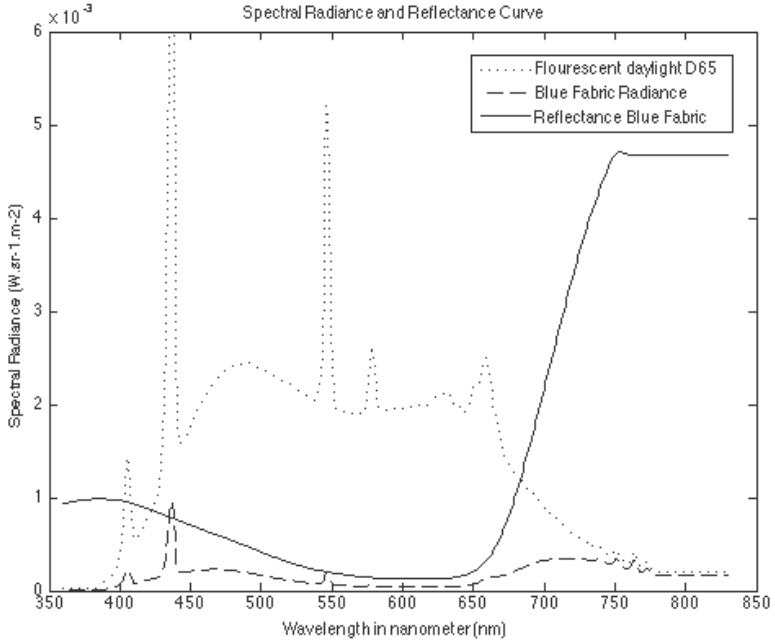

***Figure 12*: Absolute spectral radiance distribution for a daylight simulator BS EN 950-1:1967[216] and resulting absolute spectral radiance distribution from a blue fabric sample viewed in a viewing cabinet. The smooth curve represents the shape of the reflectance distribution obtained from the fabric sample scaled to fit the radiance scale of the graph.**

2.8.8 The observed colour is complementary to the colour of the dyes. However, according to McLaren[231], a perceived colour is not only depended on the absorption wavelength band but also on the number of dyes, width (pale or intense colour), profile of the wavelength band (governs chroma), molar extinction coefficient (intensity), and wavelength of maximal absorption. Narrow absorption bands with sharp peaks describe bright, and broad absorption bands with no peaks refer to dull colours. *Table 2* lists absorbed light and its approximately complementary colour seen in average daylight.

2.8.9 'Scattering' occurs when light interacts with matter as such photon energy is absorbed by atoms or molecules (electrons) and remitted at the same wavelength but in varies directions. If there is a large amount of scattered light reflected from a material than it refers to diffuse scattering. The amount of light that is scattered depends on the difference in the refractive index, and on the size of the particles. If the particles are smaller than the wavelength of the incident light than scattering is enhanced. The result of this phenomenon can be seen in the blue and red sky when the sunlight is scattered by the air's molecules. This is known as Rayleigh scattering, according to Strutt[232]. The scattering power of blue light is approximately 4 times as high as the scattering power of red light. About 95% of red and 75% of blue light are

transmitted through the earth's atmosphere when the sun is at the zenith; and 20% for the red and 0.001% for the blue at sunrise and sunset. When the particle diameter is larger than the wavelength, scattering is less dependent on the wavelength of the light. The white colour of fog and clouds are the results from diffuse scattering of larger particles.

Wavelength	*Absorbed Colour*	*Perceived Colour*
400-435nm	Violet	Green-Yellow
435-480nm	Blue	Yellow
480-490nm	Green-Blue	Orange
490-500nm	Blue-Green	Red
500-560nm	Green	Purple
560-580nm	Yellow-Green	Violet
580-595nm	Yellow	Blue
595-605nm	Orange	Green-Blue
605-750nm	Red	Blue-Green

***Table 2*: Absorbed wavelength, colour name, and complementary colour.**

2.8.10 When an object transmits light, then it is said to be transparent. It can be colourless when it transmits all of the incident light apart from small amounts that are reflected from the two surfaces. Reflection and scattering of light occurs when the refractive index of two materials differ. The index calculates the difference between velocities of light in a vacuum compared to the velocity of light in a second material. The larger the value is, the more the velocity of light is reduced. A typical refractive index for materials such as air and glass is around '1' and '1.5', respectively. Two possible outcomes were observed when a light beam hits a boundary of a transparent material; (**1**) parts of the incident light is reflected (*Equation 9*), and (**2**) a light beam changes its direction depending on the refractive index (*Equation 8*), angle of incidence, and partly dependent on the wavelength of the light (*Equation 6*). For a glossy smooth surface the reflection is of specular form characterised by a reflection angle that is similar to the incident angle. Also, the spectral composition is the same as the incident light.

2.8.11 Refraction and surface reflection of monochromatic light is governed by 'Snell's' and 'Fresnel's law', respectively (*Equation 8* and *9*). Dispersion or the relationship between refractive index and wavelength can be empirical described, for instance, with '*Sellmeier's* equation' as described mathematically in *Equation 10*, according to Jenkins and White[233].

Eq. 8: $n_1 \sin(r_1) = n_2 \sin(r_2)$, where

angle of refraction ('r_2') is given by the angle of incident light ('r_1') and two refractive indexes ('n_1', 'n_2') for two materials in use. If the angle of incident light is perpendicular to the surface of a material (air – glass) than the monochromatic light will not be refracted, but will change velocity. The refractive angle is approximately 27 degrees from the normal for incident light (45°) at wavelength 589.3 nm from air ('n_1=1') to glass ('n_2=1.5'), and 30.23 degrees for the same light beam entering the eye ('n_2 =1.34'). The incident light, which is reflected from a surface with a different refractive index, can be approximated by 'Fresnel's law' (*Equation 8*).

Eq. 9: $p = \frac{(n-1)^2}{(n+1)^2}$, where

('p') means reflected unpolarised incident light and ('n') refers to refractive indices ('n_2/n_1'). Two per cent of a light beam incident at the surface of the eye at normal angles ('n_1' = '1' and 'n_2' = '1.34') will be reflected. The amount of light that is reflected depends also on incident angle, and whether the light was polarised, or not.

2.8.12 Dispersion of light in transmissive material depends on wavelength; so that refractive angle also various with wavelength. Shorter wavelengths of rays (blue) are dispersed stronger than longer wavelengths (red). *Equation 10* can be used to determine the refractive index for various wavelengths but is strictly correct only for normal dispersion in the visible wavelength range, according to Sellmeier[234].

Eq. 10: $n^2(\lambda) = 1 + \sum\left(\frac{B\lambda^2}{\lambda^2 - C}\right)$, where

('n') means refractive index, ('λ') refers to wavelength in micrometre ('μm') and ('B' = '1.039', '0.231', '1.010') and ('C' = '6.01' x '10^{-3}', '2.002' x '10^{-2}', '1.036' x '10^{2}' μm^2) are empirically derived coefficients for crown glass. Refractive angles ('r') for monochromatic light at 250, 400, 589.3 and 780 nm were calculated as 25.6°, 26.4°, 26.7°, and 26.8° at incident angle of 45°, respectively. Generally, when natural or artificial 'white' light is transmitted or reflected from a colourless object than the incident light remains approximately the same. If a coloured object transmits or reflects white light, than the incident light reflects only the wavelength range that we see. If the surface of an object is irregular than the incident light is reflected diffusely producing a matte appearance of a colour compared to a glossy reflectance from a glass surface. Scattering can also change a colour of an object, or lead to translucency.

2.9 The human eye

2.9.1 The next step in producing a colour sensation in a human observer induced by a light source and object is concerned with the human visual system. Of interest here is how the radiant or photon flux enters and travels along the optical system of the eye (*Figure 13*). A simplified generalisation of the human visual system is approximated when we compare the eye with a photographic imaging system. This includes a subject (subject to be photographed or visualised), the optical system (camera: lens/aperture – eye: cornea and eyelid/pupil/lens), the body of the system (camera: light tight box/air – eye: vitreous body/jelly), and the photo sensitive material at the back of the camera or eye (camera: silver halide film or silicon sensor – eye: photo pigment/rhodopsin inherent in the photoreceptors 'rods' and 'cones'). The visual system and post processing stage (pigments/neural system/brain) can be also partly approximated with the post processing stage of a digital camera (i.e. moving images) including compression of redundant data (silicon/sensor/analogue to digital conversion and data compression).

2.9.2 The size of the human eye is of spherical shape and about 12 mm in radius. The iris is of annular shape with a 1.5 mm diameter at bright light, becoming larger in dim conditions with a maximum diameter of 8 mm. This translates to an aperture range from f-stop 2 to f-stop 11 suggesting that 16 times the amount of light is entering the eye when the iris changes its size from 1.5 to 8 mm, according to Jacobson[235]. However, this is not always enough to compensate for the amount of light that can be experienced in nature, so that we are forced to were sunglasses, or have to shade our eyes, once we enter from a dark room into daylight. The image or object focal length of the eye is about 16.5 mm from which the refractive power (D) is calculated (inverse of 0.0165 = 60).

2.9.3 The lens shape is of biconvex form becoming thinner while focusing on objects in the distance, and thicker for objects situated closer to the eye, according to Hunt[236]. Radial muscles (ciliary) pull or release tension via attached fibres that can bend or flatten the lens. This stronger 'bending' for near objects changes the refractive power (optical power) so that incoming rays focal on the retina, whereas otherwise the image would fall just in front, or behind it[237]. Also, the index of refraction is higher in the middle than around the edges of the lens. Again, a blurred image would be the result if the lens could not accommodate between near and distant objects. The main function of the lens is to focus on objects at various distances, according to Hubel[238]. The lens divides the eye into two parts. The two chambers are filled with fluid (in front of the lens) and a transparent 'gelatine - like' material (behind the lens). The refractive indices for both fluids are similar to that of water. The cornea is the outer layer of the eye from which the light enters the eye. It is of convex form and transparent. The amount of the incident light that is absorbed is about 10 % at wavelengths around 800 nm and 20 % at 400 nm. In the region of 300

nm the cornea absorbs more than 99% per cent of the incident light as such protecting the eye from damage caused by ultraviolet radiation. The fluids in the eye (virtuous and aqueous humour) absorb about 10 % of the light at all wavelengths. Also, the lens pigments absorb strongly light in the short wavelength range. Increasing age also produces an increase in light scattering within the lens, thickness of the lens, and increase of lens pigments and absorptions in the shorter wavelength range.

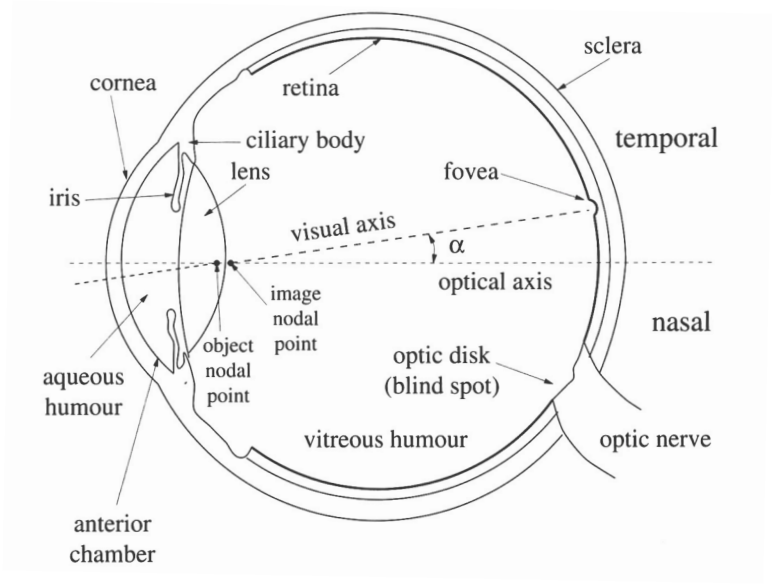

***Figure 13*: Schematic cross section of the human eye. The most important parts for our purpose are the cornea, lens, iris, fovea, retina and the optic nerve (Source: H.-C. Lee 2005, page 272)**

2.9.4 A network of capillaries within the retina filter incoming light (blood/haemoglobin absorbs light in the short wavelength range) and macular pigments absorb light between the wavelength range from 400 to 550 nm. Age related effects are stronger in the short wavelength range (approximately after the age of 30) and can alter colorimetric measurements significantly, according to Packer and Williams[239]. However, colour vision may also be altered by neural mechanism to provide similar colour appearance measures despite of a change in macular density known as yellowing in the ocular media, according to Neitz *et al.*[240]. About 3% of the incident light is reflected from the cornea; 0.8 parts of the incident light is transmitted, and about 20% of the light is scattered in the eye before it reaches the retina[241]. The partial light that is not reflected or absorbed from the eye travels from the cornea via the lens to the retina located at the back of the eye initiating chemical and electrical events that generate nerve impulses.

2.9.5 The retina is a light sensitive tissue that covers a large area at the back of the inner eyeball about 1100 mm^2 in size. Its material is of transparent nature and consists of a structure of cells that can be regarded as stocked layers of neurons on top of each. The cells are interconnected by

synapses. The retina (brain tissue) is an extension of the brain that is connected via the optic nerve. The initial stage of vision is determined by the external stimulus and its inherent radiant flux. The flux is modified while entering the eye via the cornea travelling trough the optical media until it penetrates the retina (physical optics). This process is not of optical form anymore once the external stimulus is absorbed by the light sensitive pigments in the rods and cones (*Figure 13*)[l]. The output from the photoreceptors (neural signals) results in action potentials in the retinal ganglion cells whose axons form the optic nerve.

2.9.6 The major regions of the retina are; (**1**) the optic disk (blind spot about 2 mm in size not sensitive to light), (**2**) the ora serrata (boundary of retina towards the front of the eye), (**3**) the fovea (5.2° angular diameter, most accurate area of the retina, no blood vessels, high density of about 100.000 - 150.000 cones, no rods present), (**4**) the rod free area, (**5**) the central avascular region (centred on the visual pole about 1.4 – 2.3° degree), (**6**) the yellow spot central area extending beyond the fovea (very slight in the fovea), which appears yellow (pigmentation) associated with a shaded spot – the 'Maxwell' spot, (**7**) the parafoveal area which surrounds the fovea, and (**8**) the peripheral area, which is the area between para fovea and ora serrata.

2.9.7 The retina (see *Figure 14*) consists of l0 distinctive layers that include nerve cells and fibres; (**1**) pigment epithelium containing non-photosensitive melanin pigments (single layer of cuboidal cells) that absorb most of the lights that travels through the retina (outer most area of retina towards the brain), (**2a**) rod and cone outer segment layer containing the light sensitive pigments, (**2b**) inner segments, (**3**) outer limit membrane made from fibres of the cells, (**4**) outer nuclear layer containing the cell bodies of rod and cone cells, (**5**) outer plexiform layer containing inner fibres of rod and cone cells and synaptic contacts, (**6**) inner nuclear layer containing nuclei of bipolar, horizontal, and amacrine cells, (**7**) inner plexiform layer containing synapses between bipolar cell axons and dendrites of ganglion and amacrine cells, (**8**) layer of ganglion cells containing the cytoplasmic body of ganglion cell that has an axiom that becomes a fibre of the optic nerve for messaging, (**9**) layer of optic nerve fibres containing fibers (axon of ganglion cells) from the ganglion cells proceeding across the retina to leave the eyeball at the optic disk, and (**10**) inner limiting membrane (Müller cell footplates). Wyszecki and Stiles[242] describe the functional properties of the neural network between (**1**) and (**10**) as (**a**) layer of photoreceptor cells, (**b**) layer of intermediate neurons, (**c**) layer of ganglion cells where (**a**) and (**b**) described the first synaptic layer that interconnected the processes of intermediate neurons, and **(b**) with (**c**) described the second synaptic layer that interconnects the processes of intermediate neurons and ganglion cells, as described by Stell[243].

---

[l] see page 68

2.10 Photoreceptors

2.10.1 The photoreceptors in the photoreceptor layer are called rods and cones (described by their shapes). There are approximately 92 million rods and 4.6 million cones in the human retina. Cones are sensitive to the direction of rays ('Stiles-Crawford effect'). However, the most important difference between rods and cones is the relative sensitivity to light. Rods are generally more sensitive in low light conditions (threshold approximately 5 x 10^{-4} until saturation at a luminance level of 3000 scotopic trolands), whereas cones require a higher intensity of light to function (larger than 3 cd m^{-2}). The overall range of luminance, in which a human eye is operational, exceeds 10^{-6} to 10^{4} cd m^{-2}. Four photoreceptors contribute to the visual response in mesopic viewing conditions when the luminance level was in the range between low and daylight conditions.

2.10.2 Rods are able to detect single-photon events and saturate once approximately 100 photons are absorbed. A rod generally consists of a cylindrical outer- and inner segment (contains ellipsoid and myoid regions). The nucleus and synaptic terminal (small and rounded for rods called the spherule, and pyramid shaped called the pedicle in the case of cones) can be found further down along the inner segment. The outer segment is the part where the light (photon) interacts with visual pigments and is of lamellar structure, whereas the inside consists of double membrane disks thus stacked on top of each other. The visual pigment molecules are situated in these disks (each approximately containing 10^{5} molecules). They are combinations of chromophores (11-cis $retinal_1$, 11-cis $retinal_2$, which are embedded in trans membrane protein molecules called opsins).

2.10.3 Pigments from land vertebrates' retinae are called rhodopsin. Micro spectrophotometry gave evidence for the existence of three pigments with absorption maxima in the short (S – cones at 419 +/- 3.6 nm), medium (M –cones at 530.8 +/- 3.5 nm), and long (L – cones at 558.4 +/- 5.2 nm) wavelength range. All rods have the same pigments with a peak absorption in the blue/green region about 496 +/- 2.3 nm, according to Dartnall, Bowmaker, and Mollon[244]. The difference in the absorption peaks is caused by the small differences in the amino sequences of the opsin in the pigments. The spatial resolution for cones (fovea area) is higher than for rods, the cones response time to light is faster than for rods, and the dynamic range is approximately 100:1 (maximum and minimum change of intensity to which rods and cones responds with a change in output). Dark adaption of the eye can take more than 15 (cones) and 50 minutes (rods) whereas adaption from dark to daylight conditions is achieved within a few seconds.

2.10.4 Photons from the external stimulus enter the retina and travels through all layers until they reach the outer layers of the rods and cones. Those photons, which are absorbed by the visual pigments in the outer segments of the photoreceptors, produce signals. Calcium ion

concentrations inside the cells membrane are lowered in a resting state of rods and cones (dark conditions).

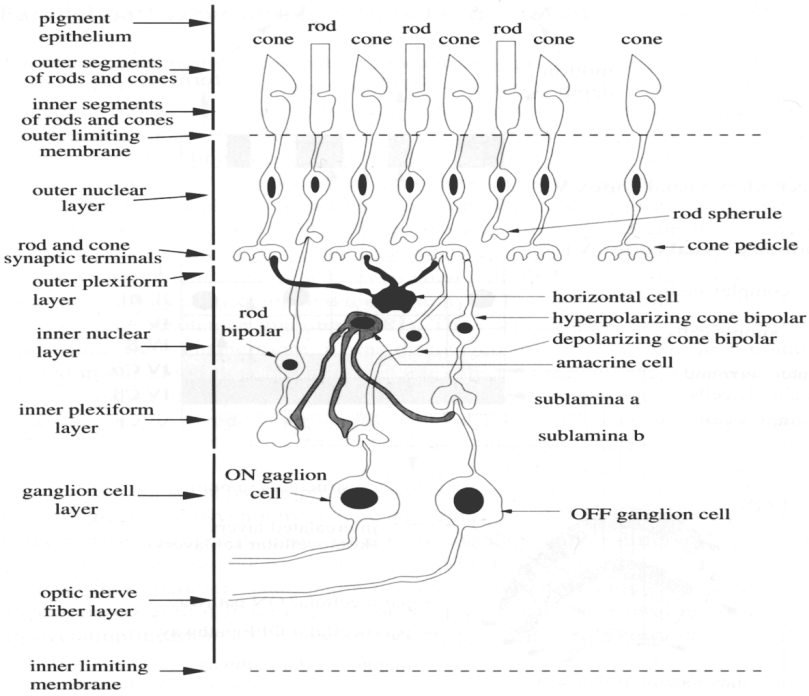

Figure 14: **Schematic diagram of the human retina. Source: Lee, H.C. (2005), page 296**

2.10.5 Rods and cones are polarised when a charge inside the cell's membrane is negative compared to a positive charge outside the cell. Depolarisation occurs when there is a positive charge in the inner cells membrane caused, for instance, by the addition of positively charged sodium ions. A pump mechanism together with the cell membrane's desire to reach balance between in- and outside constitutes the dark current flow in the resting state. Typical neurons have a resting potential of -70 mV, a typical rod resting potential is about -37 mV, and -47 mV for cones. If, the photoreceptors are excited by the absorption of photons, less glutamate is released and transmitted to bipolar cells. The photoreceptor response is, in contrast to the action potential of neural responses, a graded potential according to Lee[245].

2.11 Signal processes

2.11.1 The theory of the processes of signal generation, transmission, and coding were based on structural data of the retina, on physiological data collected from single cells, and on psychophysical data. Wyszecki and Stiles[246] described those processes as the action of absorption of photons that generates signals that were transmitted to rod synaptic bodies that connects to other nerves cells (rod-bipolar cells and horizontal cells). Rod receptors are also connected to horizontal cells, which in turn connect to other rod and cone receptors. Photons, which are absorbed in the cone receptors, produce neural signals that followed generally the

same path as described for rod signals. However, cone pedicles contain 15-30 invaginations (including synapses) from which a particular synapses transmits signals to midget bipolar cells. Another synapses transmit the signals to horizontal cells, and a third synapses is connected to flat bipolar cells.

2.11.2 There are three types of horizontal cells; 'A', 'B' and 'C'. 'A' cells receive non-opponent additive input from 'L' - and 'M'- cones, but not from 'S' - cones; 'B' cells receive also additive inputs from 'L' - and 'M' – cones, but additionally connect to a large number of 'S' - cones. The 'A' cells provide surround responses to the luminance channel in the bipolar cells, 'B' cells provide yellow surround via the cones (contact with 'L' - and 'M' - cones) to the 'S' - cone bipolar and ganglion cells, 'B' and 'C' horizontal cells may provide opponent surround for midget bipolar cells.

2.11.3 Cone bipolar cells are subdivided based on their contacts; (**1**) with cone pedicles, (**2**) extent of their dendritic field (midget and diffuse), (**3**) their response polarity ('ON' and 'OFF'), and (**4**) their synaptic contacts with amacrine and ganglion cells. 'ON' and 'OFF' bipolar cells are increasing the response resolution thus providing a larger dynamic range, 'ON' bipolar cells respond to a light spot that is induced on the centre of their receptive field with depolarisation, 'OFF' cells respond with hyperpolarisation.

2.11.4 Amacrine cells are located between bipolar and ganglion cells; the most common one linking the rod bipolar to the ganglion cells. Those amacrine cells provide rod signals with neural circuits to connect to 'ON' and 'OFF' ganglion cells. In the dark, these amacrine cells are strongly coupled so that signals from various rods are summed to increase the sensitivity to light, and decoupled in daylight conditions, as described by Lee[247].

2.11.5 There are various classes of ganglion cells in the retina, the major two groups known as parasol 'M' and midget 'P' ganglion cells (or Pα and Pβ cells) contributing over 90% of the ganglion cell population of approximately 1.25 millions per eye. Midget ganglion or 'P' - cells carry the colour opponent signals to the parvocellular layers of the 'LGN', small parasol or 'M' cells carry a lower temporal frequency broadband luminance signals to the same layer, Midget or P – ganglion cells have also 'ON' and 'OFF' centre responses[247].'ON' centre cells are excited and discharges (increased firing rate of electrical signals) when illuminated by a small spot of light in the centre of the receptive field, whereas 'OFF" centre cells stop firing when illuminated by a smalls spot of light. The firing rate stopped (inhibited) for 'ON' surround cells (increased firing rate for 'OFF' surround cells) when illuminated by a spot of light. They are called opponent cells. A fraction of all ganglion cells project to the superior collicules ('SC') in the mid brain, an older part of the brain. The cells are of minor types and their role is associated for instance with eye movement, according to Lennie[248].

2.11.6 Signals from all photoreceptors are compared and coded in opponent processes once they reach the ganglion cells. Lee[249] described the method of generating opponent signals as the increase in impulses for a small spot of light in the long wavelength range (illuminating the centre of a receptive field), and a decrease in impulses for a larger spot of light in the medium wavelength range (illumination of the surround of a receptive field). Derrington, Krauskopf, and Lennie[250] analysed chromatic properties of neurones. Chromatic opponency was said to be a distinctive feature of many ganglion cells in the retina. Those cells fall into distinct and homogeneous groups; two chromatically opponent classes in the parvocellular layers and a separate magnocellular group. A colour space was named after the authors ('DKL' colour space) that consists of one luminance axis ''L' + 'M''; (represents CIE photopic luminance[m]) and two chromatic axes either 'a constant 'S' with different 'L' and/or 'M' responses' and 'a constant 'L' - and 'M' axis but with varying 'S' responses. However, psychophysical colour appearance data did not correlate well with those that were measured from neurons.

2.12. Colour vision models

2.12.1 Hunt and Pointer[251] suggested a simple framework (*Figure 15*) for a colour vision model that explained how three connection paths between retinal and nerve fibres can be modelled. The signals are represented by the symbols 'ρ', 'γ', 'β' (associated with cones sensitivity for the long, medium, and short wavelength range) representing the strength of the signals that are generated by the absorption of photons in three cones (among other factors). Generally, colour vision models are described either by the idea of trichromacy and opponency or a combination of them. Models were developed, for instance, by Walraven and Voss[252] (known as the stage theory in 1971), Müller[253] and Judd's[254,255] zone theory, Adams model of colour vision[30], Hurvich and Jameson[256] working on Hering's opponent colour theory, or Land's retinex theory[257], amongst others.

2.12.2 *Figure 15* shows three distinctive paths; (**1**) one achromatic channel where all rods ('S' - for scotopic vision) and cones feed in the ratios of 40:20:1 for long, middle, and short wavelength sensitivity into the overall signal of brightness, (**2**) a colour opponent signal either red or green given by the subtraction of 'γ' - from 'ρ' signals (medium minus long wavelength sensitivities signals), and (**3**) opponent signals either yellow (provided by addition of 'ρ' - and 'γ' signals) or blue signals ('β' signals) given by the subtraction of 'ρ- γ'+ '2β' – signals.

---

[m] see CIE colour specification, page 83ff

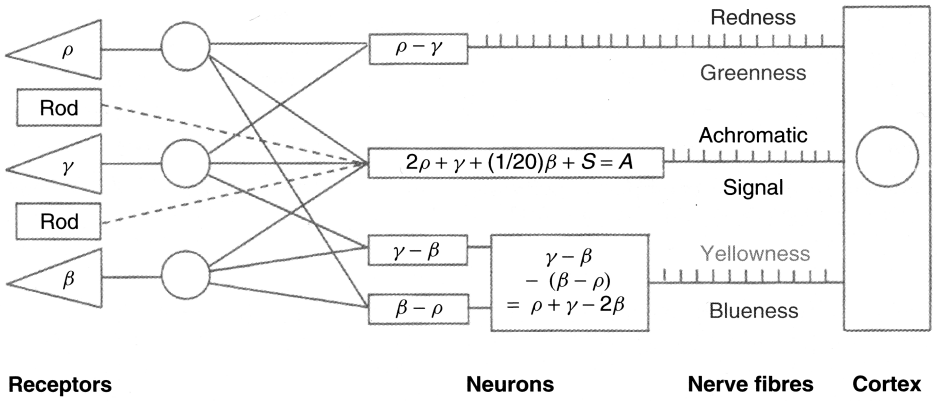

***Figure 15*: Representation of possible types of connections between some retinal receptors and some nerve fibres. Source: Hunt and Pointer (2012, p. 8)**

2.13 Photometry

2.13.1 Rods produce signals from small amounts of photon catches in scotopic viewing conditions. These catches by pigments (rhodopsin), the graded decrease of released neurotransmitter, and the reduced firing rate of nerve signals, provides monochromatic vision. Colour vision is initiated from three different photo pigments, which are sensitive to different wavelength ranges. The graded responses from rods produce shades of grey depending on the intensity and wavelength of a stimulus (brightness sensation). Hunt[257] described the attribute of brightness as a sensation according to which *'...an area appeared to exhibit more or less light'*. The photosensitive pigment rhodopsin is most sensitive (highest absorption band) in the blue/green wavelength region around 500 nm. The responses of rods to equally bright monochromatic lights over the visible wavelength range were plotted against wavelength. The result was given as a relative spectral luminous efficiency curve. This curve describes a weighted response of the human visual system to equal radiation per small bandwidth in very low viewing conditions. A similar approach was used for daylight ('photopic') viewing conditions (*Figure 16*)[n].

2.13.2 Spectral responses to radiation from the human visual system resulted in photocurrents that could be measured by direct means. However, robust instrumental techniques were not available when the CIE system was introduced in 1924 and 1931. The perception of brightness from a stimulus was than compared to a known reference stimuli by matching each other. Those brightness matching results were obtained by judging a stimuli of 2° degree angular subtense with another stimuli; by comparing similar colours (close or next to each other in regards to

[n] see page 76

their wavelengths), or using a flicker method when the frequency of repetitions for a reference stimuli matched a stimuli with the results of a (**1**) additively mixed colour stimulus (i.e. 'yellow') that was produced by a flicker frequency of 30 hertz (Hz) for the red and green stimuli, but also (**2**) provided evidence whether a match in brightness between green and red was achieved once the flicker sensation stopped (for repetition rates in the range between 30 – 50 Hz).

2.13.3 Three different cones are active in photopic viewing conditions. The task of brightness matching would, therefore, result in three types of weighting functions according to the contribution from each single type of cone. However, a single luminous efficiency function for photopic vision was regarded as most appropriate since the contributions of 'β' - cones to the overall brightness response was smallest (photon catches in the short, medium, and long wavelength were approximately in the ratio 1:20:40, respectively). Also, experimental results showed that sensitivity curves belonging to the medium and long wavelength range overlapped, significantly, as explained by Hunt and Pointer[258].

2.13.4 The normalised luminous efficiency functions 'V(λ)' and 'V'(λ)' are generally specified over the wavelength range from '360' – '830' nm (see CIE[175] for exceptions). They represent the sensitivity of a human observer to brightness sensations in either scotopic or photopic viewing conditions. These functions were obtained from many observers and therefore regarded as the sensitivities of an 'ideal average observer', respectively. Independent experimental determinations of the luminous efficiency functions for monochromatic stimuli over the visible wavelength range were determined by methods of; (**1**) minimum flicker using '125' observers[259], (**2**) step by step method using twenty-nine observers in the wavelength range from 500 – 660 nm[260] (**3**) the same method as (**2**) using fifty-two observers[37], and (**4**) by direct brightness matching using nine observers at the red end of the spectrum[261], and twenty observers matching colours at the blue end of the spectrum[262], according to Wyszecki and Stiles[263]. However, experimental results showed that weighting function 'V(λ)' needed larger values in the blue region. Judd[255] modified the 'V(λ)' function and the CIE[264] recommend in 1988 a supplement weighting function to be used, whenever appropriate (*Figure 16*). The recommended visual field for colour brightness matching is of 2° angular subtense for photopic and scotopic vision. The CIE recommends also a luminous efficiency function for a 10° field 'V_{10} (λ)'. This curve is equivalent to the CIE 1964 10° colour matching function '$\overline{y}'_{10}(\lambda)$[o]. Differences between experimental results for brightness matching were, according to Wyszecki

---

[o] see page 82

and Stiles[265], mainly caused by the magnitude in intensity of the stimuli to be matched (Purkinje shift), field size (macular pigmentation), and age (yellowing), amongst other reasons.

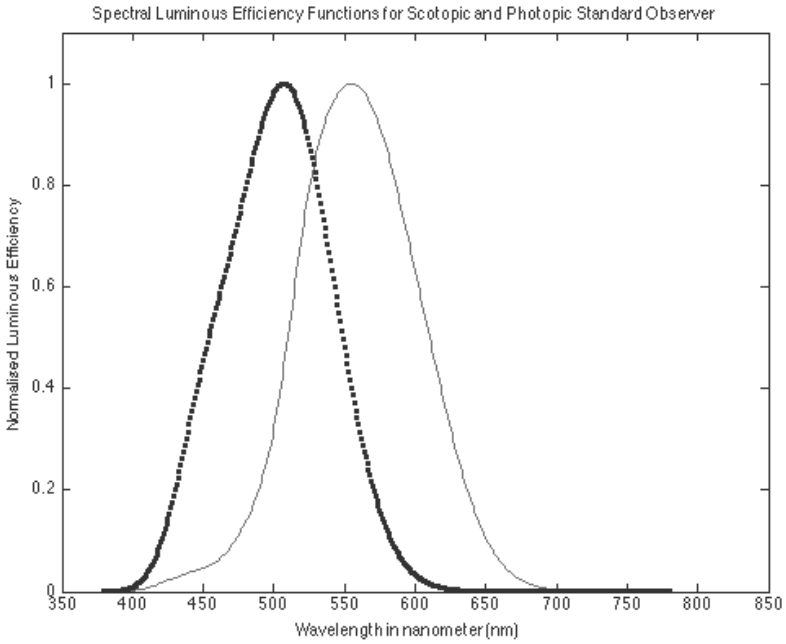

***Figure 16*: Spectral luminous efficiency functions for scotopic (…) and supplement photopic (__) standard observer normalised at peak absorption wavelengths at 507 and 555 nm.**

Generally, a mixture of radiation from different wavelengths are then weighted according to the luminous efficiency functions as a measure of brightness that is perceived by the average human observer[266]. The functions are relative functions of wavelength since they are normalised to unity at the strongest absorption peak for photopic vision at 555 nm and 507 nm for sotopic vision. The link between photopic luminous flux and radiant flux (same method for scotopic vision) is described by a factor 'K_M' (*Equation 11* and *12*).

2.13.5 The corresponding photometric measure of brightness is the 'luminous flux' in units of lumen (*Equation 13*), which is defined as '…the luminous flux (one steradian (sr) emmitted within unit solid angle by a point source having a uniform luminous intensity of one candela' (*Equation 14*). The candela ('cd') as a basic photometric unit is the '*luminance intensity*' in a given direction of a source ('luminous flux per unit solid angle'), according to Wyszecki and Stiles[267], which is emitting monochromatic radiant energy with a frequency of 540 x 10^{12} Hz (at 555 nm), and whose radiant intensity in that direction is '1/683' watt per steradian ('W·sr^{-1}').

Eq. 11: $\mathrm{K}(\lambda) = \frac{P_{\mathrm{v},\lambda}}{P_{\mathrm{e},\lambda}}$

Eq. 12: $\mathrm{K}(\lambda) = K_{\mathrm{M}}\mathrm{V}(\lambda)$

Eq. 13: $\mathrm{lm} = \mathrm{cd} \cdot sr^{-1}$, where

Eq. 14: $\Phi_{\mathrm{v}} = K_{\mathrm{m}} \int \Phi_{\mathrm{e}}\,(\lambda)\mathrm{V}(\lambda)\mathrm{d}\lambda$, where

'P_v' and 'P_e' refer to luminous and radiant flux per wavelength, 'K(λ)' equals the ratio between both at each wavelength, 'K_M' relates the luminous weighting function 'V(λ)' at a particular wavelength to radiant flux at the same wavelength and described as a factor value of '683' (2°) and '1700' lumen per watt ('lm·W^{-1}') for photopic and scotopic vision (maximum luminous efficacies), ('lm') refers to lumen, ('cd') to candela, and ('sr') to steradian. 'Φ_v' refers to the spectral concentration of luminous flux (i.e. 'lm'), 'Φ_e' represents the spectral concentration of radiant flux (i.e. watt per small constant width wavelength in '1', '5', '10' or '20' nm steps) covering a range from 360 – 830 nm, 'V' referred to the spectral value of the weighting function 'V(λ)' at the corresponding wavelength interval, and 'K_m' referred to a constant. If 'K_m' ('K'_m' for scotopic vision) was given in absolute values as '683', '683.6' or '1700' (BSI[268]) for photopic and scotopic viewing field (2° and 10°) than 'L' is given in units of candela per square meter ('cd m^{-2}') only if the units of the radiance 'P_i' were given in watts per steradian and per square metre ('W sr^{-1} m^{-2}'). Important quantities in photometric practice such as luminous flux 'P_v' in lumen ('lm'), luminous intensity or candela 'I_V', ('c' or 'lm sr^{-1}'), luminance 'L_v' ('cd m^{-1}' or 'lm sr^{-1} m^{-2}'), and illuminance 'E_v' ('lx' or 'lm m^{-2}') are related to radiometric quantities radiant flux or power 'P_e' in Watt ('W'), radiant intensity 'I_e' ('W sr^{-1}'), radiance 'L_e' ('W sr^{-1} m^{-2}'), and irradiance 'E_e' ('W m^{-2}') by substituting 'L' and 'P', accordingly.

2.13.6 The relationship between these two systems can be used to transfer energy or power in radiometry by luminous weighting functions to calculate corresponding photometric quantities[269]. The luminous weighting functions were derived from brightness matching assuming four principle laws that were based on 'Grassmann additivity laws' for colour matching[p]. However, the proportionality and additivity law are said to be invalid in brightness matching. The photometric measure of brightness does not correlate well with how bright a stimulus actually appears to a human observer since a sensation of brightness is also affected by the viewing conditions. Also, no proportional relationship between them is found. Additionally, even though colours have the same luminance they may appear brighter with increasing colourfulness of a colour ('Helmholtz-Kohlrausch effect'). *Equation 14* assumes that the contribution of light for all wavelengths are additive. Achromatic signals in photopic vision are generated by three different cones with an output that may be approximately described as a square root function, when compared to photon absorption, according to Hunt[270].

---

[p] see page 78

2.14 Colour specification system

2.14.1 A colour specification system ought to quantify colour providing unambiguous colour specification values. Colour systems can be based on colour mixing (mixed amount of coloured lights to match a test colour), or colour appearance systems (based on human perception of material standards under specific viewing conditions as described by the Munsell system). The appearance of a colour is a subjective psychological impression that includes additional sensory elements. These can be, for instance, texture or the conditions of the environment a sample is viewed in. Colour specifications that are commonly used in colour mixing systems are; lightness, chroma, and hue. Colour appearance attributes can be a series of attributes such as lightness, chroma, hue but also brightness, colourfulness, and saturation. The use of colour specifications depends also on whether a colour is seen in isolation of other colours (unrelated), or if they are seen in relation to other colours (related). The colour sensation experienced from a colour stimulus in a colour mixing system does not consider the factor of a surround.

2.14.2 Instead of measuring cone responses directly in the retina[244] with suitable instruments, a colour stimulus can be also specified indirectly by mixing three coloured lights (red, green and blue). The radiant powers of each stimulus in the mixture that matches a reference stimulus are called tristimulus values in a trichromatic system[271]. Experiments provided evidence that almost any colour is synthesized by mixing red [R], green [G], and blue [B] lights by controlling the amounts (intensities) for each stimulus. Such a colour match is described in mathematically form by a colour equation (*Equation 15*).

Eq. 15: $[F1] \equiv [F2]$, where

'F1' is the colour stimuli to be matched (≡) and 'F2' refers to the mixed light that matches 'F1'. These experimental results of colour matching were summed up in the trichromatic generalisation. Grassmann[15] summarised those experiments and provided three simple laws that can be applied using general mathematical equations. These laws were further extended thus providing a stronger interpretation[272].

1. *Symmetry Law*: If colour stimulus 'A' matches colour stimulus 'B', then colour stimulus 'B' matches also colour stimulus 'A'.
2. *Transitivity Law*: If 'A' matches 'B' and 'B' matches 'C', then 'A' matches 'C'.
3. *Proportionality Law*: If 'A' matches 'B', then 'αA' matches 'αB', where 'α' is a positive factor by which the radiant power of the colour stimulus is increased or reduced, while its relative spectral distribution is kept the same.

4. *Additivity Law*: If ‘A’, ‘B’, ‘C’, ‘D’ are any four colour stimuli, then if any two of the following three colour matches ‘A’ matches ‘B’, ‘C’ matches ‘D’, and (‘A’ + ‘C’) matches (‘B’ + ‘D’) holds good, then so does the remaining match (‘A’ + ‘D’) matches (‘B’ + ‘C’), where (‘A’ + ‘C’), (‘B’ + ‘D’), (‘A’ + ‘D’), (‘B’ + ‘C’) denote, respectively, additive mixtures of ‘A’ and ‘C’, ‘B’ and ‘D’, ‘A’ and ‘D’, and ‘B’ and ‘C’.

2.14.3 However, three important considerations were ignored in above generalisation of colour matching; (**1**) the dependency of observational conditions under which two colour stimuli are compared (only valid for the same viewing conditions), (**2**) the possible effects on a match of different previous exposures of the eyes to light (after images), and (**3**) differences in the colour matches made by different observers (observer metamerism). As an example, a vector colour matching equation describes a match once stimulus [F] is matched by the addition of the products of the suitable radiant powers (‘R’, ‘G’, and ‘B’) of stimuli [R], [G], and [B] as given in *Equation 16*.

Eq. 16: $$[\mathrm{F}] \equiv R[\mathrm{R}] + G[\mathrm{G}] + B[\mathrm{B}]$$

The radiant powers ‘R’, ‘G’, and ‘B’ are positive factors; their unit amounts are determined by an observer triggering stimuli [R], [G], and [B] until their additive mixture matches an achromatic stimulus. The scalar multipliers ‘R’, ‘G’, and ‘B’, measured in units of the primary stimuli [R], [G], [B] to match stimuli [F], can be regarded as three coefficients (also called tristimulus values of stimuli [F]) that are needed to adjust the primaries until they matches [F].

2.15 Colorimetry

2.15.1 Colorimetry is the science specifying numerically the colour of a physical defined stimulus in a way such as ‘*…the numbers comprising the specification are continuous functions of the physical parameters defining the spectral radiant power distribution of the stimuli’,* according to Wyszecki and Stiles[273]. Thus a colour stimulus can be described by its spectral radiant power distribution normally at short wavelength intervals (‘1’, ‘5’, ‘10’, ‘20’ nm) over the visible wavelength range from 360 to 830 nm. The resulting curve, values of the spectral radiant powers for each wavelength width plotted against wavelength, can be regarded as a unique fingerprint of the physical quantity of this colour stimulus. The idea in colorimetry is to provide a numerical specification for a spectral radiant power distribution from a colour stimulus that takes into account how a human observer perceives it. Different matching curves are generally obtained since three cones, varying in broad sensitivities according to the short, medium, and long wavelength range, are present in the retina.

2.15.2 Observers were asked to match colours over the visible wavelength range. The colours to be matched were of the same radiant power for each small wavelength width. All colour matching coefficients (tristimulus values), which were obtained in such a way, were plotted against their wavelength widths, respectively. These curves define the 'colour matching functions' from a human observer. The functions were derived as mathematically described in *Equation 17*.

Eq. 17: $[E_\lambda] \equiv \bar{r}(\lambda)[R] + \bar{g}(\lambda)[G] + \bar{b}(\lambda)[B]$, where

'E_λ' refers to the equal energy stimulus at a particular wavelength, [R], [G], [B] refer to red, green and blue real primary stimulus, and $\bar{r}(\lambda), \bar{g}(\lambda), \bar{b}(\lambda)$ refer to the colour matching functions for the chosen primaries at a particular wavelength (λ). RGB tristimulus values for a colour stimulus is then calculated by using *Equation 18 – 20*.

Eq. 18: $R = \int_a^b P_\lambda \bar{r}(\lambda) d\lambda$

Eq. 19: $G = \int_a^b P_\lambda \bar{g}(\lambda) d\lambda$

Eq. 20: $B = \int_a^b P_\lambda \bar{b}(\lambda) d\lambda$, where

'RGB' refer to the tristimulus values for a given colour stimuli, 'P_λ' describes the spectral radiant power at a particular wavelength for this stimuli, $\bar{r}(\lambda)$, $\bar{g}(\lambda)$, $\bar{b}(\lambda)$ are the colour matching functions at a particular wavelength for this stimuli, '$d\lambda$' described the wavelength integrals that are summed over the visible wavelength range. Generally, the colour matching functions differ once the primaries are changed for each observer and method that is used for deriving them. The CIE recommended therefore colour-matching functions from a group of normal colour vision observers. They can be regarded as the ideal 'average' human observer from a larger population of observers. This ideal observer makes matches in accordance to the 'stronger form of trichromatic generalisation'[q].

2.15.3 The CIE introduced two standard colorimetric observers in 1931 and 1964 (CIE[175,274]). The recommendation for two theoretical observers applied to matching tasks for differences in visual field sizes for observers with normal colour vision. Whether to use the 1931 standard colorimetric observer or the 1964 supplement standard colorimetric observer, depends only on the size of the stimuli that are to be matched. The colour matching functions for the 1931

---

[q] see page 79

standard colorimetric observer is recommended when a stimulus falls within a visual field size of angular subtense from about 1° to 4° in photopic viewing conditions. The 10° observer is recommended for judging samples occupying visual field sizes larger than 4° (up to 10°) angular subtenses. The important features of these theoretical observers are the use of colour matching functions but also to use the luminous efficiency functions obtained from brightness matching. The decision, to distinguish between field sizes, was mainly based and related to the topography of the retina and the distribution of photoreceptors. Rods are not present within the fovea (approximately 1.5° subtense), but increases in numbers as the field size increases so that rod intrusion to vision may occur at larger field sizes when the level of illumination is low. Also, when large field sizes are occupied by a large uniform stimulus then they appear non-uniform. This is caused by the so-called 'Maxwell spot[275]', which differs in colour when compared with the rest of the viewing field. This yellow macular pigment, which occupies the area of the fovea in the retina, causes this non-uniformity for viewing fields that are larger than 4° angular subtenses. The 1964 CIE supplement standard colorimetric observer colour-matching functions were derived in such a way to avoid the central circle of the viewing field by omitting it during visual experiments. It was possible to select a set of colour matching functions, which would coincident with the luminous efficiency function for brightness matching. The CIE 1931 standard observer includes both; (**1**) the brightness matching function for visual fields of 2° angular subtense, and (**2**) the colour matching functions for visual fields of 2° angular subtense. It is assumed that brightness matching by the flicker method is an additive process, and that the luminous efficiency functions 'V(λ)' is a linear combination of these colour matching functions. The luminous V(λ) function describes exactly the '$\bar{y}$' – colour matching function, as such combining both '*…colour-matching and heterochromatic brightness matching properties in a single quantitative scheme*[276]*'*.

2.15.4 The initial advantage of incorporating the brightness matching functions 'V(λ)' into the colour matching functions for the 1931 2° Standard Observer, is to provide a colour specification value ('Y' - tristimulus value) that corresponds to an absolute photometric quantity (sensation of brightness for instance given in cd m^{-2})[r]. The luminous efficiency functions and colour matching functions for the; (**1**) 1931 CIE 2° Standard Colorimetric Observer '$\bar{x}(\lambda)$, $\bar{y}(\lambda)$, $\bar{z}(\lambda)$' and the (**2**) 1964 CIE 10° Supplementary Standard Colorimetric Observer '$\bar{x}_{10}(\lambda)$, $\bar{y}_{10}(\lambda)$, $\bar{z}_{10}(\lambda)$' are given as in *Figure 18*[s]. The initial experimental work that led to those functions was mainly contributed by Guild[38] in 1931 and Wright[39] in 1928 using seven and ten observers,

---

[r] see page 76

[s] see page 83

respectively. They used broadband primary stimuli in a trichromatic colorimeter at peak wavelengths (λ) 659, 530, and 460 nm while producing monochromatic stimuli to be matched between a wavelength range from 400 – 700 nm. The results were then converted into those that would have been obtained if matching were carried out at peak wavelengths at 700, 546.1, and 435.8 nm measured in such a way that equal quantities of [R], [G], [B] matched the equal energy white (ratio in relative luminances of 1:4.5907:0.0601), respectively. These transformations ensured; (**1**) the equality of 'V(λ)' with '$\bar{y}(\lambda)$', (**2**) that values of '$\bar{x}(\lambda)$', '$\bar{y}(\lambda)$', '$\bar{z}(\lambda)$' are all positive, (**3**) that values of '$\bar{z}(\lambda)$' are zero for wavelengths longer than 650 nm, (**4**) that values of '$\bar{x}(\lambda)$' are almost zero at wavelengths around 505 nm, (**5**) that values at short wavelength range for '$\bar{x}(\lambda)$', '$\bar{y}(\lambda)$' are small, and (**6**) that the energy spectrum is specified by equal amounts of 'XYZ' – tristimulus values (CIE[277]).

2.15.5 The work, which contributed to the development of the colour matching functions for the CIE 1964 supplementary standard colorimetric observer, was based on experiments conducted by Stiles and Burch[278] and Speranskaya[279] as seen in *Figure 17*. Larger field of views are prone to rod intrusion requiring experimental setups to operate at sufficient photopic levels. A total of 67 observers matched monochromatic stimuli in the range form 390 – 830 nm by mixing primaries at peak wavelengths 444.4, 526.3, and 645.2 nm, respectively. The units for all quantities of [R_{10}], [G_{10}], [B_{10}] were chosen appropriately until they matched the equal energy spectrum. The transformation was similar to the one that was used for deriving the 1931 CIE Standard Observer; however, the data were not fitted to the 'V(λ)' luminous efficiency function with the result that 'Y_{10}' - tristimulus values were not proportional to a absolute luminance quantity.

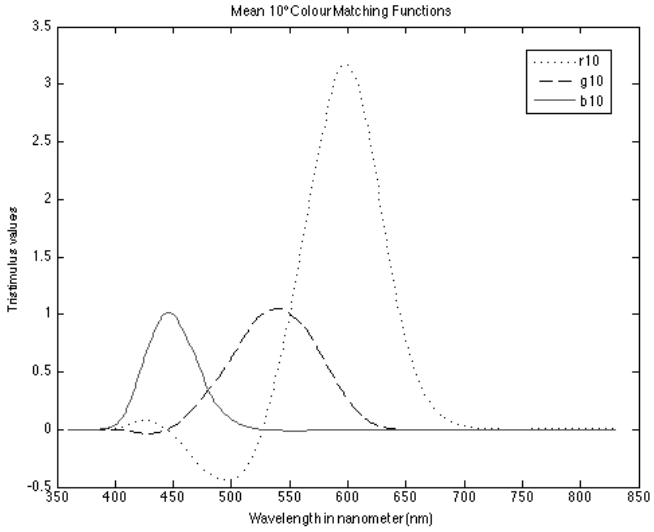

***Figure 17*: Stiles and Burch (1959); Mean 10° Colour Matching Functions, Source: Wyszecki and Stiles (2000), p.815**

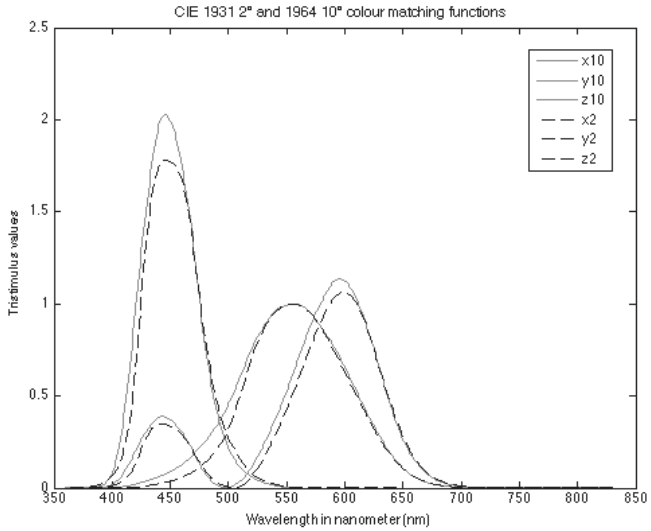

***Figure 18*: The colour matching functions for the CIE 1931 2° Standard Colorimetric Observer and 1964 10° Supplementary Standard Colorimetric Observer.**

The constant 'K_M' according to *Equation 14*[t] can be set to a factor of 683.6 so that 'Y_{10}' - tristimulus values equal absolute values of a photometric quantities, according to 'ISO 23539:2005(E)/CIE S 010/E:2004[280]', 'BS EN ISO 11664-1:2011[281]', or 'CIE S 014-1/E:2006[207]'. The values of the CIE 1964 colour matching functions '$\bar{x}_{10}(\lambda)$', '$\bar{y}_{10}(\lambda)$', and '$\bar{z}_{10}(\lambda)$' are provided on a wavelength basis in the range from 360 – 830 nm.

2.15.6 So far, it is possible to provide a colour specification for a colour stimulus in the form of 'RGB' tristimulus values derived from an 'ideal average observer' using *Equation 18*, *19*, and *20*[u]. It was evident in *Figure 17* that some values of the spectral colour matching functions $\bar{r}(\lambda)$, $\bar{g}(\lambda)$, and $\bar{b}(\lambda)$ for both visual fields, which were used to match the equal energy white on a wavelength basis, were of negative form. This appeared to be inappropriate, and for mathematical reasons, the CIE transformed real 'RGB' tristimulus to imaginary 'unreal 'XYZ' – tristimulus values. They are lying outside the spectrum locus and purple boundary. However, this transformation results in a triangle, formed by the chromaticity points of the primary stimuli 'XYZ', in which all 'xyz' – chromaticity coordinates and the corresponding 'XYZ' – tristimulus values are not negative[282].

2.15.7 The CIE[277] suggests methods to calculate 'XYZ' – tristimulus values for colour stimuli in conjunction with the CIE 1931 (1° and 4° visual field) or 1964 (larger than 4° visual field) standard observer once the spectral distribution for a stimulus is known. Two methods are suggested either; (**1**) for reflectance and transmitting objects, or (**2**) self-luminous light sources.

---

[t] see page 76

[u] see page 80

Generally, the standard method is defined as a summation at 1 nm intervals over a wavelength range from 360 – 830 nm. The calculation of 'XYZ' - tristimulus values for self-luminous sources are given as in *Equation 21*, *22*, and *23*.

Eq. 21: $X = k\sum_{830}^{360} \varphi_\lambda\,(\lambda)\bar{x}(\lambda)\Delta\lambda$

Eq. 22: $Y = k\sum_{830}^{360} \varphi_\lambda\,(\lambda)\bar{y}(\lambda)\Delta\lambda$

Eq. 23: $Z = k\sum_{830}^{360} \varphi_\lambda\,(\lambda)\bar{z}(\lambda)\Delta\lambda$, where

'k' describes a normalising constant (see *Equation 24*), 'φ_λ' refers to the spectral colour stimulus function (per wavelength interval), '$\bar{x}(\lambda)$', '$\bar{y}(\lambda)$', '$\bar{z}(\lambda)$' are the spectral colour matching functions (per wavelength interval), and '$\Delta\lambda$' defines the interval in nm. The constant 'k' are set to a factor of '683' or '683.6' '$(\mathrm{lm}\cdot\mathrm{W}^{-1})$' for the 1931 or 1964 Standard colorimetric observer, if the 'Y_L' – tristimulus value is evaluated in terms of a photopic photometric quantity. The spectral concentration of a radiometric quantity for the stimuli '$\varphi_\lambda(\lambda)$' corresponds to the photometric quantity that is required. For cases of reflecting or transmitting object colours, a colour stimulus function is replaced by the relative colour stimulus function '$\varphi(\lambda)$', which is defined as the product of the relative spectral distribution of the illuminant 'S(λ)' for each wavelength interval with either a spectral reflectance factor 'R(λ)', spectral radiance factor 'β(λ)', spectral reflectance 'ρ(λ)', or spectral transmittance 'τ(λ)'. The constant 'k' is chosen so that the 'Y' tristimulus value becomes a value of '100' for objects for which 'R(λ)', 'β(λ)', 'ρ(λ)', 'τ(λ)' equals '1' for each short wavelength interval as given in *Equation 24*.

Eq. 24: $k = 100/\sum_{830}^{360} S(\lambda)\bar{y}(\lambda)\Delta\lambda$

Equation 21 - 24 are also applied for the CIE 1964 Standard colorimetric system substituting colour matching functions '$\bar{x}(\lambda)$', '$\bar{y}(\lambda)$', '$\bar{z}(\lambda)$' with '$\bar{x}_{10}(\lambda)$', '$\bar{y}_{10}(\lambda)$', '$\bar{z}_{10}(\lambda)$', and substituting 'X', 'Y', 'Z' - tristimulus values and constant 'k' for 'X_{10}', 'Y_{10}', 'Z_{10}' and 'k_{10}' thus obtaining relative or normalised 'XYZ_{10}' - tristimulus values ('Y_{10}' describing a percentage value from 1 - 100 for the perfect diffuser), or 'X_L', 'Y_L', 'Z_L' for absolute tristimulus values by changing constant 'k' from 683 to a value of 683.6.

2.15.8 Abridged methods were introduced for '5', '10', or '20' nm wavelength intervals by using weightings that can improve the precision of calculations for 'XYZ' and 'XYZ_{10}'-tristimulus values according to ASTM[201]; Li, Luo, and Rigg[283]; and the CIE[175]. Also, it is possible to simplify those calculations by reducing the integration wavelength range as long as results are similar to those that were obtained for a recommended wavelength range (360 – 830 nm). However, caution needs to be taken whenever the spectral radiance distribution of

illuminants is expected to be of narrow band and spiky in form. 'XYZ' – tristimulus values provide a colour specification for a sample but cannot describe how a colour appears to a human observer.

A 'Y' - tristimulus value can be regarded as a percentage reflectance or transmitting factor, but also regarded as a percentage luminance factor as such correlating with the perceptual attribute of lightness[284]. Tristimulus 'X' and 'Z' values do not correlate with any perceptual attributes as it the case for lightness and the associated 'Y' tristimulus value. However, colour attributes can be derived from relative magnitudes of 'XYZ' - tristimulus values as given in *Equation 25 – 27*.

Eq. 25: $x = X/(X + Y + Z)$

Eq. 26: $y = Y/(X + Y + Z)$

Eq. 27: $z = Z/(X + Y + Z)$

The 'x' and 'y' chromaticity coordinates can be used to construct a two-dimensional chromaticity diagram. This diagram can provide approximately correlates of perceptual attributes for hue and saturation known as complementary wavelength 'λ_c' and excitation purity 'ρ_e'. Also, it provides a colour difference measure (difference in chromaticity), described by the distances between two samples in the 'xy' - diagram. However, distances between colour difference samples for the same perceptual difference varied significantly within the diagram.

2.15.9 A new CIE 1976 uniform chromaticity scale diagram ('UCS') was introduced, in which a perceptual similar colour difference distance, was reduced to a ratio of 4:1 compared to 20:1 in the case of the 'xy' – chromaticity diagram. The new $u'v'$ - chromaticity coordinates are a projective transformation of 'xy' – chromaticity coordinates, so that straight lines remain also straight in the new diagram. Coordinates can be calculated using *Equation 28* and *29*.

Eq. 28: $u' = \frac{4x}{-2x+12y+3} = \frac{4X}{X+15Y+3Z}$

Eq. 29: $v' = \frac{9y}{-2x+12y+3} = \frac{9Y}{X+15Y+3Z}$

2.15.10 Two new measures based on the 'CIE 1976 UCS' - diagram were provided to correlate more uniformly with the attributes of 'hue' and 'saturation'. They are referred to CIE's 1976 $u'v'$– hue angle ('h_{uv}') and '$u'v'$' - saturation ('s_{uv}'). They can be determined using *Equation 30* and *31*.

Eq. 30: $h_{uv} = \arctan\left[(v' - v'_n)/(u' - u'_n)\right]$

Eq. 31: $s_{uv} = 13[(u' - u'_n)^2 + (v' - v'_n)^2]^{1/2}$, where

'u'_n', 'v'_n' refer to the values of 'u', v'' for a reference white. These values are calculated using *Equation 25 - 27* but substituting denominator 'X', 'Y', 'Z' with 'X_n', 'Y_n', 'Z_n'; and denominator 'x', 'y', 'z' with 'x_n', 'y_n' , 'z_n' in accordance to *Equation 28* and *29*. 'X_n', 'Y_n', 'Z_n' - tristimulus values referred to a calculated white object stimulus (normally provided in terms of a spectral radiant power distribution as given by one of the recommended CIE daylight stimuli D50, D55, D65, D75, C, or illuminant A - CIE[285]).

2.15.11 In 1976 the 'CIE' recommended a non-linear function to provide a measure for lightness in terms of the ratio of the 'Y' - tristimulus value of a colour to that of a reference white 'Y_n' as given in *Equation 32* and *33*.

Eq. 32: $L^* = 116f\left(\frac{Y}{Y_n}\right) - 16, \text{for} \frac{Y}{Y_n} > 0.008856$

Eq. 33: $L^* = 903.3\left(\frac{Y}{Y_n}\right) + 0.1379, \text{ for} \frac{Y}{Y_n} \leq 0.008856$

A colour stimulus can then be described using three perceptual attributes; lightness ('L^*'), hue angle ('h_{uv}'), and chroma ('C_{uv}'). Hunt[286] defines perceptual attributes into five categories such as; (**1**) lightness, which *'...is the brightness of an area judged relative to the brightness of a similarly illuminated area that appears to be white or highly transmitting – whereby brightness is the attribute of a visual sensation according to which an area appears to exhibit more or less light.';* (**2**) hue, which *'...is the attribute of a visual sensation according to which an area appears to be similar to one, or two proportions of two, of the perceived colours red, yellow, green and blue.',* (**3**) chroma, which *'...is the colourfulness of an area judged in proportion to the brightness of a similarly illuminated area that appears to be white or highly transmitting.'*, (**4**) saturation, which *'...is the colourfulness of an area judged in proportion to its brightness.'*, (**5**) colourfulness, which *'...is the attribute of a visual sensation according to which an area appears to exhibit more or less of its hue.'*

2.15.12 An approximately uniform colour space is produced by plotting rectangular coordinates from the quantities 'L^*', 'u^*' and 'v^*'. The CIE introduced in 1976 the 'CIE' 1976 '$L^*u^*v^*$' ('CIELUV') and the 1976 '$L^*a^*b^*$' ('CIELAB') colour space as a three-dimensional approximately uniform colour space (CIE[287,288]). The CIELUV colour space was used in the lighting and television industry, in which additive mixtures of light stimuli are the main methods to produce coloured lights. The associated parameters can be calculated as described in *Equation 32*, *33*, *34*, and *35*.

Eq. 34: $u^* = 13L^*(u' - u'_{\mathrm{n}})$

Eq. 35: $v^* = 13L^*(\mathrm{v}' - \mathrm{v}'_{\mathrm{n}})$, where

'Y_{n}' describes the 'Y' tristimulus value of a reference light, '$u'_{\mathrm{n}}v'_{\mathrm{n}}$' refers to the chromaticity coordinates of a reference white, and 'L^*' refers to a perceptual attribute of lightness. The CIE 1976 ($L^*u^*v^*$) – space replaced MacAdams and Wyszecki's initial yet adopted CIE 1960 ($U^*V^*W^*$) uniform colour space. CIELAB parameters are expressed in three-dimensional orthogonal coordinates as given in *Equation 32* or *33*, *36*, and *37*.

Eq. 36: $a^* = 500\left[\mathrm{f}\left(\frac{\mathrm{X}}{X_{\mathrm{n}}}\right) - \mathrm{f}\left(\frac{\mathrm{Y}}{Y^{\mathrm{n}}}\right)\right]$

Eq. 37: $b^* = 200[\mathrm{f}\left(\frac{\mathrm{Y}}{Y_{\mathrm{n}}}\right) - \mathrm{f}\left(\frac{\mathrm{Z}}{Z_{\mathrm{n}}}\right)]$, where and if

any ratio of the terms 'f(X/X_{n})' 'f(Y/Y_{n})', and 'f(Z/Z_{n})' is equal to or larger than 0.008856, it is replaced with the terms '$(\mathrm{X}/X_{\mathrm{n}})^{1/3}$', '$(\mathrm{Y}/Y_{\mathrm{n}})^{1/3}$', or '$(\mathrm{Z}/Z_{\mathrm{n}})^{1/3}$'. If, the ratios are equal to or smaller than 0.008856, the term 'f(X/X_{n})' is replaced with the term '7.787*(X/X_{n}) + 16/116'. This is also valid for (Y/Y_{n}) and (Z/Z_{n}). 'X_{n}', 'Y_{n}', and 'Z_{n}' refer to the values of the chosen reference white. The reference white can vary depending on the intended use. Either, being a theoretical perfect diffuser or, in the case of a reflection print or displayed image, it may be associated with a white area in the image itself. The CIE 1976 '$L^*a^*b^*$' chroma ('C^*_{ab}') and hue-angle ('h_{ab}' - in radians) are calculated as described in *Equation 38 – 39*. CIE 1976 'u' and 'v' – chromaticity coordinates, hue angle ('h_{uv}'), and chroma ('C^*_{uv}') are of similar form but replacing the 'a^*' and 'b^*' terms in *Equation 40* and *41* with 'u^*' and 'v^*', as explained by Hunt and Pointer[289].

Eq. 38: $C^*_{\mathrm{ab}} = (a^{*2} + b^{*2})^{\frac{1}{2}}$

Eq. 39: $h_{\mathrm{ab}} = \arctan\left(\frac{b^*}{a^*}\right)$

The limitation in both colour spaces are described by Lee[290] as the missing of two important attributes; (**1**) spatial-temporal variations of the colour stimuli, and (**2**) the interplay between the object properties and the 'interpreted' colour. As such, the systems are only valid for limited viewing conditions. Other colour spaces that are based or related to object colours are known as Munsell, OSA-UCS, *CIECAM*$_{02}$, *DIN*$_{99}$, amongst other colour spaces[291]. These perceptual uniform colour spaces can also be used to derive colour difference formulae.

2.16 Colour difference formulae - Maths

2.16.1 The Adams - Nickerson 'LAB' colour difference formula - ANLAB

The Adams-Nickerson uniform colour space was developed with the objective to derive a distance measure in a colour space that is proportional to a perceived colour difference[74]. The Adam-Nickerson colour difference formula is mathematically described in *Equation 40*.

Eq. 40: $\Delta E_{\mathrm{AN}} = \{[0.23\Delta V_{\mathrm{y}}]^2 + [\Delta(V_{\mathrm{x}} - V_{\mathrm{y}})]^2 + [0.4\Delta(V_{\mathrm{y}} - V_{\mathrm{z}})]^2\}^{1/2}$, where

'ΔE_{AN}' refers to an overall difference sensation in colour, 'ΔV_{y}' describes the difference in lightness, '$\Delta(V_{\mathrm{x}} - V_{\mathrm{y}})$' describes the difference between two samples in respect to the yellow/blue axis, and '$\Delta(V_{\mathrm{y}} - V_{\mathrm{z}})$' describes the difference between two samples in the red/green axis. A constant ('40', '42', '43.909', '50') was often applied to the results that were obtained from *Equation 40* so to provide more meaningful units. Nickerson suggested that one unit in the red/green was equal to '8.75' chroma steps and two chroma steps equalled one value ('V_{Y}') step, so to derive a scaling factor of '0.23'. The coordinates of the Adam-Nickerson 'UCS' are given in *Equation 41 – 43*, and an alternative representation of *Equation 40* and corresponding colour difference formula ('ANLAB42') is described in *Equation 44*.

Eq: 41: $L_{42} = 42 \cdot 0.23V_{\mathrm{y}}$

Eq. 42: $A_{42} = 42(V_{\mathrm{x}} - V_{\mathrm{y}})$

Eq. 43: $B_{42} = 42 \cdot 0.4(V_{\mathrm{y}} - V_{\mathrm{z}})$

Eq. 44: $\Delta E_{\mathrm{AN42}} = \{(\Delta L_{42})^2 + (\Delta A_{42})^2 + (\Delta B_{42})^2\}^{1/2}$

The terms 'V_{y}', 'V_{x}', 'V_{z}' in *Equation 40* are related to CIE 'XYZ' - tristimulus values as given in *Equation 45*, where 'Y' is replaced with '1.0197*X' or '0.8458*Z', and 'V_{y}' with 'V_{x}' or 'V_{z}' on the right hand side, according to Ohta and Robertson[292]. The expression on the left hand side is altered so to refer to the standard illuminant 'C' reflected from a perfect diffuser.

Eq. 45:

$\mathrm{Y} = 1.2219V_{\mathrm{y}} - 0.23111V_{\mathrm{y}}^2 + 0.23951V_{\mathrm{y}}^3 - 0.021009V_{\mathrm{y}}^4 + 0.0008404V_{y}^5$

2.16.2 A modified Adams – Nickerson 'LAB' colour difference formula - ANLAB

ANLAB40 was adopted by the Society of Dyers and Colourists for uses in the textile industry and became also British standard in the plastic industry, according to McDonald[114]. McLaren[106,128] was using multiple regression analysis and techniques so to improve the correlation between formula and visual results.

McDonald investigated the ANLAB formula with a scale factor of '50' using bright, dull, and grey colour thread winding card colour difference sample pairs. Those sample pairs were then compared with four samples of a matching grey scale (5cm x 5cm soft cotton thread cards dyed with varies concentrations of *Sirius Supra Grey GG*). The objectives were to determine whether a mathematical equation could describe a relationship between equal numerical results and the variation in visual results obtained from different areas in the ANLAB50 colour space. A minimum of five cards was selected for each of the sixteen colour and eleven grey centres. The lightness values were chosen in the range between 'L' equal to '56' and '80'. Linear regression analysis were carried out on the initial grading of the observer results so to find a relationship between 'ΔE_{AN50}' and the following variables for the individual 'Grades' of matches; 'r' (saturation), *'l'* (lightness), 'Θ' (hue angle), 'r^{2}' (saturation^2), and 'Θ^{2}' (hue-angle^2). The regression analysis was conducted by means of fitting an equation to the scatter plots of derived data. Visual colour difference results were contrasted against numerical results and, in addition, also contrasted against saturation level for each individual 'Grade'. The variation amongst results for each grading and saturation level was reduced to a minimum once calculated 'ΔE_{AN50}' colour difference values were transformed with an optimised saturation equation (*Equation 48*). The results showed that the most significant relationship was indeed between 'ΔE_{AN50}' and 'r' (saturation) values as described in *Equation 46, 47, and 48*:

Eq. 46: $$r = 1/2[(a_1^2 + b_1^2)^{1/2} + (a_2^2 + b_2^2)^{1/2}$$

Eq. 47: $$\Delta E_{AN50} = mr + \Delta E_a$$

Eq: 48: $$\Delta E_a = \Delta E_{AN50}/(1 + 0.022r)$$, where

'r' refers to a saturation measure in ANLAB's colour space, 'm' describes the regression coefficient for 'r', 'ΔE_a' refers to a saturation modified colour difference prediction, and 'ΔE_{AN50}' refers to a colour difference value according to ANLAB50's colour coordinates. The correlation coefficient 'r' (-0.68) for 'ΔE_a' colour difference values compared with visual results was significantly improved when compared with other colour difference formulae at that time.

2.16.3 The Commission Internationale de L'Éclairage 1976 $L^*a^*b^*$ and $L^*u^*v^*$ colour difference formulae – CIELAB and CIELUV

Experiments provided evidence that the CIE 'XYZ' - tristimulus colour space was not perceptual uniform. For instance, a distance measure for the same perceptual colour difference is represented five times larger in the green area of the 'xy' – chromaticity diagram when compared with the blue area. Also, colour matching results in the form of ellipses from MacAdam[54,88] shows large variations in size and orientation. Several types of transformations with the intent to map those ellipses into circles of the same radii were made, according to Lee[293].

After several proposals and revisions, the CIE finally suggested the use of two new formulae in 1976 (CIE[287,288]). The 1976 CIE '$L^*A^*B^*$' ('CIELAB') formula is based on ANLAB yet using a simplified square root function (rather than a fifth order polynomial function) for mapping 'XYZ' - tristimulus values to a 'quasi' perceptual uniform Munsell lightness scale. The 1976 CIE '$L^*U^*V^*$' ('CIELUV') formula is based on projective transformation from 'XYZ' - tristimulus values. The lightness function ('L^*')[v] can be calculated for both formulae as given in *Equation 32* and *33*. The calculations of colour coordinates for the CIELAB and CIELUV colour space are described mathematically in *Equation 34, 35, 36* and *37*[w]. The CIELAB and CIELUV colour differences 'ΔE^*_{ab}' and 'ΔE^*_{uv}' between two colour stimuli are calculated as simple Euclidean distances between two points in both spaces as given in *Equations 49 – 52*.

Eq. 49: $$\Delta E^*_{ab} = [(\Delta L^*)^2 + (\Delta a^*)^2 + (\Delta b^*)^2]^{1/2}$$

Eq. 50: $$\Delta E^*_{ab} = [(\Delta L^*)^2 + (\Delta C^*_{ab})^2 + (\Delta H^*_{ab})^2]^{1/2}, \text{ where}$$

Eq. 51: $$\Delta E^*_{uv} = [(\Delta L^*)^2 + (\Delta u^*)^2 + (\Delta v^*)^2]^{1/2}$$

Eq. 52: $$\Delta E^*_{uv} = [(\Delta L^*)^2 + (\Delta C^*_{uv})^2 + (\Delta H^*_{uv})^2]^{1/2}$$

'ΔH^*_{ab}' is calculated as described in *Equation 53*, chroma 'ΔC^*_{ab}' is described in *Equation 38*[x], and hue angle 'h_{ab}' is defined in *Equation 39*. The same equations are used for CIELUV, respectively.

Eq. 53: $$\Delta H^*_{ab} = 2(C^*_{ab,1} \cdot C^*_{ab,2})^{\frac{1}{2}} \sin\left(\frac{\Delta h_{ab}}{2}\right), \text{ where}$$

---

[v] see page 86

[w] see page 87

[x] see page 87

The subscripts '$_0$' and '$_1$' refer to a reference and batch sample[y] for calculating colour differences in the direction of one of the colour scales, for instance 'ΔL^{*}'. It is generally required to subtract the scale value for a reference or standard sample from a batch sample. Alternative methods for deriving 'ΔH^{*}_{ab}' and 'ΔH^{*}_{uv}' were reported by Sêve[294,295], and Stokes and Brill[296]. If, the angular subtense of a sample exceeded 4°, a subscript '$_{10}$' was added to all symbols and equations for the 'CIELAB' and 'CIELUV' formulae, respectively. The 'CIELAB' and 'CIELUV' colour difference formulae did not accurately quantify small to medium size colour differences.

2.16.4 The J. P. Coates 1979 colour difference formula – *JPC*$_{79}$

The disadvantage of using 'CIELAB' and 'ANLAB' colour difference formulae for pass/fail matching, as reported by McDonald[129,130], was caused by the non-uniformity of both colour spaces since individual tolerance values for each colour centre were required. Only, a few experimental colour difference datasets were available at that time for predicting the reliability of any new designed formula. Available sets were, for instance, those of; Davidson and Friede[92] (wool textile samples); Jaeckel[297] (854 textile samples); Morley, Munn and Billmeyer[298] (using painted samples), and Kühni[299,300] (polyester/cotton fabric and '180' textile samples). However, as reported by McLaren[112] and McDonald[129], those data sets were not satisfactory for the use in the textile industry. Reasons for their opinion were associated with the inconsistency of datasets in terms of using observers that were not experienced in industrial colour matching assignments; many colour differences were much larger than normally experienced in a dye house production cycle; perceptibility and acceptability controversy, weighting placed on hue were larger than obtained from other industrial data; many datasets were obtained form measurements that were made on colorimeter and, therefore, regarded as not precise enough for the development of a colour difference formula, and/or only thirteen colour centres with a limited number of colours were considered. These unsatisfactory circumstances let McDonald produce a comprehensive set of visual matching samples (spun polyester sewing thread winding cards) containing colour difference magnitudes that were normally encountered in J.P. Coats Ltd dye house routine work. The average colour difference occurring in standard formula dye lots for visual pass/fail colour matching and instrumental correction was reported as 1.9 'ΔE_a' (ANLAB50) units. All samples were produced as to form two concentric shells around each colour centre with a predicted colour difference value of '1' 'ΔE_a' and '2' 'ΔE_a' units (*Equation 48*)[z]. Fifty-five colour centres

---

[y] subscripts will be consistently applied for any other formula in this thesis

[z] see page 89

at four lightness levels ('L' equalled a value of '42' and '91') were produced in a way that they differed either only in lightness, chroma, or hue. Measurements were obtained from a spectrophotometer in 'D65/10°' mode with diffuse illumination at zero degree viewing conditions ('d/0') with specular components included ('SPIN'). Visual assessments (90°/45° illumination/viewing angle) were made using a colour-matching booth (black background, artificial fluorescent daylight according to BS EN 950-1:1967[216], two 5ft 80 watts tubes, illumination level of 130 lm/ft^2). Observers were asked whether those produced colour differences between each standard and batch samples were acceptable (or not) when compared with an anchor grey pair that gave a measured colour difference of '1.9' 'ΔE_{a}' units at lightness value 'L' equal to fifty. The results were used to fit tolerance ellipsoids around each colour centre in ANLAB50's colour space. Also, the orientations of ellipsoids, in terms of their semi-axes 'Lt', 'Ct', and 'Ht', were constraint to the directions of psychophysical important colour difference attributes (lightness, metric chroma, and hue). The objective was to fit ellipsoids to obtained pass/fail data such as acceptable matches stayed inside- and not-accepted matches outside the boundaries of a tolerance ellipsoid. Generally, a colour difference from a tolerance ellipsoid was calculated mathematically as given in *Equation 54*.

Eq. 54: $\Delta Et_{\mathrm{AN}} = [(\Delta L_{\mathrm{AN}}/\mathrm{Lt})^2 + (\Delta C_{\mathrm{AN}}/\mathrm{Ct})^2 + (\Delta H_{\mathrm{AN}}/(\mathrm{Ht})^2\ )]^{1/2}$, where

'ΔL_{AN}', 'ΔC_{AN}', 'ΔH_{AN}' refer to the lightness, metric chroma, and hue differences in ANLAB's colour space, and 'Lt', 'Ct', and 'Ht' refer to visual tolerance limits in the form of ellipsoid's semi axis in those directions, respectively. Several methods were introduced as how to fit tolerance ellipsoids to the data mainly by optimising them until they provided better correlation with visual results. Optimising criteria varied in such ways as; (**1**) to maximise the correlation coefficient from linear regression between acceptable and 'ΔEt' – values (prone to erroneous results once data where close to near zero values of 'ΔEt'), (**2**) using the standard deviations of colour matching from all observers and transform all associated 'ΔEt' to '% Acceptability' values of the normal ogive; optimising then those generated '%A' values with obtained '%A' data until the sum of squares were minimised between '50% Acceptability' - values and 'ΔEt' ellipsoid formula values (some trials were necessary prior starting the computations yet to find a suitable standard deviation value for the observers), and (**3**) to maximise correlation coefficients between 'ΔEt' – values and visual acceptability decisions expressed as standard normal deviates from visual matching tolerances using linear regression methods while omitting acceptability data less than ten- and higher than ninety percent values (acceptability decision distributions follow generally an ogive curve).

The results suggested that ellipsoid sizes in the direction of chroma, hue, and lightness increases with increasing metric chroma and lightness level of the standards for all three optimisation techniques. Those results obtained from McDonald also suggested that acceptability ellipsoids differed in hue dimension with the variations in hue angle of the standards. More data were obtained from McDonald[131] and analysed, accordingly. Plots of visual colour difference values for 'ΔL_{AN}' and 'ΔC_{AN}' against lightness and chroma values for a variety of standards were reported as of curve-linear form. Constants for either chroma or lightness tolerance limits for each equation were determined by iteration methods and are described in *Equation 55* and *56*.

Eq. 55: $\mathrm{Lt} = 0.149 \cdot L_{0,\mathrm{AN50}}/(1 + 0.0155 \cdot L_{0,\mathrm{AN50}})$,

Eq. 56: $\mathrm{Ct} = 0.105 \cdot C_{0,\mathrm{AN50}}/(1 + 0.115 \cdot C_{0,\mathrm{AN50}}) + 1.2$, where

'$L_{0,\mathrm{AN50}}$' and '$C_{0,\mathrm{AN50}}$' refer to lightness and chroma values for their standards, respectively. 'Lt' and 'Ct' refer to the lightness and metric chroma tolerance limits described as the length of each semi axis from a ellipsoid and particular ANLAB colour space. Hue plots, derived in the same way as for chroma and lightness colour differences, were reported to show also a curve-linear relationship between hue tolerance limits plots against metric chroma values for all chroma standards. However, hue tolerance limits 'Ht' were about half the size when compared to chroma tolerance limits 'Ct'. McDonald described those variations in ratios by varying values of 'Ht' for each individual hue sector (expressed as a fraction of 'Ct') until disagreements between 'ΔEt' from *Equation 54* and visual results were smallest. 'Ht' is mathematically described in *Equation 58*. *Equation 59* describes a factor 'T' that adjusts hue metric chroma tolerance limits 'Ht' in regards to the hue angle of the standard by modifying metric chroma tolerance limits 'Ct'. An optimised 'Ct' function was later rescaled by a factor of 1.1 so to provide lowest variances together with an optimum 'Ht' value as given in *Equation 57*.

Eq. 57: $\mathrm{Ct} = 0.116 \cdot (C_{0,\mathrm{AN50}})/(1 + 0.0115 \cdot C_{0,\mathrm{AN50}}) + 1.32$

Eq. 58: $\mathrm{Ht} = \mathrm{T}.\mathrm{Ct}$

Eq. 59: $\mathrm{T} = 0.56 + |0.2\cos(\theta + 168)|$, when $164° < \theta < 345°$

$\mathrm{T} = 0.36 + |0.4\cos(\theta + 35)|$, when $345° < \theta < 164°$

This formula, including a modification for neutral grey colours in which the hue angle dependent factor 'T' was set to '1' (*Equation 58,* ellipsoids axes 'Ht' equals 'Ct' within the neutral circle) for all standard colours with a metric chroma value '$C_{0,\mathrm{AN50}}$' smaller than '1.32' ANLAB50 units, became the J & P Coats Ltd 1979 colour difference formula ('JPC_{79}'). The performance of the formula based on one dyehouse-manager gave a total of 9.7% disagreements

compared to any observer in a matching panel[130]. A practical trial use of the formula revealed a disagreement figure of 8.2 per cent. McDonald and McLaren[301] also provided a scaling factor '43.909', which makes lightness '$L_{43.909}$' values equal to 'Y'- tristimulus values '100' so to provide generally similar colour difference results between CIELAB and ANLAB's formula. The Society of Dyers and Colourists Colour Measurement Committee ('CMC') also encouraged users to scale ellipsoids tolerance limits in regards to other data sets, for instance, for those observer tolerance limits that were different when compared to JPC_{79}'s limits obtained from various products. The corresponding final equations in regards to a dataset provided by Davidson and Friede[92] are mathematically described in *Equation 60*, *61*, and *62*.

Eq. 60: $$\mathrm{Lt} = (0.08195L_{0,\mathrm{AN43.909}})/(1 + 0.01765L_{0,\mathrm{AN43.909}})$$

Eq. 61: $$\mathrm{Ct} = (0.0638C_{0,\mathrm{AN43.909}})/(1 + 0.0131C_{0,\mathrm{AN43.909}}) + 0.638$$

Eq. 62: $$\mathrm{Ht} = \mathrm{T} \cdot Ct_{\mathrm{AN43.909}}$$

The colour difference formula gave satisfactorily results and was approved as an alternative method to be used in visual colour matching pass/fail assignments. Also, this formula could be regarded as a prototype that provided methods as how to fit functions to experimental results for optimising the prediction of colour differences, according to Kühni[302].

2.16.5 The Society of Dyers and Colourists Colour Measurement Committee colour difference formula – CMC(*l:c*)

Clarke, McDonald, and Rigg[136] modified the JPC79 formula by applying a constant for the lightness tolerance limits 'Lt' for standard colours with lightness values 'L_0' smaller than '16'. Predictions of hue colour differences for colours at the near neutral boundary were further improved by introducing a function 'f' for calculating the hue dependent factor 'T_n'. The new factor 'T_n' regulates metric hue tolerance limits providing a smooth transition for metric hue standard colours with increasing chroma values for standard colours away from the neutral point and boundary. The Society of the Dyers and Colourist's Colour Measurement Committee ('CMC') also recommended allowing for different relative weightings applied either for acceptability or perceptibility data for lightness and chroma differences, or for acceptability predictions for various substrates such as textiles, paint, or leather. The length of the semi axes 'L_T', 'C_T', and 'H_T' defining unit 'ΔE_{JPC79}' were replaced by the terms 'S_L', 'S_C', and 'S_H'. The formula is abbreviated 'CMC(*l:c*)', where relative tolerances for *'l'* and *'c'* are specified for the use for various applications. Generally, unit weightings were recommended for perceptibility judgements. The range of *'l'* weighting values obtained from several datasets varied, according to Clarke *et al.*[136], from '0.67' to '5' and '1' to '4' for perceptibility and acceptability matches,

respectively. The range of values for weighting *'c'* varied from '0.5' to '3' and '1' to '2' (perceptibility/acceptability). Colour difference calculations for the CMC(*l:c*) formula are mathematically described as in *Equations 63ff.*

Eqs. 63ff: $\Delta E_{\mathrm{CMC}} = [(\frac{\Delta L^*}{lS_{\mathrm{L}}})^2 + (\frac{\Delta C^*_{\mathrm{ab}}}{cS_{\mathrm{C}}})^2 + (\frac{\Delta H^*_{\mathrm{ab}}}{S_{\mathrm{H}}})^2]^{\frac{1}{2}}$, where

$S_{\mathrm{L}} = 0.040975L^*_0/(1 + 0.01765L^*_0)$, unless

$L^*_0 < 16$ when $S_{\mathrm{L}} = 0.511$

$S_{\mathrm{C}} = 0.0638C^*_{\mathrm{ab},0}/\left(1 + 0.0131C^*_{\mathrm{ab},0}\right) + 0.638$

$S_{\mathrm{H}} = S_{\mathrm{C}}(\mathrm{Tf} + 1 - \mathrm{f})$

$\mathrm{f} = \{(C^*_{\mathrm{ab},0})^4/[(C^*_{\mathrm{ab},0})^4 + 1900]\}^{1/2}$

$\mathrm{T} = 0.36 + \left|0.4\cos\left(h_{\mathrm{ab},0} + 35\right)\right|$, unless 164° < $h_{\mathrm{ab},0}$ > 345° when

$\mathrm{T} = 0.56 + \left|0.2\cos\left(h_{\mathrm{ab},0} + 168\right)\right|$, where

'L^*_0', '$C^*_{\mathrm{ab},0}$', and '$h_{\mathrm{ab},0}$' refer to the standard of a pair of samples and differences in 'ΔL^*', 'ΔC^*_{ab}', and 'ΔH^*_{ab}' are determined according to the 1976 CIE '$L^*a^*b^*$' colorimetric system[aa]. Colour difference calculations are also described in detail in the publication BS 6923:1988 from the British Standard Institution[303].

2.16.6 The University of Bradford colour difference formula – BFD(*l:c*)

A new colour difference formula 'BFD(*l:c*)' for predicting small too medium colour differences for surface colours and different materials was developed by Luo and Rigg[138] in 1987, which in its structure is similar to that of the 'CMC(*l:c*)' formula, apart from two distinctive exceptions. A rotation term is applied, which is most effective in the blue region, tilting the major ellipsoid axis counter clockwise away from the neutral point in CIE's 'a^*b^*' - diagram. The BFD lightness function applies a logarithmic term to the 'Y' – tristimulus values in contrast to a cube root term in CIELAB's lightness function (included in CMC's formula). However, both lightness functions describe visual results for the same low lightness difference values in the range from '0' to '30' rather different. The same can be said for hue angle colour differences for low hue values, according to Luo.

[aa] see page 85 - 87 and 90 - 91

Various perceptibility (2775 sample paris) and acceptability data sets (1613 sample pairs) were combined and brought to a common visual scale for data analysis and the development of the 'BFD' – formula. Sample pairs wee made of wool, ink, paint, and/or textile materials. The formula's parameter, for instance, 'G', 'T'', and 'D_c', were optimised for those datasets, which hereby explains partly the differences in parameters between the BFD and CMC lightness, metric chroma, and hue tolerance limits. The calculations to obtain a colour difference value using the 'BFD' colour difference formula are described in *Equations 64ff*:

Eqs. 64ff:

$$\Delta E_{\mathrm{BFD}} = [(\frac{\Delta L_{\mathrm{BFD}}}{l})^2 + (\frac{\Delta C^*_{\mathrm{ab}}}{cD_{\mathrm{C}}})^2 + (\frac{\Delta H^*_{\mathrm{ab}}}{D_{\mathrm{H}}})^2 + \ldots$$

$$R_{\mathrm{T}}(\frac{\Delta C^*_{\mathrm{ab}}}{D_{\mathrm{C}}})(\frac{\Delta H^*_{\mathrm{ab}}}{D_{\mathrm{H}}})]^{1/2}, \text{ where}$$

$$L_{\mathrm{BFD}} = 54.6\, log_{\mathrm{bb}}(\mathrm{Y} + 1.5) - 9.6$$

$$D_{\mathrm{C}} = (0.035\bar{C}^*_{\mathrm{ab}})/(1 + 0.00365\bar{C}^*_{\mathrm{ab}}) + 0.521$$

$$D_{\mathrm{H}} = D_{\mathrm{C}}(\mathrm{G}T' + 1 - \mathrm{G})$$

$$\mathrm{G} = [\bar{C}^{*4}_{\mathrm{ab}}/\bar{C}^{*4}_{\mathrm{ab}} + 14000)]^{\frac{1}{2}}$$

$$T' = 0.627 + 0.055\cos(\bar{h}_{\mathrm{ab}} - 254^{\circ}) - 0.040\cos \ldots$$

$$\ldots(2\bar{h}_{\mathrm{ab}} - 136° + 0.070\cos(3\bar{h}_{\mathrm{ab}} - 32°) + 0.049\cos \ldots$$

$$\ldots(4\bar{h}_{\mathrm{ab}} + 114°) - 0.015\cos(5\bar{h}_{\mathrm{ab}} - 103°)$$

$$\mathrm{RT} = R_{\mathrm{H}}R_{\mathrm{C}}$$

$$R_{\mathrm{H}} = -0.260\cos(\bar{h}_{\mathrm{ab}} - 308°) - 0.379\cos(2\bar{h}_{\mathrm{ab}} - 160°) \ldots$$

$$\ldots - 0.636\cos(3\bar{h}_{\mathrm{ab}} + 254°) + 0.226\cos(4\bar{h}_{\mathrm{ab}} + 140°) \ldots$$

$$\ldots - 0.194\cos(5\bar{h}_{\mathrm{ab}} + 280°)$$

$$\mathrm{RC} = \{[(\bar{C}^*_{\mathrm{ab}})^6/[(\bar{C}^*_{\mathrm{ab}})^6 + 7 \cdot 10\text{^}7]\}^{1/2}$$

The terms '$\bar{C}^*_{\mathrm{ab}}$' and '$\bar{h}_{\mathrm{ab}}$' refer to the mean chroma and hue values for the standard and trial or batch sample, whereas the terms 'ΔC^*_{ab}' and 'ΔH^*_{ab}' refer to CIELAB's formula and associated numerical calculations. Using the mean values for calculating the weighting functions improved the shortcomings of the CMC(*l:c*) formula. Luo and Rigg suggested using a value of '1.5' for the lightness weighting '*l*', and a value of '1' for the chroma weighting '*c*' for predicting the

[bb] not consistently used in the literature either described as the common, natural, or binary log

acceptability of colour differences. For predicting the 'perceptibility' of colour differences the weighting '*l*' and '*c*' should be set to '1'. Furthermore, Luo and Rigg[139] explained that both formulae, BFD and CMC, improved the prediction of colour differences significantly when compared to CIELAB's formula. In addition, the new formula can be used for predicting larger colour differences although some inconsistencies for some datasets were reported presumably caused by scaling techniques applied to some visual results. Differences in predicting acceptability and perceptibility data were only visible in a change of the weighting factor '*l*', but not so in weighting '*c*'. The authors also emphasised on the fact that discontinuities for the lightness and hue tolerance limits as seen in CMC ('S_L' and factor 'T') were avoided. It was reported that it made programming and testing tasks considerably easier for the BFD formula.

2.16.7 The 1994 Commission Internationale de L'Éclairage colour difference formula - $CIE_{94}(k_L{:}k_C{:}k_H)$

Suggestions from Völz[145] in 1991, the work from Alman *et al.*[133] designing a dataset for colour difference evaluation, the reports and work from CIE's committees TC 1-28 and 29[304], analysis from Berns *et al.*[144,147] at the Rochester Institute of Technology (RIT) in 1993, and efforts from other workers resulted in a recommendation for exploiting and testing a new colour difference formula. This formula was initially abbreviated as 'CIELCH' ('ΔE_{CH}' units) and was later brand-named as 'CIE_{94}' ('ΔE^*_{94}' units) indicating the year the formula was recommended for evaluation and use. Mainly three data sets were considered for deriving new colour tolerance limits; those from Witt[143,173], Luo and Rigg[139], and Berns *et al.*'s dataset[144]. The latter consisting of glossy acrylic paint pairs for forty-five colour difference vectors sampling five directions in nine colour centres and varying from zero to four 'ΔE^*_{ab}' colour difference units. Those pairs were judged by fifty observers in terms of whether a perceived colour difference was larger or smaller compared to an anchor pair describing a combined lightness and chromatic colour difference of one 'ΔE^*_{ab}' unit. This unit was generally regarded as an industrial tolerance boundary for various products. Provisional tolerance limits were determined, applied, and various formulae performances were compared with each other. In a second phase, more sample pairs were produced so to determine population tolerances for '151' colour difference vectors for '19' colour centres. The choice of samples varied according to all three important directions from a colour centre in the CIELAB colour space. The visual results were then used to investigate the CIE_{94} colour difference formula and to compare it with CMC's formula. CIE_{94} contains simpler weighting functions, which are described mathematically in *Equations 65ff.*

Eqs. 65ff: $$\Delta E^*_{94} = [(\frac{\Delta L^*}{k_L S_L})^2 + (\frac{\Delta C^*_{ab}}{k_C S_C})^2 + (\frac{\Delta H^*_{ab}}{k_H S_H})^2]^{\frac{1}{2}}, \text{ where}$$

$S_L = 1$
$S_C = 1 + 0.045C^*_{ab,0}$
$S_H = 1 + 0.015C^*_{ab,0}$, and

'$C^*_{ab,0}$' refers to the chroma value 'C^*_{ab}' of a standard sample for a colour difference pair so to avoid asymmetry when batch and standard samples were interchanged, according to Hunt and Pointer[305]. Calculations of difference values followed also CIELAB's recommendations. Relative weightings 'k_L', 'k_C', and 'k_H' were now classified as parametric factors, which can vary once the reference conditions in the experimental setup are altered, for instance, by a change in luminance level of the background, texture, sample separation, and so on. The reference conditions in the experimental setup for colour difference evaluation are described as follows;

. the specimens shall be visually homogeneous in structure,
. the colour difference should be between zero and five 'ΔE^*_{ab}',
. they should be placed in nearest possible contact,
. each specimen should subtends a viewing angle greater than 4°,
. they should be illuminated with 1000 lux by a daylight simulator,
. and be seen in object mode against a uniform neutral grey background of 'L^*' = 50.

CIE reporter Witt[149] requested in 1995 workers to follow those simple guidelines, and also to report new results for further considerations. Performance results and analysis were obtained from work by Heggie *et al.*[151], Melgosa *et al.*[179,306], Griffin and Sepheri[307], McDonald and Smith[150], among others. Kühni[308] reported a method how to modify the CIE94 formula resulting in correlation results that were significant better than compared to those obtained from *Equations 65ff.* Thomsen[156] reported a similar method for CIELAB's colour difference formula. The first step according to Kühni's modification is to modify; (**1**) the '$\bar{x}$' - colour matching function (*Equation 86*), and (**2**) to derive a lightness scale that is dependent on the lightness of the surround as given in *Equation 66, 67, and 68*.

Eq. 66: $\bar{x}_{10,\,mod} = 1.1\bar{x}_{10} - 0.1\bar{z}_{10}$, where
Eq. 67: $L\hat{} = 116[(\frac{Y}{Y_0})^{0.333} - (\frac{Y_s}{Y_0})^{0.333}]$
Eq. 68: $\Delta L = \frac{\Delta L\hat{}}{S_L}$, where

'Y_s' refers to the luminous reflectance of the surround, 'Y_0' describes the reflectance value of the illuminant, and the lightness tolerance limit 'S_L' function is given in *Equation 69*.

Eq. 69: $S_L = 1 + 0.010L\hat{}$

2.16.8 The University of Leeds colour difference formula - 'LCD(k_L:k_{CH})'

Kim and Nobbs[155] used glossy acrylic paint pairs for conducting visual assessments with the aid of a pair comparison and grey scale method for an overall number of '347' colour difference pairs around twenty-one colour centres with an average value of 1.6 'ΔE_{ab}' units. Each pair was assessed for on average '30' times under each viewing conditions by ten to fifteen, or twelve to fifteen observers. The formula was intended to modify CIELAB's formula so to fit both scaling methods and datasets, and also Bradford University's perceptibility dataset ('BFD-P'), in a best possible way. The formula is abbreviated as 'LCD'. Individual parametric factors 'k_C' and 'k_H' terms are not used separately, but a common factor 'K_{CH}' is applied, instead. The 'LCD' colour difference formula is similar to *CIE*$_{94}$'s formula in aspects of simplicity but also alters the lightness tolerance limits for bright colours larger than 'L^*' equal to '50', and the predictions for standard samples around CIELAB's blue color region. The 'LCD' formula is described in *Equations 70ff.*

Eqs. 70ff:

$$\Delta E_{\mathrm{LCD}} = \left[\frac{\left(\frac{\Delta L^*}{S_L}\right)^2}{k_L^2} + \frac{\left(\frac{\Delta C^*_{ab}}{S_C}\right)^2 + \left(\frac{\Delta H^*_{ab}}{S_H}\right)^2 + S_R \Delta C^*_{ab} \Delta H^*_{ab}}{k_{CH}^2}\right]^{\frac{1}{2}}$$

$$S_L = 1 - 0.01L_0^* + 0.0002L_0^{*2}, \text{ when } L_0^* < 50 \text{ then } S_L = 1$$

$$S_C = \left(1 + 0.045C^*_{ab,0}\right)S_{CH}$$

$$S_H = \left(1 + 0.015C^*_{ab,0}\right)S_{HH}$$

$$S_R = \left[\frac{-C^*_{ab,0}}{(2+0.07C^*_{ab,0})^3}\right]\sin(2\Delta\Theta)$$

$$\Delta\Theta = 30\exp\{-[(h_{ab,0} - 275°)/25)^2\}$$

$k_L = k_{CH} = 1$ for non-textile samples

$k_L = 1.5, k_{CH} = 1$ for textile samples

$S_{CH} = S_{HH} = 1$, when $C^*_{ab,0}$ is smaller or equal to '4', otherwise

$$S_{CH} = 1 + 0.07\sin(h_{ab}) - 0.16\cos(2h_{ab} + 250) - 0.05\cos(3h_{ab}) - 0.03\cos(4h_{ab})$$

$$S_{HH} = 1 + 0.03\cos(h_{ab} + 60) + 0.12\cos(2h_{ab}) + 0.12\cos(3h_{ab}) - 0.07\cos(4h_{ab} - 45)$$

The results obtained from LCD's colour difference formula, are according to Kühni[309], similar to those obtained from the BFD formula.

2.16.9 Deutsches Institut für Normung - Farbabstandsformel - *DIN*$_{99}$

The basic concept of the German colour standard order system was to find a series of equidistant scales. The DIN hue concept is based on a constant dominant wavelength for each hue; the order of equal saturation and lightness level for a hue circle was found by visual experiments, and also extended as such for other hues. DIN does not differ from other colour order systems in terms of hue and saturation *per se* but does so for brightness. Equally saturated colours are obtained from their relative luminance factor ('Y') compared to the luminous factor ('Y_0') of an optimal colour. Relative in the sense that a luminous reflectance value for a sample is divided by the reflectance value from an optimal colour for the same chromaticity. A sphere segment was chosen for describing the relationship between DIN's scales 'D' for lightness, 'T' degree of longitude, and saturation 'S' as the degree of latitude from the north pole as described by Richter and Witt[167]. A colour difference formula for predicting small colour differences was derived from this solid as described in DIN6164 and *Equation 71 and 72*.

Eq. 71: $\Delta E_{6164} = 25[(\frac{\mathrm{S}}{6}\frac{(10-\mathrm{D})}{9}\Delta T)^2 + (\frac{10-\mathrm{D}}{9}\Delta S)^2 + (\Delta D)^2$, where

Eq. 72: $\mathrm{D} = 10 - 6.1723\log(40.7\frac{\mathrm{Y}}{Y_0} + 1)$

Witt proposed a formula that also can predict larger colour differences. That colour solid is based on a lightness-chromaticness model providing a definition of chromaticity very similar to those described in CIE 1976 '$L^*u^*v^*$' colour system[cc]. This colour difference equation is described in *Equation 73*, *74*, and *75*.

Eq. 73: $\Delta E_{\mathrm{TS}} = 33[(\Delta D_n)^2 + (\Delta u_{\mathrm{TS}})^2 + (\Delta v_{\mathrm{TS}})^2]^{1/2}$, where

Eq. 74: $u_{\mathrm{TS}} = 0.071u'_{\mathrm{TS}}(10 - D_{\mathrm{n}});\ v_{\mathrm{TS}} = 0.071v'_{\mathrm{TS}}(10 - D_{\mathrm{n}})$

Eq. 75: $u'_{\mathrm{TS}} = \mathrm{S}\cdot\cos[15^{\circ}(7-\mathrm{T})];\ v'_{\mathrm{TS}} = \mathrm{S}\cdot\sin[15^{\circ}(7-\mathrm{T})]$, where

'D_{n}' is described in *Equation 74*. A different DIN colour difference formula (DIN6176:2001-03) was developed in 1999 based on *CIE*$_{94}$'s formula and ideas from Rohner and Rich as described in the '*DCI*$_{95}$' – colour difference formula[164]. The authors applied an integration method and transformed CIELAB's colour coordinates directly in a logarithmic fashion to a new colour space; similar approaches as to modify CIE's coordinates were reported by Völtz [310,311,312] and Thomsen[156]. All transformations from CIELAB's into *DIN*$_{99}$'s colour space are achieved in four steps; (**1**) by rotating CIELAB's 'a^*b^*'- axes, (**2**) by weakening the yellow/blue

---

[cc] see page 86-87

axis by a factor of 0.7, (**3**) by compressing high saturated colours, and (**4**) by a logarithmic transformation of CIELAB's lightness scale 'L^*' (compression of bright and enhancement of dark colours). The advantage of this approach was to be able to use a simple Euclidean colour difference formula for predicting colour differences in *DIN*$_{99}$'s colour space. The transformation of coordinates and calculation of colour differences are described in *Equations 76ff*. The basic parameters are all associated with CIELAB's '$L^*a^*b^*$'- coordinates.

Eqs. 76ff:

$$\Delta E_{99} = [(\Delta L_{99})^2 + (\Delta a_{99})^2 + (\Delta b_{99})^2]^{1/2}, \text{ alternatively}$$

$$\Delta E_{99} = [(\Delta L_{99})^2 + (\Delta C_{99})^2 + (\Delta H_{99})^2]^{1/2},$$

$$L_{99} = \left(\frac{1}{k_{\mathrm{e}}}\right) 105.51(\ln(1 + 0.0158L^*),$$

$$C_{99} = (\ln(1 + 0.045\mathrm{G}))/(0.045k_{\mathrm{CH}}k_{\mathrm{e}}),$$

$$\Delta H_{99} = -(a_{99,1}b_{99,0} - a_{99,0}b_{99,1})/(0.5\begin{pmatrix}C_{99,1}C_{99,0} + a_{99,1}a_{99,0}\\ +b_{99,1}b_{99,0}\end{pmatrix})^{1/2},$$

$$\mathrm{e} = a^* \cos(16°) + b^* \sin(16°),$$

$$\mathrm{f} = -0.7\, a^* \sin(16°) + 0.7\, b^* \cos(16°),$$

$$\mathrm{G} = (e^2 + f^2)^{1/2},$$

$$h_{\mathrm{ef}} = \arctan\left(\frac{\mathrm{f}}{\mathrm{e}}\right),$$

$$h_{99} = h_{\mathrm{ef}} \cdot 180/\mathrm{pi},$$

$$a_{99} = C_{99}\cos(h_{99}),$$

$$b_{99} = C_{99}\sin(h_{99}), \text{ where}$$

factor 'k_{CH}' and 'k_{E}' are adjustable as to account for variations in external or experimental conditions that are different from those usually experienced in academia. However, Rösler[313] recommended not using any other value than '1' for the calculations of 'C_{99}' values. Cui *et al.*[165] modified this formula reporting improvements by introducing two modifications as given in *Equation 77* and 7*8ff*. An overall 'size' parametric factor 'k_{e}' was introduced and a denominator parametric factor 'k_{L}' was included to the lightness colour difference term for the *DIN*$_{99}$ formula, as it was also done for other advanced colour difference formula at that time. The second improvement was associated with a modified 'X' - tristimulus value as suggested by Kühni[154] in 1999. Otherwise, Cui *et al.* optimised colour difference tolerance parameter so to fit four datasets in a best possible way (BFD-P, RIT-DuPont, Leeds, and Witt data sets).

Eq. 77:

$$\Delta E_{99\mathrm{b}} = \frac{1}{k_{\mathrm{E}}}\sqrt{(\Delta L_{99}/k_{\mathrm{L}})^2 + (\Delta a_{99})^2 + (\Delta b_{99})^2}$$

Eqs. 78ff:

$$\Delta E_{99\mathrm{d}} = \frac{1}{k_{\mathrm{E}}}\sqrt{(\Delta L_{99\mathrm{d}})^2 + (\Delta a_{99\mathrm{d}})^2 + (\Delta b_{99\mathrm{d}})^2}$$

$$X' = 1.12X - 0.12Z,$$

$$L_{99\mathrm{d}} = 325.22ln(1 + 0.0036L^*),$$

$$\mathrm{e} = a^* \cos(50°) + b^* \sin(50°),$$

$$\mathrm{f} = 1.14[-a^* \sin(50^\circ) + b^* \cos(50^\circ)],$$

$$\mathrm{G} = \sqrt{e^2 + f^2},$$

$$C_{99\mathrm{d}} = 22.5ln\,(1 + 0.06G),$$

$$h_{99\mathrm{d}} = \arctan\left(\frac{\mathrm{f}}{\mathrm{e}}\right) + 50°,$$

$$a_{99\mathrm{d}} = C_{99\mathrm{d}} \cos\,(h_{99\mathrm{d}}),$$

$$b_{99\mathrm{d}} = C_{99\mathrm{d}} \sin\,(h_{99\mathrm{d}})$$

The modified DIN_{99} formulae significantly improved the correlation between calculated and visual data for small colour differences.

2.16.10 Optical Society of America Uniform Colour Order System (OSA-UCS) and associated colour difference formulae.

The Optical Society of America ('OSA') developed a uniform colour order system (also known as a colour appearance system) between the years 1947 and 1974 based on the method of perceptual uniformity of colour scales. A large number of paint chips were produced and viewed under daylight conditions ('D65') against a grey background colour with a reflectance value of approximately 30%. Colorimetric data were specified according to CIE's 1964 colorimetric system. A production of a 558-chip set was completed in 1976 so to satisfy a best possible approximation of three-dimensional uniform visual spacing of colours on a global as on a local scale in the form of a rhombohedral lattice, according to Billmeyer[291].MacAdam[117] conducted experiments in 1974 using a limited number of samples ('43' paint ceramic tile colours of matt finish all having a luminous reflectance factor of 30%). The chromaticity of those samples were all equally different when compared with each other and as such triangularly arranged. The experimental setup separated both samples of a colour difference pair from each other by a gap of 3 - 4 mm. The surround or background was of a grey colour of 30% relative reflectance that was illuminated by daylight of at least 500 lm/m^2. Seventy-six observers participated in this pair comparison assignment. Spectrophotometric measurements (illumination perpendicular to the sample; all of the reflected light was collected) and visual results were related and scaled with each other ('D65', CIE 10° standard observer) by using cube-root functions. MacAdam derived a three dimensional colour space from those data by non-linear transformations of the CIE 1931 'xy' – chromaticity diagram. The third dimension followed Judd's suggestions, the chairman of the OSA Uniform Color Committee at that time,

to include the influence of the background in deriving a uniform lightness scale. CIE's 'XYZ_{10}' – tristimulus values are transformed to OSA 'L' (lightness), 'j' (yellowness-blueness), 'g' (greenness-redness) using *Equations 79ff*, *80ff*, and *81ff*. Luminous reflectance ('$\bar{Y}_{10}$') refers to a grey object colour that appears similar in luminance when compared to the sample colour ('Y_{10}', 'x_{10}', 'y_{10}'); Semmelroth's intermediate lightness[181] ('L_{i}'), which takes crispening into account when the grey background is of 30% reflectance[314], are described in *Equations 79ff*.

Eqs. 79ff:
$$\bar{Y}_{10} = Y_{10}(4.4934x_{10}^2 + 4.3034y_{10}^2 - 4.276x_{10}y_{10} \ldots -1.3744x_{10} - 2.5643y_{10} + 1.8103),$$
$$L_{\mathrm{i}} = 5.9[(\bar{Y}_{10}^{\frac{1}{3}} - \tfrac{2}{3}) + 0.042(\bar{Y}_{10} - 30)^{\frac{1}{3}}],$$

CIE 'XYZ_{10}' - tristimulus values are converted to cone sensitivity values as given in *Equations 81ff*; lightness 'L', and OSA's 'j' and 'g' are calculated according to *Equations 83ff*.

Eqs. 80ff:
$$R_{10} = 0.799X_{10} + 0.4194Y_{10} - 0.1648Z_{10},$$
$$G_{10} = -0.4493X_{10} + 1.3265Y_{10} + 0.0927Z_{10},$$
$$B_{10} = -0.1149X_{10} + 0.3394Y_{10} + 0.717Z_{10},$$

Eqs. 81ff:
$$\mathrm{L} = L_{\mathrm{i}} - 14.4)/2^{1/2},$$
$$\mathrm{g} = \mathrm{C}\left(-13.7R_{10}^{1/3} + 17.7G_{10}^{1/3} - 4B_{10}^{1/3}\right) = \mathrm{Ca},$$
$$\mathrm{j} = \mathrm{C}\left(1.7R_{10}^{1/3} + 8G_{10}^{1/3} - 9.7B_{10}^{1/3}\right) = \mathrm{Cb},$$
$$\mathrm{C} = 1 + 0.042(\bar{Y}_{10} - 30)^{\frac{1}{3}}/((\bar{Y}_{10})^{\frac{1}{3}} - \tfrac{2}{3}), \text{ where}$$

'$\bar{Y}_{10}$' adjusts lightness and chromaticness ('Helmholtz-Kohlrausch effect') using a formula modified by Sanders and Wyszecki[315], and factor 'C' adjusts Semmelroth's crispening effect of chromatic differences. However, MacAdam suggested not using 'L', 'g', and 'j' for designing a colour difference formula for predicting small but also large colour differences because all judged differences were more than twenty times a just noticeable difference, according to Billmeyer[84]. The coefficients in *Equations 80ff* for deriving 'RGB_{10}' - tristimulus values were based on specific primary stimuli. However, Oleari *et al.*[186] used the uniform colour opponencies scales on the OSA-UCS geodesic lines to find a transformation of 'XYZ_{10}' - tristimulus values to fit OSA's 'j'- and 'g'- scales. This was mathematically achieved by; (**1**) linear transformations of 'XYZ_{10} - tristimulus values to main stimuli 'A', 'B', and 'C' (found by iteration technique so to minimize an index), which also serves as fix points for a three component diagram, and (**2**) by logarithmic compression. Based on these transformations, Huertas *et al.*[185] developed a new formula ('ΔE_{GP}') that includes the original OSA 'L_{OSA}'

lightness function, according to the authors. The tolerance limits and parameters were obtained by fitting ellipses to four data sets that were also used for the development of the *CIEDE*$_{2000}$ formula. Following this approach, Oleari *et al.*[316] described in 2009 a new Euclidean colour difference formula 'E_E' using chroma log – compression on the basis of OSA's colour space[317]. The calculations for (**1**) and (**2**) are described in *Equation 82* and *83*.

Eq. 82:
$$\begin{pmatrix} A \\ B \\ C \end{pmatrix} = \begin{bmatrix} 0.6597 & -0.4492 & -0.1089 \\ -0.3053 & 1.2126 & 0.0927 \\ -0.0374 & 0.4795 & 0.5579 \end{bmatrix} \begin{pmatrix} X_{10} \\ Y_{10} \\ Z_{10} \end{pmatrix},$$

Eq. 83:
$$\begin{pmatrix} J \\ G \end{pmatrix} = \begin{bmatrix} S_J & 0 \\ 0 & S_G \end{bmatrix} \begin{bmatrix} -\sin\alpha & \cos\alpha \\ \sin\beta & -\cos\beta \end{bmatrix} \begin{pmatrix} \ln\left(\frac{A/B}{A_n/B_n}\right) \\ \ln\left(\frac{B/C}{B_n/C_n}\right) \end{pmatrix}, \text{ where}$$

'J' and 'G' refer to perceptual coordinates relating to 'j' and 'g' in OSA's colour space (*Equations 81ff*), 'S_J' and 'S_G' refer to linear normalization factors for OSA's 'L_{OSA}' lightness scale, ratios 'A_n/B_n' and 'B_n/C_n' refer to transformed tristimulus values from the 'D65' white point, and angles 'α' and 'β' are given as '-10.31°' and '71.46°' degrees values. Once all parameter are determined, it is possible to calculate a colour difference 'ΔE_E' in an approximately Euclidean colour space as given in *Equations 84ff*.

Eqs. 84ff:
$$\Delta E_E = \sqrt{(\Delta L_E)^2 + (\Delta G_E)^2 + (\Delta J_E)^2},$$
$$L_E = \left(\frac{1}{b_L}\right) \ln[1 + \frac{b_L}{a_L}(10 L_{OSA})],$$
$$L_{OSA} = \left\{5.9\left[\left(\bar{Y}_{10}^{1/3} - \frac{2}{3}\right) + 0.042(\bar{Y}_{10} - 30)^{1/3}\right] - 14.4\right\}\frac{1}{\sqrt{2}},$$
$$a_L = 2.890 \text{ and } b_L = 0.015,$$
$$G_E = -C_E \cos(h),$$
$$J_E = C_E \sin(h),$$
$$h = \arctan\left(-\frac{J}{G}\right),$$
$$C_E = \left(\frac{1}{b_C}\right) \ln[1 + \frac{b_C}{a_C}(10 C_{OSA})],$$
$$a_C = 1.256 \text{ and } b_C = 0.050,$$
$$C_{OSA} = \sqrt{G^2 + J^2}.$$

The authors concluded that empirical small to medium colour differences show a regularity that is not seen in CIELAB. The prediction performance of colour differences was said to be similar to those generated from the *CIEDE*$_{2000}$ formula.

2.16.11 The 2000 Commission Internationale de L'Éclairage colour difference formula - $CIEDE_{2000}$ (k_L:k_C:k_H)

Contributions from well-known researchers in colour science towards the development of advanced colour difference formulae, as such discussed during the development of the JPC_{79}, CMC, BFD, LCD, CIE_{94}, and DIN_{99} formula, were combined to derive a new CIE recommended colour difference formula for evaluating small to medium colour differences for surface colours. Parameters were optimised so to fit four comprehensive datasets that were available at that time, and a combination of them (CIE[175,169]). Cui *et al's*[318] work, accounting for those major contributions in the form of an optimised formula ('M2b'), became approved by the CIE in 2001. Five corrections in regards to CIELAB's formula were applied in the form of a improved lightness weighting function 'S_L' ('V' - shaped function), a chroma weighting function 'S_C', a hue weighting function 'S_H', an interactive term 'RT' between chroma and hue differences, and a term '1+G' for rescaling CIELAB's 'a^*' - scale. The new formula and its terms are calculated as given in *Equations 86ff.* The underlying parameters for all basic $CIEDE_{2000}$'s terms are associated with CIELAB's coordinates and as such modified as given in *Equations 85ff.*

Eqs. 85ff:

$$L' = L^*,$$

$$a' = (1 + \mathrm{G})a^*,$$

$$b' = b^*,$$

$$C' = \sqrt{a'^2 + b'^2},$$

$$h' = \tan^{-1}\left(\frac{b'}{a'}\right), \text{ where}$$

$$\mathrm{G} = 0.5\left(1 - \sqrt{\frac{\bar{C}_{ab}^{*7}}{\bar{C}_{ab}^{*7} + 25^7}}\right),$$

$$\Delta L' = L'_1 - L'_0,$$

$$\Delta C' = C'_1 C'_0,$$

$$\Delta H' = \sqrt[2]{C'_1} C'_0 \sin\left(\frac{\Delta h'}{2}\right),$$

$$\Delta h' = h'_1 - h'_0,$$

Eqs. 86ff:

$$\Delta E_{00} = \sqrt{\left(\frac{\Delta L'}{k_L S_L}\right)^2 + \left(\frac{\Delta C'}{k_C S_C}\right)^2 + \left(\frac{\Delta H'}{k_H S_H}\right)^2 + R_T\left(\frac{\Delta C'}{k_C S_C}\right)\left(\frac{\Delta H'}{k_H S_H}\right)},$$

$$S_L = 1 + \frac{0.015(\bar{L}' - 50)^2}{\sqrt{20 + (\bar{L}' - 50)^2}},$$

$$S_C = 1 + 0.045\bar{C}',$$

$S_{\mathrm{H}} = 1 + 0.015\bar{C}'\mathrm{T}$, where

$$\mathrm{T} = 1 - 0.17\cos\left(\bar{h}' - 30°\right) + 0.24\cos\left(2\bar{h}'\right) + \cdots$$
$$\ldots 0.32\cos\left(3\bar{h}' + 6°\right) - 0.20\cos\left(4\bar{h}' - 63°\right),$$

$$R_{\mathrm{T}} = -\sin(2\Delta\Theta)\, R_{\mathrm{C}},$$
$$\Delta\Theta = 30\exp\{-[\tfrac{h'-275°}{25}]^2\},$$
$$R_{\mathrm{C}} = \sqrt[2]{\frac{\bar{C}'^7}{\bar{C}'^7+25^7}}.$$

The values of '$\bar{L}'$', '$\bar{C}'$', '$\bar{h}'$, '$\bar{C}_{\mathrm{ab}}^{*7}$' refer to the arithmetic means of 'L'', 'C'', 'h'', and 'C_{ab}^{*}' -values for a pair of samples. Subscripts '$_0$' and '$_1$' refer to a batch and standard sample so to be consistent with earlier formulae mentioned in this thesis (other literature sources prefer subscript '$_b$' and '$_s$'). The formula improved the predictions statistically significant for small colour differences when compared to CIELAB's formula, according to Melgosa *et al.*[319]. And this, in itself, was said to be a valuable contribution to many critical applications, as reported by Lee[320]. The reference conditions to be used to determine colour differences according to above formula were similar to those used for the CIE_{94}[dd] formula. Sharma *et al.*[321] provided guidelines for implementing $CIEDE_{2000}$ either in a Matlab or Excel software environment. A critical and constructive paper from Kühni[322] emphasizes mainly on three issues in regards to the latest recommendation from the CIE as such asking; (**a**) whether the CIELAB colour space is a good basis for colour difference calculations, (**b**) whether $CIEDE_{2000}$'s 'T' function is applicable for all levels of chroma and lightness, and (**c**) whether a factor in $CIEDE_{2000}$ compensating for the crispening effect constrained at a background luminance of 'L^*' equal to '50' is appropriate enough for predicting colour differences for sample pairs seen against various backgrounds. However, the CIE considers the latest developments in the form of the $CIEDE_{2000}$ formula as a provisional international standardised colour difference formula, as described in CIE DS 014-6/E:2012[323].

[dd] see page 97

2.16.12 The 2002 Commission Internationale de L'Éclairage colour appearance model (*CIECAM*$_{02}$) and associated colour difference formula for small colour differences - *CIECAM*$_{02}$(SCD)

Conditions in colour difference perceptions are mainly based on (**a**) the variations in light stimuli colour matching (threshold), (**b**) judgements of small colour differences (material samples from threshold to moderate colour differences), and (**c**) colour appearance scaling (visual scaling of individual colour samples – normally compromising large colour differences). Two kinds of models that describe those data are of empirical (CIELUV, $U^*V^*W^*$), or theoretical form (CIELAB). A major innovation was the invention of hybrid models ('JPC_{79}'), in which empirical models were combined with theoretical models including visual mechanism that influences colour vision such as cone excitation, chromatic adaption, opponent processes, and non-linear compression, as described by the CIE[49]. Early colorimetry was concerned with describing and predicting the nature of human vision under simplified and reproducible experimental conditions. At a later stage, several colour vision models were developed so to widen the scope for predicting more complex scenario, for instance, the appearance of colours under a range of viewing conditions[324]. The most extensive studies and models were generated by Nayatani *et al.*[191] and Hunt[190,325]. Other models are associated with Bartleson[326], Fairchild and Berns[327], Luo *et al.*[197,199], Li *et al.*[198], Pointer[328], and Richter[329], among other researchers. A colour appearance model (CAM) is able to transform physical measurement of stimuli and viewing conditions into perceptual correlates by mathematical means. These perceptual correlates can then be used to construct a colour space. The major two important parts of a CAM are the chromatic adaption transformation and the definition of appearance correlates. The combined efforts of several authors[ee] resulted in CIE's CIECAM97s and, after revision, in *CIECAM*$_{02}$[46]. The *CIECAM*$_{02}$ model is based on a set of corresponding colours, which are used to optimise a chromatic adaption transform[45] (an example of a 'CAM' is the 'Bradford-CAT'), and the degree of adaption by a factor 'D'. Perceptual correlate attributes are, according to Moroney *et al.*[330], based on physiological data, for instance, derived from various phases of the 'LUTCHI' data set and/or Munsell's Book of Color. Those models predict colour appearance attributes such as brightness and colourfulness in addition to hue, lightness, saturation, and chroma as predicted by CIELAB's and CIELUV's colour specification systems. *CIECAM*$_{02}$ describes also; (**a**) the surround effect predicted by a colourfulness scale ('M'), (**b**) the surround effect predicted by a lightness scale ('J'), and (**c**) the lightness contrast effect (various 'J' against

---

[ee] see page 44-48

various 'Y' luminous factors)[ff]. Li *et al.*[331] used several large colour difference datasets, and a combined set of them, to predict visual sample pair colour differences in modified $CIECAM_{02}$ colour appearance spaces. Those datasets were generated from;

(**1**) Zhu *et al.*'s set[332] consisting of '144' CRT generated colour difference pairs (average colour difference value of '10' 'ΔE^*_{ab}' - units), which were scaled by observers from one end to the other for each scale;

(**2**) OSA set consisting of 128 perceived colour differences obtained from '76' and '49' observers judging '43' and '16' matt painted ceramic tiles using a ratio judgement method under D65/10° conditions (average 'ΔE^*_{ab}' unit value of '14');

(**3**) a selection of Kuo- and Luo's dataset consisting of 292 wool samples colour difference pairs judged by ten observers twice in simulated daylight conditions using a grey scale method (average 'ΔE^*_{ab}' unit value of '11');

(**4**) the Bradford - Badu data set consisting of 238 nylon sample pairs judged by twenty observers in similar conditions as with an average colour difference value of '12' 'ΔE^*_{ab}' units,

(**5**) Pointer and Attridge's set consisting of '28' colour centres generated from '1308' printed colour differences samples with an average value of 9 'ΔE^*_{ab}' units judged with a greyscale; and

(**6**) a selection of '844' colour difference paint chip pairs from the Munsell Renotation system with an average 'ΔE^*_{ab}' value of '10' units judged in terms of illuminant 'C' and CIE's 1931 standard observer.

In contrast, a second dataset combined from the BFD, RIT-DuPont, Leeds, and Witt data[gg] consisting of '3657' sample pairs with an average colour difference value of '2.6' 'ΔE^*_{ab}' units was used to optimise a formula for predicting small colour differences in $CIECAM_{02}$ colour's appearance space. Also, a colour difference set derived from illuminant 'A' was generated and tested. $CIECAM_{02}$'s lightness ('J'), colourfulness ('M'), and hue angle ('h') attributes were then scaled and optimised so to fit a small, large, and a combined colour difference dataset. Li *et al.*[198,199] provided a general colour difference formula based on those datasets that can be applied, accordingly as given in *Equations 87ff*, by varying the parameter for '$k_{L'}$, 'c_1', and 'c_2'.

[ff] see page 47

[gg] see page 48

Eqs. 87ff: $\Delta E' = \sqrt{(\frac{\Delta J'}{k_{\mathrm{L}}})^2 + \Delta a_{\mathrm{M}}'^2 + \Delta b_{\mathrm{M}}'^2}$,

$J' = \frac{(1+100\cdot c_1)\cdot \mathrm{J}}{1+c_1\cdot \mathrm{J}}$,

$a_{\mathrm{M}} = \mathrm{M}\cdot\cos(\mathrm{h})$,

$b_{\mathrm{M}} = \mathrm{M}\cdot\sin(\mathrm{h})$,

$M' = (\frac{1}{c_2})\cdot \ln(1 + c_2\cdot \mathrm{M})$,

$\mathrm{M} = \mathrm{C}F_{\mathrm{L}}^{0.25}$,

$F_{\mathrm{L}} = 0.2k^4(5L_{\mathrm{A}}) + 0.1(1-k^4)^2(5L_{\mathrm{A}})^{1/3}$,

$\mathrm{k} = 1/(5L_{\mathrm{A}} + 1)$,

$L_{\mathrm{A}} = \frac{1}{5}$of the luminance in cd $\mathrm{m}^{-2}$for the adapting field,

$\mathrm{C} = t^{0.9}\,(\mathrm{J}/100)^{0.5}(1.64 - 0.29^n)^{0.73}$,

$\mathrm{J} = 100/(\mathrm{A}/A_{\mathrm{W}})^{\mathrm{cz}}$,

$\mathrm{c} = 0.69, 0.59,$ or 0.525;

$z = 1.48 + n^{0.5}$,

$\mathrm{n} = Y_{\mathrm{b}}/Y_{\mathrm{w}}$,

$Y_{\mathrm{w}} =$ adopted white in test conditions,

$Y_{\mathrm{b}} =$ adapted background in test conditons,

$A = [2\rho_a + \gamma_a + \left(\frac{1}{20}\right)\beta_{\mathrm{a}} - 0.305]N_{\mathrm{bb}}$,

$A_w\left[2\rho_{\mathrm{aw}} + \gamma_{\mathrm{aw}} + \left(\frac{1}{20}\right)\beta_{\mathrm{aw}} - 0.305\right]N_{\mathrm{bb}}$,

$\rho_{\mathrm{a}} = \{[400((F_{\mathrm{L}}\,\rho)/(100)^{0.42}]/[27.13 + (F_{\mathrm{L}}\rho/100)^{0.42}]\} + 0.1$,

$\gamma_{\mathrm{a}} = \{[400((F_{\mathrm{L}}\,\gamma)/(100)^{0.42}]/[27.13 + (F_{\mathrm{L}}\gamma/100)^{0.42}]\} + 0.1$,

$\beta_{\mathrm{a}} = \{[400((F_{\mathrm{L}}\,\beta)/(100)^{0.42}]/[27.13 + (F_{\mathrm{L}}\beta/100)^{0.42}]\} + 0.1$,

$\mathrm{t} = \left[\left(\frac{50000}{13}\right)N_{\mathrm{c}}N_{\mathrm{cb}}\right][e_t(a^2 + b^2)^{0.5}]/[\rho_{\mathrm{a}} + \gamma_{\mathrm{a}} + \left(\frac{21}{20}\right)\beta_{\mathrm{a}}]$,

$N_{\mathrm{c}} = 1.0, 0.9,$ or 0.8;

$N_{\mathrm{cb}} = N_{\mathrm{bb}} = 0.725(1/n)^{0.2}$,

$e_{\mathrm{t}} = \left[\frac{1}{4}\right][\cos\left(\mathrm{h}\frac{\pi}{180} + 2\right) + 3.8]$,

$\mathrm{a} = \rho_{\mathrm{a}} - (12\gamma_{\mathrm{a}}/11) + (\beta_{\mathrm{a}}/11)$,

$\mathrm{b} = (1/9)(\rho_a + \gamma_a - 2\beta_{\mathrm{a}})$,

$\mathrm{h} = tan^{-1}\left(\frac{\mathrm{b}}{\mathrm{a}}\right)$, where

'k_L', 'c_1' and 'c_2' are optimised and set set to '1.24', '0.007', and '0.0053' for predicting small colour differences. The adapting field refers to the total environment a colour is seen in (normally 20% on average in an image); adopted white refers to the illuminant, and adapted background in the test condition refers to the background surrounding a sample (about 10° from the edge of a sample's proximal field), according to Hunt and Pointer[333]. The comparison with colour difference formulae for the same datasets were said to be comparable, according to the authors of this formula. The *CIECAM*$_{LCD}$ colour difference formula predicted larger colour differences, for instance, with similar results when compared with CIELAB and GLAB; and gave similar results for predicting small colour differences when compared with the *CIEDE*$_{2000}$ and *DIN*$_{99d}$ formula. Berns and Zue[334] constructed an optimised weighted colour difference formula from *CIECAM*$_{02}$ attributes using the RIT-DuPont and Qiao *et al.*'s dataset containing glossy automotive paints and printing papers. Their approach describes the integration of line elements from optimised weighting functions for a defined set of data. The form of the functions they used was similar to those included in *CIE*$_{94}$'s formula. The form of the lightness weighting function is described as an exponential function. The authors transformed, in order to obtain Euclidean distances, the colour space in accordance to the positional weightings along the path of each attribute. A colour difference in *CIECAM*$_{02}$'s colour space is based on the attributes 'J' (correlate for lightness), 'C' (correlate for chroma), and 'h' (measure of hue in hue-angle), which were transformed by integration into Euclideanised 'J^E', 'C^E', and 'h^E' as given in *Equations 88ff*.

Eqs. 88ff:

$$J^{\mathrm{E}} = 0.99 \cdot \frac{200}{\sqrt{2}} \arctan \frac{\sqrt{2.5}}{100} \cdot \mathrm{J},$$

$$C^{\mathrm{E}} = 0.94 \cdot 50 \ln\left(1 + 0.02\mathrm{C}\right),$$

$$h^{\mathrm{E}} = \mathrm{h},$$

$$a^{\mathrm{E}} = C^{\mathrm{E}} \cos\left(h^{\mathrm{E}}\right), b^{\mathrm{E}} = C^{\mathrm{E}} \sin\left(h^{\mathrm{E}}\right),$$

$$\Delta E_{\mathrm{Euclidean}} = [(\Delta J^{\mathrm{E}})^2 + (\Delta a^{\mathrm{E}})^2 + (\Delta b^{\mathrm{E}})^2]^{1/2}, \text{ where}$$

the scalar values '0.99' and '0.94' were optimised to compress mainly the chroma scale for minimising the performance factor 'PF/3', and the average maximum disagreement 'MD', between a weighted- and Euclideanised equation. The disagreement values were '2.0%' and '1.02%', respectively. The formula performed similar or slightly better than CIEDE2000's formula for all employed datasets. Both formulae require comprehensive calculations prior to applying a simple Euclidean formula as given in *Equations 89ff*. The reader may be redirected to Thomsen's model[156], where the integration is applied directly to CIELAB's 'a^*b^*' - axis.

2.17 Parametric factors

2.17.1 Parametric factors are introduced when experimental conditions, in which observer judgements are obtained, differ significantly from those that are unambiguously described as reference conditions. A significant factor as such is described as one that changes the sensitivity of colour difference discrimination of an observer significantly in relation to some reference conditions. Once sufficient information is collected from two experimental conditions (phases according to some attributes against a reference phase), a correction factor for the change in colour difference perception is quantified as described mathematically in *Equation 90* and *91*. The parametric factor 'k_E' describes an overall factor that either reduces or enlarges a reference colour difference value calculated from a colour difference formula ('ΔE').

Eq. 89: $$\Delta E' = \Delta E / k_E,$$

Eq. 90: $$k_E = \frac{\sum_{i=1}^{N}(\frac{\Delta V_R}{\Delta V_T})}{N},$$

Eq. 91: $$k_E = \frac{\sum_{i=1}^{N}(\frac{\Delta V/\Delta E_R}{\Delta V/\Delta E_T})}{N},$$ where

'ΔV_T' and 'ΔV_R' refer to visual colour difference predictions obtained from a test and a reference experimental setup, respectively. If, for instance, for experimental reasons (i.e. physical sample pair reproduced on a display) numerical 'ΔE' units differ to some extent in both conditions, then *Equation 91* can be used to determine a parametric factor. This factor refers then to differences in ratios of visual against numerical colour differences for two sets. On the other hand, if numerical colour difference values ('ΔE') for both conditions and sample pairs are the same, then only visual results 'ΔV' are needed to determine an overall factor. The sum of parametric factors for all (ideally matched) pairs are then divided by the number of pairs ('N') so to derive an average that can be applied across all calculated or predicted colour difference values for sample pairs seen in those reference conditions. The concept of an overall factor can also be extended and applied to each individual colour difference scale attribute so that either 'ΔL^*', 'Δa^*', 'Δb^*', or metric chroma 'ΔC_{ab}' and 'ΔH_{ab}' are compared with each other. A parametric factor for the reference conditions should ideally result in a value of '1'. The general form of formulae including parametric factors is described in *Equations 84ff*.

Eq. 92ff: $$\Delta E' = [(\Delta L^*/k_L)^2 + (\Delta C^*_{ab}/k_C)^2 + (\Delta H^*_{ab}/k_H)]^{1/2},$$

$$\Delta E' = [(\Delta L^*/(k_L)^2 + \frac{(\Delta a^*)^2+(\Delta b^*)^2}{k^2_{CH}}]^{1/2},$$

$$\Delta E' = \frac{1}{k_E}[(\Delta L^*/k_L)^2 + (\frac{\Delta C^*_{ab}}{k_C})^2 + (\frac{\Delta H^*_{ab}}{k_H})^2]^{1/2},$$ where

'k_L', 'k_C' and 'k_H' refer to parametric factors for each metric colour difference scale direction, and 'k_{CH}^2' is described as a parametric factors for total chromatic differences. The assumption is made that parametric factors do not change the Euclidean form and structure of the formula, according to CIE 101:1993[126]. Parametric factors larger than '1' indicate a loss, and factors smaller than '1' indicate a gain in sensitivity, according to *Equation 90* and *91*.

2.17.2 Experimental conditions may vary according to mainly two types of parameter; (**1**) due to human factors (psychophysical) inherent in the inspection of colour samples, and (**2**) due to physical changes (stimuli and optical system) in the presentation of colour samples. Human factors are described as those;

(**1a**) caused by the human visual system that is less sensitive to very high frequency, spatial, and temporal differences as described by Kaiser and Boynton[335];

(**1b**) caused by simultaneous contrast when a colour is surrounded by other colours so to become lighter when seen against darker backgrounds, or darker when seen against lighter backgrounds; red induces green, blue induces yellow (chromatic induction), and vice versa according to Fairchild[336];

(**1c**) caused by the crispening effect that increases the perceived magnitude of a colour difference pair when the background, on which two samples are presented, are of similar colour as, for instance, described by Semmelroth[181], Xin[337], Cui[338].

(**1d**) caused by spreading when a colour blended in with the background but was still discrete and visible, as described by Chevreul[339],

(**1e**) caused by a shift of hue towards blue or yellow once luminance changes for monochromatic light shorter or longer than 500 nm (up to - 30 nm shift); this known as the Bezold-Brücke hue shift,

(**1f**) caused by the perception of hue changes when a white light is added to a monochrome stimuli (Abney effect),

(**1g**) caused by the Helmholtz-Kohlrausch effect (brightness increase with saturation),

(**1h**) related to the Hunt effect (perceptual colourfulness increases with luminance for same chromaticity),

(**1i**) related to Stevens effect (contrast increases with luminance),

(**1j**) known as the Helson-Judd effect (lighter achromatic surfaces take on colour of illuminant whereas darker achromatic surfaces take on complementary colour of illuminant colour, as described by Fairchild[340].

2.17.3 Physical changes were classified as those;

(**2a**) caused by the sample size as shown by Brown[89] resulting in a recommendation of using two different types of observer (2° and 10° Standard Observer as recommended by the CIE[274]),

(**2b**) caused by the separation of colour difference sample pairs where the distance between two samples affected the judgment of threshold and small colour differences, according to Sharpe and Wyszecki[341]; also they reported that lightness discrimination is more affected than chromaticity discrimination,

(**2c**) caused by the illumination level and light source temperature,

(**2d**) caused by the surface structure (texture) that changed the colour difference perception, according to Kansi *et al.*[342] and Xin *et al.*[343]. The texture of textile samples and their diffuse dividing line reduced colour discrimination (higher tolerance value especially for lightness differences) compared to homogeneous paint surfaces with sharp lines as described by the CIE[126].

Parametric effects that were of interest during this project were related to background colour, sample size, spreading effects, and surface structure of the samples ('1c', '2a', '1d', '2d')

2.18. Ellipses and ellipsoids

2.18.1 A colour discrimination ellipsoid or ellipse can represent a contour of perceptually equal colour differences distributed in all directions from a standard colour centre in a particular colour space. The prediction performances of existing colour difference formulae can be determined by plotting them, for instance, against those ellipses or ellipsoids that are constructed from experimental results. If 'ΔE_{eli}' or 'ΔE_{elo}' (distance from a centre to the boundary of an ellipse or ellipsoid, respectively) is taken as a constant value (for instance, '1') then defining those surfaces for various colour centres in CIELAB's colour space can be accomplished by using *Equation 93* and *94*. The original definitions[344] for ellipses and ellipsoids formulae, as described by Melgosa *et al.*[345], were altered so that 'Δx', 'Δy', 'ΔY' and original coefficients 'g_{ff}' where replaced by CIE L^* a^* b^*'s 'Δa^*', 'Δb^*', and 'ΔL^*' - values, respectively.

Eq. 93: $$\Delta E_{\mathrm{el}} = \sqrt{b_{11}(\Delta a_{\mathrm{i}}^*)^2 + 2b_{12}\Delta a_{\mathrm{i}}^*\Delta b_{\mathrm{i}}^* + b_{22}(b_{\mathrm{i}}^*)^2}$$

Eq. 94:

$$\Delta E_{\mathrm{elo}} = \sqrt{b_{11}(\Delta a_{\mathrm{i}}^*)^2 + 2b_{12}\Delta a_{\mathrm{i}}^*\Delta b_{\mathrm{i}}^* + b_{22}(\Delta b_{\mathrm{i}}^*)^2 + 2b_{13}\Delta a_{\mathrm{i}}^*\Delta L_{\mathrm{i}}^* + 2b_{23}\Delta b_{\mathrm{i}}^*\Delta L_{\mathrm{i}}^* + \mathrm{b}_{33}(\Delta L_{\mathrm{i}}^*)^2},$$

where 'ΔL^*', 'Δa^*', 'Δb^*' refer to the difference between measured standard sample's coordinates and associated visual or numerical results. Ellipsoid or ellipse's parameter such as semi major axis ('A'), semi minor axis ('B'), ratio between semi-major and semi-minor axis ('A/B'), orientation angle ('θ'), and ellipses area ('πAB') can be used to describe and contrast them. Experimental visual results 'ΔV', or calculated results from a colour difference formula 'ΔE', are related to 'ΔE_{eli}' or 'ΔE_{elo}' from an ellipsoid or ellipse equation by varying coefficients '$b_{11\text{-}13,\,23,\,33}$' until they fit those results with a minimum of error.

2.18.2 An optimisation technique is normally employed so to minimise those fitting errors, for instance, in the form of the 'sum of squares' between '$\Delta E_{eli,elo}$' and 'ΔV' for each colour centre[346] as mathematically described in *Equation 95*.

Eq. 95: $S^2 = \sum_{i=1}^{N}(\Delta V_i - \Delta E_i)^2$, where

'N' refer to the number of sample pairs distributed around a colour centre. Other formulae can be used to minimize the error such as suggested by Robertson[125] and Friele[347]. Other least square methods (algebraic or geometric) were employed in digital pattern recognition, for instance, by Fitzgibbon *et al.*[348] so to provide least square error minimisation constrained to fit a conic into an ellipse. The coefficients for a simplified ellipsoid- '$b_{11,\,12,\,22,\,33}$' and ellipse equation '$b_{11,\,12,\,22}$' are defined as given in *Equations 96ff.*

Eq. 96ff: $b_{11} = \frac{cos^2\theta}{A^2} + \frac{sin^2\theta}{B^2}$, and $b_{12} = \left(\frac{1}{A^2} - \frac{1}{B^2}\right)\sin\theta\cos\theta$,

$b_{22} = \frac{sin^2\theta}{A^2} + \frac{cos^2\theta}{B^2}$, and $b_{33} = \frac{1}{C^2}$, where

'A' and 'B' refer to the ellipse and ellipsoid's semi-axes, 'θ' refers to the angle of orientation here inclined in relation to CIELAB's 'a^*' axis, and 'C' refers to the 'lightness' - axis in regards to an ellipsoid. 'A', 'B', 'C', and 'θ' can be determined mathematically by known parameter 'b_{11}', 'b_{12}', 'b_{22}', and 'b_{33}' as described in *Equations97ff.*

Eq. 97ff: $A = \frac{1}{\sqrt{b_{12}+b_{22}\cot\theta}}$, and $B = \frac{1}{\sqrt{b_{11}-b_{12}\cot\theta}}$,

$C = \frac{1}{\sqrt{b_{33}}}$, and $\theta = \frac{1}{2}tan^{-1}(\frac{2b_{12}}{b_{11}b_{12}})$, where

the angle 'θ' is smaller than '90°' when the value of 'b_{12}' is smaller than '0', and when the angle 'θ' is larger than '90°' when the value of 'b_{12}' is greater than '0'. The values for the coefficients 'b_{11ff}' vary with visual results, according to Wyszecki and Stiles[349].

2.19 Performance measure for colour difference formulae

2.19.1 Statistical measures were introduced for quantifying the performances of colour difference formulae by comparing visual with predicted results from human observations. These measures are generally used either;

(**1**) to describe the relationship (linear correlation or strength) between two variables (for instance, data from numerical and visual colour difference judgements) and also to predict one variable with another,
(**2**) and/or for determining the magnitude of differences between predicted and experimental data in the form of an overall factor,

(**3**) to determine whether one formula predicted colour differences significantly better than another for a specific dataset,

(**4**) or to determine which of the individual components within a formula has a significant influence on the overall prediction results.

2.19.2 Basic, but important characteristics in data are associated with; the centre value of a dataset (average or median), the variation (variance or standard variation) as a measure of spread within a data set, the distribution characteristic of a dataset (bell shaped, skewed, kurtios, multinomial distribution, etc), the concept of outliers, and time (BS ISO[350,351]). The main distinctive difference between choices of statistical methods depends on the characteristic of the data. Mainly parametric or non-parametric tests can be used for describing and analysing data. The assumptions that need to be met for using parametric statistical test are associated with (**a**) normal distributed data, (**b**) homogeneity of variance, (**c**) interval data, and (**d**) independence of data, according to Field[352].

2.19.3 Observers are normally asked to scale colour differences during psychophysical experiments, for instance, by judging a pair of sample that varies in one of the three colour attribute scales, until their perception matches one of the steps in a grey scale. Those scaled visual results refer to 'ΔV' - values (scaled by the numerical colour difference values of a chosen grey scale step). The description of the relationship between 'ΔV_i' and 'ΔE_i' can be then obtained from a graph of paired data by plotting a regression line. This line is generally of linear form (but can come in different forms depending on the relationship, for instance, when a quadratic form describes a non linear curved relationship) with an intercept 'b_0' and a slope 'b_1'. A regression line is mathematically described as in *Equations 98ff*. This equation can then be used to predict 'ΔV_p' from calculated 'ΔE_i' - values.

Eqs. 98ff: $\Delta V_{\mathrm{p,i}} = b_0 + b_1 \Delta E_{\mathrm{i}} + \varepsilon_{\mathrm{i}}$,

$$b_1 = \frac{\mathrm{n}(\sum \Delta E_{\mathrm{i}} \Delta V_{\mathrm{i}}) - (\sum \Delta E_{\mathrm{i}})(\sum \Delta V_{\mathrm{i}})}{\mathrm{n}(\sum \Delta E_{\mathrm{i}}^2) - (\sum \Delta E_{\mathrm{i}})^2},$$

$$b_0 = \Delta \overline{V} - b_1 \Delta \overline{E},$$

Eq. 99: $$S_{\mathrm{e}} = \sqrt{\frac{\sum (\Delta V_{\mathrm{i}} - \Delta V_{\mathrm{P,i}})^2}{\mathrm{n-df}}},$$

Eqs. 100ff: $\Delta V_{\mathrm{P},1} - \mathrm{E} < \Delta V_{\mathrm{i}} < \Delta V_{\mathrm{P},1} + \mathrm{E}$,

$$E_{\mathrm{i}} = t_{\alpha/2} S_{\mathrm{e}} \sqrt{1 + \frac{1}{\mathrm{n}} + \frac{\mathrm{n}(\Delta E_{\mathrm{i}} - \Delta \overline{E})^2}{\mathrm{n}(\sum \Delta E_{\mathrm{i}}^2) - (\sum \Delta E_{\mathrm{i}})^2}},$$ where

'ε_i' refers to the error between predicted '$\Delta V_{\mathrm{p,i}}$' and regressed 'ΔE_{i}' - values from any formula and colour discrimination data set. The standard error (or spread) 'S_{e}' of predictions '$\Delta V_{\mathrm{p,1}}$' from *Equations 98ff* compared to observed data is explained in *Equation 99*; 'df' refers to 'degrees of freedom', 'n' refers to the total number of sample pairs, the prediction interval (*Equations 100ff*) for one observed value of 'ΔV_{i}' is calculated by determining 'E_{i}' using the associated 'ΔE_{i}'- value, whereas '$t_{\alpha/2}$' (two tailed) refers to a test statistic value 't' for 'n-2' degrees of freedom (value can be obtained from statistical tables). The best fit for a regression line can be found by a method of least squares that minimizes the sum of the squares from the values of the vertical differences between regression line and 'real' observed 'ΔV_{I}' - values. The sum of these squared values provides an overall measure as such describing the goodness of fit; the individual differences between pairs of data are known as residuals 'r_{U}' (unexplained deviation from a regression equation). This concept can be extended to each of the colour scale attributes, for instance, when used to determine tolerance limits when a linear relationship between observed and calculated scale differences in lightness, chroma, and/or hue is present in a dataset.

2.19.4 Modelled '$\Delta V_{\mathrm{p,i}}$' - values are also compared with the mean observed value '$\Delta \overline{V}$' for a dataset so to determine the explained deviations 'r_{E}' by a regression equation in relation to the simplest model in the form of the mean value for all observations. The total variation 'r_{T}' in regards to the mean is given either (**1**) by the sum of the squared explained 'r_{E}' and unexplained deviation 'r_{U}', or (**2**) by the sum of the squared values from the differences between mean '$\Delta \overline{V}$' and observed 'ΔV_{i}' data points. A useful measure is derived by division of 'r_{E}' with 'r_{T}', as described by Triola[353], resulting in a percentage measure of 'r_{E}' as described with *Equation 101*. The term '$r^2_{\mathrm{E\%}}$' explains the variation in the outcome described by the model compared to the mean. For simple regression equations a square root of '$r^2_{\mathrm{E\%}}$' provides a correlation coefficient 'r_{c}' (*Equation 102*).

Eq. 101: $r_{E\%}^2 = (\frac{r_E}{r_T}) \cdot 100,$

Eq. 102: $r_C = \sqrt{(\frac{r_E}{r_T})},$

Eq. 103: $F_t = \bar{r}_E / \bar{r}_U,$

2.19.5 Another use of sums of squared values is to describe the characteristics of a prediction model with the use of the Fisher test statistic 'F_t'. It provides a ratio value between improved predictions and the unexplained deviations from the model as described in *Equation 103*. The mean values are used with appropriate degrees of freedom. A good model should result in a large 'F_t'- value. However, prediction performances from two formulae can also be contrasted, for instance, to determine whether one formula performs significantly better than another as described in *Equation 104*. Important is the fact that 'F' – tests require normal distributed residual data for results to be meaningful, or a sufficient number of paired data points (so to assume the requirement of normality). Alternatively, methods known as 'Count Five' or 'Levene-Brown-Forsythe' can be used for comparing variances.

Eq. 104: $F_t = \frac{\sum(\Delta V_1 - \Delta V_{p,1})^2/N-2}{\sum(\Delta V_1 - \Delta V_{p,2})^2/N-2}$, where

'ΔV_1' refers to the observed colour difference value for a particular observation and data set, '$\Delta V_{p,1}$' and '$\Delta V_{p,2}$' refer to modelled colour difference values from two different formulae as described in *Equation 98ff*, respectively. The critical test statistic 'F_{crit}' for each test can be taken from statistical tables, for instance, as described by Alman[354].

2.19.6 Other measures, which describe the relationship between visual and predicted values, were given by Schultz[355], who introduced a measure of variance 'V_{ab}' (*Equations 105ff*); a similar measure is known as the 'Spearman's rank correlation test'; Coats *et al.*[356] used a statistical measure independent of a particular unit known as the coefficient of variation 'CV' in a 'scaled form' by introducing a factor to minimise the difference between 'ΔV' and 'ΔE' (*Equation 106ff*) and a gamma factor ('γ') as described in *Equation 107*[357] (decimal instead of natural log was used at times), a combined performance measure 'PF/3' (*Equation 108*), and STRESS measure (*Equation 109*) related to multidimensional scaling.

Eq. 105ff: $V_{ab} = \sqrt{\frac{1}{N}\sum_{i=1}^{N} \frac{(\Delta E_i - F\Delta V_i)^2}{\Delta E_i \cdot F\Delta V_i}}$, where

$$F = \sqrt{\frac{\sum_{i=1}^{N} \frac{\Delta E_i}{\Delta V_i}}{\sum_{i-1}^{N} \frac{\Delta V_i}{\Delta E_i}}}$$

Eq. 106ff: $\mathrm{CV} = \frac{\sqrt{\frac{1}{\mathrm{N}}\sum_{\mathrm{i}=1}^{\mathrm{N}}(\Delta E_{\mathrm{i}} - \mathrm{f}V_{\mathrm{i}})^2}}{\Delta \bar{E}_{\mathrm{i}}} \cdot 100$, where

$\mathrm{f} = \frac{\sum_{\mathrm{i}=1}^{\mathrm{N}}(\Delta E_{\mathrm{i}} \cdot \Delta V_{\mathrm{i}})}{\sum_{\mathrm{i}-1}^{\mathrm{N}}(\Delta V_i)^2}$,

Eq. 107: $\ln(\gamma) = \sqrt{\frac{1}{\mathrm{N}}\sum_{\mathrm{i}=1}^{\mathrm{N}}[\ln(\frac{\Delta E_{\mathrm{i}}}{\Delta V_{\mathrm{i}}}) - \ln(\frac{\overline{\Delta E_{\mathrm{i}}}}{\Delta V_{\mathrm{i}}})]^2}$,

Eq. 108: $\mathrm{PF3} = 100(\gamma - 1 + V_{\mathrm{ab}} + \frac{\mathrm{CV}}{100})/3$,

A 'PF3' value would approach zero for a perfect agreement between observed and predicted colour differences for any formula and dataset. A 'PF3' value of '20' was said to indicate an average overall disagreement figure of 20% between observed and predicted data.

2.19.7 An alternative method for comparing performances for different colour difference formulae was introduced by Garcia *et al.*[358]. This method is known as the 'STRESS' measure referring to the index of 'standardized residual sum of squares'. The main advantage of using 'STRESS' instead of 'PF/3' is described as the advantage of applying a Fisher – test ('F_{t}') directly to squared STRESS values for two different colour difference formulae.

Eq. 109ff: $\mathrm{STRESS} = 100 \cdot (\frac{\sum(\Delta E_{\mathrm{i}} - \mathrm{F}\Delta V_{\mathrm{i}})^2}{\sum F^2 \Delta V_{\mathrm{i}}^2})^{1/2}$,

$F_1 = \frac{\sum \Delta E_{\mathrm{i}}^2}{\sum \Delta E_{\mathrm{i}} \Delta V_i}$, where

'F_1' describes a factor minimizing the differences between predicted 'ΔE_{i}' and observed 'ΔV_{i}', respectively. Recently, the authors also recommended using STRESS to determine (**1**) intra-observer and (**2**) inter-observer variability (observer's own repeatability and observer's accuracy compared to the mean value for all observers, respectively). Melgosa *et al.*[359] suggested to use STRESS including a scaled 'F' – term for determining the inter-observer variability (**1**), and not a value of 1, as some researchers suggested so far. The calculations for both measures (**1**) and (**2**) are given as in *Equation 110ff*.

Eq. 110ff: $\mathrm{Intra} = 100 \cdot (\frac{\sum(\Delta V_1 - \mathrm{F}\Delta \bar{v}_2)^2}{\sum F^2 \Delta \bar{v}_2^2})^{1/2}$, where

$\mathrm{F} = \frac{\sum \Delta V_1^2}{\sum \Delta V_1 \Delta V_2}$, (alternatively, F = 1)

$\mathrm{Inter} = 100 \cdot (\frac{\sum(\Delta V_{\mathrm{i}} - \mathrm{F}\Delta \bar{v}_{\mathrm{i}})^2}{\sum F^2 \Delta \bar{v}_2^2})$, where

$\mathrm{F} = \frac{\sum \Delta V_{\mathrm{i}}^2}{\sum \Delta V_{\mathrm{i}} \Delta \bar{v}_{\mathrm{i}}}$

'$\Delta \bar{v}_i$' describes the mean observed value from a group- or a set of repetition observations.

2.19.8 Kirchner and Dekker[360] questioned whether STRESS is an appropriate alternative for evaluating colour difference formula performances. The main argument is that STRESS implies

a restricted regression model with a line passing through the origin (zero). However, it has been shown that greyscale measurements may deviate from such kind of origin, for instance, caused by the design limitations between the 'Grade Standard' and 'Grade 5'. Often, measurements between both batches do not result in the same colorimetric specification (a monitor based grey scale may introduce variations caused by spatial non-uniformity across the display). Also, some stimuli may need a certain threshold value until the visual system recognises a change in colour difference scales. Those cases suggested using an intercept to correct for non-zero origins. The authors generally recommended to use scatter diagrams and a standardised product moment correlation coefficient as described in *Equation 102* or *111*[361,362].

Eq. 111: $$r = \frac{\sum[\frac{(\Delta E_i - \Delta\bar{E})}{S_{\Delta E}} \cdot \frac{(\Delta V_i - \Delta\bar{V})}{S_{\Delta V}}]}{n-1}$$, where

'$S_{\Delta E}$' and '$S_{\Delta V}$' refer to the standard deviation for all 'ΔE' and 'ΔV' paired samples for a particular sample set. A test statistic 't' can be found as described in *Equation 112*; critical values for 't' can be found in statistical tables[363].

Eq. 112: $$t = \frac{r}{\sqrt{\frac{1-r^2}{n-2}}}$$

This project required testing (*Experiment A*, *C*, and *D*) as such to determine whether the same modelled colour difference magnitudes but judged in different presentation modes (in the form of a 'Single Needle Lockstitch', 'Buttonhole stitch type', or 'Thread Winding Card' sample) resulted in the same visual colour difference values. Hence, the hypothesis 'H_0' tests for equality of the observations from the same observer group for different presentation modes. Also, equality is tested for two different observer groups (*Experiment B* and *C*; naive and professional observers) judging the same 'Single Needle Lockstitch' data set.

2.19.9 The first method, which can be used to determine whether there is a significant difference in perception of colour differences due to the variation in sample presentations, is known as the 'paired t – test' (dependent matched pairs). The requirements are that; (**1**) samples were drawn randomly from a population and, (**2a**) that either the number of matched pairs is large (n > 30) or (**2b**) that the differences between matched pairs is following approximately a normal distribution. The hypothesis test statistic for matched pairs is given in *Equation 113.*

Eq. 113: $$t = \frac{\bar{d} - \mu_d}{\frac{S_d}{\sqrt{n}}}$$, where

the degrees of freedom is equal to 'n-1', '$\bar{d}$' refers to the mean value of the differences 'd' for all matched pairs, 'μ_d' refers to the mean value of differences 'd' for the population for all matched pairs (equals 0 for null hypothesis), 'S_d' standard deviation of differences 'd' for the paired data

set, and 'n' refers to the number of samples pairs. 'P' – and critical '$t_{\alpha/2}$' – values can be found in statistical tables and confidence intervals can be derived from *Equations 114ff.*

Eq. 114ff: $\bar{d} - E < \mu_d < \bar{d} + E$, where

$$E = t_{\alpha/2} \frac{S_d}{\sqrt{n}}$$

2.19.10 When two different groups (for instance, professional observer against naive observers as employed in *Experiment B* and *C*) are asked to judge the same sample pair selection, statistical inference is obtained from a two sample 't-test'. The requirements are; (**1**) that the populations standard deviation '$\sigma_{1,2}$' are not known, (**2**) that the samples are independent and randomly chosen, (**3a**) and either both samples sizes are large (n > 30), or (**3b**) come from normal distributed data (approximation). The hypothesis test statistic for two means and independent samples are described in *Equations 115ff.*

Eq. 115ff: $t = \frac{(\bar{x}_1 - \bar{x}_2) - (\mu_1 - \mu_2)}{\sqrt{\frac{S_1^2}{n_1} + \frac{S_2^2}{n_2}}}$, where df equals

$$df = \frac{(A+B)^2}{\frac{A^2}{n_1 - 1} + \frac{B^2}{n_2 - 1}}, \text{ and}$$

$$A = \frac{S_1^2}{n_1}, B = \frac{S_2^2}{n_2}, \text{ where}$$

'$S_{1,2}$'refer to the standard deviation for each data set, 'P' – and critical values can be obtained from statistical tables. The confidence interval estimates of two independent samples are calculated as described in *Equation 116ff.*

Eq.116ff: $(\bar{x}_1 - \bar{x}_2) - E < (\mu_1 - \mu_2) < (\bar{x}_1 - \bar{x}_2) + E$, where

$$E = t_{\alpha/2} \sqrt{\frac{S_1^2}{n_1} + \frac{S_2^2}{n_2}}, \text{ where}$$

degrees of freedoms 'df' is described as in *Equations 116ff*. For large sample sizes 'Z' – test statistic can be used since the central limit theorem states, according to Hughes and Hase[364], that a sample distribution are expected to be normal distributed once the number of samples exceeds thirty.

2.19.11 A *non- parametric* test is used instead when a sample distribution is not normal distributed. Either, the 'Wilcoxon's signed rank test' for matched pairs of samples, or 'Wilcoxon's rank sum test' for a two sample t-test, are methods that can be used to determine for equality of medians, as described by Triola[365]. For the determination of mean visual colour difference values 'ΔV' for a particular colour sample pair and experiment, measures were implemented either to identify outliers for each individual colour difference pair (in those cases outliers were replaced by average values according to *Chauvenet's criterion*[366]).

Chapter 3:

3.1 *Experimental*: General considerations

3.1.1 The project was divided into four experiments. The focus of the first experiment (*Experiment A*) was to contrast visual responses that were obtained from two different sample type presentations. Both data sets described the same numerical colour differences. The number of physical samples, which were available for judging colour differences, was limited. It was therefore decided to obtain visual data from two, grey and blue, colour centres[hh] so to; (**1**) establish whether there is a difference in colour perception when judgements are obtained from Thread Winding Cards ('TWC') or Buttonhole Stitch type samples ('BH'), and (**2**) to reproduce both datasets on a digital screen for (**a**) verifying those results obtained from physical samples in (**1**), and also (**b**) to correlate visual colour difference results from physical samples with results obtained from digital reproductions. The blue and grey colours were the latest improvement in formula design and as such used for comparison reasons (CMC/$CIEDE_{2000}$).

3.1.2 The second experiment (*Experiment B*) was limited in regards to the numbers and time professional observers (twelve participants) were available for attending psychophysical experiments. That was the main reasons why just one type of sample set was used for that experiment. The set consisted of synthesized 'digital' thread sewn into fabric samples (Single Needle Lockstitch – 'ST'). Batch samples were designed around ten colour centres either varying in lightness and/or chromaticity. All experimental results were then used to establish whether perceptual colour differences obtained from Single Needle Lockstitch samples were significantly different when they were compared with their associated calculated colour difference values obtained from several formulae. Also, it was of interest to compare colour difference formulae in terms of their prediction performances before and after optimisation of parametric factors and various other parameters.

3.1.3 The third experiment (*Experiment C*) consisted of three different digital sample data sets ('ST', uniform 'TWC', 'BH'), all sample pairs displaying the same modelled colour differences to human observers. Visual data were obtained from naïve observers for six colour centres with batches either varying in lightness and/or chromaticity. Also, the results obtained from *Experiment C* for 'ST' – samples were compared with those results that were established during *Experiment B*. The results were also used to determine whether there are differences in perceptual judgements of colour difference sample pairs between professional and naive observers.

[hh] page 37

3.1.4 The fourth experiment (*Experiment D*) was designed to verify results from *Experiment A – C* in terms of; (**a**) whether differences in human perception can be caused by the sample presentation for either physical ('BT', 'ST', 'TWC') and also synthesized digital samples ('BH', 'ST'), and (**b**) to verify results in (**a**) by using captured images from a digital camera for the same 'ST' and 'BH' samples (back up verification for synthesized method)) as to verify all observed experimental trends during this project. Finally, it was of interest to determine whether the direction of their presentations to the observer has had a significant influence on the perception of colour differences (directional parametric effect).

3.2 Psychophysical layout

3.2.1 The experimental setup for *Experiment A, B,* and *C* followed generally the outline as described in *Graph 1* (samples were judged in a viewing cabinet, and their digital reproductions were viewed on a digital screen). A grey scale according to 'ISO 105-A02:1993' was used during *Experiment D* for scaling perceptual colour differences in regards to physical samples observed in a viewing cabinet. Five grey scale fabric cotton patches were used in *Experiment A* for scaling physical samples in a viewing cabinet. Absolute CIE '$XYZ_{L,10}$' – tristimulus values for the grey background colour, and all physical samples that were measured in the viewing cabinet in *Experiment D*, were also reproduced in absolute terms on a digital screen for psychophysical experiments, respectively. A standard and batch colour sample in this context refers either to a 'TWC', 'UNI', 'BH', or 'ST' colour difference sample pair in physical- or digital form.

3.2.2 Each observer was asked to find a grey 'GRADE' batch sample ('G B') that together with the 'Grey Standard' sample ('STD G') formed a difference pair that was required to be perceptual similar in comparison to a colour difference sample pair ('STD' and 'B'). The wording and instructions for scaling colour difference pairs for all datasets with the aid of a greyscale were generally given in written form to each observer before starting each session as follows:

Wording:

"Given a thread sewn into a fabric sample that forms a colour difference pair (between thread and underlying fabric) you are required to quantify those differences with the aid of a grey scale. The grey scale in front of you consists of a grey standard sample (STD) and five grey GRADE samples (GRADE 1 – 5).

You are subsequently asked to scale and contrast a visual colour difference, which are presented as either a 'Single Needle Lockstitch – ST', 'Uniform Patch – UNI', 'Buttonhole – BH', or 'Thread Winding Card –TWC' sample pair, using the grey STD and one of the grey

'GRADE' samples until the visual differences for both sample pairs appear to be the same (or very similar) to you.

If you think that a visual colour difference value for a colour sample pair is perceived inbetween two GRADE values – then specify your chosen value as such. You can use decimal numbers so to fit them exactly with your visual perceptions.

***For example**: You should specify a decimal value between GRADE 3 and 4 (for instance '3.5') once a perceived visual difference between GRADE 4 and the grey standard sample appears to you smaller, and the difference between GRADE 3 and the standard sample appears to be larger to you, if compared with a colour difference pair that is to be matched. Please, do not hesitate to ask if you have got any questions.*

***Graph 1*: The arrangement of a grey scale and colour difference images displayed against a grey background (L^* 50) for psychophysical experiments as used during this project. A standard colour ('STD'), batch colour ('B'), standard grey ('STD G'), and batch GRADE ('B G') samples were randomly interchanged in regards to their locations on the screen. The difference in contrast between 'STD G' and one of the 'GRADES' were largest for 'GRADE 1', and the contrast was the same for 'GRADE 5'. 'STD' and 'B' colour sample pairs were either replaced by 'BH', 'ST', 'TWC' or 'UNI' (uniform) colour samples.**

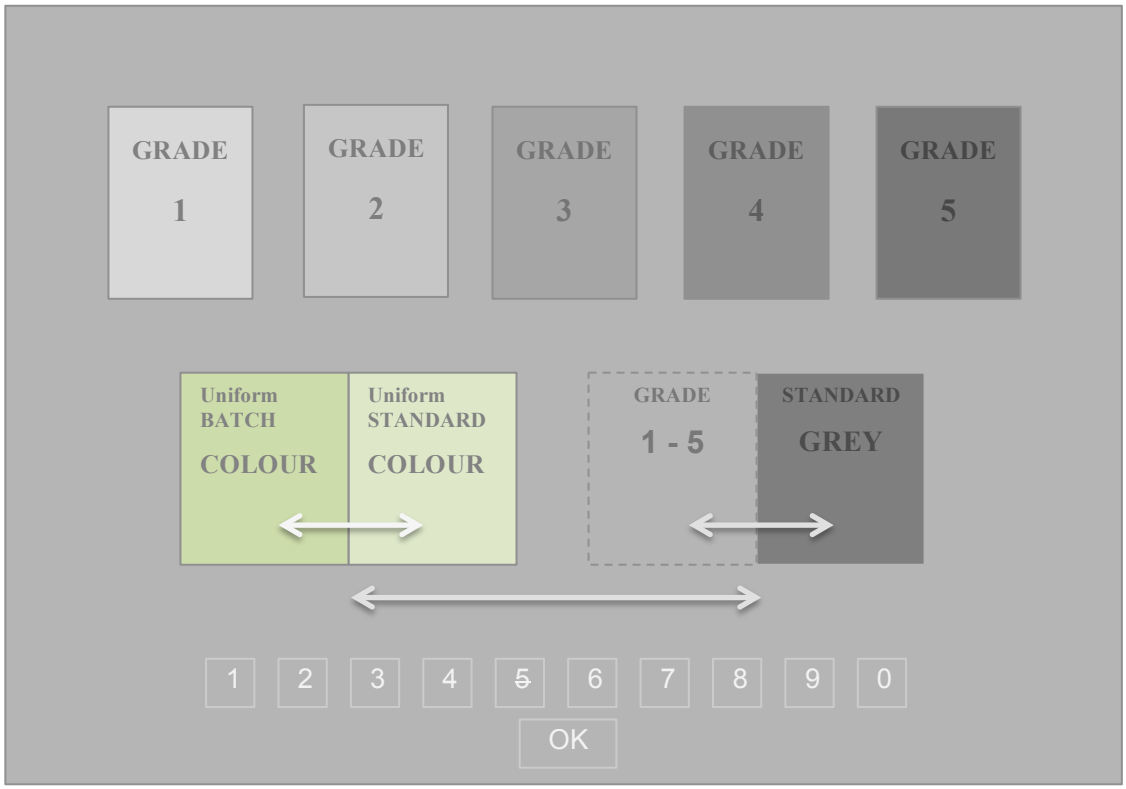

3.2.3 Observer's judgements, which were obtained from psychophysical experiments with physical samples viewed in a cabinet, were verbally communicated and recorded in Excel. All sample pairs were presented to each observer in random order (Excel function '*rand*' and

'*randbetween*') avoiding any possible biases caused by the locations of 'STD', 'B', 'STD G', and 'B G' samples within the cabinet and viewing field.

3.2.4 Observers specified their GRADE judgements for digital colour difference samples using the software environment on a digital screen as given in *Graph 1*. They were asked to click the appropriate button on screen once a GRADE decision was made, and a second time for specifying any decimal places, if necessary. At this stage, it was possible to correct an entry, but once the 'OK' button was pressed, a GRADE value was permanently stored into the computer's storage system. The sample and greyscale patches were again randomly presented to each observer and experiment in terms of sequence and position on screen. Each experiment was constrained to a time limit of no longer than '45' minutes. Observers were advised to take their time to ascertain their decisions but to act in a timely manner once they had done so.

3.2.5 Training was provided in the form of a mock test run ('20' – '30' randomly chosen samples) for each observer for both physical and digital samples so to ensure that they were adapted to the experimental environment and to make them familiar with the procedure, especially in terms of how to provide 'GRADE' values verbally to the presenter, or in digital form by entering values into the system with the aid of a software. Also, it was of importance to adjust the height of the chair in front of the screen for each observer until the axis of transmitted light from the images reproduced on screen was perpendicular in regards to observer's eyes. They were asked to keep their position without altering their height and viewing angle during each experimental session. The same procedure in terms of height and position was applied for each observer for judging physical samples in the viewing cabinet. A random presentation order was applied for each observer and session; all four sample's resting positions were marked and fixed so to avoid any prejudices caused by the variation in terms of location and/or any spatial influences caused by the fixed position of the light source and change in viewing angle.

3.2.6 Observers were also screened for colour deficiency at the start of their experimental phase. Either the 'Ishihara-' (*Experiment A* and *D*) and/or the 'Farnsworth-Munsell 100 Hue – test' (*Experiment C* and *D*) was used to determine any possible deviations from normality in observer's colour vision. Some observers were asked to repeat the Farnsworth-Munsell test up to three times. Basic statistical description of observer's age, gender, and experiences in colour matching can be found in Chapter 4, 5, 6, and 7 for *Experiment A, B, C, and D.*

3.3 Colour measurement

3.3.1 The experimental setups required colorimetric measurements from either physical or digital samples measured in a viewing cabinet or on screen so to obtain spectral reflectance or spectral radiance values over a defined wavelength range. The measurement instruments, which

were used during those experimental preparations, were a spectrophotometer (XRITE Gretag MacBeth 7000A – see *Table 3*) for measuring physical samples, and a tele-spectroradiometer (Minolta CS1000) for measuring digital samples on screen.

	Gretag Macbeth – Color Eye 7000A	*Minolta – CS1000*
Repeatability	0.01 ΔE_{ab}	0.1 % (cd/m^2)
Spectral Range	360 – 750 nm	380 – 780 nm
Wavelength accuracy	0.1 nm	0.3 nm
Wavelength precision	0.05 nm	0.3 nm
Wavelength interval	10 nm	5 nm
Bandpass	10 nm	5 nm
Aperture	from 0.3 – 2.5 cm circular to rectangular shape	8 mm (distance 45 cm) f50 mm lens
Optical configuration	Diffuse/8° illumination/measurement	0° measurement
Measurement time	< 1 second	40 msec to 60 seconds

***Table 3*: Manufacturer's specification for (1) Minolta CS-1000 and (2) Color-Eye 7000A; Sources:**

(1) http://www.konicaminolta.com/instruments/products/display/spectroradiometer/cs1000ast/specifications.html
(2) http://www.xrite.com/documents/literature/gmb/en/gmb_7000a_manual-en_en.pdf

3.3.2 A tele-spectroradiometer (Minolta CS-1000) was tested for measurement accuracy in 2008 by the Colour and Imaging Group of Colour Science at the University of Leeds. The peak values for a red and yellow LED confirmed within two nanometres between a reference instrument (a Bentham tele-spectroradiometer) and Minolta's CS1000 tele-spectroradiometer. The average deviation from CIE's 'XYZ' – tristimulus values was '0.02', and '0.015' for 'xy' – chromaticity coordinates. A repeated measure (ten successive measurements in a short time and four measurements within 8 hours) from a white tile obtained from a spectrophotometer was well within the manufacturer's specifications ('0.008' ΔE_{ab} ±'0.005' STD).

3.3.3 All measurements and calculations that were obtained from a tele-spectrophotometer were constraint to a wavelength range from 380 to 780 in '1' nm intervals. Calculations of CIE 'XYZ_{10}' – tristimulus values were completed in accordance to CIE's guidelines[275,277,285]. A constant 'K' – factor of '683.6' was applied for the calculation of 'XYZ_{10}'- tristimulus values for the CIE 10° - degree standard observer[ii], whenever absolute photometric quantities were necessary. Calculated colorimetric tristimulus values that were limited in the wavelength range from 380 – 780 nm for some test samples were identical to those values that were obtained from distributions in the range from 360 – 830 nm for the same samples.

[ii] see page 84 for Equations 21-24

3.4 Devices

3.4.1. Mainly four devices were employed during this project. A liquid crystal display ('LCD') was used for presenting digitized and synthesized reproductions of different physical samples ('TWC', 'ST', 'BH', 'UNI') to human observers. A digital scanner was used to capture so called 'Master' texture images, which were at a later stage altered in all three important colour attribute scales, so to generate required batch samples around each standard colour centre. This was achieved either by varying the colour attributes of the thread and fabric master samples, or by changing the colour attributes of the Master 'Thread Winding Card' samples. A digital camera was used to capture 'BH' and 'ST' physical samples, which were later displayed to observers on a LCD. And, a viewing cabinet was used for displaying physical samples ('TWC', 'BH", 'ST) to human observers for determining visual colour differences. Technical specifications for all digital devices were obtained from the manufacturer's websites as summarised in *Table 4*.

3.5 LCD – General considerations

3.5.1 Liquid crystal displays ('LCD') allow light either to pass-, or prevent to pass, through various layers. The molecules of this substance are more elongated (long range order) in one or two directions for a range of temperatures. They are said to have lower free energy when they are arranged with their long axes parallel to each other. The refractive index is dependent on the directions of the molecules. The direction determines whether light is propagating along the axes or propagating perpendicular to it. Also, when molecules are placed within an electrical field, they start to polarise into electrical dipoles, changing their direction until they are aligned to an applied electrical field. The direction of two crossed polarisation filters, and the direction of liquid crystals between them, defines the amounts of light being transmitted through the various layers of a LCD display, according to Lee[367].An un-polarised light beam passes through the first filter and becomes polarised; the beam will be then twisted in its direction by liquid crystals (in the case of TN twisted nematic cells), so that the twisted light is transmitted through the second polarisation filter. Once, an electrical field is induced by a high voltage (10mV) between bottom and top plate, those twisted cells changes their directions (on – state) so to let polarised light pass them unaltered. However, this un-twisted light is now blocked by the second 'crossed' polariser in 'on' state. A pixel, the smallest part of an entire imaging area, consists of three sub pixels, generally acting as small light stimuli coloured by filters in front of them (red, green, and blue filters). Additive mixing, and controlling the strength of the electrical field for each sub pixel, can reproduce thousands of shades of colours. By addressing each pixel

separately, and given a sufficient amount of pixels defining an image area, a reproduction of real objects can be achieved as suggested by Hunt[368].

3.5.2 Various technologies are employed in liquid crystal displays; a 'SA-TFT' LCD refers to a 'self-aligned' thin film transistor liquid crystal display. This type of display is said to inhibit better image quality due to the structure of the uniform and small capacitances between gates and drain overlaps, according to Lüder[369]. The main light source in this LCD, which was used during this project, was a cold fluorescence tube[370], as described in *Figure 12*[jj].

3.5.3 Standardised methods were implemented when appropriate so to ensure objective assessment and characterisation of the LCD device for colour reproduction[371]. The method of calibration was altered as such to fit experimental requirements. Methods varied from proposed standardised methods mainly due to the position of displayed samples on a digital screen for the use in psychophysical experiments.

	LaCie 321 LCD display	***Nikon D2x(s) digital camera***	***Epson V350Photo digital scanner***
Technology	SA-TFT	CMOS DX	Color Epson Matrix CCD™ Line Sensor
Resolution (dpi)	1600 x 1200	4288 x 2848	4800
Dot pitch	0.2700 mm	0.0055 mm	0.0053 mm
Nyquist	2 cycles/mm	90 cycles/mm	94 cycles/mm
Bits depth per channel	12	12 (RAW)	16
Light	6 CCFL	*	CCFL
Luminance	250 cd/m^2	*	*
Contrast	500:1		3.2 Dmax density

***Table 4*: Manufacturer's specification for LCD display (1), digital camera (2), and digital scanner (3):**
(1) http://www.lacie.com/download/datasheet/300series_en.pdf
(2) http://www.nikonusa.com/Nikon-Products/Product-Archive/Digital-SLR-Cameras/25215/D2X.html
(3) http://files.support.epson.com/pdf/prv35_/prv35_pg.pdf

3.5.4 The characterisation of a LCD display can be generally described in two steps; (**1**) non-linear stage relating input monitor 'RGB' values to measured luminance 'Y' – tristimulus values for each primary (it is also possible to use $R_1G_2B_3$ linked directly to CIE $X_1Y_2Z_3$ – tristimulus values), and (**2**) linear stage to transform device dependent values to device independent data (in the form of CIE 'XYZ' – tristimulus values). Several models were developed. Non-linear functions can be of various forms such as of; (**a**) 'second-order polynomial', (**b**) 'logarithmic',

[jj] see page 64

(**c**) 'second – order logarithmic', (**d**) 'LUT – Tables' form[372] derived from various interpolation methods coupled with optimisation techniques, amongst others as described by Kang[373]. Recent models addressed 'crosstalk' issues between neighbouring pixels. However, all models followed generally a two-stage pattern. The voltage luminance transfer curve from some displays can also follow, according to Lee[374], a sigmoid curve. Both, lower and upper, ends of the curve often described different gamma values (steepness) making it necessary in those cases to use more elaborated functions to predict them, precisely.

3.6 Preliminary LCD testing

3.6.1 The LCD 'LaCie 321' was calibrated and tested as to determine; (**1**) the appropriate display settings in terms of contrast, brightness, sharpness, and white point that were desired to be used during this project, (**2**) how long the display needed to stabilise its output values until it produces robust and reliable results, (**3**) the voltage transfer function against a black background by varying the input 'RGB' values in steps of eight digital counts in the range from '0' – '255' for each channel, (**4**) whether and how a grey background colour (*Graph 1*) influences the colorimetric values of a reproduced image, (**5**) whether the display is producing the same colorimetric values for the same image despite its location on the screen, (**6**) whether each primary light transmission is additive in respect to a white image measured at the same location on screen, and (**7**) whether the device is able to reproduce the same colour over time.

3.6.2 Reproduced images on screen were of appropriate size in terms of viewing distance compared to their physical counterparts that were seen in a viewing cabinet. All images were measured at the same location on screen as they were seen and judged by observers. Grey scale colour differences (between 'GRADE 1 – 5' and 'Standard Grey') on screen were measured at all *four* positions and averaged giving the random order and locations of samples displayed to observers. It was also desirable to increase the peak '$Y_{10,L}$' tristimulus value as much as possible so to (**a**) avoid rod intrusion, and (**b**) to match 128odeled. magnitude of illumination in a viewing cabinet (*Experiment D*).

3.6.3 The short ('24' hours) and mid term ('96' hours) variations in luminance '$Y_{10,L}$' and chromaticity 'u'_{10}' and 'v'_{10}' for the LCD are provided in *Figure 19* and *Figure 20*. The LCD needed to warm-up for approximately '2' hours ('$Y_{10,L}$' equalled '204.38' cd/m^2 ± '0.35' STD after warming up); chromaticity coordinates values equalled '0.206' for 'u'_{10}' and '0.483' for 'v'_{10}' (with a STD of '0.0002') and remained stable during a day's work. The medium term stability (four days) for the LCD resulted in a '$Y_{10,L}$' value equal to '200.29' cd/m^2 ('0.36' '$Y_{10,L}$' STD) and '0.206' for 'u'_{10}' and '0.482' for 'v'_{10}' with a standard deviation of '0.00005'.

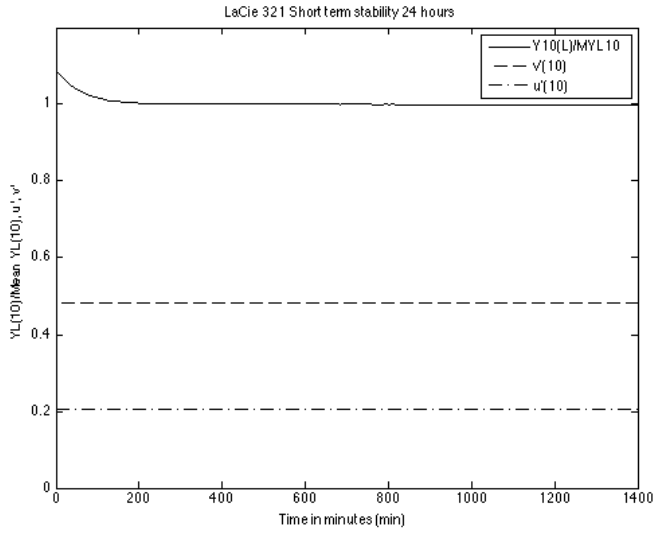

***Figure 19*: Short term stability LCD LaCie 321 absolute luminance ('$Y_{10,L}$') divided by average absolute luminance; chromaticity coordinates 'u'_{10}', 'v'_{10}' for 24 hours (13.03.2011).**

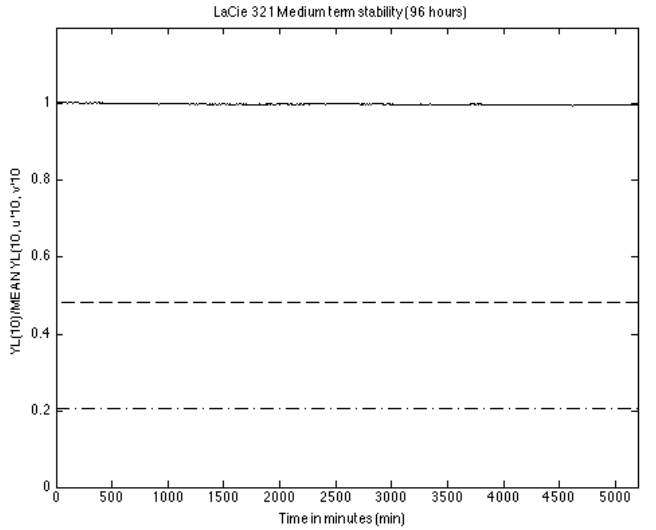

***Figure 20*: Medium term stability LCD LaCie 321 absolute luminance ('$Y_{10,L}$') divided by average absolute luminance; chromaticity coordinates 'u'_{10}', 'v'_{10}' for 96 hours (15.03.2011).**

The absolute '$Y_{10,L}$' values varied in the range from '212' cd/m^2 at the beginning of the project in 2008 to '196' cd/m^2 until the last experiment in 2012. The temperature in the laboratory had an affect on those values. The chromaticity coordinates remained stable for the time duration of each experiment. The LCD was re-calibrated and re-characterised prior to each individual experiment; the longest time duration for an observational experiment lasted for approximately six weeks (*Experiment C* and *Experiment D*), and the shortest duration (*Experiment B*) for exactly one week.

3.6.4 The LCD was set to a 'sRGB' colour space with a white point similar to daylight (display's setting D65), brightness was set to a value of '100' and contrast to a value of '50'. The display's setting remained as such throughout the entire project. The normalised white point for the display, and chromaticity coordinates for each experiment, were recorded and are listed in *Table 5*.

Date	X_{10}	Y_{10}	Z_{10}	u'_{10}	v'_{10}	*CT*
April 2009	96.20	100	102.76	0.202	0.473	5950
February 2010	95.35	100	97.93	0.202	0.476	5800
October 2010	95.40	100	93.80	0.203	0.480	5600
August 2011	95.60	100	89.90	0.205	0.482	5400

***Table 5*: Normalised 'XYZ_{10}'- tristimulus values for white point for LaCie 321 LCD display taken at different times, CT referred to colour temperature, and '$u'_{10}v'_{10}$' referred to corresponding chromaticity coordinates.**

3.6.5 Twenty-five points on screen were measured using the entire display area (R = '255', G = '255', B = '255') for testing its uniformity as given in *Table 6*. It was evident from *Table 5* that there were considerably differences in lightness, but also in chromatic content, among all measurements and positions.

Position	$\Delta u'$	$\Delta v'$	$\Delta u'v'$	ΔL^*	ΔC^*_{ab}
1	0.0002	0.0013	0.0013	**-1.5902**	**-0.5731**
2	0.0076	0.0010	0.0076	**-2.3236**	**-0.0829**
3	0.0005	0.0015	0.0016	**-1.8669**	**0.0035**
4	0.0004	0.0025	0.0026	**-2.2853**	**0.3498**
5	0.0010	0.0044	0.0045	**-1.8480**	**0.6176**
6	-0.0005	0.0019	0.0020	**-1.4524**	**-0.9146**
7	0.1564	0.0012	0.1564	**-0.4933**	**-0.3077**
8	0.1562	0.0008	0.1562	**-0.5976**	**-0.1887**
9	-0.0012	0.0026	0.0028	**-0.3161**	**2.0682**
10	0.0049	0.0049	0.0069	**-1.0168**	**1.1641**
11	0.1565	0.0029	0.1566	**-1.4211**	**-0.7579**
12	0.1562	0.0015	0.1562	**-0.8931**	**0.3800**
13	0.0000	0.0000	0.0000	**0.0000**	**0.0000**
14	-0.0008	0.0029	0.0030	**-0.2186**	**0.4734**
15	-0.0003	0.0049	0.0049	**-1.4149**	**0.8726**
16	-0.0001	0.0034	0.0034	**-0.9116**	**-0.0542**
17	-0.0004	0.0021	0.0022	**-0.7020**	**-0.0324**
18	-0.0002	0.0017	0.0017	**-0.6344**	**0.2313**
19	0.0002	0.0041	0.0041	**-0.8129**	**0.3095**
20	0.0003	0.0052	0.0052	**-1.7095**	**1.4732**
21	0.0002	0.0042	0.0042	**-2.2280**	**-1.5543**
22	-0.0001	0.0038	0.0038	**-2.2535**	**-1.1468**
23	0.0001	0.0039	0.0039	**-1.8922**	**-0.4455**
24	0.0006	0.0052	0.0053	**-2.2662**	**0.2907**
25	0.0011	0.0057	0.0058	**-2.5088**	**0.9483**

***Table 6*: Uniformity measures against patch number 13 (5 x 5 Matrix) from top row starting left to right and down to position 25 (measured in April 2008)**

3.7 LCD Model

3.7.1 The voltage luminance transfer curves were determined by measuring several uniform grey patches that were displayed on screen against a black background at the same position as 'TWC', 'ST', 'UNI' and 'BH' colour difference sample pairs were displayed to observers on the same screen (*Graph 1*). These patches were created in steps of eight digital counts in the range from '0' – '255' (8 bit display). In addition, the spectral radiance distributions, r(λ), g(λ), b(λ), and w(λ) for peak red, green, blue and a white patch were measured with a tele-spectroradiometer in the wavelength range from 380 – 780 nm. The spectral radiance distributions and transfer curves are described as in *Figure 21* and *22*. These transfer curves were used to construct one dimensional lookup tables ('1D – LUT') for each primary channel either by plotting LCD 'RGB' input- against CIE 'XYZ_{10}' – tristimulus values for each combination, or 'XYZ_{10}' – tristimulus to LCD 'RGB' values describing the non-linear stage for predicting LCD 'RGB' input values from linearized scalars ('d_r', 'd_g', 'd_b'), or predicting scalar values from input LCD 'RGB' values.

3.7.2 The peak red ('R'), green ('G'), and blue ('B') transmissive primaries were also used to derive a forward and inverse '3 x 3' matrix for linearily transforming either CIE 'XYZ_{10}' – tristimulus values to scalars ('d_r', 'd_g', 'd_b'), or by transforming given scalars to predicted 'XYZ_{10}' – tristimulus values. The conversion matrices are given in *Table 7.* The forward training model predicted LCD 'RGB' values from input CIE 'XYZ_{10}' tristimulus values. A backward model predicted display's input 'RGB' values to CIE 'XYZ_{10}' – tristimulus values with a variation on average of '0.0005' 'ΔE_{00}' units.

Forward Model	X_{10}	Y_{10}	Z_{10}	*Inverse Model*	X_{10}	Y_{10}	Z_{10}
Peak Red	47.0242	23.9802	1.2382	**Peak Red**	0.0293	0.0113	0.0004
Peak Green	33.8863	62.5016	6.3933	**Peak Green**	-0.0156	0.0223	-0.0015
Peak Blue	14.8742	13.4923	80.9434	**Peak Blue**	-0.0028	0.0016	0.0125

***Table 7*: Forwarded matrix for (1) calculating (predicted) 'XYZ_{10}' – tristimulus and '$L^*a^*b^*$ - values from scalars ('d_r', 'd_g', 'd_b'), and (2) calculating (predicted) display input RGB values from desired 'XYZ_{10}' – tristimulus and '$L^*a^*b^*$' – values.**

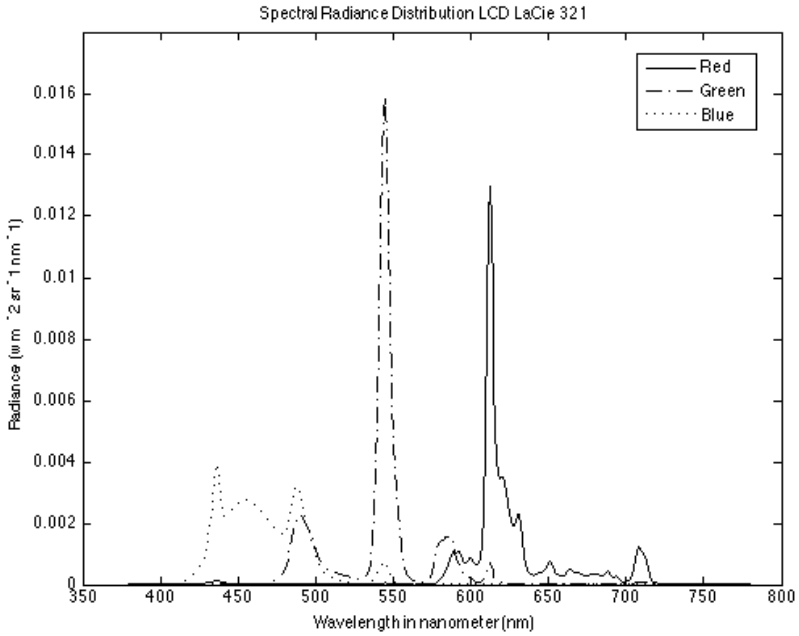

***Figure 21*: Spectal radiance distribution for the red ('R'), green ('G'), and blue ('B') channel for a peak red, green, and blue patch displayed on LCD 'LaCie 321'.**

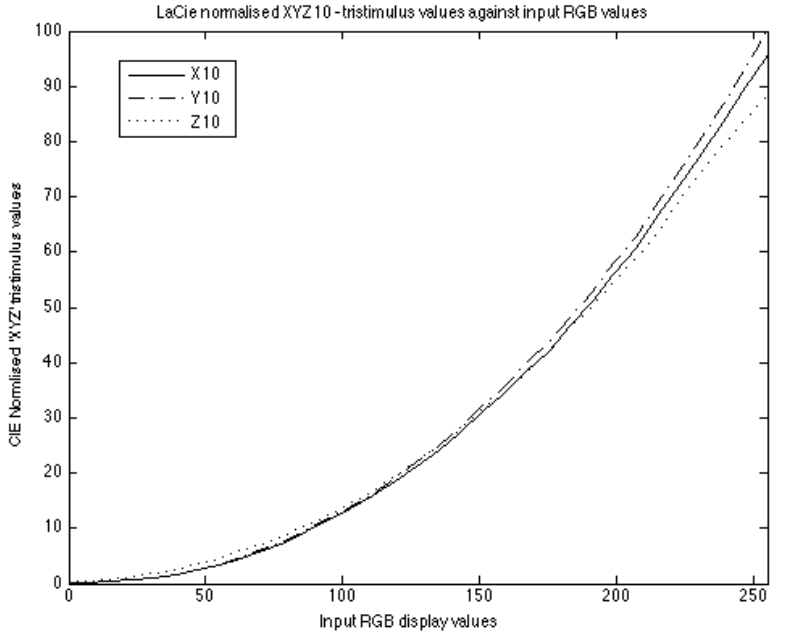

***Figure 22*: Transfer curves between LaCie display digital RGB input values (grey scale) and measured normalised CIE 'XYZ_{10}' – tristimulus values.**

3.8 Optimised liquid crystal display

3.8.1 A second step in the characterisation process for the LCD for this project was to determine whether a displayed colour image on screen is affected by the grey background colour inherent in the experimental software design (see *Graph 1*). A training model for a digital display is generally based on measurements obtained from a series of grey images (or individual red, green, and blue step scales) varying only in intensities seen against a black background. The experimental setup in *Graph 1* suggested that images are viewed versus a grey background approximating a lightness value of 'L^{*}' equal to '50' (specifications in *Experiment D* were strictly met with those measurement data that were obtained from physical samples and background in a viewing cabinet – see *Chapter 7*). Therefore, a series of grey images against a grey and black background were measured on screen. Several trial measurement results were considered for a final model, which generally describes the colorimetric behaviour of the LCD display if used with various background colours, so to predict and derive robust colorimetric data for psychophysical experiments on screen. The average of a collection of data over a prolonged period of time for a series of grey images in the range '0' – '255' digital counts were plotted in terms of differences between CIE 'XYZ_{10}' tristimulus values from a mid grey and black background as described in *Figure 23*.

3.8.2 A colorimetric modelled image against a black training background on screen was altered by the immediate surrounding (and size of the image) as given by the differences in CIE 'XYZ_{10}'- tristimulus values. A modelled and measured image on a black background (training) plotted against measurements for the same sample against a grey background (prediction model), was described by oscillating channel responses in the vertical direction for grey images brighter than '128' digital counts. Also, a decline in measured CIE 'XYZ_{10}' – tristimulus values for grey images, brighter than '200' digital counts displayed against a grey background compared to a black background, was evident for this particular 'LaCie 321' display. The modelled average response curves for either the red, green, or blue channel is given in *Figure 24*. A similar comparison in terms of background influence using the same experimental software environment for a Thinkpad X200 tablet (fluorescent light source) and Apple MacBook pro 13.3 (LED light source – see *Figure 25*) resulted in larger CIE 'XYZ_{10}' – tristimulus values for images measured against a grey background as expected (addition of light); but, were more consistent and showed no oscillating behaviour. Three '1D' – LUTs were constructed by interpolation and included within the final LCD characterisation model for determining an average grey background effect for displayed images on screen. This background influence was either subtracted from input CIE 'XYZ_{10}' – tristimulus values for predicting LCD RGB display values, or finally added to predict CIE 'XYZ_{10}' – tristimulus values that are were derived from scalar values.

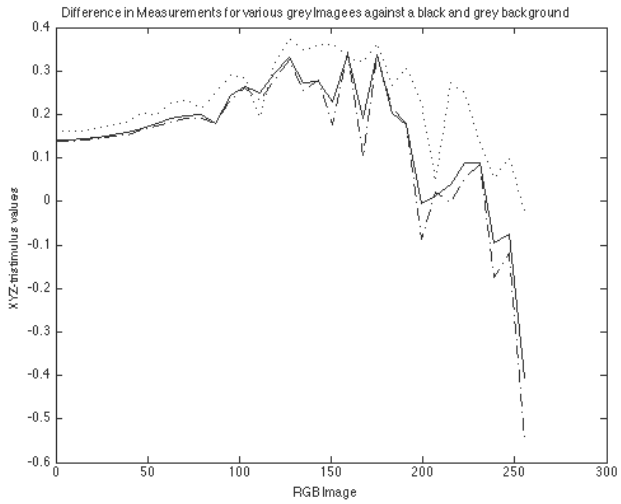

***Figure 23*: Plot of differences in '$X(\ldots),Y(-.-),Z_{10}(-)$' – tristimulus values from a grey and black background for various grey level images (Light source: CCFL).**

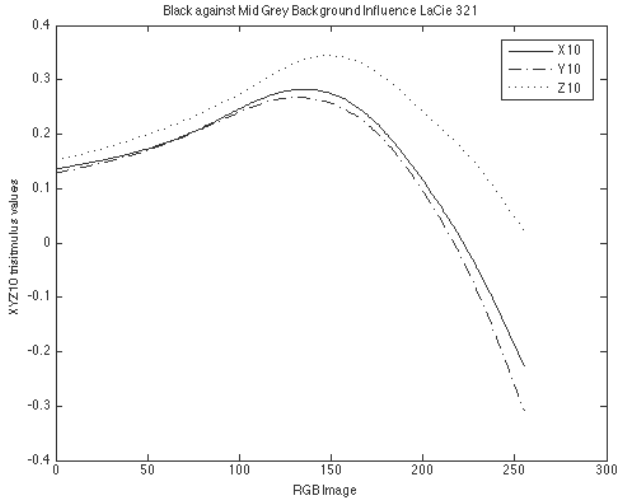

***Figure 24*: LaCie 321 modelled differences in 'XYZ_{10}' – tristimulus values for grey and black background influence for various grey images by interpolation.**

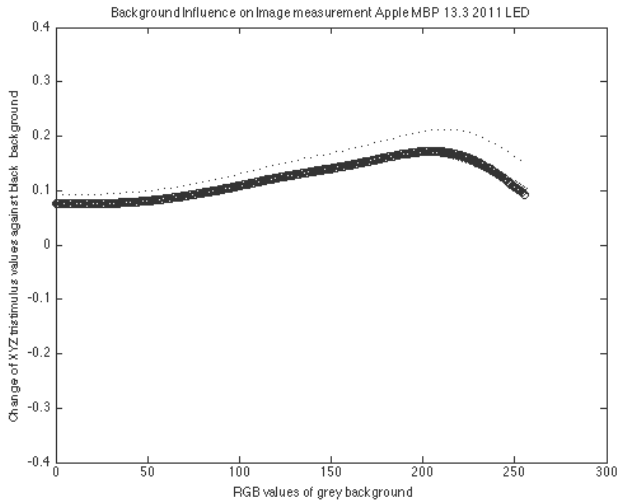

***Figure 25:* Apple MacBook Pro 13.3 (2011) modelled differences in 'XYZ_{10}' – tristimulus for grey and black background influence for various grey images by interpolation (LED).**

3.9 LCD performance and model flowchart

3.9.1 The prediction performance in 'ΔE_{00}' units for the '1D-LUT' LCD LaCie321 display model that was used during this project for a test data set of '107' uniform patches within the experimental setup *(Graph 1)* resulted, for measured and predicted 'XYZ_{10}' – tristimulus and '$L^*a^*b^*$ - values from various uniform 'RGB' images covering a wide colour gamut (see *Figure 26* and *27*), in a mean difference value of 0.2515 'ΔE_{00}' units (median '0.22', standard deviation '0.11', maximum '0.64'). Those predicted and calculated data were also plotted in CIE's *u*'*v*' – chromaticity diagram against the standard RGB's colour gamut as given in *Figure 28*. The displays prediction performances were satisfactory considering recent literature, in which LCDs were screened for performances in terms of their prediction abilities. However, the long-term stability in terms of colour temperature and colour space maintenance was not stable, if we consider the same display's settings that were used for all experiments during this project over a long period of time. Calibration and characterisation models were designed before each individual experiment.

3.9.2 The final LCD model followed those general principles as described in *Graph 2*; (**1**) for predicting overall image RGB values from desired CIE 'XYZ_{10}' – tristimulus values and CIE $L^*a^*b^*$ - coordinates, and (**2**) for predicting CIE 'XYZ_{10}' – tristimulus values and CIE $L^*a^*b^*$ coordinates from input LCD RGB – values.

***Graph 2*: Backward and forward model for predicting LCD 'RGB' from input $L^*a^*b^*$ - values, and $L^*a^*b^*$ - values from LCD input 'RGB' – values f including image background effect .**

Backward LCD modelling:

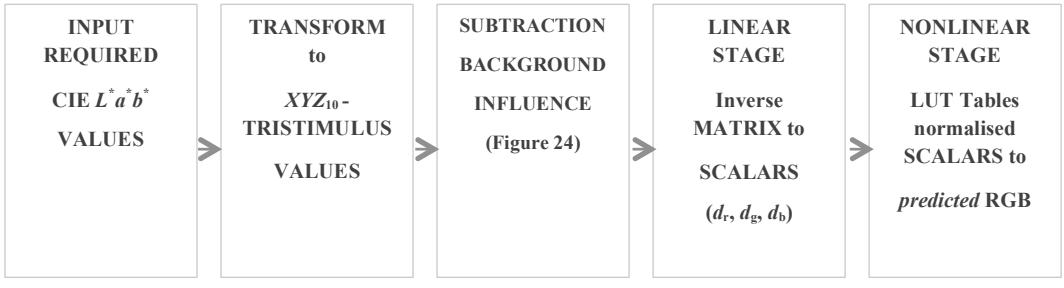

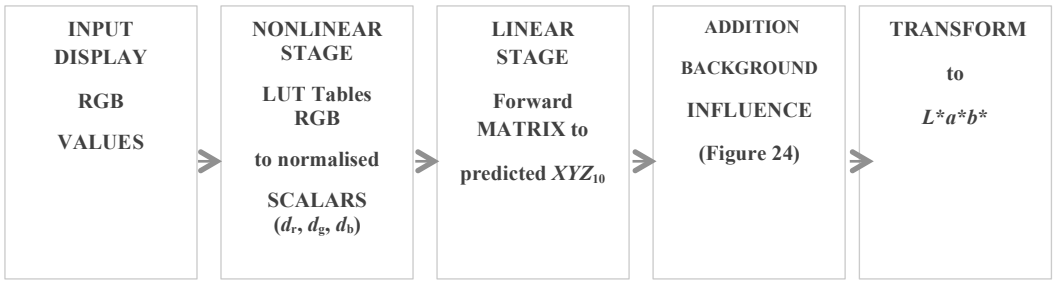

Forward LCD modelling:

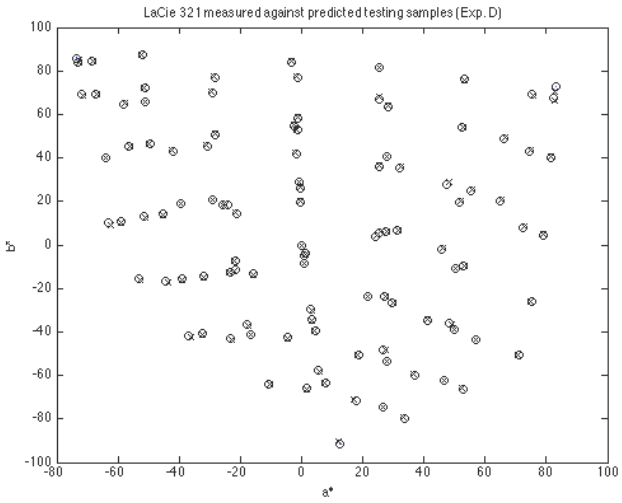

***Figure 26*: Relative testing dataset for LCD LaCie 321. Measured data (o) against predicted data (x) for 107 test samples.**

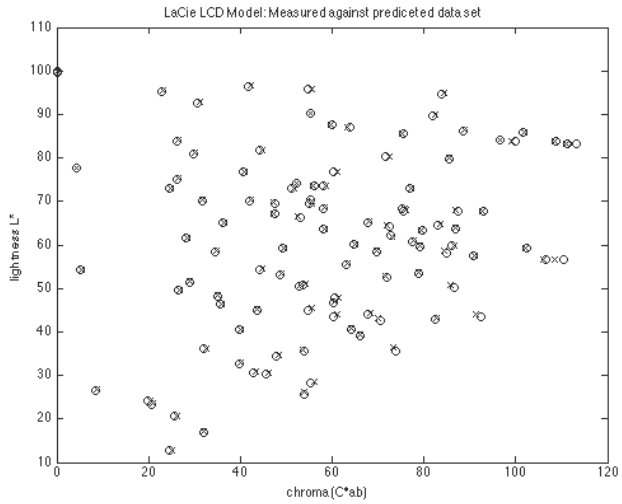

***Figure 27*: Testing datset for LCD LaCie 321: Measured data (o) against predicted data (x) for CIE L^* against C^*_{ab}.**

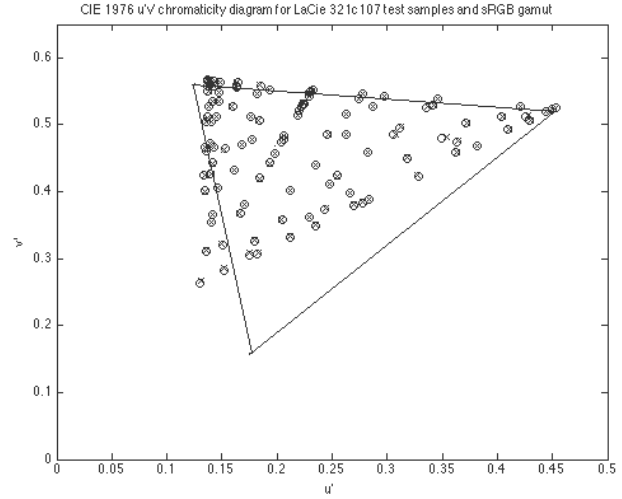

***Figure 28*: LaCie LCD 107 measured and predicted test colours (~D55) plotted in CIE *u'v'* – chromaticity diagram against boundaries of sRGB primaries (D65)**

3.10 Digital image design

3.10.1 Four different types of digital datasets were produced ('TWC', 'UNI', 'ST', and 'BH') to determine whether there was a significant difference in colour difference perception caused by those variations in sample presentations. Two methods were used to design all images. The first method was based; (**1**) on a 'master' texture image that can be obtained from a suitable physical master 'thread sewn into fabric' sample by means of linearised monochrome responses from a digital scanner (see *Image 1* and *2* for 'ST'- and 'BH' samples). A three channel coloured RGB master image was designed by using that same green one-dimensional monochrome channel response (see *Figure 34*) for all other channels. Simple mathematical multiplications by a suitable factor for each pixel in the red and blue channel provided an average mid grey master texture image so to match an average mid grey value on screen. This master image was then used for further digital processing in a pixel-by-pixel fashion in an MS Excel environment so to design all required images and colorimetric specifications.

3.10.2 Digital masks for 'ST' and 'BH' thread type samples (see *Image 3* and *4*) were designed to separate thread and fabric content from an LCD RGB image. These digital masks were used to; (**a**) separate a thread stitch ('BH' or 'ST') from the underlying fabric sample by subtraction in a pixel-by-pixel fashion. This digital separation into thread and fabric content generated either 'BH' or 'ST' threads master texture images (see *Image 5* and *6*), but could be also used to generate master fabric texture images once a positive mask was used, instead. A digitized grey intensity 'TWC' sample served as a master 'TWC' image (see *Image 8*), from which all other digital 'TWC' images and datasets were produced.

3.10.3 Once a fabric sample and thread were separated into two individual images, it was possible to apply colour specifications to each of them. This was done by means of individual digital image processing before re-combining both together so to form a colour difference sample pair in the form of an image. The first method for deriving those difference pairs for a fabric sample, a standard, and thread stitch, a batch sample (see *Images 5* and *6*) is described in *Graph 3*. The first method was implemented in MS Excel on a 'pixel-by-pixel' basis for fabric texture samples ('FA'); thread winding cards samples ('TWC'), Buttonhole ('BH'), and Single Needle Lockstitch ('ST') samples. Uniform patches ('UNI') were designed in Matlab.

Graph 3: ***Inverse workflow description for designing texture images 'FA', 'TWC'. 'BH', and 'ST' for desired $L^*a^*b^*$ - values***

1. Input colour specified as CIE $L^*a^*b^*$ - Values	2. Subtract/Add texture from average input L^* value for each pixel	3. Transform $L^*a^*b^*$ texture image to 'XYZ_{10}'- tristimulus for each pixel	4. Subtract background influence on image from 'XYZ_{10}'	5. Transform 'XYZ_{10}' - tristimulus values into scalars using inverse Matrix	6. Use LUT and transform scalars to RGB pixel values

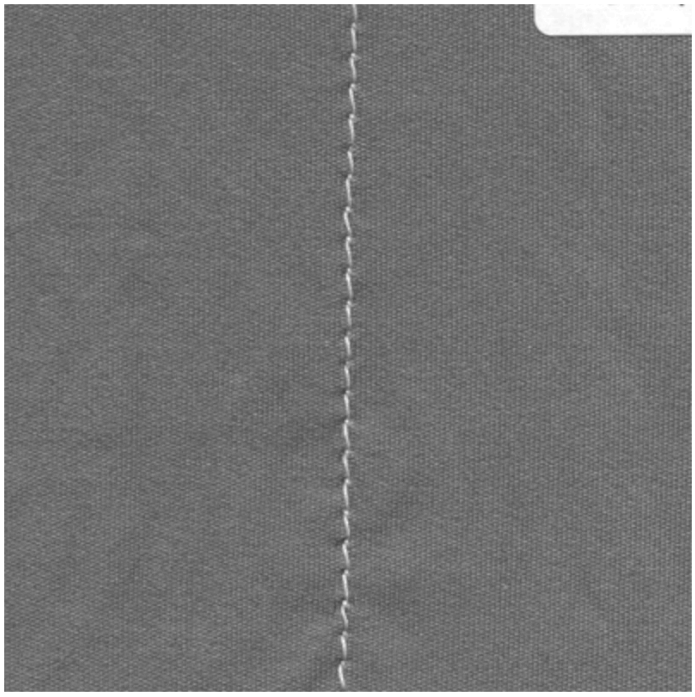

***Image 1*: Monochrome scan from original stitch type; Single Needle Lockstitch Master Image (EPIC 50)**

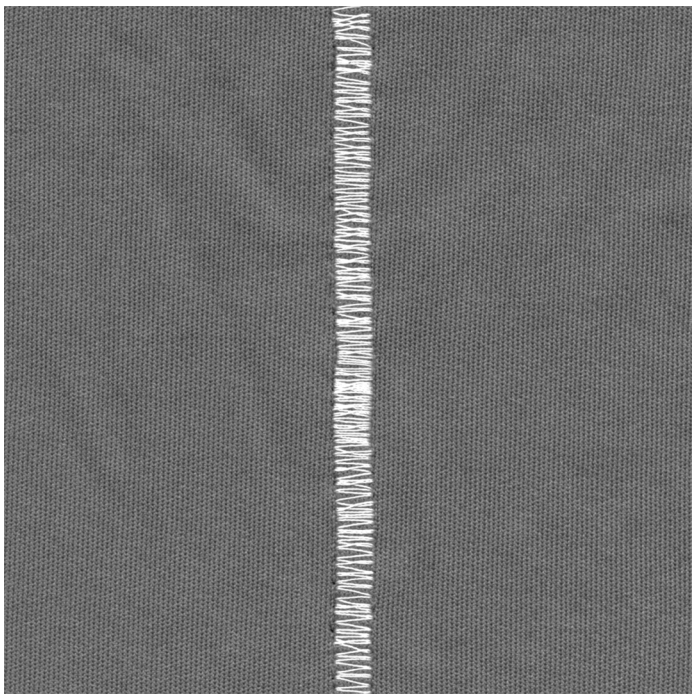

***Image 2*: Monochrome scan from original Master Buttonhole Image**

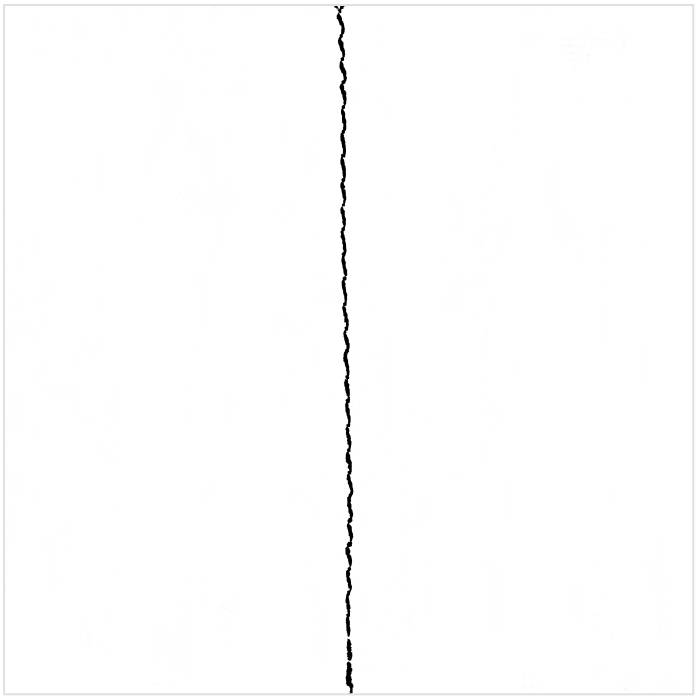

***Image 3*: Digital negative mask for separating background from Buttonhole stitch thread type**

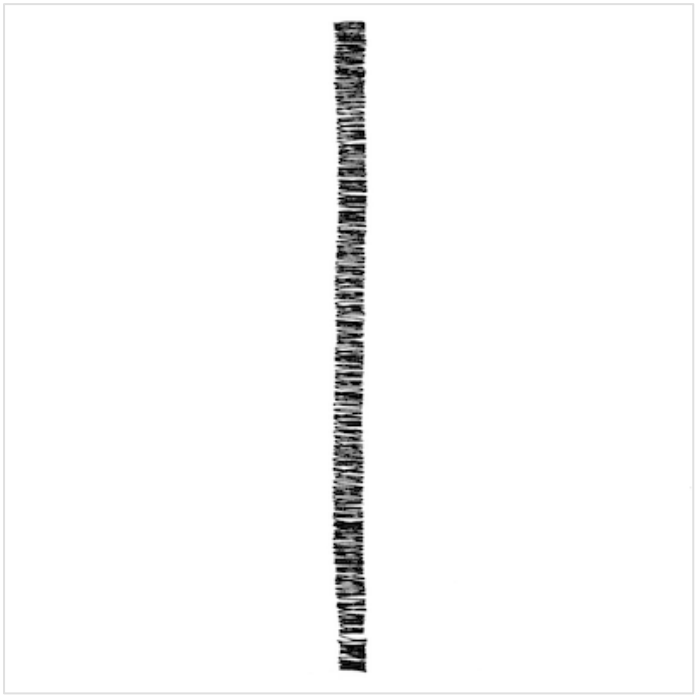

***Image 4*: Digital negative mask for separating background from Single Needle Lockstitch sample (Epic 50)**

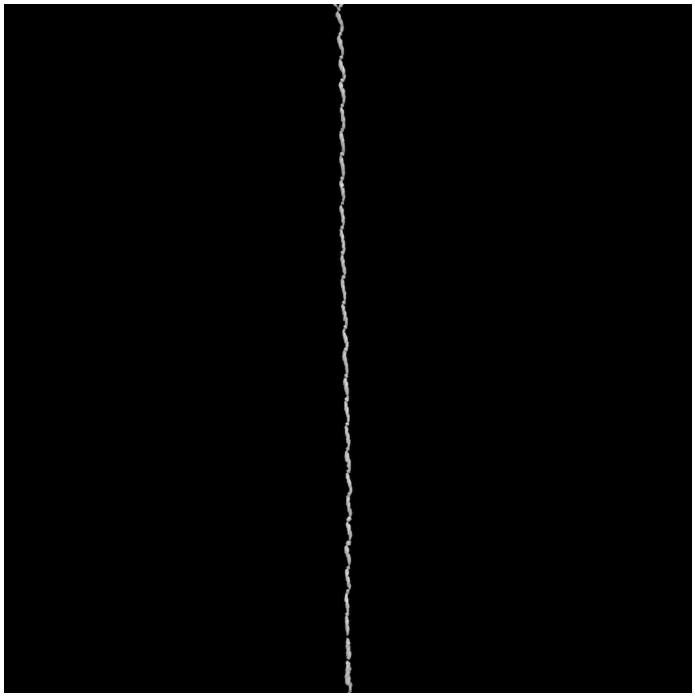

***Image 5*: Master Single Needle Lockstitch texture sample**

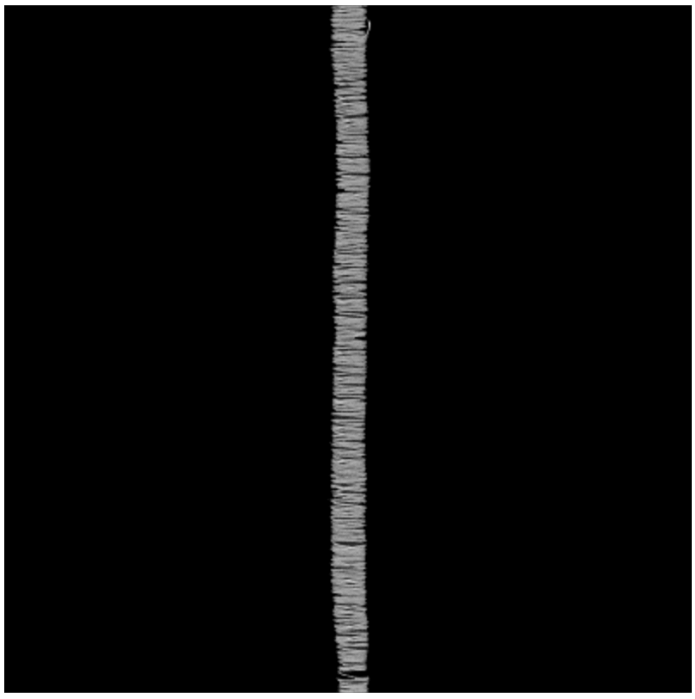

***Image 6*: Master Buttonhole texture sample**

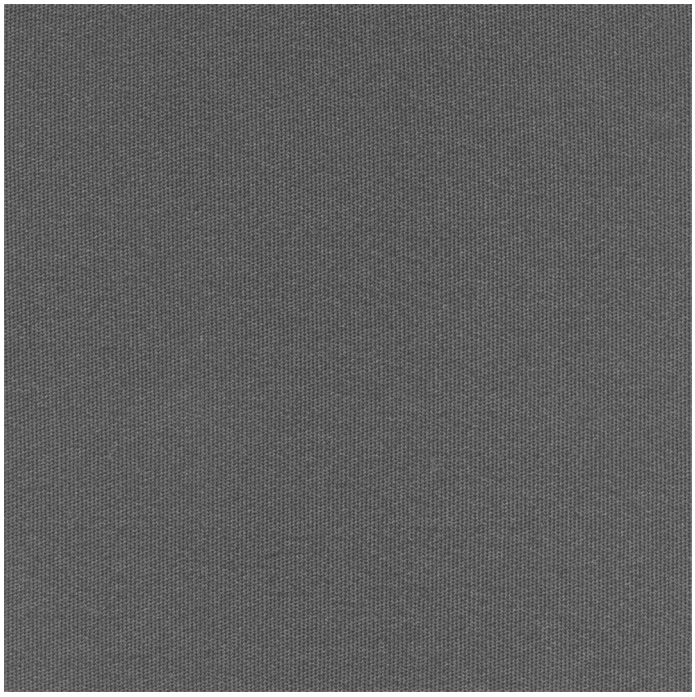

***Image 7*: Scanned Master Fabric Texture Image.**

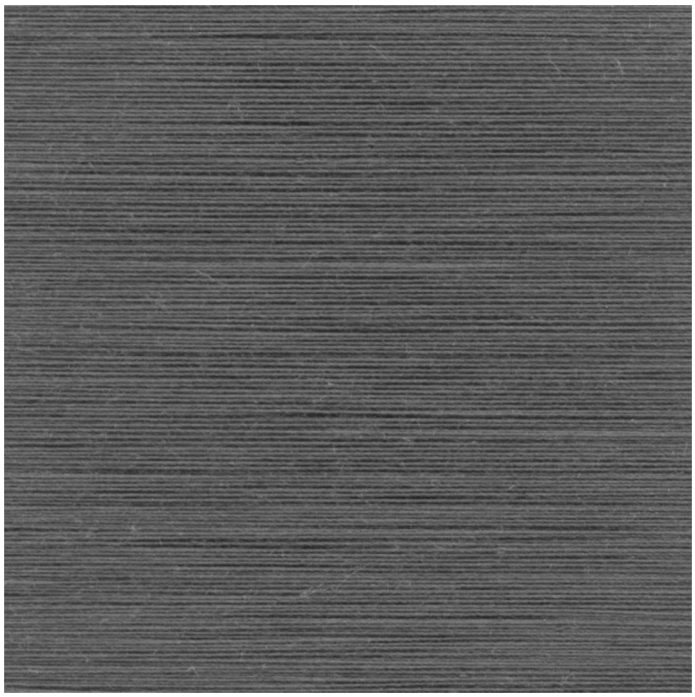

***Image 8*: Scanned Master Thread Winding Card Image**

3.10.4 A colour difference sample pair was designed by either producing two colorimetric defined 'TWC' samples, a 'BH' stitch type that was seen against a fabric sample ('FA'), or a 'ST' – stitch type image sample judged against a standard fabric image sample, once all desired $L^*a^*b^*$ colorimetric values were specified and entered into the model in a MS Excel environment so to produce corresponding LCD 'RGB' image values. A texture was added to these images by either subtracting or adding deviations in lightness values 'L^*' at each spatial location from the average lightness value '$\overline{L}^*$' that was obtained from a master texture image.

3.10.5 A second method (*Model 2*) was based on a technique described by Shen and Xin[375]. A function was written in Matlab for producing 'TWC', 'FA', 'BH', and 'ST' image samples following generally a similar approach by adding texture to an image as described in '*Model 1*', but starting from input LCD 'RGB' values, instead. These uniform 'RGB' images were altered in each channel at each spatial location by a value in regards to the deviations from the mean intensity value obtained from a master texture image. Image statistics in the form of deviations for each colour channel from the mean texture image in the 'R', 'G', or 'B' – channel, and the deviations at each pixel location from the mean intensity value, were weighted with each other before altering a specified RGB value with the associated intensity deviation. A formula that generates a textured image for each channel from a master texture image is described in *Equation 117*. All four types of RGB images were then processed again using a forward model (*Graph 4*) so to determine either; (**1**) the differences between *Model 1* and *2*, and (**2**) the average quantification error between desired $L^*a^*b^*$ - values and resulting RGB values for predicting the same $L^*a^*b^*$- values.

Eq.117: $$\text{Image pixel } (R_{\text{i}}G_{\text{i}}B_i) = \text{RGB} + \left(\frac{\text{STD } R_iG_iB_i}{\text{STD } L_i^*}\right) \cdot \Delta L_i^*, \text{ where}$$

'$R_iG_iB_i$' refers to a specified red, green or red pixel value, 'STD $R_iG_iB_i$' refers to the standard deviation among pixel values in either the red, green or blue channel, 'STD L_i^*' refers to the standard deviation among pixel values in the intensity channel, and 'ΔL_i^*' refers to an individual pixel deviation from the average lightness pixel value in the luminance channel for the same master texture image. A median filter, and a filter that regulates the contrast between 'STD $R_{\text{i}}G_{\text{i}}B_{\text{i}}$' and 'STD L_i^*', was built into the algorithm. The equation was applied to each pixel in all three channels. Generally, this method worked as expected as long as the pixel distribution of a textured image was of normal form (see *Figure 31*). However, Buttonhole and Single Needle Lockstitch texture samples were described by a slightly different underlying statistical distribution. 'BH' and 'ST' colour difference sample images were predicted generally with larger colour differences, if compared with *Model 1* predicted colour difference samples. *Model 1* was finally used to produce 'FA','BH','ST', and 'TWC' – samples (see *Image 7* and *13-15*).

Histograms for a master 'TWC', 'ST', and 'BH' – image sample are presented in *Figure 29, 30* and *31*.

***Graph 4*: Forward model for testing Model 1 and 2; for deriving quantisation error between $L^*a^*b^*$ - RGB – $L^*a^*b^*$.**

1. Transform Image $R_iG_iB_i$ pixels to scalars ($d_i r_i g_i$) by using LUTs	2. Use LCD model to transform scalars to 'XYZ_{10}' with forward matrix	3. Add back-ground influence 'XYZ_{10}' to each pixels 'XYZ_{10}'.	4. Transform modified 'XYZ_{10}' to $L^*a^*b^*$ for each pixel

3.11 Digital camera characterisation

3.11.1 The third method used a digital camera for capturing those physical samples in a viewing cabinet. Several methods of digital camera characterisation were introduced; for instance, by EN[376], Hong *et al.*[377], Hunt and Pointer[378], ISO[379], and Westland and Ripamonti[380]. Two methods were implemented for the aim of characterising a Nikon D2X digital camera (D2X's' software update, Micro Nikkor f55mm f2.8 lens). Characterisation ought to relate camera's output RGB pixel values to either CIE 'XYZ_{10}' – tristimulus values or calculated camera '$XYZ_{10,CAM}$' – tristimulus values by using; (**1**) a Bentham FSGM150 monochromator (narrow band quasi monochromatic light over the visible spectrum) to identify camera's sensitivity functions (*Figure 32*) for calculating device dependent '$XYZ_{10,CAM}$' – tristimulus values, or by (**2**) using CIE colour matching functions (*Figure 18*) to get device independent CIE 'XYZ_{10}' tristimulus values for a set of training samples. Training samples were measured with a tele-spectroradiometer in a viewing cabinet so to obtain spectral radiance distributions for each of the training samples. First, (**1**) camera's RGB image values for each sample were paired with 'calculated' camera '$XYZ_{10,CAM}$' – tristimulus values using D2X's sensitivity functions; thus camera tristimulus values were then mapped (**b**) to CIE 'XYZ_{10}' – tristimulus values for the same samples, and (**2**) CIE 'XYZ_{10}' tristimulus values were mapped directly to camera's average output RGB values for above training samples. The mapping procedure from either '$XYZ_{10,CAM}$' or 'RGB' – camera output values to CIE 'XYZ_{10}' – tristimulus values followed (**a**) a non-linear transform function to obtain linearized RGB values prior mapping (function derived from output RGB to $XYZ_{10}/XYZ_{10,CAM}$ for a series of grey scale images varying between 0 – 255 RGB values), and (**b**) by mapping linearized RGB (from '**1'** or '**2'**) to CIE 'XYZ_{10}' – tristimulus values using either 'neural networks' or 'polynomial' modelling. *Image 9* and *10* shows the set up for Bentham's monochromator diffuser box and *Figure 32* represents obtained spectral sensitivity functions for Nikon's D2x digital camera in regards to a 'ICC-sRGB' pixel output.

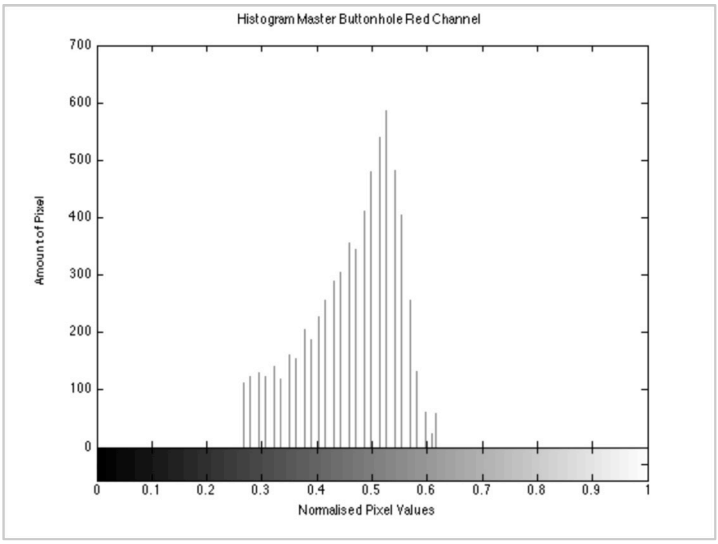

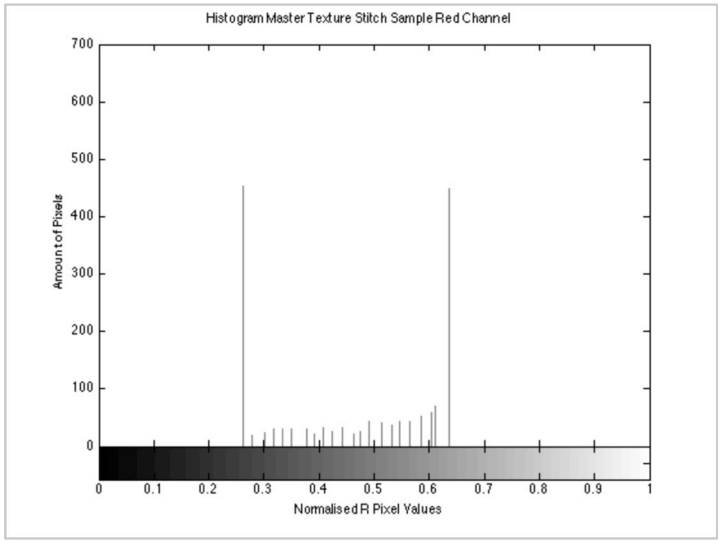

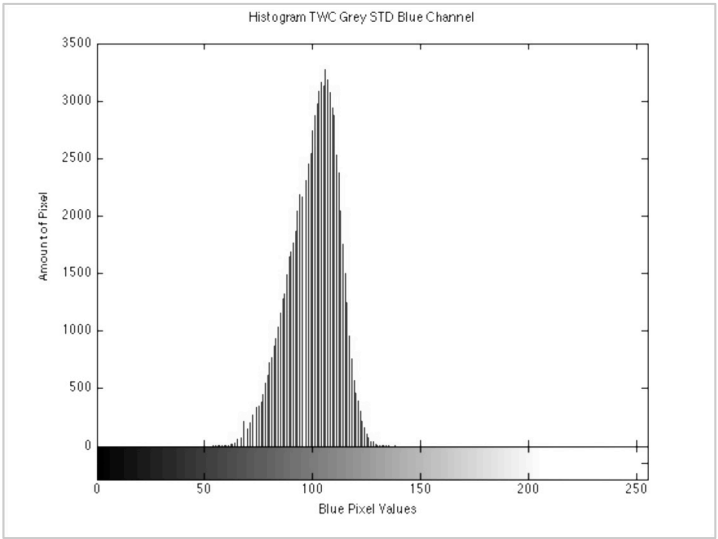

***Figure 29, 30, 31*: Histogram for Master BH, ST, TWC sample. The same histogram was also obtained for the other channels.**

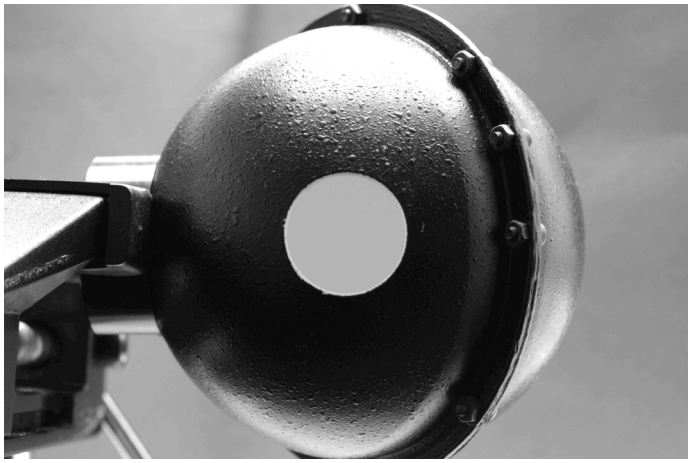

***Image 9*: Diffuser box Bentham FSGM150 monochromator set up.**

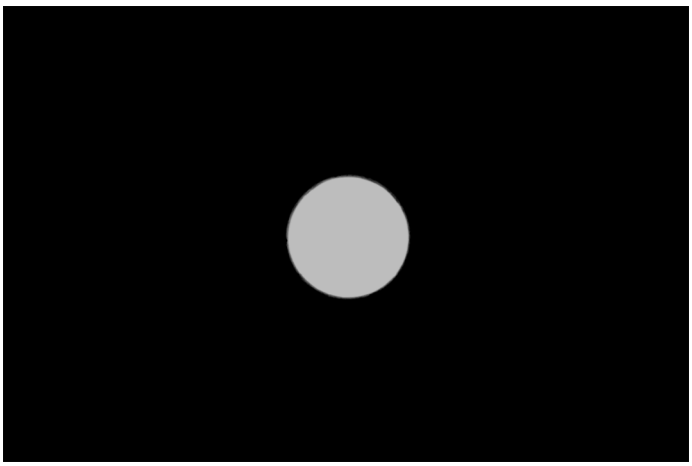

***Image 10*: Recorded and measured (TSR) image from D2x camera for various quasi monochromatic colours from 380 – 780 nm in '5' nm steps in dark laboratory conditions.**

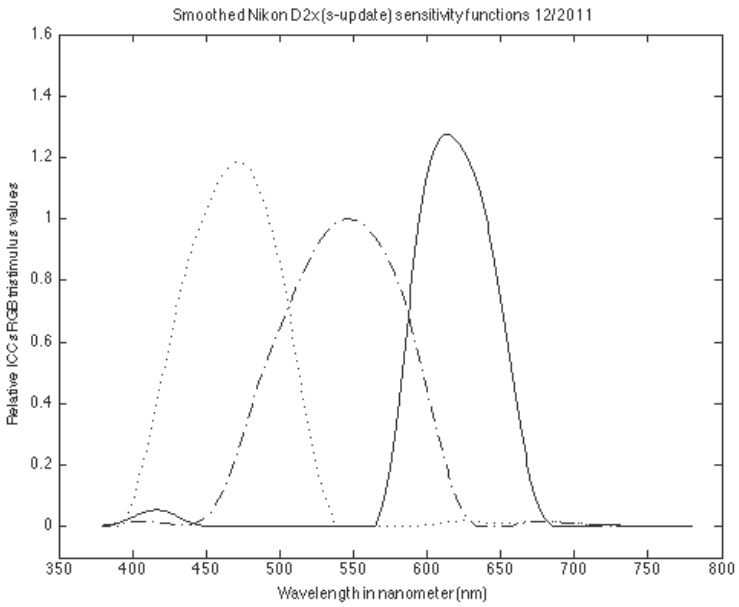

***Figure 32*: Smoothed colour sensitivity function for Nikon D2x(s) digital camera, normalised to green channel 'G' at unity ('ICC-sRGB').**

3.11.2 Three sample datasets were used to train three types of neural networks and various degrees of polynomials ('3x4', '3x7', '3x11', '3x17', '3x20'). The training samples were either provided in the form of a MacBeth 'ColorChecker Chart' ('24' samples), digital 'ColorChecker Chart' ('237' samples), and a combination of 'Thread Winding Card – TWC' and fabric ('FA') samples ('52' samples). Camera's raw image data were processed into four colour spaces ('ICC sRGB', 'Nikon sRGB', 'Adobe RGB', 'Adobe Wide RGB' – see *Figure 32, 36, 37,* and *38*) for determining the most suitable colour space in regards to those digital devices and samples that were used in this imaging chain. A general workflow for designing a colour difference pair on screen, which were used as a physical sample during *Experiment D* (*Part – A*), is described in *Graph 5*.

***Graph 5*: Model for obtaining colour difference images on LCD from Nikon D2X captured physical samples in a viewing cabinet.**

1. Obtain *grey scale* images for deriving a non-linear function. Normalise those RGB data for all *grey images*.	2. Calculate 'XYZ_{CAM}' (or use measured 'XYZ_{10}' values) from this *grey scale* and plot values from (1) with normal. values from (2) and fit a curve.	3. Use curve fitting equation from (2) for linearizing RGB training samples to derive linRGB – values for all of them.	4. Design a neural network or polynomial so to map *linRGB* (3) for any image to normalised CIE '*XYZ_{10}*'-*tristimulus values*	5. Use LCD model to obtain RGB values for each CIE '*XYZ_{10}*' *tristimulus values* from (4) in a pixel by pixel manner.

The camera was mounted and positioned on a sturdy tripod so that the imaging plane from the camera's imaging sensor approximately matched the average position of the observer's eyes. Both datasets ('BH', 'ST') were obtained with a digital camera while setting the aperture to stop '*f*11' with an exposure time of '¼' seconds so to fit depth of field requirements. Also, the exposure time was chosen to achieve *approximately* 'R/G/B' values of '128/128/128' for the red, green and blue channel from the camera response after white point balancing against an illuminated grey background cardboard laid out in a viewing cabinet. Samples were flattened and stitched firmly over a grey card's surface prior capture (0°/45°).

3.12 Neural networks

3.12.1 Neural networks can have several classes according to Westland and Ripamonti[380]; one of them is described as a 'multilayer' perceptron. Each of them consisted of layers of processing units (neurones). Each neuron received input and performed an output using a transfer function (non – or of linear form). The hidden layers can vary in numbers and were defined as such until a suitable number were determined given a measure, for instance, in terms of smallest error (mean square error –'*mse*'). The process of training required adjusting weights and biases values of a network so to optimize the performance between in- and output. A transfer function and the error can be described mathematically as given in *Equation 117* and *118*.

Eq. 117: $\mathrm{f(x)} = 1/(1 + e^{-\mathrm{x}})$

Eq. 118: $\mathrm{F} = mse = \frac{1}{\mathrm{N}}\sum_{\mathrm{i}=1}^{\mathrm{N}}(e_{\mathrm{i}})^2 = \frac{1}{\mathrm{N}}\sum_{\mathrm{i}=1}^{\mathrm{N}}(t_{\mathrm{i}} - a_{\mathrm{i}})^2$, where

't_{i}' refers to targets points and 'a_{i}' to inputs for a neural network. Two steps were normally necessary to determine a neural network model; (**1**) a training input dataset to design a neural network, and (**2**) a testing dataset to determine the output performance of a neural network. A Matlab function ('*neuralnet2.m*') was created using existing training algorithms known as 'Levenberg-Marquardt', 'Bayesian Regularisation', and a 'Resilient Backpropagation' thus generally based on gradient or Jacobian method, according to Beale, Hagan and Demuth[381]. The function required a training dataset input defined as 'linearized RGB' values from camera images and their associated measured CIE 'XYZ_{10}' tristimulus values described as output values. A third input parameter was required to specify the number of layers that were used to train the network. Training was obtained from three colour data sets; and testing, was either conducted by comparing networks with (**1**) different datasets, or (**2**) the same dataset. The performance for a final network model, in regards to a training sample set that was displayed on screen (reduced datastet), was on average '0.44' 'ΔE_{00}' ('0.03' SE) units. The procedure to calculate mathematically the camera's 'XYZ_{10}' – tristimulus values is described in *Equations 119 – 121.*

Eq. 119: $X_{10,\mathrm{CAM}} = \mathrm{k}\sum_{780}^{380}\varphi_{\lambda}\,(\lambda)\bar{\mathrm{r}}(\lambda)\Delta\lambda$

Eq. 120: $Y_{10,\mathrm{CAM}} = \mathrm{k}\sum_{780}^{380}\varphi_{\lambda}\,(\lambda)\bar{\mathrm{g}}(\lambda)\Delta\lambda$

Eq. 121: $Z_{10,\mathrm{CAM}} = \mathrm{k}\sum_{780}^{380}\varphi_{\lambda}\,(\lambda)\bar{\mathrm{b}}(\lambda)\Delta\lambda$, where

'φ_{λ}' describes a combination of a light source and the resulting spectral radiance distributions for physical samples, '$\bar{\mathrm{r}}(\lambda)$, $\bar{\mathrm{g}}(\lambda)$, $\bar{\mathrm{b}}(\lambda)$' refers to spectral colour matching functions for Nikon's digital camera, and '$\Delta\lambda$' defines the integral in nm. Otherwise, the method follows same pattern as for the calculations for CIE 'XYZ_{10}' – tristimulus values. Some of the expected training and testing results between measured 'XYZ_{10}' – tristimulus values and predicted 'XYZ_{10}' – tristimulus values for polynomial modelling ('POL') and neural networks ('NNT') are listed in *Table 8*. Values are provided in 'ΔE_{00}' units. *For example*, normalised '$R_{\mathrm{i}}G_{\mathrm{i}}B_{\mathrm{i}}$' – values from a colour checker chart are plotted in *Figure 33, 34,* and *35* against calculated and normalised *'$XYZ_{CAM,10}$' - tristimulus values* (o) as such describing a systematic non-linear response trend. A function approximated by a third order polynomial model described those trends. Using this function for linearising all colour checker chart's samples resulted in linearised RGB values (+), and a neural network mapped those linarised RGB values to measured CIE 'XYZ_{10}' tristimulus values onto the straight line (·).

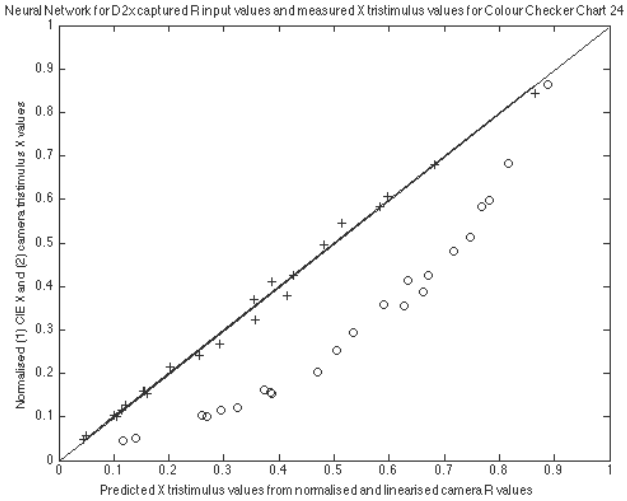

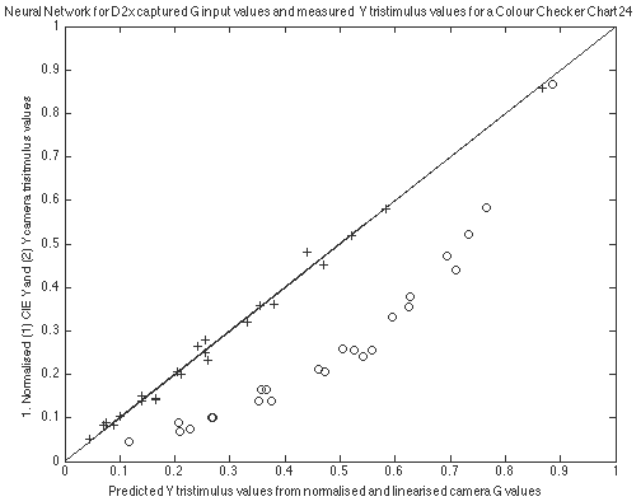

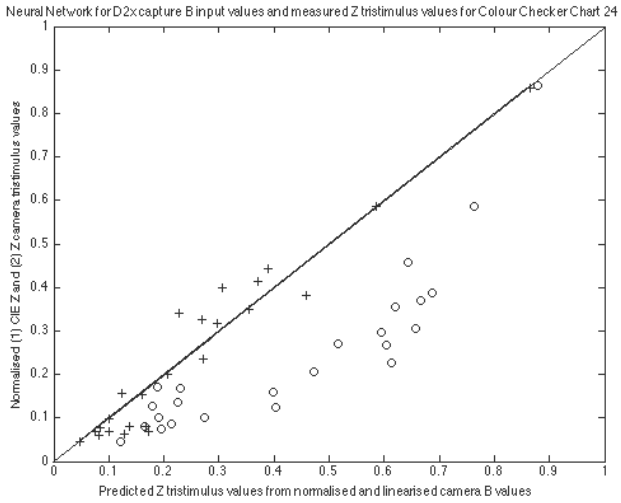

***Figure 33, 34, 35*: Predicted 'XYZ_{10}'- tristimulus values (•), linearized RGB (+), and normalised Adobe RGB (o) – values for individual RGB channels (NNT:Feedforward Net, 15 Layers – 24 Colour Checker Chart).**

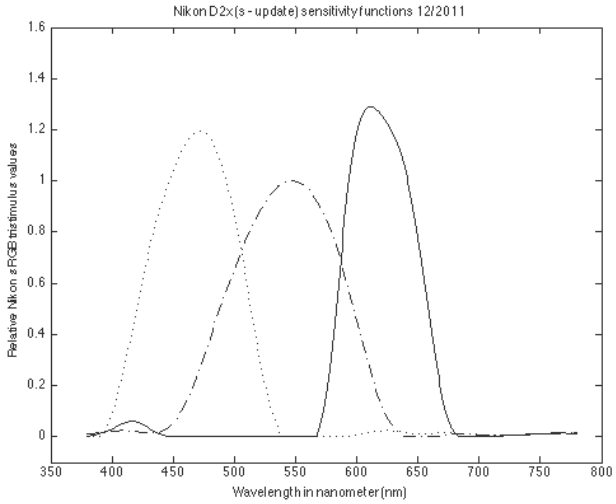

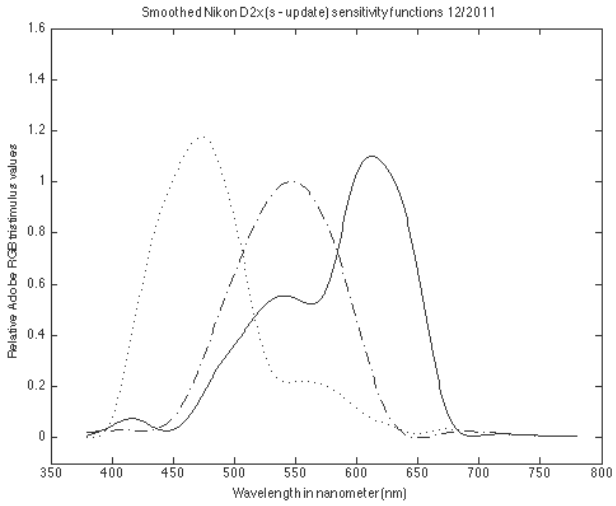

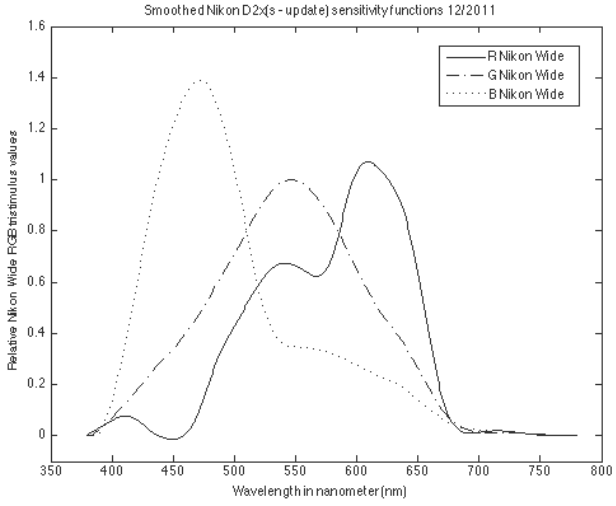

***Figure 36, 37, 38*: D2x camera sensitivity function for various RGB colour spaces**

3.13 Polynomial modelling

3.13.1 A training sample set, which generally includes a sequence of grey patches increasing in $R_iG_iB_i$ – values, was measured in the viewing cabinet with a tele-spectroradiometer resulting in spectral radiance distributions for each patch. *Equations 21 – 23* were used to calculate CIE '$XYZ_{i,10}$'- tristimulus values for each training sample. A plot of averaged and normalised camera output $R_iG_iB_i$ – values for an increasing sequence of grey scale samples against their averaged and normalised CIE '$XYZ_{i,10}$' – tristimulus values (curve similar to *Figure 33 – 35*) can be mathematically approximated by a third degree polynomial (cubic) as described in *Equation 113*; other approximation might be necessary depending on the relationship between two paired data sets.

Eq. 122: $Z_p = aB^3 + bB^2 + cB + d$, where

'B' refers to a normalised averaged output pixel value in the blue channel (for instance, processed as an output value from one of the RGB colour spaces as described in *Figure 36, 37*, and *38*, 'Z_p' refers to a predicted and normalised CIE '$X_{i,10}$' tristimulus value, 'and 'd' refers to a residual value describing the error estimate. This fitting procedure was also applied to the averaged and normalised red 'R' and green 'G' camera channel output responses and thus plotted against measured and normalised CIE '$X_{i,10}$' and '$Y_{i,10}$' – tristimulus values. All three obtained approximation equations were then used to linearize camera's output $R_iG_iB_i$ – values for various training samples (physical samples captured as digital images).

3.13.2 Matrix algebra can be used to obtain coefficients that maps between camera's normalised and linearised $R_iG_iB_i$ – and measured and normalised CIE '$XYZ_{i,10}$'- tristimulus values. The relationship can generally be described in mathematical form as in *Equation 123***,** according to de Levie[382].

Eq. 123: $nXYZ_{10,p,i} = coef \cdot linRGB$, where

'$nXYZ_{10,p,i}$' refers to predicted and normalised CIE '$XYZ_{i,10}$' tristimulus values from camera linearized and normalised '$R_iG_iB_i$' channel responses from a series of physical training samples captured in a viewing cabinet. The coefficients 'coef' were derived from *Equation 124* and *125*.

Eq. 124: $coef = linRGB^{+}XYZ_{10}$, where

Eq. 125: $linRGB^{+} = (linRGB^{T}linRGB)^{-1}linRGB^{T}$

'linRGB^{+}' refers to a pseudo inverse of 'linRGB' as given in *Equation 125*, 'linRGB^{T}' refers to transformed 'lin*RGB*' matrix, and the term $(\ldots)^{-1}$ describes the inverse matrix of the term in the parentheses. Training and testing results were always best for the same sample type. Mixing various types may introduce additional errors so to decrease the performance of a model.

Method	***NNT***	***NNT***	***NNT***	***POL***	***POL***	***POL***
Train	*CCH24*	*CCH237*	*TWC/FA*	*CCH24*	*CCH237*	*TWC/FA*
Mean	0.23	0.73	0.44	0.39	1.04	0.51
Median	0.16	0.57	0.34	0.19	0.82	0.40
Max	0.74	2.74	1.26	1.73	3.82	2.62

***Table 8*: Model performances for neural networks and polynomial modelling for train/test digital camera model.**

3.13.3 Measured and predicted sample data are plotted together in CIE's 'a^*b^*' - diagram as presented in *Figure 39*. All 'BH' and 'ST' samples were then transformed to device independent CIE 'XYZ_{10}' – tristimulus values by using a neural network for further considerations; mainly to be transformed for display on a digital screen in *Experiment D*.

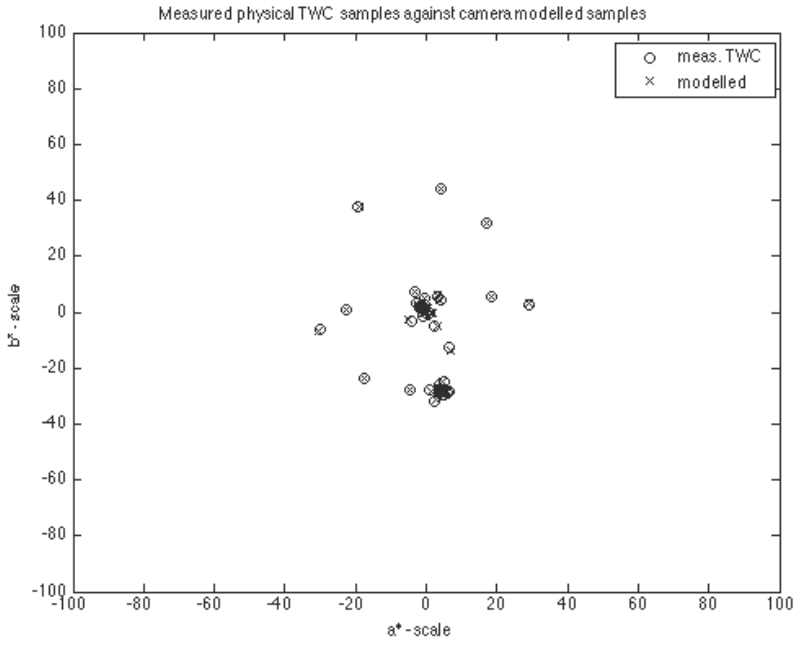

***Figure 39*: Measured physical 'TWC' samples in a viewing cabinet and predicted data using a neural network (fitnet, 15 layers).**

3.14 Scanner

3.14.1 A consumer scanner was employed to scan and digitize a 'master texture image' for Buttonhole 'BH', Single Needle Lockstitch 'ST', and Thread Winding Card 'TWC' samples. The output values of a scanner ('$R_iG_iB_i$') are generally not of linear form as described, for instance, by CENELEC[384], Johnson[385], Kang[373], and Lee[386]. A simplistic requirement at first was therefore to derive a linearised output from a master texture image for each stitch type that was used for the image design stage[kk]. This non-linear transform function of a scanner is general described as in *Equation 126.*

Eq. 126: $lin\text{RGB} = o_{\text{RGB}} + R^{\gamma_{\text{RGB}}}$, where

'*lin*RGB' describes linearised scanner 'RGB' channel outputs, 'o_{RGB}' refers to any possible offset for each channel, and 'R' normally describes the reflectance values for each channel (but can also be described by measured and normalised CIE 'XYZ_{10}' tristimulus values for a series of grey patches, for instance, as seen in a viewing cabinet that was used during this project), and gamma 'γ' describes the slope of the resulting curve between scanner's output 'RGB' – values and reflectance or CIE 'XYX_{10}' tristimulus values for a specific illuminant. The resulting transfer functions are mathematically described as in *Equations 127 – 129* and graphical in *Figure 40*, *41*, and *42* (points close to the vertical line describe linearised scanner output values).

Eq. 127: $R_{\text{lin}} = 1.008 \cdot X_{\text{norm.}}^{1.5584}$

Eq. 128: $G_{\text{lin}} = 0.9337 \cdot Y_{\text{norm.}}^{1.6003}$

Eq. 129: $B_{\text{lin}} = 0.8824 \cdot Z_{\text{norm.}}^{1.6674}$

3.14.2 A polynomial ('3' 'XYZ_{10}' x '17' 'RGB' augmented matrix) was used to map those linearized scanner value output values for a colour checker chart with measured CIE 'XYZ_{10}' tristimulus values considering LaCie's LCD light source (*approximately* D55). The training model performance was on average '0.9' 'ΔE_{00}' colour difference units (median '0.64', STD '1.03', maximum '2.9') between measured and predicted 'XYZ_{10}' tristimulus values, or '1.1' 'ΔE_{00}' units (median '0.52', STD '1.14', maximum '3.67') once the 'K' – term '1' was replaced with '0'. However, only the scanner's green channel responses according to *Equation 128* were used for designing digital texture images ('ST', 'BH', 'TWC').

[kk] see page 138ff

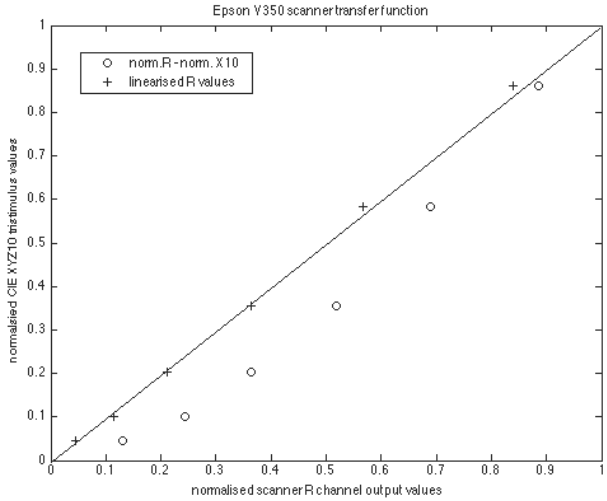

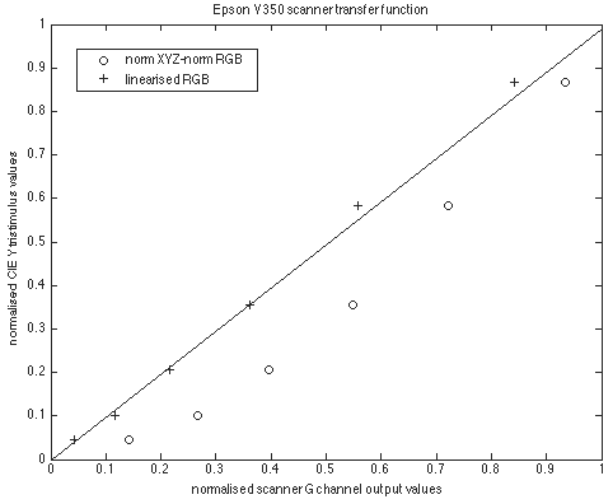

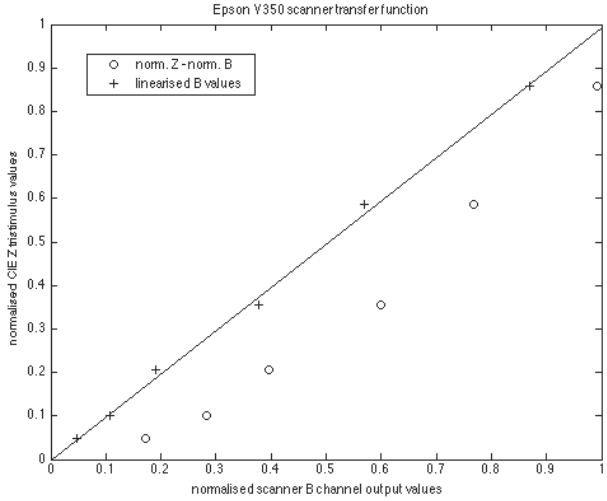

***Figure 40 - 42*: Epson scanner RGB channel outputs against CIE 'XYZ_{10}' - tristimulus values (o) for LCD light source and linearised responses close to the vertical line from Equations 127 – 129.**

3.15 Viewing cabinet

3.15.1 Two different viewing cabinets were used either for *Experiment A* or *Experiment D*. Both viewing cabinets inside walls were either painted with grey colour or covered with grey cardboard (close to Munsell's N5 value). Two fluorescent tubes approximating daylight 'D65' with a high colour-rendering index were used to illuminate samples that were judged during psychophysical experiments. A diffuser was placed between the light sources and the cabinet's floor. Both viewing cabinets were designed for visual assessments of colour samples in accordance to British Standard 950:Part – 1 directives and international standards. A high diffusive white plaque was placed on the floor in the middle of each viewing cabinet and measured with a tele-spectroradiometer. The plaque's reflectance values were determined by taking spectrophotometric measurements (see *Figure 43*). The spectral radiance distributions for both light sources (see *Figure 44*), which were used in those viewing cabinets, were approximated using *Equation 120*.

Eq. 120: $I_{\mathrm{i}}(\lambda)\Delta\lambda = \frac{S_{\mathrm{i}}(\lambda)\Delta\lambda}{R_{\mathrm{i}}(\lambda)\Delta\lambda}$, where

'$I_{\mathrm{i}}(\lambda)\Delta\lambda$' refers to the light source's approximated spectral radiance at a specific wavelength interval[ll], '$S_{\mathrm{i}}(\lambda)\Delta\lambda$' refers to the spectral radiance value for a specific wavelength interval from the plaque in the viewing cabinet, and '$R_{\mathrm{i}}(\lambda)\Delta\lambda$' refers to the reflectance value obtained from the plaque from a spectrophotometer at the same specific wavelength interval.

3.15.2 The illumination in the viewing cabinet was controlled in *Experiment D* so that background and sample luminances and absolute CIE 'XYZ_{10}' tristimulus values (viewing cabinet's grey background equalled '$Y_{\mathrm{L},10}$' ~ 40 cd/m^2, white point '$Y_{\mathrm{L},10}$' ~ 172 cd/m^2) were approximately matched with background and digital sample's colorimetric values on the display (grey background '$Y_{\mathrm{L},10}$' ~ 40 cd/m^2, white point '$Y_{\mathrm{L},10}$' ~ 196 cd/m^2). The peak luminance of the light source in *Experiment D* differed significantly in comparison to *Experiment A* ('$Y_{\mathrm{L},10}$' ~ 415 cd/m^2). CIE normalised 'XYZ_{10}' – tristimulus values for both viewing cabinet's light sources were 'X_{10}' = 94.27, 'Y_{10}' = 100, 'Z_{10}' = 100.45 (*Experiment A*) and 'X_{10}' = 95.17, 'Y_{10}' = 100, and 'Z_{10}' = 100.82 for *Experiment D*. Both light sources referred to a colour temperature of approximately 6000K.

3.15.3 Short and mid term measurements indicated a warm up time prior experimental observations for approximately 60 minutes. The chromaticity coordinates and lightness level remained stable over a period of 50 hours (see *Figure 45)*.

[ll] see page 83 - 84 for calculations of 'XYZ_{10}' - tristimulus values

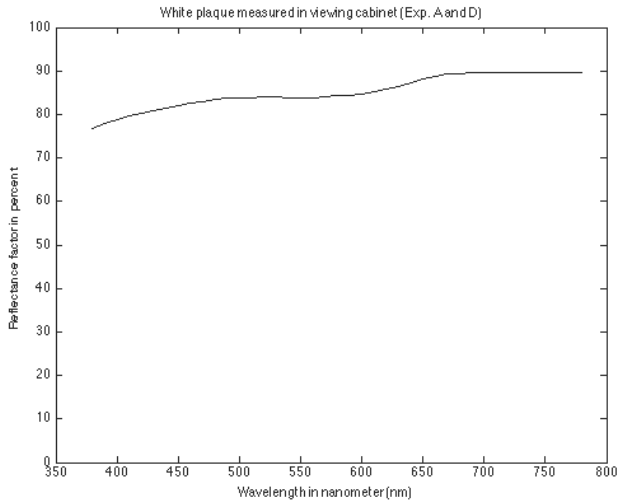

***Figure 43*: Reflectance measurement of a white plaque used in a viewing cabinet to determine SPD's light source.**

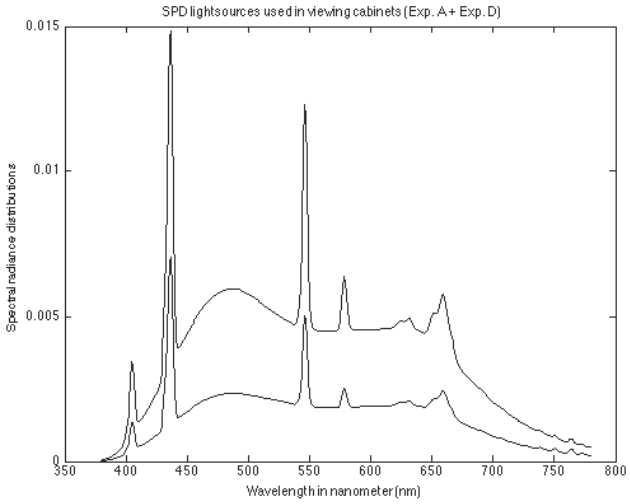

***Figure 4:* SPD of light sources used in viewing cabinets for *Experiment A* (higher radiances) and *Experiment D* (lower radiances).**

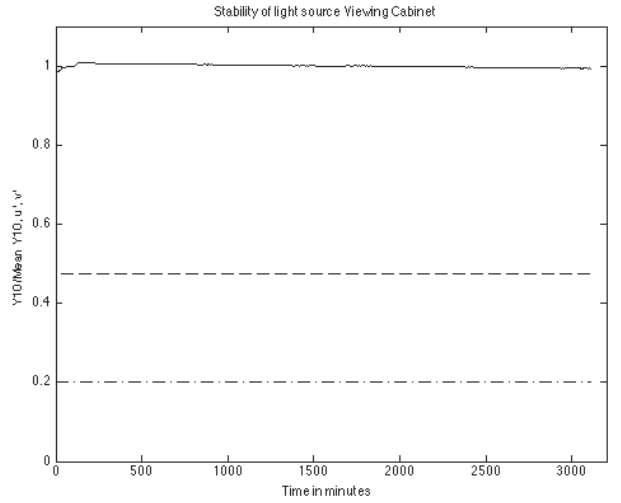

***Figure 45*: Viewing Cabinet's light source stability over time.**

3.16 Images

3.16.1 Examples of camera captured and characterised images for display on a LCD screen and synthesized images from scanned texture master images, which were used during this project, are given here as *Image 11* (camera captured 'BH' sample) and *Image 12* (camera captured 'ST' sample), and *Image 13* (synthesized 'BH' sample), *Image 14* (synthesized 'ST' sample) and *Image 15* (synthesized 'TWC' sample), respectively. The direction of a thread stitch was either applied in North-South direction (*Image 11*) or in East-West direction (*Image 15*). Images are only shown as grey scale images for archival and presentation purposes here in the thesis and do as such not represent the real colour of them.

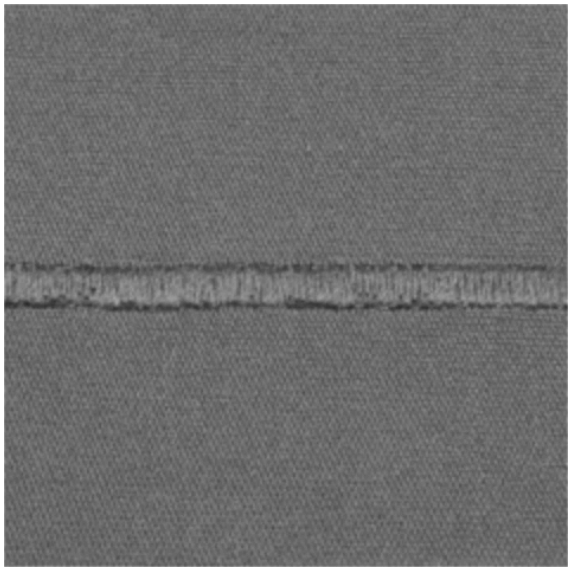

***Image 11*: Camera captured and characterised 'BH' sample**

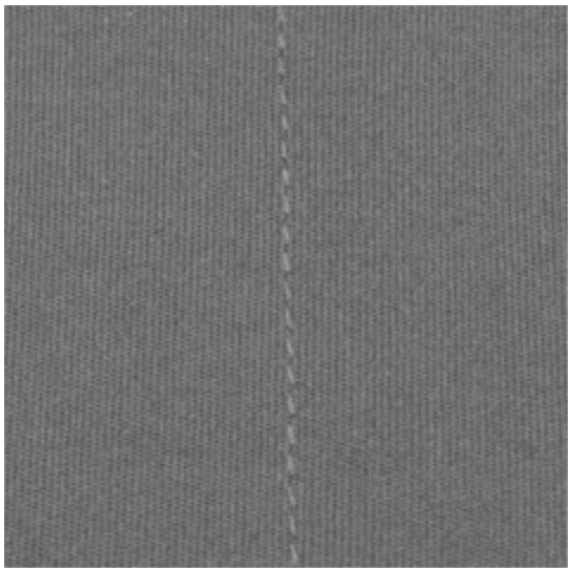

***Image 12*: Camera captured and characterised 'ST' sample**

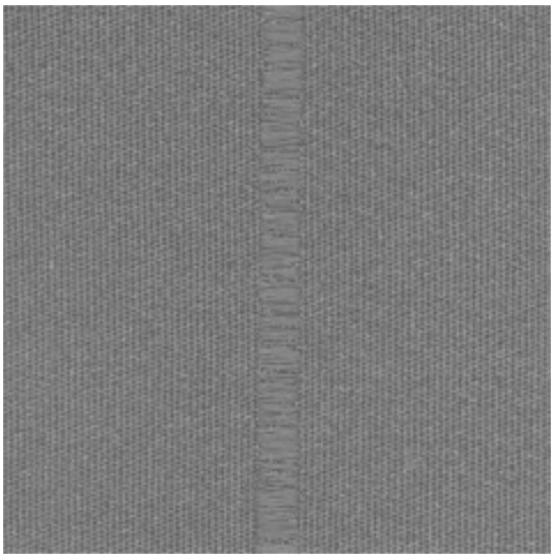

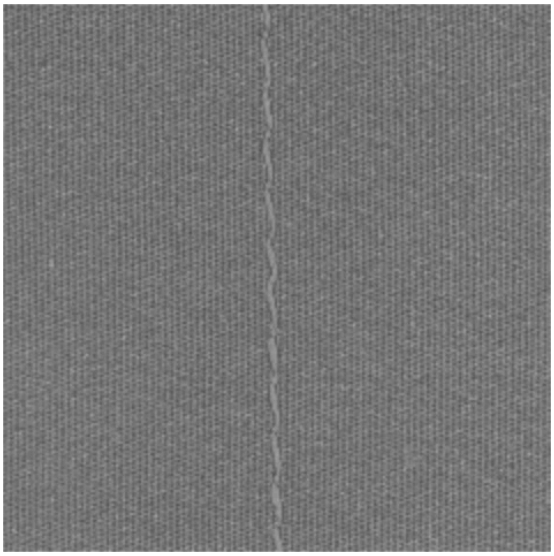

***Images 13-15*: Synthesized Monochrome Images 'BH', 'ST', 'TWC'**

Chapter 4:

4.1 *Experiment A – Part A*: General considerations

4.1.1 A pilot study was conducted to determine whether there are significant changes in the perception of colour differences caused only by the variation in stitch types that were used, and how they were presented and seen by observers, for instance, as within a final product. The sponsor's 'day to day' industrial thread production and visual quality control results suggested that visual colour differences that are perceived by judging, for example, a thread that is stitched into a fabric sample, is altered in colour difference magnitude compared to those results that are solely obtained from instrumental measurements. Generally, it is expected that a colour difference judgement would be enlarged when a background colour (fabric) is similar to the colour of the foreground (stitched thread serves here as a batch sample). This phenomenon is known as lightness crispening in cases of grey colour difference pairs judged against a similar bright grey background colour. This was also reported for chromatic colour difference pairs judged against a similar coloured background (chromatic crispening). The JPC_{79} formula[mm] developed at Coats plc, of which a modified version became the CMC(*l*:*c*) formula[nn] , was designed from psychophysical experiments using a comprehensive thread winding card dataset ('TWC'), which was tested in an industrial environment. The procedure to obtain visual results suggested that colour difference pairs of typical industrial magnitude (small colour differences of approximately 1 – 3 'ΔE_{ab}' units) were judged 'side by side' in a viewing cabinet against a grey scale.

4.1.2 The CIE[3] provided guidelines as how to evaluate colour difference formulae, especially in terms of viewing conditions and the number of colour centres that 'ideally' should be employed for visual evaluation. These reference conditions were approximately matched during this project. However, the choice of colour centres (standards) and number of physical samples (batches) were limited due to constraints in time and available resources. The history of colour difference evaluation suggested that visual colour difference results for grey and blue colour centres[oo] were inconsistent and only recently dealt with when new experimental data were made available, and compared with instrumental data. Hence, it was suggested to use those critical colour centres for evaluation purposes for this pilot study.

[mm] see page 31 and 91

[nn] see page 32

[oo] see page 31-32 limitation JPC_{79}, CMC(*l*:*c*)

4.2 Physical samples

4.2.1 Physical samples were produced around a grey and blue colour standard. Just 'threshold' or 'noticeable' visual colour differences in varies directions around a colour standard were described in the literature as ellipses (see *Figure 5*), or as ellipsoids when a third direction, a lightness scale, was added. Colour specifications for batch samples were determined and placed in semi circles around both standards with a predicted colour difference distance of '0.6', '1.2', and '2.4' '$\Delta E_{\mathrm{CMC}}(2{:}\,1)$' units – ('D65/10°', specular content included, diffuse/8) – varying either in '$\Delta a^{*}\Delta b^{*}$' or '$\Delta L^{*}\Delta a^{*}$' – values (see *Figure 46 – 49*). Coats plc quality control measures suggested that a total colour difference tolerance limit of '1.2' '$\Delta E_{\mathrm{CMC}}(2{:}\,1)$' units is still commercially accepted. Finally, three datasets were kindly produced by Coats plc according to above requirements in the form of; (**1**) thread winding card samples ('TWC'), (**2**) single needle lockstitch type samples ('ST'), and (**3**) buttonhole stitch type samples ('BH').

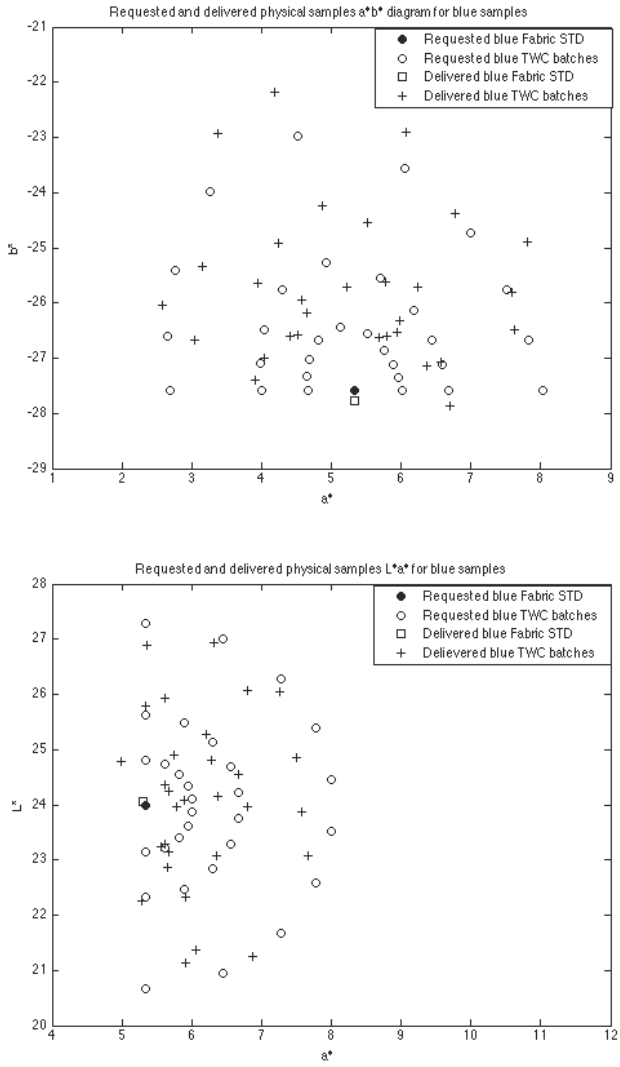

***Figure 46 and 47*: Physical sample distributions as requested and delivered for blue standard and batch variations in '$\Delta a^{*}\Delta b^{*}$' and '$\Delta L^{*}\Delta a^{*}$'- directions.**

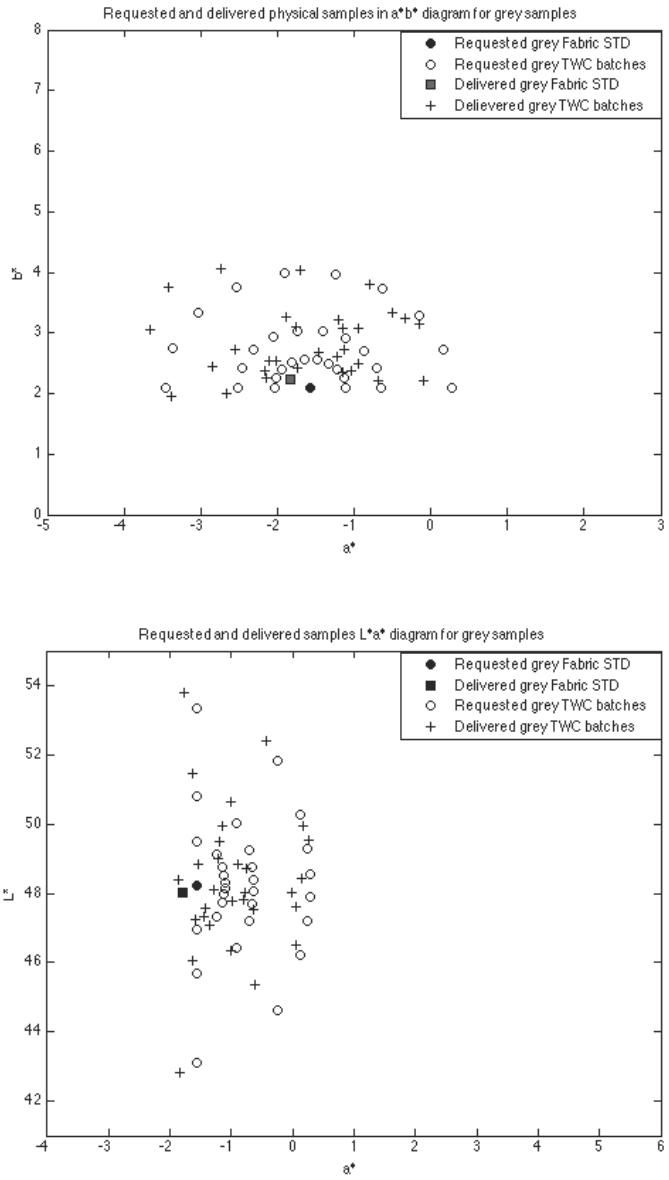

***Figure 48 and 49*: Physical sample distributions as requested and delivered for grey standard and batch variations in '$\Delta a^* \Delta b^*$' and '$\Delta L^* \Delta a^*$'**

4.2.2 Requested batch colour difference specifications are listed in *Table 9* against those that were delivered and measured for the blue and grey fabric standard samples ('FA'), and their associated thread winding card batches ('TWC'). All colour differences between standard and batches were calculated in '$\Delta E_{CMC}(2:1)$' units while considering those viewing conditions that were present in a viewing cabinet (approximately 6000K). Measurements for 'FA' and 'TWC' samples were obtained from a spectrophotometer in North-South and East-West directions. The results for both sample's reflectance values were averaged and used for calculating CIE 'XYZ_{10}' – tristimulus values. The inclusion or exclusion of 'UV' – content did not alter CIE 'XYZ_{10}' – tristimulus values in the wavelength range from 380 -780 nm for ten test samples. Also, parametric effects are listed for colour difference pairs according to '0.6', '1.2', or '2.4' '$\Delta E_{CMC}(2:1)$' sample subgroups.

	Requested CMC(2:1)	*Delivered CMC(2:1)*	*'BH' $\Delta V/\Delta E$*	*'TWC' $\Delta V/\Delta E$*	*PARAMETRIC FACTOR*
Sample STD/Batches	***Mean***	***Mean***	***Mean***	***Mean***	k_{CH}, k_L
Grey $\Delta a^*\Delta b^*$ 1-10	0.6	0.65	7.11	5.49	1.30
Grey $\Delta a^*\Delta b^*$ 11-20	1.2	1.20	4.17	3.54	1.18
Grey $\Delta a^*\Delta b^*$ 21-30	2.4	2.23	2.57	2.59	0.99
Grey $\Delta L^*\Delta a^*$ 1-10	0.6	0.66	6.88	4.63	1.48
Grey $\Delta L^*\Delta a^*$ 11-20	1.2	1.24	4.20	3.57	1.18
Grey $\Delta L^*\Delta a^*$ 21-30	2.4	2.41	2.56	2.64	0.97
Blue $\Delta a^*\Delta b^*$ 1-10	0.6	0.74	4.97	4.60	1.18
Blue $\Delta a^*\Delta b^*$ 11-20	1.2	1.30	3.97	2.92	1.36
Blue $\Delta a^*\Delta b^*$ 21-30	2.4	2.32	2.48	2.39	1.04
Blue $\Delta L^*\Delta a^*$ 1-10	0.6	0.53	6.20	4.94	1.26
Blue $\Delta L^*\Delta a^*$11-20	1.2	1.10	3.73	2.71	1.38
Blue $\Delta L^*\Delta a^*$21-30	2.4	1.89	2.59	2.26	1.15

***Table 9*: Requested and delivered numerical colour differences CMC(2:1) between 'TWC' batches and 'FA' or 'TWC' standards and corresponding visual results for physical 'TWC' and 'BH' samples 'ΔV_{CMC}(1:1)'; resulting parametric factors for lightness '$\Delta L^*\Delta a^*$' and chroma '$\Delta a^*\Delta b^*$' – directions.**

4.2.3 After inspection of all physical sample pairs, and the consideration of observers, most of them participating for their very first time in observational experiments, it was decided to start with those colour difference datasets that were clearly visible to observers. Physical 'TWC' and 'BH' samples were presented in a random order to each observer in a viewing cabinet. The arrangement of samples was generally very similar to the one that was introduced as a digital setup as described in *Graph 1***.** A grey scale was formed from five squared (5 x 5 cm) flat wool panels varying mainly in lightness (see *Table 10*) when compared with a fixed grey standard panel. Twenty observers participated in this pilot study judging both datasets in four sessions. All observers passed the Ishihara test ('10' male/'10' female, between 22 – 55 years old, average of 31 years, no prior experiences in colour matching assignments). The 'BH' – dataset consisted of '117' samples (including '12' repetitions); the same number of samples was used for the 'TWC' dataset. Over '5200' observations were obtained from physical samples during *Experiment A – Part A*. Grey scale samples were measured at the beginning, mid term, and the end of a experiment **(**d/8º, SPIN, cabinet's light source). A transfer function (smooth spline interpolation between 'GRADE' values) was modelled so to transfer perceptual GRADE values (between '1' and '5') to visual colour difference units for any chosen colour difference formula, for instance, CMC(*l*:*c*) and given 'ΔV_{CMC}(1:1)' units. The results were compared with predicted results. The transfer function values are presented in *Figure 50.*

GRADE	*SUM*	$(\Delta L^*/lS_L)^2$	$(\Delta C^*_{ab}/cS_c)^2$	$(\Delta H^*_{ab}/S_H)^2$	CMC(1:1)	ΔL^* %	ΔC^*_{ab} %	ΔH^*_{ab} %	*SUM*
1	183.34	182.04	0.096	1.212	**13.54**	99.28	0.05	0.66	100
2	53.30	52.23	0.314	0.761	**7.30**	97.98	0.59	1.43	100
3	30.51	26.43	2.778	1.307	**5.52**	86.61	9.11	4.28	100
4	14.39	13.51	0.286	0.594	**3.79**	93.89	1.99	4.12	100
5	0.29	0.22	0.001	0.075	**0.54**	74.52	0.19	25.29	100

***Table 10*: Measured colour differences 'GRADE' against a fixed grey standard and component differences in per cent**

4.3 Observational results

4.3.1 Observational results in the form of '$\Delta V_{CMC}(1:1)$' values were then compared with predicted results 'ΔE_{var}' for approximately the same colour difference sample pairs either obtained from the CIELAB, CMC, or *CIEDE*$_{2000}$ formula. Ratios between visual results '$\Delta V_{CMC}(1:1)$' and predicted values in '$\Delta E_{var}(1:1)$' and '(2:1)' units between 'TWC' and 'BH' samples were compared with each other (see *Equation 91*, *Figure 51* and *52*). Generally, and for all sample pairs, it was evident that ratios for 'BH' samples were judged with a larger colour difference magnitude when compared with ratios for 'TWC' sample pairs. A Wilcoxon rank sum test rejected the null hypothesis of equal medians at a 5% significance level for the full 'BH'- and 'TWC' ratio data set ('p' – value equal to 5.78e-05). The overall visual parametric effect was approximately 28% larger on average in magnitude for the same modelled colour difference between 'BH' (*Image 11*) and 'TWC' (*Image 15*) samples. However, a more detailed analysis for *Table 9* revealed a possibly texture effect for 'BH' sample groups. This effect seemed to vanish once colour difference magnitudes of '2.4' '$\Delta E_{CMC}(2:1)$' units were judged. Those judgements between 'BH' and 'TWC' samples became similar. The parametric factor between predicted and judged colour differences were largest for small colour difference sample pairs (approximately a factor of '1.35' for 'BH' against 'TWC' samples), larger for critical colour matching work at Coats plc for difference sample pairs in the region around '1.2' '$\Delta E_{CMC}(2:1)$' units (approximately a factor of '1.27'), and smallest for 'BH' colour difference sample pairs in the region '2.4' '$\Delta E_{CMC}(2:1)$' units and larger (factor of '1.06').

4.4 Formulae performances

4.4.1 The performances of existing formulae were analysed and optimised in terms of 'STRESS' units[pp] so to derive a formula for each dataset that was able to increase the prediction and correlation between visual 'ΔV_{CMC}' and instrumental data 'ΔE_{var}'. STRESS values for the physical 'BH' dataset and several formulae are listed in *Table 11*. Performance values for the physical 'TWC' dataset are listed in *Table 12*. Parametric factors 'k_L', 'k_C', and 'k_H' are listed for various values; '$\Delta V/\Delta E$ 'r'' describes a Pearson's correlation coefficient for visual against predicted colour differences for a particular setting and formula; and '$\Delta V/\Delta E$ 't'' provides a critical statistical 't'-test value for a particular setting and formula. An overall factor was applied so to reduce absolute differences between visual and predicted results. A large average residual figure suggests higher variances and lower precision. A 'PF/3' value and component performance values are also provided.

[pp] see page 118

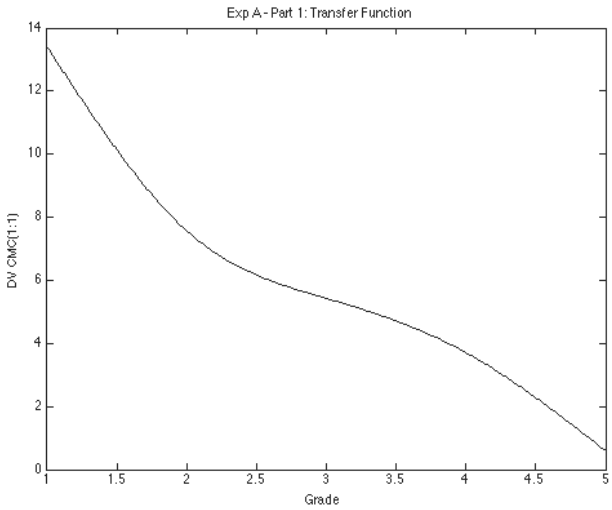

***Figure 50*: Transfer Function Grade to ΔV_{CMC} (1:1) for Exp. A – Part 1: Physical samples**

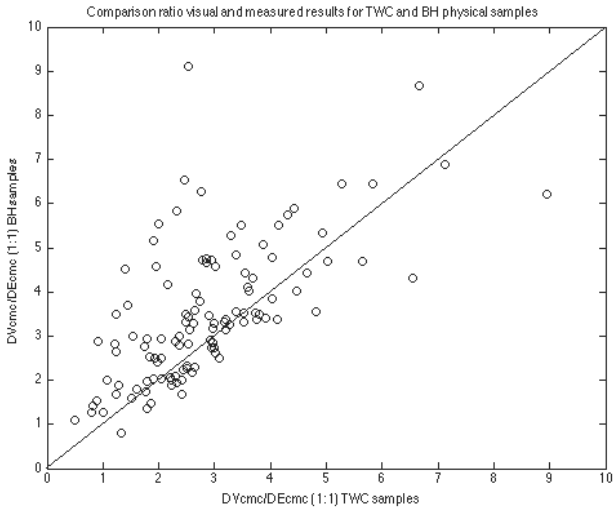

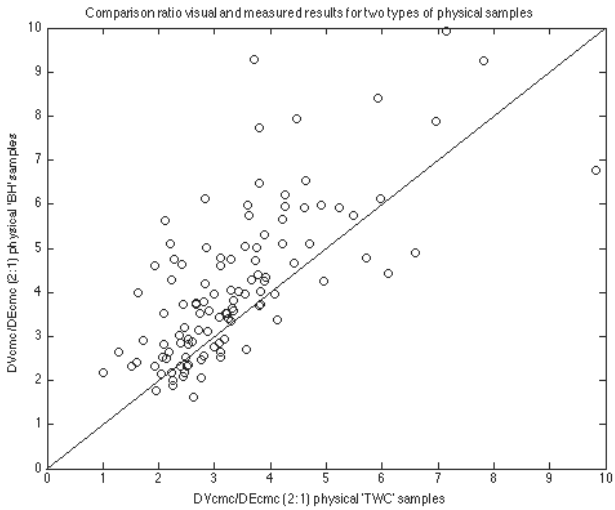

***Figure 51 and 52*: Comparison between ratios 'ΔV_{CMC}' and 'ΔE_{CMC}' for all 'BH' and 'TWC' samples.**

PHY. BH	***CMC***	***ΔV_{CMC}(1:1)***				***Best Setting***
k_L	2	1	2.14	2.23	**CV**	39.64
k_C	1	1	1	1.12	**VAB**	43.3
					Gamma	1.54
Δ*V*/Δ*E* 'r'	0.54	0.3	0.55	0.56	**Factor**	3.24
Δ*V*/Δ*E* 't'	6.76	3.38	6.98	7.12	**Mean residual**	1.66
STRESS	***34.53***	***41.88***	***34.49***	***34.35***	***PF/3***	***45.76***
BLUE	CMC					
k_L	2	1	2.14	2.24		
k_C	1	1	1	1.12		
	1	1	1	1		
STRESS	28.22	37.7	28.27	28.21		
GREY	CMC					
k_L	2	1	2.14	2.24		
k_C	1	1	1	1.12		
	1	1	1	1		
STRESS	38.42	44.13	38.37	38.04		
OVERALL	***$CIEDE_{2000}$***					***Best Setting***
k_L	2	1	1.92	1.94	**CV**	42.72
k_C	1	1	1	0.92	**VAB**	42.67
k_H	1	1	1	1.05	**Gamma**	1.52
Δ*V*/Δ*E* 'r'	0.67	0.47	0.66	0.66	**Factor**	3.32
Δ*V*/Δ*E* 't'	9.5	5.7	9.34	9.41	**Mean residual**	1.73
STRESS	***36.22***	***40.36***	***36.21***	***36.04***	***PF/3***	***45.81***
BLUE	$CIEDE_{2000}$					
k_L	2	1	1.92	1.94		
k_C	1	1	1	0.92		
k_H	1	1	1	1.05		
STRESS	30.99	29.3	30.73	31.02		
GREY	$CIEDE_{2000}$					
k_L	2	1	2.14	1.94		
k_C	1	1	1	0.92		
k_H	1	1	1	1.05		
STRESS	38.57	45.96	38.7	38.41		
OVERALL	***CIELAB***					***Best Setting***
k_L	2	1	1.21	1.24	**CV**	44.58
k_C	1	1	1	0.66	**VAB**	47.12
k_H	1	1	1	1.36	**Gamma**	1.61
Δ*V*/Δ*E* 'r'	0.43	0.34	0.53	0.44	**Factor**	2.35
Δ*V*/Δ*E* 't'	5.09	3.81	6.67	5.17	**Mean residual**	1.83
STRESS	***45.33***	***43.92***	***41.29***	***32.24***	***PF/3***	***53.39***
BLUE	CIELAB					
k_L	2	1	1.21	1.24		
k_C	1	1	1	0.66		
k_H	1	1	1	1.36		
STRESS	44.07	35.83	43.12	43.36		
GREY	CIELAB					
k_L	2	1	1.21	1.24		
k_C	1	1	1	0.66		
k_H	1	1	1	1.36		
STRESS	47.95	50.46	39.77	34.95		

***Table 11*: Optimised formulae (weighting functions only) for physical 'BH' samples (*Experiment A – Part A*).**

PHY. TWC	***CMC***	***ΔV_{CMC}(1:1)***				***Best Setting***
k_L	2	1	2.58	2.75	**CV**	29.14
k_C	1	1	1	1.24	**VAB**	50.04
					Gamma	1.59
$\Delta V/\Delta E$ 'r'	0.85	0.57	0.88	0.9	**Factor**	3
$\Delta V/\Delta E$ 't'	17.01	7.35	19.96	21.72	**Mean residual**	0.87
STRESS	***26.94***	*41.55*	***25.9***	***25.24***	***PF/3***	***45.95***
BLUE	CMC					
k_L	2	1	2.58	2.75		
k_C	1	1	1	1.24		
STRESS	29.32	47.09	27.43	27.42		
GREY	CMC					
k_L	2	1	2.58	2.75		
k_C	1	1	1	1.24		
STRESS	24.66	37.57	24.16	23.08		
OVERALL	***$CIEDE_{2000}$***					***Best Setting***
k_L	2	**1**	1.96	1.96	**CV**	31.37
k_C	1	1	1	1.00	**VAB**	48.95
k_H	1	1	1	1.00	**Gamma**	1.57
$\Delta V/\Delta E$ 'r'	0.95	0.77	0.94	0.94	**Factor**	3
$\Delta V/\Delta E$ 't'	29.91	12.72	29.46	29.55	**Mean residual**	0.96
STRESS	***25.97***	***33.8***	***25.96***	***25.96***	***PF/3***	***46.04***
BLUE	$CIEDE_{2000}$					
k_L	2	1	1.96	1.96		
k_C	1	1	1	1.00		
k_H	1	1	1	1.00		
STRESS	28.74	29.02	28.57	28.57		
GREY	$CIEDE_{2000}$					
k_L	2	1	1.96	1.96		
k_C	1	1	1	1.00		
k_H	1	1	1	1.00		
STRESS	22.35	35.34	22.47	22.47		
OVERALL	***CIELAB***					***Best Setting***
k_L	2	1	1.59	1.31	**CV**	40.06
k_C	1	1	1	0.60	**VAB**	57.02
k_H	1	1	1	1.39	**Gamma**	1.71
$\Delta V/\Delta E$ 'r'	0.66	0.56	0.64	0.76	**Factor**	1.97
$\Delta V/\Delta E$ 't'	9.2	7.15	8.88	12.48	**Mean residual**	1.24
STRESS	***41.08***	***43.29***	***41.29***	***34.59***	***PF/3***	***55.95***
BLUE	CIELAB					
k_L	2	1	1.59	1.31		
k_C	1	1	1	0.60		
k_H	1	1	1	1.39		
STRESS	44.74	38.86	42.33	35.79		
GREY	CIELAB					
k_L	2	1	1.59	1.31		
k_C	1	1	1	0.60		
k_H	1	1	1	1.39		
STRESS	38.99	46.12	39.87	34.07		

***Table 12*: Optimised formulae (weighting functions only) for physical 'TWC' samples (*Experiment A – Part A*).**

4.4.2 *Table 11* and *12* provided evidence as how much predictive results were altered by varying weightings either for differences in lightness 'ΔL^*', chromatic content 'ΔC^*_{ab}', or in hue content 'ΔH^*_{ab}'. The prediction performances from formulae were generally better for 'TWC' samples than for 'BH' – type samples (the CMC formula was developed using a comprehensive 'TWC' sample dataset). There was no significant difference in prediction performances between $CIEDE_{2000}$ (best setting) and CMC (best setting), but between CIELAB (1:1:1) and all other formulae according to the 'STRESS' measure (see *Table 13*).

BH	***STRESS^2***	*1179.92*	*1298.88*	*1928.97*	*1546.06*
STRESS^2	***FORMULA***	***CMC***	***CIEDE$_{2000}$***	***CIELAB***	***CIELAB W***
1179.92	**CMC**	**A/B**	0.908	**0.612**	0.763
1298.88	***CIEDE$_{2000}$***	1.101	**A/B**	**0.673**	0.840
1928.97	**CIELAB**	**1.635**	**1.485**	**A/B**	1.248
1546.06	**CIELAB W**	1.310	1.190	0.801	**A/B**
TWC	***STRESS^2***	*765.08*	*823.69*	*1728.06*	*1204.09*
STRESS^2	***FORMULA***	***CMC***	***CIEDE$_{2000}$***	***CIELAB***	***CIELAB W***
637.06	**CMC**	**A/B**	0.773	**0.369**	**0.529**
673.92	***CIEDE$_{2000}$***	0.881	**A/B**	**0.390**	**0.560**
1874.02	**CIELAB**	**2.449**	**2.275**	**A/B**	1.212
1196.47	**CIELAB W**	**1.564**	**1.453**	**0.692**	**A/B**
DF degrees of freedom: 116		**Range (0.7359 – 1.3589)**			

***Table 13*: 'F'-test for several formulae and physical 'BH' and 'TWC' samples *Experiment A: Part – A*. Highlighted numbers indicates a significant difference in performances between two formulae.**

4.4.3 The main difference in prediction performances was associated with grey samples. Blue samples were predicted with similar results for both datasets and advanced formulae. $CIEDE_{2000}$ predictions for blue samples were not altered significantly by the variation of weighting functions, whereas 'CMC' prediction performances for blue colours were altered when 'k_L' was set to a value of '1'. A buttonhole stitch type thread sewn into a fabric sample caused two distinguished differences when compared to thread winding card samples. These two differences can be explained by; (**1**) a texture difference induced by the 'BH' stitch texture in 'East/West' direction upon a fabric sample's texture ('$\Delta V_{CMC}(1:1)$' threshold for physical 'BH' samples around a value of '3'), and (**2**) by a boundary effect between the fabric sample and 'BH' stitch type with an effect of enhancing the contrast when a dark line (or shadow between stitch edge and fabric) inbetween two areas increased visually the contrast between both areas. Both visual effects increased colour difference judgements in addition to lightness and chromatic crispening effects caused by a similar coloured background. There was also evidence that a texture effect was more prominent in small colour difference sample pairs and diminished gradually for larger colour differences (see *Table 9*). The general recommendation for judging colour differences within textile samples with a lightness weighting function of '2' was approximately confirmed considering 'BH and 'TWC' lightness weighting settings for

CMC(l:1) ‘2.14’/‘2.58’ (‘BH’/’TWC’) and ‘1.94’/‘1.96’ (‘BH’/’TWC’) for $CIEDE_{2000}$(k_L:1:1) in *Experiment A – Part A*, respectively. The linear factor, a value for minimizing the sum of the square root of squared differences between visual and predicted results, gave an indication of how far on average a best setting for a particular formula according to STRESS was compared to visual results in absolute units. A factor of three indicated to multiply a predicted colour difference on average by three times. The correlation coefficient ‘r’ gave an indication of the strength of the linear relationship between visual and predicted results and would approach a value of ‘1’ for a perfect agreement. A ‘r’ value of ‘0.55’ (for ‘BH’ samples) and ‘0.88’ (for ‘TWC’ samples) for the CMC(2:1) formula explained those differences in STRESS values between both data sets. The higher variation in residuals may also explain overall quality and/or (in)-consistency in the design and handling of physical samples that were judged in a viewing cabinet[qq]. *Figures 53 – 60* for ‘BH’ and *Figures 61 – 68* for ‘TWC’ samples indicated normal distributed residuals for the $CIEDE_{2000}$ and CMC formula for both datasets, whereas the distribution for CIELAB(weighted) and CIELAB were especially ‘not-normal distributed’ in the case of ‘BH’ samples. This provided some indications how to interpretate those results.

4.4.4 In summation, it can be said that the ratio, between predicted and visual results, was largest for smaller colour difference pairs and decreased towards larger colour difference sample pairs. The effect of observing a colour difference end product as a ‘BH’ sample resulted on average in larger visual colour differences about 30% per cent higher when compared with visual colour difference results obtained from ‘TWC’ samples. This texture and contrast effect (see *Image 11*) was significant. Adjusting weighting factors increased linear correlation between visual and numerical results (‘BH’ sample correlation values ‘r’ for the CMC formula were in the range from ‘0.3’ – ‘0.56’ and for ‘TWC’ samples in the range from ‘0.57’ – ‘0.9’). However, grey samples gave larger variations in prediction performances for both datasets if compared to predictions obtained from blue colour samples. Although, most optimised lightness weighting functions were more or less matched with the setting that is generally recommended for colour difference evaluation for textile products, the absolute differences between predicted and visual result were large. An overall size parametric factor maybe necessary, if more accurate results are required.

[qq] see page 156-157 comparison of digital images

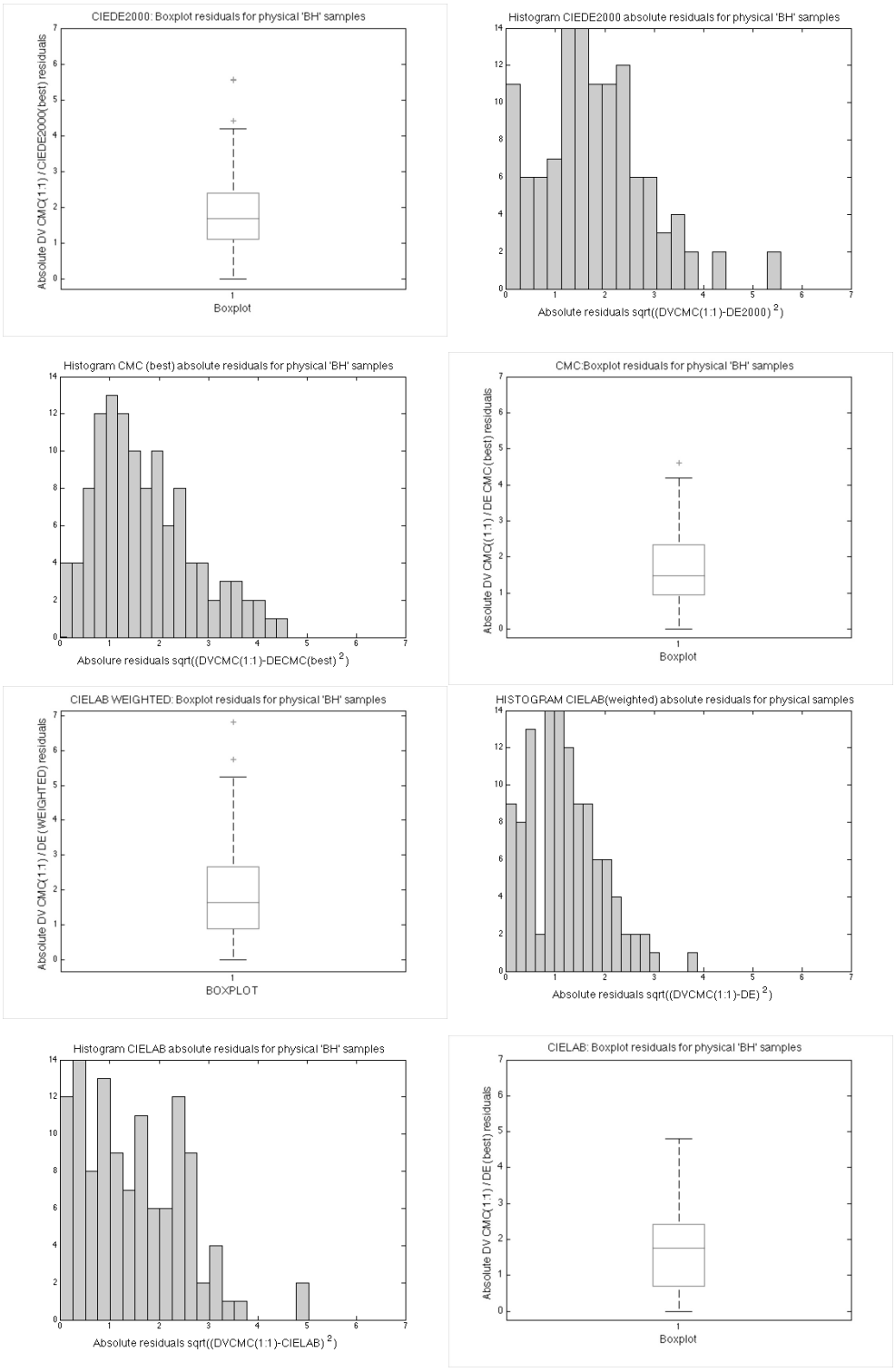

***Figure 53-60*: Residual boxplots and histograms for *CIEDE*$_{2000}$, CMC, CIELAB(W), and CIELAB (from top to bottom) and physical 'BH' buttonhole stitch type samples for best fitting modes according to *Table 11* (*Experiment A – Part A*).**

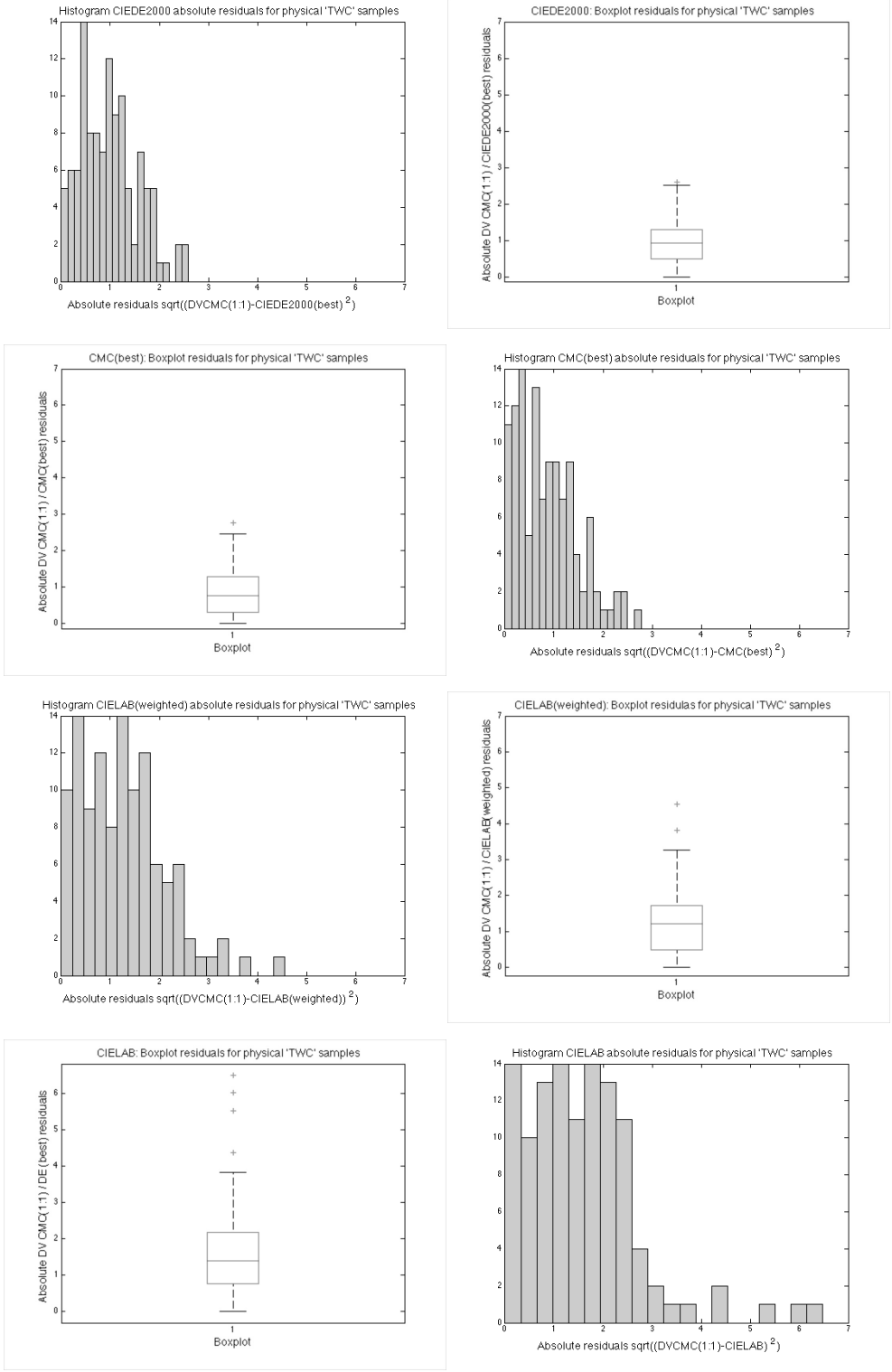

***Figure 61-68*: Residuals boxplots and histograms for $CIEDE_{2000}$, CMC, CIELAB(W), and CIELAB for physical 'TWC' samples for best fitting modes as given in *Table 12* (*Experiment A – Part A*). Residuals between visual and predictive colour differences were approximately normal distributed for all formulae (see 'F' – test – *Table 13* for comparison of significant differences in prediction performances STRESS)**

4.5 *Experiment A – Part B*: Digital samples

4.5.1. Physical samples were limited in terms of numbers and colour centres so that it became desirable to find; (**1**) a correlation between visual results that were obtained from physical samples and those that can be obtained from digital reproductions, and (**2**) once a relationship was established, more colour centres and batches could be designed by digital processing and psychophysically evaluated without the need of a large amount of individual produced physical samples (see *Image 16* and *17*). Therefore, a similar experiment was conducted using most of the observers from *Part – A* but now judging digital reproductions on a LCD screen instead of physical samples (*Experiment A – Part B*).

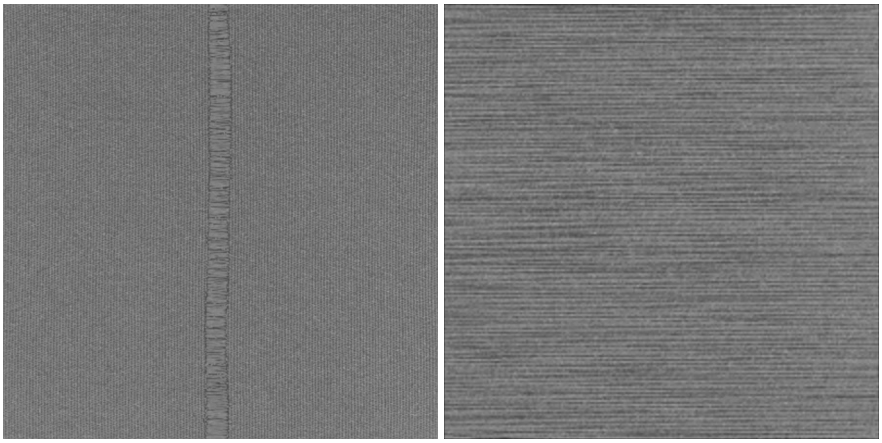

***Image 16 and 17*: Digital synthesized buttonhole 'BH' and synthesized thread winding card 'TWC' image used for *Experiment A – Part B*.**

4.5.2 Datasets were produced so to provide colour difference sample pairs with magnitudes in the range '1.2', '2.4' and '3.6' ΔE_{CMC} (2:1) units mainly differing in two directions ('$\Delta L^* \Delta a^*$' and '$\Delta a^* \Delta b^*$') in regards to both standard samples. The average colour difference between modelled and measured samples on screen for the 'TWC' sample set was on average '0.42' 'ΔE_{00}' units. The distribution of batches followed the same pattern as described in *Figure 46, 47, 48* and *49*. Twenty observers (average age of '29' years) participated in *Part B* (fifteen of them participated also in *Part A*) judging '129' samples for each data set within '2' to '3' sessions. Overall more than '5000' judgments were made for digital 'TWC' and 'BH' samples. Observers inter-repeatability values[rr] for both experiments were for physical/digital 'TWC' samples '30'/'27' STRESS units and '23'/'24' STRESS units for 'BH' samples, respectively. The intra-observer variations for physical/digital 'TWC' samples were '19'/'16' and '20'/'17' STRESS units for physical/digital 'BH' samples. All visual results were transformed from interpolated 'GRADE'- to 'ΔV_{CMC}(1:1)' values as given in *Table 14*.

[rr] see page 118: *Equations 109ff*; 'F' equals 1

GRADE	5	4	3	2	1
CMC(1:1)	0.809	1.963	3.592	6.734	13.7

***Table 14*: Measured grey scale over time to construct a transfer function interpolated between 'GRADES' (cubic spline).**

4.5.3 All digital colour sample pairs (same number of batches either as such '1.2' and '2.4' '$\Delta E_{CMC}(2:1)$' units away from the standards as described in in *Part – A*) were displayed to observers, who were asked to judge them on a digital screen. Each observer provided a GRADE number (decimal numbers were allowed) for each colour difference pair by comparing various grey patches with a standard (GRADE number was attached to each pair) until it became the same perceptual colour difference as seen in one of the colour difference pair samples that were to be judged. The results were compared in two ways as to determine; (**1**) whether there was a difference in visual colour difference perception between 'TWC' and 'BH' samples (ratios '$\Delta V/\Delta E$' for each dataset were calculated and compared with each other since the colour specifications for 'BH' standards ('FA' – samples) and 'TWC' standards differed), and (**2**) how those digital results were related to those results that were obtained from physical samples (*Table 16*). Also, colour difference formulae CIELAB, CIELAB (weighted), CMC, and $CIEDE_{2000}$ were optimised and contrasted with each other in terms of performances (see *Table 17* and *18*). Parametric factor quantification results for digital samples are listed in *Table 15*.

DIGITAL SAMPLES	*Requested*	*Measured*	*'BH'*	*'TWC'*	*Sample*
	TWC CMC (1:1)	*TWC CMC (1:1)*	$\Delta V/\Delta E$	$\Delta V/\Delta E$	*FACTOR*
Sample STD/Batches	*Mean*	*Mean*	*Mean*	*Mean*	k_{CH}, k_L
Grey $\Delta a^*\Delta b^*$1-10	1.2	1.20	2.35	1.16	2.01
Grey $\Delta a^*\Delta b$ 11-20	2.4	2.41	1.64	0.97	1.71
Grey $\Delta L^*\Delta a^*$ 1-10	1.2	1.45	2.64	1.61	1.46
Grey $\Delta L^*\Delta a^*$11-20	2.4	2.44	2.08	1.57	1.32
Blue $\Delta a^*\Delta b$ 1-10	1.2	1.20	1.74	1.51	1.14
Blue $\Delta a^*\Delta b$ 11-20	2.4	2.40	1.32	1.22	1.08
Blue $\Delta L^*\Delta a^*$ 1-10	1.2	1.39	1.70	1.40	1.17
Blue $\Delta L^*\Delta a^*$11-20	2.4	2.43	1.41	1.27	1.11
ALL SAMPLES	**1.80**	**1.87**	**1.84**	**1.41**	**30%**

***Table 15*: Requested and measured numerical colour differences 'ΔE_{CMC}(1:1)' for digital 'TWC' and 'BH' samples; corresponding visual/predictive ratio results for digital 'BH' and digital 'TWC' samples; parametric factors[ss] for '$\Delta L^*\Delta a^*$' and chroma '$\Delta a^*\Delta b^*$' – directions, and overall average parametric effect in percent between digital 'TWC' and 'BH' samples.**

4.5.4 Overall ratio results in *Table 15* suggested that digital 'BH' samples were judged on average 30% higher when compared with those results from visual colour difference judgements obtained from digital 'TWC' samples (see *Figure 69*). This confirmed with overall results from observational experiments using physical samples that are listed in *Table 9*. Also, the same trend of decreasing overall parametric factor values (texture content and crispening) for increasing

[ss] see pages 112ff for parametric factors

colour difference magnitudes (to be judged) were observed with those digital data sets. However, there were subtle differences between those ratio results between 'TWC' and 'BH' samples in digital and physical form. If we consider only those modelled samples in the range from '1.2' to '2.4' '$\Delta E_{CMC}(1:1)$' units then chromatic parametric factors were larger in the viewing cabinet between 'BH' and 'TWC' samples compared to digital chromatic parametric factors (higher luminance in the viewing cabinet), and especially lightness parametric factors between 'TWC' and 'BH' samples were enlarged on a digital screen if compared to those in the viewing cabinet. Also, the absolute ratio magnitudes of visual colour differences were significant larger from physical samples. *Figure 70 – 71* represented plots of ratios between digital and physical 'TWC' and 'BH' samples for either directions; (**1**) changes in '$\Delta a^*\Delta b^*$' or (**2**) '$\Delta L^*\Delta a^*$'. *Table 16* listed magnitude differences between either digital 'BH' or 'TWC' and physical 'BH' or 'TWC' ratio results.

TWC and BH SAMPLES COMPARISON: DIGITAL AGAINST PHYSICAL SAMPLE OBSERVATIONS												
TWC	***DIG***	$\Delta a^*\Delta b^*$	$\Delta E/\Delta V$	***PHY***	$\Delta a^*\Delta b^*$		***DIG***	$\Delta L^*\Delta a^*$	$\Delta E/\Delta V$	***PHY***	$\Delta L^*\Delta a^*$	
TWC	*DV*	$\frac{DE}{CMC}$	***RATIO***	***DV***	$\frac{DE}{CMC}$	***RATIO***	***DV***	$\frac{DE}{CMC}$	***RATIO***	***DV***	$\frac{DE}{CMC}$	***RATIO***
ΔV or ΔE	2.27	1.82	1.30	4.66	1.81	2.67	2.92	1.48	2.05	4.00	1.48	2.84
TWC	RATIO DIGITAL/PHYSICAL						RATIO DIGITAL/PHYSICAL					
DIG/PHY	**2.06**						**1.36**					
BH	***DIG***	$\Delta a^*\Delta b^*$	$\Delta E/\Delta V$	***PHY***	$\Delta a^*\Delta b^*$		***DIG***	$\Delta L^*\Delta a^*$	$\Delta E/\Delta V$	***PHY***	$\Delta L^*\Delta a^*$	
BH	*DV*	$\frac{DE}{CMC}$	***RATIO***	***DV***	$\frac{DE}{CMC}$	***RATIO***	***DV***	$\frac{DE}{CMC}$	***RATIO***	***DV***	$\frac{DE}{CMC}$	***RATIO***
ΔV or ΔE	3.05	1.75	1.81	5.97	2.07	3.08	4.27	2.38	1.91	5.96	2.37	2.90
BH	RATIO DIGITAL/PHYSICAL						RATIO DIGITAL/PHYSICAL					
DIG/PHY	**1.65**						**1.40**					

***Table 16*: Comparison between physical and digital '$\Delta a^*\Delta b^*$' and '$\Delta L^*\Delta a^*$' ratios for digital and physical 'TWC' and 'BH' samples**

4.5.5 *Table 16* recommended factors to be used so to relate results from digital samples judged on screen with results obtained from physical samples that were judged in a viewing cabinet. Two main observations were established such as; (**1**) ratios between visual and predicted results were larger in magnitude for physical samples no matter what kind of stitch type was presented to observers, and (**2**) lightness difference ratios ('2.28' and '1.89' for grey and blue 'TWC' samples) were on screen larger when compared to chromatic difference ratios on screen for 'TWC' samples ('1.15' and '1.29'). Chromatic differences for digital 'BH' samples were larger ('1.84' and '1.59'), and lightness ratios for digital grey 'BH' samples were similar in magnitude to physical grey 'BH' lightness samples (ratio of '0.98').

4.5.6. Two possible reasons have contributed to those results, (**1**) chromatic differences observed from physical samples in a viewing cabinet were more prominent to observers (viewing cabinet's light source luminance equalled 415 cd/m^2 compared to 196 cd/m^2 for a LCD's white point measurement), and (**2**) lightness 'crispening effects' on screen were larger than similar effects observed for physical samples.

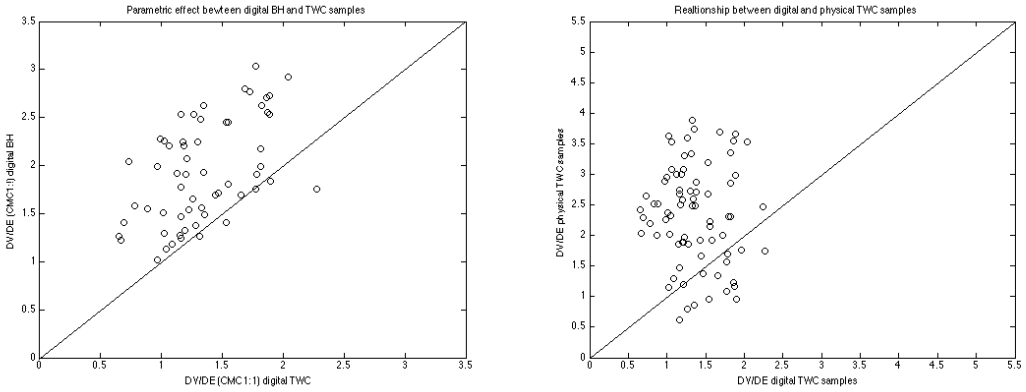

Figure 69: Plot of ratios '$\Delta V/\Delta E$' (left) for digital 'TWC' and 'BH' samples and overall for Fig. 70-71 (right)

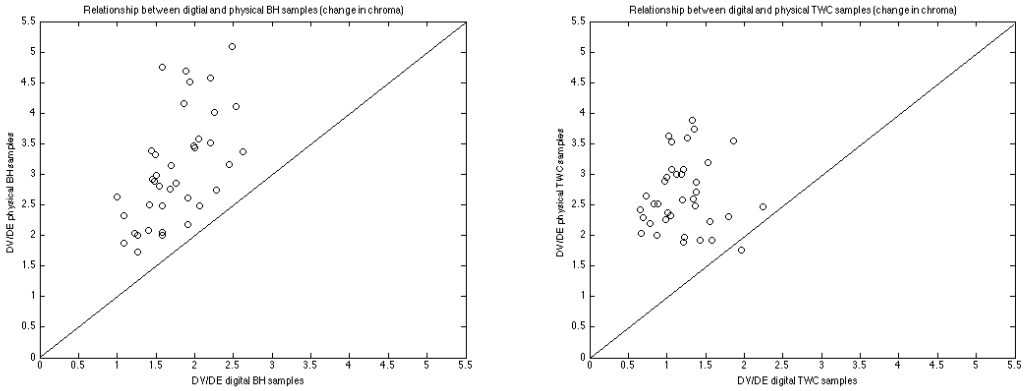

Figure 70: Ratios 'ΔV/ΔE' change in chroma for digital and physical 'BH' (left) and 'TWC' (right) samples

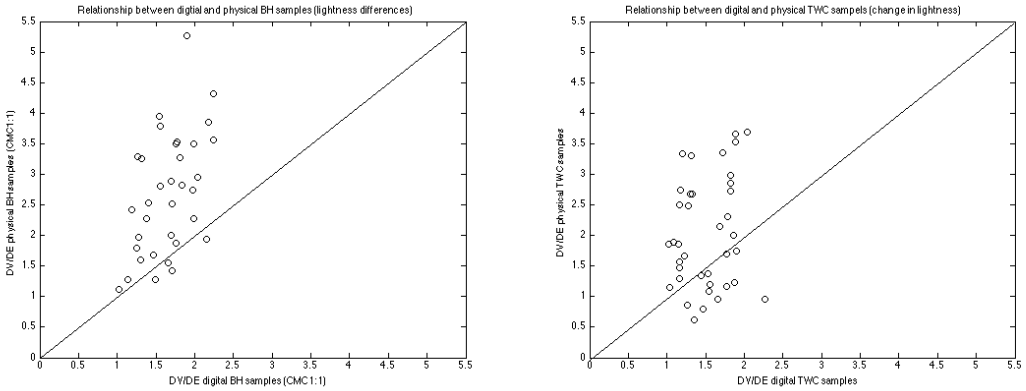

***Figure 71*: Ratios '$\Delta V/\Delta E$' change in lightness for digital and physical 'BH' (left) and 'TWC' (right) samples**

4.6 Formula performances

4.6.1 Fomulae performances in STRESS units are listed in *Table 17* and *18* for $CIEDE_{2000}$, CMC, CIELAB(weighted), and CIELAB for various parametric factors. In *Table 17* and *18* optimised weighting factors are listed for the predictions of digital colour difference sample pairs. Significant differences were observed in 'k_L' weighting values between physical and digital samples as such varying from '2.14' to '2.58' (physical 'BH' and 'TWC' sample pairs) and '0.94' to '0.78' for digital 'BH' and 'TWC' sample pairs in the case of the CMC formula; from '1.94' to '1.96' for physical 'BH' and 'TWC' sample pairs and '0.73' to '0.64' for digital 'BH' and 'TWC' sample pairs in the case of the $CIEDE_{2000}$'s formula.

Digital BH	***CMC***					***Best Setting***
k_L	2	1	0.94	1.05	**CV**	28.69
k_C	1	1	1	1.33	**VAB**	27.07
					Gamma	1.31
ΔV/ΔE 'r'	0.52	0.76	0.77	0.82	**Factor**	1.62
ΔV/ΔE 't'	6.53	12.29	12.66	14.39	**Mean residual**	0.87
STRESS	***36.63***	***27.88***	***27.78***	***25.40***	***PF/3***	***28.90***
BLUE	CMC					
k_L	2	1	0.94	1.05		
k_C	1	1	1	1.33		
STRESS	31.52	27.59	28.36	25.17		
GREY	CMC					
k_L	2	1	0.94	1.05		
k_C	1	1	1	1.33		
STRESS	39.24	28.25	27.72	26.70		
Digital BH	***CIEDE$_{2000}$***					***BEST Setting***
k_l	2	1	0.73	0.74	**CV**	21.8
k_C	1	1	1	1.05	**VAB**	22.64
k_H	1	1	1	1.00	**Gamma**	1.25
Δ*V*/Δ*E* 'r'	0.61	0.87	0.94	0.94	**Factor**	1.61
Δ*V*/Δ*E* 't'	8.16	18.78	29.19	29.51	**Mean residual**	0.67
STRESS	***36.2***	***22.96***	***19.65***	***19.62***	***PF/3***	***23.22***
BLUE	$CIEDE_{2000}$					
k_l	2	1	0.73	0.74		
k_C	1	1	1	1.05		
k_H	1	1	1	1.00		
STRESS	41.7	29.66	21.71	21.37		
GREY	$CIEDE_{2000}$					
k_l	2	1	0.73	0.74		0.808
k_C	1	1	1	1.05		1.039
k_H	1	1	1	1.00		0.978
STRESS	33.72	19.16	18.53	18.65		**14.95**
Digital BH	***CIELAB***					***Best Setting***
k_l	2	1	0.59	0.36	**CV**	34.68
k_C	1	1	1	0.41	**VAB**	38.61
k_H	1	1	1	1.00	**Gamma**	1.46
Δ*V*/Δ*E* 'r'	0.19	0.49	0.7	0.78	**Factor**	0.67
Δ*V*/Δ*E* 't'	2.09	5.9	10.37	13.26	**Mean residual**	1.12
STRESS	***52.72***	***42.18***	***36.96***	***30.46***	***PF/3***	***39.86***
BLUE	CIELAB					
k_l	2	1	0.59	0.36		
k_C	1	1	1	0.41		
k_H	1	1	1	1.00		
STRESS	58.8	49.97	37.68	31.53		
GREY	CIELAB					
k_l	2	1	0.59	0.36		
k_C	1	1	1	0.41		
k_H	1	1	1	1.00		
STRESS	49.98	38.18	36.91	30.11		

***Table 17*: Optimised formulae (weighting functions only) for digital Buttonhole stitch type samples for *Experiment A – Part B*.**

Digital TWC	***CMC***					***BEST Setting***
k_L	2	1	0.78	0.99	**CV**	24.6
k_C	1	1	1	1.64	**VAB**	23.22
					Gamma	1.26
ΔV/ΔE 'r'	0.43	0.76	0.83	0.87	**Factor**	1.27
ΔV/ΔE 't'	5.01	12.51	15.57	18.59	**Mean residual**	0.59
STRESS	***39.54***	***26.76***	***24.86***	***21.97***	***PF/3***	***24.7***
BLUE	CMC					
k_L	2	1	0.78	0.99		
k_C	1	1	1	1.64		
STRESS	27.36	26.75	22.35	21.37		
GREY	CMC					
k_L	2	1	0.78	0.99		
k_C	1	1	1	1.64		
STRESS	46.7	31.8	26.24	21.78		
Digital TWC	***CIEDE$_{2000}$***					***BEST Setting***
k_l	2	**1**	0.64	0.65	**CV**	15.01
k_C	1	1	1	1.20	**VAB**	17.9
k_H	1	1	1	0.90	**Gamma**	1.19
Δ*V*/Δ*E* 'r'	0.55	0.87	0.99	0.99	**Factor**	1.15
Δ*V*/Δ*E* 't'	6.93	18.77	79.46	81.89	**Mean residual**	0.38
STRESS	***37.4***	***21.8***	***13.87***	***13.66***	***PF/3***	***17.43***
BLUE	*CIEDE$_{2000}$*					
k_l	2	1	0.64	0.65		
k_C	1	1	1	1.20		
k_H	1	1	1	0.90		
STRESS	36.35	23.98	13.55	13.76		
GREY	*CIEDE$_{2000}$*					
k_l	2	1	0.64	0.65		
k_C	1	1	1	1.20		
k_H	1	1	1	0.90		
STRESS	38.68	20.06	12.58	12.34		
Digital TWC	***CIELAB***					***BEST Setting***
k_l	2	1	0.60	0.35	**CV**	26.58
k_C	1	1	1.00	0.45	**VAB**	31.13
k_H	1	1	1.00	1	**Gamma**	1.36
Δ*V*/Δ*E* 'r'	0.21	0.53	0.79	0.9	**Factor**	0.58
Δ*V*/Δ*E* 't'	2.275	6.7	13.8	22.02	**Mean residual**	0.66
STRESS	***52.72***	***40.41***	***30.88***	***23.13***	***PF/3***	***31.26***
BLUE	CIELAB					
k_l	2	1	0.6	0.35		
k_C	1	1	1	0.45		
k_H	1	1	1	1		
STRESS	53.82	45.02	33.96	23.29		
GREY	CIELAB					
k_l	2	1	0.6	0.35		
k_C	1	1	1	0.45		
k_H	1	1	1	1		
STRESS	52.02	36.35	28.09	22.3		

***Table 18*: Optimised formulae (weighting functions only) for digital Thread Winding Card samples for *Experiment A – Part B*.**

Observers were more sensitive to lightness differences on screen than they were sensitive to lightness differences contained in physical samples. The prediction performances of formulae were generally improved on screen mainly due to the same underlying texture content within digital samples (created from the same master texture monochrome sample). *Figures 72 – 79* presents plots from observations for digital 'TWC' samples using either the CMC or $CIEDE_{2000}$ formula for predicted and observed colour differences for best weighting settings (*Table 18*) for grey and blue colours in regards to changes in '$\Delta a^* \Delta b^*$' or '$\Delta L^* \Delta a^*$' – directions. *Figures 80 – 87* presents the similar plots but for digital 'BH' – sample prediction and observed data.

4.6.2 The CMC formula (weightings '1.05:1.33' and '0.99:1.64') performed less well if compared with the $CIEDE_{2000}$ formula ('0.74:1.05:1.00' and '0.65:1.20:0.90') given STRESS values of '25.40'/'21.97' and '19.62'/'13.66', respectively. Comparisons between observed plots of digital 'TWC' samples and predictions plots obtained from results for the digital 'BH' samples revealed two distinguish differences; (**1**) visual grey lightness and chromatic differences were still underestimated in the case of 'BH' samples (larger visual results compared to predicted results after optimisation of weighting functions – see *Figure 80, 81, 82* and *83*[tt]), and (**2**) the slope for blue chromatic differences (changes in '$\Delta a^* \Delta b^*$') were not of ideal linear form as suggested normally by a 45º slope line (see *Figure 85*[uu]).

4.6.3 It was also of interest to determine whether both formulae can be further optimised by including important functions within an optimisation process (see *Table 19*[vv] and *Figures 88 – 91*[ww]). Especially, the 'S_L', 'S_C', and 'S_H' functions were of interest and as such to determine whether a significant improvement in colour difference predictions can be achieved once they were altered, but also the 'T' – function and the 'f' term were considered for further refinements. Both plots for 'TWC' and 'BH' samples showed approximately similar distributions; average residuals values were '0.26' 'ΔE_{00}(0.68:1.23:0.89)' units for digital 'TWC' samples (factor '1.04'), and '0.26' 'ΔE_{00}(0.75:1.19:1.06)' units for digital 'BH' samples (factor '1.16'). Residuals values were on average '0.26' 'ΔE_{CMC}(1.04:1.78)' units for 'TWC' samples (factor '1.42') and '0.38' 'ΔE_{CMC}(1.2:1.65)' units for digital 'BH' samples (factor '1.80'). An overall linear factor was applied to minimise differences between '$\Delta V/\Delta E$'. Factor ratio values were '1.12' and '1.27.'

[tt] see page 177

[uu] see page 178

[vv] see page 180

[ww] see page 179

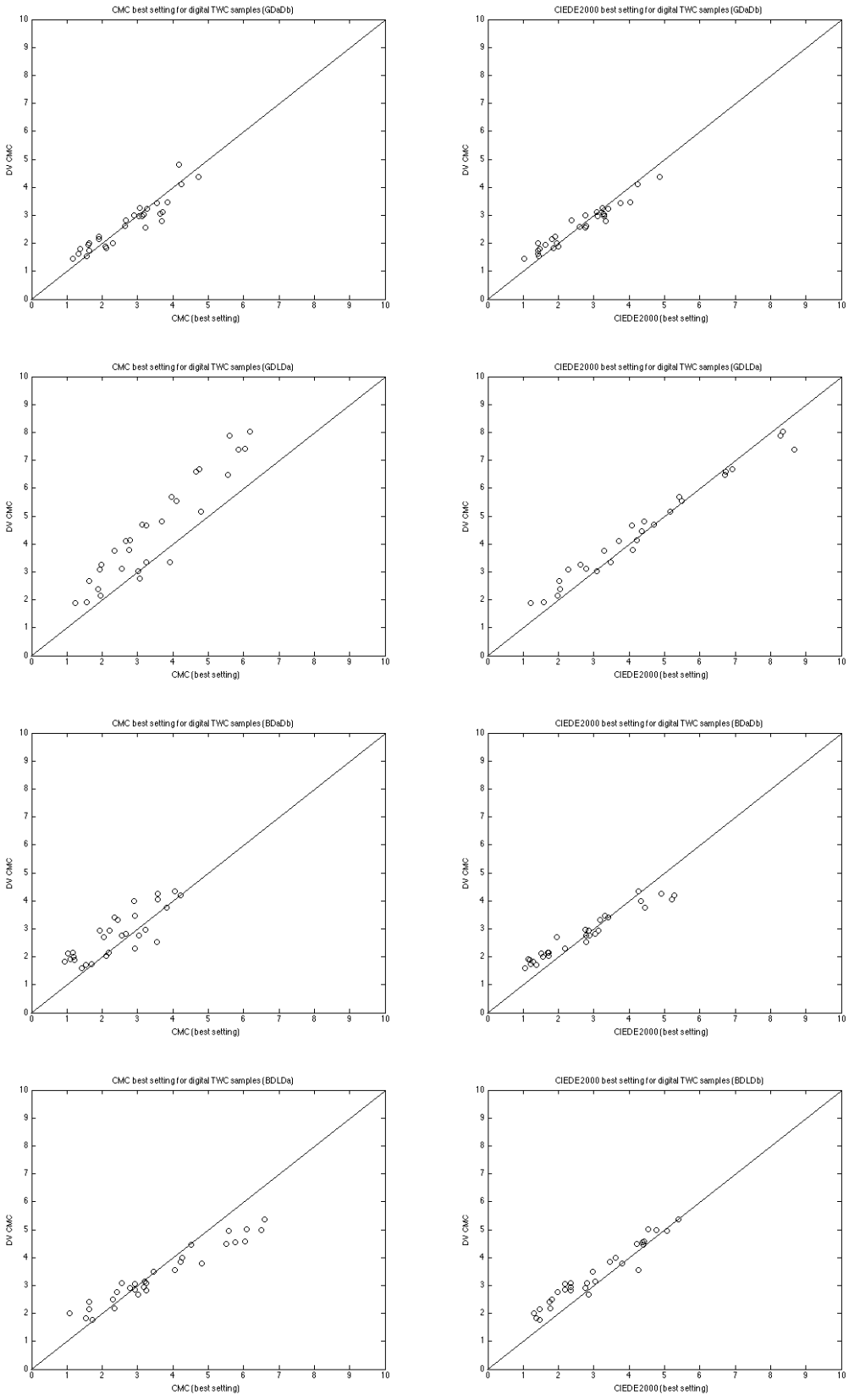

***Fig. 72 – 79*: Best setting (only weighting functions) for formulae CMC (left) and *CIEDE*$_{2000}$ (right) against visual results for colour difference changes in '$\Delta a^* \Delta b^*$' (row '1' and '3') and '$\Delta L^* \Delta a^*$' (row '2' and '4') for grey (row '1' and '2') and blue colours (row '3' and '4') – digital 'TWC' samples.**

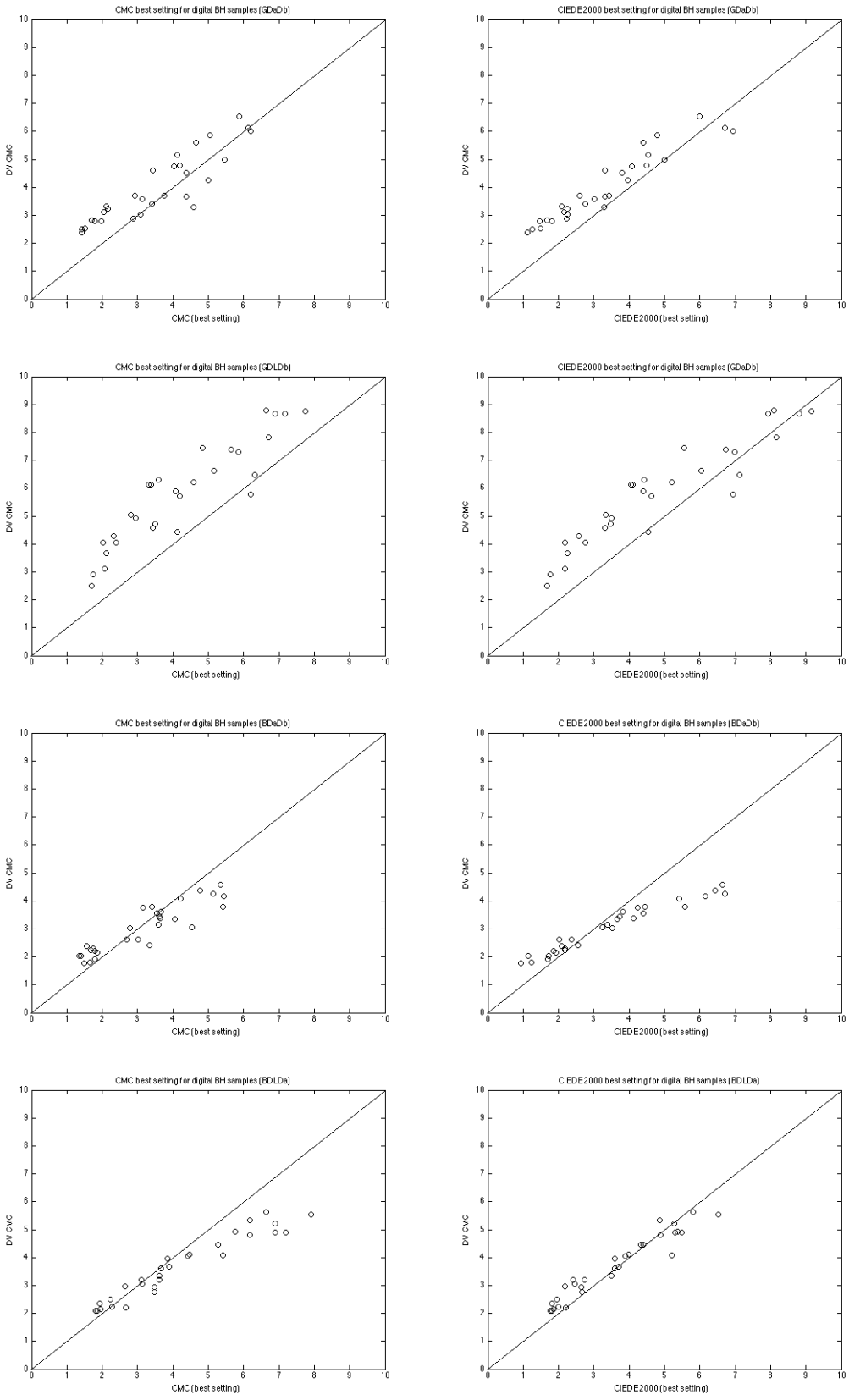

***Fig. 80 – 87*: Best setting (only weighting functions) for formula CMC (left) and *CIEDE*$_{2000}$ (right) against visual results for colour difference changes in '$\Delta a^* \Delta b^*$' (row '1' and '3') and '$\Delta L^* \Delta a^*$' (row '2' and'4') for grey (row '1' and '2') and blue colours (row '3' and '4') – digital 'BH' samples.**

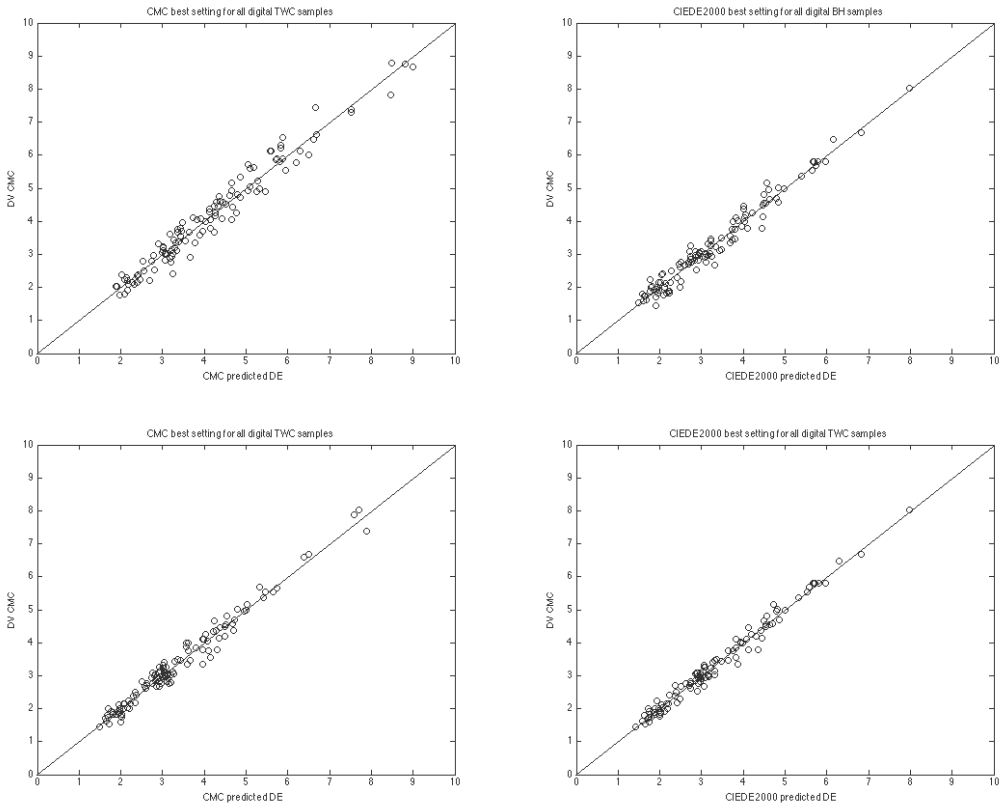

***Figure 88 – 91*: Best setting CMC and $CIEDE_{2000}$ prediction results against visual results (optimised functions) for digital 'BH' and 'TWC' samples.**

4.6.4 Significance tests between the $CIEDE_{2000}$ formula and CMC for a comparison of performances for optimised digital sample pairs ('TWC' and 'BH') are listed in *Table 20*. Modelled colour differences, observed colour differences, and optimised predicted colour differences for 'BH' and 'TWC' visual results according to changes in '$\Delta a^* \Delta b'^*$ are contrasted for physical and digital blue and grey colours for the CMC formula in *Figure 92 – 97*. The sizes of the ellipses differed significantly across those stitch types and presentation modes (digital and physical samples). A smaller ellipse refers to a larger perception since a fixed modelled sample difference of '2.4' '$\Delta E_{CMC}(1:1)$' units is perceived at a shorter distance in respect to the standard; and, also, in comparison to any other obtained distances that were perceived from other stitch type samples.

4.6.5 The residuals were approximately normal distributed so that the summed squared residuals were comparable with each other ('F' value obtained by division between formula 'A' and 'B'). CMC- and $CIEDE_{2000}$ ratios for 'TWC' and 'BH' sample observations were within a critical range and, therefore, the 'H_0' hypothesis was accepted (two colour difference formulae were not significant different in their prediction performances – 95% certainty). $CIEDE_{2000}$'s and CMC's formula (best setting according to *Table 19*) became then of the form as given in *Equations 121 – 124*.

CIEDE$_{2000}$	***DIGITAL BH***	***RES.***	***0.32***		
Factor	1.16	**Δ*V*/Δ*E* 'r'**	0.99	**T MOD.**	
k_L	0.75	**CV**	12.65	-28.60	
k_C	1.19	**VAB**	14.19	-17.26	
k_H	1.06	**GAMMA**	1.15	-7.69	
STRESS	***11.26***	***PF/3***	***14.01***	***13.67***	
Orig./Mod. G 'L^*'	Orig./Mod. G 'a^*'	Orig./Mod. G 'b^*'	Orig./Mod. B 'L^*'	Orig./Mod. 'a^*'	Orig./Mod. 'b^*'
48.42	-1.64	2.50	24.74	5.31	-26.88
48.10	-1.56	2.35	24.43	5.79	-28.06
-0.32	0.07	-0.15	-0.31	0.48	-1.18
CIEDE$_{2000}$	***DIGITAL TWC***	***RES.***	***0.26***		
Factor	1.04	**Δ*V*/Δ*E* 'r'**	1.00	**T MOD.**	
k_L	0.68	**CV**	10.38	-3.34	
k_C	1.23	**VAB**	10.04	-2.81	
k_H	0.89	**GAMMA**	1.10	-3.11	
STRESS	***9.23***	***PF/3***	***10.31***	***4.56***	
Orig./Mod. G 'L^*'	Orig./Mod. G 'a^*'	Orig./Mod. G 'b^*'	Orig./Mod. B 'L^*'	Orig./Mod. 'a^*'	Orig./Mod. 'b^*'
48.42	-1.64	2.50	24.74	5.31	-26.88
47.86	-1.05	1.88	23.95	6.35	-28.75
-0.56	0.58	-0.62	-0.79	1.04	-1.87
CMC	***DIGITAL BH***	***RES.***	***0.38***		
Factor	1.80	**Δ*V*/Δ*E* 'r'**	0.99	**T**	0.57
k_L	1.20	**CV**	12.14	**f**	1900
k_C	1.65	**VAB**	11.71	**SL**	**opt.**
		GAMMA	1.13	**SC**	opt.
STRESS	***10.71***	***PF/3***	***12.13***	***SH***	***opt.***
Orig./Mod. G 'L^*'	Orig./Mod. G 'a^*'	Orig./Mod. G 'b^*'	Orig./Mod. B 'L^*'	Orig./Mod. 'a^*'	Orig./Mod. 'b^*'
48.42	-1.64	2.50	24.74	5.31	-26.88
45.70	-2.04	3.52	24.64	5.53	-28.88
-2.72	-0.40	1.02	0.10	0.22	-2.01
CMC	***DIGITAL TWC***	***RES.***	***0.26***		
Factor	1.42	**Δ*V*/Δ*E* 'r'**	1.00	**T**	0.58
k_L	1.04	**CV**	10.25	**f**	1900
k_C	1.78	**VAB**	10.65	SL	opt.
RES.		**GAMMA**	1.11	**SC**	opt.
STRESS	***9.20***	***PF/3***	***10.71***	***SH***	***opt.***
Orig./Mod. G 'L^*'	Orig./Mod. G 'a^*'	Orig./Mod. G 'b^*'	Orig./Mod. B 'L^*'	Orig./Mod. 'a^*'	Orig./Mod. 'b^*'
48.19	-1.08	2.00	24.27	5.77	-27.26
46.77	-1.28	2.63	24.52	5.84	-29.61
-1.42	0.20	0.63	0.26	0.07	-2.35

***Table 19*: Optimised formulae (weighting + standards) for digital 'BH' and 'TWC' samples for the CMC and *CIEDE$_{2000}$* formula.**

Exp. A – Part B **F-TEST (Eq. 90ff)**	***CIEDE$_{2000}$* DIG. BH**	***CIEDE$_{2000}$* DIG. TWC**	**CMC DIG. BH**	**CMC DIG. TWC**
***CIEDE$_{2000}$* DIG BH**	A/B	**0.64**	1.31	**0.58**
***CIEDE$_{2000}$* DIG TWC**	**1.56**	A/B	**2.06**	0.91
CMC DIG BH	0.76	**0.49**	A/B	**0.58**
CMC DIG TWC	**1.72**	1.10	**2.26**	A/B
CRIT RANGE (0.05)	**0.73 – 1.36**			

***Table 20*: 'F'-test for CMC/*CIEDE$_{2000}$* for digital 'BH' and 'TWC' samples *Experiment A: Part – B*. Bold numbers indicate a significant difference in performances between two formula.**

Eq. 121: $\text{digital}\,\Delta E_{\text{BH}} = 0.9355 \cdot \Delta E_{00} + 0.3054$

Eq. 122: $\text{digital}\,\Delta E_{\text{TWC}} = 0.9705 \cdot \Delta E_{00} + 0.1964$

Eq. 123: $\text{digital}\,\Delta E_{\text{BH}} = 0.7201 \cdot \Delta E_{\text{CMC}} + 0.8788$

Eq. 124: $\text{digital}\,\Delta E_{\text{TWC}} = 0.9320 \cdot \Delta E_{\text{CMC}} + 0.2623$, where

'digital $\Delta E_{\text{BH,TWC}}$' refers to an optimised formula, and '$\Delta E_{\text{CMC,00}}$' refers to predicted colour differences obtained from the *CIEDE*$_{2000}$ or CMC formula in optimised conditions. The offset and slope of linearity gave indications for improvement for predicting visual results as seen in *Figures 88 - 91*. STRESS values were further reduced (on average STRESS 7), and the average colour difference values between predicted and observed sample data were '0.27'/'0.21' 'ΔE_{00}' and '0.30'/'0.20' 'ΔE_{CMC}' for digital 'BH' and 'TWC' samples, respectively. However, those experiments were limited to just two colours (grey and blue), but provided as such directions for further studies. The texture effect was more dominant for physical samples containing smaller colour differences. Data that were derived from 'F' – tests (*Equations 98ff* or *Equation 104*) for CMC's colour difference formula components for predicting digital and physical 'BH' and 'TWC' sample sets (for optimised weighting values) are listed in *Table 21*. Two datasets for each stitch type and colour (average value of '1.4' and '2.6' 'ΔE_{CMC}(1:1)' for each data set) were contrasted with each other (see legends in *Figure 92* and *94* for data set and ellipses identification). The same numerical colour differences resulted in smaller distances between centre and boundary of an ellipse for 'BH' samples (for both physical and digital samples). Predicted ellipses using CMC formula (best setting) for digital BH samples were given as in *Figure 96* and *97*. Ellipses confirmed findings from *Table 9* and *15* thus suggesting larger colour difference observations for 'BH' samples when compared with 'TWC' samples (for the same modelled colour differences).

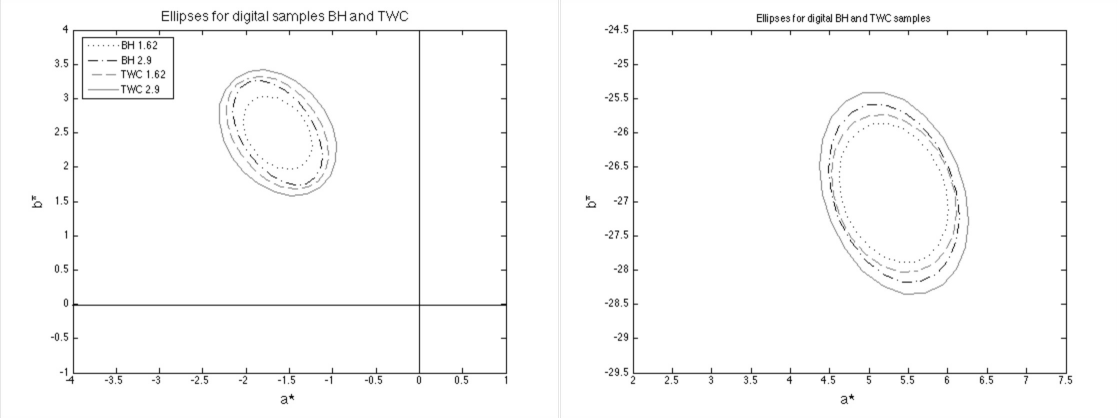

***Figure 92 – 93*: Ellipses for observed digital 'BH' and 'TWC' samples for grey (left) and blue (right) colours.**

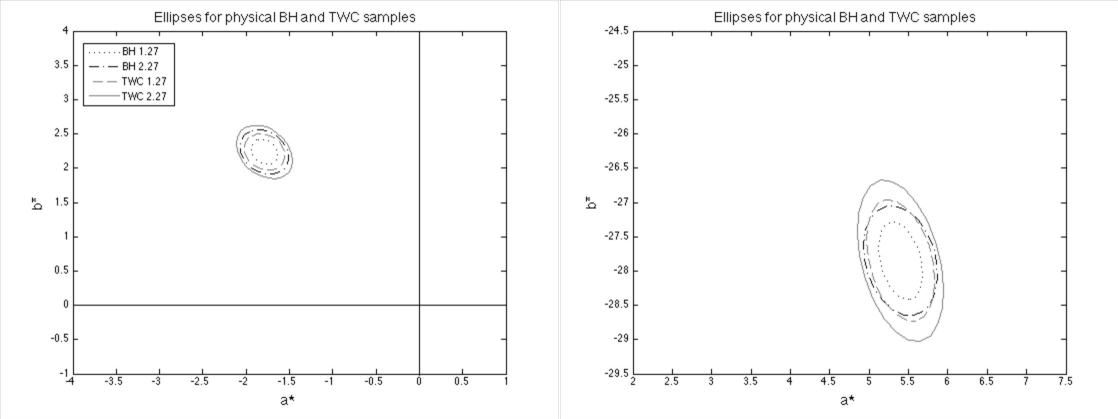

***Figure 94 – 95*: Ellipses for observed physical 'BH' and 'TWC' samples for grey (left) and blue (right) colours.**

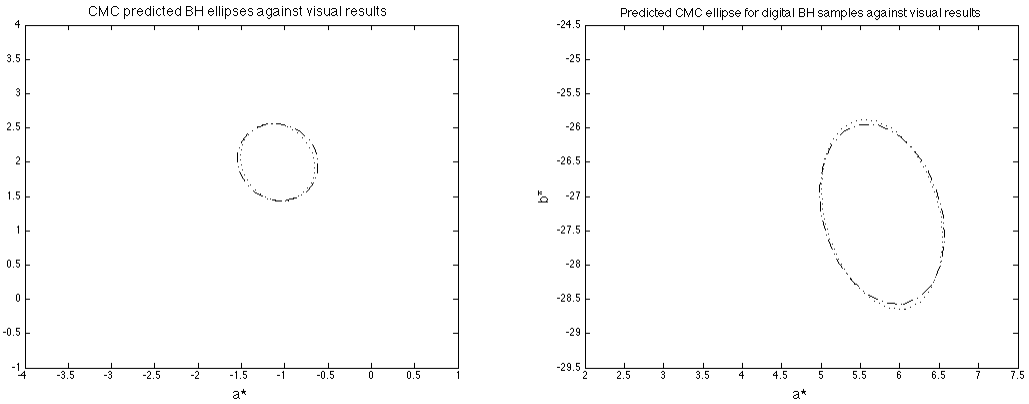

***Figure 96 – 97*: Predicted CMC (optimised) ellipses against visual ellipses for grey and blue digital 'BH' samples.**

4.6.6 Two major findings were observed from *Table 21*[xx]; (**1**) significant improvements in prediction performances for digital samples and the CMC formula was achieved by altering 'STD' grey and blue sample specifications (reduction of lightness on average by a value of '2', and an increase of chroma 'b^*' by a value of '1.5'), and (**2**) by altering CMC's 'S_L' function (if, step (**1**) was not applied). Formula performances for physical samples were also increased once a standard sample for a blue or grey colour was altered; however, a normal distribution of residuals derived from visual and predicted results for physical 'BH' samples in the case of 'CMC' was only approximated when compared to digital 'BH'/'TWC' or physical 'TWC' samples. CMC formula prediction performances for physical samples were improved by altering weighting function 'S_C' opposed to 'S_L' for digital samples. The outcome of an optimised formula predicting visual results in the case of 'CMC(*l*:*c*)' formula and visual colour difference results obtained from experiments with 'BH' samples on a digital screen are given in *Figure 96* and *97*.

[xx] see page 183

CMC		*Critical*			
DIG. TWC	***SUM RESIDUALS***	***Range***		***F – test***	***STRESS***
Opt. k_L k_C	65.95	0.7349	1.3608	1	21.97
Opt.. S_L	33.2	0.7349	1.3608	**1.99**	15.85
Opt. S_C	63.91	0.7349	1.3608	1.03	21.66
Opt. T	60.28	0.7349	1.3608	1.09	22.06
Opt. STD	20.34	0.7349	1.3608	**3.24**	10.18
CMC		***Critical***			
DIG. BH	***SUM RESIDUALS***	***Range***		***F – test***	***STRESS***
Opt. k_L k_C	131.08	0.7349	1.3608	1	26.94
Opt.. S_L	86.18	0.7349	1.3608	**0.76**	21.75
Opt. S_C	94.49	0.7349	1.3608	0.7	23.52
Opt. T	99.74	0.7349	1.3608	0.66	24.49
Opt. STD	65.95	0.7349	1.3608	**1.58**	11.26
CMC		***Critical***			
PHY TWC	***SUM RESIDUALS***	***Range***		***F – test***	***STRESS***
Opt. k_L k_C	52.93	0.7349	1.3608	1	25.24
Opt.. S_L	50.83	0.7349	1.3608	1.04	24.71
Opt. S_C	33.02	0.7349	1.3608	**1.6**	**24.01**
Opt. T	49.36	0.7349	1.3608	1.07	24.21
Opt. STD	42.01	0.7349	1.3608	1.27	17.24
CMC		***Critical***			
PHY BH	***SUM RESIDUALS***	***Range***		***F – test***	***STRESS***
Opt. k_L k_C	75.28	0.7349	1.3608	1	34.35
Opt.. S_L	75.24	0.7349	1.3608	0.99	34.34
Opt. S_C	74.99	0.7349	1.3608	1.09	34.31
Opt. T	75.26	0.7349	1.3608	1.01	34.34
Opt. STD	75.63	0.7349	1.3608	1.31	22.21

***Table 21*: CMC colour differences formula component analysis for digital and physical samples in terms of significance. All changes for optimised components were compared with an optimised weighting function formula – CMC(*l*:*c*).**

4.7 Summary

. Results from visual colour difference experiments for 'buttonhole stitch type' samples ('BH') and 'thread winding cards' samples ('TWC') provided evidence that observer's perception was significant altered by how a colour difference sample pair was presented to them. The same numerical colour difference value obtained from instrumental measurements for a buttonhole sample pair (fabric and thread winding card) was judged larger in magnitude when compared to a thread winding card sample pair with the same measured colour difference between a thread and the thread standard.

. Observers perceived larger colour differences (on average 30% larger in total colour difference 'ΔE' magnitude) when 'BH' samples were compared with 'TWC' samples. Lightness/chromatic crispening and texture effects (higher contrast between fabric and thread content) were enhanced for smaller colour difference sample pairs but diminished for larger colour difference pairs equal or larger than '2.4' '$\Delta E_{CMC}(2:1)$' units. Judging colour differences around Coats

tolerance limit of '1.2' '$\Delta E_{CMC}(2:1)$' units revealed about 20% larger visual colour differences for 'BH' samples when compared with 'TWC' sample pairs.

. The same observers also perceived colour differences between digital buttonhole stitch type and thread winding card samples on average 30% higher in regards to all colour difference sample pairs. However, absolute visual colour differences magnitudes were smaller for digital colour samples, especially if chromatic content was the main difference. Also, grey colour differences on screen, especially in the lightness direction, were enhanced when compared to lightness differences contained in physical samples.

. No significant differences in prediction performances between the CMC and $CIEDE_{2000}$ formula (STRESS measure) for optimised weighting functions and physical sample observations were evident. Weighting factors for 'k_L' were '2.14/1' (CMC) and '1.92/1/1' ($CIEDE_{2000}$) for physical 'BH', and '2.58/1' and '1.96/1' for physical 'TWC' samples. Weighting factors for 'k_L' and 'k_C' were given as '2.23/1.12' (CMC) and '1.94/0.92/1.05' ($CIEDE_{2000}$) for physical 'BH', and '2.75/1.24' and '1.96/1/1' for physical 'TWC' samples. The variation in visual results for a physical 'BH' dataset was higher when compared with variations in visual results for a physical 'TWC' dataset.

. Significant differences in prediction performances between CMC and $CIEDE_{2000}$ (in STRESS units) for optimised weighting and digital sample observations were observed. Weighting factors for 'k_L' were optimised to values of '0.94/1' (CMC) and '0.74/1/1' ($CIEDE_{2000}$) for digital 'BH', and '0.78/1' and '0.64/1' for digital 'TWC' samples. Weighting factor for 'k_L' and 'k_C' were given as '1.05/1.33' (CMC) and '0.74/1.05/1' ($CIEDE_{2000}$) for digital 'BH', and '0.99/1.64' (CMC) and '0.65/1.20/0.90' ($CIEDE_{2000}$) for digital 'TWC' samples.

. There was no significant difference in prediction performances once all weighting factors and either all- or some of the functions 'S_L', 'S_C', 'S_H', 'T', and 'f' between CMC and $CIEDE_{2000}$ for digital samples were optimised (*Table 19)*. STRESS values of less than 'eight' could be achieved in this way.

. 'F' – tests for formula components (*Table 19* and *21*) suggested that either; (**1**) a change in the specifications of the standard samples (mainly a reduction in lightness 'L^*' of '2'), or (**2**) an optimised 'S_L' parameter were responsible for significant improvements in colour difference prediction performances once weightings were optimised.

4.8 Conclusion

. Two different sample presentations altered observer's perception of colour differences, significantly. 'BH' samples were on average judged higher in colour difference magnitudes when compared with 'TWC' samples containing the same calculated colour differences.

. A similar trend was obtained for differences between physical 'BH' and 'TWC' sample sets and colour difference results obtained between digital 'BH' and 'TWC' sample sets. A texture effect dimished for larger colour difference pairs and was more pronounced for the critical range in Coats plc. colour matching work. In those cases, 'BH' samples (as provided in the form as seen in *Image 11*) may enhance an observer's colour difference perception in magnitude of about 20%.

. All colour difference formula performances suggested that observational results from digital samples correlated better with numerical results when compared to psychophysical results from physical samples (possibly caused by the larger variations in visual results for the physical 'BH' sample set).

. Considering statistical distributions analysis as plots of residuals between visual and predicted colour difference data may suggest to derive a suitable correlation factor (reference factor) between physical and digital samples by using 'TWC' visual data as used in *Experiment A – Part A* and *B*. Optimised weighting functions were significant different between digital and physical visual data sets.

Chapter 5:

5.1. *Experiment 5*: General considerations

5.1.1 *Experiment A* provided evidence that observer's colour difference perceptions varied among different sample types ('TWC' and 'BH'). Also, it was concluded that there was a systematic trend between results from two different presentation modes (physical samples seen in a viewing cabinet and digital samples seen on screen). Although, colour differences on screen were judged smaller in absolute magnitudes compared to physical samples judged in a viewing cabinet, the overall ratio between visual and numerical results between them were similar. Research on colour difference evaluation using digital screens (for instance, 'cathode ray tube' displays 'CRT') such as by Cui[386], Cheung and Rigg[141], or Alman *et al.*[133] provided some evidence that observed colour differences on a digital screen were perceived on average '1.5' – '2' times smaller in magnitude then perceived colour differences obtained from observational studies using physical samples judged in a viewing cabinet.

5.1.2 A third dataset was designed so to obtain visual data for more colour centres, but also to provide another type of stitch that was required so to fulfil the sponsor's business needs. The number and colour of physical samples that could be used for this project was limited. The sponsor's requirement in a 'day by day' manufacturing environment was to produce threads that are generally used for stitching, for instance, into fabric samples using a single needle lock stitch type. Ten colour centres were produced having batches surrounding them in semi circles mainly in two directions; either (**1**) in the '$\Delta a^* \Delta b^*$' – directions, ten samples varying in hue angle (18˚ degrees) from each other within a distances of '2.4' '$\Delta E_{CMC}(1:1)$' units away from each standard, or (**2**) in the '$\Delta L^* \Delta a^{*'}$ – directions; six batch samples varying in hue angle (0˚, 25˚, 65˚, 115˚, 180˚) given a colour difference distance of '2.4' '$\Delta E_{CMC}(1:1)$' units away from each standard sample.

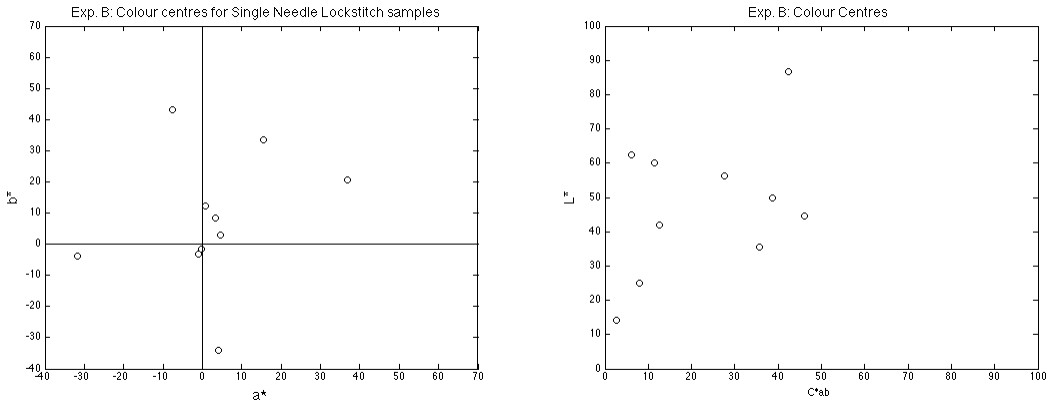

***Figure 98 and 99*: Colour coordinates for ten colour centres for *Experiment B* for single needle lockstitch samples.**

Standards, from which all batch samples deviated into both directions, were of red, green, blue, yellow, grey, beige, orange, olive, brown, and black colour. The choice of colour centres was narrowed down to either satisfy CIE's reference colour centres or to provide industrial interest to five of Coats plc '*bread and butter*' thread colours. Also, making Coats plc professional observers available for *Experiment B* within a time limit of a week provided some guidance for that experimental setup.

5.1.3. The colorimetric specifications for all colour centres (standards) are listed in *Table 22* and plotted in a diagram as provided in *Figure 98* and *99.* Two contrasting colour schemes in terms of their locations in the CIELAB 'a^*b^*' – diagram are evident. CIE's recommended colour centres are of high chromatic content whereas Coats plc colour set was less chromatic and duller in appearance. A synthesized single needle lockstitch sample ('ST') that was used for psychophysical evaluation in *Experiment B* is presented here as *Image 18*.

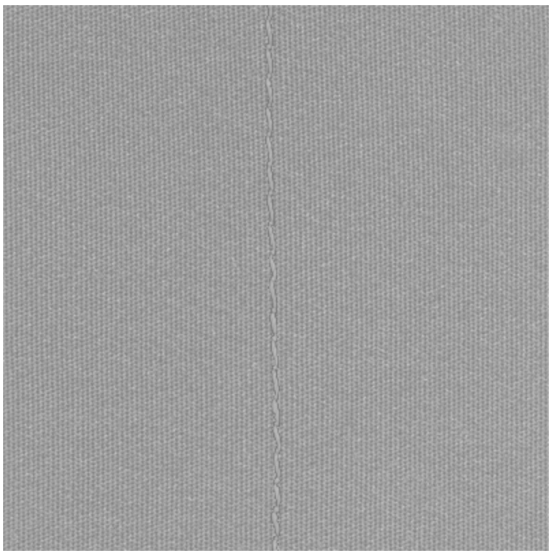

***Image 18*: Single needle lockstitch type image designed for *Experiment B* judged by professional observers.**

Standard	L^* *mod.*	a^* *mod.*	b^* *mod.*	C^*_{ab}	h_{ab}
Blue	35.60	4.17	-33.90	186.58	277.02
Red	44.70	36.74	20.67	42.15	29.37
Green	56.30	-31.73	-3.66	31.94	186.58
Grey	62.50	-0.94	-3.17	3.30	253.52
Yellow	86.60	-7.72	43.28	43.96	100.11
Coats 1 – beige	60.00	3.38	8.31	8.97	67.89
Coats 2 – orange	50.00	15.43	33.59	36.97	65.32
Coats 3 – olive	42.00	0.73	12.36	12.38	86.64
Coats 4 – brown	25.00	4.66	2.96	5.52	32.45
Coats 5 – black	14.10	-0.24	-1.61	1.63	261.38

***Table 22*: Colour coordinates for ten colour centres for *Experiment B* modified for LCD white point (X_{10} = 95.35, Y_{10} = 100, Z_{10} = 97.93) to match approximately CIE and Coats plc 'D65' daylight conditions.**

5.2 Image design and performance

5.2.1 Standards were produced according to an image and display model[yy] for fabric ('FA') samples (*Graph 3*, *Image 1* and *7*). Those standards were displayed on screen within the experimental setup as shown in *Graph 1*[zz]. A tele-spectroradiometer was used to measure all fabric standard colours for determining a reproduction performance measure for values obtained from modelled and displayed image samples. Those results are listed in *Table 23* and provided in 'ΔE_{00}' units.

5.2.2 The colour difference measured between desired, modelled, and reproduced 'FA' images on screen was on average '0.22' 'ΔE_{00}' units (+/- '0.025' mean standard error – mse -). This deviation may be explained by quantisation errors in the calculations of CIE '$L^*a^*b^*$'-, resulting '$XYZ_{10,I}$' – tristimulus values, and transformed '$R_iG_iB_i$' – scalar values for a final image. A grey, black, and beige colour standard resulted in larger deviations when compared with all other fabric colour standards on screen (see *Table 23)*.

FABRIC	*LaCie*			*XYZ_{10} pred.*			*Model RGB*			*Wanted-Pred.*	*Wanted-Meas.*
STANDARDS	*X_{10} wanted*	*Y_{10} wanted*	*Z_{10} wanted*	*X_{10} pred.*	*Y_{10} pred.*	*Z_{10} pred.*	*X_{10} meas.*	*Y_{10} meas.*	*Z_{10} meas.*	*ΔE_{00} prediction*	*ΔE_{00} measured*
CIE Blue	9.31	8.81	23.07	9.31	8.81	23.07	9.26	8.72	23.29	0.07	0.14
CIE Red	21.30	14.33	7.34	21.30	14.30	7.34	21.14	14.19	7.35	0.13	0.18
CIE Green	17.57	24.32	26.40	17.57	24.32	26.40	17.47	24.17	26.30	0.22	0.10
CIE Grey	30.82	31.04	33.36	30.82	31.04	33.36	30.80	31.02	33.54	0.18	0.36
CIE Yellow	65.90	69.51	29.93	65.90	69.51	29.93	66.23	69.77	29.89	0.08	0.17
Coats1 beige	29.00	28.13	23.28	29.00	28.13	23.28	29.11	28.20	23.33	0.22	0.28
Coats2 orange	21.53	18.33	6.40	21.53	18.37	6.40	21.47	18.27	6.31	0.13	0.17
Coats3 olive	12.50	12.41	8.42	12.50	12.40	8.42	12.55	12.42	8.38	0.22	0.22
Coats4 brown	4.84	4.47	3.94	4.84	4.47	3.94	4.65	4.29	3.80	0.20	0.25
Coats5 black	1.75	1.75	1.93	1.74	1.75	1.93	1.63	1.63	1.82	0.27	0.30

Table 23*: LCD reproduction performances for colour fabric standards in 'ΔE_{00}' – units for *Experiment B.

All measurement results were reasonably close to modelled and predicted image colour specifications. Therefore, the same LCD model for designing fabric ('FA') samples were used to design 'ST' batch samples around standards in mainly two directions with a numerical colour difference of '2.4' '$\Delta E_{CMC}(1:1)$' units. More than '300' colour difference sample pairs were produced and displayed on screen (including '80' repetition samples).

5.2.3 All measurements derived from standard fabric samples were transformed to '$u'v'$' – chromaticity coordinates and plotted together with the LCD primaries so to derive device's

---

[yy] see page 135: *Graph 2*

[zz] see page 123: *Graph 1*

colour gamut boundaries as provided in *Figure 103*. Also, display's 'RGB' channel ramps (input 'R', 'G', or 'B' from '0' – '255' digital counts in '17' steps) were contrasted against CIE 'XYZ_{10}' tristimulus values. It was of interest here to determine whether the sum of three individual 'X_{10}', 'Y_{10}', or 'Z_{10}' – tristimulus values for each digital 'R_i', 'G_i', and B_i' – count at a particular step were the same as the 'X_{10}', 'Y_{10}', or 'Z_{10}' – tristimulus value measured from grey images containing the same 'RGB' – values at a particular ramp step (*Figures 100 -103*). All those measured data used for additivity testing are listed in *Table 24*.

5.2.4 The 'RGB' range of images that were judged during *Experiment B* were mainly between '31' – '223' display input 'RGB' values. The summation between 'X_{10}', 'Y_{10}', and 'Z_{10}' – tristimulus values for each channel compared to 'X_{10}', 'Y_{10}', or 'Z_{10}' – tristimulus values obtained from measurements of grey patches at the same steps differed especially at low input display 'RGB' values ('0' – '31').

Scale	*RGB*	*Grey*	*Patches*		*SUM*	*R+G+B*		*CMC in %*			*CMC*
No	*VALUES*	X_{10}	Y_{10}	Z_{10}	X_{10}	Y_{10}	Z_{10}	$\Delta L^*/K_L S_L$	$\Delta C^*/K_c S_C$	$\Delta H^*/S_H$	*1:1*
1	**0**	0.00	0.00	0.01	0.01	0.01	0.01	7.17	0.64	92.19	0.90
2	**15**	0.00	0.00	0.01	0.01	0.01	0.02	87.64	12.31	0.05	9.15
3	**31**	0.01	0.01	**0.02**	0.01	0.01	0.03	98.82	0.10	**1.09**	7.47
4	**47**	**0.02**	**0.02**	**0.04**	0.03	0.03	0.04	**95.36**	**1.06**	**3.58**	4.44
5	**63**	**0.04**	**0.04**	**0.06**	0.05	0.05	0.07	**94.25**	**2.04**	**3.71**	1.42
6	**79**	**0.07**	**0.07**	**0.09**	0.07	0.08	0.10	**32.22**	**12.07**	**55.71**	0.82
7	**95**	**0.11**	**0.11**	**0.13**	0.11	0.11	0.13	**0.14**	**23.80**	**76.06**	0.66
8	**111**	**0.15**	**0.16**	**0.18**	0.15	0.16	0.18	**15.51**	**24.08**	**60.41**	0.67
9	**127**	**0.21**	**0.22**	**0.24**	0.20	0.21	0.23	**97.81**	**2.18**	**0.01**	0.72
10	**143**	**0.27**	**0.28**	**0.30**	0.27	0.28	0.29	**44.08**	**33.01**	**22.91**	0.80
11	**159**	**0.34**	**0.36**	0.38	0.33	0.35	0.37	**33.90**	**21.79**	44.30	0.93
12	**175**	**0.43**	**0.45**	0.46	0.41	0.43	0.45	**48.65**	**50.93**	0.42	0.92
13	**191**	**0.52**	**0.54**	0.56	0.51	0.53	0.53	**37.07**	**57.14**	5.79	1.02
14	**207**	**0.62**	**0.65**	0.66	0.60	0.63	0.63	**19.44**	**80.44**	0.12	1.28
15	**223**	**0.73**	**0.76**	0.76	0.71	0.75	0.74	**24.37**	**66.56**	9.07	0.96
16	**239**	0.85	0.89	0.89	0.84	0.88	0.86	9.45	75.22	15.33	1.22
17	**255**	0.95	1.00	0.98	0.97	1.02	0.98	9.06	90.94	0.00	1.59

***Table 24*: Additivity measure for LaCie display for summed individual channel ramps against grey patches**

Larger deviations in colour differences between measured additive and grey patches were mainly caused by lightness differences up to 'RGB' '63' input values and hue differences ('RGB' range from '79' – '111'). Otherwise, all additivity differences in critical image 'RGB' input ranges were evenly distributed in each of the three colour difference scales in the directions of lightness, chroma and hue (35%, 37% and 28%, respectively). The LCD was switched on each morning two hours before starting observational experiments. Professional observers (eight males and four females with an average age of 34 years), generally involved in critical colour matching work, were employed for *Experiment B*. Observers judged all samples

within five sessions; one observer went through the data set twice without prior knowledge of doing so. The final results were compiled from more than '3600' observations. All observers conducted a 'Farnsworth-Munsell 100 – Hue test'; the recorded results were provided by Coats plc and suggested that all participants were of 'superior discrimination' type observers[387].

5.2.5 A grey scale, which was displayed on screen, was measured each morning and evening over a period of a week. A transfer function from 'GRADE' to visual '$\Delta V_{CMC}(1{:}1)$' units followed a similar procedure as described in *Experiment A – Part A*[aaa]; however, the GRADE scale was adjusted in magnitude considering an overall modelled colour difference value of '2.4' '$\Delta E_{CMC}(1{:}1)$'. The final colorimetric measurement results for that scale are provided in *Table 25*. All observations were then transformed to '$\Delta V_{CMC}(1{:}1)$' units and compared with predicted results from various formulae. Important as such was a comparison between the CMC and $CIEDE_{2000}$ formula with those results that were obtained from *Experiment A*.

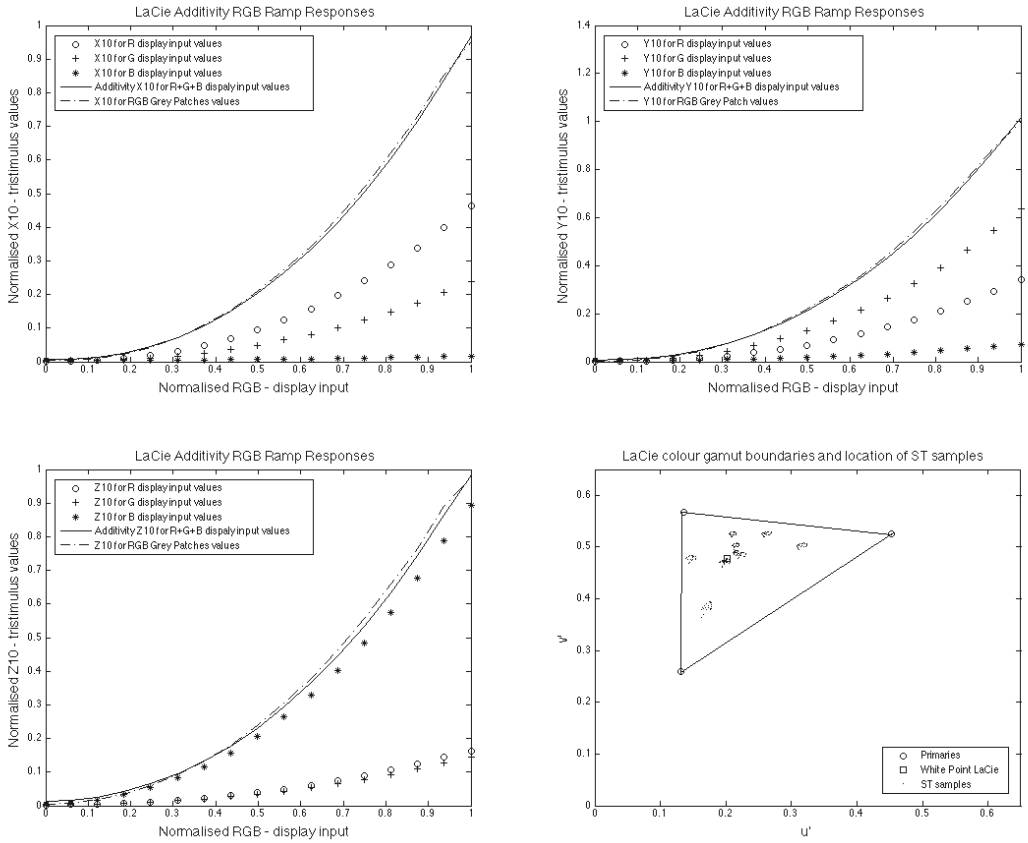

***Figure 100 -103*: LaCie additivity plots of each channel's summed 'XYZ_{10}' – tristimulus values against 'X_{10}', 'Y_{10}', or 'Z_{10}' - tristimulus values from grey patches considering the same 'R', 'G', or 'B' display input; sample set plotted in u',v'- diagram.**

[aaa] see page 161

GRADE	*SUM*	$(\Delta L^*/lS_L)^2$	$(\Delta C^*_{ab}/cS_c)^2$	$(\Delta H^*_{ab}/S_H)^2$	*CMC(1:1)*	*ΔL %*	*ΔC %*	*ΔH %*	*SUM*
5	0.70	0.004	0.129	0.565	**0.83**	0.61	18.44	80.95	100
4	1.66	0.746	0.406	0.508	**1.28**	44.97	24.45	30.58	100
3	3.87	3.157	0.199	0.517	**1.97**	81.51	5.14	13.35	100
2	12.89	11.692	0.639	0.561	**3.59**	90.69	4.96	4.35	100
1	45.15	44.137	0.312	0.701	**6.72**	97.76	0.69	1.55	100

Table 25: Measured grey scale on screen for transforming 'GRADE' to visual 'ΔV_{CMC}(1:1)' for *Experiment B*.

5.3 Results

5.3.1 The average 'GRADE' value for all sample pair judgements, except for the observations for the red colour centre, was '2.99' (median '3.04'). This average GRADE value translated to a visual colour difference value of '1.99' ΔE_{CMC}(1:1) units (median '1.94') for a modelled colour difference pair data set of '2.4' ΔE_{CMC}(1:1) units. Average GRADE values mainly differing in the lightness direction '$\Delta L^* \Delta a^*$' were given an average a GRADE value of '2.63' (median '2.62' – '2.46' lower and '2.81' upper boundary based on '1000' bootstrap samples), and GRADE '3.21' (Median '3.21', lower '3.11' and upper '3.31' boundaries for '1000' bootstrap samples) for chromatic differences. Those values were transformed to '2.44' ΔV_{CMC}(1:1) units (median value of '2.40', lower '2.21' and upper '2.71' boundary values based on '1000' bootstrap samples) for lightness differences, and '1.78' ΔV_{CMC}(1:1) units (median value of 1.78 – lower 1.70 / upper 1.87 boundary values) for chromatic differences, respectively. GRADE values were then analysed in terms of their distributions around their mean values mainly in two directions; (**1**) for differences in '$\Delta a^* \Delta b^*$', and (**2**) '$\Delta L^* \Delta a^*$' – coordinates.

5.3.2 The distribution of average GRADE and 'ΔV_{CMC} (1:1)' units are given as in *Figure 104 – 107*, *Table 25* and *26*. Especially, yellow and orange colour difference predictions from modelled '2.4' ΔE_{CMC}(1:1) units difference pairs were judged on average larger than all other colour batches. It became evident that professional observers judged chromatic colour difference for 'ST' sample pairs very consistently resulting in normal distributed GRADE values. Transforming those into 'ΔV_{CMC}(1:1)' units provided a similar shape. Generally, observational results from 'ST' difference sample pairs differing in lightness were less normal distributed (but still not significant 'not-normal' distributed with a 'p' – value of '0.11'). This may suggested some bias for professional matching work for lightness differences in the textile industry where colour matcher might be less sensitive to lightness differences. All judgments 'in the general directions of '$\Delta L^* \Delta b^*$' followed the same pattern. All data were then processed (except the red colour centre, which was produced with an average 'ΔE_{CMC}(1:1)' value of '1.4') and summarised in terms of average values for further considerations as listed in *Table 26*. A weighted overall mean resulted in '2.01' ΔV_{CMC}(1:1) units.

5.3.3 The results suggested that on average digital 'ST' colour difference pairs were judged with smaller colour difference magnitudes when compared with numerical colour measurement results. The overall ratio '$\Delta V_{CMC}(1:1)$'/'$\Delta E_{CMC}(1:1)$' between measured against visual results were '0.90' for *Experiment B*. Splitting the ratios in lightness and chromatic differences for the entire dataset resulted in ratios of '1.04' and '0.75', respectively.

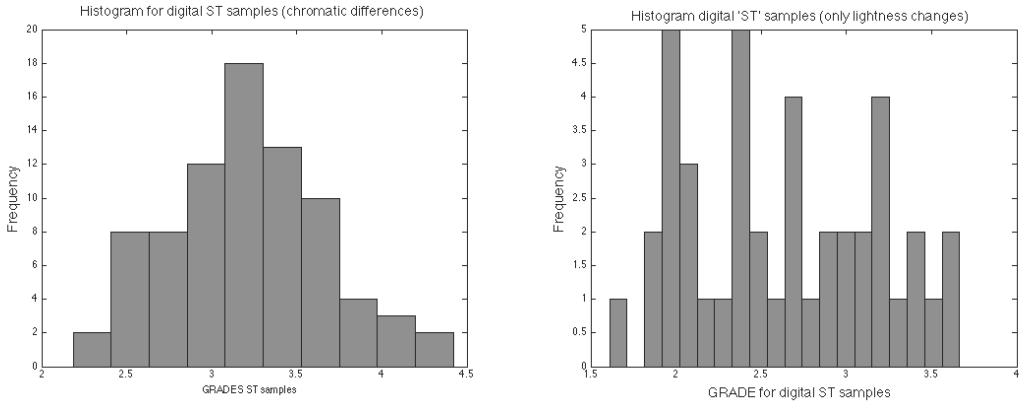

***Figure 104 and 105*: GRADE distribution for 'ST' samples differing only in '$\Delta a^* \Delta b^*$' and '$\Delta L^* \Delta a^*$' – directions**

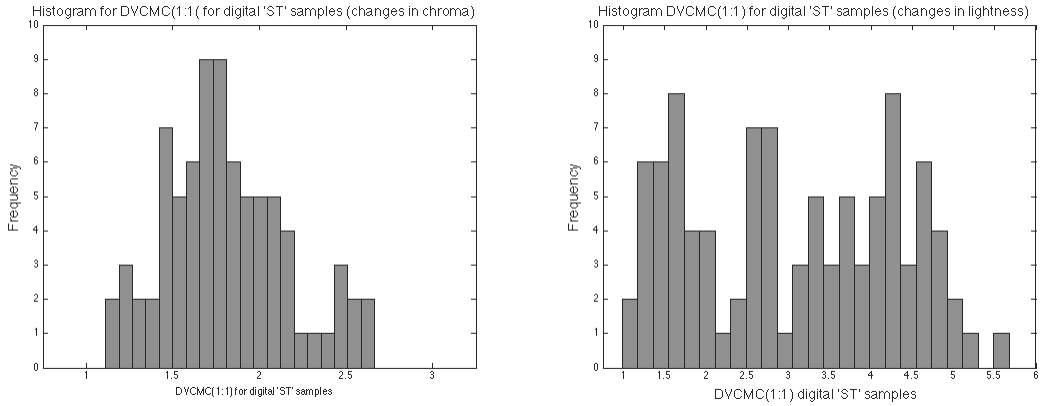

***Figure 106 and 107*: '$\Delta V_{CMC}(1:1)$' distributions for 'ST' samples differing only in '$\Delta a^* \Delta b^*$' or '$\Delta L^* \Delta a^*$' – directions**

All chromatic 'ST' judgments were smaller in magnitude than average modelled '2.4' '$\Delta E_{CMC}(1:1)$' colour differences, whereas lightness judgments were larger for the grey, yellow, beige and green colour centre on screen, and smaller for all other colour centres. Visual results for the digital blue and grey colour difference ratios were '0.79/0.91' and '0.88/1.23' for chromatic and lightness 'ST' sample pairs compared to '1.22/1/27' and '0.97/1.57' for digital 'TWC' samples, and '1.32/1.41' and '1.64/2.08' for digital 'BH' samples. All data were used to determine intra– and inter-observer variability using the STRESS measure for '60' repetition samples, and a dataset of '220' 'ST' samples, respectively. Intra-observer variation (average result of 15.37 STRESS units) gave evidence of how close a repeated judgment for the same samples and observer was made provided in terms of the STRESS measure. Inter-observer variation indicated how much an individual observer's judgment results confirmed to the average result obtained from all observers ('33.53' STRESS). The intra-observer variability

measure for '$\Delta a^* \Delta b^*$' and '$\Delta L^* \Delta a^*$ - Δb^*' observations were given as '30.82' and '38.68' STRESS units.

Samples (without red)		*CHROMA MEAN*		*LIGHTNESS MEAN*	
Mean 'ΔV_{CMC}(1:1)'	**2.16**	**$\Delta a^* \Delta b^*$ Mean**	**1.82**	**$\Delta L^* \Delta a^* b^*$ Mean**	**2.44**
STD	0.74	$\Delta a^* \Delta b^*$ STD	0.42	$\Delta L^* \Delta a^* b^*$ STD	0.81
STD ERROR	0.05	$\Delta a^* \Delta b^*$ STD Error	0.042	$\Delta L^* \Delta a^* b^*$ STD	0.22
Approx. confidence 95%		Approx. confidence intervals		Approx. confidence intervals	
Lower	2.06	**$\Delta a^* \Delta b^*$** Lower	1.74	**$\Delta L^* \Delta a^* b^*$** Lower	2.00
Upper	2.26	**$\Delta a^* \Delta b^*$** Upper	1.90	**$\Delta L^* \Delta a^* b^*$** Upper	2.87
		CIE Chroma Mean		***CIE Lightnes Mean***	
		$\Delta a^* \Delta b^*$Mean	**2.03**	**$\Delta L^* \Delta a^* b^*$ Mean**	**2.74**
		$\Delta a^* \Delta b^*$ STD	0.83	$\Delta L^* \Delta a^* b^*$ STD	0.83
		$\Delta a^* \Delta b^*$ STD	0.12	$\Delta L^* \Delta a^* b^*$STD	0.11
		Approx.confidence intervals		Approx.confidence intervals	
		$\Delta a^* \Delta b^*$ Lower	1.80	**$\Delta L^* \Delta a^* b^*$** Lower	2.53
		$\Delta a^* \Delta b^*$ Upper	2.26	**$\Delta L^* \Delta a^* b^*$** Upper	2.95
		Coats Chroma Mean		***Coats Lightness Mean***	
		$\Delta a^* \Delta b^*$ Mean	**1.66**	**$\Delta L^* \Delta a^* b^*$ Mean**	**2.20**
		$\Delta a^* \Delta b^*$ STD	0.26	$\Delta L^* \Delta a^* b^*$ STD	0.73
		$\Delta a^* \Delta b^*$	0.04	$\Delta L^* \Delta a^* b^*$ STD	0.09
		Approx. confidence intervals		Approx. confidence intervals	
		$\Delta a^* \Delta b^*$Lower	1.58	$\Delta L^* \Delta a^* b^*$ Lower	2.01
		$\Delta a^* \Delta b^*$ Upper	1.73	$\Delta L^* \Delta a^* b^*$ Upper	2.38

Table 26*: Overall visual results for digital 'ST' images in 'ΔV_{CMC}(1:1)' units for *Experiment B.

5.4. Formulae performances

5.4.1 The $CIEDE_{2000}$ and CMC formula were compared directly using results in 'ΔV_{CMC}(1:1)' units for a digital 'ST' colour difference sample set by varying weighting factors 'k_L' or 'l', 'k_C' or 'c', and 'k_H', if applicable. Weighting factors were added to CIELAB's formula, and also a 'S_L' function was created from existing lightness difference 'ST' data (*Experiment A – Part B;* significant improvement in prediction performances were obtained by optimizing 'S_L' functions) after factor scaling (linear factor to minimize '$\Delta V_{CMC}/\Delta E_{CMC}$' for lightness differences only). *Table 27* listed results for optimized weighting factors and *Table 28* listed both optimized weighting factors and functions. Residuals were referred to an absolute measure (average value for each individual square root from the squared differences between '$\Delta V_{CMC}/\Delta E_{CMC}$' after scaling given in '$\Delta E_{various}$' units). Similar trends were evident for digital 'ST' samples when compared with physical samples. 'k_L' weighting for 'ST' samples was reduced to '0.57' compared to '2' for physical samples, '1.20' for digital 'BH', '1.04' and 'TWC' samples in the case of the CMC formula, respectively.

DIG. 'ST'	***CMC ALL CENTRES***					***Best Setting***
k_L	2	1	0.58	0.57	**CV**	27.47
k_C	1	1	1	0.96	**VAB**	26.39
					Gamma	1.3
ΔV/ΔE 'r'	-0.41	0.15	0.6	0.61	**Factor**	0.75
ΔV/ΔE 't'	-6.56	2.3	11.14	11.15	**Residual**	0.45
STRESS	***42.67***	***32.37***	***25.93***	***23.91***	***PF/3***	***27.94***
BLUE	CMC BLUE					
k_L	2	1	0.58	0.62		
k_C	1	1	1	0.93		
STRESS	41.54	33.81	30.75	30.42		
STRESS B	32.81	21.71	25.7	23.1		
GREY	CMC GREY					
k_L	2	1	0.58	0.62		
k_C	1	1	1	0.93		
STRESS	45.84	39.14	33.32	33.94		
DIG. 'ST'	***All CIEDE$_{2000}$***					***BEST Setting***
k_L	2	1	0.54	0.55	**CV**	22.59
k_C	1	1	1	0.95	**VAB**	23.25
k_H	1	1	1	1.05	**Gamma**	1.26
ΔV/ΔE 'r'	-0.14	0.38	0.77	0.77	**Factor**	0.86
ΔV/ΔE 't'	-2.11	6.01	17.67	17.77	**Residual**	0.37
STRESS	***42.47***	***30.71***	***21.18***	***21.05***	***PF/3***	***23.94***
BLUE	*CIEDE$_{2000}$*					
k_L	2	1	0.54	0.55		
k_C	1	1	1	0.95		
k_H	1	1	1	1.05		
STRESS	41.3	32.21	24.63	24.48		
STRESS B	34.12	23.2	17.37	17.06		
GREY	*CIEDE$_{2000}$*					
k_L	2	1	0.54	0.55		
k_C	1	1	1	0.95		
k_H	1	1	1	1.05		
STRESS	44.93	36.43	27.97	27.88		
DIG. 'ST'	***WEIGHTED CIELAB***					***Best Setting***
k_L	2	1	0.44	0.58	**CV**	22.2
k_C	1	1	1	1.67	**VAB**	23.54
k_H	1	1	1	1.00	**Gamma**	1.26
ΔV/ΔE 'r'	0.06	0.36	0.8	0.83	**Factor**	0.69
ΔV/ΔE 't'	0.86	5.77	21.12	22.29	**Residual**	0.36
STRESS	***47.28***	***36.34***	***23.2***	***20.11***	***PF/3***	***24.02***
BLUE	WEIGHTED CIELAB					
k_L	2	1	0.44	0.58		
k_C	1	1	1	1.67		
k_H	1	1	1	1.00		
STRESS	47.57	37.43	25.96	22.75		
STRESS	50.038	38.23	27.35	25.4		
GREY	WEIGHTED CIELAB					
k_L	2	1	0.44	0.58		
k_C	1	1	1	1.67		
k_H	1	1	1	1.00		
STRESS B	42.99	38.24	23.37	17.24		

Table 27: Optimised formulae (weighting functions only) for digital 'ST' samples for *Experiment B.*

5.5 Optimising formulae

5.5.1 Significant improvements in prediction performances was achieved by varying weighting factors especially evident in those cases when the 'k_L' weighting factor were altered. Chromatic weighting 'k_C' was optimal at a value of approximately '1' for CMC's formula and digital 'ST' samples compared with weighting factors of '1.33'/'1.64' for digital 'BH' and 'TWC' samples. The absolute average residuals value was reduced to '0.30' '$\Delta E_{various}$' units. A factor ('F') described an average multiplicator that was used to alter numerical differences until overall differences between visual and predicted results were minimized. Those overall factors for CMC (best setting) for predicting digital 'BH', TWC', and 'ST' sample pairs were '1.62', '1.27' and '0.75', respectively. These factors suggested that digital 'BH' samples were judged 27% higher than 'TWC' samples (only blue and grey colour centres), and digital 'ST' samples were judged about 30% smaller if compared to a 'TWC' sample set. However, the 'ST' sample set was formed from ten digital colour centres and judged by professional observers so that a comparison between them was only approximately valid if we consider results from a different group of observers judging digital 'BH'- and 'TWC' sample pairs.

WEIGHTED CIELAB	***DIGITAL ST***	***RES.***	***0.28***		
Factor	0.32	**DV/DE 'r'**	0.85	S_L	opt
k_L	0.66	**CV**	20.95	S_C	opt.
k_C	1.00	**VAB**	22.67		
k_H	1.50	**GAMMA**	1.25		
STRESS	*17.44*	***PF/3***	*22.95*		
MOD. 'L^*'	MOD 'a^*'	MOD 'b^*'			
0.56	-0.58	0.62			
CIEDE$_{2000}$	***DIGITAL ST***	***RES.***	***0.23***		
Factor	0.62	**DV/DE 'r'**	0.91	T	Yes
k_L	0.60	**CV**	14.44	f	Yes
k_C	1.00	**VAB**	14.60	S_L	opt.
k_H	1.00	**GAMMA**	1.22	S_C	opt.
STRESS	*13.48*	***PF/3***	*14.90*	S_H	opt.
MOD. 'L^*'	MOD 'a^*'	MOD 'b^*'			
-1.69	-0.48	0.13			
CMC	***DIGITAL ST***	***RES.***	***0.32***		
Factor	0.76	**DV/DE 'r'**	0.80	T	Yes
k_L	0.64	**CV**	20.53	F	Yes
k_C	1.01	**VAB**	20.13	S_L	opt.
		GAMMA	1.22	S_C	opt.
STRESS	*19.19*	***PF/3***	*20.95*	S_H	*opt.*
MOD. 'L^*'	MOD 'a^*'	MOD 'b^*'			
-0.17	0.28	-0.17			

***Table 28*: Best settings for digital 'ST' sample set for optimized weighting and functions ('S_L'- function for weighted CIELAB – see *Figure 111*)**

A 'F' – test between the $CIEDE_{2000}$ and CMC formula in optimized mode as listed in *Table 28* (best setting) for digital 'ST' samples suggested a significant difference in prediction performances between them ('F' – value of '1.53' for a critical range of '0.80' – '1.25' – 95%, '213' degree of freedom, approximately normal distributed residuals). Also, 'F' – tests were conducted so to identify those functions that were significantly improving formulae's prediction performances (see *Table 29*).

DIG. ST	*SUM Residuals*	*Critical Range (95%)*		*F-Test*	*STRESS*
CMC					
FULLY OPT.	33.29	0.7977	1.2535	1	19.3
minus STD	41.27	0.7977	1.2535	1.24	21.46
minus 'S_L'	57.36	0.7977	1.2535	**1.72**	**23.96**
minus 'S_C'	63.93	0.7977	1.2535	**1.92**	**25.96**
***CIEDE*$_{2000}$**					
Fully OPT	16.84	0.7977	1.2535	1	13.27
minus STD	25.69	0.7977	1.2535	1.25	20.54
minus 'S_L'	40.78	0.7977	1.2535	**2.42**	**21.16**
minus'S_C', 'S_H'	42.73	0.7977	1.2535	**2.53**	**21.5**

***Table 29*: 'F' – test for functions for fully optimized *CIEDE*$_{2000}$ and CMC formula for digital 'ST' sample set.**

5.5.2 A significant improvement in $CIEDE_{2000}$ colour difference predictions was achieved by reducing mainly lightness 'L^*' by an average value of '1.69' when applied to all standard colour centres. Optimising the 'S_L' parameter improved all predictions furthermore when compared to visual colour differences obtained from a digital 'ST' sample set. These trends were also similar to those listed in *Table 21*. Adding weighting factors to CIELAB's formula, and optimizing the added 'S_L' function (- 2 STRESS units), resulted in similar results as obtained from CMC's formula. The 'k_L' weighting factor for digital 'ST' samples was reduced to '0.60' compared to approximately '2' for physical samples, '1.20' for digital 'BH', and '1.04' for digital 'TWC' samples, respectively (for the CMC formula). The $CIEDE_{2000}$ and CMC[bbb] formula became then of the form as given in *Equation 124* and *125* in a best setting mode.

Eq. 124: digital $\Delta E_{ST,1} = 0.608 \cdot \Delta E_{00} + 0.0781$

Eq. 125: digital $\Delta E_{ST,2} = 0.6371 \cdot \Delta E_{CMC} + 0.1089$, where

[bbb] see page 181 for comparison with

'$\Delta E_{ST,i}$' refers to a predicted colour difference value approaching those visual results for digital 'ST' samples either by using a optimized *CIEDE*$_{2000}$ or CMC formula according to *Table 29*. Those results for both formulae were then plotted in terms of 'ΔV_{ST}' against 'ΔE_{opt}' as given in *Figure 108* and *109.*

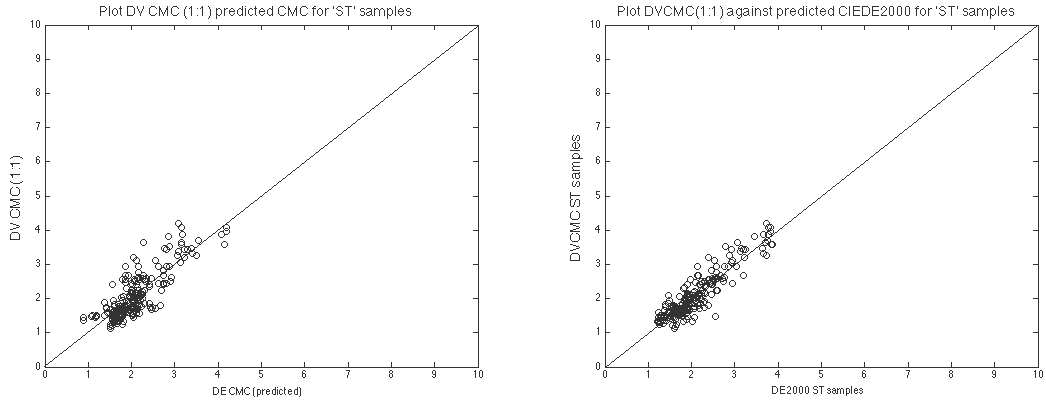

***Fig. 108 and 109*: Plot visual results against predicted results for 'ST' samples for using CMC and *CIEDE*$_{2000}$ formula.**

The result showed a better linear correlation for the *CIEDE*$_{2000}$ formula; but, it was also evident that both plots were generally less well distributed when compared with plots from 'BH' and 'TWC' samples as seen in *Figures 88 – 91*[ccc]. Visual results from 'ST' observations were plotted as ellipse contours in CIELAB's 'a^*b^*' - diagram and contrasted with discrimination ellipses that were calculated from *Experiment A – Part B* data for approximately '2.4' 'ΔE_{CMC}(1:1)' modelled distances.

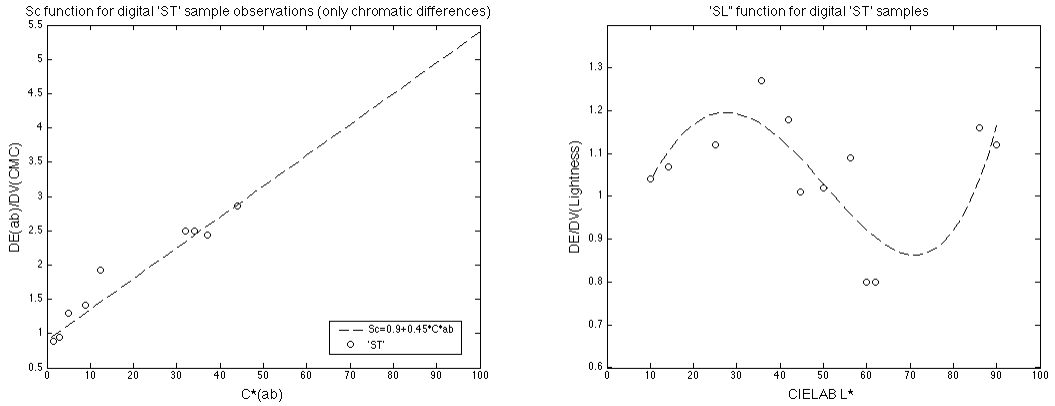

***Fig 110 and 111*: 'S_L' and 'S_C' function from 'ST' samples varying only in lightness (after scaling) and chroma directions (before scaling).**

[ccc] see page 179 for comparison

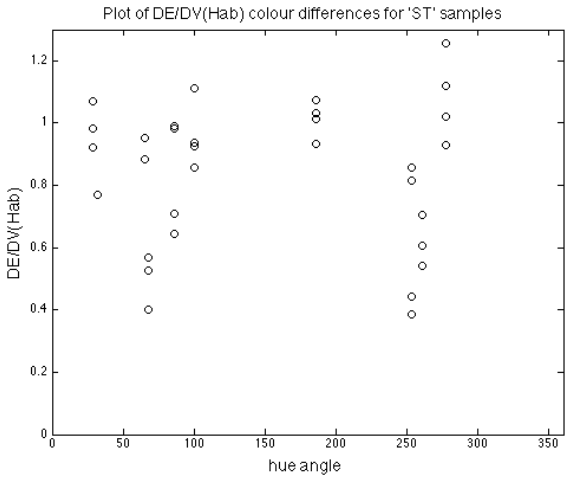

Figure 112: Plot '$\Delta E/\Delta V(H^*_{ab})$' for digital 'ST' samples (*Experiment B*)

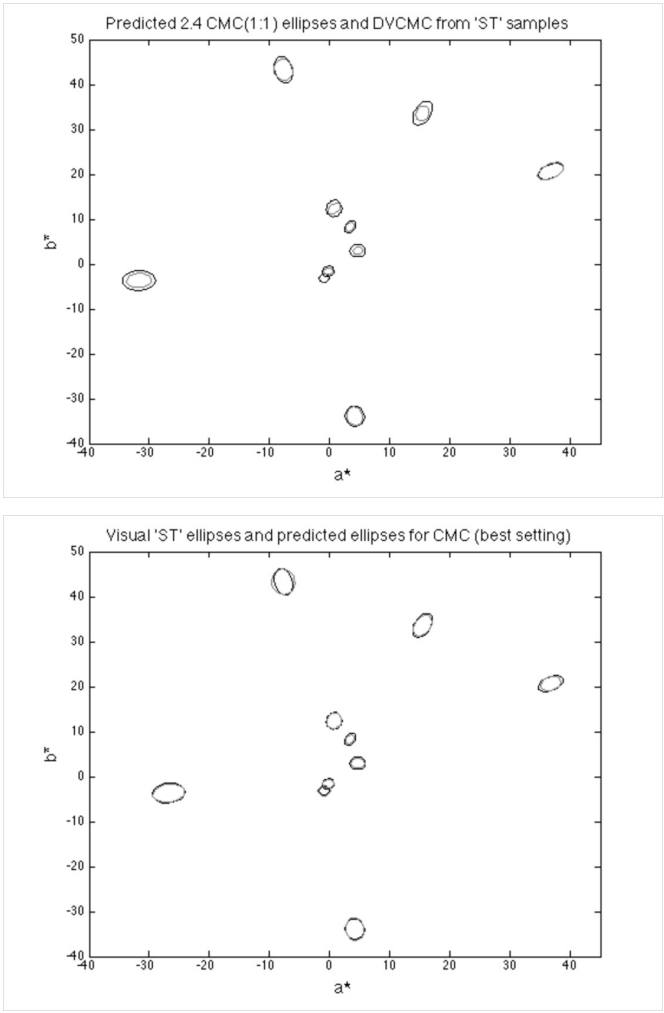

***Fig 113 and 114*: Predicted '2.4' CMC(1:1) ellipses against visual results (top), and optimised predicted CMC(best) ellipses against visual results for 'ST' samples.**

5.5.3 *Figure 113* and *114* shows visual and predicted (best setting) '2.4' 'ΔE_{CMC}(1:1)' units contour ellipses within CIELAB's 'a^*b^*' – diagram. Also, other formulae were optimized and compared with visual results for the digital 'ST' dataset. The STRESS measure was applied for different weightings and optimized standards as given in *Table 30.*

5.5.4 CIELAB improved significantly once all standard colour centres were optimized mainly in the lightness direction (reducing 'L^*' by a value of '2') altering the STRESS value from '29.61' to a value of '17.4'. The inclusion of a 'S_c' weighting function did not improve the predictions for digital 'ST' colour difference sample pairs once the optimization of the standards colour specifications was conducted; but, the optimization for the 'S_L' function did so albeit with only an insignificant amount from a statistical point of view (about '2' STRESS values). Also, colour differences ('$\Delta V_L/\Delta E_{CMC}$') for digital 'ST' samples mainly differing in the lightness direction, may suggested using a waveform form function (largest colour difference values were recorded for standards between 'L^*' 55 – 60).

CIE94				***STD Op.***	***LCD***				***STD OPT.***
k_L	2	1	0.81	0.83	k_L	2	1	0.766	0.77
k_C	1	1	1.1	1.11	k_{CH}	1	1	1	1
k_H	1	1	1.09	1.06					
STRESS	***38.41***	***24.58***	***21.39***	***20.01***	***STRESS***	***37.8***	***24.2***	***21.71***	***20.03***
$L^*a^*b^*$		-0.056	-0.338	0.16	$L^*a^*b^*$		-0.014	-0.305	0.187
DIN_{99}					***CIELAB***				***STD OPT***
k_l	2	1	0.79	0.76	k_L	2	1	0.5	0.5
k_e	1	1	1	1	k_C	1	1	1.05	1.05
					k_H	1	1	1.6	1.46
STRESS	***37.61***	***24.6***	***22.72***	***21.87***	***STRESS***	***52.02***	***43.77***	***29.61***	***17.44***
$L^*a^*b^*$		0.086	-0.213	0.15	$L^*a^*b^*$		-2.054	-1.136	0.698
DIN_{99c}					***DIN_{99d}***				
k_L	2	1	0.55		k_l	2	1	0.61	
k_e	1	1	1		k_e	1	1	0.99	
STRESS	***40.41***	***27.47***	***16.07***		***STRESS***	***38.26***	***23.95***	***15.95***	

***Table 30*: Prediction performances of various formulae in terms of weighting and optimizing standard colour centres.**

A fitted 'S_C' function differing only in chromatic content 'C^*_{ab}' for digital 'ST' samples followed a similar pattern as the 'S_C' function contained in CIE_{94}'s and $CIEDE_{2000}$'s formula (here given in the form as described in *Equation 126*). Also, a 'S_L' function as described in *Equation 127* was fitted to visual results from lightness difference sample pairs. A digital 'ST' formula could be then of the form as given in *Equation 128.*

Eq. 126: $$S_{C,ST} = 0.9 + 0.045 * L^*$$

Eq. 127: $$S_{L,ST} = (7E-08) * L^{*3} - (4E-06) * L^{*2} + 0.0315L^* + 0.7508$$

Eq. 128: $$E_{ST} = \text{ST factor} \cdot \sqrt{(\frac{\Delta L^*}{S_{L,ST}K_L})^2 + (\frac{\Delta C^*_{ab}}{K_C})^2 + (\frac{\Delta H^*_{ab}}{K_H})^2}, \text{ where}$$

weighting factors refer to approximate values of '0.5', '1', '1.5' for k_L', 'k_C' and 'k_H', and the overall size factor for 'ST' samples was given as a value of '0.75'. Significant tests between colour difference formulae are listed i*n Table 31* based on the assumption that residuals between optimised '$\Delta E_{Various}$' and '$\Delta V_{CMC}(1:1)$' were approximately normal distributed.

FORMULA		*CIE_{94}*	*DIN_{99}*	*DIN_{99c}*	*DIN_{99d}*	*LCD*	*CIELAB*
	STRESS^2	400.40	478.30	258.24	254.40	401.20	304.15
CIE_{94}	400.40	**A/B**	**1.1945**	0.6450	0.6354	**1.0020**	0.7596
DIN_{99}	478.30	**0.8371**	**A/B**	0.5399	0.5319	**0.8388**	0.6359
DIN_{99c}	258.24	1.5505	1.8521	**A/B**	**0.9851**	1.5536	**1.1778**
DIN_{99d}	254.40	1.5739	1.8801	1.0151	**A/B**	1.5770	**1.1956**
LCD	401.20	**0.9980**	**1.1922**	0.6437	0.6341	**A/B**	0.7581
CIELAB	304.15	1.3164	1.5726	**0.8491**	**0.8364**	1.3190	**A/B**
CRITICAL RANGE 95%		0.8	1.25				

***Table 31*: Significant test between various formulae. Bold figures indicate no significant differences in prediction performances between two formulae.**

5.5.5 The results showed significant differences in prediction performances between two groups of formulae; (**1**) $DIN_{99c,d}$ and modified CIELAB, and (**2**) LCD, CIE_{94}, and DIN_{99}. Also, a comparison of prediction performances for individual colour centres was conducted for various formulae so to identify those colour centres that were possibly critical for modeling purposes. Generally, those formulae were optimized for a best weighting factor settings and then analyzed in terms of prediction performances for each colour centre as listed in *Table 32* for the digital 'ST' sample data set. The prediction performance for grey colours was generally less well correlated with visual results that were obtained from other colours. $CIEDE_{2000}$ predicted batches around a blue centre best, whereas DIN_{99c} performed best for dark colours such as brown and black, when compared with CMC's formula. Generally, it was necessary to optimized weighting factors for minimizing differences between visual and numerical results.

STRESS	*$CIEDE_{2000}$*	*$CIEDE_{2000}$*	*DIN_{99c}*	*DIN_{99c}*	*CMC*	*CMC*
k_L/k_{CH}	0.540	0.552	1.000	0.750	1.000	0.560
k_C/k_e	1.000	0.938	1.000	1.250	1.000	0.958
k_H	1.000	1.058				
BEIGE	***16.090***	***14.120***	***27.010***	***15.150***	***34.130***	***20.100***
k_L/k_{CH}	0.540	0.552	1.000	0.750	1.000	0.560
k_C/k_e	1.000	0.938	1.000	1.250	1.000	0.958
k_H	1.000	1.058				
ORANGE	***14.400***	***14.780***	***19.750***	***10.430***	***28.710***	***11.130***
k_L/k_{CH}	0.540	0.552			1.000	0.560
k_C/k_e	1.000	0.938	0.701	0.750	1.000	0.958
k_H	1.000	1.058	1.000	1.250		
BLUE	***14.910***	***14.670***	***22.840***	***20.850***	***21.050***	***23.440***
k_L/k_{CH}	0.540	0.552			1.000	0.560
k_C/k_e	1.000	0.938	1.000	0.750	1.000	0.958
k_H	1.000	1.058	1.000	1.250		

GREY	***24.290***	***24.060***	***27.12***	***25.530***	***36.270***	***26.300***
k_L/k_{CH}	0.540	0.552			1.000	0.560
k_C/k_e	1.000	0.938	1.000	0.750	1.000	0.958
k_H	1.000	1.058	1.000	1.250		
OLIVE	***19.260***	***18.050***	***25.200***	***18.110***	***26.920***	***17.980***
k_L/k_{CH}	0.540	0.552			1.000	0.560
k_C/k_e	1.000	0.938	1.000	0.750	1.000	0.958
k_H	1.000	1.058	1.000	1.250		
RED	***20.930***	***20.010***	***27.750***	***18.880***	***33.030***	***19.970***
k_L/k_{CH}	0.540	0.552			1.000	0.560
k_C/k_e	1.000	0.938	1.000	0.750	1.000	0.958
k_H	1.000	1.058	1.000	1.250		
BROWN	***14.740***	***16.420***	***18.330***	***7.670***	***15.060***	***13.220***
k_L/k_{CH}	0.540	0.552			1.000	0.560
k_C/k_e	1.000	0.938	1.000	0.750	1.000	0.958
k_H	1.000	1.058	1.000	1.250		
GREEN	***11.360***	***10.190***	***30.630***	***14.270***	***30.320***	***12.870***
k_L/k_{CH}	0.540	0.552			1.000	0.560
k_C/k_e	1.000	0.938	1.000	0.750	1.000	0.958
k_H	1.000	1.058	1.000	1.250		
BLACK	***18.270***	***16.780***	***20.630***	***13.200***	***30.970***	***23.670***
k_L/k_{CH}	0.054	0.552			1.000	0.560
k_C/k_e	1.000	0.938	1.000	0.750	1.000	0.958
k_H	1.000	1.058	1.000	1.250		
YELLOW	***8.940***	***9.290***	***16.230***	***11.120***	***23.180***	***12.580***

***Table 32*: STRESS measure for each colour centre for the $CIEDE_{2000}$, CMC, and DIN_{99c} formula.**

5.6 Summary

. Twelve professional observers judged '300' digital Single Needle Lockstitch' type samples ('ST') around ten colour centres. The modelled and measured colour differences from batch fabric samples around each standards in various directions on screen resulted in an average '2.4' '$\Delta E_{CMC}(1:1)$' unit (+/- 0.2) value.

. The average visual result for all colour difference judgments was GRADE '2.99'. This translated to a visual colour difference value of '1.99' '$\Delta V_{CMC}(1:1)$' units. Lightness judgments were larger in magnitude (especially for high chromatic colours), whereas chromatic observations for all colour batches and centres were consistently lower in magnitude compared to instrumental measurements of on average '2.4' '$\Delta E_{CMC}(1:1)$' unit.

. The overall ratio between '$\Delta V_{CMC}(1:1)$' and '$\Delta E_{CMC}(1:1)$' for all colour samples was on average '0.9' ('0.75' and '1.04' for chromatic and lightness differences, respectively). *Experiment A – Part B* provided ratios of on average '1.25' ('1.10' to '1.42' for difference in

'C^*_{ab}' and in '$L^{*'}$) for blue and grey digital 'TWC' samples, and '1.61' ('1.48' to '1.75' for differences in 'C^*_{ab}' and in 'L'^*) for blue and grey digital 'BH' samples. All modelled differences for 'ST', 'BH' and 'TWC' samples were on average '2.4' $\Delta E_{CMC}(1:1)$ units.

. Formulae were significant improved by varying weightings according to 'k_L','k_C', and'k_H'. Lightness weighting 'k_L' for 'ST' samples were optimized to a value of '0.60' compared to '0.78' and '0.94' for digital 'TWC' and 'BH' samples. Those results provided evidence for parametric effects caused by the variation in sample presentations.

. A linear overall factor 'k_e' minimizing those total visual and predicted colour difference results were given as 0.75, 1.27, and 1.62 for 'ST', 'TWC' and 'BH' samples (values smaller than '1' would suggest that visual results were smaller in magnitude than numerical results, and vice versa). This provided evidence that visual colour difference values varied significantly in magnitude depending only on stitch type and presentation mode.

. Significant improvements in prediction performances was achieved by optimizing weighting factors, by changing colour standard coordinates (on average 'L^*' – 2), or optimizing the 'S_L' function. The CIEDE2000 formula prediction performance for a digital 'ST' colour data set was given as STRESS '13.48' ('0.23' 'ΔE_{00}' units difference on average between visual and predicted results). Grey colours were generally less well predicted; $CIEDE_{2000}$ predicted digital blue 'ST' samples best, whereas dark colours (black and brown batches) were predicted best using the DIN_{99c} formula.

5.7 Conclusion

. *Experiment B* provided evidence that colour difference magnitudes for 'ST' samples were judged smaller when compared with instrumental results from various colour difference formulae. Furthermore, human perception of colour differences was altered by the way they were presented to them. Results obtained from *Experiments A* and *B* suggested that 'ST' sample pairs were judged smallest, 'TWC' sample pairs larger, and 'BH' sample pairs largest in comparison given the same modelled colour difference magnitude for each data set.

. However, professional observers were, when compared to naive observers, presumably biased towards smaller judgments in the lightness direction. Therefore, a combined experiment was introduced (*Experiment C*) using naive observers at the University fo Leeds judging digital uniform 'TWC', digital 'BH', and digital 'ST' sample pairs around six colour centres with an average colour difference distance from the standards of '2.4' '$\Delta E_{(CMC)}(1:1)$' units.

Chapter 6:

6.1 *Experiment C*: General considerations

6.1.1. *Experiment A* and *B* provided evidence that the variation in sample presentation alters observer's colour difference perception. The magnitude of those visual data from smallest to largest average value for approximately the same instrumental values were in the order 'ST' < 'TWC' < 'BH' samples. However, two different groups (professional and naive observers) participated in psychophysical studies for the 'ST' data set. Also, it might be the case that professional observers are biased in their 'day to day' colour critical matching work. It is known that professional observers are less sensitive in the lightness direction compared to naive observers for textile samples when compared to chroma but, especially, for the hue difference direction.

6.1.2 Therefore, a new combined digital dataset was produced consisting of digital 'ST', 'BH', and 'UNI' samples that were judged in psychophysical assessments by naive observers at the University of Leeds. It was desired to let the same participants judge all three datasets, one set after another. Digital samples were designed while using the same LCD – and image models, but with new derived parameters. Those models were implemented according to *Graph 2* and *3* finally resulting in '26' batch samples surrounding six colour centres for three datasets. Twelve of them differed solely in CIELAB's 'a^*b^*' – direction with a colour difference distance of '2.4' '$\Delta E_{CMC}(1:1)$' units from a standard with an angle inclination of 0º, 15º, 30º, 45º, 60º, 75º, 90º, 105º, 120º, 135º, 150º, 165º, and 180º degrees (counter-clockwise in regards to CIELAB's 'a^*' – axis). Seven batches differed in the 'L^*a^*'- direction with a distance of '2.4' '$\Delta E_{CMC}(1:1)$' units from a standard with an angle inclination of 0º, 30º, 60º, 90º, 120º, 150º, 180º degrees in regards to CIELAB's 'a^*' –axis; another seven samples differed in the lightness direction 'L^*b^*' with a distance of '2.4' '$\Delta E_{CMC}(1:1)$' units differences from a standard in a similar fashion as all batches in CIELAB's 'L^*a^*' – direction.

6.1.3 The standard centres for *Experiment C* were of orange, olive, green, blue, brown, and grey colour. A dataset consisted of '186' samples including '30' repetition samples. Observers were asked to judge '558' sample pairs, altogether. Twenty-one observers participated in '*Experiment C – Part 1*' (uniform 'UNI' samples); nineteen observers participated in '*Part 2*' ('BH' stitch type samples), and eighteen observers participated in '*Part 3*' ('ST' stitch type samples) providing '10.788' visual colour difference judgments for analysis. The location of the colour centres and batches are plotted in CIELAB's – diagrams as given in *Figures 115 – 117.* All images were processed accordingly; however, edge enhancement were reduced for 'BH' and 'ST' samples (see *Image 11* –page 156- compared to *Image 13* - page 157 - for 'BH' samples and *Image 18* - page 187 - and *Image 14* - page 157 - for 'ST' samples) so to focus on colour

and lightness (also size and background effect) rather than texture differences (*Experiment A – Part A* and *B*).

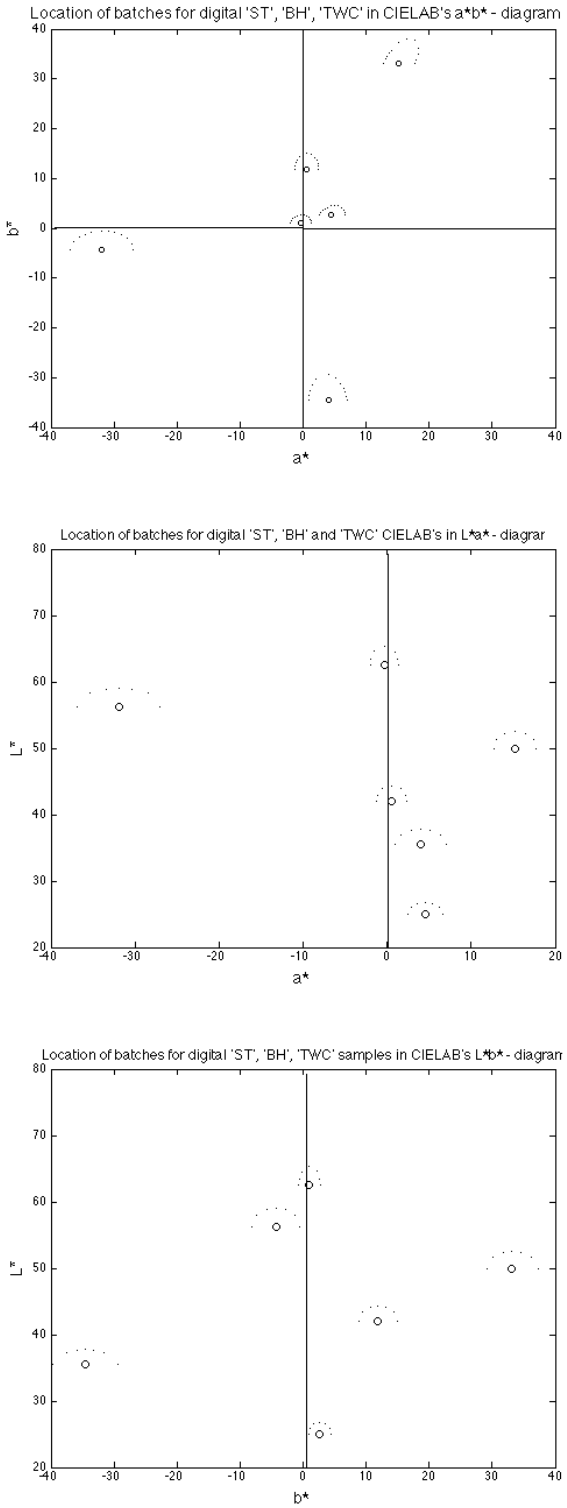

***Figure 115-117*: Location of batches and standards for *Experiment C* in 'a*b*' -, 'L*a*' - and 'L*b*' - directions.**

6.2 Performance of liquid crystal display model

6.2.1 The uniform 'TWC' sample data set was displayed on a LaCie LCD within the digital software setup as they were presented to observers (see *Graph 1*). Reflectance data were obtained from a tele-radiospectrometer for all uniform samples in the range from 380 – 780 nm. The CIE 10° standard observer's colour matching functions and spectral power distribution of the LCD's white point were used to calculate CIE 'XYZ_{10}' – tristimulus values. The white point was given as 'X_{10}' = '95.61', 'Y_{10}' = '100', and 'Z_{10}' = '92.82'. Absolute CIE '$XYZ_{10,L}$' – tristimulus values were calculated so to give on average; '$X_{10,L}$' = '203.01', '$Y_{L,10}$' = '212.33', and '$Z_{10,L}$' = '197.08', whereas '$Y_{L,10}$' refers to a luminance of '212.33' cd/m^2. Measurements of the LCD's white point were taken several times during *Experiment C* and are listed in *Table 33.*

LACIE	*White Point Measurement*								*Correlated*
Date	***X_{10}***	***Y_{10}***	***Z_{10}***	***x***	***y***	***Y***	***u***	***v***	***Colour Temperature***
16.10.10	95.52	100	93.06	0.3310	0.3465	100	0.2038	0.3201	5600
18.10.10	95.54	100	92.67	0.3315	0.3470	100	0.2040	0.3202	5600
19.10.10	95.46	100	93.08	0.3308	0.3466	100	0.2037	0.3200	5600
21.10.10	95.52	100	92.66	0.3315	0.3470	100	0.2039	0.3203	5600
22.10.10	95.61	100	92.39	0.3320	0.3472	100	0.2042	0.3204	5600
25.10.10	95.56	100	92.11	0.3322	0.3476	100	0.2042	0.3205	5600
28.10.10	95.80	100	93.37	0.3313	0.3458	100	0.2043	0.3198	5600
29.10.10	95.82	100	93.41	0.3313	0.3457	100	0.2043	0.3198	5600
01.11.10	95.77	100	93.20	0.3314	0.3461	100	0.2043	0.3199	5600
05.11.10	95.51	100	92.29	0.3319	0.3474	100	0.2040	0.3204	5600
	95.6145	***100***	***92.8270***	***0.3315***	***0.3467***	***100***	***0.2041***	***0.3202***	***5600***
						STD	***0.0002***	***0.0003***	

***Table 33*: White point measurement LaCie 321 for *Experiment C*.**

The absolute luminance '$Y_{10,L}$' for LaCie LCD's white point varied over time in the range from '$Y_{10.L}$' – '205' cd/m^2 to '$Y_{L,10}$' – '215' cd/m^2 . Chromaticity coordinates and the correlated colour temperature of the white point remained stable over a period of '3' weeks time. It was unlikely that a colour change over a period of '4' – '6' weeks time (time for modelling and observations) occurred during *Experiment C.*

6.2.2. The LCD model performances for all colour centres was determined by measuring uniform 'TWC' samples on screen. It was of interest to determine how well a model was able to predict required colour coordinates for a particular dataset. Colour distances between standard and batches were for all samples and directions '2.4' 'ΔE_{CMC}(1:1)' units. The measured colour difference distances for a reproduced uniform dataset and standards was on average '2.37' 'ΔE_{CMC}(1:1)' units ('0.2' standard deviation). The 95% confidence intervals for the mean values for all colour centres was in the range from '2.34' to '2.41' 'ΔE_{CMC} (1:1)' units according to those data listed in *Table 34.*

MEASURED UNIFORM SAMPLES ON SCREEN IN CMC (1:1) UNITS							
	BLUE	***BROWN***	***GREEN***	***GREY***	***OLIVE***	***ORANGE***	***MEAN***
a^*b^*	2.42(±0.12)	2.85(±0.07)	2.55(±0.05)	2,39(±0.06)	2,24(±0.04)	2.48(±0.08)	**2.42(±0.08)**
L^*a^*	2.14(±0.14)	2.06(±0.15)	2.42(±0.06)	2,44(±0.05)	2,25(±0.08)	2.32(±0.09)	**2.27(±0.06)**
L^*b^*	2.23(±0.11)	1.89(±0.25)	2.32(±0.08)	2,56(±0.11)	2.29(±0.09)	2.46(±0.07)	**2.29(±0.09)**
OVERALL	***2.26(±0.08)***	***2.38(±0.13)***	***2.46(±0.04)***	***2.45(±0.05)***	***2.26(±0.04)***	***2.43(±0.05)***	***2.37(±0.04)***

***Table 34*: Measurement of batch uniform 'TWC' samples on screen in' ΔE_{CMC}(1:1)' units.**

6.3 Grey scale

6.3.1 A grey scale consisting of 5 'GRADE' patches on screen were designed so to differ only in CIELAB's or CMC's lightness 'L^*' direction. The desired 'ΔL^*' differences between GRADE and standard grey scale sample (STD) were; GRADE '5' and STD equalled exactly '0' **'**ΔL^*' units**,** GRADE '4' and STD equalled '0.85' **'**ΔL^*' units**,** GRADE 3 and STD equalled '1.7' **'**ΔL^*' units, GRADE '2' and STD equalled '3.4' **'**ΔL^*' units, and GRADE '1' and STD equalled '6.8' **'**ΔL^*' units. The STD patch compared with GRADE '5' on screen next to each other (see *Graph 1*) resulted in an calculated colour difference of '0.66' **'**ΔE^*_{ab}' units. STD against GRADE '4', '3', '2', and '1' resulted in '1.06' (+/- 0.1 standard error of the mean -SEM-), '1.83' (+/- 0.2 SEM), '3.31' (+/- 0.2 SEM), and '6.48' (+/- 0.4 SEM) 'ΔE^*_{ab}' units. Those differences from a fixed location on screen (model performance independent of spatial variation) were '0.00', '0.83', '1.75', '3.32', and '6.60' 'ΔE^*_{ab}' units. The difference between both measurement scales, for a fixed- and variable positions, was mainly caused by the inherent non-uniformity of the LCD. The fixed scale did not change its location; hence, the colour differences between GRADE patches were close to those values that were predicted from the model. The variation in location included four different positions on screen; left/right column on the right side– and left/right column on the left side on the screen.

6.3.2 A change of position (placed next to each other) added an additional amount of chroma and hue content to those expected differences in 'ΔL^*'. This spatial effect decreased with the increase of lightness differences towards smaller GRADE numbers. Scale measurements were made in each of the four possible positions, and were as such recorded over time. Measurement data for the grey scale on screen are listed in *Table 35* in CIELAB and CMC(1:1) colour differences units. The CMC(1:1) formula was used to transfer GRADE values to 'ΔV_{CMC}(1:1)' units (see *Table 25*[ddd]).

[ddd] see page 191: Transfer function for *Experiment B*

GREYSCALE	*CIELAB*					*CMC(1:1)*				
DIFF. L/R	*Right*	*Left*	*Mean L/R*	*STD R*	*STD L*	*Right*	*Left*	*Mean L/R*	*STD R*	*STD L*
STD	0.66	0.66	**0.66**	0.06	0.06	0.97	0.89	**0.93**	0.10	0.07
GRADE 4	1.03	1.10	**1.06**	0.16	0.10	1.26	1.27	**1.27**	0.26	0.11
GRADE 3	1.76	1.90	**1.83**	0.16	0.14	1.93	2.01	**1.97**	0.17	0.16
GRADE 2	3.19	3.44	**3.31**	0.11	0.11	3.34	3.53	**3.43**	0.15	0.11
GRADE 1	6.23	6.72	**6.48**	0.22	0.22	6.38	6.79	**6.58**	0.23	0.24

***Table 35*: Averaged grey scale GRADE measurements over time for *Experiment C*.**

6.3.3 An 'exponential function' was designed for transforming GRADE to visual '$\Delta V_{\mathrm{CMC}}(1{:}1)$' units. The exponential function that was used to interpolate between measured GRADE values was of the form as given in *Equation 129*.

Eq. 129: $\Delta E_{\mathrm{CMC}}(1{:}1) = c1 + c2 \cdot exp^{c3 * \mathrm{GRADE}}$, where

parameter '$c1$' equals '0.640' (0.02 SEM), 'c2' equals '12.595' (0.07 SEM), and '$c3$' equals '0.752' (0.006 SEM). The model's residual sums of squares values were '0.00028' and '0.99997' for the adjusted 'R'-Square values for that interpolation curve approaching all five points.

6.4 Observers

6.4.1 Twenty-one, nineteen, and eighteen observers ('13' females and '8' males, average age of '30.61' years) participated in three experiments estimating visually colour differences on a digital screen. Observers were between '21' and '52' years of age with origins from China, England, France, Germany, and South Korea. All participants conducted a 'Farnsworth – Munsell 100 Hue' test for the examination of their colour discrimination ability. This test generally separates observers into classes of superior, average, and low colour discrimination. Also, it was possible to detect zones of colour confusion. Results obtained from past colour discrimination tests revealed that average discrimination observers achieved a total error score between '20' and '100' on a first test run. Superior observers according to 'Farnsworth-Munsell' test achieved scores between '0' and '16' errors, whereas low discrimination observers scored more than '100' errors units. The observer data were recorded and are listed as such in *Table 36.*

6.4.2 Those observers with only little or no experience in colour discrimination experiments were provided with a '20' minutes training session before they started the recorded experiments. Also, this procedure made observers familiar with the digital experimental setup. Each observer started the observational study for *Experiment C* with the uniform 'TWC' sample set followed by the 'BH' and 'ST' data set. Date and time of conducted observations for observers working dueing the daytime were primarily done in the evenings or weekends. However, a randomness

of dates and times for each observer experiment was maintained whenever possible, whereas the choice of samples for observations was randomised in order and position on screen for each data set. All observers conducted a colour discrimination test before and during sessions, if possible.

	TWC		*BH*		*ST*				*experienced*	*Farnsworth Munsell Hue test*		
Observer	*Session 1*	*Session 2*	*Session 3*	*Session 4*	*Session 5*	*Session 6*	*Sex*	*Age*	*Matcher?*	*1. Atempt*	*2.*	*3.*
1	Yes	Yes	No	No	No	No	Female	31-35	No	96	60	x
2	Yes	Yes	Yes	Yes	Yes	Yes	Female	21-25	No	36	32	x
3	Yes	Yes	Yes	Yes	Yes	Yes	Male	21-25	No	48	28	20
4	Yes	Yes	Yes	Yes	Yes	Yes	Female	26-30	Yes	36	4	x
5	Yes	Yes	Yes	Yes	Yes	Yes	Female	21-25	No	80	76	12
6	Yes	Yes	Yes	Yes	Yes	Yes	Female	26-30	No	88	84	32
7	Yes	Yes	Yes	Yes	Yes	Yes	Female	36-40	Yes	68	56	x
8	Yes	Yes	Yes	Yes	Yes	Yes	Male	21-25	Yes	20	x	x
9	Yes	Yes	Yes	Yes	Yes	Yes	Male	51-55	Yes	50	12	x
10	Yes	Yes	Yes	Yes	Yes	Yes	Female	21-25	No	28	16	x
11	Yes	Yes	Yes	Yes	Yes	Yes	Male	41-45	Yes	20	12	8
12	Yes	Yes	Yes	Yes	No	No	Male	41-45	Yes	20	12	x
13	Yes	Yes	Yes	Yes	Yes	Yes	Male	21-25	No	50	16	x
14	Yes	Yes	Yes	Yes	Yes	Yes	Female	31-35	No	2	x	x
15	Yes	Yes	Yes	Yes	No	No	Female	25-31	Yes	28	21	x
16	Yes	Yes	Yes	Yes	Yes	Yes	Male	31-35	No	108	92	x
17	Yes	Yes	No	No	Yes	Yes	Female	36-40	Yes	68	56	x
18	Yes	Yes	Yes	Yes	Yes	Yes	Female	26-30	Yes	68	24	x
19	Yes	Yes	Yes	Yes	Yes	Yes	Male	31-35	No	96	44	x
20	Yes	Yes	Yes	Yes	Yes	Yes	Female	21-25	No	72	60	52
21	Yes	Yes	Yes	Yes	Yes	Yes	Female	21-25	No	80	76	12

***Table 36*: Observer information for *Experiment C* and error scores for colour discrimination test after Farnsworth/Munsell.**

Discrimination error results for all observers decreased with the number of attempts they had (see *Table 36*). Those results for *Experiment C* suggested classifying all participants into nine superior and twelve average colour discrimination type of observers.

6.4.3 At first, the visual results for each paired 'BH', 'ST' and 'TWC' sample pair were ordered according to their magnitude estimates from each individual observer. They were classified into classes of smallest, medium, and largest visual colour differences '$\Delta V_{CMC}(1{:}1)$'. The classification results were then counted up for each class, observer, sample type, and colour difference direction. The results are listed in *Table 37*.

GRADES	***SMALLEST DE***	***MIDDLE DE***	***HIGHEST DE***
All Observers	*Counts*	*Counts*	*Counts*
UNI 'TWC' $\Delta V\, a^*b^*$	**8**	**8**	4
'ST' $\Delta V\, a^*b^*$	**12**	5	1
'BH' $\Delta V\, a^*b^*$	0	4	**15**
UNI 'TWC' L^*a^*	**20**	0	0
'ST' L^*a^*	0	**20**	0
'BH' L^*a^*	0	0	**20**
UNI 'TWC' L^*b^*	**20**	0	0
'ST' L^*b^*	0	**20**	0
'BH' L^*b^*	0	0	**20**

***Table 37*: Count of magnitude classes for each sample type and direction.**

Smallest magnitudes were assigned to uniform 'TWC' samples for both lightness directions, medium magnitudes for 'ST' sample and lightness directions, and largest for 'BH' samples. 'BH' samples were also given largest magnitude percentage in chromatic directions, whereas

'ST' samples and uniform 'TWC' gave mixed results with a tendency as seen in *Experiment A* and *B*.

6.5 Visual results analysis

6.5.1 '$\Delta V_{CMC}(1:1)$' results for each dataset and directions were then analysed in terms of distribution histograms as given in *Figures 118 - 125*. 'TWC' visual results were normal distributed; 'ST' observations (*Figure 119* for all samples, *Figure 122* for lightness differences, and *Figure 125* for chromatic differences) were distributed in a way suggesting to be of multi-normal form. '$\Delta V_{CMC}(1:1)$' values for all three datasets were analysed in terms of 'RAW' – data (original observer data) and revised data (unusual data points removed). First of all, it was of interest to compare each dataset's average visual values with each other for determining whether there was a variation in perception of colour differences between three different sample presentations. Average values were obtained for three datasets in '$\Delta V_{CMC}(1:1)$' units in the directions for changes in 'a^*b^*', 'L^*a*', and 'L^*b^*'. Those visual data from all observers' judgments for each particular sample pair were revised in terms of erroneous data points. Human observer judgements can be subjective and therefore may alter results depending just on the motivation, mood, or physical state of one particular observer at that day of the experiment. The main interest here was to obtain the 'ideal' average visual colour difference values that can as such describe a value that would have been obtained if the entire population of observers were asked to judge those sample pairs. So to define a legitimate average result for any colour difference pair in the dataset, it was necessary to identify those individuals' values that were distributed far away from the average value of all observations for a particular sample pair.

6.5.2 Two methods were applied to obtain a robust average value for a specific colour difference pair. The first method (**1**) assumed that the observation data for each pair were normally distributed. Those points that were two standard deviations away from the mean value for a particular sample pair were set to the overall mean value for all observations for that particular sample. This method refers to a 'role of thumb' measure. Secondly, and adopted from error analysis techniques, 'Chauvenet's criterion' was applied for determining those data points that were not legitimate, or likely to be not a value that would have been obtained from an ideal average population observer. The 'Chauvenet's Criterion' and the 'thumb of role' method uses the spread in data points (standard deviation –STD-) to determine whether one data point was a legitimate measurement, or not. A legitimate value can be determined by the probability of how many times its 'STD' differs from a mean value. If, the result was less than '0.5' (Chauvenet's Criterion), than the data point is generally discarded. This method provides evidence and direction towards those values that are unlikely when compared to all other observation values

for a particular sample pair. Also, it can detect observers who are likely not an average population observer. The combined results for the CMC(1:1) formula are listed in *Table 38.*

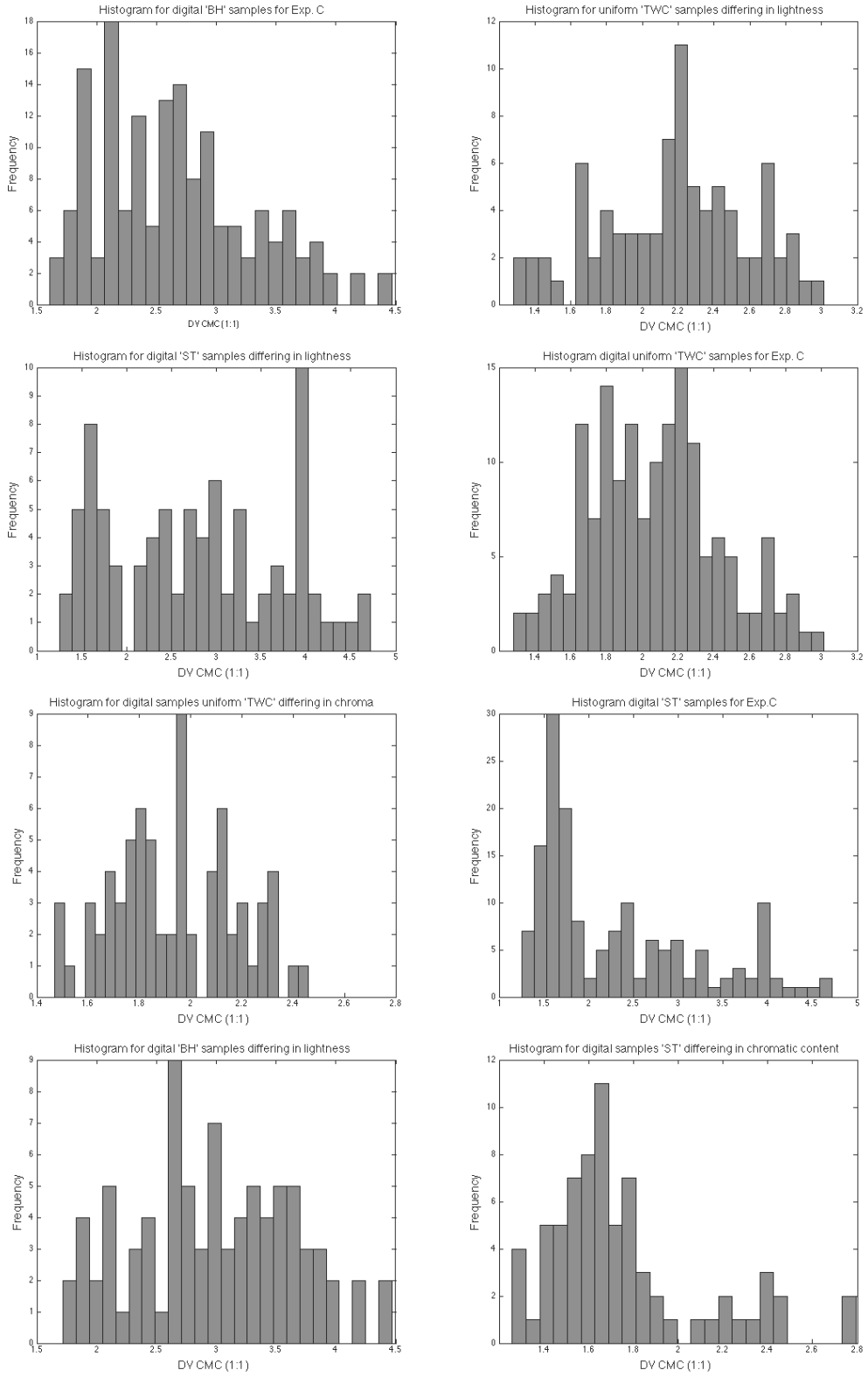

***Figure: 118 – 125*: Plots of 'ΔV_{CMC}(1:1)' for 'TWC', 'ST', and 'BH' samples for all, '$\Delta L^* \Delta a^* b^*$' and '$\Delta a^* \Delta b^*$' directions.**

CMC (1:1)	*CH.CRIT*	*CH.CRIT*	*RAW DATA*	*RAW DATA*	*MEASURED*
UNIFORM	*Weighted Mean DV*	*Mean DV*	*Weighted Mean DV*	*Mean DV*	*DATA*
All a^*b^*	1,8171	1,8816	1,8534	**1,94±0.02**	**2,4902**
All L^*a^*	2,1410	2,1463	2,2207	**2,19±0.03**	**2,2087**
All L^*b^*	2,0962	2,1030	2,1452	**2,15±0.04**	**2,3019**
BUTTONHOLE	*Weighted Mean DV*	*Mean DV*	*Weighted Mean DV*	*Mean DV*	
Sum a^*b^*	2,1895	2,3265	2,2664	**2,41±0.03**	
Sum L^*a^*	3,0296	3,0430	3,0741	**3,10±0.07**	
Sum L^*b^*	2,9858	2,9672	3,0000	**3,04±0.08**	
SINGLE STITCH	*Weighted Mean DV*	*Mean DV*	*Weighted Mean DV*	*Mean DV*	
Sum a^*b^*	1,5812	1,7399	1,6309	**1,77±0.03**	
Sum L^*a^*	2,7413	2,7710	2,7881	**2,81±0.05**	
Sum L^*b^*	2,8375	2,8051	2,8273	**2,83±0.06**	

Table 38*: Measurement data of uniform colour centres on screen for *Experiment C.

For instance, 'ΔV_{CMC}(1:1) values obtained from 'Observer 10' for the single needle lockstitch data set resulted in '90' outliers out of '156' sample pairs. This observer was far away from all other observations made during this experiment but scored considerably better in another experiment. Reasons for these anomalous results were identified because of stress related issues during a lunch break, time constraints, and probably motivation issues. However, the decision whether the data were used, or discarded, from the data set was being made available due to that criterion. All 'ΔV_{CMC}(1:1)' – values were then used to derive an arithmetic mean from all mean values from each data point for a colour centre and direction. The second method followed the same rule but weighted each individual mean sample pair value according to its associated uncertainty (standard deviation). The idea was to give priority to those data points that were less uncertain in regards to the standard deviation, or spread of the observer data, for each colour pair. However, the uncertainty or spread of data in terms of 'ΔV_{CMC}(1:1)' values was associated with the direction of batches around the colour centres (see *Table 39*). The spread was larger in the lightness direction compared to chromatic - differences. Hence, weighting were applied for each individual direction and data set.

CMC	*RAW* $\Delta V_{CMC}(1:1)$	*RAW* $\Delta V_{CMC}(1:1)$	*RAW* $\Delta V_{CMC}(1:1)$	*RAW* $\Delta V_{CMC}(1:1)$	*RAW* $\Delta V_{CMC}(1:1)$	*RAW* $\Delta V_{CMC}(1:1)$	*MEAS.* $\Delta E_{CMC}(1:1)$
SAMPLE	***BH***	***BH***	***ST***	***ST***	***UNIFORM***	***UNIFORM***	***UNIFORM***
ORANGE	*WEIGHTED MEAN*	*MEAN*	*WEIGHTED MEAN*	*MEAN*	*WEIGHTED MEAN*	*MEAN*	*MEAS. MEAN*
a^*b^*	1,99	2,08	1,58	1,65	1,62	1,71	2,48
L^*a^*	3,04	3,13	3,01	3,04	2,22	2,18	2,27
L^*b^*	3,14	3,28	3,11	3,11	2,33	2,34	2,50
OLIVE	*WEIGHTED MEAN*	*MEAN*	*WEIGHTED MEAN*	*MEAN*	*WEIGHTED MEAN*	*MEAN*	*MEAS. MEAN*
a^*b^*	2,40	2,52	1,66	1,67	1,95	2,03	2,24
L^*a^*	3,17	3,13	2,53	2,64	2,33	2,22	2,25
L^*b^*	2,98	2,98	2,70	2,68	2,32	2,22	2,30
GREEN	*WEIGHTED MEAN*	*MEAN*	*WEIGHTED MEAN*	*MEAN*	*WEIGHTED MEAN*	*MEAN*	*MEAS. MEAN*
a^*b^*	2,31	2,58	1,87	2,12	1,95	1,98	2,55
L^*a^*	3,24	3,36	3,40	3,40	2,21	2,18	2,35
L^*b^*	3,41	3,44	3,42	3,40	2,25	2,25	2,33

GREY	*WEIGHTED*	*MEAN*	*WEIGHTED*	*MEAN*	*WEIGHTED*	*MEAN*	*MEAS.*
a^*b^*	2,53	2,55	1,59	1,75	1,98	2,06	2,39
L^*a^*	3,41	3,52	3,00	3,11	2,38	2,36	2,47
L^*b^*	3,08	3,25	2,91	3,02	2,05	2,14	2,66
BROWN	***WEIGHTED***	***MEAN***	***WEIGHTED***	***MEAN***	***WEIGHTED***	***MEAN***	***MEAS.***
a^*b^*	2,07	2,15	1,43	1,48	1,79	1,84	2,85
L^*a^*	2,59	2,56	2,19	2,12	1,81	1,79	1,87
L^*b^*	2,38	2,34	2,07	1,98	1,40	1,46	1,76
BLUE	***WEIGHTED***	***MEAN***	***WEIGHTED***	***MEAN***	***WEIGHTED***	***MEAN***	***MEAS.***
L^*a^*	2,98	2,92	2,59	2,55	2,38	2,41	2,04
L^*b^*	3,00	2,97	2,77	2,79	2,54	2,51	2,27
All	***WEIGHTED***	***MEAN***	***WEIGHTED***	***MEAN***	***WEIGHTED***	***MEAN***	***MEAS.***
a^*b^*	**2,27**	**2,41**	**1,63**	**1,77**	**1,85**	**1,94**	**2,49**
L^*a^*	**3,07**	**3,10**	**2,79**	**2,81**	**2,22**	**2,19**	**2,21**
L^*b^*	**3,00**	**3,04**	**2,83**	**2,83**	**2,15**	**2,15**	**2,30**
STD	0,20	0,23	0,14	0,23	0,14	0,13	0,21
mse	0,08	0,09	0,06	0,09	0,06	0,06	0,08

***Table 39*: Average 'DV_{CMC} (1:1)' values for each colour centre and dataset for *Experiment C*.**

6.5.3 Three different sample presentations altered visual colour difference perceptions. 'ST' visual results were similar to those results that were obtained from professional observers in *Experiment B* for the same colour centres. Chromatic results for *Experiment B* was on average '1.76' '$\Delta V_{CMC}(1:1)$' units compared to '1.77' '$\Delta V_{CMC}(1:1)$' for *Experiment C*. The main difference was evident in visual lightness results for digital 'ST' samples where the average was given as '2.80' '$\Delta V_{CMC}(1:1)$' units for *Experiment C* compared to '2.3' '$\Delta V_{CMC}(1:1)$' for *Experiment B*. Two possible explanations for those lightness differences were; (**1**) that professional observer were less sensitive to lightness differences compared to hue differences (judging the colour difference rather than the total 'combined' difference), and (**2**) texture content for thread batches in *Experiment C* was reduced compared to batches in *Experiment B* so to enhance lightness perception on screen (texture content was to little to add texture colour difference amounts to the overall visual result).

6.5.4 Digital 'BH' samples for grey and blue standards were judged larger compared to digital 'ST' samples in the lightness direction '3.22' '$\Delta V_{CMC}(1:1)$' compared to '2.82' '$\Delta V_{CMC}(1:1)$' and for chromatic difference on average '2.55' '$\Delta V_{CMC}(1:1)$' compared to '1.87' '$\Delta V_{CMC}(1:1)$' for digital 'ST' blue and grey samples (35 % higher chromatic magnitude for 'BH' against 'ST'). The overall ratio between '$\Delta V_{CMC}(1:1)$' and '$\Delta E_{CMC}(1:1)$' results for digital 'BH' samples obtained during *Experiment C* was '1.20'. The ratio for 'BH' observations obtained from *Experiment A* against observations obtained from *Experiment C* for chromatic differences was '1.5' (50 % higher in *Experiment A* caused by the addition of texture content and a possibly enhanced chromatic content due to higher illumination level in the viewing cabinet), and a ratio of '1.29' in regards to lightness differences. The ratios between '$\Delta V_{CMC}(1:1)$ and '$\Delta E_{CMC}(1:1)$' for digital 'TWC' sample observations in *Experiment A* and digital uniform (no texture) 'TWC' samples in *Experiment C* was '1.26' (chromatic ratio 1.10 to 1.42 lightness ratio) against '0.87'

(0.81 and 0.92). This was on average about '1.38' times higher than those results that were obtained from *Experiment C*. The same ratio values were obtained for 'BH' sample pairs between *Experiment A* and *C*. Digital 'BH' and digital 'TWC' sample observations followed a systematic trend but 'ST' samples did not in terms of chromatic content; but, were as such approximately similar in magnitude between *Experiment B* and *C* albeit judged by two different observer groups. The ratio results between digital uniform 'TWC', 'BH', and 'ST' sample data sets were plotted either for mainly lightness (*Figures 129 – 131*) or chromatic differences (*Figures 126 – 128)* in a scatter diagram.

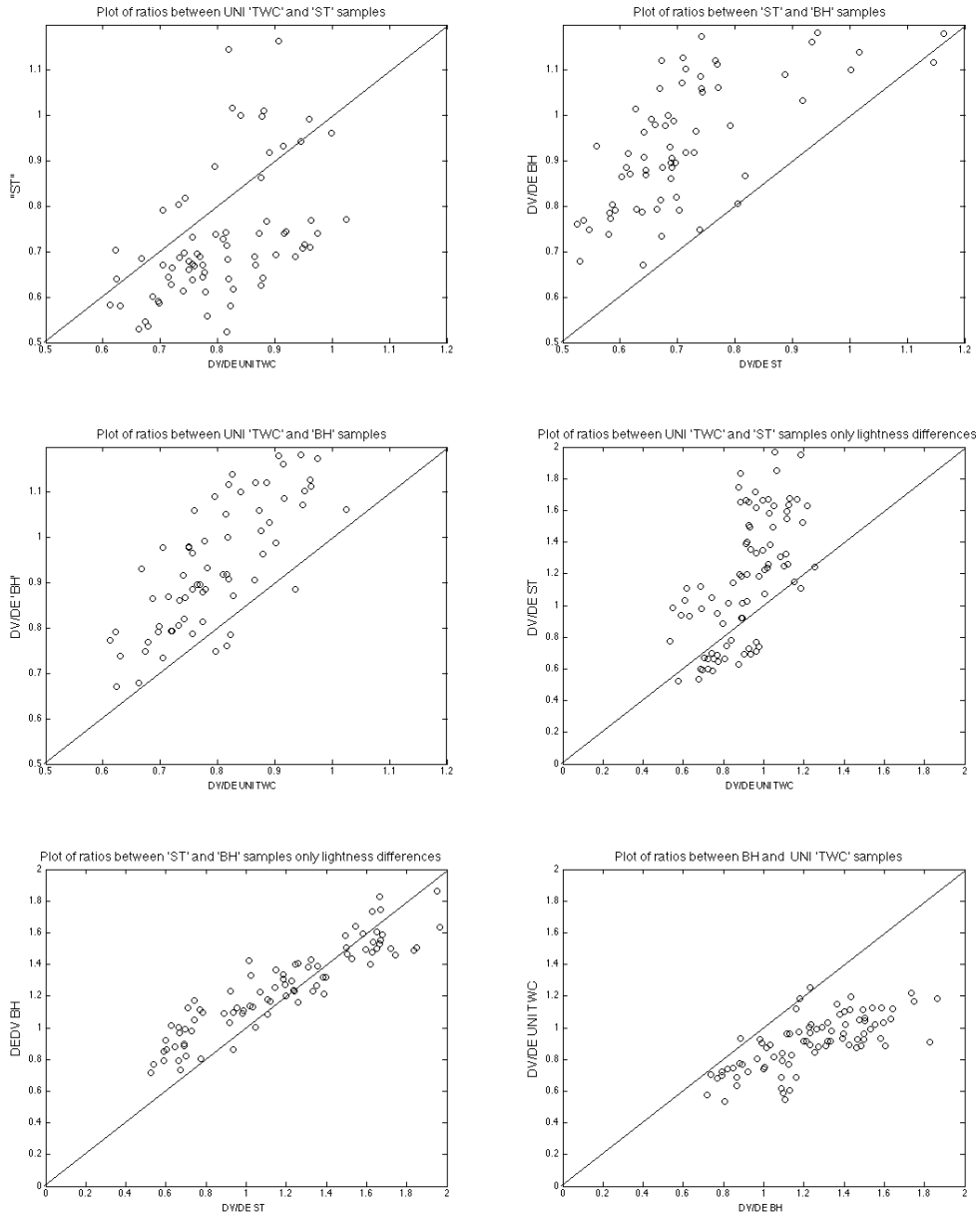

***Figure 126 – 131*: Plots of ratios '$\Delta V/\Delta E$' for CMC's formula for digital uniform 'TWC', 'ST' and 'BH' samples for *Experiment C*.**

6.6 Observer performances

6.6.1 Prediction performances for individual observers against all observations in terms of mean 'ΔV_{CMC}(1:1)' units for each sample pair and dataset, and a repeatability measure for each observer, were calculated using the STRESS measure (minimizing factor 'F' was not applied). The method for calculating those measures is given in *Equations 109 and 110ff*. However, STRESS values in this sense are not comparable with STRESS values obtained from performance quantifications for colour difference formulae. Therefore, it seemed to be sensible, to introduce also absolute differences in 'DV_{CMC} (1:1)' units for determining a repeatability measure for each observer (average value for a dataset) and, also, to determine how close one observer judged on average colour differences compared to the group mean value for a specific data set. This provided a value for each observer as such quantifying a deviation from the overall mean colour difference values (see *Table 40***,** *41***,** and *42*)

6.6.2 Averaged STRESS values were '29.69', '29.24', and '29.08' for the uniform 'TWC', 'BH', and 'ST' data set, respectively. These values matched approximately results from past research work in which inter-observer variation was given on average a value of '30' (STRESS). Average residuals, or average deviations from the mean value for a particular data set, was either '0.48', '0.64', or '0.58' 'ΔV_{CMC} (1:1)' units according to those three datasets.

6.6.3 The intra-observer repetitions values were obtained using just three sample pairs varying in CIELAB's 'a^*b^*' – direction for the blue and grey colour centres and dataset. These pairs formed data points at locations approximately 0°, 90°, and 180° degrees inclined to CIELAB's 'a^*' – axis; chosen in this manner because chromatic observations around each colour centre are expected to form ellipses (or ellipsoids, if a lightness direction is included). Six repeated observations were then obtained for each sample pairs at those three locations, averaged, and all deviations from the mean value in absolute 'ΔV_{CMC} (1:1)' units were calculated. The STRESS values for those repetitions are listed in *Table 43, 44*, and *45*.

6.6.4 Variations in performances between datasets and observers were compared with the numbers of outliers that were identified in each set; '91', '133', and '157' outliers for uniform 'TWC', 'BH' and 'ST' sample pairs, respectively. Outliers refer here to values that were unusual in terms of the discussed criteria, and as such given as the sum for each individual observer and data set. Generally, the average variation for uniform 'TWC' sample pairs showed a smaller spread when compared to other datasets. Also, the variation given as the magnitude of visual results (labelled residuals in *Tables 40 – 42*) for the 'BH' and 'ST' data set was larger. Overall, there was no 'unexpected' difference amongst data sets in terms of observer inter- and intra-observer variability; except those results obtained from observer number '10' for the 'ST' data set.

OBSERVER	*FARNSWORTH*			*Type*	*STRESS*	*Outlier*	*ΔV_{CMC} Residual*	*STD*	*ems*
1.	96	60	X	UNI	**33,07**	1	0,6061	0,3390	0,0271
2.	36	32	X	UNI	**23,32**	0	0,4024	0,2793	0,0224
3.	48	28	20	UNI	**32,77**	5	0,4896	0,4845	0,0388
4.	36	4	X	UNI	**35,88**	4	0,5778	0,4843	0,0388
5.	80	76	12	UNI	**38,04**	1	0,7225	0,3407	0,0273
6.	88	84	32	UNI	**50,38**	23	0,7792	0,7166	0,0574
7.	68	56	X	UNI	**27,87**	4	0,4433	0,3827	0,0306
8.	68	56	X	UNI	**25,63**	3	0,4279	0,3267	0,0262
9.	20	X	X	UNI	**27,71**	2	0,4623	0,3537	0,0283
10.	28	16	X	UNI	**41,77**	9	0,5751	0,6635	0,0531
11.	20	12	8	UNI	**14,14**	0	0,2473	0,1647	0,0132
12.	20	12	8	UNI	**17,46**	0	0,2986	0,2132	0,0171
13.	50	X	X	UNI	**29,90**	2	0,4852	0,3992	0,0320
14.	28	21	X	UNI	**20,34**	1	0,3478	0,2484	0,0199
15.	68	24	X	UNI	**37,06**	12	0,5537	0,5478	0,0439
16.	96	44	X	UNI	**27,46**	3	0,4449	0,3675	0,0294
17.	72	60	52	UNI	**22,68**	0	0,3800	0,2876	0,0230
18.	2	X	X	UNI	**32,79**	7	0,4824	0,4921	0,0394
19.	50	12	X	UNI	**20,07**	0	0,3327	0,2591	0,0207
20.	80	76	12	UNI	**35,66**	12	0,5173	0,5424	0,0434
21.	108	92	X	UNI	**29,56**	2	0,4647	0,4122	0,0330
MEAN	***55,33***	***42,50***	***20,57***		***29,69***	***91***	***0,4781***	***0,3955***	***0,0317***
OBSERVER	***FARNSWORTH***			***Type***	***STRESS***	***Outlier***	***ΔV_{CMC} Residual***	***STD***	***ems***
1.	96	60	X	Button	**X**	X	X	X	X
2.	36	32	X	Button	**20,10**	2	0,4068	0,4006	0,0321
3.	48	28	20	Button	**27,21**	0	0,6680	0,3883	0,0311
4.	36	4	X	Button	**42,21**	21	0,9920	0,6737	0,0539
5.	80	76	12	Button	**30,18**	5	0,6381	0,5732	0,0459
6.	88	84	32	Button	**23,79**	2	0,5500	0,3921	0,0314
7.	68	56	X	Button	**26,36**	1	0,6107	0,4335	0,0347
9.	20	X	X	Button	**28,58**	3	0,7041	0,4035	0,0323
10.	28	16	X	Button	**45,32**	28	0,9544	0,8646	0,0692
11.	20	12	8	Button	**19,25**	0	0,3198	0,2476	0,0198
12.	20	12	8	Button	**19,89**	0	0,3296	0,2567	0,0206
13.	50	X	X	Button	**19,89**	0	0,3296	0,2567	0,0206
14.	28	21	X	Button	**20,48**	0	0,3389	0,4835	0,0387
15.	68	24	X	Button	**45,17**	24	0,9460	0,8677	0,0695
16.	96	44	X	Button	**39,51**	22	0,8987	0,6723	0,0538
17.	72	60	52	Button	**22,12**	2	0,3945	0,5865	0,0470
18.	2	X	X	Button	**30,42**	14	0,7426	0,5836	0,0467
19.	50	12	X	Button	**30,71**	2	0,7398	0,4621	0,0370
20.	80	76	12	Button	**29,60**	4	0,6665	0,5127	0,0411
21.	108	92	X	Button	**34,71**	3	0,8525	0,4954	0,0397
MEAN	***55,33***	***42,50***	***20,57***		***29,24***	***133***	***0,6359***	***0,5029***	***0,0403***
OBSERVER	***FARNSWORTH***			***Type***	***STRESS***	***Outlier***	***ΔV_{CMC} Residual***	***STD***	***ems***
1.	96	60	X	Single	**X**	X	X	X	X
2.	36	32	X	Single	**19,85**	3	0,4011	0,3239	0,0259
3.	48	28	20	Single	**22,74**	0	0,4519	0,3806	0,0305
4.	36	4	X	Single	**21,60**	0	0,4048	0,3887	0,0311
5.	80	76	12	Single	**37,36**	15	0,6875	0,6854	0,0549
6.	88	84	32	Single	**24,79**	2	0,5088	0,3945	0,0316
7.	68	56	X	Single	**18,52**	0	0,3612	0,3179	0,0255
8.	68	56	X	Single	**15,94**	0	0,3378	0,3016	0,0241
9.	20	X	X	Single	**22,07**	0	0,4653	0,3349	0,0268
10.	28	16	X	Single	**77,05**	95	1,7051	1,0469	0,0838
11.	20	12	8	Single	**24,36**	0	0,5073	0,3784	0,0303
12.	20	12	8	Single	**25,03**	0	0,5053	0,4094	0,0328
13.	50	X	X	Single	**X**	X	X	X	X
14.	28	21	X	Single	**24,44**	1	0,4830	0,4121	0,0330
15.	68	24	X	Single	**26,40**	11	0,6916	0,6598	0,0528
16.	96	44	X	Single	**33,37**	2	0,7190	0,4840	0,0388
17.	72	60	52	Single	**29,12**	4	0,5713	0,9729	0,0779
18.	2	X	X	Single	**35,22**	6	0,7399	0,5381	0,0431
19.	50	12	X	Single	**24,26**	1	0,5180	0,3587	0,0287
20.	80	76	12	Single	**41,23**	17	0,4647	0,4122	0,0330
MEAN	***55,33***	***42,50***	***20,57***	***Single***	***29,08***	***157***	***0,5846***	***0,4889***	***0,0391***

***Table 40 – 42*: Inter observer variability measurement for three datasets for *Experiment C*.**

BUTTONHOLE OBSERVER	*BlDaDb1 STRESS*	*BlDaDb7 STRESS*	*BlDaDb12 STRESS*	*GrDaDb1 STRESS*	*GrDaDb7 STRESS*	*GrDaDb12 STRESS*	*MDM STRESS*	*MDM ΔV CMC*
2	0.1640	0.1420	0.1250	0.1932	0.1537	0.1176	**14.79**	0.3681
3	0.0710	0.0729	0.0467	0.1978	0.0768	0.2188	**11.29**	0.2214
4	0.1178	0.1929	0.2156	0.1018	0.1244	0.1214	**13.95**	0.5099
5	0.1915	0.2230	0.2475	0.1415	0.1051	0.2985	**20.12**	0.5707
6	0.1612	0.2542	0.1239	0.2531	0.1827	0.1973	**19.87**	0.5468
7	0.0605	0.0965	0.1630	0.1157	0.1295	0.0717	**10.63**	0.2109
8	0.1821	0.2312	0.0956	0.1389	0.1473	0.1568	**15.39**	0.3119
9	0.1453	0.1993	0.2714	0.2415	0.1658	0.1583	**19.35**	0.6130
10	0.0918	0.0781	0.1059	0.0840	0.0643	0.1026	**8.89**	0.2141
11	0.0515	0.1173	0.1533	0.1114	0.0608	0.0783	**9.56**	0.2288
12	0.0878	0.1907	0.1503	0.1200	0.0951	0.1328	**12.58**	0.3232
13	0.0562	0.0653	0.1109	0.0888	0.1293	0.0833	**8.88**	0.2071
14	0.0817	0.2054	0.1524	0.2346	0.3201	0.1337	**18.54**	0.4967
15	0.1222	0.2890	0.2031	0.2581	0.2134	0.2536	**21.67**	0.6964
16	0.0476	0.0891	0.1091	0.0975	0.1765	0.1181	**10.88**	0.3118
18	0.0563	0.0806	0.1244	0.1266	0.1984	0.2766	**14.37**	0.3736
19	0.1176	0.2951	0.1182	0.1788	0.1961	0.2419	**18.68**	0.3427
20	0.2401	0.2714	0.1312	0.2566	0.1751	0.1721	**19.97**	0.5194
21	0.0697	0.1355	0.2131	0.2348	0.0501	0.2322	**16.27**	0.3509
MEAN	0.1112	0.1611	0.1506	0.1671	0.1455	0.1666	**15.04**	0.3832
MEAN STD	0.0557	0.0681	0.0566	0.0638	0.0654	0.0698	**6.33**	0.1519
Standard error	0.0127	0.0156	0.0130	0.0146	0.0150	0.0160	**1.451**	0.0349

UNIFORM OBSERVER	*BlDaDb1 STRESS*	*BlDaDb7 STRESS*	*BlDaDb12 STRESS*	*GrDaDb1 STRESS*	*GrDaDb7 STRESS*	*GrDaDb12 STRESS*	*MDM STRESS*	*MDM ΔV CMC*
1	0,0900	0,3539	0,1574	0,1720	0,2978	0,1966	**21.13**	0,1914
2	0,2505	0,1173	0,3339	0,1011	0,3333	0,2292	**22.76**	0,2283
3	0,2589	0,1662	0,2096	0,1694	0,1997	0,1978	**20.03**	0,3059
4	0,2305	0,3144	0,5011	0,2243	0,2044	0,2526	**28.79**	0,4217
5	0,0711	0,2958	0,4384	0,1559	0,0927	0,1819	**20.60**	0,1492
6	0,1816	0,2996	0,2235	0,3459	0,0960	0,1395	**21.43**	0,3129
7	0,3914	0,2995	0,4121	0,1839	0,2197	0,2492	**33.60**	0,4678
8	0,3402	0,2326	0,1624	0,3127	0,1921	0,1867	**23.78**	0,3448
9	0,1081	0,1474	0,3426	0,0748	0,1271	0,0382	**13.97**	0,1666
10	0,3272	0,2401	1,0279	0,0960	0,1332	0,2716	**34.93**	0,3863
11	0,1467	0,1046	0,1286	0,0912	0,1107	0,1630	**12.42**	0,1426
12	0,1377	0,2776	0,1864	0,1342	0,0676	0,0820	**14.76**	0,1688
13	0,2452	0,2668	0,2580	0,2486	0,2546	0,3464	**26.99**	0,3934
14	0,1912	0,1396	0,2946	0,4115	0,2912	0,2518	**26.33**	0,4418
15	0,2242	0,2947	0,2949	0,1963	0,1832	0,2211	**23.57**	0,3243
16	0,0556	0,0564	0,0970	0,0710	0,0381	0,0609	**6.32**	0,0761
17	0,1107	0,3696	0,5459	0,0739	0,0661	0,0428	**20.15**	0,1817
18	0,3971	0,0859	0,3076	0,1150	0,1712	0,1375	**20.24**	0,1946
19	0,2310	0,1920	0,3801	0,3239	0,3082	0,3801	**30.25**	0,3722
20	0,2883	0,1612	0,3433	0,1127	0,1302	0,1448	**19.68**	0,1968
21	0,3082	0,1387	0,3528	0,3056	0,4385	0,0583	**26.70**	0,2920
MEAN	0,2184	0,2168	0,2956	0,1867	0,1884	0,1825	**21.47**	0,2742
MEAN STD	0,1018	0,0930	0,2118	0,1020	0,1031	0,0945	**6.931**	0,1138
Standard error	0,0222	0,0203	0,0462	0,0223	0,0225	0,0206	**1.512**	0,0248

SINGLESTITCH OBSERVER	*BlDaDb1 STRESS*	*BlDaDb7 STRESS*	*BlDaDb12 STRESS*	*GrDaDb1 STRESS*	*GrDaDb7 STRESS*	*GrDaDb12 STRESS*	*MDM STRESS*	*MDM ΔV CMC*
2	0,1193	0,1364	0,2509	0,1522	0,2976	0,3257	**21.37**	0,3759
3	0,0410	0,1408	0,0767	0,0528	0,1435	0,0905	**9.09**	0,1176
4	0,0668	0,0918	0,1641	0,2390	0,0709	0,0801	**11.88**	0,1872
5	0,1997	0,4818	0,2317	0,2602	0,3407	0,3585	**31.21**	0,4737
6	0,1457	0,2602	0,0815	0,2006	0,3353	0,1874	**20.18**	0,2575
7	0,0852	0,1671	0,0780	0,1775	0,1446	0,0822	**12.24**	0,1760
8	0,1601	0,2080	0,1779	0,1375	0,2336	0,1733	**18.17**	0,2483
9	0,1926	0,4032	0,1418	0,1893	0,3320	0,1987	**24.29**	0,2721
10	0,3458	0,2761	0,4298	0,2146	0,2267	0,1488	**27.37**	0,7555
11	0,0851	0,2223	0,0858	0,1152	0,1843	0,1058	**13.31**	0,1790
12	0,1145	0,0926	0,1277	0,0986	0,1270	0,0451	**10.09**	0,1197
14	0,3471	0,1973	0,1501	0,0765	0,1440	0,1773	**18.21**	0,2528
15	0,1500	0,0815	0,0727	0,1728	0,2769	0,0668	**13.68**	0,2015
17	0,1672	0,1943	0,1656	0,1814	0,1617	0,0942	**16.07**	0,2636
18	0,1939	0,1769	0,1805	0,1767	0,1816	0,2160	**18.76**	0,2255
19	0,4154	0,4204	0,4065	0,0865	0,3859	0,1370	**30.86**	0,3323
20	0,2067	0,1334	0,2170	0,2379	0,1857	0,2067	**19.79**	0,3382
21	0,2975	0,3027	0,0000	0,5082	0,0000	0,2741	**23.04**	0,4520
MEAN STRESS	0,1852	0,2215	0,1688	0,1821	0,2096	0,1649	**18,45**	0,2687
MEAN STD	0,1047	0,1169	0,1111	0,1005	0,1027	0,0890	**6.67**	0,1534
mse	0,0247	0,0276	0,0262	0,0237	0,0242	0,0210	**1.571**	0,0362

***Table 43 – 45*: Repetition values in STRESS units and 'ΔV_{CMC}(1:1)' for 'BH', uniform 'TWC', and 'ST'- samples.**

6.6.5 Generally, all results showed similarities in variability amongst data sets and observers. STRESS values, in terms of how well observers repeated their judgements for the same sample pairs, were on average ’18.45’ (‘6.67’ STD) and ’15.04’ (6.33 STD) units for ‘ST’ and ‘BH’ samples. ‘BH’ samples were repeated with higher precision when compared with values obtained from ‘ST’ sample pairs. Those STRESS values refer to absolute colour difference values of ‘0.269’ (‘0.15’ STD) and ‘0.3823’ (‘0.15’ STD) in ‘$\Delta V_{CMC}(1:1)$’ units on average. An important finding was that observers judged consistently well once they were trained and became more familiar with the tasks. Naive observers judged sample sets with similar precision as professional observers did; and, in some cases, even lower STRESS values were obtained. Some observers attended all four experiments during this project period of four years and this certainly was helpful to achieve good discrimination results. It became evident that observers were easily distracted because of personal motivation, stress levels, physical health conditions (morning – evening, working day – weekend observations, etc.).

6.7 Formulae performances

6.7.1 Prediction performances obtained for various colour difference formulae and visual results were quantified while applying several measures. Those measures considered for *Experiment C* were; ‘STRESS’, ‘PF/3’, ‘CV’, ‘$V_{ab'}$, Gamma ‘γ’, and residuals in ‘ΔE_{var}’ units depending on the formula that was used. The average residual, in this context described as the sum of the square root of squared difference between ‘$\Delta V_{CMC}(1:1)$’ and ‘$\Delta E_{CMC}(1:1)$’ values divided by the number of sample pairs, were minimised by optimising STRESS values by varying parametric factors and weighting functions.

6.7.2 In an ideal scenario a formula will fit predicted and observed colour difference values until the average residual for all sample pairs in a dataset becomes zero. Since, average visual results for each sample pair was expected to be affected by outliers in the data, a comparison between methods for outlier detection and removal for the raw data set, ‘role of thumb’ data, and ‘Chauvenet’s criterion’ data was conducted for determining the effect it has on a final STRESS value. The results are listed in *Table 46.*

6.7.3 The results in STRESS values for the optimised ‘k_L’ parametric factor for the CMC(*l*:*c*) formula were; ’14.90’/’14.93’/’14.97’ for uniform ‘TWC’ samples; ’15.78’/’16.19’/’16.19’ for ‘BH’ samples; and ’19.05’/’20.04’/’19.96’ for ‘ST’ samples for the ‘raw-‘, ‘rule of thumb-’, and ‘Chauvenet’s criterion’ method data sets. It was concluded from *Table 46* that there was no significant difference in prediction performances (‘STRESS’/’PF3’) between different outlier removal methods (however, the mean ‘$\Delta V_{VAR}(1:1)$’- value, for a sample pair or colour centre, may be altered).

1. CMC FORMULA – RAW DATA – STRESS PERFORMANCE						
Uniform						
k_L	2,00	1,00	0,80	0,81	**GAMMA**	**1,18**
k_C	1,00	1,00	1,00	1,06	**CV**	**14.80**
STRESS	**31.111**	**17.24**	**14.90**	**14.82**	**VAB**	**0,16**
					PF3	**15.85**
1. CMC FORMULA – RAW DATA – STRESS PERFORMANCE						
Buttonhole						
k_L	2,00	1,00	0,66	0,68	**GAMMA**	**1,18**
k_C	1,00	1,00	1,00	1,05	**CV**	**15,96**
STRESS	**37.507**	**22.45**	**15.78**	**15.74**	**VAB**	**0,16**
					PF3	**16.64**
1. CMC FORMULA – RAW DATA – STRESS PERFORMANCE						
SingleStitch						
k_L	2,00	1,00	0,48	0,48	**GAMMA**	**1,21**
k_C	1,00	1,00	1,00	0,98	**CV**	**19,98**
STRESS	**50.04**	**34.87**	**19.05**	**19.04**	**VAB**	**0,19**
					PF3	**20.11**
2. CMC FORMULA – 2STD OUTLIER REMOVED - STRESS						
Uniform						
k_L	2,00	1,00	0,86	0,82	**GAMMA**	**1,17**
k_C	1,00	1,00	1,00	1,06	**CV**	**14,98**
STRESS	**30.96**	**17.15**	**14.93**	**14.84**	**VAB**	**0,16**
					PF3	**16.00**
2. CMC FORMULA – 2STD OUTLIER REMOVED - STRESS						
Buttonhole						
k_L	2,00	1.00	0,65	0,66	**GAMMA**	**1,18**
k_C	1,00	1.00	1,00	1,03	**CV**	**16,44**
STRESS	**38.39**	**23.29**	**16.19**	**16.18**	**VAB**	**0,17**
					PF3	**17.09**
2. CMC FORMULA – 2STD OUTLIER REMOVED - STRESS						
SingleStitch						
k_L	2,00	1,0000	0,47	0,46	**GAMMA**	**20,05**
k_C	1.00	1,0000	1,00	0,96	**CV**	**21,11**
STRESS	**51.220**	**36.22**	**20.05**	**20.04**	**VAB**	**0,20**
					PF3	**20.83**
3. CMC FORMULA – CHAUVENET's CRITERION – STRESS PERFORMANCE						
Uniform					**GAMMA**	**1,17**
k_L	2,00	1,00	0,79	0,81	**CV**	**14,98**
k_C	1,00	1,00	1,00	1,05	**VAB**	**0,16**
STRESS	**31.32**	**17.38**	**14.97**	**14.92**	**PF3**	**15,98**
3. CMC FORMULA – CHAUVENET's CRITERION – STRESS PERFORMANCE						
Buttonhole					**GAMMA**	**1,18**
k_L	2,00	1,00	0,66	0,67	**CV**	**16,39**
k_C	1,00	1,00	1,00	1,04	**VAB**	**0,17**
STRESS	**38.210**	**23.130**	**16.19**	**16.15**	**PF3**	**17.00**
3. CMC FORMULA – CHAUVENET's CRITERION – STRESS PERFORMANCE						
SingleStitch					**GAMMA**	**1,22**
k_L	2.00	1.00	0,4633	0,46	**CV**	**21,02**
k_C	1.00	1.00	1.00	0.96	**VAB**	**0,20**
STRESS	**51.52**	**36.51**	**19.96**	**19.94**	**PF3**	**20.78**

***Table 46*: STRESS performances for various methods and CMC formula for *Experiment C*.**

Also, a weighted STRESS measure was applied, in which an individual mean '$\Delta V_{CMC}(1{:}1)$' value was weighted by the spread of data points around its mean value (standard deviation) so to determine its contribution to the final result. The comparisons between both STRESS measure methods are listed in *Table 47* for a weighted CIELAB formula.

UNIFORM TWC							*OPT.*
CIELAB WEIGHTED	**STRESS**	**STRESS**	**STRESS**	**WEIGHTED**	**BEST OPT.**		
k_L	2.00	1.00	0.53	0.48	0,62	**Gamma**	1.41
k_C	1.00	1.00	1,00	1,00	1.50	**CV**	30.12
k_H	1.00	1.00	1.00	1,00	0.87	**V**	0.35
STRESS	**48.20**	**39.02**	**32.14**	**33.36**	**28.72**	**PF3**	**35.30**
Buttonhole BH							
CIELAB WEIGHTED	**STRESS**	**STRESS**	**STRESS**	**WEIGHTED**	**BEST OPT.**		
k_L	2.00	1.00	0.43	0.38	0.52	**Gamma**	1.40
k_C	1.00	1.00	1.00	1.00	1.55	**CV**	27.72
k_H	1.00	1.00	1.00	1.00	0.89	**V**	0.34
STRESS	**52.53**	**42.00**	**29.13**	**33.88**	**26.02**	**PF3**	**34.06**
SingleStitch ST							
CIELAB WEIGHTED	**STRESS**	**STRESS**	**STRESS**	**WEIGHTED**	**BEST OPT.**		
k_L	2.00	1.00	0.31	0.29	0.40	**Gamma**	1.32
k_C	1.00	1.00	1.00	1.00	1.54	**CV**	21.25
k_H	1.00	1.00	1.00	1.00	1.03	**V**	0.28
STRESS	**60.77**	**49.12**	**26.17**	**27.15**	**19.11**	**PF3**	**27.34**

***Table 47*: Comparison between weighted and 'normal' STRESS value performances.**

6.7.4 The weighted STRESS method resulted in larger STRESS values when compared to conventional methods. Chauvenet's criterion and a weighted STRESS measure were also used for a comparison between formulae performances for all three datasets while optimising; (**1**) the 'k_L' factor, (**2**) 'k_L' and 'k_C' factors, and (**3**) 'S_L' , 'S_C', and 'S_H' weighting parameters. CIELAB, CIELAB (weighted), $CIELAB_{92}$, CMC, LCD, CIE_{94}, DIN_{99c}, and $CIEDE_{2000}$ were considered for this comparison. Those comparison results are listed in *Table 48* and *50* for the digital data sets used during *Experiment C*.

UNIFORM	S_L	S_C	S_H	k_L	k_C	k_H	*STRESS*
CIELAB				**0.4799**	1	1	**33.36**
$CIELAB_{92}$	1	0.047	0.014	**0.9736**	1	1	**19.95**
CMC	0.01765	0.0131	1900	**0.9276**	1		**21.30**
CIE_{94}	1	0.045	0.015	**0.9788**	1	1	**20.10**
DIN_{99c}	317.65	23		**0.7945**			**14.97**
$CIEDE_{2000}$	0.0150	0.0450	0.0150	**0.7867**	1	1	**13.87**
BUTTON	S_L	S_C	S_H	k_L	k_C	k_H	*STRESS*
CIELAB				**0.3765**	1	1	**33.88**
$CIELAB_{92}$	1	0.047	0.014	**0.7373**	1	1	**17.51**
CMC	0.01765	0.0131	1900	**0.6227**	1		**17.79**
CIE_{94}	1	0.045	0.015	**0.7360**	1	1	**17.56**
DIN_{99c}				**0.6292**			**12.26**
$CIEDE_{2000}$	0.0150	0.0450	0.0150	**0.6207**	1	1	**13.10**
SINGLE	S_L	S_C	S_H	k_L	k_C	k_H	*STRESS*
CIELAB				**0.2887**	1	1	**27.15**
$CIELAB_{92}$	1	0.047	0.014	**0.4662**	1	1	**17.32**
CMC	0.01765	0.0131	1900	**0.3992**	1	1	**18.68**
CIE_{94}	1	0.045	0.015	**0.4600**	1	1	**17.41**
DIN_{99c}	317.65	23		**0.4265**			**13.30**
$CIEDE_{2000}$	0.0150	0.0450	0.0150	**0.4085**	1	1	**14.22**

***Table 48*: Comparison of performances for an optimised 'k_L' weighting function.**

There was a significant difference in formulae prediction performances evident between results that are listed in *Table 48* and *50;* thus to a larger extent for optimised results that were obtained from the CMC formula. This effect also changed to a larger effect the values of optimised parameters for the CMC formula (see *Table 50*). Optimised parameters for the DIN_{99} and $CIEDE_{2000}$ formula remained almost unchanged when they were compared between both tables and optimisation methods. In *Table 49* other performance measures (as discussed in *Chapter 2*, pp.117–120) are listed for the optimised 'k_L' parametric factor; also, absolute residuals given in

'ΔE_{VAR}' units for each formulae (see *Table 48*), and an overall factor that minimises visual and predicted 'optimised' results for three different sample data sets and formulae.

UNIFORM	*GAMMA*	*CV*	*VAB*	*PF3*	*Factor*	*ΔV/ΔE*	*RESIDUAL*
CIELAB	1,46	34.53	38.74	39.94	1.85	1.00	0.4084
***CIELAB*$_{92}$**	1,20	18.45	18.74	19.23	1.08	1.00	0.2813
CMC	1.18	16.17	16.75	17.02	1.21	1.00	0.2634
***CIE*$_{94}$**	1.20	18.51	18.87	19.35	1.08	1.00	0.2847
***DIN*$_{99c}$**	1.15	14.33	14.72	14.95	1.10	1.00	0.2392
***CIEDE*$_{2000}$**	1.14	14,10	13.81	14.26	1.25	1.00	0.1941
BUTTONHOLE	*GAMMA*	*CV*	*VAB*	*PF3*	*Factor*	*ΔV/ΔE*	*RESIDUAL*
CIELAB	1.46	32.50	38.45	39.01	1.49	1.00	0.6918
***CIELAB*$_{92}$**	1.19	16.96	17.94	18.15	0,86	1.00	0.3456
CMC	1.18	16.64	16.66	17.12	1.03	1.00	0.3706
***CIE*$_{94}$**	1.19	16.87	17.91	18.10	0,86	1.00	0.3425
***DIN*$_{99c}$**	1.13	12.15	12.67	12.76	1.01	1.00	0.2600
***CIEDE*$_{2000}$**	1.14	14.10	13.18	13.36	1,00	1.00	0.2536
SINGLESTITCH	*GAMMA*	*CV*	*VAB*	*PF3*	*Factor*	*ΔV/ΔE*	*RESIDUAL*
CIELAB	1.35	23.59	30.13	29.84	1.99	1.00	0.2680
***CIELAB*$_{92}$**	1.19	17.50	18.73	18.45	1.25	1.00	0.3030
CMC	1.22	22.54	22.02	21.72	1.43	1.00	0.3721
***CIE*$_{94}$**	1.19	17.76	18.21	18.63	1.26	1.00	0.3079
***DIN*$_{99c}$**	1.15	14.22	14.22	14.72	1.40	1,00	0.2535
***CIEDE*$_{2000}$**	1.16	14.10	15.17	15.97	1.39	1.00	0.2478

***Table 49*: Comparison of formulae performances measured for optimised 'k_L' parametric factor.**

6.7.5 Factor in *Table 49* refers to scalars that are used to minimise mean visual and optimised predicted results for a particular data set and formula. Residuals are given as average values that provide an *absolute* difference measure between visual and optimised predicted results. The DIN_{99c} and CMC's formula weighted STRESS values after optimisation were given as '13.31'/'14.56' (*Table 48:* '14.97' and '21.30') for the uniform 'TWC' dataset, '9.8'/'13.02 (*Table 48:* '12.26'/ '17.79') for the digital 'BH' data set, and '9.96'/'13.33' (*Table 48*: '13.30'/'18.68') for the 'ST' data set opposed to '13.57', '11.86', and '13.52' (Table 48: '13.87', '13.10', and '14.22') for the CIEDE2000 formula, respectively.

6.7.6 This provided evidence that it was possible to achieve better predictions results, if parametric and weighting factors were altered within a formula. But, it also showed that weightings functions were designed for a particular dataset. The $CIEDE_{2000}$ formula was designed from four major datasets and, therefore, it was expected that this formula provides a possibly better fit (or more stable fit) to a larger range of data sets compared to a formula that was designed from just one specific type of sample set. The $CIEDE_{2000}$ 'k_C' and 'k_H' parametric factors were almost similar for the uniform 'TWC', 'BH', and 'ST' data sets but differed for the 'k_L' – factor from '0.84', '0.72', to '0.42' (see also *Table 48*: '0.79', '0.62', '0.41') thus providing evidence for a parametric factor that was caused by size, texture, and type of presentation. Those results confirmed well with those results obtained from *Experiment A* and *B*. The average residuals value was reduced to about '0.21' 'ΔE_{00}' units between visual and predicted results for all three digital data sets.

UNIFORM TWC	S_L	S_C	S_H	k_L	k_C	k_H	*WEIGHT.*	*Mean Residuals*
CIELAB	0.66	1.67	1.0				**30.15**	0.3903
***CIELAB*$_{92}$**	1.25	0.077	0.027	**0,988**	1.036	1.000	**18.32**	0.2594
CMC	1060.99	0,0044	6011.51	**0.926**	1.000		**14.56**	0.2118
***CIE*$_{94}$**	1.25	0.074	0.028	**1.014**	1.086	1.000	**18.42**	0.2581
***DIN*$_{99}$**	250,64	23,00		**0.895**			**13.31**	0.2101
***CIEDE*$_{2000}$**	0.0126	0.052	0.0183	**0.842**	0.976	1.013	**13.57**	0.1921
BUTTONHOLEE	S_L	S_C	S_H	k_L	k_C	k_H	*WEIGHT.*	*Mean Residuals*
CIELAB	0.55	1.90	1.00				**29.40**	0.5282
***CIELAB*$_{92}$**	1.05	0,0523	0.0172	**0.462**	0.995	0.988	**17.20**	0.3010
CMC	26.58	0.004	5781.33	**0.622**	1.000		**13.02**	0.2851
***CIE*$_{94}$**	1.28	0.079	0.0301	**0.766**	1.089	1.000	**15.03**	0.3082
***DIN*$_{99}$**	246.39	23.00		**0.629**			**9.80**	0.1900
***CIEDE*$_{2000}$**	0.0025	0.0520	0.0186	**0.715**	0.979	1.010	**11.86**	0.2265
SINGLESTITCH	S_L	S_C	S_H	k_L	k_C	k_H	*WEIGHT.*	*Mean Residuals*
CIELAB	0.36	1.48	1.00				**24.98**	0.2278
***CIELAB*$_{92}$**	0.004	0.047	0.015	**0.754**	1.048	1.000	**14.96**	0.3089
CMC	441.47	0.0143	6635.54	**0.399**	1.000		**13.33**	0.2690
***CIE*$_{94}$**	1.032	0.049	0.0172	**0.465**	1.031	0.997	**17.33**	0.2988
***DIN*$_{99}$**	275.37	23.00		**0.264**			**9.96**	0.1900
***CIEDE*$_{2000}$**	0.004	0.033	0.013	**0.417**	1.01	0.991	**13.52**	0.2309

***Table 50*: Optimised weighting factors and function for various sample types for *Experiment C*.**

6.7.7 Also, a comparison between each individual colour centre for the CIELAB, CMC, DIN_{99c} and $CIEDE_{2000}$ formula was applied so to identify those colours that were predicted better than others while using various formulae. The results are listed in *Table 51*. Smaller STRESS values refer to better prediction performances for a particular colour centre and formula. Here, the transfer functions for each formula were used in a different form, for instances, 'GRADE' – 'ΔV_{00}(1:1)'or 'GRADE' – 'ΔV_{99c}(1:1)' for $CIEDE_{2000}$ and DIN_{99} formula, respectively.

STRESS PERFORMANCE FORMULA FOR EACH COLOUR CENTER												
	'TWC' ***CIE*$_{00}$**	**'TWC'** ***DIN*$_{99}$**	**'TWC' CMC**	**'TWC' LAB**	**'ST'** ***CIE*$_{00}$**	**'ST'** ***DIN*$_{99}$**	**'ST' CMC**	**'ST' LAB**	**'BH'** ***CIE*$_{00}$**	**'BH'** ***DIN*$_{99}$**	**'BH' CMC**	**'BH' LAB**
ORANGE												
a^*b^*	8.04	10.6	10.2	40.8	15.44	1.417	12.94	28.74	7.78	8.84	8.70	36.61
L^*a^*	17.99	9.50	11.31	18.13	12.24	7.07	8.09	11.37	13.32	8.23	11.4	14.97
L^*b^*	5.02	8.07	8.28	11.18	13.31	6.43	8.87	13.78	12.86	7.81	10.0	16.06
OLIVE												
a^*b^*	6.20	14.38	10.49	38.32	9.85	8.18	8.99	30.78	11.29	15.07	11.2	39.62
L^*a^*	6.14	12.92	10.71	26.94	8.82	6.19	7.71	17.23	8.80	12.77	13.1	31.27
L^*b^*	11.27	10.32	10.33	11.45	16.89	11.40	15.68	14.52	7.75	5.29	7.97	09.89
GREEN												
a^*b^*	10.50	9.68	8.49	26.60	18.20	11.59	17.42	31.53	18.86	15.44	18.0	42.66
L^*a^*	20.30	19.03	18.05	35.36	11.17	6.40	12.18	13.26	13.27	13.10	14.5	27.54
L^*b^*	16.35	15.74	12.12	20.56	11.01	8.41	13.43	12.17	10.35	7.22	10.9	12.58
GREY												
a^*b^*	15.62	11.31	11.82	54.89	11.41	13.63	10.37	45.77	14.38	4.77	8.99	55.96
L^*a^*	13.59	11.99	13.94	40.74	14.63	4.77	14.67	25.72	14.01	5.92	13.1	38.58
L^*b^*	14.60	22.42	20.32	27.49	21.40	8.53	12.42	22.26	20.45	5.15	7.29	31.00
BROWN												
a^*b^*	10.67	10.43	10.47	38.87	11.74	7.94	10.87	26.16	8.98	6.49	14.6	36.48
L^*a^*	6.01	12.48	15.14	32.45	9.86	6.61	7.37	12.63	11.10	6.74	7.14	22.58
L^*b^*	9.21	22.66	29.70	33.48	14.33	9.57	11.10	14.21	18.29	7.62	9.47	14.09
BLUE												
a^*b^*	23.37	10.06	17.85	36.30	20.28	11.19	19.70	34.80	16.81	13.67	22.3	38.28
L^*a^*	19.78	14.54	15.98	16.03	15.27	13.63	21.46	17.30	8.65	5.98	10.5	14.59
L^*b^*	22.31	20.24	20.22	22.69	8.94	8.97	13.18	19.09	7.07	6.16	11.2	19.51
ALL	***13.02***	***13.04***	***13.54***	***32.01***	***13.82***	***9.64***	***12.78***	***24.54***	***12.59***	***9.19***	***12.29***	***31.33***
a^*b^*	12.40	11.08	11.56	39.31	14.49	11.12	13.38	32.96	13.02	10.71	14.0	41.60
L^*a^*	13.97	13.41	14.19	28.28	12.00	7.44	11.91	16.25	11.53	8.79	11.6	24.92
L^*b^*	13.13	16.57	16.83	21.14	14.31	8.88	12.45	16.01	12.79	6.54	9.49	17.19

***Table 51*: STRESS prediction performances for all colour centres and various formulae for *Experiment C*.**

There were no significant performance differences evident between formulae and the 'TWC' data set. The prediction performances between DIN_{99} and CMC/$CIEDE_{2000}$ varied for the 'BH' and 'ST' dataset.

6.8 'F' – tests, ellipses, and boxplots

6.8.1 'F' – tests were conducted so to verify whether there was a significant difference in the prediction performances between the CMC, $CIEDE_{2000}$, and DIN_{99c} – formula in a best possibly setting. The transfer function for this test, from 'GRADE' to visual 'ΔV', followed the same rule as practised in *Experiment A* and *B* – as such from **'**GRADE'- values to '$\Delta V_{CMC}(1:1)$' units for all three formulae. Distributions of visual results against paired predictions in best possibly setting for the CMC, $CIEDE_{2000}$, and DIN_{99} formula and the digital 'ST' sample set judged by naive observers during *Experiment C* can be seen in *Figure 132, 133,* and *134*.

6.8.2 The results from 'F' – tests, as given in *Table 52,* suggested significant differences in prediction performances between the $CIEDE_{2000}$ and CMC/DIN_{99} formulae, if residual analysis were applied. Differences between chromatic and lightness visual/predicted results were described either by the lower or upper location as seen in *Figure 132*, *133*, and *134*. Clustered points refer to chromatic 'ΔV'/'ΔE' - differences.

DIGITAL 'ST' EXP. C		***DIN99***	***CMC***	***CIEDE2000***
BEST SETTING	***RESIDUALS***	16.93	14.44	9.99
DIN_{99}	16.93	1	0.85	**0.59**
CMC	14.44	1.17	1.00	**0.69**
$CIEDE_{2000}$	9.99	**1.69**	**1.44**	1
STRESS		7.025	12.28	10.25
MEAN $\Delta V/\Delta E$		0.26	0.24	0.19
Factor		0.529	0.69	0.71
Critical Range	0.7678	1.3023	155 degrees of freedom	

***Table 52*: 'F' – test between formulae for digital 'ST' data set.**

6.8.3 Also, chromatic ellipses for the digital uniform 'TWC', 'ST', and 'BH' visual data sets were plotted in CIE's 'a^*b^*' – diagram as presented in *Figures 135 – 140*. Here, it was of interest to determine graphically how visual judgments for the same numerical chromatic differences were altered in size due different sample presentations. Box plots were then constructed for all data sets in the chromatic and lightness direction so to identify their distributions (see *Figures 141* and *142*). Those visual results in *Figure 135 – 140* showed significant size differences especially between 'BH' and 'ST' visual colour difference results. The distributions for differences in chromatic content '$\Delta V_{CMC}(1:1)$' units was approximately normal distributed ('ST' green and three blue colour batches were judged larger compared to all other 'ST' samples). Statistical tests for 'BH' against 'TWC' and 'ST' against 'BH' clearly indicated significant differences in the mean or median values between them; hence, the null-hypothesis 'h_0' that they came from the same underlying population was rejected. 'Uniform 'TWC' visual chromatic distributions compared to 'ST' data were either significant or not

significant different according to the type of test that was applied. Differences only in the lightness direction were significant different between the uniform 'TWV' and 'ST'/'BH' visual sample data sets, but not between 'ST' and 'BH' data sets (see 'p'- and 'F' values in *Section 6.10*).

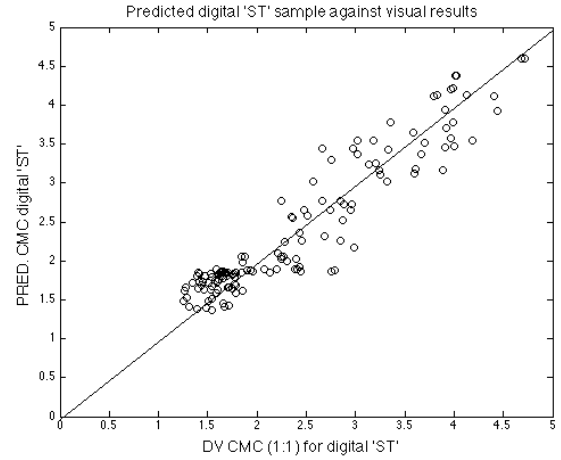

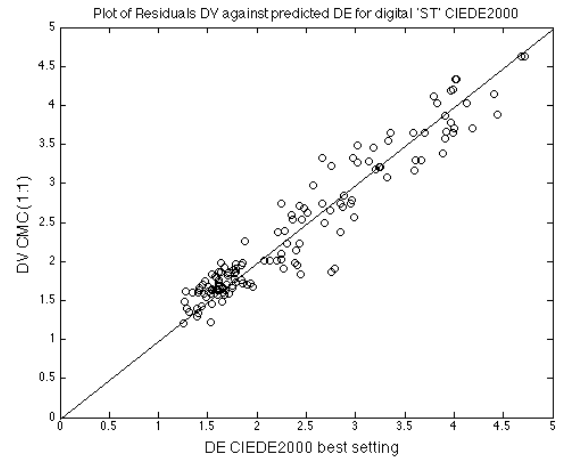

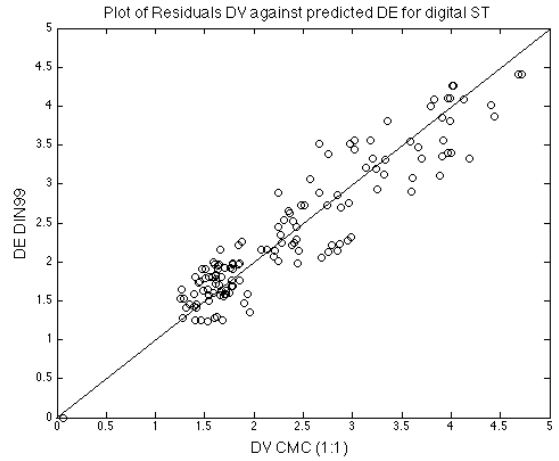

Figure 132 -134*: Plots of predicted against visual 'ST' colour difference sample pairs for CMC, $CIEDE_{2000}$, and DIN_{99} formula for *Experiment C.

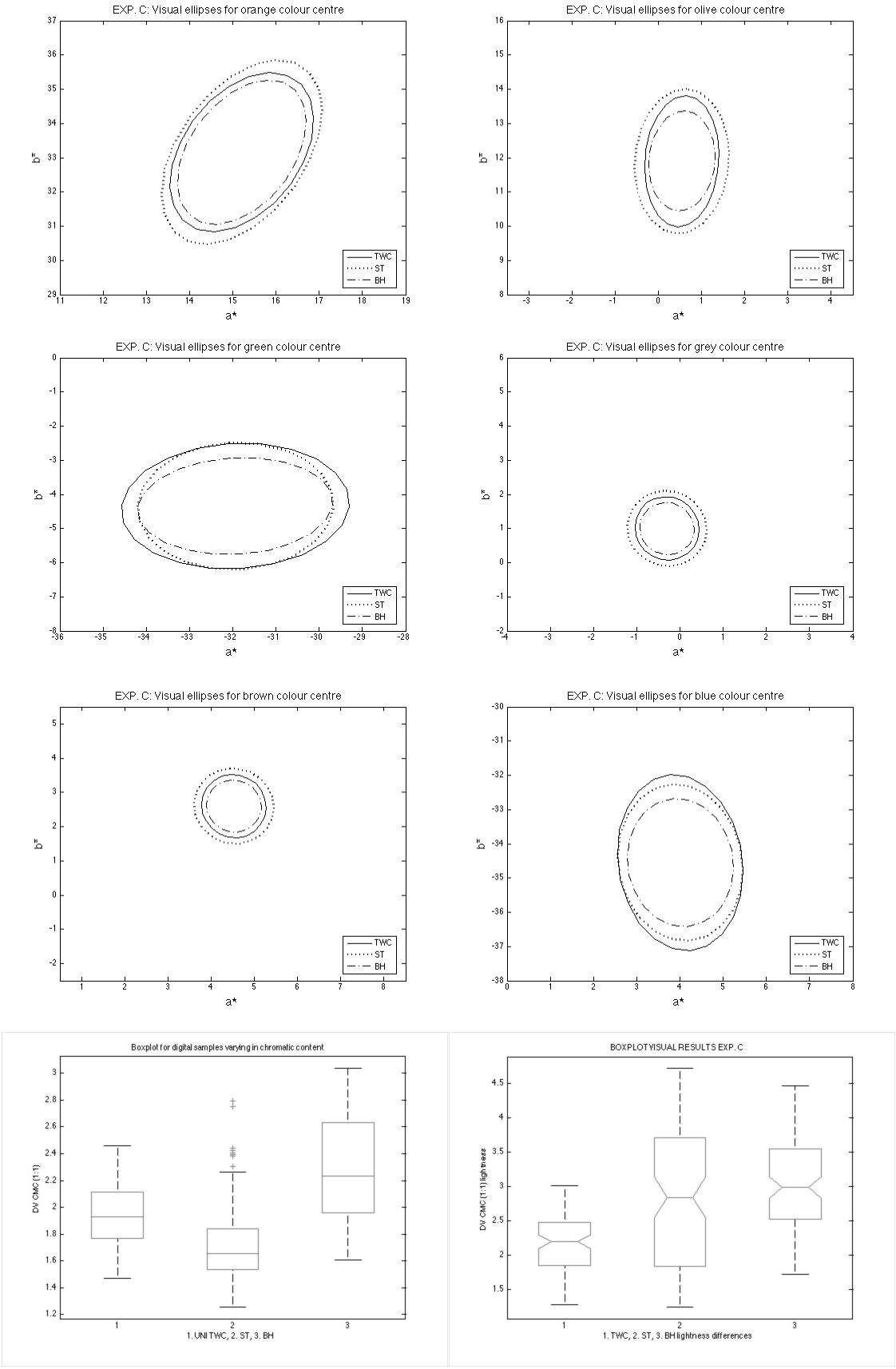

***Fig. 135 – 142*: Plots of ellipses from visual results for *Experiment C* and 'ΔV_{CMC}(1:1)' distributions for chromatic and lightness differences for uniform 'TWC', 'ST', and 'BH' sample pairs.**

6.8.4 Formula were tested and those results were used to determine which of the components of a colour difference formula were significant for improving the correlation between predicted and visual results for the 'ST' sample set observations. Altering the standard coordinates (mainly 'L^*' by a value of '- 1') for the $CIEDE_{2000}$ formula resulted in a 'F' – test value of '1.49' for a optimised formula (critical range for the test statistic '0.77' – '1.30'). Altering CMC's formula function 'S_L' resulted in significant prediction improvements; but, altering the standards colour coordinates 'L^*', 'a^*', and 'b^*' did not so. The optimised $CIEDE_{2000}$ and CMC formula became then of the form as mathematically described in *Equation 130 – 131*.

Eq. 130: digital $\Delta E_{ST,1} = 1.0359 \cdot \Delta E_{00} + 0.063$

Eq. 131: digital $\Delta E_{ST,2} = 1.0263 \cdot \Delta E_{CMC} + 0.00337$,

given parametric settings of 'ΔE_{00}(0.86:1.06:1.08)' and 'ΔE_{CMC}(0.47:0.95)' resulting in absolute mean residuals 'ΔE_{VAR}' units of '0.19' (STRESS '10.24') and '0.24' (STRESS '12.24').

6.8.5 The optimization process in this case revealled not much differences in the overall coefficients for *Equation 130* and *131* suggesting that parametric factors of approximately '0.5' for lightness and '1' for chroma weighting are suitable after optimization of the 'S_L' – function in the case of the CMC formula. However, also an overall multiplicator factor of '0.75' (*Experiment B*: '0.76', CMC(0.56:0.96), STRESS 19.91) was applied so to minimize the differences between visual and predicted results for digital 'ST' samples judged on screen.

6.9 Cross validation tests

6.9.1 All formulae during *Experiment C* were optimized while using all visual data obtained from observations with 'ST' sample pairs. Normally, a colour difference formula is designed from data obtained from a training set (using samples from a large population) and tested with different samples from the same population. This can determine the performance of a formula in testing mode but also estimate any error between training and testing performances. However, there were only data for six colour centres available for *Experiment C*. A colour difference model may introduce two issues in regards to optimization processes when using all available samples for training; (**1**) a formula may be biased towards a few data samples and sample type, and/or (**2**) that the processes of optimization parameter for any formula may overfit those available data (such as noise from incorrect data points), with the result of a decreasing predicting performance for data points that were not used for training.

6.9.2 A way to find an estimated error between training and testing performances for a small data set is described by the method of cross validation. One method in this sense is to test a formula on a sample set that was not used for training. And, this was done for each of the six colour centres that were available during *Experiment C*. Each colour centre was removed for testing the optimized formula, and the remaining five colour centres were used for training. The performance measure for each training and testing colour centre are given in STRESS values.

STRESS MEASURE	*ALL COLOURS TRAINED*	*MINUS ORANGE TRAINED*	*MINUS OLIVE TRAINED*	*MINUS GREEN TRAINED*	*MINUS GREY TRAINED*	*MINUS BROWN TRAINED*	*MINUS BLUE TRAINED*	*EACH COLOUR TESTED*
Orange	12.86	**test**	12.89	11.46	12.64	12.77	12.63	**16.53**
Olive	8.761	7.981	**test**	8.461	8.141	7.801	8.511	**9.731**
Green	14.54	13.31	14.53	**test**	14.02	14.51	14.72	**15.95**
Grey	12.37	12.31	12.31	11.88	**test**	12.08	11.99	**22.03**
Brown	10.27	10.09	9.301	10.84	9.211	**test**	10.61	**14.01**
Blue	14.37	14.59	14.31	15.05	13.98	14.01	**test**	**14.55**
MEAN	***12.21***	***12.46***	***12.17***	***12.27***	***13.33***	***14.31***	***12.17***	***15.47***

Table 53: **Performance comparison between training sets and testing sets (leave one out cross validation)**

6.9.3 It was evident, according to *Table 53,* that testing performances were less well performed compared to those performances that were obtained from training sets (as expected). The average STRESS value (for training all colour centres) increased from ’12.21’ (summation of individual colour centres) to ’15.47’ (the average from all tested colour centres), this is a difference of ‘3.26’ STRESS units. That value translates to an absolute error estimate between the training and testing performance of ‘0.07’ ‘ΔV_{CMC}(0.47:0.95)’ units (an overall experimental size factor of ‘0.76’ was applied), a change from an average absolute deviation value ‘0.26’ to ‘0.33’ between observed and predicted colour differences. Optimised ‘k_L’ and ‘k_C’ parametric factors are listed in *Table 144*, as STRESS values, ‘factor’ values, and as parameters for ‘S_L’ and ‘S_C’ weighting functions are.

FORMULA PARAMETER	*ALL COLOURS*	*MINUS ORANGE*	*MINUS OLIVE*	*MINUS GREEN*	*MINUS GREY*	*MINUS BROWN*	*MINUS BLUE*
	TRAIN SET	TRAIN SET	TRAIN SET	TRAIN SET	TRAIN SET	TRAIN SET	TRAIN SET
k_L	0.47	0.50	0.47	0.48	0.44	0.47	0.45
k_C	0.97	1.00	0.95	1.01	0.95	1.00	0.97
STRESS	**12.21**	**12.23**	**13.17**	**11.84**	**12.31**	**12.75**	**12.3**
Factor	**0.76**	**0.77**	**0.76**	**0.75**	**0.76**	**0.82**	**0.73**
S_L	1088059.91	1079331.25	1601794.92	413794.22	911539.02	1152383.17	6416749.51
	1099366.96	1114942.72	1628732.06	432052.69	943576.09	1042334.89	6411499.09
	0.511	0.511	0.511	0.511	0.511	0.511	0.511
S_C	0.1131	0.1425	0.1446	0.106	0.0302	0.0890	0.107
	0.0495	0.0768	0.0688	0.040	0.001	0.0279	0.0475
	0.5858	0.5616	0.5581	0.572	0.968	0.6623	0.5705

Table 54: **List of parameter for weighting functions and parametric factors, overall factor, and STRESS values for cross – validation test for digital ‘ST’ sample set used in *Experiment C*.**

6.9.4 Two major findings were observed *in Table 54* such as; (**1**) the parameters for the weighting function contained in ‘S_C’ did not change much while proceeding through the individual steps of the cross validation tests (no significant prediction performance gains while optimizing CMC’s ‘S_C’ function), and (**2**) the change in parameters for CMC’s ‘S_L’ function

was large as was a significant gain in prediction performances (approximately from '20' to '13' STRESS units). The prediction performance increase by optimizing CMC's 'S_H' function was in-significant. Furthermore, according to *Table 143*, a testing performance significantly decreased for grey colour difference samples, if those were not included in the training set (from approximately '12' to '20' STRESS units). This provided evidence for the fact to include grey sample pairs for designing and/or optimizing a colour difference formula. Optimisation of the $CIEDE_{2000}$ weighting functions 'S_L', 'S_C', and 'S_H' did not change contained parameters significantly as they also did not improve the prediction performances in the same sense. Optimising parametric factors for both formulae improved the prediction performances, significantly.

6.10 Statistical tests

6.10.1 It was of interest to determine statistically whether all three digital data sets were drawn form the same population. Generally, there are four assumptions that need to be matched so to determine what type of statistical test can be applied to those datasets[eee]. The residuals here were obtained as absolute differences between modelled (predicted) '2.4' '$\Delta V_{CMC}(1:1)$' and obtained visual data (average '0.46', '-0.003', and '0.584' for uniform 'TWC', 'BH', and 'ST' sample pairs) for chromatic differences. The null-hypothesis 'h_0' was given that all three samples were from continuous samples with equal medians. A Wilcoxon rank sum non-parametric test (similar to Mann-Whitney U-test) was applied to test between; (**1**) 'BH' and 'ST', (**2**) 'BH' and 'TWC', and (**3**) between uniform 'TWC' and 'ST' – residual data sets. The results of all tests were provided as 'p'– and 'H' values (either '0' or '1' where '1' rejects 'h_0' at a 5% level) as such; (**1**) 'p' equalled '8.82e-14' and 'H' equalled '1' (suggesting that there is a significant difference between visual results for 'BH' and 'ST' sample sets in chromatic content), (**2**) 'p' equalled '1.08e-12' and 'H' equalled '1', and (**3**) 'p' equalled '0.0084' and 'H' equalled '1'. A parametric test assuming normal distributed data ('ANOVA') in a similar sense provided 'p'- values for; (**1**) '1.51e-07' ('F' equal to '2.76e+13'), (**2**) '1.25e-07' ('F' equal to '4.14e+13), and (**3**) '1' ('F' equal to '-3.26e+13'). The same tests were applied to residuals (difference between modelled '2.4' '$\Delta V_{CMC}(1:1)$' units and resulting visual results) form sample pairs differing mainly in the lightness directions. The non-parametric test resulted in 'p' and 'H'- values for; (**1**) '0.3590' and '0' (no significant differences in the lightness direction for digital 'BH' and 'ST' sample pairs), (**2**) '1.94e-16' and '1', and (**3**) '8.57e-08' and '1'. Boxplots for the 'ST' dataset is also provided in *Figure 141* and *142*.

[eee] see page 115

6.11 Summary

. Twenty-one, nineteen, and eighteen observers judged three digital datasets with a modelled colour difference distance of '2.4 $\Delta E_{CMC}(1:1)$' units in the chromatic and/or lightness directions between standard and batch samples. The average '$\Delta V_{CMC}(1:1)$' value for each dataset was '2.09' ('1.94' and '2.17' for chromatic and lightness differences) for uniform digital 'TWC' samples, '2.47' ('1.77' and '2.82') for digital 'ST' samples, and '2.85' ('2.41' and '3.07') for digital 'BH' samples. Evidence was collected that different stitch types altered observer's colour difference perception, significantly. There was a clear difference in the results between chromatic and lightness perceptions. Edge content and texture was reduced in the image design for *Experiment C*. This fact resulted in smaller chromatic colour differences for 'BH' samples, when compared to *Experiment A – Part B*. Visual differences in the lightness direction was enhanced compared to chromatic differences (ratios for '$\Delta V_{CMC}(1:1)$' /'$\Delta E_{(CMC)}(1:1)$' of '1.33' and '1.50' for 'BH' and 'ST' sample pairs).

. A single needle lockstitch thread type is smaller in size when compared to a buttonhole thread stitch type; and, those modelled differences, if seen against a similar background, may spread and merge together, so that chromatic discrimination between similar colours were decreased. The size and texture content in 'BH' samples enhanced chromatic colour difference perception providing higher magnitudes when compared to 'ST' sample pairs. Colour difference discrimination between 'BH' and 'ST' samples resulted in 30% higher magnitudes for 'BH' samples. Lightness weighting 'k_L' for 'ST' samples (CMC raw-data) was optimized to approximately '0.5' compared to 0.70 for 'BH', and 0.80 for uniform 'TWC' samples.

. Significant improvement for all advanced colour difference formula was achieved when parametric factors were optimized. Further significant improvement was achieved for CMC's formula while optimizing its 'S_L' weighting function.

6.12 Conclusion

. A combined experiment including three different types of colour difference sample pairs with an average modelled colour distance of '2.4' '$\Delta E_{CMC}(1:1)$' units between standard and batches in various directions resulted in significant differences in observer's magnitude estimates. These findings were comparable with those results obtained from *Experiment A* and *B*. However, 'ST' sample types were only judged as digital samples on screen. Therefore, and for verification reasons, a reduced physical data set containing blue and grey 'ST', 'BH', and 'TWC' samples were used for *Experiment D* for verifying results from *Experiment A, B, and C*.

Chapter 7:

7.1 *Experiment D*: General considerations

7.1.1 Twenty-one observers participated in *Experiment D – Part A* judging physical colour difference pairs presented in a viewing cabinet. Thirteen female and eight male observers with an average age of '31' years, some with no and some with experience (mostly gained during the time of this project), conducted the Ishihara test at the beginning of *Experiment D – Part A* with no signs of any colour deficiencies in their colour vision.

7.1.2 Three types of sample sets were used; (**1**) a selection of single needle lockstitch samples ('ST'), (**2**) a selection of thread winding card samples ('TWC'), and (**3**) a selection of buttonhole stitch type samples ('BH'). Fourteen grey and twelve blue 'ST' sample pairs, ten grey and ten blue 'BH' samples, and ten grey and ten blue 'TWC' sample pairs were judged by each observer. Also, four samples for each 'TWC' and 'BH' set, and six samples for the 'ST' stitch type set, were presented twice to observers so to produce '24', '24', and '32' observations for each observer and direction. All sample pairs were presented in two directions in a way that the actual thread was either running along the North/South– ('NS') or East/West ('EW') direction from an observers's point of view. Altogether, '3360' observations were produced during *Experiment D – Part A*.

7.1.3 Samples were masked with a suitably tailor made mid grey paper card that was also used to cover the cabinet's floor and surrounding walls. The light source was of a fluorescent type make approaching artificial daylight with a correlated colour temperature of approximately 6000 Kelvin. The luminance was calculated while using a constant 'K_M' factor of '683.6' resulting in a luminance value of approximately 177 cd/m^2. Measurements, which were taken close to a sample's surface on the floor of the viewing cabinet, suggested an average illuminance of 1000 lux (Gossen Mastersix instrument and a flat diffuser attached to it for providing lux readings). All samples, which were used during *Experiment D – Part A*, were covered with a flat grey card. A hole, cut out with a scissor in the middle of the card, rectangular in size, having a side ratio similar to those from the grey scale device, which was used for scaling colour difference sample pairs used during *Experiment D – Part A*, provided a window for visually assessing, but also for measuring, a sample. All measurements for fabric samples (standards) were obtained from four different positions within the grey card's window as such taken close to the actual thread stitch type. Those measurements were averaged so to provide a robust instrumental colorimetric value for it. The same method was applied for 'TWC' samples in a viewing cabinet. The measurement instrument, a tele-spectroradiometer, was fixed on a tripod at the same position as the eyes of an observer were located when they were judging sample pairs in that viewing cabinet. The chromaticity varied little accross measurements for

most samples; but, lightness values varied significantly for some 'TWC' samples, thus mainly depending on the physical conditions of them.

7.2 Grey scale measurements

7.2.1 A grayscale method was introduced to observers so to help them scaling their colour difference perceptions from presented colour difference sample pairs. A 'nine'-step grey scale was measured before, between, and after completion of all experimental sessions for *Experiment D – Part A*. Those measurement results from that grey scale are listed in *Table 55*.

CMC(1:1)			CMC(1:1)		lightness	chroma	hue				CMC(1:1)
$\Delta L^*/lS_L$	$\Delta C^*_{ab}/cS_C$	$\Delta H^*_{ab}/cS_C$	ΔE_{CMC}	$\Delta E_{CMC}{}^2$	%	%	%	ΔE_{CMC}	ΔE_{CMC}	ΔE_{CMC}	ΔE_{CMC}
0.007	0.0010	0.000	**0.089**	0.008	86.803	12.482	0.714	0.077	0.011	0.000	**0.089**
1.019	0.2963	0.089	**1.185**	1.404	72.541	21.105	6.353	0.859	0.250	0.075	**1.184**
2.989	0.5181	0.004	**1.874**	3.511	85.128	14.757	0.114	1.595	0.276	0.002	**1.873**
6.188	0.5582	0.006	**2.599**	6.752	91.640	8.267	0.092	2.381	0.214	0.004	**2.598**
7.570	0.0925	0.064	**2.778**	7.727	97.973	1.197	0.828	2.723	0.033	0.023	**2.779**
7.564	0.1028	0.063	**2.780**	7.730	97.850	1.330	0.819	2.720	0.037	0.022	**2.780**
16.318	1.9619	0.013	**4.277**	18.29	89.205	10.724	0.070	3.815	0.453	0.003	**4.277**
32.901	0.8056	0.000	**5.806**	33.70	97.608	2.3900	0.001	5.667	0.138	0.000	**5.806**
74.155	1.0533	0.020	**8.674**	75.29	98.573	1.4001	0.026	8.549	0.121	0.002	**8.673**
148.73	0.2691	0.001	**12.212**	149.4	99.819	0.1805	0.000	12.190	0.022	0.000	**12.21**

***Table 55*: Transfer function for 'GRADE' - values to 'ΔV_{CMC}(1:1)' for *Experiment D – Part A* using physical samples.**

A smoothing spline function was then used to extrapolate data from visual GRADE ('1' – '5' in half steps) to visual colour difference values given in 'ΔV_{CMC}(1:1)' – units.

7.3 Inter- and Intra-observer variability

7.3.1 Observer performances amongst each other in terms of STRESS values are listed in *Table 56.* The average STRESS value for all twenty-one observers was '25.40' for all physical samples and both directions ('NS' equaled '25.87' and 'EW' equalled '24.94' STRESS units). The breakdown of grey and blue sample pairs into either 'NS'- or 'EW' direction did not reveal any significant deviations between them.

Experiment D – Part A (physical samples) *Inter-observer variability*						
Direction	EAST/WEST Buttonhole Grey	EAST/WEST SingleStitch Grey	EAST/WEST Thread WC Grey	EAST/WEST Buttonhole Blue	EAST/WEST SingleStitch Blue	EAST/WEST Thread WC Blue
STRESS	***23.69***	***21.82***	***20.02***	***25.89***	***32.36***	***31.41***
STD	6.44	4.30	7.53	5.71	8.35	6.26
MAX	34.63	30.88	27.40	36.13	44.63	48.66
MIN	14.96	14.42	11.02	15.30	14.47	23.32
Direction	NORTH/SOUTH Buttonhole Grey	NORTH/SOUTH SingleStitch Grey	NORTH/SOUTH Thread WC Grey	NORTH/SOUTH Buttonhole Blue	NORTH/SOUTH SingleStitch Blue	NORTH/SOUTH Thread WC Blue
STRESS	***23.56***	***25.85***	***24.52***	***23.64***	***24.46***	***27.58***
STD	7.42	9.49	8.02	5.76	7.63	6.78
MAX	39.33	44.95	41.59	33.80	39.73	41.82
MIN	12.90	11.86	11.15	11.69	11.39	15.09

***Table 56*: Inter-observer variations using STRESS units.**

Generally, it is evident from the values in *Table 56* that performance variations between individual observers was in fact large considering an average STRESS value of approximately '8' units. It was then of concern to determine how consistent observers were in respect to their judgements when they were presented with the same colour difference sample pairs. Either four or six randomly repeated sample pairs were presented to observers without letting them know that were actually judging those sample pairs twice. All observational judgments were then converted to '$\Delta V_{CMC}(1:1)$' units for each sample type, colour, and sample direction. The intra-observer variability calculations are described in *Equations 110ff*[fff]; all obtained average STRESS values are listed in *Table 57*.

Obs	*TWC EW Grey*	*TWC NS Grey*	*BH EW Grey*	*BH NS Grey*	*ST EW Grey*	*ST NS Grey*	*TWC EW Blue*	*TWC NS Blue*	*BH EW Blue*	*BH NS Blue*	*ST EW Blue*	*ST NS Blue*	*Mean*	*STD*	*SE M*
1	22.9	27.7	17.3	21.4	44.1	61.4	21.5	24.8	21.4	28.6	10.4	21.5	25.1	13.4	3.9
2	21.3	25.8	30.5	39.5	17.6	48.9	42.0	41.3	33.1	35.0	1.4	21.6	30.8	13.1	3.8
3	27.4	13.6	33.9	37.8	17.9	20.6	30.6	30.7	11.5	10.7	28.1	26.4	24.1	9.1	2.6
4	62.4	23.3	29.0	23.7	25.6	16.4	25.0	29.0	17.1	9.4	14.4	29.3	23.3	13.3	3.8
5	20.4	15.6	32.9	34.5	29.8	33.6	22.5	18.6	13.0	28.3	21.7	9.8	23.6	8.4	2.4
6	107	66.4	58.3	68.9	23.7	22.7	70.2	62.6	73.9	50.8	29.1	59.1	56.3	24.1	7.0
7	20.3	28.1	32.2	30.6	12.9	36.8	79.7	64.6	79.2	44.6	61.9	49.1	44.8	22.2	6.4
8	35.2	26.9	29.7	32.1	24.9	13.3	32.5	49.6	40.1	43.2	14.5	3.4	29.3	13.3	3.8
9	33.2	35.4	51.7	31.7	32.6	14.0	84.7	61.1	44.7	33.3	41.8	44.9	41.0	17.8	5.1
10	20.6	31.7	15.1	20.0	17.2	27.9	37.8	51.9	15.1	27.4	14.5	29.1	24.2	11.2	3.2
11	34.0	42.5	24.8	65.3	20.8	38.6	32.5	50.3	37.8	88.3	67.9	81.9	47.6	22.2	6.4
12	94.2	57.4	24.3	21.6	34.8	25.0	46.3	34.9	91.7	28.1	24.6	23.5	39.1	25.9	7.5
13	9.0	27.1	6.0	25.1	25.9	34.2	30.7	10.8	35.0	23.7	47.1	30.4	25.2	11.9	3.4
14	46.2	21.5	55.1	95.6	29.7	74.4	30.6	37.0	59.4	30.7	30.6	32.9	42.7	22.1	6.4
15	78.2	81.6	18.6	28.6	20.5	28.6	33.7	32.5	13.9	24.5	20.6	13.3	30.0	22.9	6.6
16	91.5	80.1	51.7	36.2	29.2	34.7	14.5	30.7	33.2	34.8	45.6	35.0	41.1	22.0	6.3
17	29.7	31.5	20.9	11.9	6.3	11.4	29.7	14.3	6.4	29.5	24.1	16.2	19.4	9.4	2.7
18	31.5	23.0	28.7	21.3	32.1	34.0	26.1	32.9	32.8	29.9	20.8	30.6	28.9	4.7	1.4
19	35.1	24.7	35.2	30.7	30.2	21.1	29.0	39.5	23.8	13.6	29.4	27.9	28.7	7.0	2.0
20	17.4	21.2	61.3	61.3	23.5	16.1	13.1	31.1	17.4	35.0	62.3	29.0	31.3	18.8	5.4
21	4.9	22.9	31.6	16.2	35.3	46.3	32.1	60.3	34.2	14.5	46.7	151.	34.0	37.9	10.9
	36.91	***31.6***	***32.2***	***33.0***	***25.6***	***29.3***	***33.6***	***38.6***	***32.1***	***29.6***	***30.3***	***30.5***	***31.9***	***16.1***	***4.67***

***Table 57*: Intra-observer variability for physical sample type 'TWC', 'BH', 'ST' in grey or blue colour and two directions for *Experiment D – Part A*.**

7.3.2 The variation of results for individual observers judging physical samples were high thus generating an average STRESS value of '16.18' units. Some observers had an average repeatability measure of '56'. The overall STRESS figure approached '32' (compared to an average value of '32' for an average observer with a standard deviation of '3.4' units) when compared to the average values for each individual sample group for four and six reapeated sample observations. Other research work provided similar figures (average around '30' units), but did not specify as such the physical state of the samples, which may be one reason for those high intra-observer figures.

[fff] see page 118

7.4. Measurement and visual results for two viewing directions

7.4.1 All sample types in *Experiment D - Part A* were presented to observers in two directions. It was of interest to determine whether a thread's running direction influenced observer's percecption of colour differences. A thread was not seen in isolation neither was a thread compared with a fabric sample while placed in a viewing cabinet just next to each other. A visual colour difference judgement might be therefore regarded as more meaningful in cases where a thread sample is seen in a real world scenario, for instance, (**1**) when seen combined with a fabric sample, and/or (**2**) seen as such in different running directions causing a change in reflective properties while changing any incident light upon them.

7.4.2 General practice in a day to day measurement assignment at Coats plc is to measure (**1**) a 'thread winding card' sample with a spectrophotometer (sphere design providing average diffuse illumination of the sample), and (**2**) measuring a fabric sample in the same way as a 'TWC' sample was measured. The differences caused by the direction of the samples presented to the spectrophotometer were insignificant with an average value of '0.15' '$\Delta E_{CMC}(2:1)$' units for both 'FA' and 'TWC' sample sets. A numerical colour difference is then calculated from both reflectance data using, for instance, the CMC(2:1) formula in combination with a CIE standard daylight source and standard observer. Here, directional and/or specular reflection is eliminated by the arrangement of a sphere and those applied lighting conditions inherent in the design of a spectrophotometer.

7.4.3 A question that arises is whether different instrumental colour diffference measurement methods can correlate well with those viewing conditions that were experienced when judging physical samples that were presented in a viewing cabinet. Also, it was of interest to determine whether those visual colour difference values are better correlated with instrumental results obtained from a (**1**) spectrophotometer, or (**2**) a tele-spectroradiometer as such being able to measure a sample in an an environment it is actually observed in. The samples were measured in both directions with a tele-spectroradiometer at the same position as they were presented to observers in a viewing cabinet (for each fabric sample 'FA' and associated 'TWC' sample). In additon, all samples were measured with a spectrophotometer (ultraviolet part of the light source excluded, 'SPIN' – any specular reflection part from the sample included -, while using the viewing cabinet's lightsource data for calculating CIE 'XYZ_{10}'- tristimulus values) and compared with corresponding visual colour difference data for both directions. The directional influence on measurement data for samples in the viewing cabinet ('ΔL^*', 'ΔC^*_{ab}', and 'ΔH^*_{ab}'), and the directional influences on visual colour difference perceptions in '$\Delta V_{CMC}(1:1)$' units, are listed in *Table 58* and *59*.

Directional difference measurements obtained from a tele-spectroradiometer in a viewing cabinet						
Difference Measurement EW / NS	GREY Buttonhole CMC(1:1)	GREY SingleStitch CMC(1:1)	GREY Thread WC CMC(1:1)	BLUE Buttonhole CMC(1:1)	BLUE SingleStitch CMC(1:1)	BLUE Thread WC CMC(1:1)
Mean	**2.464**	**2.427**	**2.440**	**1.334**	**1.245**	**1.375**
STD	0.316	0.331	0.511	0.280	0.234	0.402
ΔL^*	***0.867**	***0.397**	***0.069**	***-0.422**	***-0.249**	***-0.007**
STD	0.217	0.741	0.590	0.315	0.380	0.613
ΔC^*_{ab}	**1.498**	**1.438**	**1.527**	**-1.453**	**-1.438**	**-1.504**
STD	0.461	0.415	0.533	0.748	0.619	0.628
ΔH^*_{ab}	**-1.020**	**-1.058**	**-1.028**	**0.910**	**0.859**	**0.858**
STD	0.395	0.422	0.437	0.314	0.248	0.279

***Table 58*: Directional influence on measurement results.**

7.4.4 Measurements of samples obtained in a viewing cabinet with a tele-sprectradiometer for both directions resulted mainly in chroma and hue changes. Lightness difference results were less robust mainly caused by the difficulty to find similar lightness magnitudes across a 'TWC' sample. Generally, the average colour difference values obtained for all samples in a viewing cabinet for both directions were '2.45' 'ΔE_{CMC}(1:1)' and '1.32' 'ΔE_{CMC}(1:1)' units. A parametric factor (more specfically as a difference caused by the orientation of a sample pair) can be determined by the devision of the ratios ('ΔV_{VAR}'/ 'ΔE_{VAR}') for each each pair and both directions ('EW'/'NS'). The sum of all indivdual results for both directions divided by the number of sample pairs provided a factor that describes an average directional parametric effect. Visual data obtained from the 'NS' - direction appeared larger than sample pairs judged with a thread running along the 'EW' - direction. On average, colour differences were perceived '0.74' 'ΔV_{CMC}(1:1)' units larger than colour differences obtained from the other direction. Especially, grey 'single needle lockstitch' type samples were perceived twice as large as all other samples. However, and if compared with instrumental results, those magnitudes were redcuced to about a half, or a third, in magnitude in regards to blue and grey instrumental differences.

Visual differences for physical samples 'EW' / 'NS' (Experiment D - Part A)						
	GREY Buttonhole CMC (1:1)	*GREY SingleStitch CMC (1:1)*	*GREY Thread WC CMC (1:1)*	*BLUE Buttonhole CMC (1:1)*	*BLUE SingleStitch CMC (1:1)*	*BLUE Thread WC CMC (1:1)*
No. 1	0.51	1.06	0.52	0.18	0.51	1.01
No. 2	0.21	1.20	0.56	1.04	0.70	0.16
No. 3	0.76	1.18	0.09	0.56	0.84	-0.04
No. 4	0.67	1.45	0.08	0.57	0.49	-0.15
No. 5	0.81	1.25	0.25	1.06	0.41	1.52
No. 6	0.43	1.28	0.61	0.22	0.46	0.96
No. 7	1.09	1.53	0.67	0.58	1.19	0.05
No. 8	0.80	1.26	0.77	0.20	0.94	0.89
No. 9	0.70	1.61	0.29	0.55	0.52	0.87
No. 10	0.65	1.70	-0.08	0.82	1.13	1.31
No. 11		1.37			0.61	
No. 12		1.18			1.03	
No. 13		2.19				
		1.57				
AVERAGE	**0.66**	**1.42**	**0.37**	**0.58**	**0.73**	**0.66**
STD	0.24	0.29	0.29	0.32	0.28	0.60

***Table 59*: Differences in 'ΔV_{CMC}(1:1)' results for both directions for physical samples (Note: Fabric standards for 'BH', 'ST' samples were visually almost identical, the 'TWC' standard was kept in the same direction for both visual judgements.**

7.4.5 The results for the observations of physical samples in the viewing cabinet are listed in *Table 60* so to compare between visual data obtained from two directions; (**1**) 'NS' and (**2**) 'EW' with (**3**) calculated instrumental colour differences in (**3a**) a viewing cabinet and (**3b**) obtained from a spectrophotometer in '$\Delta E_{CMC}(1:1)$' units. Average '$\Delta V_{CMC}(1:1)$' and '$\Delta E_{CMC}(1:1)$' units refer to average visual instrumental data. A 'mean residual' value refers here to an average sum of squared differences value between '$\Delta V_{CMC}(1:1)$' and '$\Delta E_{CMC}(1:1)$' units for all paired sample. The values listed in *Table 60* suggested directional differences between sample presentations. *Experiment C* revealled smaller visual results for 'ST' sample pairs when compared with 'BH' samples pairs for the same numerical colour differences. Both measurement methods (either obtained from a 'TSR' or spectrophotometer) suggested that all blue samples were judged on average smaller in magnitude when compared with numerical values calculated for the same samples set. Visual and instrumental grey 'ST' samples were similar in visual magnitude value mainly caused by larger values in the lightness direction. Also, physical 'BH' sample pairs were judged larger than those visual results obtained from 'ST' sample pairs, however and foremost considered here as a first approximation. Especially, spectrophotometric measurements seemed to be more consistant with the results that were obtained from *Experiment A, B, and C*.

		TSR/ CABINET		*TSR/ CABINET*		*SPECTROPHOTOMETER*		*SPECTROPHOTOMETER*	
Buttonhole (BH)		**G EW**	**B EW**	**G NS**	**B NS**	**G EW**	**B EW**	**G NS**	**B NS**
Mean	CMC (1:1)	1.13	0.89	1.22	0.94	0.91	0.85	1.16	1.18
Mean ΔV	CMC (1:1)	2.81	2.64	3.46	3.29	2.81	2.64	3.46	3.29
Mean ΔE	CMC (1:1)	1.67	2.36	2.60	2.68	2.02	2.40	2.58	2.60
BH	***STRESS***	***15.77***	***42.64***	***36.26***	***25.82***	***28.75***	***34.51***	***34.81***	***35.41***
SINGLE STITCH (ST)		**G EW**	**B EW**	**G NS**	**B NS**	**G EW**	**B EW**	**G NS**	**B NS**
Mean	CMC (1:1)	0.37	0.74	0.74	0.51	0.63	0.77	1.24	0.55
Mean ΔV	CMC (1:1)	1.96	1.29	3.29	2.27	1.96	1.29	3.29	2.27
Mean ΔE	CMC (1:1)	1.96	2.00	2.61	2.16	2.00	2.00	2.55	2.34
ST	***STRESS***	***21.74***	***37.76***	***31.01***	***25.42***	***38.42***	***29.79***	***33.82***	***24.48***
THREAD WINDING		**G EW**	**B EW**	**G NS**	**B NS**	**G EW**	**B EW**	**G NS**	**B NS**
Mean	CMC (1:1)	0.99	0.69	0.73	0.46	***0.42***	***0.47***	0.54	0.32
Mean ΔV	CMC (1:1)	2.13	1.94	2.67	2.30	***2.13***	***1.94***	2.67	2.30
Mean ΔE	CMC (1:1)	2.18	2.29	2.08	1.87	***1.96***	***2.06***	2.36	2.17
TWC	***STRESS***	***36.38***	***27.81***	***30.67***	***15.37***	***23.45***	***24.11***	***24.32***	***21.89***

Table 60*: Visual and measurement results for CMC's formula for physical 'TWC', 'BH', and 'ST' sample types for the 'NS' and 'EW" direction, and two types of mesaurement instruments used in *Experiment D – Part A.

7.4.6 Visual results for TWC' sample pairs and their associated calculated 'ΔE_{CMC}' values from spectrophotometric measurements revealed almost similar average values. This was confirmed by the results of lower residual values when compared to 'BH' and 'ST' sample observations. It is vital to have clean and well maintained physical samples placed thouroughly in a viewing cabinet since any directional illumination influence and/or imperfection within a sample can alter those measurement results, significantly. To this extent, more than it might be the case for measurements obtained from sphere diffused operating spectrophotometers. Results obtained in 'NS' direction enlarged visual colour differences and as such also to the overall ratios between visual and instrumental measurements. A thread seen in the 'EW' direction correlated better

with measurements from a spectrophotometer. Also, it was evident that CMC's formula performs well for 'TWC' colour difference samples, but decreased in prediction performances for the 'BH' and 'ST' sample set. The results for physical samples in *Table 60* suggested that 'BH' samples were judged with a larger colour difference magnitude when compared to 'TWC' sample pairs (regarded as a reference condition when compared with other sample sets). The 'ST' samples pairs provided smallest magnitudes once they were judged in 'East/West' direction in a viewing cabinet and, importantly, correlating well with those results for 'ST' sample sets that were judged on screen as in *Experiment A – Part B* and *Experiment B* .

7.5 Formula performances

7.5.1 Various formulae were then optimized so to predict visual data obtained from physical samples judged in a viewing cabinet in *Experiment D – Part A*. Optimization was achieved by minimising STRESS units by varing parametric factors in a formula, as such mainly weighting factors 'k_L' and 'k_C'. Also, a size factor (overall sensitivity) was introduced so to minimize the average value of the sum of the square root of individual difference between '$\Delta V_{CMC}(1:1)$' and 'ΔE_{VAR}' values. A further breakdown into chromatic and lightness directions and optimised factors for each of them can be found in *Appendices A*. Those results that were obtained from physical samples showed that $CIEDE_{2000}$, $CIECAM_{02}$, OSA_{GP}, DIN_{99c}, and especially CMC's formula performed very well in predicting colour differences for 'TWC' colour difference sample pairs. This was the case for measurements with a spectrophotometer (diffuse illumination of the samples) and viewing conditions in 'EW' – directions ('9.62' and '9.67' for the grey and blue physical 'TWC' sample set providing average residuals of '0.23' and '0.21' '$\Delta E_{CMC}(2.05:1.30)$' units). A 'TWC' sample viewed in East/West – directions did not contain visible specular reflected light and, therefore, matched those measurement conditions well. The only difference that needed to be adjusted was an overall factor so to adjust visible with instrumental obtained colour differences (average factor of '1.25'). The performance for 'BH' and 'ST' samples in 'EW' direction for CMC's formula showed similarities for either tele-spectroradiometer measurements or those obtained from a spectrophotometer.

7.5.2 However, a difference between both measurements methods were indicated for samples in which a thread run along the 'North/South' – direction from a viewer's point of view. That direction added specular components to the reflected light thus changing the appearance of the colour especially in the lightness direction that was reaching the viewer's eye. Those effects to the observers were generally stronger for 'BH' and grey samples. Instrumental measurements from a tele-spectroradiometer for physical 'ST' samples in North/South provided better correlation with visual results than a spectrophotometer can possibly measure (diffuse average lighting). The results are listed in *Tables 61*, *62*, and *63*.

EXP. D-PART A	*Telespectrophotometer + Viewing Cabinet/Visual*				*Spectrophotometer/Visual Data*			
Buttonhole (BH)	*DV East/West Thread*		*DV North/South*		*DV East/West*		*DV North/South*	
$CIEDE_{2000}$	**GREY EW**	**BLUE EW**	**GREY NS**	**BLUE NS**	**GREY EW**	**BLUE EW**	**GREY NS**	**BLUE NS**
k_L BH	2.07	1.43	6.49	1.03	1.73	1.07	2.03	1.10
k_C BH	1.65	0.94	1.55	0.79	0.75	0.98	0.67	0.86
k_H BH	1.00	1.00	1.00	1.00	1.00	1.00	1.00	1.00
Factor	2.61	1.43	2.03	1.08	1.73	1.19	2.23	1.38
Mean Residual	0.44	0.51	0.50	0.47	0.32	0.51	0.45	0.73
STRESS	***17.29***	***20.28***	***15.26***	***15.68***	***12.86***	***20.01***	***14.06***	***23.84***
$CIECAM_{02}$								
BH	**GREY EW**	**BLUE EW**	**GREY NS**	**BLUE NS**	**GREY EW**	**BLUE EW**	**GREY NS**	**BLUE NS**
k_L BH	1.37	1.00	2.03	0.80	2.56	0.85	3.10	0.68
STRESS	***17.73***	***23.82***	***17.27***	***22.61***	***27.03***	***31.19***	***25.58***	***25.14***
$CIECAM_{02}$ UNIVERSIAL								
BH	**GREY EW**	**BLUE EW**	**GREY NS**	**BLUE NS**	**GREY EW**	**BLUE EW**	**GREY NS**	**BLUE NS**
k_L BH	3.56	4.83	13.83	4.07	5.40	2.83	6.81	3.05
Factor	5.67	4.50	5.63	3.59	4.32	2.89	5.98	3.48
Mean Residual	0.52	0.61	0.46	0.57	0.57	0.58	0.57	0.60
STRESS	***16.92***	***23.59***	***11.66***	***22.61***	***22.53***	***22.81***	***23.37***	***16.63***
GP OSA								
BH	**GREY EW**	**BLUE EW**	**GREY NS**	**BLUE NS**	**GREY EW**	**BLUE EW**	**GREY NS**	**BLUE NS**
k_L BH	5.77	1.33	1.57	1.05	2.04	1.00	2.08	0.99
k_C BH	1.06	1.00	1.24	0.85	1.82	0.96	5.41	0.82
k_H BH	1.00	1.00	1.00	1.00	1.00	1.00	1.00	1.00
Factor	1.57	0.90	1.38	0.72	1.36	0.70	2.19	0.80
Mean Residual	0.47	0.42	0.45	0.35	0.50	0.32	0.44	0.38
STRESS	***19.08***	***21.83***	***17.93***	***15.13***	***14.26***	***15.88***	***17.69***	***16.04***
CMC								
BH	**GREY EW**	**BLUE EW**	**GREY NS**	**BLUE NS**	**GREY EW**	**BLUE EW**	**GREY NS**	**BLUE NS**
k_L BH	1.86	2.68	3.00	2.02	2.11	2.01	3.94	2.51
k_C BH	0.48	1.54	1.76	0.41	0.37	1.62	2.22	1.10
Factor BH	1.00	1.76	2.13	1.08	1.20	1.38	2.93	1.68
Mean Residual	0.25	0.43	0.76	0.42	0.34	0.56	0.90	0.62
STRESS	***10.76***	***20.58***	***19.40***	***13.30***	***14.90***	***26.01***	***26.36***	***28.60***
DIN_{99c}								
BH	**GREY EW**	**BLUE EW**	**GREY NS**	**BLUE NS**	**GREY EW**	**BLUE EW**	**GREY NS**	**BLUE NS**
k_L BH	1.18	1.83	1.58	1.18	0.73	1.96	0.94	2.67
k_C BH	0.95	0.83	0.50	0.70	1.16	1.27	1.29	1.67
Factor	1.63	1.27	0.82	0.98	1.56	1.61	2.33	1.80
Mean Residual	0.48	0.60	0.70	0.64	0.51	0.53	0.61	1.13
STRESS	***16.34***	***21.94***	***19.80***	***19.18***	***17.91***	***18.47***	***17.20***	***15.23***

***Table 61*: Optimised physical 'BH' sample set for various formulae.**

EXP. D-PART A	*Telespectrophotometer + Viewing Cabinet/Visual*				*Spectrophotometer/Visual*			
Single Stitch (ST)	*DV East/West*		*DV North/South*		*DV East/West*		*DV North/South*	
$CIEDE_{2000}$	**GREY EW**	**BLUE EW**	**GREY NS**	**BLUE NS**	**GREY EW**	**BLUE EW**	**GREY NS**	**BLUE NS**
k_L ST	4.15	0.92	2.00	0.99	1.75	0.69	1.91	0.79
k_C ST	1.84	0.72	0.75	1.02	0.66	0.65	0.79	0.88
k_H ST	1.00	1.00	1.00	1.00	1.00	1.00	1.00	1.00
Factor	1.67	0.67	1.29	0.96	0.81	0.59	1.47	1.07
Mean Residual	0.38	0.37	0.61	0.52	0.27	0.32	0.70	0.56
STRESS	***19.50***	***27.49***	***23.29***	***25.42***	***26.70***	***24.50***	***25.31***	***27.18***
$CIECAM_{02}$ (+kl factor) **ST**	**GREY EW**	**BLUE EW**	**GREY NS**	**BLUE NS**	**GREY EW**	**BLUE EW**	**GREY NS**	**BLUE NS**
k_L ST	1.60	1.00	2.83	0.55	2.69	0.71	2.67	0.74
STRESS	***20.92***	***31.02***	***22.74***	***27.01***	***30.74***	***32.10***	***32.31***	***32.02***
$CIECAM_{02}$ UNIVERSAL **ST**	**GREY EW**	**BLUE EW**	**GREY NS**	**BLUE NS**	**GREY EW**	**BLUE EW**	**GREY NS**	**BLUE NS**
k_L ST	4.25	3.41	7.00	2.72	4.42	2.72	4.43	2.60
Factor	3.44	1.83	4.59	2.33	3.47	1.80	5.95	2.86
Mean Residual	0.45	0.46	0.85	0.64	0.39	0.35	1.31	0.65
STRESS	***20.91***	***31.31***	***21.09***	***26.48***	***29.82***	***32.91***	***31.78***	***33.67***
GP OSA **ST**	**GREY EW**	**BLUE EW**	**GREY NS**	**BLUE NS**	**GREY EW**	**BLUE EW**	**GREY NS**	**BLUE NS**
k_L ST	1.86	1.10	2.24	1.61	1.81	0.78	2.09	0.80
k_C ST	0.60	0.76	0.88	1.44	0.88	0.72	0.97	0.88
k_H ST	1.00	1.00	1.00	1.00	1.00	1.00	1.00	1.00
Factor	0.67	0.46	1.04	0.77	0.83	0.42	1.33	0.67
Mean Residual	0.29	0.35	0.49	0.42	0.26	0.26	0.65	0.45
STRESS	***18.43***	***32.31***	***23.29***	***27.28***	***33.37***	***23.73***	***33.19***	***27.63***
CMC(best) **ST**	**GREY EW**	**BLUE EW**	**GREY NS**	**BLUE NS**	**GREY EW**	**BLUE EW**	**GREY NS**	**BLUE NS**
*k*L ST	3.28	2.05	2.15	1.61	2.14	1.50	2.08	1.17
k_C ST	1.59	1.54	1.05	1.17	1.07	1.05	1.18	1.03
Factor ST	1.58	0.83	1.41	0.92	1.18	0.72	1.87	0.94
Mean Residual	0.36	0.41	0.99	0.56	0.27	0.33	0.85	0.61
STRESS	***13.87***	***27.57***	***18.51***	***25.04***	***29.12***	***22.20***	***28.64***	***27.02***
DIN_{99c} **ST**	**GREY EW**	**BLUE EW**	**GREY NS**	**BLUE NS**	**GREY EW**	**BLUE EW**	**GREY NS**	**BLUE NS**
k_L ST	2.13	1.70	1.35	1.06	1.60	2.42	1.71	2.34
k_C ST	0.87	1.43	0.62	1.00	1.51	1.88	1.58	2.30
Factor	1.01	0.97	0.88	0.84	1.33	1.37	2.31	1.80
Mean Residual	0.53	0.44	0.74	0.62	0.36	0.50	1.07	0.95
STRESS	***23.84***	***27.27***	***23.80***	***25.83***	***29.31***	***27.49***	***30.52***	***32.16***

***Table 62*: Optimised physical 'ST' sample set for various formulae.**

EXP. D-PART A	*Telespectrophotometer + Viewing Cabinet/Visual*				*Spectrophotometer/Visual Data*			
Thread Winding Card (TWC)	*DV East/West*		*DV North/South*		*DV East/West*		*DV North/South*	
$CIEDE_{2000}$	**GREY EW**	**BLUE EW**	**GREY NS**	**BLUE NS**	**GREY EW**	**BLUE EW**	**GREY NS**	**BLUE NS**
k_L TWC	1.23	1.56	2.35	0.77	2.30	1.12	1.94	1.00
k_C TWC	0.68	0.39	1.13	0.93	1.35	1.22	1.17	2.05
k_H TWC	1.00	1.00	1.00	1.00	1.00	1.00	1.00	1.00
Factor	0.71	0.64	1.48	1.06	1.48	1.15	1.52	1.46
Mean Residual	0.47	0.54	0.39	0.52	0.21	0.26	0.42	0.68
STRESS	***22.27***	***29.00***	***17.36***	***23.86***	***11.07***	***13.18***	***18.61***	***26.78***
$CIECAM_{02}$ ***(+kl factor)***								
TWC	**GREY EW**	**BLUE EW**	**GREY NS**	**BLUE NS**	**GREY EW**	**BLUE EW**	**GREY NS**	**BLUE NS**
k_L TWC	1.00	1.00	2.91	0.40	2.71	0.78	2.37	0.69
STRESS	***30.10***	***36.02***	***17.85***	***28.54***	***10.89***	***18.08***	***16.94***	***28.74***
$CIECAM_{02}$ ***UNIVERSAL**								
TWC	**GREY EW**	**BLUE EW**	**GREY NS**	**BLUE NS**	**GREY EW**	**BLUE EW**	**GREY NS**	**BLUE NS**
k_L TWC	6.36	3.77	7.52	2.05	7.45	3.44	6.04	3.07
Factor	3.08	2.39	5.25	2.80	4.90	3.19	5.11	4.01
Mean Residual	0.74	0.70	0.52	0.74	0.31	0.28	0.50	0.82
STRESS	***32.60***	***31.51***	***17.08***	***28.26***	***11.49***	***12.63***	***16.30***	***27.06***
GP OSA								
TWC	**GREY EW**	**BLUE EW**	**GREY NS**	**BLUE NS**	**GREY EW**	**BLUE EW**	**GREY NS**	**BLUE NS**
k_L TWC	3.45	1.72	2.37	1.11	2.22	1.14	1.79	0.95
k_C TWC	2.77	0.37	1.39	1.22	1.63	1.36	1.46	1.58
k_H TWC	1.00	1.00	1.00	1.00	1.00	1.00	1.00	1.00
Factor	1.46	0.46	1.26	0.96	1.21	0.78	1.21	0.89
Mean Residual	0.27	0.42	0.40	0.54	0.16	0.23	0.33	0.53
STRESS	***15.07***	***29.85***	***20.10***	***27.72***	***11.02***	***14.49***	***18.56***	***27.36***
CMC(best)								
TWC	**GREY EW**	**BLUE EW**	**GREY NS**	**BLUE NS**	**GREY EW**	**BLUE EW**	**GREY NS**	**BLUE NS**
*k*L TWC	1.82	2.83	2.38	1.45	2.01	2.13	1.61	1.93
k_C TWC	1.12	0.53	1.54	0.92	1.62	1.07	1.54	1.36
Factor	1.08	0.82	1.77	1.21	1.66	1.20	1.71	1.52
Mean Residual	0.83	0.39	0.50	0.60	0.23	0.21	0.44	0.60
STRESS	***21.39***	***19.26***	***17.61***	***24.80***	***9.62***	***9.67***	***16.18***	***21.53***
DIN_{99c}								
TWC	**GREY EW**	**BLUE EW**	**GREY NS**	**BLUE NS**	**GREY EW**	**BLUE EW**	**GREY NS**	**BLUE NS**
k_L TWC	2.18	1.23	1.31	0.96	2.10	2.61	2.83	2.91
k_C TWC	0.88	0.75	0.63	0.84	0.76	1.27	1.15	1.83
Factor	0.96	0.91	0.93	1.06	1.09	1.66	1.80	1.80
Mean Residual	0.80	0.58	0.56	0.58	0.30	0.32	0.43	0.97
STRESS	***30.21***	***29.33***	***19.99***	***24.31***	***12.19***	***14.42***	***16.93***	***18.18***

***Table 63*: Optimised physical 'TWC' sample set for various formulae.**

7.6 Analysis of results for physical samples

7.6.1 Visual results from three limited data sets according to physical 'TWC', 'BH', and 'ST' colour difference sample pairs were then contrasted with each other in terms of scatter plots between 'ΔV_{CMC}(1:1)' against 'ΔE_{CMC}(*opt.*:1)' units. Sample pairs differing only in the lightness direction ('ΔL^*' > '0.9') were excluded and analysed, separately. Here, it was of interest to determine whether results from psychophysical assessments between different sample types differed in magnitude as results obtained during *Experiment A*, *B*, and *C* suggested. Especially, from a Coats plc business point of view, it was of interest to determine whether 'ST' samples were judged with smaller magnitudes, when compared to instrumental obtained colour differences calculated in accordance to generally accepted standards.

7.6.2 A parametric factor, for the use in the textile industry for the prediction of colour differences, in the lightness direction is generally set to a value of '2'. The results so far suggested that, for instance, the CMC formula performed best for 'TWC' sample pairs. Different factors were applied so to minimise the differences between visual and predicted results. Assessments of 'TWC' samples should ideally result in a ratio of '1' for contrasting '$\Delta V/\Delta E$' data for paired samples. Only the the 'k_L' factor for the CMC and CIEDE2000 formula in this graphical comparison was optimised for contrasting three data sets (as such to adjust for the remaining lightness components in all hue and chromatic difference sample pairs). Also, an overall scaling factor was applied so to minimise the difference for visual and predicted data for the 'TWC' data set. The comparison between data sets were applied with those settings for samples judged in 'EW' and in the 'NS' direction for both measurement methods (spectro- and tele-spectroradiometer) for physical samples judged in a viewing cabinet.

7.6.3 The results are presented in *Figures 143 – 150* for further considerations. The parametric 'k_L' factor and optimised overall sensitivity factor for physical samples applied to various conditions are listed in *Table 64*, respectively. The ''l' or 'k_L' factors here for physical 'TWC' sample pairs were close to a recommended value of '2' that is suggested for assessing colour differences in the textile industry when weighted against parametric factor 'k_C' or 'c', respectively. What is of interest here is the overall sensitivity (or size factor) for 'ST' and 'BH' sample pairs compared to a reference 'TWC' sample set.

Experiment D - Part A		*Spectrophotometer 7000A*		*Tele-spectroradiometer CS1000*	
		Parametric	*overall*	*parametric*	*overall*
Formula	Direction	k_L – factor	factor	'k_L' - factor	factor
CMC	'EW'	1.88	1.18	1.84	1.06
$CIEDE_{2000}$	'EW'	1.71	1.23	2.09	1.24
CMC	'NS'			1.80	1.14

***Table 64*: Parametric factor and overall sensitivity setting for physical 'TWC' samples for comparing physical 'TWC', 'BH', and 'ST' sample sets obtained from psychophysical assessment during *Experiment D – Part A*.**

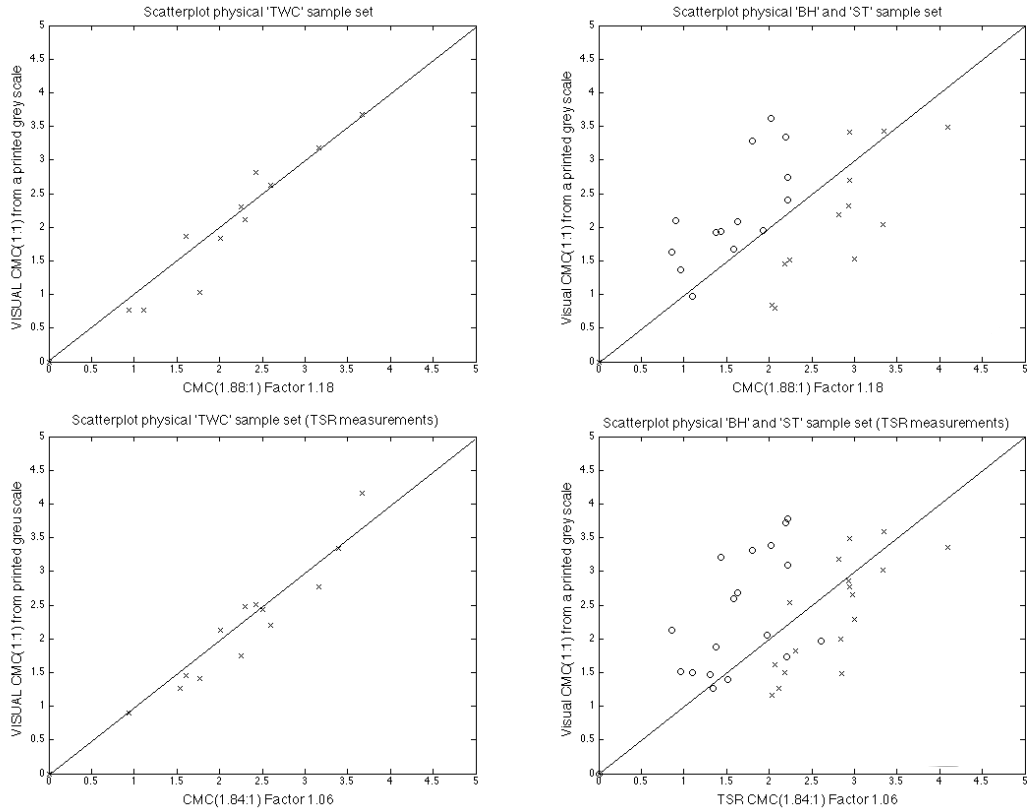

***Figure 143 – 146*: CMC's formula scatter-plot comparison for physical 'TWC' samples pairs on the left, 'BH'('o') and 'ST'('x') on the right side; top row for spectrophotometric- and bottom row for tele-spectroradiometric measurements.**

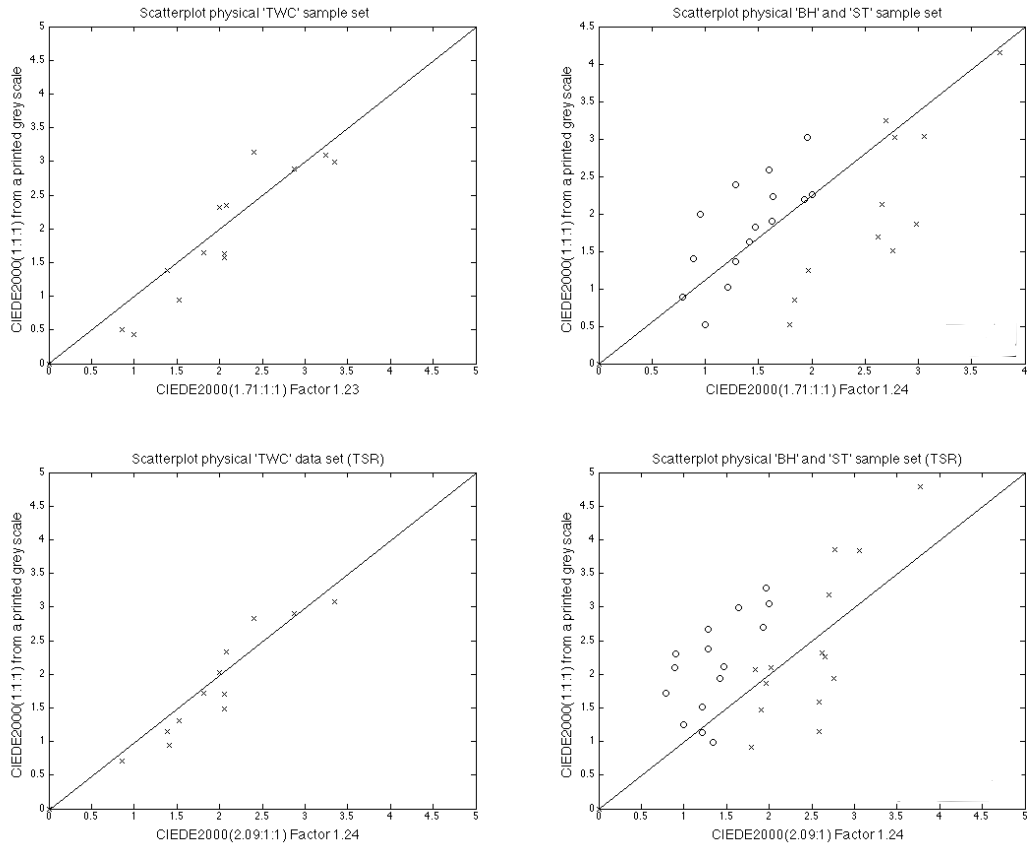

***Figure 147 – 150*: $CIEDE_{2000}$ formula scatter-plot comparison for physical 'TWC' on the left, 'BH'('o') and 'ST'('x') samples pairs on the rigth side; top row for spectrophotometric- and bottom row for tele-spectroradiometric measurements.**

7.6.4 It was evident that observations obtained from different thread type samples altered the magnitude of visual colour differences. The setting was optimised for 'TWC' samples (only 'k_L') and compared with the locations of 'BH' and 'ST' samples in the diagram. The individual plots refer to a comparison of '$\Delta V_{CMC}(1{:}1)$' against paired '$\Delta E_{VAR}(l_{opt}{:}1)$' values for each sample pair. Those results correlated well with the results that were obtained from *Experiment A*, *B*, and *C*. However, this was only valid for assessment of physical samples in a viewing cabinet presented in the 'East/West' – thread running direction. For comparison, those contrasted sample pair comparisons are also listed in *Figure 151* and *152* for CMC's formula for samples containing a stitched thread running in the 'North/South'-direction measured with a tele-spectroradiometer in a viewing cabinet ('FA' and associated 'TWC' – samples).

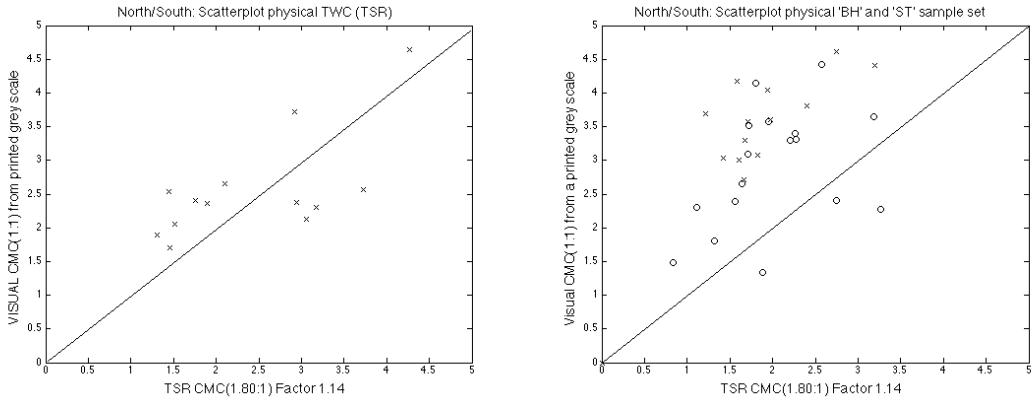

***Figure 151 – 152*: CMC's formula scatter-plot comparison for physical 'TWC' samples pairs on the left, 'BH'('o') and 'ST'('x') on the right side seen in North/South direction; top row for spectrophotometric- and bottom row for tele-spectroradiometric measurements.**

7.6.5 The results provided evidence that both sample types were judged larger in 'NS' – direction when compared to instrumental measurements. Although, all presented samples in a viewing cabinet were illuminated with diffused light, there was a significant alteration in the amount and direction of the reflected light from the samples (see *Table 58*[ggg]). Larger visual results here suggested that light was reflected in a specular manner opposed to light reflected from 'BH' and 'ST' sample pairs presented in the 'EW' – direction (see *Table 59*[hhh]). This may be explained by the technical aspect of how a thread is stitched into a fabric sample (on top of a fabric sample and knitted at both ends so to change the level of the thread upon a fabric) and, as a result, how incident light is reflected from a thread. This is not an added parameter in a spectrophotometric measurement method (insignificant directional differences were recorded

---

ggg see page 233

hhh see page 233

for ‘TWC’ and fabric ‘FA’ samples) when a thread winding card and a fabric sample are measured using a fairly large aperture size. However, a change in the directional presentation proofed to be a significant parameter to the observer’s eye. The highest magnitude differences for ‘EW’ and ‘NS’ – directional observations were recorded for ‘ST’ sample pairs, especially for grey coloured samples.

7.7 Digital camera samples

7.7.1 So far, digital colour difference samples used for assessments during *Experiment A – Part B*, *Experiment B*, and *Experiment C* were designed from synthesised (scanned master texture) ‘TWC’, ‘BH’, and ‘ST’ sample pairs. One significant difference for digital and physical observations (‘EW’ – direction) was a high enlargement of visual colour difference values in the lightness direction when assessed on screen compared to physical samples assessed in a viewing cabinet; and, this to a larger extent for most of the grey sample pairs. Whether, this was caused by the method of synthesising images from a master texture images and altering texture content, or could be generally described by the technical aspects of the design of a LCD screen (polarised light), was still to be answered. Another method of obtaining colour difference images was therefore introduced as such to capture physical ‘BH’ and ‘ST’ sample pairs, which were used during *Experiment D – Part A*, with a digital camera for display on a digital screen. The advantage over synthesised images was to replicate exactly the same images as they were also seen by observer in a viewing cabinet. The disadvantage could be described by the replication of the same larger variation in the underlying quality of each physical sample pair.

7.7.2 Eighteen observers, ten females and eight males, with an average age of ‘29’ years, participated in *Experiment D – Part B* judging digital camera captured ‘BH’ snd ‘ST’ samples in ‘EW’ and ‘NS’ running direction on screen (most of them participated also in *Part A*). They were judging ten grey and ten blue digital camera ‘BH’, and twelve grey and fourteen blue ‘ST’ sample pairs. Four ‘BH’ and six ‘ST’ sample pairs were added for each data set so to provide an estimate how well one observer can repeat the same visual assignment. Altogether, ‘2880’ observations were recorded for those camera captured digital images presented on a digital screen.

7.7.3. All physical samples were captured and displayed on screen according to the camera’s characterisation and LCD’s model as described in *Graph 5*[iii] (use steps ‘3’ – ‘5’) and *Graph 2*[jjj]. It is stressed here that all images on screen were reproduced exactly to the same photometric

---

[iii] see page 146

[jjj] see page 135

specifications that were obtained from measurements from the samples in a viewing cabinet (samples assessed in *Experiment A – Part A* and *B* were of relative colorimetric matches). For instance, the grey background measured in a viewing cabinet was reproduced as a grey display background colour in absolute tristimulus values of '$X_{10,L}$' = 37.57, '$Y_{10,L}$'= 39.09, and '$Z_{10,L}$'= 39.61. Those measured colorimetric values from the cabinet's grey background were altered as such to obtain exactly the same specifications on the digital screen considering a white point of '$X_{10,L}$'= 192.96, '$Y_{10,L}$'= 200.64, and '$Z_{10,L}$' = 177.37 for Lacie's display opposed to a white point colorimetric measure of '$X_{10,L}$'= 162.63, '$Y_{10,L}$'= 170.59, and '$Z_{10,L}$' = 171.79 for the viewing cabinet. Both devices employed fluorescent illumination/lumination; but, with a difference in colour temperature of about 500 K (of 6000 K to 5500 K for the viewing cabinet and LCD screen, respectively).

7.8 Digital greyscale

7.8.1 A digital greyscale was designed on screen used for scaling observer's assessments and measured before, between, and after all experimental sessions for *Experiment D – Part B*. A smoothing spline function was used to extrapolate data between GRADE steps. Those values are listed in *Table 65* for 'ΔV_{CMC}(1:1)' values.

	Five step greyscale				
GRADE	1	2	3	4	5
CMC(1:1)	7.30	4.10	2.15	1.35	0.78

Table 65: **Digital greyscale in CMC(1:1) units for *Experiment D – Part B*.**

7.9 Inter- and intra-observer variability

7.9.1 Observer performances for repeated measurements and against the average performance from all observers measured in STRESS units were contrasted with each other. The values are listed in *Table 66* for the digital 'BH' and 'ST' dataset for both viewing directions.

	Intra-observer variability				*Inter-observer variability*			
Observer	*BH 'EW'*	*BH 'NS'*	*ST 'EW'*	*ST 'NS'*	*BH 'EW'*	*BH 'NS'*	*ST 'EW'*	*ST 'NS'*
1	32.49	30.53	8.76	28.32	34.41	22.67	14.06	28.28
2	31.29	11.95	13.83	30.00	35.90	28.34	15.40	19.52
3	20.62	23.10	28.57	32.31	29.02	30.01	21.50	28.12
4	22.61	23.22	30.92	21.74	23.40	22.91	28.91	45.49
5	50.32	43.00	27.92	35.98	24.47	30.31	18.32	40.45
6	55.54	29.20	19.89	23.85	25.31	21.49	18.80	22.70
7	10.96	43.86	18.75	34.12	25.66	31.41	15.31	30.01
8	43.84	50.01	16.86	40.37	26.50	35.63	27.35	47.66
9	32.81	32.18	9.73	23.65	8.40	4.44	18.90	51.90
10	13.48	6.55	28.48	50.71	37.92	28.34	25.74	33.81
11	60.85	36.89	31.51	16.90	34.23	29.95	27.51	48.44
12	20.33	71.73	15.77	28.68	44.80	30.99	21.86	35.47
13	9.73	14.33	10.13	13.51	23.61	14.80	14.34	16.47
14	26.22	24.45	15.03	24.58	33.26	28.94	13.49	37.33
15	23.18	24.49	18.61	32.58	29.90	31.28	24.11	54.05
16	27.41	19.44	13.49	24.91	32.39	22.37	16.25	27.29
17	18.19	34.06	26.41	27.66	27.97	26.51	14.73	13.94
18	47.26	29.20	31.61	14.10	25.31	21.49	12.45	14.58
Trimmean	***29.78***	***29.37***	***20.37***	***27.48***	***29.33***	***26.36***	***19.23***	***32.97***

Table 66: **Intra- and inter-observer variability for digital camera 'BH' and 'ST' sample pairs.**

7.9.2 Those results suggested similar results as obtained from physical observations in the viewing cabinet (around '26' STRESS units), especially with less variances for 'ST' sample pairs in the 'EW' – direction. Generally, the results confirmed similar results between physical and digital sample in terms of inter- and intra-observer variability, as expected.

7.10 Measurement and visual results for two viewing directions

7.10.1 The results from those digital camera image observations (sample pairs with only lightness differences 'L^*' > '90' were not considered in this comparison) are listed in *Table 67*. The comparison with those results in *Table 60* for the same but physical sample pairs showed similar trends. 'BH' sample pairs were judged in 'EW' direction with larger magnitudes by a factor of '1.43' (grey samples '1.72' with a higher ratio compared to blue sample pairs '1.13' compared to '1.12' and '1.68' for physical samples). Camera 'ST' images were judged on screen smaller in magnitude compared to instrumental results given a overall ratio of '0.74' (ratio of '0.92' for grey and '0.56' for blue samples compared to '1' and '0.64' for the same physical samples, respectively).

CMC(1:1)	***digital screen 'EW'***			***digital screen 'NS'***		
Buttonhole 'BH'	GREY EW	BLUE EW	Mean	GREY NS	BLUE NS	Mean
MEAN RESIDUAL	0.91			1.01		
MEAN DV	3.76	2.55	3.16	4.27	2.92	3.60
MEAN DE	2.18	2.25	2.22	2.21	2.52	2.37
RATIO DV/DE	1.72	1.13	1.43	1.93	1.16	1.55
STRESS	***31.56***			***34.54***		
Singlestitch 'ST'	GREY EW	BLUE EW	Mean	GREY NS	BLUE NS	Mean
MEAN RESIDUAL	0.51			0.64		
MEAN DV	2.33	1.39	1.83	4.62	2.36	3.49
MEAN DE	2.48	2.42	2.45	2.51	2.01	2.26
RATIO DV/DE	0.95	0.59	0.77	1.84	1.17	1.51
STRESS	***29.61***			***31.56***		

Table 67: **Comparison of visual with instrumental colour differences for CMC's formula for digital camera 'BH' and 'ST' sample pairs assessed on a digital screen.**

7.10.2 Results from observations in the 'NS' – direction followed the same trend when compared to the same physical sample set; however, the ratios for '$\Delta V_{CMC}(1:1)$' and '$\Delta E_{CMC}(1:1)$' data were larger for grey sample pairs when compared with blue samples. Optimised parameter for the CMC formula for digital camera 'BH' and 'ST' sample pairs are listed in *Appendices B*. Those visual results from *Experiment D – Part B* for 'BH' and 'ST' sample pairs were then contrasted in a similar way as in Figure *145* and *146* for a magnitude comparison (see *Figure 153* and *154*).

7.10.3 The results of a comparison between physical and the same, but captured and digitised, samples showed the same trend for both directions. Again, the 'EW' viewing direction for physical samples correlated better with those results obtained from digital assessments. The

difference in magnitude perception for those results were then determined by scaling; (**1**) the results from physical sample sets ('TWC', 'BH', and 'ST') to a common average '$\Delta E_{CMC}(1:1)$' value for all three data sets and comparing then the ratios between all paired samples for both data sets.

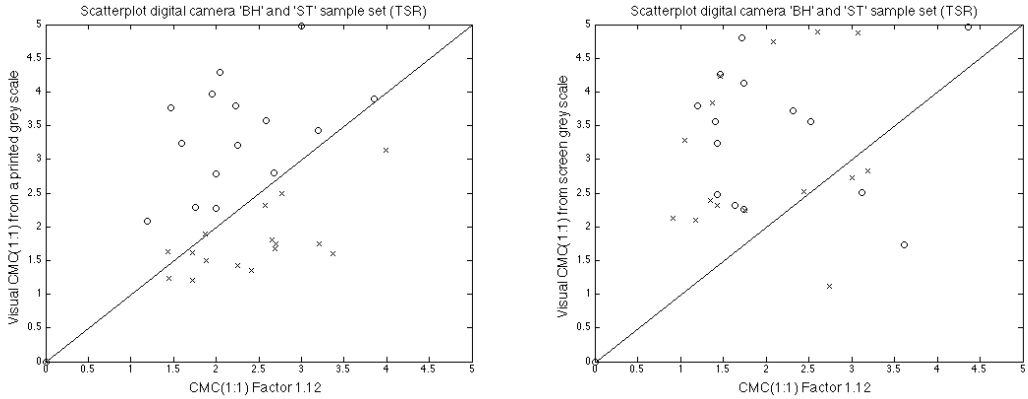

***Figure 153 – 154*: CMC's formula scatter-plot comparison for digital camera 'BH'('o') and 'ST'('x') sample pairs for 'EW' (left) and 'NS' (right) direction for tele-spectroradiometric measurements.**

7.11 Parametric overall sensitivity factor

7.11.1 The average factor for each set was taken as the overall parametric factor. A percentage measure was then calculated by normalising 'BH' and 'ST' ratio factors by the factor for the reference 'TWC' sample assessments. Those values are listed in *Table 68*.

Parametric factors for physical samples							
Measure	Type	Blue EW	Grey EW	Overall EW	Blue NS	Grey NS	Overall NS
7000A	TWC	1.11	1.43	1.25			
7000A	BH	1.47	1.47	1.47			
7000A	ST	0.69	0.95	0.82			
TSR	TWC	1.15	1.16	1.15	1.19	1.13	1.16
TSR	BH	1.28	1.28	1.28	2.08	2.08	2.08
TSR	ST	0.71	0.85	0.78	1.41	1.67	1.54

***Table 68:* Parametric factors for physical 'TWC', 'ST', and 'BH' sample pairs for two measurement methods and directions.**

Those results translated to a value of 35% smaller magnitude judgements for physical 'ST' sample pairs compared to the 'TWC' set. Physical 'BH' sample pairs were judged 18% larger than 'TWC' sample pairs. The average numerical colour difference value for the physical 'BH' sample set was approximately '2.02' '$\Delta E_{CMC}(1:1)$' units. Texture content diminishes towards larger '2.4' '$\Delta E_{CMC}(1:1)$' units (see *Experiment A – Part A*); hence, a reduction from an expected value of 30% for differences in the range of '1.2' units. The digital camera data sets were scaled in the same manner thus resulting in about 38% smaller judgements when compared with a physical 'TWC' parametric factor of '1.25; that, also meant that digital camera 'BH' samples were judged in magnitude 15% larger than the physical 'TWC' references data set. The ratios between '$\Delta V_{CMC}(1:1)$' and '$\Delta E_{CMC}(1:1)$' for physical 'TWC', 'BH' and 'ST' samples in the

case of viewing cabinet measurements were ‘1.15’, ‘1.28’, and ‘0.78’. The comparison in magnitude sizes in the ‘NS’ – direction for ‘TWC’ (reference data set), ‘ST’, and ‘BH’ sample pairs were in per cent 79% larger values for ‘BH’ sample pairs, and 33% per cent larger colour difference magnitudes for ‘ST’ assessments, when compared to a reference ‘TWC’ data set.

7.12 Summary and conclusion

. Twenty-one observers judged physical ‘BH’, ‘ST’, and ‘TWC’ sample pairs in a viewing cabinet. The same, but digital captured images, were judged by eighteen observers on a digital screen. The results showed similar trends and confirmed those findings that were found during *Experiment A, B* and *C*. Differences in sample presentation and texture content altered observer’s perception of colour differences, significantly. Parametric effects (overall size effect) were similar in size for either the physical or digital sample set.

Chapter 8:

8.1 Overview

8.1.1 This project was sponsored by Coats plc. a manufacturer of industrial spun polyester sewing and needlework threads. Coats in-house research efforts during the 1970's led to a breakthrough in colour difference predictions. The result was a new colour difference formula 'JPC_{79}', which was tested in a commercial environment providing fewer wrong decisions when compared with the best colour matcher from a group at Coats plc.

8.1.2 The formula was designed from a large number of thread winding card samples from which colour difference pairs were formed with a magnitude of '1' and '2' 'ΔE_a' units. The scaling was done by a pass/fail method against a grey anchor grey pair with a calculated difference of '1.9' 'ΔE_a' units. The formula was later modified and became a standard in the textile industry known as the CMC(l:c) colour difference formula.

8.1.3 However, colour differences seen between two thread samples may not reflect on a real world scenario, for instance, when a thread is to be matched while stitched upon or within another kind of material, such as a fabric or leather sample. A colour of an object is normally associated with a term known as the 'colour appearance' of a sample. The appearance can be altered because the lighting conditions were changed, or due to the change of the underlying material that was used (a textured fabric sample opposed to a uniform paint sample), and/or by how a sample was presented to a viewer.

8.2 Study reminder

8.2.1 Therefore, it was of interest to assess both sample scenarios; (**1**) thread winding card colour difference pairs, and (**2**) thread sewn into fabric samples using a grey scale method for assessing visual colour differences between both sample types during psychophysical experiments. Two types of thread sewn into fabric samples were used; (**1**) one type used for stitching thread around buttonholes, and (**2**) a single needle lockstitch type for determining whether size and orientation of a thread may change the colour appearance of a sample pair.

8.2.2 The number of physical sample pairs that were produced for comparison was limited to just two colour centres. Other research work employed digital substitutes that were assessed on a digital screen, instead. The question was therefore whether those physical samples could be reproduced on a digital screen, and also numerically extended to more than two colour centres. This required two models to be designed; (**1**) a model that describes the colorimetric behaviour of a digital screen, and (**2**) a model that enables the user to design those digital substitutes for 'BH', 'ST', and 'TWC' sample pairs.

8.2.3 Also, it was of interest to modify existing formulae once there was an alteration in the perceptibility of colour differences caused by the sample presentation. Finally, an optimisation process was applied to existing formulae so to increase the correlation between visual and instrumental results. Any parametric factors were quantised and recorded.

8.3 *Experiment A:* Aims 1 – 3

8.3.1 Observers perceived larger colour differences when 'BH' samples were compared with 'TWC' samples for the same instrumental colour differences (on average 30% larger 'ΔE' units). The texture effect for physical 'BH' samples was larger for smaller colour differences but diminished for larger pairs equal or larger than '2.4' '$\Delta E_{CMC}(l{:}1)$' units (higher contrast between fabric and thread content for 'BH' samples - see *Image 16*). Judging colour differences sample pairs around a tolerance limit of '1.2' '$\Delta E_{CMC}(l{:}1)$' units revealed approximately 20% larger visual colour difference values between 'BH' and 'TWC' sample pairs. The same observers also perceived colour differences for digital 'BH' on average 30% larger when compared to digital 'TWC' sample pairs. However, absolute visual colour differences magnitudes were smaller for digital colour sample pairs, especially, for chromatic content differences. Grey colour differences, especially in the lightness direction, were larger on screen when compared to lightness differences obtained from physical samples assessed in a viewing cabinet when compared to 'TWC' sample pairs (normalising factor).

8.3.2 Digital samples were designed from a texture master sample for the digital 'BH' and 'TWC' sample set. The average colour difference between a modelled and displayed uniform image data set was on average '0.25' 'ΔE_{00}' units. Inter- and intra-observer variability measures for physical observations were on average '30'/'23' and '27/24' STRESS units for the digital 'TWC' and 'BH' samples set.

8.3.3 The prediction performances of formulae for those visual results were on average '34.35'/'36.04' and '25.24'/'25.96' STRESS units for the physical 'BH' and 'TWC' sample set according to CMC's and the $CIEDE_{2000}$ formula. The prediction for the digital 'BH' and 'TWC' sample set was '25.40'/'19.62' and '21.97'/'13.66' for the CMC and $CIEDE_{2000}$ formula. The factors that were applied so to minimise the differences between visual and predicted results was '1.62'/'1.27' (ratio of '1.28') for CMC's formula and digital 'BH' and 'TWC' samples opposed to '3.24'/'3' (ratio of '1.08') for physical samples used in *Experiment A – Part A*. The average residual value was recorded as '1.66' and '0.87' for the physical 'BH' and 'TWC' sample set; '0.87' and '0.57' for the digital sets. The parametric factors for 'k_L' or 'l' and 'k_C' or 'c' were optimised so to give values of '2.23:1.12' and '2.75:1.24' for physical 'BH' and 'TWC' samples; '1.05/1.33' and '0.99/1.64' for digital 'BH' and 'TWC' samples,

‘1.94:1.29:1.05’ and ‘1.96:1:1’, ‘0.74:1.05:1’ and ‘0.65:1.20:0.9’ for the physical and digital ‘BH’ and ‘TWC’ sample set predicted by $CIEDE_{2000}$’s formula.

8.4 *Experiment B:* Aims 1 – 3

8.4.1 Twelve professional observers judged ‘300’ digital Single Needle Lockstitch’ type samples (‘ST’) around ten colour centres. The average visual result for all colour difference judgments was a GRADE ‘2.99’ value. This translated to an average visual colour difference value of ‘1.99’ ‘$\Delta V_{CMC}(1:1)$’ units. Lightness differences were judged larger in magnitude (especially for high chromatic colours), whereas chromatic observations for all colour batches and centres were consistently lower in magnitude compared to instrumental measurements. The overall ratio between ‘$\Delta V_{CMC}(1:1)$’ and ‘$\Delta E_{CMC}(1:1)$’ for all colour samples was on average given as a ratio value of ‘0.9’ (‘0.75’ and ‘1.04’ for chromatic and lightness differences, respectively).

8.4.2 Digital samples were designed from a master texture fabric ‘FA’ and master ‘ST’ sample. The average colour difference between a modelled and displayed fabric image standard data set (ten samples) was on average ‘0.22’ ‘$\Delta E_{CMC}(1:1)$’ units for an model dataset of ‘2.4’ ‘$\Delta E_{CMC}(1:1)$’ units on screen. The inter- and intra-observer variability measure for those observations obtained from professional observers was on average ’33.56’ and ’15.37’ STRESS units, respectively.

8.4.3 The prediction performances of formulae for digital ‘ST’ sample pairs were on average ‘23.91’ and ’21.05’ for the CMC and $CIEDE_{2000}$ formula. Further optimisation was achieved by changing the parameter for the ‘S_L’ and ‘S_C’ weighting functions. The STRESS values were further reduced to ’19.19’ and ‘13.48’ STRESS units, respectively. The factors that were applied so to minimise the differences between visual and predicted results were ‘0.75’(‘0.76’ full optimised) and ‘0.86’(‘0.62’) for the CMC and $CIEDE_{2000}$ formula, respectively. The average residual value was recorded as ‘0.45’ and ‘0.37’ and 0.’32’ and ‘0.23’ for the CMC and $CIEDE_{2000}$ formula for optimised parametric factors, and full-optimised parameters (including weighting functions), respectively.

8.4.4 The parametric factors for ‘k_L’ or ‘l’, ‘k_C’ or ‘c’, and ‘k_H’ for digital ‘ST’ samples were given as CMC(0.57:0.96) or (0.64:1.01), and $CIEDE_{2000}$(0.55:0.95:1.05) or (0.6:1:1) for fully optimised parameter, respectively.

8.4.5 Those data were used to construct weighting functions. These functions followed generally the same underlying parameter contained in the weighting functions that are used for the $CIEDE_{2000}$ formula. Factors for minimising visual and predicted data for digital ‘ST’, ‘BH’, and ‘TWC’ sample pairs were given as ‘1.62’ to ‘1.27’ to ‘0.75’ suggesting 28% larger visual

results for ‘BH’ sample pairs when compared to ‘TWC’ digital data; and, 34% smaller visual magnitudes for ‘ST’ sample pairs, respectively.

8.5 *Experiment C:* Aims 1 – 3

8.5.1 Twenty-one, nineteen, and eighteen observers (‘13’ females and ‘8’ males, average age of ’30.61’ years) participated in three experiments assessing visually colour difference sample pairs on a digital screen. The standard centres for *Experiment C* were of orange, olive, green, blue, brown, and grey colour. A dataset consisted of ‘186’ samples including ‘30’ repetition samples. Observers were asked to judge ‘558’ sample pairs for either uniform ‘TWC’, ‘BH’, or ‘ST’ sample pairs resulting in ‘10.788’ visual colour difference judgements.

8.5.2 The average visual ‘$\Delta V_{CMC}(1:1)$’ value for each dataset was ‘2.09’ (‘1.94’ and ‘2.17’ for chromatic and lightness differences) for the ‘TWC’ set, ‘2.47’ (‘1.77’ and ‘2.82’) for the digital ‘ST’ set, and ‘2.85’ (‘2.41’ and ‘3.07’) for the digital ‘BH’ set. Texture content was reduced for ‘BH’ and ‘ST’ samples (see *Images 13* and *14*), which resulted in an increase of lightness difference magnitudes on screen, when compared to physical samples assessed in a viewing cabinet. Chromatic colour difference results were smallest for the digital ‘ST’ set and largest for the digital ‘BH’ sample set.

8.5.3 The LCD model performance was determined by measuring the uniform ‘TWC’ sample set on screen. The measured colour difference for that reproduced dataset was on average ‘2.37’ ‘$\Delta E_{CMC}(1:1)$’ units (‘0.2’ standard deviations) for an average modelled data set of ‘2.40’ ‘$\Delta E_{CMC}(1:1)$’ units. The inter- and intra-observer variability measure for observations obtained from three data sets from naive observers was on average ’29.69’/’29.24’/’29.08’ and ’21.47’/’15.04’/’18.45’ STRESS units for the digital uniform ‘TWC’, ‘BH’, and ‘ST’ data set, respectively.

8.5.4 The prediction performance values for the CMC and $CIEDE_{2000}$ formula were on average ‘14.56’/’13.02’/13.33’ and ‘13.57’/’11.86’/’13.52’ for digital ‘TWC’, ‘BH’, and ‘ST’ sample pairs, respectively. The residuals values were determined as ‘0.21’/’0.29’/’0.27’ $\Delta E_{CMC}(l{:}c)$ and ‘0.19’/’0.23’/’0.23’ $\Delta E_{00}(k_L{:}k_C{:}k_H)$ units, accordingly. Parametric factors for ‘k_L’ or ‘l’, ‘k_C’ or ‘c’, and ‘k_H’ were optimised so to provide values of ‘0.93:1.01’ (‘TWC’), ‘0.62:1.00’ (‘BH’), and ‘0.40:1.00’ (‘ST’) for the CMC formula, and ‘0.84:0.98:1:1.00’ (‘TWC’), ‘0.72:0.98:1.01’ (‘BH’), and ‘0.42:1.01:0.99’ (‘ST’) for the $CIEDE_{2000}$ formula.

8.5.5 Weighting functions were optimised for the CMC and $CIEDE_{2000}$ formula. Significant improvements in prediction performances were achieved while optimising CMC’s ‘S_L’ weighting function. $CIEDE_{2000}$’s weighting functions were robust and less prone to large

changes in parameters for various optimised data sets. Significant improvements in prediction performances for the $CIEDE_{2000}$ formula were achieved by optimising parametric factor 'k_L'.

8.6 *Experiment D:* Aims 1 – 3

8.6.1 Three types of physical sample sets were used; (**1**) a selection of single needle lockstitch samples ('ST'), (**2**) a selection of thread winding card samples ('TWC'), and (**3**) a selection of buttonhole stitch type samples ('BH'). All sample pairs were presented in two directions in a viewing cabinet so that the actual thread was either running along the North/South– ('NS**'**) or East/West ('EW') direction from an observers's point of view. Altogether, '3360' observations were produced during *Experiment D – Part A*. Eighteen observers participated in *Experiment D – Part B* judging digital camera captured 'BH' snd 'ST' samples in 'EW' and 'NS' running direction on screen. Altogether, '2880' observations were recorded for those camera captured digital images presented on a digital screen.

8.6.2 Scaled ratios for 'ΔV_{CMC}'/'ΔE_{CMC}' values for physical 'BH' sample pairs were given as '1.28' ('1.43' for spectrophotometric measurements), '1.15' ('1.28') for physical 'TWC', and '0.78' ('0.82') for physical 'ST' sample pairs. Physical 'BH' sample pairs were judged 18% larger compared to the physical 'TWC' sample set; physical 'ST' sample pairs were judged 38% smaller than physical 'TWC' colour difference sample pairs. The average numerical colour difference value for physical 'BH' and 'ST' samples were approximately '2.02' 'ΔE_{CMC}(1:1)' units. Those results were only valid for observations in the 'EW' direction. Visual results from the 'North/South' - direction enlarged visual results, furthermore. Ratios of '$\Delta V_{CMC}/\Delta E_{CMC}$' for digital camera images were '0.77' and '1.43' for 'ST' and 'BH' samples. Those results were similar to those obtained from the same samples in physical form.

8.6.3 The LCD model performance provided the same average colour difference value between a modelled and tested set as seen in all other experiments. The camera model for fabric 'FA' and 'TWC' samples using a neural network model gave a colour difference value of '0.42' 'ΔE_{00}(1:1:1) ' units. The inter- observer variability measure obtained from three data sets from naive observers was on average '25.40' STRESS units; the intra-observer variability values were calculated and resulted in '30.69' and '20.37' STRESS units for the digital 'BH' and 'ST' data set, respectively.

8.6.4 The prediction performance values for the CMC formula was on average '21.56'/'20.45'/'9.65' STRESS units for physical 'BH', 'ST', and 'TWC' sample pairs, respectively. The performance for 'BH' and 'ST' sample pairs for digital camera images for the CMC formula was '31.56' and '29.61' STRESS units. Parametric factors for '*l*' or '*c*' were optimised so to provide values for the physical data sets of '2.05:0.99' ('BH'), '1.82:1.06' ('ST'), and '2.06:1.36' ('TWC') for the CMC formula. Values for the parametric factors

optimised for digital camera samples were ‘0.69:1’ and ‘0.88:1’ for ‘ST’ and ‘BH’, respectively. The overall sensitivity factors were recorded as ‘0.79’ and ‘1.44’ for ‘ST’ and ‘BH’ samples for those digital camera images. Those values translated to 37% smaller visual colour difference magnitudes when compared to a reference ‘TWC’ data set (factor ‘1.25’), and 15% larger magnitudes for the digital camera ‘BH’ sample set, respectively.

8.7 Project summary

(**1**) Visual colour difference magnitudes were altered by; (**a**) the sample type employed (for the same measured colour differences), and (**b**) by the orientation of those samples presented in respect to the viewing direction of an observer.

(**2**) Physical ‘ST’ stitch type samples were judged with smaller colour difference magnitudes; on average about 30% smaller than a reference ‘TWC’ sample set assessed in a viewing cabinet in ‘East/West’ – direction. This phenomenon may be explained by the effect a small thread, which is seen against a similar coloured background, has to the observer’s eye as such merging and blending together with the background colour of a relatively homogeneous textured fabric sample so to reduce the contrast and perceived colour difference magnitude between them (‘spreading effect’). The same physical ‘ST’ sample pairs assessed in ‘North/South’ – direction resulted in larger colour difference magnitudes (approximately 40% compared to a reference ‘TWC’ sample set). Those results can be explained by added specular reflected light from the ‘ST’ thread content within a sample pair.

(**3**) Physical ‘BH’ stitch type sample assessments resulted in larger colour difference magnitudes when seen in a viewing cabinet in ‘East/West’- direction; on average 20% larger in magnitude compared to a reference ‘TWC’ sample set (while considering a tolerance limit of ‘1.2’ CMC(2:1) units). This was mainly attributed to the added texture effect a ‘BH’ colour difference sample pair had to the observer’s eye. The dark shadowed line between fabric and stitched ‘BH’ thread type (see *Image 11*), and the two different texture directions for both materials, enhances the contrast between them, and so the visual perception of a colour difference. The same physical ‘BH’ sample pairs assessed in a viewing cabinet in ‘North/South’ direction resulted in larger colour difference magnitudes (on average 79% higher when compared to a reference ‘TWC’ sample set) mainly contributed to the added amount of specular reflected light when compared to a ‘TWC’ reference set assessed in ‘NS’ - direction (see *Table 68*). Naive observers may find it difficult to distinguish between either a colour and/or texture difference, if those colour difference sample pairs are scaled against a grey scale (see *Experiment B* and *C* for ‘ST’ sample pairs).

(**4**) Reproductions of digital ‘BH’, ‘ST’, and ‘TWC’ colour difference sample pairs resulted in similar visual trends; however, it was of fundamental importance to reproduce a texture content

of a reproduced sample, correctly. Crispening in the lightness direction appeared to be more visible on a digital screen, especially for grey colours, when compared to physical colour difference samples assessed in a viewing cabinet. A colour may appear in fact brighter and less chromatic in cases of geometrical forms as given from 'ST' or 'BH' colour difference sample pairs when seen against a similar coloured background (see *Images 13* and *14*). The reduced texture content for digital 'ST' and 'BH' sample pairs in *Experiment C* did enhance this effect furthermore (simultaneous contrast and lightness crispening), especially evident, when compared to those results obtained from observations in *Experiment A – Part B*. Absolute colour difference magnitudes were given smaller values on a digital screen.

(**5**) Results from instrumental measurements obtained from physical samples in a viewing cabinet did vary significantly; those differences in colorimetric values were mainly caused by the presentation direction of 'thread winding card' samples in respect to the measurement angle. Also, any physical imperfection of colour difference sample pairs and presentation to the observer can alter those measurement results; and, this to a larger extent for measurements in the lightness direction. Spectrophotometric measurements did not reveal any directional differences. Those measurements correlated better with visual results obtained in the 'East/West' – direction. Measurements taken from a tele-spectroradiometer were more consistent with visual results obtained from samples in a viewing cabinet presented in the 'North/South' – direction.

(**6**) A LCD characterisation model using three '1D – LUT' tables, and a model for determining the background effect on a displayed image within the software environment that was used to display images to observers, resulted in an absolute reproduction error of '0.25' 'ΔE_{00}(1:1)' units for testing '107' colour patches on screen. The main limitations of the screen was either; (**1**) the inherent spatial non-uniformity, which resulted in a large amount of measurements, for instance, for determining the LCD's model parameters and grey scale values from four different positions on screen, and (**2**) the shift in colour temperature for the same settings employed during this project from approximately 5900 to 5400 K, and (**3**) the inconsistent influence of the grey background on the colorimetric values of a displayed colour difference sample pair.

(**7**) Image models were based on a 'pixel by pixel' based method so to add only lightness differences from master texture images to a uniform chromatic content image. The advantage of using a texture master image is to apply the same underlying statistical distribution for each sample pair (obtained from a scanner's monochromatic green channel responses). It is therefore likely that visual results may reflect only on the difference in one of the important colour difference scales. The performances of formulae for those digital sample sets were therefore generally better than those obtained from all physical samples sets (larger error variations).

However, a possibly limitation is to find the right amount of texture content so to match the physical sample's texture content.

(**8**) A second method was introduced so to capture all physical 'BH' and 'ST' sample pairs with a digital camera. Two methods were used to characterise a camera either by polynomial modelling, or by designing a neural network, so to map camera's 'RGB' values, or camera's 'XYZ' - tristimulus values, in a 'pixel by pixel' manner to CIE 'XYZ' - tristimulus values for further considerations. Both non-linear methods provided similar model prediction performances. This resulted in a reproduction error of 0.42 'ΔE_{00}(1:1)' units for '52' fabric and 'thread winding card 'samples. The advantage of this method was to reproduce exactly the same samples on screen as they were seen and assessed in a viewing cabinet. The effect of this method was seen in the results of almost identical parametric effects (size effect) when compared to observations made for the same samples, but in physical form.

(**9**) Colour difference formulae predicted visual results for physical and digital 'TWC' sample set best. Optimisation of parametric factors improved results for all datasets, furthermore. The correlation coefficient for the optimised CMC(2.58:1) formula was '0.88' compared to '0.55' for provided physical 'TWC' and 'BH' samples (CMC(2.14:1)), respectively. Significant improvement in the prediction of colour differences was achieved by changing the average colorimetric value of the lightness 'L^*' value for the standard samples for both, physical and digital, sample sets. 'F' – tests also revealed that CMC's 'S_L' function (after optimisation of parametric factors) provided significant gains in prediction performances for all digital sample sets. However, more important was the discovery that absolute differences between visual and predicted results differed significantly amongst three sample sets. An overall size parametric factor for the CMC formula reduced average residual values to '0.30', '0.45', and '0.22' 'ΔE_{CMC}(best:1)' units for the 'BH', 'ST', and 'TWC' sample set, respectively. So, how reliable are those values? The repeated measurements of samples with a spectrophotometer are consistent in the short run but also over time; and, the differences between them so small that they are normally not detectable by the naked eye (approximately '0.08' ΔE^*_{ab} units). The errors in those associated visual assessments were much larger. Error measures are normally provided as STRESS values but were here also provided as mean residual units. Those values were determined for an individual observer's repeated visual assessments; and, as an overall measure for each individual observer against the average value obtained from all observers' visual assessments. The average residual for repeated measurements obtained from an individual observer for physical 'BH' samples can be as high as '0.57' 'ΔE_{CMC}(2:1)', and '0.78' 'ΔE_{CMC}(2:1)' units for the overall average difference of one observer's assessments against the mean value obtained from all observers. However, these are only approximations since the uncertainty of those values (error) are likely to occur in all three important colour difference

scale directions; and, those scales are not independent from each other since they interact with each other (colour matching functions are of broadband form overlapping each other)[389,390,391].

8.8 Project conclusion and recommendations

The recommended parametric factors (2:1) for the use of evaluating colour differences for textile samples were approximately confirmed while assessing physical 'TWC', 'BH', and 'ST' colour difference sample sets. However, visual magnitudes differed significantly for a 'BH' and 'ST' data set despite the fact that sample pairs for both data sets contained the same numerical colour difference values. An overall parametric factor of '0.75' for the use with the CMC formula (2:1) for physical 'ST' thread sewn into fabric samples is recommended so to minimise the differences for predicted and visual colour difference results. A factor of '1.2' shall be applied to colour difference values calculated for physical fabric 'BH' sample pairs around a tolerance limit of '1.2' 'ΔE_{CMC}(2:1) units. This minimises the differences between calculated values and associated visual colour difference results. Both factors shall be multiplied with a conventional calculated colour difference value using the CMC(2:1) formula, respectively. The tolerance limits, when calculated for 'ST' (or 'BH') samples in a conventional way, is therefore altered to '1.6' (or '0.96') 'ΔE_{CMC}(1:1)' units once sewn into a fine textured 'homogeneous' fabric sample. Whenever, a colour difference is measured for a thread and a fabric sample ('ST' - type) with a difference of '1.6' 'ΔE_{CMC}(2:1) units, than it is likely that a consumer will still regard this difference between a thread and a fabric sample as an acceptable match. Those recommended multiplicative factors changes to '1.4' and '1.8' for 'ST' and 'BH' sample pairs when assessed in the 'North/South' – direction so to minimise the difference between instrumental and visual results. The tolerance limits for visual colour difference results obtained from 'ST' and 'BH' samples presented in the 'North/South' – direction are in this case reduced from a reference '1.2' to '0.86' and '0.66' 'ΔE_{CMC}(2:1) units, respectively (according to the samples that were provided for assessments for this project). If 'ST' and 'BH' colour difference sample pairs shall be assessed on a digital screen, than the lightness parametric factor 'k_L or 'l' needs to be reduced by a factor of '2 - 3' ('TWC' < 'BH' < 'ST'), compared to a factor that is normally applied for assessing physical textile samples. The results are then comparable with physical samples judged in the 'East/West' – direction in a viewing cabinet.

8.9 Future work

It has been shown that a thread that is seen in a final product is likely to change its colour appearance. Texture content and stitch type are important experimental factors. They need as such to be quantised for reducing the differences between visual and calculated colour difference values. Therefore, it would be of interest to determine those visual changes for

various background fabric samples so to design an algorithm accounting for the changes in visual colour difference perceptions induced by varying the background texture.

Weighting functions can be designed for each stitch type from a large number of physical 'thread sewn into fabric' samples. Especially, CMC's lightness weighting function parameters had to be altered for increasing the correlation between visual and instrumental results on a digital screen. The $CIEDE_{2000}$ weighting functions were more robust in this aspect. All new advanced colour difference formulae were able to predict visual results well once parametric factors were optimised, and an overall factor was applied for the 'ST' and 'BH' colour difference sample set. The prediction performances of those formulae are dependent very much so on the quality of the training samples.

Bibliography

1. G. Allen, *The Colour-Sense: Its Origin and Development*; Paul, Trench, Trübner & Co Ltd., London, 1879.

2. J.D. Mollon, 'The Origins of Modern Color Science', in *The Science of Colour*, ed. S. Shevell, Elsevier, Oxford UK, 2003, Chapter 1, 2-39.

3. J.D. Mollen, 'Cherries among the Leaves. The Evolutionary Origins of Color Vision', in *Color perception: philosophical psychological, artistic, and computational perspectives*, ed. S. Davis, Oxford University Press, New York USA, 2000, Chapter 2, 10-30.

4. G.H. Jacobs, 'The Distribution and Nature of Colour Vision among the Mammals', *Biological Reviews*, 1993, **68**, 3, 413-471.

5. J.D. Mollon, '"Tho'she kneel'd in that place where they grew..." the uses and origins of primate colour vision', *Journal of Experimental Biology*, 1989, **146**, 21-38.

6. F. Viènot and P. Walraven, 'Color-Matching Functions: Physiological', In *Colorimetry: Understanding the CIE system*, ed. J. Schanda, John Wiley & Sons Inc., Hoboken, New Jersey USA, 2007, Chapter 9, 219-244.

7. A.R. Wallace, *Darwinism.* Macmillian and Co., London UK, 1889.

8. I. Newton, 'New Theory about Light and Colours', in *Philosophical Transactions of the Royal Society.* Publisher from Cambridge, Cambridge England, 1671, 75-87.

9. O.M. Lilien, *Jacob Christoph Le Blon*, A. Hiersemann, Stuttgart Deutschland, 1985.

10. T. Mayer, *De affinitate colorum commentatio*, G.C. Lichtenberg, Göttingen Deutschland, 1775.

11. J.H. Lambert, *Beschreibung einer mit dem Calauschen Wachse ausgemalten Farbenpyramide wo die Mischung jeder Farben aus Weiss und drey Grundfarben angeordnet*, dargelegt und derselben *Berechnung und vielfacher Gebrauch, mit einer ausgemahlten Kupfertafel*, Haude and Spener, Berlin Deutschland, 1772.

12. G. Palmer, 'Théorie des couleurs et de la Vision', Prault, Paris France, 1777.

13. T. Young, 'Outlines of experiments and inquiries respecting sound and light', *Philosophical Transactions of the Royal Society*, 1800, 106-150.

14. H. von Helmholtz, 'Über die Theorie der zusammengesetzten Farben', *Annalen der Physik*, 1852, **163**, 9, 45-66.

15. H. Grassmann, 'Zur Theorie der Farbenmischung', *Annalen der Physik,* 1853, **89**, 69-84.

16. G. Wyszecki and W.S. Stiles. *Color Science, Concepts and Methods, Quantitative Data and Formulae.* Wiley Classic Library Edition, New York USA, 2nd edition, 2000, 118.

17. J.C. Maxwell, 'Experiments on colour as perceived by the eye with remarks on colour blindness'*, Transaction of the Royal Society of Arts in Edinburg,* 1855, **XXI**, 1857, 275-298.

18. J.C. Maxwell, 'On the theory of colours in relation to colour blindness', *Transaction of the Royal Society of Arts in Edinburg,* 1856, **IV**, 394-400.

19. J.C. Maxwell, 'On the theory of the compound colours and the relations of the colours in the spectrum', *Philosophical Transactions of the Royal Society in Edinburg*, 1860**,** 57-84.

20. H. von Helmholtz, *Handbuch der Physiologischen Optik.* Voss, Leipzig und Hamburg Deutschland, 2nd edition, 1866.

21. M.D. Fairchild, *Color Appearance Models*, John Wiley & Sons, West Sussex England, 2nd edition, 2005.

22. G. Wyszecki and W.S. Stiles. *Color Science, Concepts and Methods, Quantitative Data and Formulae.* Wiley Classic Library Edition, New York USA, 2nd edition, 2000, 583.

23. E. Hering, *Zur Lehre vom Lichtsinne,* Carl Gerold's Sohn, Wien Österreich, 1878.

24. N. Ohta and A.R. Robertson, *Colorimetry. Fundamentals and Applications*, John Wiley and Sons Ltd., Chichester, West Sussex England, 2005, 42.

25. G.E. Müller, 'Grundzüge der Theorie der Farbenempfindungen', in *dem Bericht über den VII. Kongreß für experimentelle Psychologie*, ed. K. Bühler, G. Fischer, Jena Deutschland, 1922, 157-161.

26. G.E. Müller, 'Über die von Chr. Ladd Franklin aufgestellte Theorie der Farbenempfindungen', *Zeitschrift für Sinnesphysiologie*, 1929, **60**, 71-88.

27. G. Wyszecki and W.S. Stiles. *Color Science, Concepts and Methods, Quantitative Data and Formulae.* Wiley Classic Library Edition, New York USA, 2nd edition, 2000, 634.

28. D. Jameson and L. M. Hurvich, 'Some quantitative aspects of an opponent-colors theory. I. Chromatic responses and spectral saturation', *Journal of the Optical Society of America*, 1955, **45**, 7, 546-552.

29. D. Jamesonand L. M. Hurvich, 'Some quantitative aspects of an opponent-colors theory. III. Changes in brightness, saturation, and hue with chromatic adaption', *Journal of the Optical Society of America*, 1956, **46**, 6, 405-415.

30. E.Q. Adams, 'A theory of color vision', *Psychological Review*, 1923, **30,** 1, 56-76.

31. E.Q. Adams, 'X-Z Planes in the 1931 I.C.I. System of Colorimetry', *Journal of the Optical Society of America*, 1942, **32**, 3, 168-173.

32. G. Wyszecki and W.S. Stiles. *Color Science, Concepts and Methods, Quantitative Data and Formulae.* Wiley Classic Library Edition, New York USA, 2nd edition, 2000, 637.

33. E.H. Land, 'The Retinex Theory of Color Vision', *Scientific American*, 1977, **37** 6, 108-128.

34. A. König und T.W. Engelmann, *Gesammelte Abhandlungen zur physiologischen Optik*, Barth Verlag, Leipzig Deutschland,1903.

35. N. Ohta and A.R. Robertson, *Colorimetry. Fundamentals and Applications*, John Wiley and Sons Ltd., Chichester, West Sussex England, 2005, 43-44.

36. H. Grassmann, 'On the theory of compound color', *Poggendorff Annalen der Physic and Chemie*, 1853, **89**, 69-84, translation in *Philosophical Magazine and Journal of Science*, 1854, **4**, 7, 254-256.

37. K.S. Gibson and E.P.T. Tyndall, 'Visibility of radiant energy', *Scientific paper of the Bureau of Standards*, 1923, **19**, 131-191.

38. J. Guild, 'The colorimetric properties of the spectrum', *Philosophical Transactions of the Royal Society A*, 1932, **230**, 681-693, 149-187.

39. W.D. Wright, 'A re-determination of the trichromatic mixture data', *Transaction of the Optical Society*, Bristol England, 1928-1929, **30**, 141-164.

40. H.C. Lee, *Introduction in Color Imaging Science*, Cambidge University Press, Cambridge England, 2005, 90.

41. J. Schanda, 'CIE Colorimetry', In *Colorimetry. Understanding the CIE system*, ed. J. Schanda, John Wiley & Sons Inc., Hoboken, New Jersey USA, 2007, Chapter 3, 25-78

42. B. Rigg, 'Colour description/specification systems', in *Total Colour Management in Textiles.* ed. J.H. Xin, Woodhead Publishing Limited, Cambridge England, 2006, Chapter 2, 26.

43. R.W.G. Hunt, 'Revised Colour Appearance Model for related and unrelated colours, *Color research and application*, 1991, **16**, 3, 146-165.

44. R.W.G. Hunt, *Measuring Colour*, Fountain Press, Kingston-upon-Thames England, 3rd edition, 1998, 209.

45. Commission Internationale de L'Éclairage, CIE 160-2004, *A Review of Chromatic Adaption Transfsorms*, CIE Central Bureau, Vienna Austria, 2004b.

46. Commission Internationale de L'Éclairage, CIE 159:2004, *A colour appearance model for colour management systems: CIECAM02,* CIE Central Bureau, Vienna Austria, 2004a.

47. M.R. Luo and C.J. Li, 'CIE Color Appearance Models and associated Color Spaces', in *COLORIMETRY, Understanding the CIE System*, ed. J. Schanda, John Wiley & Sons Inc., Hoboken, New Jersey USA, Chapter 11, 2007, 261-294.

48. R.W.G. Hunt, 'The Future of Colorimetry in the CIE' In *Colorimetry, Understanding the CIE system*, ed. J. Schanda, John Wiley & Sons, Inc., Hoboken, New Jersey USA, 2007, Chapter 14, 355-362.

49. Commission Internationale de L'Éclairage, CIE 116-1995, *Industrial Colour Difference Evaluation,* CIE Central Bureau, Vienna Austria, 1995.

50. K. Witt, 'CIE Colour Difference Metric', In *Colorimetry; system, Understanding the CIE system*, ed. J. Schanda, John Wiley and Sons Inc., Hoboken, New Jersey USA, 2007, Chapter 4, 79-100.

51. K. McLaren, *The Colour Science of Dyes and Pigments.* A. Hilger Ltd., Bristol England, 2nd edition, 1986.

52. B. Rigg, 'Colorimetry and the CIE system', In *Colour Physics for Industry*, ed. R. McDonald, Society of Dyers and Colourists, Bradford, West Yorkshire England, 1997, 2nd edition, Chapter 3, 81-120.

53. R.W.G. Hunt and R.M. Pointer, *Measuring Colour*, John Wiley & Sons Ltd., Chichester England, 4th edition, 2011, 42ff.

54. D.L. MacAdam, 'Visual Sensitivites to Color Differences in Daylight', *Journal of the Optical Society of America*, 1942, **32**, 5, 247-274.

55. G. Wyszecki and W.S. Stiles. *Color Science, Concepts and Methods, Quantitative Data and Formulae.* Wiley Classic Library Edition, New York USA, 2nd edition, 2000, 306.

56. N. Ohta and A.R. Robertson, *Colorimetry. Fundamentals and Applications*, John Wiley and Sons Ltd., Chichester, West Sussex England, 2005, 136-138.

57. W.D. Wright, 'The sensitivity of the eye to small colour differences', *Proceedings of the Physical Society in London,* London UK, 1941, **53**, 2, 93-112.

58. W.D. Wright and F.H.G. Pitt, 'Hue discrimination in normal color-vision', *Proceedings of the Physical Society in London*, London, 1934, **46**, 3, 459-473.

59. Fairchild, M.D., *Color Appearance Models*, John Wiley & Sons, West Sussex England, 2nd edition, 2005.

60. Lee, H.C., *Introduction in Color Imaging Science*, Cambidge University Press, Cambridge England, 2005, 323-324.

61. G. Wyszecki and W.S. Stiles. *Color Science, Concepts and Methods, Quantitative Data and Formulae.* Wiley Classic Library Edition, New York USA, 2nd edition, 2000, 493.

62. K.J. Smith, 'Colour-order systems, colour spaces, colour difference and colour scales', In *Colour Physics for Industry*, ed. R. McDonald, Society of Dyers and Colourists, Bradford England, 1997, 2nd edition, Chapter 4, 123.

63. S.M. Newhall, D. Nickerson, and D.B. Judd, 'Final Report of the O.S.A. Subcommitee on the Spacing of the Munsell Colors', *Journal of the Optical Society of America*, 1943, **33**, 7, 385-418.

64. D.B. Judd, 'Chromaticity sensibility to stimulus differences', *Journal of the Optical Society of America*, 1932, **22**, 2, 72-108.

65. Judd, D.B., 'A Maxwell Triangle yielding uniform chromaticity scales', *Journal of the Optical Society of America*, 1935, **25**, 1, 24-35.

66. R.G. Kühni, *Color Space and its division*, John Wiley and Sons Inc., Hoboken, New Jersey USA, 2003.

67. K.J. Smith, 'Colour-order systems, colour spaces, colour difference and colour scales', In *Colour Physics for Industry*, ed. R. McDonald, Society of Dyers and Colourists, Bradford England, 1997, 2nd edition, Chapter 4, 131.

68. D.L. MacAdam, 'Projective Transformations of ICI Color Specifications', *Journal of the Optical Society of America*, 1937, **27**, 8, 294-297.

69. R.S. Hunter, 'Photoelectric Tristimulus Colorimetry with Three Filters, *Journal of the Optical Society of America*, 1942, **32**, 9, 509-538.

70. D.B. Judd, 'Hue, saturation, and lightness of surface colors with chromatic illumination', *Journal of Research of the National Bureau of Standards*, 1940, **24**, 3, 293.

71. E. Hering, *Outlines of a theory of light sense,* translated by L.M. Hurvich and D. Jameson, Harvard University Press, Cambridge, Massachusetts USA, 1964.

72. R.S. Berns, *Billmeyer and Saltzmann's Principles of Color Technology*, John Wiley & Sons Inc., New York USA, 3rd edition, 2000.

73. F. Scofield, 'A Method for Determination of Color Differences', *Circular 664 of the National Paint, Varnish, and Lacquer Association*, 1943.

74. K. McLaren, 'The Adams-Nickerson Colour Difference Formula', *Journal of the Society of Dyers and Colourists*, 1970, **86**, 8, 354-356.

75. E.Q. Adams, 'Chromatic Valence as a Correlate of Munsell Chroma', *Journal of the Optical Society of America*, 1943, **33**, 12, 679-679.

76. K. McLaren, 'The Development of the Geometric Grey Scales for Fastness Assessment: Fastness Tests Co-ordinating Committee', *Journal of the Society of Dyers and Colourists*, 1953, **69**, 11, 404-409.

77. American Association of Textile Chemists and Colorists, AATCC Evaluation Procedure 1, '*Gray Scale for Color Change*', AATCC, USA, 2007.

78. American Association of Textile Chemists and Colorists, AATCC Evaluation Procedure 2, '*Gray Scale for Staining*', AATCC, USA, 2007.

79. American Society for Testing and Materials, ASTM D2616-12, '*Standard Test Method for Evaluation of Visual Color Difference With a Gray Scale*', ASTM, Subcomittee E12-11, PA USA, 2012.

80. British Standard Institution, BS EN 20105-A02:1995 (ISO 105-A02:1993), *Textiles – Test for colour fastness – Part A02: Greyscale for assessing change in colour*, BSI EN ISO, London UK, 1995.

81. D. Nickerson, 'The specification of color tolerances', *Textile Research*, 1936, **6**, 505-514.

82. R.S. Hunter and R.W. Harold, *The Measurement of Appearance*, John Wiley & Sons Inc., New York USA, 2nd edition, 1987.

83. I.A. Balinkin, 'Measurement and designation of small colour differences', *The Bulletin of the American Ceramic Society*, 1941, **20**, 392-402.

84. F.W. Billmeyer and M. Saltzman, *Principles of Color Technology*, John Wiley & Sons Inc., New York USA, 2nd edition, 1981, 98.

85. D. Nickerson and F.K. Stultz, 'Color Tolerance Specification', *Journal of the Optical Society of America*, 1944, **34**, 9, 550-570.

86. B.R. Bellamy and S.M. Newhall, 'Attributive Limens in Selected Regions of the Munsell Color Solid', *Journal of the Optical Society of America*, 1942, **32**, 8, 465-473.

87. I.H. Godlove, 'Improved Color Difference Formula with Applications to the Perceptibility and Acceptability of Fadings', *Journal of the Optical Society of America*, 1951, **41**, 11, 760-772.

88. D.L. MacAdam, 'Specfication of Small Chromaticity Differences', *Journal of the Optical Society of America*, 1943, **33**, 1, 18-26.

89. W.R.J Brown, 'Color Discrimination of Twelve Observers', *Journal of the Optical Society of America*, 1957, **47**, 2, 137-143.

90. R.M. Rich, F.W. Billmeyer, and W.G. Howe, 'Methods for Deriving Color Difference Perceptibility Ellipses for Surface Color Samples', *Journal of the Optical Society of America*, 1975, **65**, 8, 956-959.

91. L. Silberstein, 'Investigations on the Intrinsic Properties of the Color Domain', *Journal of the Optical Society of America*, 1938, **28**, 3, 63-85.

92. H.R. Davidson and E. Friede, 'The Size of Acceptable Color Differences, *Journal of the Optical Society of America,* 1953*,* **43**, 7, 581-589.

93. F.T. Simon and W.J. Goodwin, 'Rapid Computation of Small Colour Differences', *American Dyestuff Reporter*, 1958, **47**, 4, 105-112.

94. R.S. Foster, 'Color Speed Computing Charts, A New Simplified System of Charts for Rapid Color Difference Calculations', *Color Engineering*, 1966, **4**, 1, 17-26.

95. D.L. MacAdam, 'Smoothed Version of Friele's 1965 Approximations for Color Metric Coefficients', *Journal of the Optical Society of America*, 1966, **56**, 12, 1784-1-1785.

96. K.D. Chickering, 'Optimization of the MacAdam-Modified 1965 Friele Color-Difference Formula', *Journal of the Optical Society of America*, 1967, **57**, 4, 537-540.

97. K.D. Chickering, 'FMC Color Difference Formula', *Journal of the Optical Society of America*, 1971, **61**, 1, 118.

98. F.T. Simon, 'Small colour differences computation and control, *Die Farbe*, 1961, **10**, 225-234.

99. F.T. Simon and W.J. Godwin, *Rapid Graphical Computation of Small Color Differences,* Bakelight Company, New York USA, 1957.

100. J.L. Saunderson and B.I. Milner, 'Modified Chromatic Value Color Space', *Journal of the Optical Society of America*, 1946, **36**, 1, 36-41.

101. D. Nickerson, 'Munsell Renotations used to study color spaces of Hunter and Adams', *Journal of the Optical Society of America*, 1950a, **40**, 2, 85.

102. D. Nickerson, 'Tables for use in computing small color differences', *American Dyestuff Reporter*, 1950b, **39**, 541-549.

103. L.G. Glasser, A.H. McKinney, C.D. Reilly, and P.D. Schnelle, 'Cube-Root Color Coordinate System', *Journal of the Optical Society of America*, 1958, **48**, 10, 736-740.

104. I.G. Priest, K.S. Gibson, and J.J. McNicholas, 'An examination of the Munsell color system I. Spectral and total reflection and the Munsell scale of value', *US National Bureau of Standards*, NW Washington, DC USA, Technical Paper 167, 1920.

105. R.G. Kühni, *Color. An introduction to Practice and Principles*, John Wiley and Sons Inc., Hoboken, New Jersey USA, 2nd edition, 2005, 100.

106. K. McLaren, 'The precision of textile color matches in relation to colour difference measurements', in *Proceedings of the Internationale Color Association*, 09.06.1969, Stockholm Sweden, 1969, 688-706.

107. G. Wyszecki, 'Proposal for a new color-difference formula', *Journal of the Optical Society of America*, 1963, **53**, 11, 1318-1319.

108 N. Ohta and A.R. Robertson, *Colorimetry. Fundamentals and Applications*, John Wiley and Sons Ltd., Chichester, West Sussex England, 2005, 135.

109. K. McLaren, *The Colour Science of Dyes and Pigments.* A. Hilger Ltd., Bristol England, 2nd edition, 1986, 132.

110. A. Berger and A. Brockes, 'Die Genauigkeit von Dreifilter-Meßgeräten bei der Messung von bedingt-gleichen Probenpaaren', *Vortrag Internationaler Farbtagung Luzern*, 1965, Tagungsbericht, 457-472.

111. E. Coates, S. Day, J.R. Provost, and B. Rigg, 'The Measurement and Assessment of Colour Differences for Industrial Use II: The Accuracy of Colour Difference Equations', *Journal of the Society of Dyers and Colourists*, 1972, **88**, 10, 363-368.

112. K. McLaren, 'The Development of the CIE 1976 (L*a*b*) Uniform Colour Space and Colour Difference Formula', *Journal of the Society of Dyers and Colourists*, 1976, **92**, 9, 338-341.

113. K. McLaren and B. Rigg, 'The SDC Recommended Colour Difference Formula: Change to CIELAB', *Journal of the Society of Dyers and Colourists*, 1976, **92**, 9. 337-338.

114. R. McDonald, 'The Effect of Non-uniformity in ANLAB Colour Space Interpretation of Visual Colour Differences', *Journal of the Society of Dyers and Colourists*, 1974, **90**, 6, 189-198.

115. R.G. Kühni, 'Acceptibility contours and small color difference formulas', *Journal of Color and Appearance*, 1971c, **1**, 1, 30-35, 42.

116. L.F.C. Friele, 'Analysis of the Brown and Brown-MacAdam Colour Discrimination Data', *Die Farbe*, 1961, **10**, 193-224.

117. D.L. MacAdam, 'Uniform Color Scales', *Journal of the Optical Society of America*, 1974, **64**, 12, 1691-1702.

118. K.J. Smith, 'Colour-order systems, colour spaces, colour difference and colour scales', In *Colour Physics for Industry*, ed. R. McDonald, Society of Dyers and Colourists, Bradford England, 1997, 2nd edition, Chapter 4, 136.

119. D. Eastwood, 'A Simple modification to improve visual uniformity of the CIE 1964 U*V*W* colour space', *Die Farbe*, 1975, **24**, 97-108.

120. K. Witt, 'CIE Colour Difference Metric', In *Colorimetry; system, Understanding the CIE system*, ed. J. Schanda, John Wiley and Sons Inc., Hoboken, New Jersey USA, 2007, Chapter 4, 79-98.

121. European Committee for Standardization, EN ISO 11664-4:2011, *Colorimetry - Part 4: CIE 1976 L*a*b* Colour Space (ISO 11664-4:2008)*, CEN, Brussels Belgium, 2011a.

122. European Committee for Standardization, EN ISO 11664-5:2011, *Colorimetry - Part 5: CIE 1976 L*u*v* Colour Space and u'v' uniform chromaticity scale diagram (ISO 11664-5:2009)*, CEN, Brussels Belgium, 2011b.

123. R.G. Kühni, 'Color-tolerance data and the tentative CIE 1976 L*a*b* formula', *Journal of the Optical Society of America*, 1976, **66**, 5, 497-500.

124. R.G. Kühni, *Color. An introduction to Practice and Principles*, John Wiley and Sons Inc., Hoboken, New Jersey USA, 2nd edition, 2005, 102-103.

125. A.R. Robertson, 'CIE Guidlines for Coordinated Research on Color-Difference Evaluation', *Color research and application*, 1978, **3**, 149-151.

126. Commission Internationale de L'Éclairage, CIE 101-1993, *Parametric Effects in Colour Difference Evaluation*, CIE Central Bureau, Vienna Austria, 1993.

127. R.S. Hunter and R.W. Harold, *The Measurement of Appearance*, John Wiley & Sons Inc., New York USA, 2nd edition, 1987.

128. K. McLaren, 'Multiple linear regression: A new technique for improving colour difference formuale', *Colour metrics, Proceedings of the Helmholtz Memorial Symposium for the International Color Association,* ed. J.J. Voß, F.C. Friele, and P.L.Walraven, 01.09.1971, Driebergen Netherlands, 1971, 296-307.

129. R. McDonald, 'Industrial Pass/Fail Colour Matching Part 1 - Preparation of Visual Colour Matching Data', *Journal of the Society of Dyers and Colourists,* 1980a, **96**, 7, 372-376.

130. R. McDonald, 'Industrial Pass/Fail Colour Matching Part II - Methods of Fitting Tolerance Ellipsoids', *Journal of the Society of Dyers and Colourists*, 1980b, **96**, 8, 418-433.

131. R. McDonald, 'Industrial Pass/Fail Colour Matching Part III - Development of a Pass/Fail Formula for use with Instrumental Measurement of Colour Difference', *Journal of the Society of Dyers and Colourists*, 1980c, **96**, 9, 486-496.

132. R. McDonald, 'A review of the relationship between visual and instrumental assessment of colour difference – Part 1', *The Journal of the Oil Color Chemists Association*, 1982, **65**, 2, 43-53.

133. D. Alman, R.S. Berns, D.G. Snyder, and W.A. Larsen, 'Performance Testing of Color-Difference Metrics Using a Color Tolerance Dataset', *Color research and application*, 1989, **14**, 3, 139-151.

134. K.J. Smith, 'Colour-order systems, colour spaces, colour difference and colour scales', In *Colour Physics for Industry*, ed. R. McDonald, Society of Dyers and Colourists, Bradford England, 1997, 2nd edition, Chapter 4, 152.

135. R.S. Hunter and R.W. Harold, *The Measurement of Appearance*, John Wiley & Sons Inc., New York USA, 2nd edition, 1987.

136. F.J.J. Clarke, R. McDonald, and B. Rigg, 'Modification to the JPC79 Colour Difference Formula', *Journal of the Society of Dyers and Colourists*, 1984, **100**, 4, 128-132, 281-282.

137. M.R. Luo and B. Rigg, 'Chromaticity - discrimination ellipses for surface colours', *Color research and application*, 1986*,* **11**, 1, 25-42.

138. M.R. Luo and B. Rigg, 'BFD(l:c) colour difference formula: Part 1 - Development of the formula', *Journal of the Society of Dyers and Colourists*, 1987a, **103**, 2, 86-94.

139. M.R. Luoand B. Rigg, 'BFD(l:c) colour difference formula Part 2 - Performance of the formula', *Journal of the Society of Dyers and Colourists*, 1987b, **103**, 3, 126-132.

140. T. Seim and A. Valberg, 'Towards a uniform Color Space: A better formula to describe the Munsell and OSA Color Scales', *Color research and application*, 1986, **11**, 1, 11-24.

141. M. Cheung and B. Rigg, 'Colour difference ellipsoids for five CIE colour centres', *Color research and application*, 1986, **11**, 3, 185-195

142. S. Badu, 'Large colour differences between surface colours, *Ph.D. thesis, University of Bradford*, 1986.

143. K. Witt, 'Three-dimensional threshold of color-difference perceptibility in painted samples: variability of observers in four CIE color regions', *Color research and application*, 1987, **12**, 3 ,128-134.

144. R.S. Berns, D.H. Alman, L. Reniff, G.D. Snyder, and M.R. Balonon-Rosen, 'Visual Determination of Suprathreshold Color Difference Tolerances Using Probit Analysis', *Color research and application*, 1991, **16**, 5, 297-316.

145. H.G. Völtz, *Industrial Color testing; Fundamentals and Techniques.* VCH Verlagsgesellschaft mbH, Weinheim Deutschland, 1995.

146. D. Alman, 'CIE Technical Committee 1-29: Industrial Color-Difference Evaluation Progress Report', *Color research and application*, 1993, **18**, 2, 137-139.

147. R.S. Berns, 'The Mathematical Development of CIE TC 1-29 Proposed Color Difference Equation: CIELCH', in *Proceedings of the 7th Congress of the International Color Association,* ed. A. Nemcsics and J. Schanda, 13.06.1993, Budapest Hungary, 1993, **B***,* C11-1C11-5.

148. K. Witt, 'Modified CIELAB formula tested using a textile pass/fail data set', *Color research and application*, 1994, **19**, 4, 273-276.

149. K. Witt, 'CIE guidelines for coordinated future work on industrial color-difference evaluation', *Color research and application*, 1995, **20**, 6, 399-403.

150. R. McDonald and K.J. Smith, 'CIE94 - a new colour-difference formula', *Journal of the Society of Dyers and Colourists,* 1995*,* **111**, 12, 376-379.

151. D. Heggie, R.H. Wardman, and M.R. Luo, 'A comparison of the colour differences computed using the CIE94, CMC(*l:c*) and BFD(*l:c*) formulae', *Journal of the Optical Society of America*, 1996, **112**, 10, 264-269.

152. M.R. Luo, Conversation with D. Alman – Chairman CIE TC 1-47, 20.01.1998.

153. R.G. Kühni, 'Analysis of Five Sets of Color Difference Data', *Color research and application*, 2001, **26**, 2, 141-150.

154. R.G. Kühni, 'Towards an Improved Uniform Color Space', *Color research and applicaton,* 1999, **24**, 4, 253-265.

155. D. Kim and J.H. Nobbs, 'New weighting functions for the weighted CIELAB colour difference formula', in *Proceedings for the 8th Congress of the International Color Association*, 25.05.1997, Kyoto Japan, 446-449.

156. K. Thomsen, 'A Euclidean Color Space in High Agreement with the CIE94 Colour Difference Formula', *Color research and application*, 2000, **25**, 1, 64-65.

157. M.R. Pointer and G.G. Attridge, 'Some aspects of the visual scaling of lare colour differences ', *Color research and application*, 1997, **25**, 2, 298-307.

158. K. Witt, 'Geometric relations between scales of small colour differences', *Color research and application*, 1999, **24**, 2, 78-92.

159. S.S. Guan and M.R. Luo., 'Investigation of Parametric Effects using small Colour Differences', *Color research and application*, 1999b, **24**, 5, 332-343.

160. S.S. Guan and M.R. Luo., 'A colour difference formula for assessing large colour differences', *Color research and application*, 1999a, **24**, 5, 344-355.

161. J.H Nobbs, Lightness difference weighting terms 'S_L', CIE Report TC1-47, 06/1999.

162. W. Chou, H. Lin, M.R. Luo, S. Westland, B. Rigg, and J. Nobbs, 'Performance of lightness difference formulae', *Coloration Technology*, 2001, **117**, 1, 19-29.

163. K. Witt, CIE Reporter Colour Difference Evaluation, Report to Devision 1, 1999.

164. E. Rohner and D.C. Rich, 'Eine angenähert gleichförmige Farbabstandsformel für industrielle Farbtoleranzen von Körperfarben', *Die Farbe*, 1996, **42**, 207-220.

165. G. Cui, M.R. Luo, B Rigg, G Rösler, and K. Witt, 'Uniform Colour Spaces based on the DIN99 Colour Difference Formula', *Color research and application*, 2002, **27**, 4, 282-290.

166. Deutsches Institut für Normung e.V., DIN 6176, *Colorimetric evaluation of colour differences for surface colours according to DIN99 – formula*, DIN, Berlin Germany, 03/2001.

167. M. Richter and K. Witt, 'The story of the DIN color system', *Color research and application*, 1986, **11**, 2,138-145.

168. M.R. Luo, Correspondence in regards to the CIE committee TC1-47 meeting in Teddington, UK, 04.04.2000.

169. Commission Internationale de L'Éclairage, CIE 142-2001, *Improvement to Industrial Colour Difference Evaluation*, CIE Central Bureau, Vienna Austria, 2001.

170. R.S. Berns, 'Derivation of a Hue-Angle Dependent, Hue Difference Weighting Function for CIEDE2000', in *Proceedings of the SPIE: 9th Congress of the International Color Association,* ed. R. Chung and R. Rodrigues, 06.06.2002*,* Rochester USA, 2002, **4421***,* 638-1735.

171. Y. Qiao, R.S. Berns, L. Reniff, and E. Montag, 'Visual determination of hue superthreshold color-difference tolerances', *Color research and application*, 1998, **23**, 5, 302-313.

172. T. Maier, T., 'Personal communication', 1992.

173. K. Witt and G. Döring, 'Parametric variations in a threshold color difference ellipsoid for green painted samples',*Color research and application*, 1983, **8**, 3, 153-163.

174. M.R. Luo, Private communication with R.S. Berns, 1999

175. Commission Internationale de L'Éclairage, CIE 015.3-2004, *Colorimetry - Technical Report*, CIE Central Bureau, Vienna Austria, 3rd edition, 2004c.

176. K. Witt, 'CIE Colour Difference Metric', In *Colorimetry; system, Understanding the CIE system*, ed. J. Schanda, John Wiley and Sons Inc., Hoboken, New Jersey USA, 2007, Chapter 4, 79-98.

177. D.H. Alman, D.H., CIE Chairman TC1-47 Progress report – CIEDE2000, 06/2000.

178. M.R. Luo, G. Cui, and B. Rigg, Performance of the CIEDE2000 Colour Difference Equation – Statistical Significance of new Terms – Report to CIE TC1-47, 05/2000

179. M. Melgosa and R. Huertas, 'Relative significance of the terms in the CIEDE2000 and CIE94 colour difference formulas', *Journal of the Optical Society of America*, 2004*,* **21**, 12, 2269-2275.

180. R.G. Kühni, *Color Space and its division*, John Wiley and Sons Inc., Hoboken, New Jersey USA, 2003.

181. C.C. Semmelroth, 'Prediction of Lightness and brightness on different backgrounds', *Journal of the Optical Society of America*, 1970, **60**, 12, 1685-1689.

182. C.C. Semmelroth, 'Adjustment of the Munsell value and W* scale to uniform lightness steps for various background reflectances', *Applied Optics*, **10**, 1, 14-18.

183. L.M. Hurvich and D. Jameson, 'Pereceived colour, induction effects, and opponent response mechanism, *The Journal of General Physiology*, 1960, **43**, 6, 63-80.

184. R.W.G. Hunt and R.M. Pointer, *Measuring Colour*, John Wiley & Sons Ltd., Chichester England, 4th edition, 2011, 183-187.

185. Huertas, R., M. Melgosa, and C. Oleari, 'Performance of a colour difference formula based on OSA-UCS space using small-medium color diffferences, *Journal of the Optical Society of America*, 2006, **23**, 9, 2077-2084.

186. C. Oleari, M. Melgosa, and R. Huertas, 'Euclidean color-difference formula for small-medium coloiur differences in log-compressed OSA-UCS space', *The Journal of the Optical Society of America*, 2009, **26**, 1, 121-134.

187. R.S. Berns and Y. Zue, 'Optimizing color-difference equations and uniform color spaces for industrial tolerancing', in *Proceedings of the Midterm Meeting of the International Color Association*, ed Y.E. Guanrong and X.U. Haisong, 12.07.2007, Hangzhuo China, 2007, 24-28.

188. P. Urban, M. Rosen, R.S. Berns, and D. Schleicher, 'Embedding non-Euclidean color spaces into Euclidean color spaces with minimal isometric disagreement', *Journal of the Optical Society of America*, 2007, **24**, 6, 1516-1528.

189. R.W.G Hunt, R.W.G. and R.M. Pointer, *Measuring Colour*, John Wiley & Sons Ltd., Chichester England, 4th edition, 2011, 315.

190. R.W.G. Hunt, 'A model of colour vision for predicting colour appearance', *Color research and application*, 1982, **7**, 2, 95-112.

191. Y. Nayatani, K. Takahama, H. Sobagaki, K. Hashimoto, 'Color appearance model and chromatic adaption transform', *Color research and application*, 1990, **15**, 4, 210-221.

192. M.D. Fairchild and R.S. Berns, 'Image color-appearance specification through extension of CIELAB', *Color research and application*, 1993, **18**, 3, 178-190

193. W.G. Kuo, M.R. Luo, and H.E. Bez, 'Various chromatic adaption transformations tested using new colour appearance data in textiles', *Color research and application*, 1995, **20**, 5, 313-327.

194. R.W.G. Hunt, 'Light and dark adaption and perception of color', *Journal of the Optical Society of America*, 1952, **42**, 3, 190-199.

195. J.C. Stevens and S.S. Stevens, 'Brightness functions: Effects of adaption', *Journal of the Optical Society of America*, 1963, **53**, 3, 375-385.

196. C.J. Bartleson and E.J. Breneman, 'Brightness perception in complex fields', *Journal of the Optical Society of America*, 1967, **57**, 7, 953-957**.**

197. M.R. Luo, X.W Gao, and S.A.R. Scriviner, 'Quantifying colour appearance, Part - 5, Simultanous contrast', *Color research and application*, 1995, **20**, 1, 18-28.

198. C.J. Li, M.R. Luo, and G.H. Cui, 'Colour-difference evaluation using colour appearance models', *Proceedings of the 11th Colour Imaging Conference IS&T and SID*, eds. B. Funt and G. Marcu, 05.11.2003, Scotsdale, Arizona USA, 2003.

199. M.R. Luo, G. Cui, and C. Li, 'Uniform Colour Spaces based on CIECAM02 Colour Appearance Model', *Color research and application*, 2006, **31**, 4, 320-330.

200. American Association of Textile Chemists and Colorists, AATCC Evaluation Procedure 9, '*Visual Assessment of Color Difference of Textiles*', AATCC, USA, 2011.

201. American Society for Testing and Materials, ASTM E308-08, '*Standard practice for computing the colors of objects by using the CIE system*', ASTM, PA USA, 2008.

202. R. McDonald, 'European Practices and Philosophy in Industrial Colour-difference Evaluation', *Color research and application*, 1990, **15**, 5, 249-260.

203. T. Steder, Private Conversation with C. Dearing – Technology Director Coats plc, 03/2012.

204. C. Soanes and S. Hawker, *Oxford English Dictionary for Students*, Oxford University Press, Oxford England, 2005.

205. E.R. Jacobson, 'Fundamentals of Light and Vision', in *The Manual of Photography,* Reed Educational and Professional Publishing Ltd., Oxford UK, 9th edition, Chapter 2, 2000, 9-15.

206. R.S. Sinclair, R.S., 'Light, light sources and light interactions', In *Colour Physics for Industry*, ed. R. McDonald, Society of Dyers and Colourists, Bradford, West Yorkshire England, 1997, 2nd edition, Chapter 1, 1-56.

207. K. Nassau, 'The Fifteen Causes of Color', in *Color for Science, Art and Technology*, ed. K. Nassau, Elsevier Science B.V., Amsterdam Netherlands, 1998.

208. H.C. Lee, *Introduction in Color Imaging Science*, Cambidge University Press, Cambridge England, 2005, 57.

209. O. Packer and D.R. Williams, 'Light, the Retinal Image, and Photoreceptors', in *The Science of Color*, ed. S.K. Shevell, *The Optical Society of America*, NW Washington, DC USA, 2003, 41-201.

210. G. Wyszecki and W.S. Stiles. *Color Science, Concepts and Methods, Quantitative Data and Formulae.* Wiley Classic Library Edition, New York USA, 2nd edition, 2000, 19.

211. N. Ohta and A.R. Robertson, *Colorimetry. Fundamentals and Applications*, John Wiley and Sons Ltd., Chichester, West Sussex England, 2005, 91-92.

212. R.S. Sinclair, 'Light, light sources and light interactions', In *Colour Physics for Industry*, ed. R. McDonald, Society of Dyers and Colourists, Bradford, West Yorkshire England, 1997, 2nd edition, Chapter 1, 17-19.

213. R.W.G. Hunt and R.M. Pointer, *Measuring Colour*, John Wiley & Sons Ltd., Chichester England, 4th edition, 2011, 88.

214. Commission Internationale de L'Éclairage, CIE 016–1970, *Daylight*, CIE Central Bureau, Vienna Austria,1970.

215. Commission Internationale de L'Éclairage, CIE 085-1989, *Solar Spectral Irradiance*, CIE Central Bureau, Vienna Austria, 1989.

216. British Standard Institution, BS EN 950-1:1967, *Specification for artificial daylight for the assessment of colour. Illuminant for colour matching and colour appraisal*, BSI, London UK, 1967.

217. H.C. Lee, *Introduction in Color Imaging Science*, Cambidge University Press, Cambridge England, 2005, 43-47.

218. G. Wyszecki and W.S. Stiles. *Color Science, Concepts and Methods, Quantitative Data and Formulae.* Wiley Classic Library Edition, New York USA, 2nd edition, 2000, 224.

219. R.W.G. Hunt and R.M. Pointer, *Measuring Colour*, John Wiley & Sons Ltd., Chichester England, 4th edition, 2011, 85-86.

220. R.S. Sinclair, 'Light, light sources and light interactions', In *Colour Physics for Industry*, ed. R. McDonald, Society of Dyers and Colourists, Bradford, West Yorkshire England, 1997, 2nd edition, Chapter 1, 15-16.

221. R.W.G. Hunt, *Measuring Colour*, Fountain Press, Kingston-upon-Thames England, 3rd edition, 1998, 74.

222. W. Budde, 'Spectral Energy Distribution of natural daylight', Private Communicatons, 1963.

223. H.R. Condit and F. Grum, 'Spectral energy distribution of daylight', *Journal of the Optical Society in America,* 1964, **54**, 7, 937.

224. S.T. Henderson and D. Hodgkiss, 'The spectral energy distribution of daylight', *The British Journal of Applied Physics*, 1963, **14**, 125.

225. Commission Internationale de L'Éclairage, CIE TC 2.2 No. 20, *Recommendations for the Integrated Irradiance and the Spectral Distribution of Simulated Solar Radiation for Testing Purposes,* CIE Central Bureau, Vienna Austria, 1972.

226. Commission Internationale de L'Éclairage, CIE 015.2-1986, *Colorimetry - Technical Report*, CIE Central Bureau, Vienna Austria, 2nd edition, 1986.

227. D.B. Judd, D.L. MacAdam, G.W. Wyszecki, H.W. Budde, H.R. Condit, S.T. Henderson, and J.L. Simonds, 'Spectral Distribution of typical daylight as a function of correlated color temperature', *Journal of the Optical Society of America*, 1964, **54**, 8, 1031-1040.

228. H.C. Lee, *Introduction in Color Imaging Science*, Cambidge University Press, Cambridge England, 2005, 13-28.

229. Commission Internationale de L'Éclairage, CIE TC 2.3 No. 38, *Radiometric and Photometric Characteristics of Materials and Their Measurement,* CIE Central Bureau, Vienna Austria, 1977.

230. R.L.M Allen, *Colour Chemistry,* Thomas Nelson and Sons Ltd., London, 1971.

231. K. McLaren, *The Colour Science of Dyes and Pigments.* A. Hilger Ltd., Bristol England, 2nd edition, 1986, 25-28.

232. J.W. Strutt, 'On the light from the sky, its polarization and colour', *Philosophical Magazine*, 1871, **XLI**, 107-120, 274-279.

233. F.A. Jenkins and H.E. White, *Fundamentals of Optics*, McGraw-Hill Education, Maidenhead UK, 4th edition, 1981.

234. W. Sellmeier, 'Zur Erklärung der abnormen Farbenfolge im Spectrum einiger Substanzen', *Annalen der Physik und Chemie*, 1871, **219**, 272-282.

235. E.R. Jacobson, 'Fundamentals of Light and Vision', in *The Manual of Photography,* Reed Educational and Professional Publishing Ltd., Oxford UK, 9th edition, Chapter 2, 2000, 11.

236. G. Wyszecki and W.S. Stiles. *Color Science, Concepts and Methods, Quantitative Data and Formulae.* John Wiley & Sons Inc., New York USA, 2nd edition, 1982, 84.

237. R.W.G. Hunt, *Measuring Colour*, Fountain Press, Kingston-upon-Thames England, 3rd edition, 1998, 19-23.

238. D. Hubel, *David Hubel's Eye, Brain, and Vision* [online], [accessed 06.07.2012] Available from: http://hubel.med.harvard.edu/book/bcontex.htm.

239. O. Packer and D.R. Williams, 'Light, the Retinal Image, and Photoreceptors', in *The Science of Color*, ed. S.K. Shevell, *The Optical Society of America*, NW Washington, DC USA, 2003, 48-49.

240. J. Neitz, J. Carroll, Y. Yamauchi, M. Neitz, and D.R. Williams, 'Color perception is mediated by a plastic neural mechanism that remains adjustable in adults', *Neurons*, 2002, **35**, 4, 783-792.

241. G. Wyszecki and W.S. Stiles. *Color Science, Concepts and Methods, Quantitative Data and Formulae.* John Wiley & Sons Inc., New York USA, 2nd edition, 1982, 84.

242. G. Wyszecki and W.S. Stiles. *Color Science, Concepts and Methods, Quantitative Data and Formulae.* John Wiley & Sons Inc., New York USA, 2nd edition, 1982, 85-86.

243. W.G. Stell, 'The morphological organisation of the vertebrate retina', in *Handbook of Sensory Physiology Vol. II/B. Physiology of Photoreceptor Organs*, eds. M.G.F. Fuortes, Springer Verlag Berlin Deutschland, 1972, 111-213.

244. H.J.A. Dartnall, J.K. Bowmaker, and J.D. Mollon, 'Human visual pigments: Microspectrophotometric results from the eyes of seven persons', in *Proceedings of the Royal Society of London*, 22.11.1983, London UK, 1983, **220**, 1218, 115-130.

245. H.C. Lee, *Introduction in Color Imaging Science*, Cambidge University Press, Cambridge England, 2005, 302-303.

246. G. Wyszecki and W.S. Stiles. *Color Science, Concepts and Methods, Quantitative Data and Formulae.* Wiley Classic Library Edition, New York USA, 2nd edition, 2000, 87.

247. H.C. Lee, *Introduction in Color Imaging Science*, Cambidge University Press, Cambridge England, 2005, 308.

248. P. Lennie, 'The Physiology of Color Vision', in *The Science of Color*, ed. S.K. Shevell, Optical Society of America, Kidlington, Oxfordshire England, 2003, Chapter 6, 218-242.

249. H.C. Lee, *Introduction in Color Imaging Science*, Cambidge University Press, Cambridge England, 2005, 311.

250. A.M. Derrington, J. Krauskopf, and P. Lennie, 'Chromatic mechanism in lateral geniculate nucleus of macaque', *The Journal of Physiology*, 1984, **357**, 241-265.

251. R.W.G. Hunt and R.M. Pointer, *Measuring Colour*, John Wiley & Sons Ltd., Chichester England, 4th edition, 2011, 8.

252. P.L. Walraven and J.J. Vos, 'On the derivation of the foveal receptor primaries', *Vision research*, 1971, **11**, 8, 799-818.

253. G.E. Müller 'Über die Farbempfindungen. Psychophysische Untersuchungen', *Zeitschrift für Psychologie,* Barth, Leipzig Deutschland, Ergänzungsband 17 und 18, 1930.

254. D.B. Judd 'Response functions for types of vision according to the Müller theory', *Journal of Research of National Bureau of Standards*, 1949, **1**, 1, 1-16.

255. D.B. Judd, 'Basic correlates of the visual stimulus', in *Handbook of Experimental Psychology*, ed. S.S. Stevens, Wiley, Oxford England, 1951, 811-867.

256. L.M. Hurvich and D. Jameson, 'Some quantitative aspects of an opponent-colors theory. II. Brightness, saturation, and hue in normal and dichromatic', *Journal of the Optical Society of America*, 1955, **45**, 8, 602-616.

257. E.H. Land, 'The Retinex Theory of Colour Vision', in *Proceedings of the Royal Institute of Great Britain*, 1974, **47**, 23-58.

258. R.W.G. Hunt and R.M. Pointer, *Measuring Colour*, John Wiley & Sons Ltd., Chichester England, 4th edition, 2011, 25.

259. Coblentz, W.W., and W.B. Emerson, 'Relative sensibility of the average eye to light of different colors and some practical applications of radiation problems', *Bulletin of the Bureau of Standards*, 1918, **14**, 167-236.

260. E.P. Hyde, W. E. Forsythe, and F.E. Cady, 'The visibility of radiation', *Astrophysical Journal.*, 1918, **48**, 65-88.

261. E.P. Hyde, W. E. Forsythe, and F.E. Cady, 'The visibility of radiation', *Astrophysical Journal.*, 1918, **48**, 65-88.

262. L.W. Hartman, 'Visibility of radiation in the blue end of the visible spectrum', *Astrophysical Journal,* 1918, **47**, 83-95.

263. G. Wyszecki and W.S. Stiles. *Color Science, Concepts and Methods, Quantitative Data and Formulae.* John Wiley & Sons Inc., New York USA, 2nd edition, 1982, 395.

264. Commission Internationale de L'Éclairage, CIE 086-1990, *CIE 1988 2° Spectral Luminous Efficiency Function for Photopic Vision,* CIE Central Bureau, Vienna Austria, 1990.

265. G. Wyszecki and W.S. Stiles. *Color Science, Concepts and Methods, Quantitative Data and Formulae.* John Wiley & Sons Inc., New York USA, 2nd edition, 1982, 252.

266. R.W.G. Hunt and R.M. Pointer, *Measuring Colour*, John Wiley & Sons Ltd., Chichester England, 4th edition, 2011, 337.

267. G. Wyszecki and W.S. Stiles. *Color Science, Concepts and Methods, Quantitative Data and Formulae.* John Wiley & Sons Inc., New York USA, 2nd edition, 1982, 255.

268. British Standard Institution, BS ISO 11664-3:2012, *Colorimetry - CIE tristimulus values*, BSI ISO, London UK, 2012.

269. G. Wyszecki and W.S. Stiles. *Color Science, Concepts and Methods, Quantitative Data and Formulae.* John Wiley & Sons Inc., New York USA, 2nd edition, 1982, 259.

270. R.W.G. Hunt, *Measuring Colour*, Fountain Press, Kingston-upon-Thames England, 3rd edition, 1998, 36.

271. N. Ohta and A.R. Robertson, *Colorimetry. Fundamentals and Applications*, John Wiley and Sons Ltd., Chichester, West Sussex England, 2005, 57.

272. G. Wyszecki and W.S. Stiles. *Color Science, Concepts and Methods, Quantitative Data and Formulae.* Wiley Classic Library Edition, New York USA, 2nd edition, 2000, 118.

273. G. Wyszecki and W.S. Stiles. *Color Science, Concepts and Methods, Quantitative Data and Formulae.* Wiley Classic Library Edition, New York USA, 2nd edition, 2000, 117.

274. Commission Internationale de L'Éclairage, CIE S 014-1/E:2006, *Colorimetry - Part 1: CIE Standard Colorimetric Observers*, CIE Central Bureau, Vienna Austria, 2006a.

275. G. Wyszecki and W.S. Stiles. *Color Science, Concepts and Methods, Quantitative Data and Formulae.* Wiley Classic Library Edition, New York USA, 2nd edition, 2000, 88.

276. G. Wyszecki and W.S. Stiles. *Color Science, Concepts and Methods, Quantitative Data and Formulae.* Wiley Classic Library Edition, New York USA, 2nd edition, 2000, 132.

277. Commission Internationale de L'Éclairage, CIE S 014-3/E:2011, *Colorimetry - Part 3: CIE tristimulus values*, CIE Central Bureau, Vienna Austria, 2011.

278. W.S. Stiles and J.M. Burch, 'Interim report to the Commission Internationale de L'Éclairage in Zürich on the National Physical Laboratory's investigations of colour matching', *Optica Acta*, 1955, **2**, 168.

279. N.I. Speranskaya, 'Determination of spectrum color co-ordinates for twenty-seven normal observers', *Optics and Spectroscopy*, 1959, **7**, 424.

280. International Organisation for Standardisation, ISO 23539:2005 (CIE S010/E:2004), *Photometry – The CIE system of physical photometry*, ISO Central Secretariat, Geneva Switzerland, 2005.

281. British Standard Institutions, BS EN ISO 11664-1:2011, *Colorimetry. CIE standard colorimetric observers,* BSI, London UK, 2009.

282. G. Wyszecki and W.S. Stiles. *Color Science, Concepts and Methods, Quantitative Data and Formulae.* Wiley Classic Library Edition, New York USA, 2nd edition, 2000, 139.

283. C.J. Li, M.R. Luo, and B. Rigg, 'A new method for computing optimum weights for calculting CIE tristimuls values', *Color reseach and applications*, 2004*,* **29**, 2, 91-103.

284. R.W.G. Hunt, *Measuring Colour*, Fountain Press, Kingston-upon-Thames England, 3rd edition, 1998, 53.

285. Commission Internationale de L'Éclairage, CIE S 014-2:E2006, *Colorimetry - Part 2: CIE Standard Illuminants for Colorimetry.* CIE Central Bureau, Vienna Austria, 2006b.

286. R.W.G. Hunt, *Measuring Colour*, Fountain Press, Kingston-upon-Thames England, 3rd edition, 1998, 25-27.

287. Commission Internationale de L'Éclairage, CIE S 014-4/E 2007, *Colorimetry - Part 4: CIE 1976 L*a*b* colour space*, CIE Central Bureau, Vienna Austria, 2007.

288. Commission Internationale de L'Éclairage, CIE S 014-5/E:2009, *Colorimetry - Part 5: CIE 1976 L*u*v* Colour Space and u'v' Uniform Chromaticity Scale Diagram*, CIE Central Bureau, Vienna Austria, 2009.

289. R.W.G. Hunt and R.M. Pointer, *Measuring Colour*, John Wiley & Sons Ltd., Chichester England, 4th edition, 2011, 57.

290. H.C. Lee, *Introduction in Color Imaging Science*, Cambidge University Press, Cambridge England, 2005, 112.

291. F.W. Jr. Billmeyer, 'Survey of Color Order Systems', *Color research and applications*, 1987, **12**, 4, 173-186.

292. N. Ohta and A.R. Robertson, *Colorimetry. Fundamentals and Applications*, John Wiley and Sons Ltd., Chichester, West Sussex England, 2005, 133.

293. H.C. Lee, *Introduction in Color Imaging Science*, Cambridge University Press, Cambridge England, 2005, 107-108.

294. R. Sêve, 'New Formula for the computation of CIE 1976 hue difference', *Color research and application*, 1991, **16**, 3, 217-218.

295. R. Sêve, 'Practical formula for the computation of CIE 1976 hue difference', *Color research and application*, 1996, **21**, 4, 314.

296. H. Brill and A. R. Robertson, 'Open Problems on the Validity of Grassmann's Laws', In *Colorimetry. Understanding the CIE system*, ed. J. Schanda, John Wiley & Sons, Hoboken, New Jersey USA, 2007, Chapter 10, 245-259.

297. S.M. Jaeckel, 'The HATRA data on colour differences and visual colour passing', *Journal of the Society of Dyers and Colourists*, 1975, **91**, 242.

298. D.I. Morley, R. Munn, and F.W. Billmeyer, 'Small and moderate colour differences II: The Morley data', *Journal of the Society of Dyers and Colourists,* 1975, **91**, 7, 229-242.

299. R.G. Kühni, 'Color difference and objective acceptability evaluation', *Journal of Color and Appearance*, 1971a, **3**, 1, 4-10, 15.

300. R.G. Kühni, 'Acceptibility contours if selected textile matches in color space', *Textile Chemist and Colorist*, 1971b, **3**, 248-255.

301. K. McLaren, 'XIII-The Development of the CIE 1976 ($L^*a^*b^*$) Uniform colour space and Colour-difference formula, *Journal of the Society of Dyers and Colourists*, 1976, **92**, 9, 338-341.

302. Kühni, R.G., *Color Space and its division*, John Wiley and Sons Inc., Hoboken, New Jersey USA, 2003.

303. British Standard Institution, BS 6923:1988, *Method for Calculation of small colour differences*, BSI, London UK, 1988.

304. R.S. Berns, 'The Mathematical Development of CIE TC 1-29 Proposed Color Difference Equation: CIELCH', in *Proceedings of the 7th Congress of the International Color Association,* ed. A. Nemcsics and J. Schanda, 13.06.1993, Budapest Hungary, 1993, **B***,* C11-1C11-5.

305. R.W.G Hunt, R.W.G. and R.M. Pointer, *Measuring Colour*, John Wiley & Sons Ltd., Chichester England, 4th edition, 2011, 337.

306. M. Melgosa, M.M. Pérez, A.E. Moraghi, and E. Hita, "Color discrimination results from a CRT device: influence of luminance, *Color research and application*, 1999, **24**,1, 38-44.

307. L.D. Griffin and A. Sepehri, 'Performance fo CIE94 for Nonreference Conditions', *Color research and application*, 2002, **27**, 2, 108-115.

308. R.G. Kühni, 'Uniform Color Space Modeled with Cone Responses', *Color research and application*, 2000, **25**, 1, 56-63.

309. R.G. Kühni, *Color Space and its division*, John Wiley and Sons Inc., Hoboken, New Jersey USA, 2003.

310. H.G. Völz, 'Die Berechnung grosser Farbabstände in nichteuklidischen Farbräumen', *Die Farbe*, 1998, **44**, 1-45.

311. H.G. Völz, 'Die Euklidisierung de CMC-Raumes zur Berechnung grosser Farbabstände', *Die Farbe*, 1999, **45**, 1-23.

312. H.G. Völz, 'Euclidization of the First Quadrant of the CIEDE2000 Color Difference System for the Calculation of Large Color Differences', *Color research and application*, 2006, **31**, 1, 5-12.

313. G. Rösler, *dfwg – Germany Society of Color Science and Application* [online], 2008 [Accessed 23.07.2012]. Available from: http://www.dfwg.de/doc/dfwg-homepage-417.htm.

314. C.C. Semmelroth, C.C., 'Prediction of Lightness and brightness on different backgrounds', *Journal of the Optical Society of America*, 1970, **60**, 12, 1685-1689.

315. C.L. Sanders and G. Wyszecki, 'Correlate for brightness in terms of CIE color matching data', in *CIE Proceedings 15th session*, CIE Central Bureau, Paris France, 1963, Paper-P.63.6.

316. C. Oleari, M. Melgosa, and R. Huertas, 'Euclidean color-difference formula for small-medium coloiur differences in log-compressed OSA-UCS space', *The Journal of the Optical Society of America*, 2009, **26**, 1, 121-134.

317. G. Wyszecki and W.S. Stiles. *Color Science, Concepts and Methods, Quantitative Data and Formulae.* Wiley Classic Library Edition, New York USA, 2nd edition, 2000, 512.

318. G.Cui, 'Colour-difference Evaluation using CRT displays', *Ph.D. thesis*, *University of Leeds*, 2000.

319. M. Melgosa, D.A. Alman, M. Grosman, L. Gómez-Robledo, A. Trémeau, G. Cui, P.A. García, D. Vázquez, C. Lin, and M.R. Luo, 'Practical Demonstration of the CIEDE2000 Corrections to CIELAB using small set of Sample Pairs', *Color research and application*, 2012, Early View, 1-8.

320. H.C. Lee, *Introduction in Color Imaging Science*, Cambidge University Press, Cambridge England, 2005, 115.

321. G. Sharma, W. Wu, and E.N. Dalal, 'The CIEDE2000 Color-Difference Formula: Implementations Notes, Supplementary Test Data, and Mathematical Observations', *Color research and application*, 2005, **30**, 1, 21-30.

322. Kühni, R., 'CIEDE2000, Milestone or Final Answer?', *Color research and application*, 2002, **27**, 2, 126-128.

323. Commission Internationale de L'Éclairage, CIE DS 014-6/E:2012, *Colorimetry - Part 6: CIEDE2000 Colour Difference Formula*, CIE Central Bureau, Vienna Austria, 2012.

324. R.W.G. Hunt, '*Measuring Colour*', Fountain Press, Kingston-upon-Thames England, 3rd edition, 1998, 208.

325. R.W.G. Hunt and R.M. Pointer, *Measuring Colour*, John Wiley & Sons Ltd., Chichester England, 4th edition, 2011, 57.

326. C.J. Bartleson, 'Changes in color appearance with variations in chromatic adaption, *Color research and applications*, 1979, **4**, 3, 119-138.

327. M.D. Fairchild and R.S. Berns, 'Image color appearance specifications through extension of CIELAB, *Color research and applications*, 1993, **18**, 3, 178-190.

328. M.R. Pointer, 'The concept of colourfulness and its use for derving grids for assessing colour appearance', *Color research and applications*, 1980, **5**, 2, 99-107.

329. K. Richter, 'Cube-Root Color Spaces and Chromatic Adaptation', *Color research and application*, 1980, **5**, 1, 25-43.

330. N. Moroney, M.D. Fairchild, R.W.G. Hunt, C. Li, M.R. Luo, and T. Newman, The CIEMAM02 Color Appearance Model, *in 10th Colour Imaging Conference: Color Science and Engineering Systems, Technologies, and Applications*, eds. P. Hubel and I. Tastl, 11/2002, Scotsdale, Arizon USA, (**10**), 2002.

331. C. Li, M.R. Luo, G. Cui, 'Colour-difference evaluation using colour appearance models', *in Proceedings of the 11th Color Imaging Conference IS&T and SID*, 13.11.2003, Scotsdale, Arizona USA, 2003, 127-131.

332. S.Y. Zhu, M.R. Luo, G. Cui, and B. Rigg, 'Comparing different colour discrimination data sets', *in Proceedings of the 11th Color Imaging Conference IS&T and SID*, 13.11.2003, Scotsdale, Arizona USA, 2003, 51-54.

333. R.W.G. Hunt and R.M. Pointer, *Measuring Colour*, John Wiley & Sons Ltd., Chichester England, 4th edition, 2011, 294.

334. Y.Zue and R. S. Berns, 'Optimizing Color-Difference Equations and Uniform Color Spaces for Industrial Tolerancing', in *Proceedings of the Midterm Meeting of the International Color Association,* eds. G. Ye and H. Xu, 12.07.2007*,* Hangzhou China, 2007, 24-28.

335. P.K. Kaiser and R.M. Boynton, *Human Colour Vision,* Optical Society of America*,* Washington, D.C USA, 1996.

336. M.D. Fairchild, *Color Appearance Models*, John Wiley & Sons, West Sussex England, 2nd edition, 2005, 113.

337. J.H. Xin, C.C. Lam, and M.R. Luo, 'Investigation of Parametric Effects using Medium Colour Differences', *Color research and application*, 2001, **26**, 5, 376-383.

338. G. Cui, M.R. Luo, B. Rigg, and W. Li, 'Colour Difference Evaluation using CRT colours - Part II: Parametric Effects', *Color research and application*, 2001, **26**, 5, 403-412.

339. M.E. Chevreul, *The Principles of Harmony and Contrast of Colors*, translated by C. Martel, Reinhold Van Nostrand, New York USA, Reprint, 1967.

340. M.D. Fairchild, *Color Appearance Models*, John Wiley & Sons, West Sussex England, 2nd edition, 2005, 122.

341. L.T. Sharpe and G. Wyszecki, 'Proximity factor in color-difference evaluations', *Journal of the Optical Society of America*, 1976, **66**, 1, 40-49.

342. S.G. Kansi, M.A. Theran, and M. Rhamati, 'Colour dependency of textile samples on the surface texture', *Coloration Technology*, 2008, **124**, 6, 348-354.

343. J.H. Xin, H.-L. Shen, and Lam C.C., 'Investigation of Texture Effect on Visual Colour Difference Evaluation', *Color research and application*, 2005, **30**, 5, 341-347.

344. G. Wyszecki and W.S. Stiles. *Color Science, Concepts and Methods, Quantitative Data and Formulae.* John Wiley & Sons Inc., New York USA, 2nd edition, 1982, 306-310.

345. M. Melgosa, E. Hita, J. Romero, and L. Jiménez del Barco, 'Some classical color differences calculated with new formulas', *Journal of the Optical Society of America*, 1992, **9**, 8, 1247-1254.

346. C. Alder, K.P. Chaing, T.F. Chong, E. Coates, B. Rigg, and B. Khalili, 'Uniform Chromaticity Scales - New Experimental Data', *Journal of the Society of Dyers and Colourists*, 1982, **98**, 1, 14-20.

347. L.F.C. Friele, 'Fine Color Metric (FCM)', *Color research and application,* 1978, **3**, 2, 53-64.

348. A.W. Fitzgibbon, M. Pilu, and R.B. Fischer, 'Direct least squares fitting of ellipses', *IEEE Transaction on Pattern Analysis and Machine Intelligence*, 1999, **21**, 5, 476-480.

349. G. Wyszecki and W.S. Stiles. *Color Science, Concepts and Methods, Quantitative Data and Formulae.* John Wiley & Sons Inc., New York USA, 2nd edition, 1982, 306-307.

350. British Standard Institution, BS ISO 3534-2:2006, *Statistics – Vocabulary and symbols – Part 2: Applied statistics*, BSI ISO, London UK, 2006.

351. British Standard Institution, BS 2846-4:1976, ISO 2854:1976, *Guide to Statistical interpretation of data – Part 4: Techniques of estimation and test relating means and variations*, BSI ISO, London UK, 1976.

352. A. Field, *Discovering Statistics using SPSS*, SAGE Publications Ltd., London UK, 2009, 133.

353. M.F. Triola, *Elementary Statistics*, Pearson Education, Boston, MA USA, 10th edition, 2006, 559.

354. D.H. Alman, 'Performance Comparison for Full and Reduced Color-Difference Models', Draft Report for CIE TC1-47, 10.05.2000.

355. W. Schultz, 'The usefulness of colour-difference formulae for fixing colour tolerances', in *Colour Metrics from the Symposium on Small Color Differences of the Internationale Association of Color in Driebergen*, 01.09.1971, Institute for Perception TNO, Soesterberg Netherlands, 1971, 245-265.

356. E. Coates, K.Y. Fong, and B. Rigg, 'Uniform Lightness Scales', *Journal of the Society of Dyers and Colourists*, 1981, **97**, 4, 179-183.

357. P.A. García, R. Huertas, G. Cui, and M. Melgosa, 'Measurement of the relationship between perceived and computed color differences', *Journal of the Optical Society of America*, 2007, **24**, 7, 1823-1829.

358. M. Melgosa, R. Huertas, and R.S. Berns, 'Performance of recent advanced color-difference formulas using the standardized residual sum of squares index', *Journal of the Optical Society of America*, 2008, **25**, 7, 1828-1834.

359. M. Melgosa, P.A. Garcìa, L. Gómez-Robledo, R. Shamey, D. Hinks, G. Cui, and M.R. Luo, 'Notes on the application of the standardized residual sum of squares index for the assessment of intra- and inter-observer variability in color-difference experiments', *Journal of the Optical Society of America*, 2011, **28**, 5, 949-953.

360. E. Kirchner and N. Dekker, 'Performance measure of color-difference equations: correlation coefficient versus standardized residual sum of squares', *Journal of the Optical Society of America*, 2011, **28**, 9, 1841-1848.

361. S. Dobbs and J. Miller, *Advanced Level Mathematics. Statistic 1*, Press Syndicate of the University of Cambridge, Cambridge UK, 2003.

362. M.F. Triola, *Elementary Statistics*, Pearson Education, Boston, MA USA, 10th edition, 2006, 529.

363. M.F. Triola, *Elementary Statistics*, Pearson Education, Boston, MA USA, 10th edition, 2006, 531.

364. I.G. Hughes and T.P.A. Hase, *Measurements and their Uncertainties*, Oxford University Press, Oxford England, 2010, 31.

365. M.F. Triola, *Elementary Statistics*, Pearson Education, Boston, MA USA, 10th edition, 2006, 607.

366. I.G. Hughes and T.P.A. Hase, *Measurements and their Uncertainties*, Oxford University Press, Oxford England, 2010, 27.

367. H.C. Lee, *Introduction in Color Imaging Science*, Cambidge University Press, Cambridge England, 2005, 532.

368. R.W.G. Hunt, *The Reproduction of Colour*, Wiley & Sons Ltd., Chichester, West Sussex England, 6th edition, 2004.

369. E. Lüder, *Liquid Crystal Displays*, John Wiley and Sons, Ltd., Chichester England, UK.

370. International Committee for Display Metrology ICDM, Society for Information Display SID, 'Information Display Measurements Standard, Version 1.03' SID, Campbell California, USA, 2012.

371. European Committee for Electrotechnical Standardization, *Multimedia systems and equipment - Colour measurement and management. Part 4: Equipment using liquid crystal display panels*, CENELEC, Brussels Belgium, 2000.

372. E.A. Day, L. Taplin, and R.S. Berns, 'Colorimetric Characterizations of a Computer-Controlled Liquid Crystal Display', *Color research and application*, 2004, **29**, 5, 365-373.

373. H.R. Kang, *Color Technology for Electronic Imaging Devices,* SPIE Optical Engineering Press, Bellingham Washington, USA, 1997.

374*.* H.C. Lee, *Introduction in Color Imaging Science*, Cambridge University Press, Cambridge England, 2005, 537.

375. H. Shen and J.H. Xin, 'Colour simulation of textiles', in *Total Colour Management in Textiles.* ed. J.H. Xin, Woodhead Publishing Limited, Cambridge England, 2006, Chapter 6, 97-116.

376. European Committee for Standardization, EN 61966-9 IEC:2003, *Multimedia systems and equipment – Colour measurement and management – Part 9: Digital cameras*, EN, Geneva Switzerland, Second edition, 11-2003.

377. G. Hong, M.R. Luo, and P.A. Rhodes, 'A Study of Digital Camera Colorimetric Characterization Based on Polynomial Modelling, *Color research and application*, **26,** 1, 2001, 76-84.

378. R.W.G Hunt and R.M. Pointer, *Measuring Colour*, John Wiley & Sons Ltd., Chichester England, 4th edition, 2011, 242.

379. International Organisation for Standardisation, ISO 17321-1:2012, *Graphic technology and photography -- Colour characterisation of digital still cameras (DSCs) -- Part 1: Stimuli, metrology and test procedures,* ISO Central Secretariat, Geneva Switzerland, 2012.

380. S. Westland and C. Ripamonti, *Computational Colour Science using Matlab,* John Wiley & Sons, Ltd, Chichester West Sussex, England, 2004, 127.

381. M.H. Beale, M.T. Hagan, and H.B. Demuth, *Neural Networks Toolbox 7: User's Guide* [online], The MathWorks, Inc., Natick MA, USA, R2012B, 1992-2012, [Accessed 08/08/2012]. Available from: http://www.mathworks.co.uk/help/pdf_doc/nnet/nnet_ug.pdf

382. R. de Levie, *Advanved Excel for scientific data analysis*, Oxford University Press, Inc., New York New York, USA, 2nd edition, 2008, 569.

383. European Committee for Electrotechnical Standardization, *Multimedia systems and equipment - Colour measurement and management - Part 8: Multimedia colour scanners*, CENELEC, Brussels Belgium, 2000.

384. T. Johnson, 'Methods for characterizing colour scanners and digita cameras', *Displays*, 1996, **16**, 4, 183-191.

385. H.C. Lee, *Introduction in Color Imaging Science*, Cambidge University Press, Cambridge England, 2005, 518.

386. G. Cui, M.R. Luo, B. Rigg, and W. Li, 'Colour Difference Evaluation using CRT colours - Part I: Data Gathering and Testing Colour Difference Formulae', *Color research and application*, 2001, **26**, 5, 394-402.

387. D. Farnsworth, 'The Farnsworth-Munsell 100 Hue Test for the examination of Color Discrimination', *Macbeth, a devision of Kollmorgwen Corp.*, 1957.

388 R. J. Hyndman, *Research Tips* [online], [Accessed 28/01/2013]. Available from: http://www.robjhyndan.com/

389 G. Wyszecki and W.S. Stiles. *Color Science, Concepts and Methods, Quantitative Data and Formulae.* John Wiley & Sons Inc., New York USA, 2nd edition, 1982, 320.

390 H.G. Völtz, *Industrial Color Testing: Fundamentals and Techniques*, VCH Verlagsgesellschaft mbH, Weinheim Deutschland, 1995, 40.

391. I.G. Hughes and T.P.A. Hase, *Measurements and their uncertainties*, Oxford University Press, Oxford England, 2010, 19.

Appendix A

CMC - PHYSICAL: BUTTONHOLE (BH) DV VC EAST/WEST - DE VC TSR									
	KL	KC	Factor	Residual	STRESS	CV	VAB	Gamma	PF/3
All Samples	**2.01**	**1.30**	**1.23**	**0.73**	**35.98**	**38.22**	**0.42**	**1.49**	**43.01**
ΔL>90%	7.01	1.91	1.70	**0.69**	**25.82**	27.71	0.36	1.41	35.05
ΔL+ΔaΔb, ΔC	0.30	1.13	1.10	**0.76**	**14.30**	14.81	0.58	1.20	30.81
All Grey	5.22	1.72	1.63	**0.48**	**20.21**	20.93	0.25	1.28	24.83
All Blue	2.50	1.20	1.19	**0.49**	**20.48**	21.98	0.25	1.28	25.17
All Samples	**1.69**	**1.00**	**1.07**	**0.78**	**36.68**	**39.12**	**0.42**	**1.48**	**42.85**
ΔL>90%	8.84	1.00	1.73	**1.23**	**25.95**	27.66	0.38	1.36	33.71
ΔL+ΔaΔb, ΔC	0.50	1.00	1.16	**0.83**	**15.84**	16.53	0.37	1.20	24.68
All Grey	2.23	1.00	1.26	**0.64**	**25.60**	27.05	0.27	1.30	27.90
All Blue	2.28	1.00	1.13	**0.51**	**21.26**	22.82	0.24	1.27	24.89
All Samples	**2.00**	**1.00**	**1.00**	**0.84**	**37.02**	**39.39**	**0.41**	**1.48**	**42.96**
ΔL>90%	2.00	1.00	1.00	**0.77**	**25.68**	27.35	0.45	1.35	35.98
ΔL+ΔaΔb, ΔC	2.00	1.00	1.00	**0.93**	**19.03**	19.98	0.46	1.25	30.16
All Grey	2.00	2.00	1.00	**0.90**	**25.71**	27.24	0.27	1.30	28.10
All Blue	2.00	2.00	1.00	**0.60**	**21.77**	23.27	0.25	1.29	25.75
All Samples	**1.00**	**1.00**	**1.00**	**0.98**	**40.72**	**44.87**	**0.45**	**1.51**	**46.91**
ΔL>90%	1.00	1.00	1.00	**0.75**	**24.90**	26.43	0.44	1.34	34.70
ΔL+ΔaΔb, ΔC	1.00	1.00	1.00	**0.92**	**17.38**	18.24	0.32	1.22	24.30
All Grey	1.00	1.00	1.00	**0.81**	**33.69**	37.45	0.33	1.32	34.26
All Blue	1.00	1.00	1.00	**0.85**	**38.83**	42.38	0.40	1.49	43.85

CMC - PHYSICAL: SINGLESTITCH (ST) DV VC EAST/WEST - DE VC TSR									
	KL	KC	Factor	Residual	STRESS	CV	VAB	Gamma	PF/3
All Samples	**2.37**	**1.26**	**0.87**	**0.47**	**31.64**	**33.69**	**0.41**	**1.49**	**40.98**
ΔL >90%	3.33	0.62	1.00	**0.46**	**26.90**	27.71	0.41	1.47	38.69
ΔL+ΔaΔb, ΔC	0.71	1.46	0.75	**0.27**	**19.51**	19.98	0.23	1.26	45.76
All Grey	2.21	1.07	0.88	**0.48**	**27.51**	29.41	0.34	1.35	32.99
All Blue	2.41	1.28	0.70	**0.34**	**29.08**	30.72	0.37	1.44	37.12
All Samples	**2.07**	**1.00**	**0.78**	**0.50**	**32.15**	**34.22**	**0.41**	**1.49**	**41.57**
ΔL>90%	3.26	1.00	1.01	**0.45**	**27.60**	28.49	0.40	1.48	38.80
ΔL+ΔaΔb, ΔC	0.76	1.00	0.69	**0.29**	**20.54**	20.70	0.25	1.27	48.66
All Grey	2.14	1.00	0.87	**0.48**	**27.57**	29.47	0.33	1.35	32.49
All Blue	2.05	1.00	0.63	**0.36**	**29.72**	31.35	0.38	1.46	38.44
All Samples	**2.00**	**1.00**	**1.00**	**0.67**	**32.17**	**34.29**	**0.47**	**1.50**	**43.75**
ΔL>90%	2.00	1.00	1.00	**0.80**	**28.88**	30.02	0.53	1.50	44.39
ΔL+ΔaΔb, ΔC	2.00	1.00	1.00	**0.55**	**22.66**	22.72	0.35	1.31	58.89
All Grey	2.00	1.00	1.00	**0.57**	**27.63**	29.65	0.30	1.35	31.50
All Blue	2.00	1.00	1.00	**0.80**	**29.74**	31.37	0.62	1.46	46.33
All Samples	**1.00**	**1.00**	**1.00**	**1.31**	**39.74**	**44.88**	**0.73**	**1.62**	**59.97**
ΔL>90%	1.00	1.00	1.00	**2.68**	**31.79**	33.46	1.02	1.56	63.98
ΔL+ΔaΔb, ΔC	1.00	1.00	1.00	**0.55**	**20.79**	20.89	0.33	1.28	54.61
All Grey	1.00	1.00	1.00	**1.07**	**35.51**	40.83	0.45	1.42	42.49
All Blue	1.00	1.00	1.00	**1.58**	**40.01**	44.08	0.96	1.63	67.83

CMC - PHYSICAL: THREAD WINDING CARD (TWC) DV VC EAST/WEST - DE VC TSR									
	KL	KC	Factor	Residual	STRESS	CV	VAB	Gamma	PF/3
All Samples	**2.47**	**1.30**	**1.46**	**0.28**	**14.41**	**15.42**	**0.17**	**1.24**	**18.93**
ΔL>90%	1.35	0.30	0.76	**0.27**	**16.18**	17.07	0.18	1.19	18.01
ΔL+ΔaΔb, ΔC	5.20	1.46	1.59	**0.11**	**10.35**	11.10	0.20	1.13	17.89
All Grey	2.78	1.59	1.64	**0.20**	**10.26**	10.98	0.14	1.29	18.08
All Blue	2.18	1.03	1.21	**0.19**	**12.52**	13.23	0.13	1.14	23.28
All Samples	**2.26**	**1.00**	**1.29**	**0.32**	**16.34**	**17.43**	**0.20**	**1.26**	**20.92**
ΔL>90%	2.06	**1.00**	1.18	**0.27**	**16.65**	17.54	0.18	1.20	18.50
ΔL+ΔaΔb, ΔC	3.03	**1.00**	1.21	**0.20**	**14.91**	16.06	0.30	1.22	28.88
All Grey	2.36	**1.00**	1.47	**0.34**	**17.19**	18.47	0.21	1.30	23.21
All Blue	2.16	1.00	1.21	**0.19**	**12.55**	13.24	0.14	1.15	1.15
All Samples	**2.00**	**1.00**	**1.00**	**0.52**	**17.05**	**18.14**	**0.20**	**1.26**	**21.44**
ΔL>90%	2.00	1.00	1.00	**0.37**	**16.66**	17.55	0.18	1.20	18.49
ΔL+ΔaΔb, ΔC	2.00	1.00	1.00	**0.35**	**15.28**	16.69	0.41	1.22	32.27
All Grey	2.00	1.00	1.00	**0.66**	**18.40**	19.78	0.23	1.31	24.53
All Blue	2.00	1.00	1.00	**0.39**	**12.94**	13.62	0.13	1.14	1.14
All Samples	**1.00**	**1.00**	**1.00**	**0.77**	**36.64**	**40.50**	**0.39**	**1.40**	**39.84**
ΔL>90%	1.00	1.00	1.00	**1.15**	**17.47**	18.50	0.18	1.20	19.07
ΔL+ΔaΔb, ΔC	1.00	1.00	1.00	**0.31**	**17.87**	20.46	0.33	1.25	31.91
All Grey	1.00	1.00	1.00	**0.83**	**37.96**	42.99	0.42	1.36	40.38
All Blue	1.00	1.00	1.00	**0.71**	**34.37**	36.98	0.33	1.39	31.93

CMC - PHYSICAL: BUTTONHOLE (BH) DV VC NORTH/SOUTH - DE VC TSR									
	KL	KC	Factor	Residual	STRESS	CV	VAB	Gamma	PF/3
All Samples	**3.88**	**0.99**	**2.23**	**0.57**	**21.76**	**22.93**	**0.23**	**1.05**	**17.21**
ΔL>90%	1.92	2.00	1.18	**0.52**	**25.19**	24.43	0.31	1.36	30.67
ΔL+ΔaΔb, ΔC	1.02	1.12	2.07	**0.58**	**19.91**	20.74	0.20	1.22	38.42
All Grey	5.50	1.14	2.65	**0.50**	**19.69**	20.12	0.23	1.28	23.64
All Blue	3.85	1.35	2.12	**0.42**	**15.24**	16.18	0.20	1.22	19.24
All Samples	**3.89**	**1.00**	**2.24**	**0.57**	**21.76**	**22.93**	**0.23**	**1.05**	**17.21**
ΔL>90%	1.38	1.00	1.00	**0.53**	**28.09**	27.21	0.38	1.45	36.53
ΔL+ΔaΔb, ΔC	1.00	1.00	2.07	**0.59**	**20.16**	21.00	0.20	1.22	39.30
All Grey	4.68	1.00	2.40	**0.52**	**19.87**	20.32	0.24	1.28	23.99
All Blue	3.39	1.00	2.03	**0.51**	**17.90**	19.15	0.21	1.23	20.98
All Samples	**2.00**	**1.00**	**1.00**	**1.70**	**30.26**	**32.14**	**0.32**	**1.07**	**23.67**
ΔL>90%	2.00	1.00	1.00	**0.82**	**31.38**	30.22	0.39	1.47	38.91
ΔL+ΔaΔb, ΔC	2.00	1.00	1.00	**2.01**	**22.02**	23.02	0.91	1.26	38.91
All Grey	2.00	1.00	1.00	**2.03**	**26.37**	27.93	0.26	1.28	27.15
All Blue	2.00	1.00	1.00	**1.33**	**26.96**	28.41	0.29	1.33	30.35
All Samples	**1.00**	**1.00**	**1.00**	**1.62**	**49.52**	**56.60**	**0.50**	**1.11**	**39.18**
ΔL>90%	1.00	1.00	1.00	**0.81**	**30.18**	29.88	0.40	1.48	39.29
ΔL+ΔaΔb, ΔC	1.00	1.00	1.00	**1.82**	**20.16**	21.00	0.77	1.22	39.29
All Grey	1.00	1.00	1.00	**1.77**	**43.18**	50.26	0.34	1.28	37.62
All Blue	1.00	1.00	1.00	**1.46**	**48.36**	53.22	0.51	1.64	56.05

CMC - PHYSICAL: SINGLESTITCH (ST) DV VC NORTH/SOUTH - DE VC TSR									
	KL	KC	Factor	Residual	STRESS	CV	VAB	Gamma	PF/3
All Samples	**2.11**	**1.10**	**1.56**	**0.94**	**35.75**	**38.16**	**0.44**	**1.54**	**45.41**
ΔL>90%	1.34	1.12	0.84	**0.65**	**24.15**	23.90	0.34	1.39	32.32
ΔL+ΔaΔb, ΔC	0.71	0.97	1.31	**0.72**	**27.06**	29.10	0.33	1.38	33.25
All Grey	3.34	1.55	2.63	**0.55**	**19.41**	20.21	0.21	1.22	20.94
All Blue	2.16	1.99	1.13	**0.56**	**31.76**	33.93	0.46	1.52	43.95
All Samples	**2.20**	**1.00**	**1.57**	**0.92**	**35.38**	**37.65**	**0.43**	**1.53**	**44.45**
ΔL>90%	1.19	1.00	0.77	**0.64**	**24.05**	24.05	0.34	1.39	32.47
ΔL+ΔaΔb, ΔC	0.73	1.00	1.33	**0.72**	**27.06**	29.09	0.33	1.38	33.26
All Grey	2.43	1.00	1.92	**0.66**	**21.98**	23.09	0.25	1.25	24.30
All Blue	1.77	1.00	1.00	**0.58**	**32.78**	35.27	0.45	1.54	44.97
All Samples	**2.00**	**1.00**	**1.00**	**1.25**	**35.54**	**37.99**	**0.65**	**1.54**	**52.06**
ΔL>90%	2.00	1.00	1.00	**0.99**	**27.86**	27.04	0.39	1.43	36.31
ΔL+ΔaΔb, ΔC	2.00	1.00	1.00	**1.37**	**37.34**	39.58	0.73	1.47	53.27
All Grey	2.00	1.00	1.00	**1.77**	**22.91**	24.42	0.77	1.25	42.02
All Blue	2.00	1.00	1.00	**0.62**	**33.15**	35.57	0.46	1.53	45.01
All Samples	**1.00**	**1.00**	**1.00**	**1.23**	**43.54**	**49.71**	**0.56**	**1.70**	**58.63**
ΔL>90%	1.00	1.00	1.00	**1.50**	**24.30**	24.46	0.58	1.40	40.78
ΔL+ΔaΔb, ΔC	1.00	1.00	1.00	**1.07**	**28.68**	30.42	0.52	1.38	40.26
All Grey	1.00	1.00	1.00	**1.31**	**35.33**	40.94	0.55	1.39	44.77
All Blue	1.00	1.00	1.00	**1.12**	**38.80**	43.56	0.58	1.68	56.65

CMC - PHYSICAL: THREAD WINDING CARD (TWC) DV VC NORTH/SOUTH - DE VC TSR									
	KL	KC	Factor	Residual	STRESS	CV	VAB	Gamma	PF/3
All Samples	**2.11**	**1.10**	**1.28**	**0.48**	**20.52**	**21.62**	**0.23**	**1.26**	**23.60**
ΔL>90%	0.96	0.57	0.68	**0.15**	**6.41**	6.51	0.06	1.06	6.29
ΔL+ΔaΔb, ΔC	2.00	1.14	1.35	**0.53**	**22.81**	24.78	0.26	1.27	25.83
All Grey	2.48	1.44	1.34	**0.55**	**22.82**	23.31	0.26	1.30	26.20
All Blue	2.89	0.64	1.23	**0.12**	**6.31**	6.63	0.09	1.09	8.35
All Samples	**2.05**	**1.00**	**1.24**	**0.48**	**20.70**	**21.77**	**0.24**	**1.25**	**23.66**
ΔL>90%	1.49	1.00	1.06	**0.17**	**7.68**	7.78	0.08	1.08	7.70
ΔL+ΔaΔb, ΔC	1.00	1.00	1.33	**0.54**	**23.52**	25.43	0.26	1.29	26.63
All Grey	1.83	1.00	1.09	**0.54**	**23.92**	24.54	0.28	1.30	27.47
All Blue	2.34	1.00	1.42	**0.30**	**14.13**	15.29	0.15	1.16	15.25
All Samples	**2.00**	**1.00**	**1.00**	**0.67**	**20.71**	**21.79**	**0.24**	**1.26**	**23.72**
ΔL>90%	2.00	1.00	1.00	**0.48**	**9.63**	9.75	0.10	1.10	10.06
ΔL+ΔaΔb, ΔC	2.00	1.00	1.00	**0.76**	**23.30**	25.18	0.43	1.28	32.24
All Grey	2.00	1.00	1.00	**0.60**	**24.00**	24.57	0.28	1.30	27.45
All Blue	2.00	1.00	1.00	**0.73**	**14.77**	15.97	0.16	1.17	16.52
All Samples	**1.00**	**1.00**	**1.00**	**0.74**	**30.48**	**33.19**	**0.34**	**1.34**	**33.98**
ΔL>90%	1.00	1.00	1.00	**0.79**	**10.40**	10.60	0.10	1.10	10.23
ΔL+ΔaΔb, ΔC	1.00	1.00	1.00	**0.76**	**23.52**	25.43	0.43	1.29	32.33
All Grey	1.00	1.00	1.00	**0.70**	**29.49**	31.37	0.35	1.29	31.85
All Blue	1.00	1.00	1.00	**0.78**	**31.49**	35.16	0.33	1.39	35.66

CMC - PHYSICAL: BUTTONHOLE (BH) DV VC EAST/WEST - DE 7000A									
	KL	KC	Factor	Residual	STRESS	CV	VAB	Gamma	PF/3
All Samples	**2.66**	**1.60**	**1.82**	**0.70**	**28.38**	**30.96**	**0.33**	**1.36**	**33.21**
ΔL>90%	2.58	0.35	1.33	**0.61**	**19.06**	20.52	0.22	1.24	22.26
ΔL+ΔaΔb, ΔC	0.69	1.26	1.28	**0.48**	**19.07**	20.32	0.26	1.28	24.80
All Grey	1.14	4.18	1.42	**0.78**	**23.00**	40.84	0.31	1.28	33.31
All Blue	2.53	1.29	1.46	**0.52**	**23.59**	25.89	0.35	1.42	34.14
All Samples	**2.11**	**1.00**	**1.41**	**0.79**	**31.30**	**34.46**	**0.36**	**1.39**	**36.39**
ΔL>90%	2.58	1.00	1.47	**0.71**	**21.13**	22.68	0.28	1.32	27.38
ΔL+ΔaΔb, ΔC	0.60	1.00	1.18	**0.52**	**19.67**	20.99	0.27	1.29	25.42
All Grey	1.94	1.00	1.86	**0.79**	**32.75**	36.84	0.31	1.28	31.90
All Blue	2.27	1.00	1.30	**0.57**	**24.95**	27.51	0.37	1.44	36.24
All Samples	**2.00**	**1.00**	**1.00**	**1.07**	**31.36**	**34.49**	**0.36**	**1.39**	**36.63**
ΔL>90%	2.00	1.00	1.00	**0.93**	**21.41**	22.89	0.28	1.33	27.31
ΔL+ΔaΔb, ΔC	2.00	1.00	1.00	**1.26**	**29.68**	33.02	0.78	1.38	49.62
All Grey	2.00	1.00	1.00	**1.32**	**33.20**	36.85	0.31	1.28	31.96
All Blue	2.00	1.00	1.00	**0.82**	**25.45**	27.91	0.38	1.46	37.48
All Samples	**1.00**	**1.00**	**1.00**	**0.99**	**39.67**	**44.50**	**0.45**	**1.49**	**46.26**
ΔL>90%	1.00	1.00	1.00	**1.09**	**22.70**	24.18	0.30	1.34	29.35
ΔL+ΔaΔb, ΔC	1.00	1.00	1.00	**0.98**	**22.90**	24.80	0.58	1.31	37.72
All Grey	1.00	1.00	1.00	**0.99**	**26.17**	41.90	0.35	1.28	34.83
All Blue	1.00	1.00	1.00	**1.01**	**40.36**	44.95	0.52	1.66	54.03

CMC - PHYSICAL: SINGLESTITCH (ST) DV VC EAST/WEST - DE 7000A									
	KL	KC	Factor	Residual	STRESS	CV	VAB	Gamma	PF/3
All Samples	**1.67**	**0.96**	**0.89**	**0.62**	**42.75**	**48.05**	**0.70**	**1.86**	**68.21**
ΔL>90%	2.19	0.19	0.82	**0.69**	**38.19**	42.18	0.51	1.61	89.89
ΔL+ΔaΔb, ΔC	1.93	1.08	0.87	**0.34**	**25.91**	27.01	0.28	1.28	70.55
All Grey	1.93	1.00	0.99	**0.69**	**40.15**	46.87	0.84	1.76	89.93
All Blue	1.90	1.05	0.71	**0.36**	**30.52**	32.72	0.40	1.48	33.53
All Samples	**1.70**	**1.00**	**0.90**	**0.62**	**42.76**	**48.06**	**0.70**	**1.86**	**68.44**
ΔL>90%	2.19	1.00	1.06	**0.90**	**49.68**	58.45	0.97	2.14	42.56
ΔL+ΔaΔb, ΔC	1.79	1.00	0.84	**0.33**	**25.82**	26.92	0.28	1.27	69.84
All Grey	1.93	1.00	0.99	**0.69**	**40.15**	46.87	0.83	1.76	89.89
All Blue	1.85	1.00	0.70	**0.36**	**30.54**	32.73	0.40	1.48	33.33
All Samples	**2.00**	**1.00**	**1.00**	**0.63**	**43.15**	**48.33**	**0.70**	**1.88**	**69.58**
ΔL>90%	2.00	1.00	1.00	**0.90**	**49.72**	58.60	0.97	2.15	42.33
ΔL+ΔaΔb, ΔC	2.00	1.00	1.00	**0.41**	**25.96**	26.85	0.25	1.27	68.83
All Grey	2.00	1.00	1.00	**0.69**	**40.18**	46.79	0.85	1.77	90.17
All Blue	2.00	1.00	1.00	**0.55**	**30.67**	32.94	0.47	1.47	28.94
All Samples	**1.00**	**1.00**	**1.00**	**1.02**	**46.44**	**54.17**	**0.68**	**1.86**	**58.48**
ΔL>90%	1.00	1.00	1.00	**1.55**	**50.91**	61.00	0.84	2.20	62.57
ΔL+ΔaΔb, ΔC	1.00	1.00	1.00	**0.59**	**43.51**	39.62	0.32	1.44	69.45
All Grey	1.00	1.00	1.00	**0.89**	**45.45**	56.56	0.54	1.65	88.26
All Blue	1.00	1.00	1.00	**1.18**	**38.28**	41.63	0.82	1.64	34.50

CMC - PHYSICAL: THREAD WINDING CARD (TWC) DV VC EAST/WEST - DE 7000A									
	KL	KC	Factor	Residual	STRESS	CV	VAB	Gamma	PF/3
All Samples	**2.24**	**1.35**	**1.46**	**0.31**	**17.47**	**18.83**	**0.21**	**1.25**	**21.16**
ΔL>90%	3.15	1.00	1.82	**0.34**	**18.15**	17.39	0.20	1.22	20.88
ΔL+ΔaΔb, ΔC	5.95	1.30	1.42	**0.33**	**17.87**	19.78	0.26	1.26	39.09
All Grey	2.39	1.67	1.68	**0.23**	**12.64**	13.56	0.19	1.28	20.08
All Blue	2.15	1.07	1.18	**0.19**	**10.67**	11.46	0.15	1.16	28.10
All Samples	**2.02**	**1.00**	**1.33**	**0.36**	**19.45**	**20.87**	**0.23**	**1.25**	**24.44**
ΔL>90%	3.15	1.00	1.82	**0.34**	**18.15**	17.39	0.20	1.22	20.88
ΔL+ΔaΔb, ΔC	1.00	1.00	1.18	**0.39**	**21.00**	22.98	0.33	1.30	22.95
All Grey	1.98	1.00	1.58	**0.38**	**19.62**	21.08	0.24	1.28	23.55
All Blue	2.10	1.00	1.18	**0.19**	**10.85**	11.62	0.15	1.16	28.75
All Samples	**2.00**	**1.00**	**1.00**	**0.57**	**19.45**	**20.87**	**0.23**	**1.25**	**24.45**
ΔL>90%	2.00	1.00	1.00	**0.65**	**23.34**	23.57	0.22	1.24	14.62
ΔL+ΔaΔb, ΔC	2.00	1.00	1.00	**0.56**	**21.00**	22.98	0.45	1.30	22.95
All Grey	2.00	1.00	1.00	**0.80**	**19.62**	21.10	0.24	1.28	23.33
All Blue	2.00	1.00	1.00	**0.34**	**11.00**	11.77	0.15	1.17	32.68
All Samples	**1.00**	**1.00**	**1.00**	**0.64**	**33.80**	**37.06**	**0.39**	**1.37**	**35.39**
ΔL>90%	1.00	1.00	1.00	**0.72**	**37.77**	39.90	0.39	1.47	37.71
ΔL+ΔaΔb, ΔC	1.00	1.00	1.00	**0.54**	**23.44**	25.56	0.41	1.33	37.71
All Grey	1.00	1.00	1.00	**0.67**	**33.25**	36.50	0.39	1.30	42.18
All Blue	1.00	1.00	1.00	**0.62**	**31.40**	34.38	0.36	1.43	33.09

CIEDE2000 - PHYSICAL: BUTTONHOLE (BH) DV VC EAST/WEST - DE VC TSR

	KL	KC	KH	Factor	Residual	STRESS	CV	VAB	Gamma	PF/3
All Samples	**1.55**	**0.93**	**0.84**	**1.16**	**0.63**	**27.51**	**30.16**	**0.33**	**1.38**	**33.76**
ΔL	3.41	0.57	1.21	1.38	**0.43**	**21.33**	22.53	0.23	1.26	23.99
ΔaΔb, ΔC, ΔH	1.30	1.58	1.55	1.66	**0.53**	**26.25**	39.89	0.41	1.42	40.65
All Grey	2.65	0.46	0.32	0.51	**0.44**	**21.14**	21.99	0.28	1.31	27.03
All Blue	1.28	1.09	1.30	1.11	**0.41**	**20.42**	22.05	0.29	1.33	27.90
All Samples	**1.85**	**1.12**	**1.00**	**1.17**	**0.58**	**27.51**	**30.16**	**0.33**	**1.38**	**33.76**
ΔL	2.82	0.47	1.00	1.14	**0.43**	**21.33**	22.53	0.23	1.26	23.99
ΔaΔb, ΔC, ΔH	0.84	1.02	1.00	1.07	**0.53**	**26.25**	39.89	0.41	1.42	40.65
All Grey	8.31	1.45	1.00	1.61	**0.44**	**21.14**	21.99	0.28	1.31	27.03
All Blue	0.99	0.84	1.00	0.86	**0.41**	**20.42**	22.05	0.29	1.33	27.90
All Samples	**1.72**	**1.00**	**1.00**	**1.09**	**0.60**	**27.68**	**30.37**	**0.32**	**1.37**	**33.25**
ΔL	2.52	1.00	1.00	1.20	**0.46**	**23.86**	25.70	0.27	1.30	27.54
ΔaΔb, ΔC, ΔH	0.83	1.00	1.00	1.05	**0.53**	**26.26**	40.33	0.41	1.41	40.84
All Grey	3.80	1.00	1.00	1.40	**0.53**	**24.21**	25.48	0.27	1.31	28.11
All Blue	1.07	1.00	1.00	1.05	**0.45**	**20.94**	22.67	0.31	1.36	30.15
All Samples	**2.00**	**1.00**	**1.00**	**1.00**	**0.66**	**27.95**	**30.66**	**0.32**	**1.37**	**33.43**
ΔL	2.00	1.00	1.00	1.00	**0.51**	**24.24**	26.26	0.25	1.29	26.85
ΔaΔb, ΔC, ΔH	2.00	1.00	1.00	1.00	**0.65**	**28.82**	24.54	0.49	1.40	38.11
All Grey	2.00	1.00	1.00	1.00	**0.80**	**26.87**	28.85	0.30	1.34	30.87
All Blue	2.00	1.00	1.00	1.00	**0.53**	**26.41**	29.51	0.33	1.39	33.98
All Samples	**1.00**	**1.00**	**1.00**	**1.00**	**0.62**	**32.75**	**36.63**	**0.36**	**1.43**	**38.70**
ΔL	1.00	1.00	1.00	1.00	**0.67**	**28.55**	31.78	0.26	1.29	28.93
ΔaΔb, ΔC, ΔH	1.00	1.00	1.00	1.00	**0.56**	**26.55**	27.04	0.45	1.40	37.46
All Grey	1.00	1.00	1.00	1.00	**0.81**	**39.50**	45.44	0.40	1.48	44.42
All Blue	1.00	1.00	1.00	1.00	**0.42**	**21.08**	22.77	0.32	1.37	30.59

CIEDE2000 - PHYSICAL: SINGLESTITCH (ST) DV VC EAST/WEST - DE VC TSR

	KL	KC	KH	Factor	Residual	STRESS	CV	VAB	Gamma	PF/3
All Samples	**1.14**	**0.66**	**0.76**	**0.46**	0.45	32.78	**36.18**	**0.44**	**1.48**	**42.86**
ΔL >90%	1.88	0.37	1.21	0.67	**0.48**	**32.00**	43.14	0.60	1.63	55.19
ΔL+ΔaΔb, ΔC,	1.15	1.70	1.87	1.13	**0.28**	**24.06**	25.90	0.34	1.41	33.59
All Grey	3.26	1.08	1.52	1.15	**0.44**	**28.16**	30.47	0.39	1.58	42.30
All Blue	2.77	2.31	3.34	1.50	**0.29**	**27.69**	29.21	0.35	1.41	35.03
All Samples	**1.50**	**0.88**	**1.00**	**0.61**	0.45	32.78	**36.18**	**0.44**	**1.48**	**42.86**
ΔL >90%	2.00	0.39	1.00	0.68	**0.50**	**32.79**	44.65	0.62	1.65	57.42
ΔL+ΔaΔb, ΔC,	0.62	0.91	1.00	0.60	**0.28**	**24.06**	25.90	0.34	1.41	33.59
All Grey	2.14	0.71	1.00	0.76	**0.44**	**28.16**	30.47	0.39	1.58	42.30
All Blue	0.83	0.69	1.00	0.45	**0.29**	**27.69**	29.21	0.35	1.41	35.03
All Samples	**1.60**	**1.00**	**1.00**	**0.66**	0.45	32.90	**36.39**	**0.43**	**1.48**	**42.45**
ΔL	2.00	1.00	1.00	0.71	**0.59**	**36.01**	40.52	0.49	1.60	50.01
ΔaΔb, ΔC, ΔH	0.65	1.00	1.00	0.64	**0.29**	**24.22**	26.11	0.33	1.39	32.98
All Grey	2.40	1.00	1.00	0.82	**0.44**	**29.17**	31.63	0.43	1.58	44.01
All Blue	1.05	1.00	1.00	0.52	**0.32**	**29.29**	31.23	0.37	1.42	36.80
All Samples	**2.00**	**1.00**	**1.00**	**1.00**	**0.66**	**33.70**	**36.79**	**0.45**	**1.49**	**43.67**
ΔL	2.00	1.00	1.00	1.00	**0.79**	**36.01**	40.52	0.54	1.60	51.64
ΔaΔb, ΔC, ΔH	2.00	1.00	1.00	1.00	**0.56**	**28.48**	30.88	0.41	1.42	37.94
All Grey	2.00	1.00	1.00	1.00	**0.62**	**29.69**	32.60	0.34	1.51	39.39
All Blue	2.00	1.00	1.00	1.00	**0.71**	**33.97**	36.66	0.55	1.43	44.92
All Samples	**1.00**	**1.00**	**1.00**	**1.00**	**1.10**	**36.52**	**42.44**	**0.61**	**1.51**	**51.26**
ΔL	1.00	1.00	1.00	1.00	**1.70**	**37.28**	43.55	0.51	1.62	52.16
ΔaΔb, ΔC, ΔH	1.00	1.00	1.00	1.00	**0.66**	**25.65**	27.67	0.43	1.40	37.02
All Grey	1.00	1.00	1.00	1.00	**1.23**	**38.86**	46.10	0.52	1.51	49.96
All Blue	1.00	1.00	1.00	1.00	**0.95**	**29.34**	31.29	0.69	1.43	47.83

CIEDE2000 - PHYSICAL: THREAD WINDING CARD (TWC) DV VC EAST/WEST - DE VC TSR

	KL	KC	KH	Factor	Residual	STRESS	CV	VAB	Gamma	PF/3
All Samples	**1.51**	**0.81**	**0.69**	**0.90**	0.31	18.88	**20.98**	**0.21**	**1.32**	**15.47**
ΔL>90%	2.61	1.32	0.90	1.39	**0.38**	**24.66**	28.27	0.34	1.41	34.47
ΔaΔb, ΔC, ΔH	1.21	1.06	0.92	1.16	**0.18**	**10.54**	11.33	0.17	1.16	14.80
All Grey	1.68	0.80	0.64	0.89	**0.16**	**8.92**	9.57	0.13	1.14	34.44
All Blue	1.86	1.65	1.58	1.92	**0.21**	**15.31**	16.51	0.17	1.18	1.18
All Samples	**2.19**	**1.17**	**1.00**	**1.31**	0.31	18.88	**20.98**	**0.21**	**1.32**	**15.47**
ΔL>90%	2.42	1.10	1.00	1.35	**0.40**	**24.83**	28.54	0.34	1.40	34.45
ΔaΔb, ΔC, ΔH	1.32	1.15	1.00	1.27	**0.18**	**10.54**	11.33	0.17	1.16	14.80
All Grey	2.65	1.26	1.00	1.40	**0.16**	**8.92**	9.57	0.13	1.14	34.44
All Blue	1.17	1.04	1.00	1.21	**0.21**	**15.31**	16.51	0.17	1.18	1.18
All Samples	**2.09**	**1.00**	**1.00**	**1.24**	0.32	19.42	**21.51**	**0.20**	**1.32**	**17.08**
ΔL	2.42	**1.00**	1.00	1.32	**0.40**	**24.85**	28.63	0.34	1.41	34.50
ΔaΔb, ΔC, ΔH	1.25	**1.00**	1.00	1.23	**0.20**	**11.75**	12.55	0.16	1.15	14.46
All Grey	2.49	**1.00**	1.00	1.33	**0.20**	**10.96**	11.74	0.16	1.17	34.53
All Blue	1.16	1.00	1.00	1.21	**0.22**	**15.37**	16.54	0.16	1.18	1.18
All Samples	**2.00**	**1.00**	**1.00**	**1.00**	0.51	19.50	**21.59**	**0.16**	**1.31**	**18.19**
ΔL	2.00	1.00	1.00	1.00	**0.54**	**25.26**	29.03	0.34	1.41	34.65
ΔaΔb, ΔC, ΔH	2.00	1.00	1.00	1.00	**0.49**	**14.15**	15.28	0.36	1.17	22.86
All Grey	2.00	1.00	1.00	1.00	**0.46**	**14.12**	15.18	0.19	1.21	34.65
All Blue	2.00	1.00	1.00	1.00	**0.56**	**24.70**	27.78	0.27	1.31	1.31
All Samples	**1.00**	**1.00**	**1.00**	**1.00**	0.59	35.43	**40.87**	**0.32**	**1.28**	**45.34**
ΔL	1.00	1.00	1.00	1.00	**0.90**	**28.79**	33.12	0.36	1.43	37.25
ΔaΔb, ΔC, ΔH	1.00	1.00	1.00	1.00	**0.37**	**13.05**	13.88	0.28	1.17	19.65
All Grey	1.00	1.00	1.00	1.00	**0.86**	**37.27**	42.72	0.42	1.51	37.25
All Blue	1.00	1.00	1.00	1.00	**0.31**	**16.61**	17.77	0.18	1.19	1.19

CIEDE2000 - PHYSICAL: Buttonhole (BH) DV VC NORTH/SOUTH - DE VC TSR

	KL	KC	KH	Factor	Residual	STRESS	CV	VAB	Gamma	PF/3
All Samples	**0.89**	**0.63**	**0.86**	**1.25**	**0.88**	**36.13**	**43.19**	**0.48**	**1.57**	**49.39**
ΔL>90%	1.07	0.20	0.60	0.48	**1.09**	**48.00**	68.42	0.75	2.01	81.25
ΔaΔb, ΔC, ΔH	2.00	0.30	0.91	0.74	**0.94**	**19.38**	37.41	0.58	1.59	51.42
All Grey	2.19	0.73	0.90	1.71	**0.67**	**31.36**	26.32	0.26	1.29	27.17
All Blue	0.81	0.85	1.28	1.59	**1.10**	**29.81**	48.09	0.58	1.75	60.34
All Samples	**1.03**	**0.73**	**1.00**	**1.45**	**0.88**	**36.13**	**43.19**	**0.48**	**1.57**	**49.39**
ΔL>90%	2.00	0.35	1.00	0.84	**1.10**	**47.49**	70.17	0.75	2.01	81.89
ΔaΔb, ΔC, ΔH	2.00	0.33	1.00	0.81	**0.94**	**19.43**	37.27	0.58	1.59	51.20
All Grey	2.44	0.81	1.00	1.91	**0.67**	**31.36**	26.32	0.26	1.29	27.17
All Blue	0.62	0.62	1.00	1.16	**1.10**	**29.74**	48.03	0.58	1.75	60.56
All Samples	**1.15**	**1.00**	**1.00**	**1.66**	**0.96**	**37.03**	**45.63**	**0.47**	**1.57**	**49.80**
ΔL>90%	1.07	1.00	1.00	0.79	**0.91**	**56.96**	56.53	0.75	2.04	78.46
ΔaΔb, ΔC, ΔH	2.00	1.00	1.00	2.12	**0.58**	**30.36**	24.09	0.23	1.25	24.03
All Grey	2.12	1.00	1.00	2.12	**0.75**	**33.42**	31.64	0.26	1.30	29.15
All Blue	0.81	1.00	1.00	1.49	**1.04**	**31.67**	45.28	0.56	1.72	57.83
All Samples	**2.00**	**1.00**	**1.00**	**1.00**	**1.72**	**42.96**	**35.38**	**0.50**	**1.60**	**48.37**
ΔL>90%	2.00	1.00	1.00	1.00	**1.21**	**60.32**	56.08	0.74	2.01	76.91
ΔaΔb, ΔC, ΔH	2.00	1.00	1.00	1.00	**1.82**	**30.36**	24.09	0.89	1.25	45.89
All Grey	2.00	1.00	1.00	1.00	**1.80**	**33.46**	33.04	0.27	1.30	30.04
All Blue	2.00	1.00	1.00	1.00	**1.65**	**51.73**	38.11	0.63	1.81	60.89
All Samples	**1.00**	**1.00**	**1.00**	**1.00**	**1.46**	**37.63**	**49.94**	**0.48**	**1.58**	**51.82**
ΔL>90%	1.00	1.00	1.00	1.00	**0.92**	**56.97**	56.58	0.75	2.04	78.58
ΔaΔb, ΔC, ΔH	1.00	1.00	1.00	1.00	**1.63**	**35.90**	19.41	0.75	1.21	38.38
All Grey	1.00	1.00	1.00	1.00	**1.62**	**41.37**	56.15	0.37	1.44	45.70
All Blue	1.00	1.00	1.00	1.00	**1.30**	**34.00**	39.89	0.56	1.71	55.52

CIEDE2000 - PHYSICAL: THREAD WINDING CARD (TWC) DV VC NORTH/SOUTH - DE VC TSR

	KL	KC	KH	Factor	Residual	STRESS	CV	VAB	Gamma	PF/3
All Samples	**1.34**	**0.81**	**0.84**	**1.24**	**0.89**	**36.65**	**42.48**	**0.52**	**1.60**	**51.56**
ΔL >90%	0.86	1.93	0.19	0.60	**1.00**	**34.79**	40.67	0.69	1.88	66.04
ΔaΔb, ΔC, ΔH	1.12	1.16	1.28	1.44	**0.74**	**32.70**	36.05	0.45	1.43	41.22
All Grey	2.18	1.12	0.55	1.71	**0.74**	**27.77**	30.20	0.48	1.54	44.08
All Blue	2.07	1.92	2.23	2.27	**0.62**	**37.35**	41.45	0.53	1.64	52.91
All Samples	**1.59**	**0.96**	**1.00**	**1.47**	**0.89**	**36.65**	**42.48**	**0.52**	**1.60**	**51.56**
ΔL >90%	4.63	10.39	1.00	3.26	**1.00**	**34.79**	40.67	0.69	1.88	66.04
ΔL+ΔaΔb, ΔC	0.87	0.91	1.00	1.12	**0.74**	**32.70**	36.05	0.45	1.43	41.22
All Grey	3.97	2.03	1.00	3.12	**0.74**	**27.77**	30.20	0.48	1.54	44.08
All Blue	1.08	1.00	1.00	1.14	**0.62**	**37.60**	41.58	0.52	1.62	51.93
All Samples	**1.62**	**1.00**	**1.00**	**1.51**	**0.89**	**36.66**	**42.45**	**0.52**	**1.60**	**51.33**
ΔL>90%	2.08	1.00	1.00	1.47	**1.05**	**37.28**	45.15	0.62	1.78	61.56
ΔaΔb, ΔC, ΔH	0.92	1.00	1.00	1.19	**0.74**	**32.79**	36.03	0.44	1.42	40.47
All Grey	2.30	1.00	1.00	1.73	**0.93**	**32.16**	35.84	0.56	1.56	49.11
All Blue	0.98	1.00	1.00	1.07	**0.62**	**37.40**	41.44	0.52	1.63	52.22
All Samples	**2.00**	**1.00**	**1.00**	**1.00**	**1.23**	**37.35**	**42.74**	**0.90**	**1.63**	**65.03**
ΔL>90%	2.00	1.00	1.00	1.00	**1.44**	**37.28**	45.18	0.83	1.77	68.46
ΔaΔb, ΔC, ΔH	2.00	1.00	1.00	1.00	**1.10**	**37.09**	40.58	0.73	1.46	53.07
All Grey	2.00	1.00	1.00	1.00	**1.57**	**32.49**	36.59	0.96	1.53	61.84
All Blue	2.00	1.00	1.00	1.00	**0.84**	**46.01**	52.17	0.82	1.69	67.69
All Samples	**1.00**	**1.00**	**1.00**	**1.00**	**0.97**	**39.68**	**48.10**	**0.60**	**1.61**	**56.34**
ΔL>90%	1.00	1.00	1.00	1.00	**1.17**	**37.74**	46.00	0.76	1.75	65.38
ΔaΔb, ΔC, ΔH	1.00	1.00	1.00	1.00	**0.84**	**32.88**	36.03	0.58	1.42	45.14
All Grey	1.00	1.00	1.00	1.00	**1.25**	**40.34**	48.97	0.64	1.56	56.20
All Blue	1.00	1.00	1.00	1.00	**0.64**	**37.41**	41.42	0.55	1.63	53.21

CIEDE2000 - PHYSICAL: THREAD WINDING CARD (TWC) DV VC NORTH/SOUTH - DE VC TSR

	KL	KC	KH	Factor	Residual	STRESS	CV	VAB	Gamma	PF/3
All Samples	**1.84**	**0.80**	**0.93**	**1.06**	**0.44**	**20.09**	**21.43**	**0.26**	**1.32**	**26.35**
ΔL>90%	1.78	0.84	1.02	1.14	**0.34**	**16.49**	16.04	0.19	1.21	18.98
ΔaΔb, ΔC, ΔH	2.00	0.89	1.02	1.16	**0.49**	**22.00**	23.82	0.33	1.32	29.68
All Grey	2.26	1.00	0.81	1.18	**0.37**	**16.62**	16.94	0.19	1.21	18.80
All Blue	2.40	0.69	1.30	1.42	**0.31**	**15.36**	16.51	0.21	1.23	20.39
All Samples	**1.99**	**0.87**	**1.00**	**1.14**	**0.44**	**20.09**	**21.43**	**0.26**	**1.32**	**26.35**
ΔL>90%	1.74	0.82	1.00	1.12	**0.34**	**16.49**	16.04	0.19	1.21	18.98
ΔaΔb, ΔC, ΔH	2.00	0.87	1.00	1.15	**0.49**	**22.00**	23.82	0.33	1.32	29.60
All Grey	2.78	1.23	1.00	1.45	**0.37**	**16.62**	16.94	0.19	1.21	18.80
All Blue	1.85	0.53	1.00	1.09	**0.31**	**15.36**	16.51	0.21	1.23	20.39
All Samples	**2.08**	**1.00**	**1.00**	**1.18**	**0.44**	**20.49**	**21.96**	**0.26**	**1.32**	**26.78**
ΔL>90%	1.98	1.00	1.00	1.26	**0.34**	**16.77**	16.30	0.21	1.24	20.40
ΔaΔb, ΔC, ΔH	2.08	1.00	1.00	1.15	**0.49**	**22.51**	24.55	0.37	1.32	31.01
All Grey	2.30	1.00	1.00	1.18	**0.35**	**17.10**	17.48	0.19	1.21	19.29
All Blue	1.21	1.00	1.00	1.32	**0.43**	**20.61**	22.92	0.27	1.31	27.23
All Samples	**2.00**	**1.00**	**1.00**	**1.00**	**0.65**	**20.51**	**21.99**	**0.26**	**1.32**	**26.79**
ΔL>90%	2.00	1.00	1.00	1.00	**0.63**	**16.77**	16.29	0.21	1.24	20.41
ΔaΔb, ΔC, ΔH	2.00	1.00	1.00	1.00	**0.66**	**22.51**	24.55	0.47	1.32	34.56
All Grey	2.00	1.00	1.00	1.00	**0.54**	**17.49**	17.95	0.20	1.22	19.95
All Blue	2.00	1.00	1.00	1.00	**0.76**	**22.77**	25.60	0.28	1.32	28.24
All Samples	**1.00**	**1.00**	**1.00**	**1.00**	**0.65**	**30.03**	**33.23**	**0.35**	**1.34**	**33.77**
ΔL>90%	1.00	1.00	1.00	1.00	**0.68**	**20.04**	19.75	0.22	1.25	22.22
ΔaΔb, ΔC, ΔH	1.00	1.00	1.00	1.00	**0.63**	**22.91**	24.89	0.46	1.33	34.64
All Grey	1.00	1.00	1.00	1.00	**0.71**	**31.12**	33.77	0.34	1.40	35.96
All Blue	1.00	1.00	1.00	1.00	**0.58**	**21.29**	23.62	0.29	1.33	28.72

CIEDE2000 FORMULA - PHYSICAL: BUTTONHOLE (BH) DV VC EAST/WEST - DE 7000A

	KL	KC	KH	Factor	Residual	STRESS	CV	VAB	Gamma	PF/3
All Samples	**4.67**	**3.33**	**2.65**	**4.18**	**0.63**	**30.26**	**37.04**	**0.34**	**1.39**	**36.72**
ΔL<90%	2.27	1.00	0.83	1.90	**0.72**	**37.06**	44.09	0.35	1.41	39.87
ΔaΔb, ΔC, ΔH	1.61	2.13	1.58	2.00	**0.63**	**26.23**	28.74	0.46	1.45	39.83
All Grey	2.14	1.17	0.61	1.33	**0.55**	**26.09**	28.07	0.27	1.30	28.35
All Blue	1.86	1.75	1.70	1.93	**0.49**	**25.12**	28.09	0.42	1.52	40.67
All Samples	**1.76**	**1.26**	**1.00**	**1.58**	**0.63**	**30.26**	**37.04**	**0.34**	**1.39**	**36.72**
ΔL<90%	2.38	2.00	1.00	2.08	**0.71**	**36.53**	43.38	0.34	1.40	38.91
ΔaΔb, ΔC, ΔH	1.02	1.34	1.00	1.26	**0.63**	**26.23**	28.74	0.46	1.45	39.83
All Grey	3.50	1.92	1.00	2.17	**0.55**	**26.09**	28.07	0.27	1.30	28.35
All Blue	1.09	1.03	1.00	1.14	**0.49**	**25.12**	28.09	0.42	1.52	40.67
All Samples	**1.61**	**1.00**	**1.00**	**1.44**	**0.68**	**30.78**	**37.41**	**0.36**	**1.43**	**38.72**
ΔL<90%	2.50	1.00	1.00	2.09	**0.70**	**37.25**	44.49	0.36	1.42	40.93
ΔaΔb, ΔC, ΔH	0.90	1.00	1.00	1.16	**0.60**	**27.40**	30.17	0.49	1.50	42.84
All Grey	2.50	1.00	1.00	1.85	**0.68**	**30.22**	32.88	0.28	1.33	31.31
All Blue	1.08	1.00	1.00	1.14	**0.49**	**25.13**	28.12	0.43	1.52	40.94
All Samples	**2.00**	**1.00**	**1.00**	**1.00**	**0.99**	**31.57**	**43.44**	**0.36**	**1.43**	**40.72**
ΔL<90%	2.00	1.00	1.00	1.00	**0.88**	**37.54**	45.13	0.38	1.46	43.16
ΔaΔb, ΔC, ΔH	2.00	1.00	1.00	1.00	**0.79**	**30.92**	34.80	0.76	1.52	54.17
All Grey	2.00	1.00	1.00	1.00	**1.04**	**30.75**	33.62	0.27	1.31	30.78
All Blue	2.00	1.00	1.00	1.00	**0.94**	**32.27**	38.08	0.42	1.52	43.95
All Samples	**1.00**	**1.00**	**1.00**	**1.00**	**0.73**	**34.67**	**34.31**	**0.41**	**1.49**	**41.37**
ΔL<90%	**1.00**	1.00	1.00	1.00	**0.63**	**40.33**	49.84	0.53	1.67	56.38
ΔaΔb, ΔC, ΔH	**1.00**	1.00	1.00	1.00	**0.79**	**27.51**	30.36	0.61	1.50	47.06
All Grey	**1.00**	1.00	1.00	1.00	**0.84**	**37.20**	42.13	0.34	1.39	38.36
All Blue	**1.00**	1.00	1.00	1.00	**0.61**	**25.33**	28.21	0.43	1.53	41.55

CIEDE2000 - PHYSICAL: SINGLESTITCH (ST) DV VC EAST/WEST - DE 7000A

	KL	KC	KH	Factor	Residual	STRESS	CV	VAB	Gamma	PF/3
All Samples	**0.77**	**0.38**	**0.73**	**0.43**	**0.53**	**39.10**	**46.02**	**0.59**	**1.10**	**38.52**
ΔL<90%	1.87	0.29	1.00	0.81	**0.69**	**42.94**	52.55	0.61	1.64	59.11
ΔaΔb, ΔC, ΔH	1.16	1.18	2.34	0.81	**0.37**	**22.72**	24.58	0.62	1.38	41.75
All Grey	2.07	0.80	1.39	0.92	**0.60**	**39.08**	45.72	0.81	1.72	66.39
All Blue	2.13	1.70	3.47	1.54	**0.33**	**30.17**	32.88	0.46	1.54	1.54
All Samples	**1.05**	**0.53**	**1.00**	**0.59**	**0.53**	**39.10**	**46.02**	**0.59**	**1.10**	**38.52**
ΔL<90%	1.87	0.29	1.00	0.76	**0.69**	**42.94**	52.55	0.65	1.64	60.37
ΔaΔb, ΔC, ΔH	0.50	0.50	1.00	0.44	**0.23**	**22.72**	24.58	0.43	1.38	35.12
All Grey	1.35	0.52	1.00	0.60	**0.61**	**39.11**	45.85	0.82	1.72	66.50
All Blue	0.61	0.49	1.00	0.45	**0.33**	**30.17**	32.88	0.46	1.54	1.54
All Samples	**1.43**	**1.00**	**1.00**	**0.79**	**0.56**	**40.80**	**48.31**	**0.64**	**1.11**	**40.86**
ΔL<90%	1.87	1.00	1.00	0.82	**0.78**	**47.69**	60.31	0.99	1.94	84.55
ΔaΔb, ΔC, ΔH	0.74	1.00	1.00	0.68	**0.30**	**27.22**	29.71	0.44	1.43	39.13
All Grey	1.99	1.00	1.00	1.09	**0.61**	**39.90**	46.78	0.69	1.76	63.91
All Blue	0.92	1.00	1.00	0.65	**0.39**	**34.34**	38.14	0.54	1.64	1.64
All Samples	**2.00**	**1.00**	**1.00**	**1.00**	**0.56**	**42.50**	**49.69**	**0.63**	**1.12**	**41.42**
ΔL<90%	2.00	1.00	1.00	1.00	**0.81**	**47.70**	60.25	0.88	1.94	80.66
ΔaΔb, ΔC, ΔH	2.00	1.00	1.00	1.00	**0.37**	**31.47**	34.97	0.36	1.42	37.48
All Grey	2.00	1.00	1.00	1.00	**0.61**	**39.90**	46.76	0.75	1.76	65.89
All Blue	2.00	1.00	1.00	1.00	**0.51**	**40.80**	47.48	0.46	1.56	1.56
All Samples	**1.00**	**1.00**	**1.00**	**1.00**	**0.77**	**42.75**	**52.28**	**0.53**	**1.10**	**38.64**
ΔL<90%	1.00	1.00	1.00	1.00	**1.26**	**48.09**	61.51	0.70	1.95	75.63
ΔaΔb, ΔC, ΔH	1.00	1.00	1.00	1.00	**0.40**	**28.06**	30.75	0.36	1.41	35.90
All Grey	1.00	1.00	1.00	1.00	**0.93**	**45.46**	57.11	0.51	1.64	57.45
All Blue	1.00	1.00	1.00	1.00	**0.59**	**34.46**	38.37	0.56	1.62	1.62

CMC FORMULA - PHYSICAL: THREAD WINDING CARD (TWC) DV VC EAST/WEST - DE 7000A

	KL	KC	KH	Factor	Residual	STRESS	CV	VAB	Gamma	PF/3
All Samples	**1.42**	**0.98**	**0.78**	**1.08**	**0.34**	**18.43**	**20.46**	**0.29**	**1.33**	**27.55**
ΔL<90%	2.05	1.00	0.70	1.28	**0.37**	**21.25**	22.85	0.25	1.24	24.00
ΔaΔb, ΔC, ΔH	1.68	1.45	1.14	1.41	**0.30**	**16.40**	18.38	0.24	1.36	26.03
All Grey	1.99	1.12	0.86	1.24	**0.19**	**10.77**	11.56	0.16	1.18	15.18
All Blue	2.07	2.26	1.81	2.18	**0.26**	**16.42**	18.23	0.36	1.42	32.15
All Samples	**1.82**	**1.26**	**1.00**	**1.38**	**0.34**	**18.43**	**20.46**	**0.29**	**1.33**	**27.55**
ΔL<90%	2.52	1.00	1.00	1.57	**0.37**	**21.45**	23.17	0.25	1.25	24.31
ΔaΔb, ΔC, ΔH	1.47	1.27	1.00	1.23	**0.30**	**16.40**	18.38	0.24	1.36	26.03
All Grey	2.30	1.30	1.00	1.44	**0.19**	**10.77**	11.56	0.16	1.18	15.18
All Blue	1.14	1.25	1.00	1.20	**0.26**	**16.42**	18.23	0.36	1.42	32.15
All Samples	**1.71**	**1.00**	**1.00**	**1.24**	**0.36**	**19.48**	**21.51**	**0.28**	**1.32**	**27.43**
ΔL<90%	2.52	1.00	1.00	1.57	**0.37**	**21.45**	23.17	0.25	1.25	24.31
ΔaΔb, ΔC, ΔH	1.40	1.00	1.00	1.20	**0.31**	**18.02**	20.04	0.24	1.35	26.38
All Grey	2.13	1.00	1.00	1.36	**0.23**	**12.80**	13.69	0.18	1.20	17.07
All Blue	1.08	1.00	1.00	1.14	**0.28**	**17.51**	19.30	0.34	1.39	30.86
All Samples	**2.00**	**1.00**	**1.00**	**1.00**	**0.57**	**20.38**	**22.61**	**0.28**	**1.32**	**27.77**
ΔL<90%	2.00	1.00	1.00	1.00	**0.62**	**21.60**	23.45	0.25	1.24	24.27
ΔaΔb, ΔC, ΔH	2.00	1.00	1.00	1.00	**0.51**	**19.04**	21.11	0.25	1.34	26.92
All Grey	2.00	1.00	1.00	1.00	**0.58**	**13.06**	13.95	0.18	1.20	17.48
All Blue	2.00	1.00	1.00	1.00	**0.56**	**27.30**	31.50	0.34	1.40	35.20
All Samples	**1.00**	**1.00**	**1.00**	**1.00**	**0.49**	**29.25**	**32.86**	**0.39**	**1.46**	**39.13**
ΔL<90%	1.00	1.00	1.00	1.00	**0.61**	**22.34**	24.47	0.25	1.25	24.69
ΔaΔb, ΔC, ΔH	1.00	1.00	1.00	1.00	**0.39**	**19.83**	22.27	0.25	1.37	28.06
All Grey	1.00	1.00	1.00	1.00	**0.67**	**32.11**	35.51	0.37	1.45	39.26
All Blue	1.00	1.00	1.00	1.00	**0.30**	**17.77**	19.54	0.35	1.41	32.00

Appendices B

CMC - DIGITAL: CAMERA BUTTONHOLE (BH) DV VC EAST/WEST - DE VC TSR

	KL	KC	FACTOR	Residual	STRESS	CV	VAB	Gamma	PF/3
All Samples	**1.94**	**0.69**	**1.26**	0.90	36.20	**38.55**	**0.37**	**1.50**	**41.94**
ΔL>90%	3.01	0.34	1.12	0.31	12.63	13.51	0.18	1.20	17.12
ΔL+ΔaΔb, ΔC, ΔH	0.60	0.98	1.18	0.73	27.24	28.45	0.36	1.38	34.30
All Blue	2.20	1.26	1.28	0.57	26.72	28.50	0.32	1.37	32.34
All Grey	1.53	0.46	1.14	0.67	22.49	23.30	0.28	1.33	28.08
All Samples	**2.26**	**1.00**	**1.60**	1.02	37.65	**40.30**	**0.39**	**1.55**	**44.99**
ΔL>90%	6.71	1.00	2.24	0.42	15.06	16.02	0.20	1.21	19.01
ΔL+ΔaΔb, ΔC, ΔH	0.88	1.00	1.48	0.87	30.00	31.40	0.32	1.37	33.68
All Blue	2.33	1.00	1.21	0.61	27.52	29.51	0.30	1.35	31.38
All Grey	1.75	1.00	2.00	1.15	31.99	34.38	0.31	1.36	34.00
All Samples	**2.00**	**1.00**	**1.00**	1.39	37.83	**40.47**	**0.40**	**1.61**	**47.33**
ΔL>90%	2.00	1.00	1.00	1.00	28.65	30.22	0.32	1.37	33.05
ΔL+ΔaΔb, ΔC, ΔH	2.00	1.00	1.00	1.52	38.98	41.84	0.75	1.46	54.32
All Blue	2.00	1.00	1.00	0.74	28.06	29.98	0.31	1.36	32.60
All Grey	2.00	1.00	1.00	2.04	32.19	34.48	0.31	1.37	34.11
All Samples	**1.00**	**1.00**	**1.00**	1.28	46.28	**51.39**	**0.51**	**2.17**	**73.13**
ΔL>90%	1.00	1.00	1.00	1.19	33.85	36.14	0.40	1.48	41.11
ΔL+ΔaΔb, ΔC, ΔH	1.00	1.00	1.00	1.31	31.56	33.14	0.60	1.38	43.80
All Blue	1.00	1.00	1.00	0.91	42.65	46.98	0.46	1.56	49.77
All Grey	1.00	1.00	1.00	1.65	36.63	40.94	0.34	1.41	38.50

CMC - DIGITAL CAMERA SINGLESTITCH (ST) DV VC EAST/WEST - DE VC TSR

	KL	KC	FACTOR	Residual	STRESS	CV	VAB	Gamma	PF/3
All Samples	**2.09**	**1.24**	**1.04**	0.65	36.74	**39.48**	**0.43**	**1.51**	**44.33**
ΔL>90%	1.53	0.44	0.68	0.48	24.70	25.30	0.41	1.41	35.76
ΔL+ΔaΔb, ΔC, ΔH	0.77	1.23	0.86	0.44	26.54	28.27	0.31	1.35	31.62
All Blue	2.20	1.26	0.70	0.41	30.21	31.97	0.41	1.40	37.61
All Grey	1.94	0.98	1.02	0.65	29.61	31.89	0.34	1.37	34.19
All Samples	**1.88**	**1.00**	**0.94**	0.64	37.05	**39.67**	**0.44**	**1.52**	**45.11**
ΔL>90%	1.38	1.00	0.65	0.57	27.21	28.24	0.39	1.45	37.32
ΔL+ΔaΔb, ΔC, ΔH	0.69	1.00	0.79	0.46	26.92	28.55	0.31	1.36	31.78
All Blue	1.88	1.00	0.61	0.41	30.61	32.39	0.42	1.42	38.79
All Grey	1.96	1.00	1.04	0.65	29.61	31.91	0.34	1.36	34.02
All Samples	**2.00**	**1.00**	**1.00**	0.65	37.11	**39.62**	**0.43**	**1.52**	**44.78**
ΔL>90%	2.00	1.00	1.00	0.58	27.46	28.35	0.45	1.44	39.17
ΔL+ΔaΔb, ΔC, ΔH	2.00	1.00	1.00	0.67	39.91	42.38	0.42	1.48	44.17
All Blue	2.00	1.00	1.00	0.62	30.70	32.44	0.44	1.41	39.21
All Grey	2.00	1.00	1.00	0.67	29.62	31.88	0.36	1.37	34.82
All Samples	**1.00**	**1.00**	**1.00**	1.09	42.64	**48.47**	**0.56**	**1.62**	**55.57**
ΔL>90%	1.00	1.00	1.00	2.67	27.28	28.39	0.97	1.45	56.63
ΔL+ΔaΔb, ΔC, ΔH	1.00	1.00	1.00	0.51	29.74	31.20	0.31	1.37	33.05
All Blue	1.00	1.00	1.00	1.35	38.64	42.98	0.74	1.57	58.03
All Grey	1.00	1.00	1.00	0.86	36.78	42.52	0.27	1.42	37.40

Appendices C

CMC - SYNTHESIZED BUTTONHOLE (BH) DV VC EAST/WEST - DE VC TSR									
	KL	KC	Factor	Residual	STRESS	CV	VAB	Gamma	PF/3
All Samples	**0.82**	**0.70**	**0.87**	0.67	28.26	**30.64**	**0.27**	**1.31**	**29.50**
ΔL>90%	5.73	0.70	3.05	0.38	12.75	13.75	0.21	1.23	19.06
ΔL+ΔaΔb, ΔC, ΔI	0.62	0.75	0.89	0.44	21.64	22.71	0.26	1.24	24.22
All Blue	1.66	1.25	1.16	0.21	9.28	9.84	0.11	1.12	10.74
All Grey	0.51	0.52	0.77	0.44	14.06	15.85	0.16	1.17	16.10
All Samples	**0.98**	**1.00**	**1.13**	0.72	29.11	**31.81**	**0.29**	**1.33**	**31.37**
ΔL>90%	7.31	1.00	3.68	0.52	14.83	15.84	0.22	1.25	21.07
ΔL+ΔaΔb, ΔC, ΔI	0.67	0.88	1.02	0.47	22.01	23.18	0.28	1.26	25.67
All Blue	1.48	1.00	1.04	0.23	11.05	11.68	0.11	1.11	11.10
All Grey	0.71	1.00	1.13	0.57	17.66	20.44	0.20	1.22	20.96
All Samples	**2.00**	**1.00**	**1.00**	1.07	37.40	**39.85**	**0.36**	**1.42**	**39.23**
ΔL>90%	2.00	1.00	1.00	2.10	24.97	26.82	0.31	1.37	31.62
ΔL+ΔaΔb, ΔC, ΔI	2.00	1.00	1.00	0.73	33.83	36.11	0.54	1.35	41.67
All Blue	2.00	1.00	1.00	0.49	15.44	16.39	0.15	1.16	15.89
All Grey	2.00	1.00	1.00	1.65	37.49	40.06	0.40	1.49	43.03
All Samples	**1.00**	**1.00**	**1.00**	0.73	29.12	**31.76**	**0.29**	**1.33**	**31.32**
ΔL>90%	1.00	1.00	1.00	1.29	29.97	32.59	0.37	1.44	37.61
ΔL+ΔaΔb, ΔC, ΔI	1.00	1.00	1.00	0.52	25.40	26.74	0.24	1.27	25.83
All Blue	1.00	1.00	1.00	0.38	18.62	19.93	0.17	1.18	18.33
All Grey	1.00	1.00	1.00	0.38	20.89	23.23	0.24	1.27	25.01

CMC - SYNTHESIZED Thread Winding Card (TWC) DV VC EAST/WEST - DE VE TSR									
	KL	KC	Factor	Residual	STRESS	CV	VAB	Gamma	PF/3
All Samples	**1.52**	**1.00**	**1.35**	0.49	22.28	**24.14**	**0.27**	**1.30**	**27.08**
ΔL>90%	1.00	0.75	0.79	0.79	26.79	29.11	0.34	1.38	33.69
ΔL+ΔaΔb, ΔC, ΔI	1.15	0.91	1.28	0.25	13.55	14.18	0.17	1.18	16.43
All Blue	2.97	1.02	1.24	0.15	9.61	9.92	0.09	1.09	9.35
All Grey	1.33	0.81	1.38	0.31	10.73	12.08	0.16	1.15	14.31
All Samples	**1.52**	**1.00**	**1.35**	0.49	22.28	**24.14**	**0.27**	**1.30**	**27.07**
ΔL>90%	1.00	1.00	0.78	0.79	26.80	29.18	0.34	1.38	33.56
ΔL+ΔaΔb, ΔC, ΔI	1.19	1.00	1.33	0.28	13.77	14.42	0.17	1.18	16.68
All Blue	2.93	1.00	1.22	0.16	9.64	9.94	0.09	1.09	9.52
All Grey	1.45	1.00	1.51	0.31	11.19	12.60	0.18	1.17	16.01
All Samples	**2.00**	**1.00**	**1.00**	0.83	24.57	**26.03**	**0.41**	**1.28**	**31.78**
ΔL>90%	**2.00**	**1.00**	**1.00**	1.03	28.02	30.19	0.46	1.41	39.03
ΔL+ΔaΔb, ΔC, ΔI	**2.00**	**1.00**	**1.00**	0.59	21.39	22.02	0.40	1.23	28.12
All Blue	**2.00**	**1.00**	**1.00**	0.33	15.00	15.33	0.20	1.16	17.17
All Grey	**2.00**	**1.00**	**1.00**	1.27	16.16	17.56	0.53	1.21	30.58
All Samples	**1.00**	**1.00**	**1.00**	0.59	26.79	**30.62**	**0.35**	**1.41**	**35.58**
ΔL>90%	**1.00**	**1.00**	**1.00**	0.84	26.80	29.18	0.46	1.38	37.82
ΔL+ΔaΔb, ΔC, ΔI	**1.00**	**1.00**	**1.00**	0.38	15.24	16.18	0.28	1.20	21.39
All Blue	**1.00**	**1.00**	**1.00**	0.63	37.68	39.59	0.39	1.44	41.00
All Grey	**1.00**	**1.00**	**1.00**	0.56	16.51	19.65	0.31	1.24	24.89